plants

Advances in Forest Ecophysiology

Stress Response and Ecophysiological Indicators of Tree Vitality

Edited by
Nenad Potočić

Printed Edition of the Special Issue Published in *Plants*

www.mdpi.com/journal/plants

MDPI

Advances in Forest Ecophysiology: Stress Response and Ecophysiological Indicators of Tree Vitality

Advances in Forest Ecophysiology: Stress Response and Ecophysiological Indicators of Tree Vitality

Editor

Nenad Potočić

MDPI • Basel • Beijing • Wuhan • Barcelona • Belgrade • Manchester • Tokyo • Cluj • Tianjin

Editor
Nenad Potočić
Croatian Forest Research
Institute
Croatia

Editorial Office
MDPI
St. Alban-Anlage 66
4052 Basel, Switzerland

This is a reprint of articles from the Special Issue published online in the open access journal *Plants* (ISSN 2223-7747) (available at: https://www.mdpi.com/journal/plants/special_issues/forest_ecophysiology).

For citation purposes, cite each article independently as indicated on the article page online and as indicated below:

LastName, A.A.; LastName, B.B.; LastName, C.C. Article Title. *Journal Name* **Year**, *Volume Number*, Page Range.

ISBN 978-3-0365-7519-3 (Hbk)
ISBN 978-3-0365-7518-6 (PDF)

Contents

About the Editor

Nenad Potočić

Dr. Nenad Potočić is a scientific advisor at the Croatian Forest Research Institute in Jastrebarsko, Croatia, and the Chair of the UNECE ICP Forests Expert panel on Crown Condition and Damage Causes. His scientific interests include forest monitoring and forest tree ecophysiology, especially tree crown condition, tree nutrition, and other indicators of tree vitality.

plants

MDPI

Editorial

Advances in Forest Ecophysiology: Stress Response and Ecophysiological Indicators of Tree Vitality

Nenad Potočić

Croatian Forest Research Institute, Division of Forest Ecology, Cvjetno naselje 41, 10450 Jastrebarsko, Croatia; nenadp@sumins.hr

Citation: Potočić, N. Advances in Forest Ecophysiology: Stress Response and Ecophysiological Indicators of Tree Vitality. *Plants* **2023**, *12*, 1063. https://doi.org/10.3390/plants12051063

Received: 3 February 2023
Revised: 21 February 2023
Accepted: 22 February 2023
Published: 27 February 2023

Back in the beginning of the year 2021, when the work on this Special Issue started, it was quite clear that the topics of tree stress response and the ecophysiological indicators of tree vitality were both current and important, but the attitude of the scientific community towards the idea of a Special Issue on the subject was yet to be determined. Now that we are closing the first, and already preparing the second volume, I am very happy to definitely confirm your high interest.

Air pollution and the changing climate are some of the greatest threats to the health and functioning of forest ecosystems, strongly jeopardizing their ecological and economic functions as well as services. The impact of increasing temperatures and extreme weather events (droughts, storms, temperature and precipitation extremes) on the vitality of forest trees is often difficult to separate from the impact of pollution, such as nitrogen deposition and tropospheric ozone, as they can exhibit synergistic effects. For example, forest soil acidification, atmospheric N deposition, and climate change are all partly responsible for the continuous decrease in foliar P concentrations in Europe, causing reduced tree growth [1,2]. The use of indicators is elementary in modern forest ecophysiological research, as they help us to disentangle complex interactions between trees and various stress-inducing factors as well as better estimate the level of damage to trees and forest ecosystems.

The initial Special Issue framework, as defined by the title and suggested topics of interest, has been broadened in the process thanks to your valuable submissions, adding terms such as heavy metals, carbon isotopes, water use efficiency, polyamines, antioxidants, or plant hormones to the list of subjects which already included photosynthetic activity and other biochemical stress indicators; nutrients in different tree compartments; tree growth; tree leaf loss and mortality; visible symptoms of stress in foliage; and microscopical markers of stress. All of these terms share one common trait: they have an important role in measuring and assessing tree stress in the context of the great ecological challenges of today.

Eleven papers are included in this Special Issue, with wide-ranging topics from various disciplines but centered around tree response to environmental stress. In line with the current trends in environmental research, climate takes clear precedence over pollution, and as many as nine of the articles discuss climate effects; tree anatomy, growth, nutrition, foliar injury, the level of antioxidants, and defoliation are used as response variables.

Three papers, by Levanič and Štraus [3], Sensuła and Wilczyński [4], and Popa et al. [5], discuss the effects of climate on tree growth, and the paper by Sensuła and Wilczyński [4] also includes the effects on water use efficiency and carbon isotopes' composition. Two papers, one by Ognjenović et al. [6] and another by Češljar et al. [7], focus on climate effects on tree crown defoliation. While the first paper tests the differences between defoliation and defoliation change as long-term and short-term indicators, respectively, of tree vitality, the second paper discusses the links between crown defoliation and tree mortality. Defoliation is again featured in the paper by Ognjenović et al. [8], where its effect on the nutritional response of beech trees to climate and stand factors is discussed. Soheili et al. [9] investigate how cell anatomical structure is affected by drought stress. Nutrition, oxidative stress,

and defoliation in four Mediterranean tree species are the focus of the paper by Lovreškov et al. [10], while Kebert et al. [11] discuss species-level differences in osmoprotectants and antioxidants under water deficit and high temperatures. Despite the prevalence of interest in climate effects, pollution-oriented papers are not less exciting: tree responses to heavy-metal-induced stress are the subject of a paper by Kebert et al. [12], and the effects of ozone and drought on oak seedlings are discussed by Baesso Moura et al. [13]. The latter paper also nicely underlines the fact that climate and pollution effects on trees, although often investigated separately, are in practice often related and intertwined.

In conclusion, the task of this Special Issue is twofold: one, to remind us that a better understanding of the physiological processes influencing tree vitality under the changing climate and air pollution pressures requires considerable research efforts and constant advancements in research methods and approaches; two, to highlight the fact that the environmental pressures instigating the use of tree stress response indicators are more present than ever, and will likely continue to affect tree vitality in the foreseeable future.

As the Guest Editor of this Special Issue, I would like to use the opportunity to thank all of the authors for their valuable submissions, their dedicated and hard work, and the continuous exchange of thoughts and ideas that form the backbone of current scientific research, pushing it ever further.

Conflicts of Interest: The author declares no conflict of interest.

References

1. Jonard, M.; Fürst, A.; Verstraeten, A.; Thimonier, A.; Timmermann, V.; Potočić, N.; Waldner, P.; Benham, S.; Hansen, K.; Merilä, P.; et al. Tree Mineral Nutrition Is Deteriorating in Europe. *Glob. Chang. Biol.* **2015**, *21*, 418–430. [CrossRef] [PubMed]
2. Talkner, U.; Meiwes, K.J.; Potočić, N.; Seletković, I.; Cools, N.; De Vos, B.; Rautio, P. Phosphorus Nutrition of Beech (*Fagus sylvatica* L.) Is Decreasing in Europe. *Ann. For. Sci.* **2015**, *72*, 919–928. [CrossRef]
3. Levanič, T.; Štraus, H. Effects of Climate on Douglas-Fir (Pseudotsuga Menziesii (Mirb.) Franco) Growth Southeast of the European Alps. *Plants* **2022**, *11*, 1571. [CrossRef] [PubMed]
4. Sensuła, B.; Wilczyński, S. Dynamics Changes in Basal Area Increment, Carbon Isotopes Composition and Water Use Efficiency in Pine as Response to Water and Heat Stress in Silesia, Poland. *Plants* **2022**, *11*, 3569. [CrossRef]
5. Popa, A.; Popa, I.; Roibu, C.C.; Badea, O.N. Do Different Tree-Ring Proxies Contain Different Temperature Signals? A Case Study of Norway Spruce (*Picea abies* (L.) Karst) in the Eastern Carpathians. *Plants* **2022**, *11*, 2428. [CrossRef] [PubMed]
6. Ognjenović, M.; Seletković, I.; Potočić, N.; Marušić, M.; Tadić, M.P.; Jonard, M.; Rautio, P.; Timmermann, V.; Lovreškov, L.; Ugarković, D. Defoliation Change of European Beech (*Fagus sylvatica* L.) Depends on Previous Year Drought. *Plants* **2022**, *11*, 730. [CrossRef]
7. Češljar, G.; Jovanović, F.; Brašanac-Bosanac, L.; Đorđević, I.; Mitrović, S.; Eremija, S.; Ćirković-Mitrović, T.; Lučić, A. Impact of an Extremely Dry Period on Tree Defoliation and Tree Mortality in Serbia. *Plants* **2022**, *11*, 1286. [CrossRef]
8. Ognjenović, M.; Seletković, I.; Marušić, M.; Jonard, M.; Rautio, P.; Timmermann, V.; Tadić, M.P.; Lanšćak, M.; Ugarković, D.; Potočić, N. The Effect of Environmental Factors on the Nutrition of European Beech (*Fagus sylvatica* L.) Varies with Defoliation. *Plants* **2023**, *12*, 168. [CrossRef] [PubMed]
9. Soheili, F.; Abdul-Hamid, H.; Almasi, I.; Heydari, M.; Tongo, A.; Woodward, S.; Naji, H.R. How Tree Decline Varies the Anatomical Features in Quercus Brantii. *Plants* **2023**, *12*, 377. [CrossRef] [PubMed]
10. Lovreškov, L.; Radojčić Redovniković, I.; Limić, I.; Potočić, N.; Seletković, I.; Marušić, M.; Jurinjak Tušek, A.; Jakovljević, T.; Butorac, L. Are Foliar Nutrition Status and Indicators of Oxidative Stress Associated with Tree Defoliation of Four Mediterranean Forest Species? *Plants* **2022**, *11*, 3484. [CrossRef] [PubMed]
11. Kebert, M.; Vuksanović, V.; Stefels, J.; Bojović, M.; Horák, R.; Kostić, S.; Kovačević, B.; Orlović, S.; Neri, L.; Magli, M.; et al. Species-Level Differences in Osmoprotectants and Antioxidants Contribute to Stress Tolerance of *Quercus robur* L., and *Q. cerris* L. Seedlings under Water Deficit and High Temperatures. *Plants* **2022**, *11*, 1744. [CrossRef] [PubMed]
12. Kebert, M.; Kostić, S.; Vuksanović, V.; Gavranović Markić, A.; Kiprovski, B.; Zorić, M.; Orlović, S. Metal- and Organ-Specific Response to Heavy Metal-Induced Stress Mediated by Antioxidant Enzymes' Activities, Polyamines, and Plant Hormones Levels in Populus Deltoides. *Plants* **2022**, *11*, 3246. [CrossRef] [PubMed]
13. Moura, B.B.; Paoletti, E.; Badea, O.; Ferrini, F.; Hoshika, Y. Visible Foliar Injury and Ecophysiological Responses to Ozone and Drought in Oak Seedlings. *Plants* **2022**, *11*, 1836. [CrossRef] [PubMed]

plants

MDPI

Article

Visible Foliar Injury and Ecophysiological Responses to Ozone and Drought in Oak Seedlings

Barbara Baesso Moura [1], Elena Paoletti [1,*], Ovidiu Badea [2,3], Francesco Ferrini [4] and Yasutomo Hoshika [1]

[1] Institute of Research on Terrestrial Ecosystems (IRET), National Research Council of Italy (CNR), Via Madonna del Piano 10, 50019 Sesto Fiorentino, Italy; bmourabio@gmail.com (B.B.M.); yasutomo.hoshoka@unifi.it (Y.H.)
[2] "Marin Drăcea" National Institute for Research and Development in Forestry, 128 Eroilor Blvd., 077190 Voluntari, Romania; ovidiu.badea63@gmail.com
[3] Faculty of Silviculture and Forest Engineering, "Transilvania" University of Brasov, 1, Ludwig van Beethoven Str., 500123 Braşov, Romania
[4] Department of Agriculture, Food, Environmental and Forestry Sciences, Section Woody Plants, University of Florence, 50019 Sesto Fiorentino, Italy; francesco.ferrini@unifi.it
* Correspondence: elena.paoletti@cnr.it

Abstract: To verify the responses of visible foliar injury (VFI), we exposed seedlings of three oak species for 4.5 months in an open air facility, using differing ozone (O_3) and drought treatments: O_3 (three levels from ambient to ×1.4 ambient), and drought (three levels of irrigation from 40% to 100% field capacity). We related the accumulated phytotoxic O_3 dose (POD_1) and cumulative drought index (CDI) to the O_3 and drought VFI and assessed growth increment (height, diameter, leaf number), biomass (of all organs), and physiological parameters: net photosynthesis per plant (P_n), photosynthetic nitrogen (PNUE) and phosphorus use efficiency (PPUE)). The results indicated that an increase in POD_1 promoted O_3 VFI in *Quercus robur* and *Quercus pubescens*, while *Quercus ilex* was asymptomatic. The POD_1-based critical level at the onset of O_3 VFI was lower for *Q. robur* than for *Q. pubescens* (12.2 vs. 15.6 mmol m^{-2} POD_1). Interestingly, drought reduced O_3 VFI in *Q. robur* but increased it in *Q. pubescens*. Both O_3 and drought were detrimental to the plant biomass. However, *Q. robur* and *Q. pubescens* invested more in shoots than in roots, while *Q. ilex* invested more in roots, which might be related to a hormetic mechanism. P_n, PNUE and PPUE decreased in all species under drought, and only in the sensitive *Q. robur* (PPUE) and *Q. pubescens* (PNUE) under O_3. This study confirms that POD_1 is a good indicator to explain the development of O_3 VFI and helps a differential diagnosis of co-occurring drought and O_3 VFI in oak forests.

Keywords: tropospheric ozone; leaf symptoms; PODy; water stress; risk assessment

Citation: Moura, B.B.; Paoletti, E.; Badea, O.; Ferrini, F.; Hoshika, Y. Visible Foliar Injury and Ecophysiological Responses to Ozone and Drought in Oak Seedlings. *Plants* **2022**, *11*, 1836. https://doi.org/10.3390/plants11141836

Academic Editor: Nenad Potočić

Received: 22 May 2022
Accepted: 11 July 2022
Published: 13 July 2022

1. Introduction

Tropospheric ozone (O_3) is an oxidative pollutant harmful to plants [1]. Ozone enters the leaves through the stomata, reacts in the mesophyll, and triggers the formation of reactive oxidative species (ROS) with a cascade of events eventually promoting cell death and, finally, the appearance of visible foliar injury (VFI), physiological impairment, and growth reduction [2–4]. Furthermore, O_3 inhibits the efficient use of nutrients such as nitrogen (N) and phosphorus (P) and thereby causes a reduction of photosynthetic N and P use efficiency (PNUE and PPUE, respectively) [5,6]. Therefore, critical levels (CL) have been investigated to assess the O_3 negative impacts on several plant species, especially those related to biomass loss [7,8]. CLs are based on cumulative O_3 indexes, e.g., AOT40, defined as the accumulated exposure over 40 ppb hourly concentrations, and PODy, defined as the phytotoxic O_3 dose above an hourly threshold y of stomatal O_3 uptake [9]. PODy is considered the most realistic index with a high correlation with the detrimental effects of O_3 [10,11]. Ozone VFI is a forest-health indicator in forest monitoring programs [12].

The estimation of CL based on O_3 VFI has been proposed as a not destructive and easily repeated observation over long-term monitoring studies [13,14].

Ozone alone can affect plant growth and development, but its effect usually occurs in combination with other factors, such as drought, which is known as the most critical environmental factor limiting plant productivity worldwide [15,16]. The adverse effects of drought are progressive and, thus, are often evaluated by the cumulative drought index (CDI), defined as the accumulated difference of soil moisture relative to field capacity [17]. Drought stress also promotes the formation of specific VFI, which can be distinguished from O_3-induced foliar injury. While O_3 VFI is usually indicated by interveinal, irregular-border, yellow to dark-brown stippling [18,19], drought VFI consists in gradients of leaf margin necrosis increasing in severity from the base to the top of a plant [20], with the injury co-occurring when plants are exposed to a combination of these stress factors.

Both O_3 and drought can limit plant carbon fixation, and the effect of both stress factors has been reported as the cause of biomass loss for *Quercus* species [21,22], which are significant components of temperate forests. Previous papers from the same experiment presented here showed that the interacting factorial impacts of O_3 and drought were species-specific, and the order of O_3 sensitivity was *Q. robur* > *Q. pubescens* > *Q. ilex* from the point of view of total biomass [22] and leaf gas exchange [23,24]. Although physiological acclimations to O_3 and drought are not fully elucidated, diverse adaptation strategies were observed for tolerating stress in different oak species. One of the reasons for the variability of strategies is related to gas exchange regulation depending on their water use strategy (isohydric and anisohydric) [24]. Under elevated O_3 with sufficient water availability, the isohydric *Q. robur* limited O_3 uptake by stomatal closure, while the anisohydric *Q. ilex* and the intermediate *Q. pubescens* activated tolerance mechanisms and did not actively show a closing response of stomata. In particular, Pellegrini et al. [25] found that *Q. ilex* had a well-regulated antioxidative defense system through phenylpropanoid pathways. However, in the combination of O_3 and drought, the anisohydric *Q. ilex* and the intermediate *Q. pubescens* exhibited stomatal closure to prevent severe oxidative damage due to excess generation of ROS.

The present study aimed to characterize the VFI induced by O_3, drought, and their combination and assess their related effects on biomass, biometry, and physiological parameters. The results will help a differential diagnosis of co-occurring drought and O_3 VFI in oak forests. In detail, we addressed the following hypotheses: (1) the development of O_3 VFI may be better explained by PODy than by AOT40, (2) the reduction in soil water availability may reduce or exacerbate the negative impacts of O_3 on VFI, and (3) O_3 VFI may be an indicator to explain biomass reduction or physiological damage in Mediterranean oaks. We postulated that the effects on the development of VFI are modulated by the plant species-specific sensitivity to oxidative stressors.

2. Materials and Methods

2.1. Plant Material and Experimental Setting

The experiment was conducted in an O_3 Free-Air Controlled Exposure (FACE) facility at Sesto Fiorentino, Italy (43°48′59″ N, 11°12′01″ E, 55 m a.s.l.). Two-year-old plants of *Q. robur* L., *Q. pubescens* Willd., and *Q. ilex* L. were obtained from nurseries and transplanted into 10-L plastic pots. They were exposed to three levels of O_3 (1.0, 1.2, and 1.4 times the ambient air concentration, denoted as AA, ×1.2, and ×1.4, respectively: 24-h averaged concentration, AA = 35.2 ppb, ×1.2 = 42.9 ppb, ×1.4 = 48.9 ppb) and three levels of water irrigation [100, 80, and 40% of field capacity (0.295 m^3 m^{-3}, Paoletti et al., 2017) on average, denoted as WW-treated (well-watered), MD-treated (moderate drought) and SD-treated (severe drought), respectively]. Three replicated plots were assigned to each treatment, with three plants per combination of species, drought, and O_3. The experiment lasted for 4.5 months, from 1 June to 15 October.

The details of the FACE facility are described in Paoletti et al. [26], and the details of the experimental design are published in Hoshika et al. [27].

2.2. Evaluation of O_3 and Drought Visible Foliar Injury

Two well-trained observers evaluated the presence of O_3 and drought VFI during the experimental period for all plants for a total of 6 evaluation dates (Table 1). We applied photo guides to verify whether O_3 and/or drought VFI was present [28–30]. VFI incidence (INC = number of injured plants/total number of plants × 100) was calculated according to Chappelka et al. [31]. POD_1-based CLs and CDI-based CLs were calculated for the corresponding day when O_3 and drought VFI onset was observed.

Table 1. Phytotoxic O_3 dose (POD_1, mmol m^{-2}) and accumulated exposure over 40 ppb hourly concentrations (AOT40, ppm h) calculated at the O_3 visible foliar injury onset, and Cumulative Drought Index (CDI) calculated at the drought visible foliar injury onset for *Q. robur* and *Q. pubescens*.

Water Regime	O_3 Treat.	Onset O_3 Injury				Onset Drought Injury	
		POD_1		AOT40		CDI	
		Q. robur	*Q. pubescens*	*Q. robur*	*Q. pubescens*	*Q. robur*	*Q. pubescens*
WW-treated	AA	12.07	Asymp.	17.78	Asymp.	Asymp.	Asymp.
	×1.2	12.40	15.69	16.41	23.77	Asymp.	Asymp.
	×1.4	11.62	20.46	15.15	33.38	Asymp.	Asymp.
MD-treated	AA	13.02	Asymp.	21.74	Asymp.	6.10	6.52
	×1.2	12.13	18.41	16.41	30.43	6.10	4.04
	×1.4	13.07	20.04	21.59	33.38	4.96	6.10
SD-treated	AA	Asymp.	Asymp.	Asymp.	Asymp.	10.20	10.20
	×1.2	Asymp.	13.13	Asymp.	30.43	10.20	10.20
	×1.4	10.72	12.81	26.23	26.23	10.20	10.20

2.3. Measure of Growth Parameters

The assessment of total annual biomass production during the experiment was performed based on dry weight per plant (DW) as described in Hoshika et al. [22], additionally discriminating the below-(roots) and above-ground biomass (stem and leaves) to calculate the ratio of root to shoot biomass (Ratio R/S). Furthermore, the total number of leaves, plant height increment (measured with a metric tape) and stem caliber increment (measured just above soil level) were expressed as the absolute values relative to the values at the beginning and end of the experiment.

2.4. Assessment of Photosynthetic Parameters

The net photosynthetic rate (P_n) was previously reported for mid-summer (July: [24]) and early and late summer and autumn (June, August, and October: [23]). Here, these published data of P_n were re-analyzed to address the cumulative effects of O_3 and drought on the photosynthetic activity. The target leaves were fully sun-exposed leaves (4–6th from the shoot tip) of the plant main shoot (one representative leaf per plant, 1 to 3 plants per replicated plot per each O_3 and W treatment). Measurements were made under light-saturated conditions (1500 μmol m^{-2} s^{-1} PPFD [photosynthetic photon flux density]) with constant CO_2 concentration (400 μmol mol^{-1}), relative humidity (40 to 50%), and leaf temperature (25 °C) using a commercial gas exchange system (CIRAS-2 PP Systems, Herts, UK). Measurements were carried out in two campaigns (8–10 June and 27 September–6 October) for all O_3 treatments and an additional campaign (6–9 August) for two O_3 levels (1.2, and ×1.4) on days with clear sky between 9:00 and 12:00 a.m. CET. The other detailed specifications for the photosynthetic measurements were described in our previous studies [23,24].

After the measurement of P_n in August and October, leaves were collected to examine the nitrogen (N) content. Nitrogen content per unit mass (N_{mass}) was determined by the dry combustion method using a LECO TruSpec C/N analyzer (Leco Corporation, St. Joseph, MI, USA). In October, the foliar phosphorus (P) content was also determined. Phosphorus content per unit mass (P_{mass}) was examined by an inductively coupled plasma-optical emission spectroscopy (ICP-OES) (iCAP7000, Thermo Fisher Scientific, Waltham, MA,

USA). We calculated photosynthetic N use efficiency (PNUE) as the product of N_{mass} and mass-based net photosynthetic rate and photosynthetic P use efficiency (PPUE) as the product of P_{mass} and mass-based net photosynthetic rate.

2.5. Calculation of Accumulated Drought and Ozone Indexes

The accumulated drought index (CDI) was calculated from the beginning of the experimental period to the date of observation as follows:

$$\text{CDI} = \sum |Sm - Fc|$$

where, *Sm* is soil moisture, and *Fc* is field capacity (0.295 m^3 m^{-3}) [26]; drought stress is considered severe when *Sm* values are lower than *Fc*.

AOT40 and POD_1 for each O_3 and drought treatment were calculated following the parameters applied by Hoshika et al. [22] according to the methodology designed by CLRTAP (Convention on Long-range Transboundary Air Pollution) [9].

2.6. Statistical Analysis

Multiple Linear Regression (MLR) analysis was used to estimate the relationship between the O_3 indexes (AOT40 and POD_1) and CDI versus growth (height, diameter, and N. leaves), biomass (Leaf, Shoot, Root, Total, and R/S), VFI (O_3 and Drought) and physiological parameters (P_n, PNUE, and PPUE). Two models were compared, i.e., Model 1 (POD_1 and CDI as predictor variables) and Model 2 (AOT40 and CDI as predictor variables). The statistical analyses were performed using the R software (R version 4.1.2 [32]), considering a significance of $p < 0.05$. Principal component analysis (PCA) was conducted by using OriginPro 2021b software. The PCA was applied considering VFI (O_3 and drought), growth (Height, Diameter, and N. of leaves), biomass (Leaf, Shoot, Root; Total and R/S), and physiological (Pn, PNUE, and PPUE) parameters in order to distinguish the groups of parameters better related to each symptomatic species; in this analysis, the asymptomatic *Q. ilex* species was not included.

3. Results

3.1. Visible Foliar Injury

The O_3 VFI in *Q. robur* was characterized by small homogeneously distributed dots between the primary leaf veins (Figure 1A). *Q. robur* plants from all water regimes but SD (AA and ×1.2) presented O_3 VFI (Tables 1 and 2). In fact, 11% of the SD-treated plants developed O_3 VFI at the end of the experiment, relative to 56% of the WW-treated plants (Table 2).

There were individual-specific differences on the day of VFI onset. The POD_1 values calculated for the O_3 VFI onset in *Q. robur* were similar across O_3 treatments (approximately 10.7 to 13.0 mmol m^{-2} POD_1, average = 12.1 mmol m^{-2} POD_1), while the AOT40 values corresponding to the O_3 VFI onset increased from 15-16 ppm h to 26.2 ppm h; for SD-treated plants, the O_3 VFI onset occurred only in ×1.4 (10.7 ppm h, Table 1). In addition, the MLR revealed a positive regression of O_3 VFI with POD_1 or AOT40 and a negative regression with CDI when tested with AOT40 (Model 2), but the effect was not significant when tested with POD_1 (Model 1) (Figure 1B; Table 3).

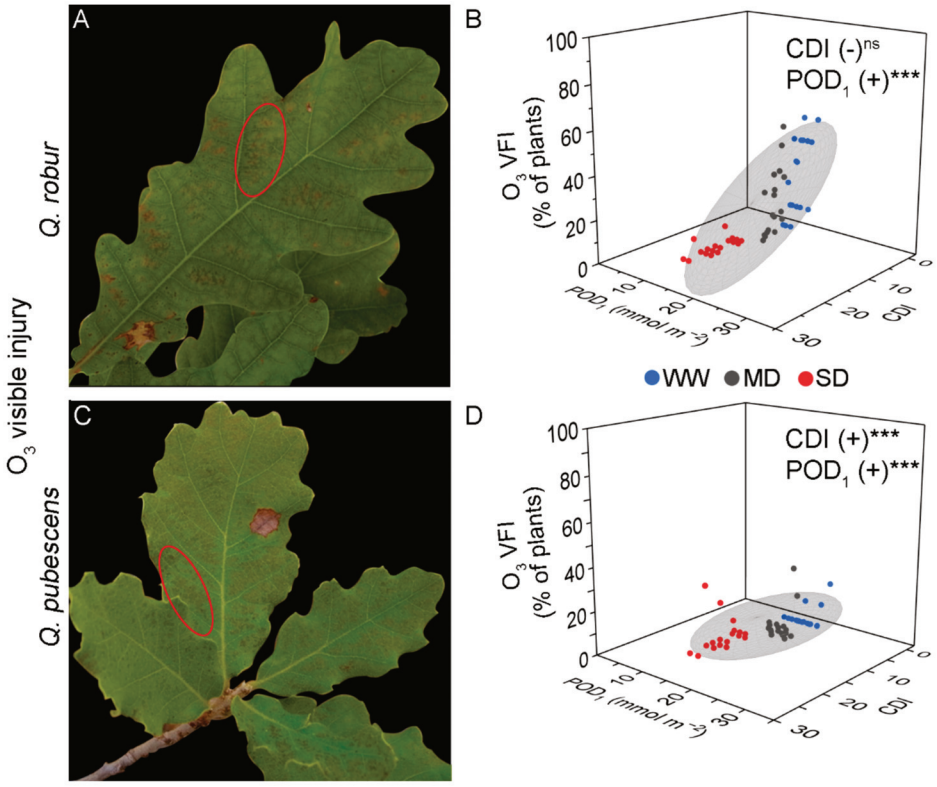

Figure 1. Illustrative examples of O_3 visible foliar injury in *Quercus robur* (**A**) and *Q. pubescens* (**C**) characterized by small homogeneously distributed dots between the primary leaf veins (ellipse). (**B**,**D**) Results from the linear multiple regression of O_3 visible foliar injury with Cumulative Drought Index (CDI) and phototoxic O_3 dose (POD_1) as predictor factors in *Quercus robur* (**B**) and *Q. pubescens* (**D**). Colored dots represent well-watered (WW-blue), moderate drought (MD-grey), and severe drought (SD-red). The grey ellipsoid represents a confidence level of 75%. (+) positive regression, *** = $p < 0.001$, ns = not significant.

Table 2. Evaluation of O_3 and drought incidence of visible foliar injury (VFI) along the experimental period for *Q. robur* and *Q. pubescens* exposed to different levels of O_3 and drought.

	Water Regime	O_3 Treat./DOY	*Q. robur*						*Q. pubescens*					
			209	218	232	240	247	266	209	218	232	240	247	266
O_3 VFI incidence	WW-treat.	AA	-	-	11	11	11	50	-	-	-	-	-	-
		×1.2	-	11	44	44	44	44	-	-	-	-	11	11
		×1.4	22	33	33	44	56	56	-	-	-	-	-	22
	MD-treat.	AA	-	-	-	11	22	44	-	-	-	-	-	-
		×1.2	-	22	22	22	44	56	-	-	-	-	-	33
		×1.4	-	-	22	33	33	33	-	-	-	-	-	22
	SD-treat.	AA	-	-	-	-	-	-	-	-	-	-	-	-
		×1.2	-	-	-	-	-	-	-	-	-	-	-	22
		×1.4	-	-	-	-	11	11	-	-	-	-	11	33
Drought VFI incidence	WW-treat.	AA	-	-	-	-	-	-	-	-	-	-	-	-
		×1.2	-	-	-	-	-	-	-	-	-	-	-	-
		×1.4	-	-	-	-	-	-	-	-	-	-	-	-
	MD-treat.	AA	-	-	33	33	50	67	-	-	-	11	11	11
		×1.2	-	-	22	58	67	67	11	11	11	22	33	33
		×1.4	-	44	33	44	50	63	-	-	22	33	33	33
	SD-treat.	AA	22	22	67	78	83	89	22	22	39	67	67	67
		×1.2	11	56	61	78	78	89	11	11	22	33	44	44
		×1.4	33	56	78	78	100	100	44	44	67	78	78	78

Table 3. Regression coefficients of the multiple linear regression for the species *Q. robur*, *Q. pubescens*, and *Q. ilex*, considering Cumulative Drought Index (CDI) and phototoxic O_3 dose (POD_1) for Model 1, and CDI and accumulated exposure over 40 ppb hourly concentrations (AOT40) for Model 2 as predictor factors, and Growth: Plant height increment (cm), Stem diameter increment (cm), and leaf number increment (N. leaves—n); Biomass: Leaf (g), Shoot (g), Root (g), Total biomass (g), and Ratio root/shoot (Ratio R/S); Visible foliar injury (O_3 and drought—% of plants); Physiological parameters: Photosynthesis (P_n—μmol $m^{-2}s^{-1}$), Photosynthetic nitrogen use efficiency (PNUE—μmol $m^{-2}s^{-1}$) and Photosynthetic phosphorus use efficiency (PPUE—μmol $m^{-2}s^{-1}$) as dependent parameters. Levels of significance (p), intercepts and determination coefficients (R^2) are shown.

	Parameters		Model 1 (POD_1, CDI)							Model 2 (AOT40, CDI)					
			POD_1	p	CDI	p	Intercept	p	R^2	AOT40	p	CDI	p	Intercept	p	R^2
Q. robur	Injury	O_3	6.736	***	−0.043	n.s	−64.967	***	0.717	0.002	***	−2−027	***	−20.600	***	0.738
	Drought		4.802	***	5.882	***	−68.059	***	0.887	0.001	***	4.524	***	−31.350	***	0.861
	Growth	Height	0.316	**	0.035	n.s	−1.197	n.s	0.308	0.159	***	−0.041	n.s	−0.213	n.s	0.501
		Diameter	0.032	n.s	−0.051	**	5.182	***	0.323	0.019	n.s	−0.059	***	5.214	***	0.338
		N. Leaves	0.068	n.s	−2.338	***	190.955	***	0.521	0.003	n.s	−2.351	***	191.913	***	0.521
	Biomass	Leaf	0.240	***	0.013	n.s	1.741	n.s	0.404	0.068	*	−0.040	n.s	3.743	***	0.191
		Shoot	−0.043	n.s	−0.176	***	12.517	***	0.404	−0.017	n.s	−0.166	***	12.268	***	0.404
		Root	−0.784	**	−0.568	***	40.098	***	0.508	−0.287	*	−0.391	***	35.097	***	0.476
		Total	−0.588	n.s	−0.732	***	54.357	***	0.428	−0.236	n.s	−0.597	***	51.108	***	0.427
		Ratio R/S	−0.063	***	−0.019	***	2.600	***	0.692	−0.022	***	−0.005	n.s	2.163	***	0.491
	Physiology	P_n	−0.629	***	−0.283	***	14.579	***	0.824	0.000	***	−0.152	**	11.930	***	0.738
		PNUE	−0.569	n.s	−0.307	*	14.724	*	0.558	−0.152	n.s	−0.175	*	10.032	**	0.558
		PPUE	−3.751	*	−1.560	**	82.525	**	0.916	−0.668	n.s	−0.671	*	41.067	*	0.767
Q. pubescens	Injury	O_3	1.827	***	0.645	***	−26.982	***	0.329	0.876	***	0.090	n.s	−16.377	***	0.387
	Drought		1.279	*	3.658	***	−23.673	*	0.787	0.660	*	3.259	***	−17.183	**	0.792
	Growth	Height	0.241	***	−0.001	n.s	−0.472	n.s	0.373	0.115	***	−0.060	*	1.039	n.s	0.371
		Diameter	−0.151	***	−0.052	***	8.020	***	0.485	−0.052	**	−0.017	n.s	6.595	***	0.244
		N. Leaves	−4.901	***	−1.801	**	175.047	***	0.390	−2.011	**	−0.644	n.s	136.376	***	0.283
	Biomass	Leaf	−0.019	n.s	−0.012	n.s	4.183	***	−0.070	−0.001	n.s	−0.008	n.s	3.865	***	−0.075
		Shoot	−0.205	**	−0.130	***	13.137	***	0.511	−0.091	**	−0.081	**	11.687	***	0.474
		Root	−0.054	n.s	−0.223	***	22.085	***	0.366	−0.039	n.s	−0.208	***	22.072	***	0.372
		Total	−0.278	n.s	−0.364	***	39.404	***	0.400	−0.132	n.s	−0.297	***	37.625	***	0.398
		Ratio R/S	−0.022	*	−0.017	***	2.132	***	0.316	−0.009	n.s	−0.012	**	1.955	***	0.277
	Physiology	P_n	−0.370	***	−0.255	***	13.500	***	0.795	0.000	***	−0.179	***	12.290	***	0.771
		PNUE	−0.485	*	−0.286	**	14.671	**	0.741	−0.173	*	−0.172	**	10.622	***	0.757
		PPUE	−2.385	*	−1.389	**	70.714	**	0.954	−0.575	n.s	−0.788	**	41.724	**	0.901
Q. ilex	Injury	O_3														
	Drought															
	Growth	Height	0.127	n.s	0.004	n.s	15.423	***	−0.050	0.051	n.s	−0.026	n.s	15.623	***	−0.357
		Diameter	0.153	**	0.031	*	0.799	n.s	0.305	0.042	**	−0.003	n.s	1.483	***	0.229
		N. Leaves	3.238	**	1.194	**	17.246	n.s	0.329	1.218	***	0.445	n.s	23.955	**	0.468
	Biomass	Leaf	−0.151	n.s	−0.035	n.s	5.825	***	0.022	−0.029	n.s	−0.002	n.s	4.846	***	−0.037
		Shoot	0.011	n.s	−0.053	n.s	7.619	***	0.158	−0.000	n.s	−0.055	*	7.750	***	0.157
		Root	0.453	**	0.064	n.s	7.027	***	0.230	0.072	n.s	−0.031	n.s	10.315	***	0.013
		Total	0.313	n.s	0.024	n.s	20.471	***	0.038	0.043	n.s	−0.089	n.s	22.911	***	−0.005
		Ratio R/S	0.095	*	0.012	n.s	0.158	n.s	0.294	0.022	n.s	−0.008	n.s	0.7669	n.s	0.068
	Physiology	P_n	0.094	n.s	−0.173	***	9.090	***	0.630	0.000	n.s	−0.196	***	9.380	***	0.624
		PNUE	−0.014	n.s	−0.122	**	5.768	**	0.840	−0.014	n.s	−0.118	***	5.939	***	0.846
		PPUE	−3.036	n.s	−1.870	*	96.073	*	0.814	−0.478	n.s	−1.124	*	71.158	*	0.772

* = $p < 0.05$, ** = $p < 0.01$, *** = $p < 0.001$, n.s = not significant.

The O_3 VFI in *Q. pubescens* was similar to that developed by *Q. robur* (Figure 1C). Independently of the water regime, plants from AA did not show O_3 VFI, while plants from ×1.2 and ×1.4 treatments presented O_3 VFI (Tables 1 and 2). The percentage of plants presenting VFI was lower than for *Q. robur,* with a maximum of 33% presenting VFI (Table 2). VFI occurred for the first time at DOY 247 or 266, i.e., around the end of the experiment. The POD_1 and AOT40 values for the O_3 VFI onset were 12.8–20.46 mmol m^{-2} POD_1 (average = 16.8 mmol m^{-2} POD_1) and 24–33 ppm h AOT40, respectively (Table 1). The MLR revealed a positive regression with the O_3 indexes (POD_1 and AOT40; Figure 1D, Table 3). Interestingly, CDI positively affected the O_3 VFI when tested with POD_1 (Model 1), but the effect was not significant when tested with AOT40 (Model 2) (Table 3).

The drought VFI of *Q. robur* was evident exclusively on the leaf edge that became dry and brownish (Figure 2A). The VFI progressively increased in MD- and SD-treated plants until the end of the experimental period, while WW-treated plants did not show any injury (Table 2). At the end of the experiment, 89–100% of the SD-treated plants showed drought VFI, relative to 63–67% of the MD-treated plants (Table 2). The CDI calculated at the drought VFI onset was the same for all SD-treated plants (CDI = 10.20 for all AA, ×1.2, ×1.4 treatments, Table 1) and similar for MD-treated plants (CDI= 4.96 to 6.10, Table 1). The MLR revealed a strong positive regression between the *Q. robur* drought VFI and CDI, although POD_1 or AOT40 also increased the extent of drought VFI (Figure 2B, Table 3).

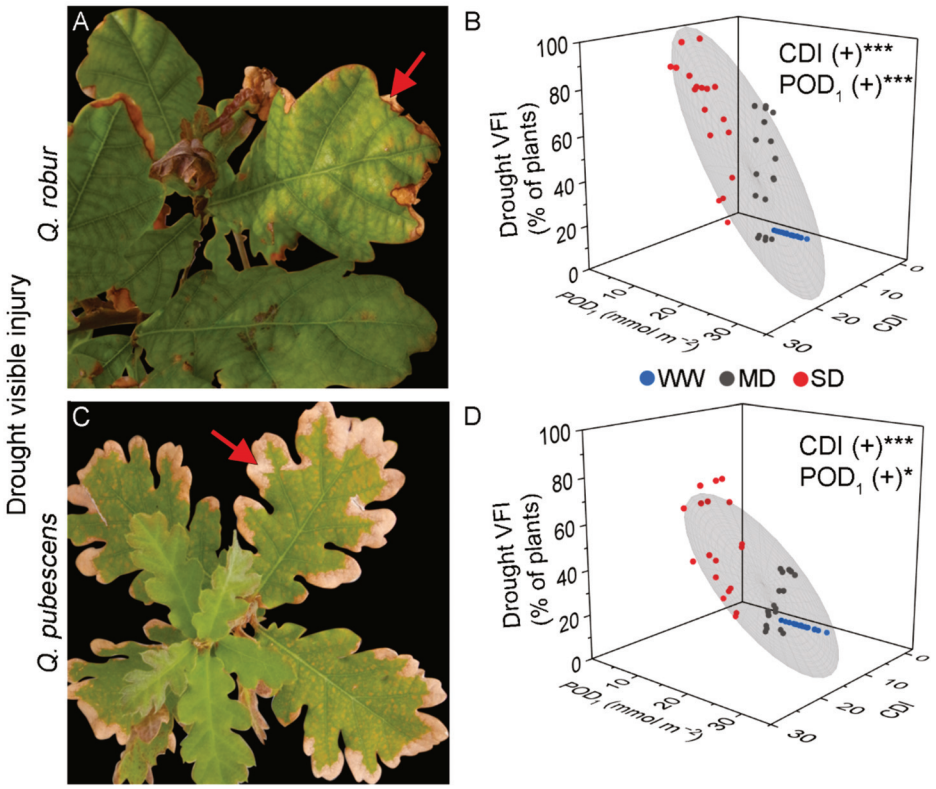

Figure 2. Illustrative examples of drought visible foliar injury in *Q. robur* (**A**) and *Q. pubescens* (**C**) characterized by dry and brownish leaf edges (arrow). (**B**,**D**) Results from the linear multiple regression of drought visible foliar injury with Cumulative Drought Index (CDI) and phototoxic O_3 dose (POD_1) as predictor factors in *Q. robur* (**B**) and *Q. pubescens* (**D**). Colored dots represent well-watered (WW—blue), moderate drought (MD—grey), and severe drought (SD—red). The grey ellipsoid represents a confidence level of 75%. (+) positive regression, * = $p < 0.05$, *** = $p < 0.001$, ns = not significant.

The drought VFI of *Q. pubescens* was similar to that developed by *Q. robur* (Figure 2C). At the end of the experimental period, *Q. pubescens* presented 44–78% of the SD-treated plants with VFI, 11–33% of the MD-treated plants, and no VFI for the WW-treated plants. As found in *Q. robur*, the CDI calculated at the drought VFI onset was the same for all SD-treated plants (CDI = 10.20 for all AA, ×1.2, ×1.4 treatments) and similar for MD-treated plants (CDI= 4.04 to 6.52, Table 1). Interestingly, the CDI values at drought VFI onset were similar in *Q. robur* and *Q. pubescens* within the same O_3 and drought treatments (Table 1). In addition, the MLR revealed a positive regression with CDI, POD_1, and AOT40 (Table 3, Figure 2D). The evergreen *Q. ilex* did not present O_3 or drought VFI.

3.2. Physiological Responses

In both *Q. robur* and *Q. pubescens*, P_n was negatively affected by POD_1 and CDI (Table 3, Figure S1B and D), but it unexpectedly increased with increasing AOT40 (Table 3). Furthermore, PNUE and PPUE were negatively related to CDI and POD_1 except for PNUE in *Q. robur* (Table 3).

For *Q. ilex*, the MLR revealed that CDI negatively affected P_n (Figure S1F), PNUE, and PPUE, with no significant relationship with the O_3 indexes (POD_1 and AOT40, Table 3).

3.3. Growth and Biomass

The MLR indicated that height increment was positively affected by POD_1 or AOT40 in *Q. robur*, while increments of diameter and number of leaves were negatively affected by CDI (Table 3). As confirmed by negative regression coefficients with CDI, most biomass

parameters of *Q. robur* were reduced by drought. On the other hand, POD_1 or AOT40 positively affected leaf biomass and negatively affected root biomass, indicating a reduction of the R/S ratio under elevated O_3 exposure (Table 3, Figure S1A).

In *Q. pubescens*, the O_3 indexes (POD_1 and AOT40) were positively related to plant height increment, while CDI was negatively related to height only when tested with AOT40 (Table 3). Increments in shoot diameter and number of leaves in this species were negatively related to POD_1 and AOT40, while they were negatively related to CDI when tested with POD_1 (Model 1, Table 3). Regarding the biomass parameters, leaf biomass was not affected by any factor, while shoot biomass was negatively affected by both O_3 indexes (POD_1 and AOT40) and CDI (Table 3). Root and total biomass were negatively related to CDI, and the R/S ratio was negatively influenced by CDI and POD_1 (Table 3, Figure S1C).

In *Q. ilex*, plant height increment was not affected by any factors, while a positive relationship between diameter increments and O_3 indexes was found (Table 3). The increment in the number of leaves was positively affected by POD_1 and AOT40 and positively affected by CDI when tested together with POD_1 (Table 3), although leaf and total biomass were not significantly affected by those factors. Shoot biomass was negatively affected by CDI only when tested with AOT40, and root biomass was positively affected only by POD_1 (Table 1). The R/S ratio was positively related only to POD_1 (Table 3, Figure S1E).

The raw data off all growth parameters for the species *Q. robur*, *Q. pubescens*, and *Q. ilex* are avaible in Table S1.

3.4. Principal Component Analysis

The PCA detected separate multivariate spaces between the two symptomatic species as groups related to different growth, biomass, and physiological parameters related to O_3 or drought VFI (Figure 3).

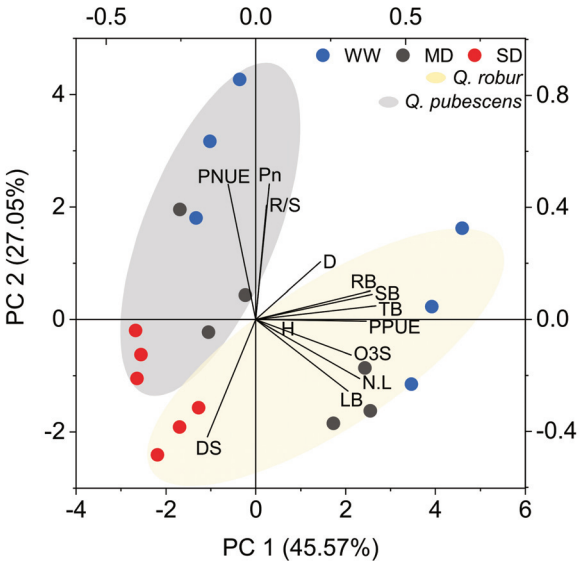

Figure 3. Bi-plot of the principal component analysis on Growth: Plant height increment (H), Stem diameter increment (S), and leaf number increment (N.L); Biomass: Leaf (L), Shoot (S), root (R), Total biomass (TB), and shoot/root ratio (R/S); Visible foliar O_3 (O_3S) and drought injury (DS); Physiological parameters: Photosynthesis (P_n), Photosynthetic nitrogen use efficiency (PNUE) and Photosynthetic phosphorus use efficiency (PPUE).

Since *Q. ilex* did not show VFI, this species was not included in the analysis. The first two components of the PCA explained 45.57 and 27.05% of the variances. The SD-treated plants of both species were grouped near the drought VFI (DS) with no other parameter following the same vector direction. The individuals of *Q. robur* (especially MD-treated

plants) were grouped near the vectors of the growth parameters number of leaves and height, leaf biomass, and O_3 VFI, which presented the same direction, thus indicating that when O_3 VFI increased, these parameters also increased. The individuals of *Q. pubescens* (specially WW-treated plants) were grouped near P_n, PNUE, and R/S, with the vectors in the opposite direction of O_3 and drought VFI, thus indicating that when O_3 and drought VFI increased, these parameters decreased.

4. Discussion

4.1. Development of Visible Injury Due to Ozone and Drought Stress

The POD_1 values corresponding to the onset of O_3 VFI for the two symptomatic deciduous oaks (on average, 14.4 mmol m^{-2}) were similar to those estimated for broadleaf species under field conditions in Italy and France (10 mmol m^{-2} s^{-1}) [10]. However, the CL for the VFI onset was lower for *Q. robur* than for *Q. pubescens*, indicating its higher sensitivity to O_3, possibly related to its lower antioxidative capacity and inability to protect the cell structure [25]. Furthermore, O_3 VFI increased with increasing POD_1 in the two deciduous oaks. This suggests that PODy is a key indicator to describe the development of O_3 VFI [33] once it is well known that O_3 damage is closely related to stomatal O_3 uptake [1]. In fact, the absence of O_3 VFI in *Q. ilex* might be related to its low g_{max} (165 mmol O_3 m^{-2} s^{-1}, compared to 225 mmol O_3 m^{-2} s^{-1} and 200 mmol O_3 m^{-2} s^{-1} of *Q. pubescens* and *Q. robur*, respectively, [22] suggesting that the development of VFI might be discussed in terms of the specific-species patterns of stomatal conductance.

For both injured species (*Q. robur* and *Q. pubescens*) at the end of the experimental period, the severe drought treatment reduced POD_1 by 30 to 40% [22], which would be expected to decrease the O_3-induced VFI in plants as reported before for ecophysiological responses in poplars [34]. In *Q. robur*, the presence of O_3 VFI was decreased under drought. On the contrary, drought stress aggravated the O_3 VFI in *Q. pubescens*. Drought has been reported to have the potential to aggravate the harmful effects of O_3 [35]. Furthermore, Hoshika et al. [24] found that the combination of O_3 and drought altered the activity of the antioxidant system so that *Q. pubescens* was not protected from the severe oxidative stress resulting from the combined stress of O_3 and drought.

For the symptomatic species (*Q. robur* and *Q. pubescens*), the progression of drought VFI could be attributed to the obstruction of conducting tissue [20], conferring to both species a high sensitivity. In the asymptomatic *Q. ilex*, this phenomenon might not happen due to its capacity to increase the cell wall thickness by reinforcing the strength and rigidity of the secondary cell walls with hemicellulose and lignin deposition (data not published). Changes in lignin might function as physical desiccation tolerance and maintenance of protein integrity in drought-tolerant species [36], thus helping the photosynthetic recovery activity after re-watering from severe drought episodes [37]. The CDI threshold for the appearance of drought VFI in the two symptomatic species was higher in SD-treated than MD-treated plants, possibly due to the interaction with leaf aging, which is an important physiological and biochemical defense factor against drought stress [38]. In fact, most plants showed drought VFI in mid- or late-summer in both SD-treated and MD-treated plants when leaves were relatively old.

4.2. Effects of Ozone and Drought Stress on Growth and Biomass Parameters

For both deciduous species (*Q. robur* and *Q. pubescens*), height increment was higher when exposed to O_3 treatment. This phenomenon was verified in other species, such as *Populus* sp. [39], and it is possibly related to promoting a new leaf development as a compensative response against O_3 damage. However, the decrease in the number of leaves was eventually found to be due to O_3 exposure, which might be related to the potential O_3 phytotoxicity that triggers programmed cell death, promoting an increase in leaf senescence [40]. When combined with drought stress, the effect can be more substantial once the lack of water and nutrients promotes a decrease in new leaf development.

Both O_3 and drought stresses were detrimental to the plant biomass increment in all the oak species. In fact, the reduction of biomass due to drought stress is reported for many species and is related to the reduction of water content, diminished leaf water potential and turgor loss, promotion of stomatal closure, and decreased cell enlargement growth [41,42]. As previously revealed by Alonso et al. [21], drought stress does not protect holm oak from O_3 effects when considering the whole plant response. However, differences between the species responses must be considered when comparing the species sensitivity. For example, we observed that *Q. robur* and *Q. pubescens* invested more in shoots than in roots when exposed to both stresses, while *Q. ilex* performed the opposite, which might be another strategy of *Q. ilex* indicating a hormetic mechanism of tolerance for increasing conducting tissue and maintaining the water flow. These tolerance mechanisms may be associated with morphological/anatomical adjustments, such as a versatile root system, conservative growth and carbon allocation patterns, and diverse adaptations in the leaf morphology [20,43]. This might increase the apoplastic water fraction [44] and promote the species tolerance to O_3 and drought stress.

4.3. Effects of Ozone and Drought Stress on Physiological Parameters

The O_3 and drought stress negatively affected the physiological parameters. Drought stress induced a decrease of P_n regardless of the different species, as confirmed by a negative relationship with CDI. A decrease in P_n with increasing POD_1 was verified for both sensitive species (*Q. robur* and *Q. pubescens*), while no such reduction was found in *Q. ilex*. The present discussion is based on the species responses to POD_1 once the flux-based index is more realistic [9]. In fact, AOT40 was positively related to P_n in the two deciduous oaks, which does not agree with a consensus about O_3 negatively affecting photosynthetic capacity [45]. In fact, the regression coefficient was very low (=0.000), although the regression slope was numerically significant. Even though data was generated from an underlying distribution, the significance is a rather unlikely biological sense. The data suggest that a biological-sound index such as POD_1 is superior to AOT40 for the studies of the O_3 effects on vegetations because it can consider the principal physiological cause of O_3 damage, i.e., stomatal O_3 uptake.

Drought stress decreased PNUE and PPUE for all three species, while O_3 stress negatively affected PNUE for *Q. pubescens* and PPUE for the sensitive species *Q. robur* and *Q. pubescens*. Drought stress is directly related to changes in the allocation of N and P to leaves, no matter the species sensitivity to O_3 stress. However, a reduced allocation of N and P to the photosynthetic apparatus [5,6,46] is more pronounced in O_3 sensitive species. The N-uptake efficiency and leaf N efficiency are important traits to improve growth under drought [47]; thus, the decline in root biomass might explain the decrease in PNUE and PPUE for those species, once reduced quantity of absorptive roots reduces water and nutrient uptake as verified for the same oak species in a previous study [48].

4.4. Is the Ozone Visible Injury an Indicator to Explain Biomass Reduction or Physiological Damage in Mediterranean Oaks?

The PCA biplot contains the strength of VFI, physiology, and growth relationships, along with the species-specific sensitivity to drought and O_3 stress. Relationships between O_3 VFI and biomass growth were discussed by other authors [49,50]. In the present study, we observed that the vector of O_3 VFI injury (O_3S) and total biomass (TB) were crossing at the right angle of each other, suggesting a weak association between these two parameters in Mediterranean oaks. However, the O_3S vector shows the same direction as those of leaf parameters (number of leaves [N.L] and leaf biomass [LB]) in plants presenting more O_3 VFI, which may indicate the promotion of carbon allocation to leaves as a compensation response against O_3 injury. In addition, opposite directions of the vectors were found for O_3 VFI (O_3S) and net photosynthesis (P_n), PNUE, and the R/S ratio, highlighting a negative correlation between O_3 VFI and these parameters. The results indicate that O_3 VFI was not a direct indicator of biomass reduction under elevated O_3 in these oaks but provides

important insights regarding the impairment of photosynthetic capacity and biomass partitioning to roots. Mediterranean oak species generally develop taproots that grow deep into the soil, enhancing resistance to abiotic stress such as drought [51]. However, small amounts of roots due to O_3 exposure imply a loss of water and nutrient uptake, suggesting that O_3 VFI should be considered a bioindicator in forests exposed to the combination of O_3 pollution and drought.

5. Conclusions

We examined O_3- and drought-induced VFI and their effects on growth, biomass, and physiological parameters by using cumulative indexes and oak species known for showing differential sensitivity to these stressors. The increase in POD_1 promoted the development of specific O_3 VFI in the isohydric *Q. robur* and the intermediate *Q. pubescens*, while the anisohydric *Q. ilex* was asymptomatic. In *Q. robur*, the presence of O_3 VFI was decreased under drought probably because drought-induced stomatal closure reduced O_3 uptake and thus limited O_3 damage. However, drought stress aggravated O_3 VFI in *Q. pubescens*. This result indicates the importance of the protective role of antioxidant activity under the combination of O_3 and drought, which may be weakened by the combined stress factors and become a dominant factor in species that are not strictly isohydric. On the other hand, the drought VFI was clearly distinguished from the O_3-induced VFI, and it developed with increasing CDI in *Q. robur* and *Q. pubescens* but not in *Q. ilex*, suggesting a high tolerance of *Q. ilex* to drought stress. Therefore, we suggest using the specific O_3 or drought VFI as a bioindicator, especially for establishing the onset injury CL.

We also confirmed that P_n was decreased progressively with POD_1 and CDI in the two deciduous oaks, in tandem with PNUE decline, suggesting a cumulative effect of O_3 and drought on photosynthetic capacity. As a result, both stress factors showed a deleterious effect on the development of VFI and biomass growth. Interestingly, the two deciduous oaks increased the allocation to shoot growth rather than to root growth when exposed to both stresses, while an opposite result was found in *Q. ilex*. The imbalance in carbon allocation to roots may reduce the stability against strong winds and impair water uptake under the warming climate expected in future climate change [52,53].

Supplementary Materials: The following supporting information can be downloaded at: https://www.mdpi.com/article/10.3390/plants11141836/s1, Figure S1: Results of the multiple linear regression for shoot/root (Ratio R/S) and Photosynthesis (P_n) parameters; Table S1: Raw data of growth parameters.

Author Contributions: Conceptualization, E.P. and Y.H.; methodology, E.P., Y.H. and B.B.M.; formal analysis, Y.H. and B.B.M.; investigation, E.P., Y.H.; resources, E.P, F.F. and O.B.; data curation, Y.H. and B.B.M.; writing—original draft preparation, Y.H. and B.B.M.; writing—review and editing, E.P, O.B., F.F. and Y.H.; visualization, B.B.M.; supervision, E.P., O.B. and F.F.; project administration, E.P. and Y.H.; funding acquisition, E.P. All authors have read and agreed to the published version of the manuscript.

Funding: This research was funded by Fondazione Cassa di Risparmio di Firenze (2013/7956), the LIFE15 ENV/IT/000183 project MOTTLES and the APC was funded by LIFE: MODERN(NEC) (LIFE20 GIE_IT_000091).

Data Availability Statement: The data presented in this study are available on request from the corresponding author. The data are not publicly available due to technical limitations and other restrictions.

Acknowledgments: We want to thank Alessandro Materassi and Gianni Fasano for designing and maintaining the ozone FACE; Moreno Lazzara for support during fieldwork; Cristina Mascalchi for administrative and logistic support; Marcello Vitale for providing the *Q. ilex* seedlings; Giulia Carriero for help during the biomass assessment; the Fondazione Cassa di Risparmio di Firenze (2013/7956) for supporting the ozone FACE installation; and the NEC Italy and MODERN(NEC) (LIFE20 GIE_IT_000091) projects coordinated by CUFAA for supporting the ozone FACE maintenance.

Conflicts of Interest: The authors declare no conflict of interest.

References

1. Mills, G.; Pleijel, H.; Malley, C.S.; Sinha, B.; Cooper, O.R.; Schultz, M.G.; Neufeld, H.S.; Simpson, D.; Sharps, K.; Feng, Z.; et al. Tropospheric Ozone Assessment Report: Present-Day Tropospheric Ozone Distribution and Trends Relevant to Vegetation. *Elementa* **2018**, *6*, 47. [CrossRef]
2. Paoletti, E. Ozone Impacts on Forests. *CAB Rev. Perspect. Agric. Vet. Sci. Nutr. Nat. Resour.* **2007**, *2*, 13. [CrossRef]
3. Dusart, N.; Gandin, A.; Vaultier, M.N.; Joffe, R.; Cabané, M.; Dizengremel, P.; Jolivet, Y. Importance of Detoxification Processes in Ozone Risk Assessment: Need to Integrate the Cellular Compartmentation of Antioxidants? *Front. For. Glob. Chang.* **2019**, *2*, 45. [CrossRef]
4. Grulke, N.E.; Heath, R.L. Ozone Effects on Plants in Natural Ecosystems. *Plant Biol.* **2020**, *22*, 12–37. [CrossRef] [PubMed]
5. Watanabe, M.; Hoshika, Y.; Inada, N.; Wang, X.; Mao, Q.; Koike, T. Photosynthetic Traits of Siebold's Beech and Oak Saplings Grown under Free Air Ozone Exposure in Northern Japan. *Environ. Pollut.* **2013**, *174*, 50–56. [CrossRef] [PubMed]
6. Hoshika, Y.; Brilli, F.; Baraldi, R.; Fares, S.; Carrari, E.; Zhang, L.; Badea, O.; Paoletti, E. Ozone Impairs the Response of Isoprene Emission to Foliar Nitrogen and Phosphorus in Poplar. *Environ. Pollut.* **2020**, *267*, 115679. [CrossRef]
7. Büker, P.; Feng, Z.; Uddling, J.; Briolat, A.; Alonso, R.; Braun, S.; Elvira, S.; Gerosa, G.; Karlsson, P.E.; Le Thiec, D.; et al. New Fl Ux Based Dose e Response Relationships for Ozone for European Forest Tree Species. *Environ. Pollut.* **2015**, *206*, 163–174. [CrossRef]
8. Hoshika, Y.; Paoletti, E.; Agathokleous, E.; Sugai, T.; Koike, T. Developing Ozone Risk Assessment for Larch Species. *Front. For. Glob. Chang.* **2020**, *3*, 45. [CrossRef]
9. CLRTAP. Mapping Critical Levels for Vegetation, Chapter III. Manual on Methodologies and Criteria for Modelling and Mapping Critical Loads and Levels and Air Pollution Effects, Risks and Trends. In *UNECE Convention on Long-Range Transboundary Air Pollution*; UNECE: Geneva, Switzerland, 2017.
10. Sicard, P.; De Marco, A.; Carrari, E.; Dalstein-Richier, L.; Hoshika, Y.; Badea, O.; Pitar, D.; Fares, S.; Conte, A.; Popa, I.; et al. Epidemiological Derivation of Flux-Based Critical Levels for Visible Ozone Injury in European Forests. *J. For. Res.* **2020**, *31*, 1509–1519. [CrossRef]
11. Bagard, M.; Jolivet, Y.; Hasenfratz-Sauder, M.-P.; Gérard, J.; Dizengremel, P.; Le Thiec, D. Ozone Exposure and Flux-Based Response Functions for Photosynthetic Traits in Wheat, Maize and Poplar. *Environ. Pollut.* **2015**, *206*, 411–420. [CrossRef]
12. Schaub, M.; Calatayud, V.; Ferretti, M.; Brunialti, G.; Lövblad, G.; Krause, G.; Sanz, M.J. Part VIII: Monitoring of Ozone Injury. In *Manual on Methods and Criteria for Harmonized Sampling, Assessment, Monitoring and Analysis of the Effects of Air Pollution on Forests*; UNECE ICP Forests Programme Coordinating Centre, Ed.; Thünen Institute of Forest Ecosystems: Eberswalde, Germany, 2016; p. 14.
13. Sicard, P.; De Marco, A.; Dalstein-Richier, L.; Tagliaferro, F.; Renou, C.; Paoletti, E. An Epidemiological Assessment of Stomatal Ozone Flux-Based Critical Levels for Visible Ozone Injury in Southern European Forests. *Sci. Total Environ.* **2016**, *541*, 729–741. [CrossRef]
14. Sicard, P.; Hoshika, Y.; Carrari, E.; De Marco, A.; Paoletti, E. Testing Visible Ozone Injury within a Light Exposed Sampling Site as a Proxy for Ozone Risk Assessment for European Forests. *J. For. Res.* **2021**, *32*, 1351–1359. [CrossRef]
15. Hanjra, M.A.; Qureshi, M.E. Global Water Crisis and Future Food Security in an Era of Climate Change. *Food Policy* **2010**, *35*, 365–377. [CrossRef]
16. Xu, C.; McDowell, N.G.; Fisher, R.A.; Wei, L.; Sevanto, S.; Christoffersen, B.O.; Weng, E.; Middleton, R.S. Increasing Impacts of Extreme Droughts on Vegetation Productivity under Climate Change. *Nat. Clim. Chang.* **2019**, *9*, 948–953. [CrossRef]
17. Peters, M.P.; Iverson, L.R.; Matthews, S.N. *Spatio-Temporal Drought Trends by Forest Type in the Conterminous United States, 1960–2013*; US Department of Agriculture, Forest Service, Northern Research Station: Madison, WI, USA, 2014.
18. Vollenweider, P.; Ottiger, M.; Günthardt-Goerg, M.S. Validation of Leaf Ozone Symptoms in Natural Vegetation Using Microscopical Methods. *Environ. Pollut.* **2003**, *124*, 101–118. [CrossRef]
19. Moura, B.B.; Alves, E.S.; Marabesi, M.A.; de Souza, S.R.; Schaub, M.; Vollenweider, P. Ozone Affects Leaf Physiology and Causes Injury to Foliage of Native Tree Species from the Tropical Atlantic Forest of Southern Brazil. *Sci. Total Environ.* **2018**, *610–611*, 912–925. [CrossRef]
20. Vollenweider, P.; Menard, T.; Arend, M.; Kuster, T.M.; Günthardt-Goerg, M.S. Structural Changes Associated with Drought Stress Symptoms in Foliage of Central European Oaks. *Trees—Struct. Funct.* **2016**, *30*, 883–900. [CrossRef]
21. Alonso, R.; Elvira, S.; González-Fernández, I.; Calvete, H.; García-Gómez, H.; Bermejo, V. Drought Stress Does Not Protect Quercus Ilex L. from Ozone Effects: Results from a Comparative Study of Two Subspecies Differing in Ozone Sensitivity. *Plant Biol.* **2014**, *16*, 375–384. [CrossRef]
22. Hoshika, Y.; Moura, B.; Paoletti, E. Ozone Risk Assessment in Three Oak Species as Affected by Soil Water Availability. *Environ. Sci. Pollut. Res.* **2018**, *25*, 8125–8136. [CrossRef]
23. Cocozza, C.; Paoletti, E.; Mrak, T.; Zavadlav, S.; Levanič, T.; Kraigher, H.; Giovannelli, A.; Hoshika, Y. Isotopic and Water Relation Responses to Ozone and Water Stress in Seedlings of Three Oak Species with Different Adaptation Strategies. *Forests* **2020**, *11*, 864. [CrossRef]
24. Hoshika, Y.; Fares, S.; Pellegrini, E.; Conte, A.; Paoletti, E. Water Use Strategy Affects Avoidance of Ozone Stress by Stomatal Closure in Mediterranean Trees—A Modelling Analysis. *Plant Cell Environ.* **2020**, *43*, 611–623. [CrossRef]

25. Pellegrini, E.; Hoshika, Y.; Dusart, N.; Cotrozzi, L.; Gérard, J.; Nali, C.; Vaultier, M.N.; Jolivet, Y.; Lorenzini, G.; Paoletti, E. Antioxidative Responses of Three Oak Species under Ozone and Water Stress Conditions. *Sci. Total Environ.* **2019**, *647*, 390–399. [CrossRef] [PubMed]
26. Paoletti, E.; Carriero, G. A New-Generation 3D Ozone FACE (Free Air Controlled Exposure). *Sci. Total Environ.* **2017**, *575*, 1407–1414. [CrossRef] [PubMed]
27. Moura, B.B.; Hoshika, Y.; Ribeiro, R.V.; Paoletti, E. Exposure- and Flux-Based Assessment of Ozone Risk to Sugarcane Plants. *Atmos. Environ.* **2018**, *176*, 252–260. [CrossRef]
28. Innes, J.L.; Skelly, J.M.; Schaub, M. *Ozone and Broadleaved Species: A Guide to the Identification of Ozone-Induced Foliar Injury/Ozon, Laubholz-Und Krautpflanzen: Ein Fuhrer Zum Bestimmen von Ozonsymptomen*; Haupt: Bern, Switzerland, 2001.
29. Vollenweider, P.; Gunthardtgoerg, M. Erratum to "Diagnosis of Abiotic and Biotic Stress Factors Using the Visible Symptoms in Foliage". *Environ. Pollut.* **2006**, *140*, 562–571. [CrossRef]
30. Günthardt-Goerg, M.S.; Kuster, T.M.; Arend, M.; Vollenweider, P. Foliage Response of Young Central European Oaks to Air Warming, Drought and Soil Type. *Plant Biol.* **2013**, *15*, 185–197. [CrossRef]
31. Chappelka, A.; Renfro, J.; Somers, G.; Nash, B. Evaluation of Ozone Injury on Foliage of Black Cherry (Prunus Serotina) and Tall Milkweed (Asclepias Exaltata) in Great Smoky Mountains National Park. *Environ. Pollut.* **1997**, *95*, 13–18. [CrossRef]
32. Team R Development Core. A Language and Environment for Statistical Computing. 2018. Available online: https://www.R-project.org/ (accessed on 21 May 2022).
33. Fernandes, F.F.; Moura, B.B. Foliage Visible Injury in the Tropical Tree Species, Astronium Graveolens Is Strictly Related to Phytotoxic Ozone Dose (PODy). *Environ. Sci. Pollut. Res.* **2021**, *28*, 41726–41735. [CrossRef]
34. Gao, F.; Catalayud, V.; Paoletti, E.; Hoshika, Y.; Feng, Z. Water Stress Mitigates the Negative Effects of Ozone on Photosynthesis and Biomass in Poplar Plants. *Environ. Pollut.* **2017**, *230*, 268–279. [CrossRef]
35. Grulke, N.E. The Physiological Basis of Ozone Injury Assessment Attributes in Sierran Conifers. *Dev. Environ. Sci.* **2003**, *2*, 55–81. [CrossRef]
36. Yoshimura, K. Programmed Proteome Response for Drought Avoidance / Tolerance in the Root of a C 3 Xerophyte (Wild Watermelon) Under Water Deficits. *Plant Cell Physiol.* **2008**, *49*, 226–241. [CrossRef]
37. Le Gall, H.; Philippe, F.; Domon, J.M.; Gillet, F.; Pelloux, J.; Rayon, C. Cell Wall Metabolism in Response to Abiotic Stress. *Plants* **2015**, *4*, 112. [CrossRef]
38. Pinheiro, C.; Chaves, M.M. Photosynthesis and Drought: Can We Make Metabolic Connections from Available Data? *J. Exp. Bot.* **2011**, *62*, 869–882. [CrossRef]
39. Pell, E.J.; Sinn, J.P.; Johansen, C.V. Nitrogen Supply as a Limiting Factor Determining the Sensitivity of Populus Tremuloides Michx. to Ozone Stress. *New Phytol.* **1995**, *130*, 437–446. [CrossRef]
40. Matyssek, R.; Sandermann, H. Impact of Ozone on Trees: An Ecophysiological Perspective. In *Progress in Botany*; Esser, K., Lüttge, U., Beyschlag, W., Hellwig, F., Eds.; Springer: Berlin/Heidelberg, Germany, 2003; ISBN 978-3-642-55819-1.
41. Jaleel, C.A.; Manivannan, P.; Wahid, A.; Farooq, M.; Al-Juburi, H.J.; Somasundaram, R.; Panneerselvam, R. Drought Stress in Plants: A Review on Morphological Characteristics and Pigments Composition. *Int. J. Agric. Biol.* **2009**, *11*, 100–105.
42. Chaturvedi, R.K.; Tripathi, A.; Raghubanshi, A.S.; Singh, J.S. Functional Traits Indicate a Continuum of Tree Drought Strategies across a Soil Water Availability Gradient in a Tropical Dry Forest. *For. Ecol. Manag.* **2021**, *482*, 118740. [CrossRef]
43. Moura, B.B.; Alves, E.S. Climatic Factors Influence Leaf Structure and Thereby Affect the Ozone Sensitivity of Ipomoea Nil "Scarlet O'Hara". *Environ. Pollut.* **2014**, *194*, 11–16. [CrossRef]
44. Serrano, L.; Peñuelas, J. Contribution of Physiological and Morphological Adjustments to Drought Resistance in Two Mediterranean Tree Species. *Biol. Plant.* **2005**, *49*, 551–559. [CrossRef]
45. Watanabe, M.; Agathokleous, E.; Anav, A.; Araminiene, V.; Carrari, E.; De Marco, A.; Hoshika, Y.; Proietti, C.; Sicard, P.; Paoletti, E. Impacts of Ozone on the Ecophysiology of Forest Tree Species. In *Tropospheric Ozone—A Hazard for Vegetation and Human Health*; Agrawal, S.B., Agrawal, M., Singh, A., Eds.; Cambridge Scholars: Newcastle, UK, 2021; pp. 277–306.
46. Shang, B.; Xu, Y.; Dai, L.; Yuan, X.; Feng, Z. Elevated Ozone Reduced Leaf Nitrogen Allocation to Photosynthesis in Poplar. *Sci. Total Environ.* **2019**, *657*, 169–178. [CrossRef]
47. Weih, M.; Bonosi, L.; Ghelardini, L.; Rönnberg-Wästljung, A.C. Optimizing Nitrogen Economy under Drought: Increased Leaf Nitrogen Is an Acclimation to Water Stress in Willow (*Salix* Spp.). *Ann. Bot.* **2011**, *108*, 1347–1353. [CrossRef]
48. Mrak, T.; Štraus, I.; Grebenc, T.; Gričar, J.; Hoshika, Y.; Carriero, G.; Paoletti, E.; Kraigher, H. Different Belowground Responses to Elevated Ozone and Soil Water Deficit in Three European Oak Species (*Quercus Ilex*, *Q. Pubescens* and *Q. Robur*). *Sci. Total Environ.* **2019**, *651*, 1310–1320. [CrossRef]
49. Somers, G.L.; Chappelka, A.H.; Rosseau, P.; Renfro, J.R. Empirical Evidence of Growth Decline Related to Visible Ozone Injury. *For. Ecol. Manag.* **1998**, *104*, 129–137. [CrossRef]
50. Marzuoli, R.; Gerosa, G.; Bussotti, F.; Pollastrini, M. Assessing the Impact of Ozone on Forest Trees in an Integrative Perspective: Are Foliar Visible Symptoms Suitable Predictors for Growth Reduction? A Critical Review. *Forests* **2019**, *10*, 1144. [CrossRef]
51. Chirino, E.; Vilagrosa, A.; Hernández, E.I.; Matos, A.; Vallejo, V.R. Effects of a Deep Container on Morpho-Functional Characteristics and Root Colonization in *Quercus Suber* L. Seedlings for Reforestation in Mediterranean Climate. *For. Ecol. Manag.* **2008**, *256*, 779–785. [CrossRef]

52. Giovannelli, A.; Traversi, M.L.; Anichini, M.; Hoshika, Y.; Fares, S.; Paoletti, E. Effect of Long-Term vs. Short-Term Ambient Ozone Exposure on Radial Stem Growth, Sap Flux and Xylem Morphology of O3-Sensitive Poplar Trees. *Forests* **2019**, *10*, 396. [CrossRef]
53. Agathokleous, E.; Saitanis, C.J.; Wang, X.; Watanabe, M.; Koike, T. A Review Study on Past 40 Years of Research on Effects of Tropospheric O3 on Belowground Structure, Functioning, and Processes of Trees: A Linkage with Potential Ecological Implications. *Water. Air. Soil Pollut.* **2016**, *227*, 33. [CrossRef]

plants

MDPI

Article

Defoliation Change of European Beech (*Fagus sylvatica* L.) Depends on Previous Year Drought

Mladen Ognjenović [1], Ivan Seletković [1], Nenad Potočić [1,*], Mia Marušić [1], Melita Perčec Tadić [2], Mathieu Jonard [3], Pasi Rautio [4], Volkmar Timmermann [5], Lucija Lovreškov [1] and Damir Ugarković [6]

1 Division for Forest Ecology, Croatian Forest Research Institute, 10450 Jastrebarsko, Croatia; mladeno@sumins.hr (M.O.); ivans@sumins.hr (I.S.); miam@sumins.hr (M.M.); lucijal@sumins.hr (L.L.)
2 Meteorological and Hydrological Service, 10000 Zagreb, Croatia; melita.percec.tadic@cirus.dhz.hr
3 Earth and Life Institute, Université Catholique de Louvain, 1348 Louvain-La-Neuve, Belgium; mathieu.jonard@uclouvain.be
4 Natural Resources Institute Finland, 00790 Helsinki, Finland; pasi.rautio@luke.fi
5 Norwegian Institute of Bioeconomy Research, 1433 Ås, Norway; volkmar.timmermann@nibio.no
6 Faculty of Forestry and Wood Technology, University of Zagreb, 10000 Zagreb, Croatia; dugarkovic@sumfak.hr
* Correspondence: nenadp@sumins.hr

Abstract: European beech (*Fagus sylvatica* L.) forests provide multiple essential ecosystem goods and services. The projected climatic conditions for the current century will significantly affect the vitality of European beech. The expected impact of climate change on forest ecosystems will be potentially stronger in southeast Europe than on the rest of the continent. Therefore, our aim was to use the long-term monitoring data of crown vitality indicators in Croatia to identify long-term trends, and to investigate the influence of current and previous year climate conditions and available site factors using defoliation (DEF) and defoliation change (ΔDEF) as response variables. The results reveal an increasing trend of DEF during the study period from 1996 to 2017. In contrast, no significant trend in annual ΔDEF was observed. The applied linear mixed effects models indicate a very strong influence of previous year drought on ΔDEF, while climate conditions have a weak or insignificant effect on DEF. The results suggest that site factors explain 25 to 30% DEF variance, while similar values of conditional and marginal R^2 show a uniform influence of drought on ΔDEF. These results suggest that DEF represents the accumulated impact of location-specific stressful environmental conditions on tree vitality, while ΔDEF reflects intense stress and represents the current or recent status of tree vitality that could be more appropriate for analysing the effect of climate conditions on forest trees.

Keywords: defoliation; monitoring; tree vitality; drought; climate change

Citation: Ognjenović, M.; Seletković, I.; Potočić, N.; Marušić, M.; Tadić, M.P.; Jonard, M.; Rautio, P.; Timmermann, V.; Lovreškov, L.; Ugarković, D. Defoliation Change of European Beech (*Fagus sylvatica* L.) Depends on Previous Year Drought. *Plants* **2022**, *11*, 730. https://doi.org/10.3390/plants11060730

Academic Editors: Frank M. Thomas and Oleg Chertov

Received: 25 January 2022
Accepted: 7 March 2022
Published: 9 March 2022

1. Introduction

Climate conditions influence the structure and function of forest ecosystems, and play an essential role in forest health [1,2]. Global warming has indisputably caused climate change, which is a significant threat to forest ecosystems [3]. The effects of climate change are generally expected to reduce tree growth and survival, predispose forests to disturbances, and ultimately change forest structure and composition at the landscape scale [4]. Therefore, there is an increasing concern in Europe over the sustainability of forest ecosystems under climate change [5].

Although vitality is a theoretical concept, it can be defined as the ability of a tree to assimilate, to survive stress, to react to changing conditions, and to reproduce [6]. As vitality cannot be measured directly, various indicators can be used to describe it [7]. Crown defoliation is a commonly used tree vitality indicator [8–10], which can be obtained cost-effectively and relatively quickly in field surveys [11]. Defoliation is defined as leaf loss in the assessable crown, as compared to a reference tree, and is observed regardless of the

cause of foliage loss [12]. Landmann [13] states that defoliation is an indicator of acute stress and subsequent recovery of forest ecosystems. However, defoliation has been criticized due to the subjectivity of the assessment, as well as it being a non-specific indicator affected by several biotic and abiotic factors [14–16]. To ensure data quality, training courses and repeated control assessments are regularly carried out on a national [17–19] and international level [20].

European beech (*Fagus sylvatica* L.) is a dominant broadleaved tree species in European forests that forms forest communities over a broad range of habitat conditions [21]. These forests provide multiple ecosystem goods and services [22]. Despite being adapted to a wide range of environmental conditions, the projected effects of climate change, particularly drought, will significantly affect the vitality of European beech [23,24].

Southeast Europe represents one of the most vulnerable regions with expected intensification of severity and duration of droughts and heat waves. As the impacts of climate change on forests in southeast Europe will be potentially stronger and faster than on the rest of the continent [25,26], this region is an ideal model for studying the impacts of changing climatic conditions. A trend of decreasing precipitation and increasing temperatures has already been observed in Croatia [27,28]. In the decade 2001–2010 alone, four drought events occurred, while only 13 took place between 1961 and 2010 [29]. In the future, the climate in Croatia is expected to be hotter and drier, with considerable impacts to be expected for the forest ecosystems. Consequently, continuous long-term forest monitoring is crucial in order to measure and assess these impacts and their consequences on ecosystem functioning.

In Europe, the International Co-operative Program on Assessment and Monitoring of Air Pollution Effects on Forests (ICP Forests) is the most comprehensive European program for the large-scale assessment of forest ecosystem health [30]. The defoliation data obtained from the ICP Forests monitoring network have led to the publication of numerous studies of climate influence in several European countries, such as Switzerland [31], Germany [32], France [33], and Spain [34]. Depending on the investigated region, different climate parameters were found to have a negative impact on crown defoliation. Studies of this kind in Croatia have previously only been regional, which has limited the applicability of results [35,36]. A recent pilot study found a pronounced lag effect of both temperature and precipitation on beech defoliation [37]. Based on these studies, we hypothesize that previous and current year droughts as a consequence of high temperatures and low precipitation contribute the most to beech defoliation across Croatia. Given the ecological and economic importance of beech, it is necessary to understand the impact of climate change on beech defoliation. Therefore, by using the ICP Forests monitoring network in Croatia, our aim was to (i) identify European beech long-term defoliation trends, and to (ii) investigate the influence of current and previous year climate conditions and various site factors on beech defoliation.

2. Results

2.1. Temporal Trends in Tree Vitality

There was a significant trend of increasing mean defoliation (DEF) by 0.39% annually over the study period (Figure 1). Annual overall mean defoliation values peaked in 2001 and 2014. The latter year is marked by the highest observed overall mean defoliation of 18.4%. In contrast, no significant trend in annual defoliation change (ΔDEF) was observed. Time series of annual defoliation change values exhibit stationarity (Dickey–Fuller = −5.81, $p < 0.01$), and generally stay close to the neutral trend line.

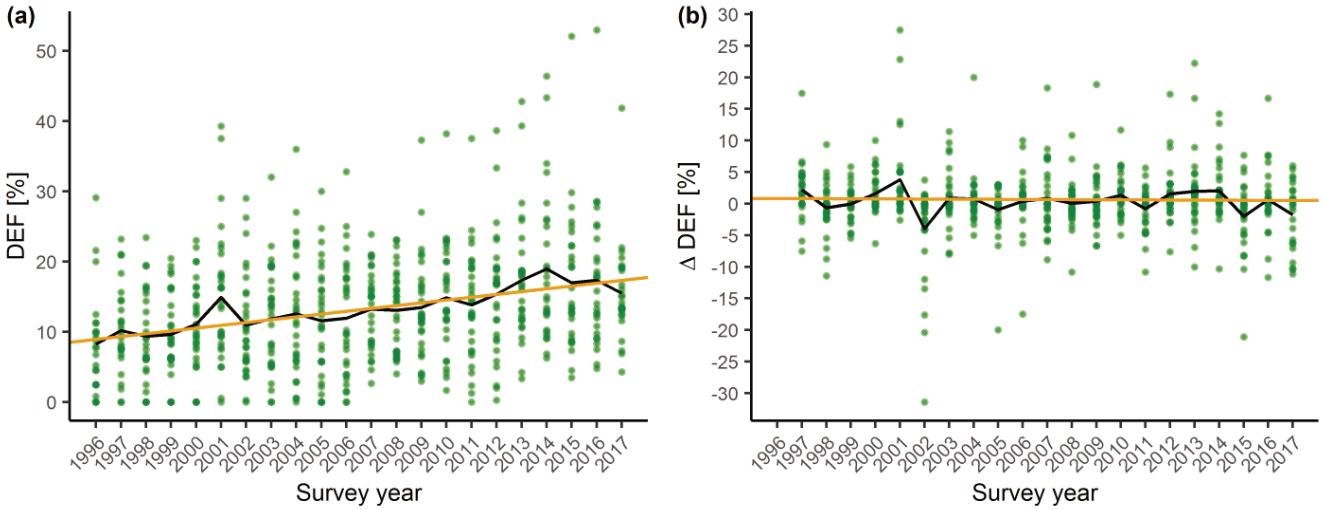

Figure 1. Overall trend of crown vitality parameters from 1996–2017. (**a**) Defoliation trend of European beech (Tau = 0.78, Sen's slope = 0.39, $p < 0.001$, orange line) and annual overall mean defoliation (DEF_i, black line). (**b**) Defoliation change trend of European beech (Tau = −0.05, Sen's slope = −0.01, $p = 0.73$, orange line) and annual overall change in mean defoliation (ΔDEF_i, black line). Points represent annual plot mean values.

Plot-scale trend analysis of DEF showed that 53% of plots have a significant and increasing trend of defoliation at an annual rate ranging from 0.25% to 1.29%. On the remaining 47% of plots, we did not observe any significant trend. The results of the q-statistics and Morans' I spatial autocorrelation coefficient did not indicate spatial stratification of plot-scale DEF trends (data not shown). We did not detect any significant ΔDEF trend at the plot-scale. Therefore, the subsequent spatial stratification tests were not conducted.

2.2. Influence of Environmental Conditions on Tree Vitality

During the selection procedure for DEF and ΔDEF models, additional variables were considered: stand age, site factors (altitude and orientation), and soil properties (soil pH, total nitrogen content in the soil, content of available phosphorus and available potassium in the soil) were tested. However, only altitude showed a significant impact. Although the influence of stand age was not significant, it was retained in the selection process due to improved model performance and the reported influence of stand age on defoliation in other studies [38,39].

The two linear mixed effects models (LMM) used to assess the impact of climatic variables on DEF revealed different influences of current and previous year SPEI (Standardized Precipitation Evapotranspiration Index). Current year SPEI is positively correlated with defoliation, while previous year SPEI has a negative effect. Although significant, this divergent effect of drought should be regarded with caution, since the estimated effects are weak (Table 1). Both the current and previous year temperature and precipitation did not have significant effects on defoliation. Plots located on higher altitudes had significantly higher mean defoliation. The annual increase in defoliation estimated in the LMM models is very similar to the positive defoliation trend assessed by the Mann–Kendall test (Figure 1). The marginal coefficient of determination (R^2) was lower than the conditional R^2 in both models, which suggests that the model random effects i.e., plot location, accounts for a high proportion of the explained DEF variance (Table 2).

Table 1. Estimated model parameters, standard errors, *t*-values, and *p*-values for mean defoliation LMM models with current year (DEF-I) and previous year climate variables (DEF-II). T—mean annual temperature, P—annual sum of precipitation, SPEI3—mean annual Standardized Precipitation Evapotranspiration Index calculated on a three-month time scale, lag—denotes previous year values.

		Estimate	Std. Error	*t* Value	*p* Value
DEF-I	Intercept	−7.924	1.591	−4.980	<0.001
	Year	0.004	8.03×10^{-4}	4.934	<0.001
	Stand age	-4.70×10^{-4}	3.16×10^{-4}	−1.486	0.138
	Altitude	1.58×10^{-4}	3.86×10^{-5}	4.095	<0.01
	T	0.007	0.004	1.954	0.051
	P	-1.07×10^{-5}	1.19×10^{-5}	−0.902	0.367
	SPEI3	0.016	0.006	2.834	<0.01
DEF-II	Intercept	−7.542	1.571	−4.799	<0.001
	Year	0.004	7.92×10^{-4}	4.767	<0.001
	Stand age	-3.68×10^{-4}	3.09×10^{-4}	−1.191	0.234
	Altitude	1.18×10^{-4}	3.82×10^{-5}	3.099	<0.01
	T_lag	0.005	0.003	1.553	0.121
	P_lag	9.67×10^{-6}	1.19×10^{-5}	0.813	0.417
	SPEI3_lag	−0.014	0.006	−2.501	<0.05

Table 2. Defoliation (DEF) and defoliation change (ΔDEF) model performance indices: Akaike Information Criterion (AIC); Conditional coefficient of determination (Conditional R^2); Marginal coefficient of determination (Marginal R^2); Intraclass Correlation Coefficient (ICC); Root Mean Square Error (RMSE).

	AIC	Conditional R^2	Marginal R^2	ICC	RMSE
DEF-I	−1906	0.89	0.60	0.71	0.061
DEF-II	−1915	0.88	0.62	0.68	0.062
ΔDEF-I	1824	0.09	0.09	1.20×10^{-8}	0.996
ΔDEF-II	1806	0.32	0.32	7.07×10^{-9}	0.984

Defoliation change LMM indicates a very strong and significant negative influence of previous year SPEI (Table 3). Positive defoliation changes were observed in years preceded by low SPEI, while negative defoliation changes were associated with high SPEI the previous year. This inverse relationship where the increase of defoliation is preceded by drought was most notable in 2001 (Figure 2). Other climate variables, including current year SPEI, did not have a significant effect and neither did stand age or elevation. Equal values of conditional and marginal R^2 suggest a uniform effect of previous year drought on European beech ΔDEF (Table 2). As expected, the models did not reveal a significant trend in the change of defoliation.

Table 3. Estimated regression parameters, standard errors, *t*-values, and *p*-values for mean defoliation change LMM models with current year (ΔDEF-I) and previous year climate variables (ΔDEF-II). T—mean annual temperature, P—annual sum of precipitation, SPEI3—mean annual Standardized Precipitation Evapotranspiration Index calculated on a three-month time scale, lag—denotes previous year values.

		Estimate	Std. Error	*t* Value	*p* Value
ΔDEF-I	Intercept	25.114	15.641	1.606	0.109
	Year	−0.013	0.008	−1.595	0.111
	Stand age	-1.91×10^{-4}	0.002	−0.104	0.917
	Altitude	-1.50×10^{-4}	3.87×10^{-4}	−0.388	0.701
	T	0.012	0.057	0.207	0.836
	P	1.47×10^{-4}	1.35×10^{-4}	1.094	0.274
	SPEI3	−0.006	0.091	−0.066	0.947
ΔDEF-II	Intercept	15.966	15.833	1.008	0.314
	Year	−0.008	0.008	−0.964	0.336
	Stand age	-2.50×10^{-5}	0.002	−0.014	0.989
	Altitude	−0.001	3.78×10^{-4}	−1.388	0.176
	T_lag	−0.047	0.055	−0.857	0.392
	P_lag	1.98×10^{-4}	1.33×10^{-4}	1.487	0.138
	SPEI3_lag	−0.388	0.089	−4.338	<0.01

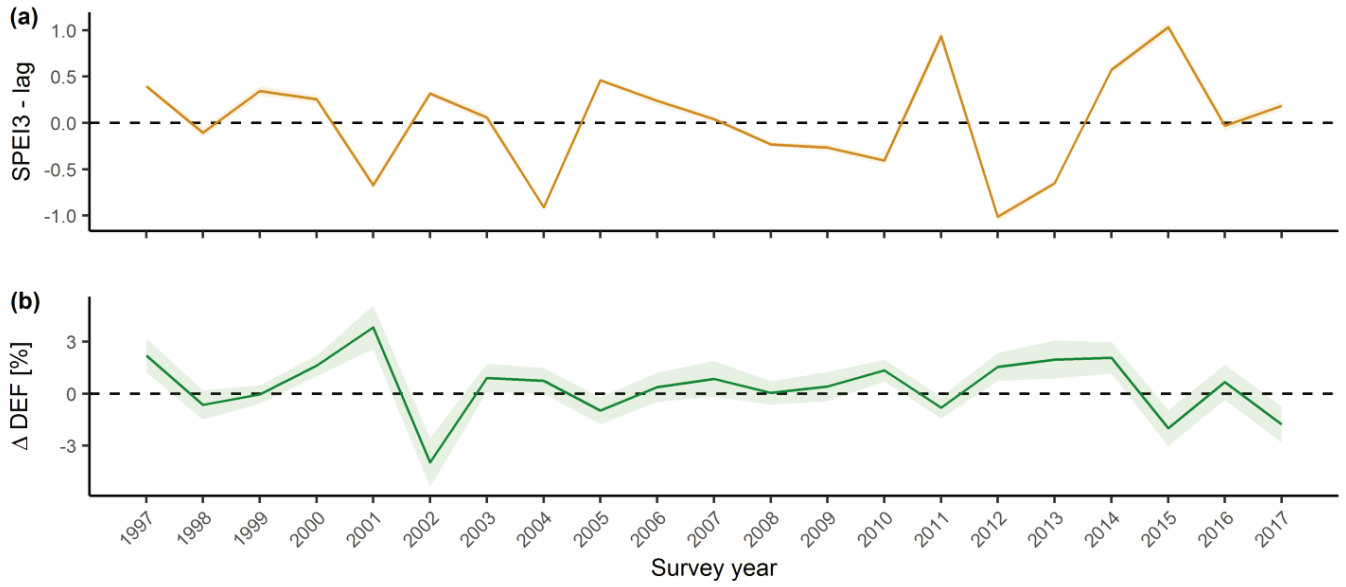

Figure 2. Inverse relationship between previous year SPEI (Standardized Precipitation Evapotranspiration Index) and defoliation change (ΔDEF_i) in Croatia from 1996–2017. (**a**) Previous year mean SPEI (orange line) and standard error (orange area), calculated on a time scale of three months. (**b**) Annual overall defoliation change (ΔDEF_i) mean (green line) and standard error (green area).

3. Discussion

3.1. Temporal Trends in Crown Vitality

Defoliation is widely accepted as a proxy indicator of tree vitality and forest health, able to provide useful information on its status and trends. Long-term defoliation data series are an important asset to explore the changes in forest ecosystem health across Europe over the past 30 years [8]. This study revealed a statistically significant trend of increasing defoliation of European beech in Croatia over time. The distinctive impulses of increasing mean defoliation in 2001 and from 2012 to 2014 (Figure 1) are preceded by the dry 2000 and the extreme drought period recorded in 2011/2012 (Figure S1) [40]. The severe drought recorded in 2003 did not result in an increase in mean defoliation in the

following years, which is consistent with our previous findings [37]. Sudden increases in mean defoliation preceded by years or periods of pronounced precipitation deficit were also recorded in studies conducted in France [33] and the Iberian Peninsula [41]. A significant, but weaker trend of increasing beech defoliation was also observed at a European level [42]. A study comparing the general defoliation trends between geographical regions found that southern Europe, including Croatia, has a more pronounced trend of increasing defoliation compared to central and northern Europe [41].

Plot-scale analysis of defoliation revealed a statistically significant increase on 53% of plots in the 1996 to 2017 period. A study applying a similar plot-scale approach in France found that as many as 70% of beech plots showed an increasing defoliation trend from 1996 to 2009 [33]. Our results also suggest that there is no spatial grouping of the defoliation trend, which is in line with other studies [9,31]. Obviously, the trend of defoliation is not influenced by geographical position, but rather by specific environmental conditions present on a particular plot.

Defoliation change (ΔDEF), defined as the difference between the defoliation assessed in the current and previous year has so far been used in only a few studies [31,43]. Unfortunately, detailed results from these studies were not provided, and therefore a straightforward comparison with our results was not possible. While differences in assessment of absolute defoliation values can be expected due to national adjustments of the methods, the differences in assessing the relative change of defoliation from year to year should be negligible, and could potentially reduce the influence of possible subjectivity of the assessment [43]. Additionally, the absence of serial correlation of defoliation change, i.e., its stationarity, enables easier development of impact models compared to using defoliation data.

3.2. Influence of Environmental Conditions on Tree Vitality

A key task at the European level is to study the impact of climate change on crown defoliation and, consequently, on forest health [44], taking into consideration a wide range of natural and anthropogenic environmental factors [45].

The established difference in marginal and conditional R^2 in crown defoliation models suggests that site factors explain 25 to 30% variance of European beech defoliation over time. A high influence of specific site attributes on defoliation was also found in other studies, e.g., lower defoliation values were observed at higher nitrogen supply levels and higher pH levels [46,47]. However, soil properties did not show a significant impact during the model selection process in our study, which is in line with several studies that did not confirm the importance of soil properties for European beech defoliation [10,43]. It is possible that the applied approach to soil sampling and analysis does not provide a sufficient level of detail to detect the significance of soil variables, given that soil properties have nevertheless been shown as significant factors in some studies of European beech [48] and Norway spruce defoliation [49]. On the other hand, effects from environmental factors that change on a long-term scale, like soil properties, will not likely be detected through annual variation of defoliation [46].

Stand age was identified as a significant predictor in different approaches to modelling defoliation [39,40,45,50]. However, the established relationship between defoliation and stand age may, in many cases, represent an interaction between various stress factors and age [4]. The absence of a significant impact of stand age on European beech defoliation in Croatia (Tables 1 and 3) can be explained by a relatively small number of plots in our sample, where stands are older than 80 years (Figure S2), while the abovementioned studies were not limited by irregular age distribution.

Numerous studies have observed a significant effect of drought on increasing defoliation [32,38,39,42,45], and increased leaf loss following spring and summer heat waves was recorded both in European [50,51] and North American forests [52]. In contrast to the clear influence of spring and summer temperatures on European beech defoliation found in Spain [34], the results of this study indicate a very weak influence of all examined tempera-

ture variables, which is consistent with results of a beech study conducted in Germany [46]. Furthermore, we did not find a significant influence of precipitation on defoliation. This is contrary to the results of a French study, where precipitation and precipitation deficit correlated with defoliation [33]. While we could not detect any effect of air temperature and precipitation when considered independently, these climate variables showed to have a clear impact on defoliation change when combined in the SPEI drought index.

The basic mechanism for regulating water loss in dry conditions is stomatal closure in plants [53]. Under conditions of increased water deficit, plants also respond by increasing water use efficiency [54], reduced growth [55], and conservative mechanisms such as limiting their photosynthetic activity [56]. Due to drought, plants can adapt their morphological structure by increasing the carbon allocation to the root system [57], reducing their leaf size [58], decreasing leaf area index [59], and ultimately shedding leaves [10]. During long lasting drought events, stomatal closure can significantly reduce carbon fixation by trees as well as their carbon reserves, which weakens trees and makes them more vulnerable to biotic and abiotic stresses. In extreme cases, this can lead to mortality by carbon starvation [60]. Severe drought during the year of bud formation, in our study indicated by low previous year SPEI and its impact on ΔDEF, decreases the number of new leaves formed in the bud thus influencing the number of leaves, leaf surface area, and twig extension in the following year [51]. In *Fagus* species, all leaves are pre-formed in winter buds [61,62] during late summer and early autumn [59]. Hydraulic failure may also occur during severe droughts leading to twig and leaf abscission, which can be seen as a drastic adaptation strategy to reduce evapotranspiration [63]. This effect is visible from the values of defoliation rising in the period from 2011 until 2014 (Figure 1), which coincides with low SPEI for the years 2011 and 2012 (Figure 2).

Equal values of conditional and marginal R^2 and the low value of ICC (intraclass correlation coefficient) suggests a uniform influence of previous year drought on the European beech ΔDEF throughout Croatia. On the other hand, the increase in the marginal R^2 of defoliation models after the inclusion of climatic variables was slight, and the influence of all observed climatic variables on DEF was weak. This indicates that defoliation is influenced by site-specific environmental or stand factors that have not been identified in this study. Mean beech defoliation shows fluctuations that coincide with the occurrence of common to abundant fructification [48,64]. However, we were not able to include fruiting as a factor due to the lack of data. The lack of a clear ΔDEF trend, as well as the pronounced impact of drought in the previous year, may indicate that this response variable reflects intense stress, while the positive DEF trend represents the accumulated impact of location-specific stressful environmental conditions on tree vitality. Since defoliation change shows the current or recent status of tree vitality, while defoliation is an integrated indicator resulting from cumulated biotic and abiotic pressures on tree vitality over many years, defoliation change could be a more appropriate indicator for analysing the effect of recent climate conditions on tree vitality.

Increasing temperatures may lead to drought thus affecting forest vitality in the region. Forest monitoring activities in southeast Europe should be intensified to determine the unknown site-specific environmental and/or stand factors that may explain a part of the variance in the present data. This could help develop adequate and locally applicable mitigation strategies to secure the future of beech forests in the region.

4. Materials and Methods

4.1. Study Area and Plot Selection

The ICP Forests Level I monitoring plots in Croatia are established on intersections of a 16 × 16 km grid that contain forest cover. These plots do not have a fixed area; rather, 24 trees are chosen for defoliation assessments using a cross-cluster system with six trees in each cluster [65]. Only plots with a minimum of five European beech trees were selected to ensure that European beech was significantly represented in the mixture of tree species. To ensure defoliation data consistency over the investigated period from 1996 to 2017,

defoliation assessment on selected plots had to have been carried out for at least 80% of the investigated period. This resulted in the selection of 28 research plots (Figure 3). In addition to defoliation, the ICP Forests database contains information on several site factors (Table S1).

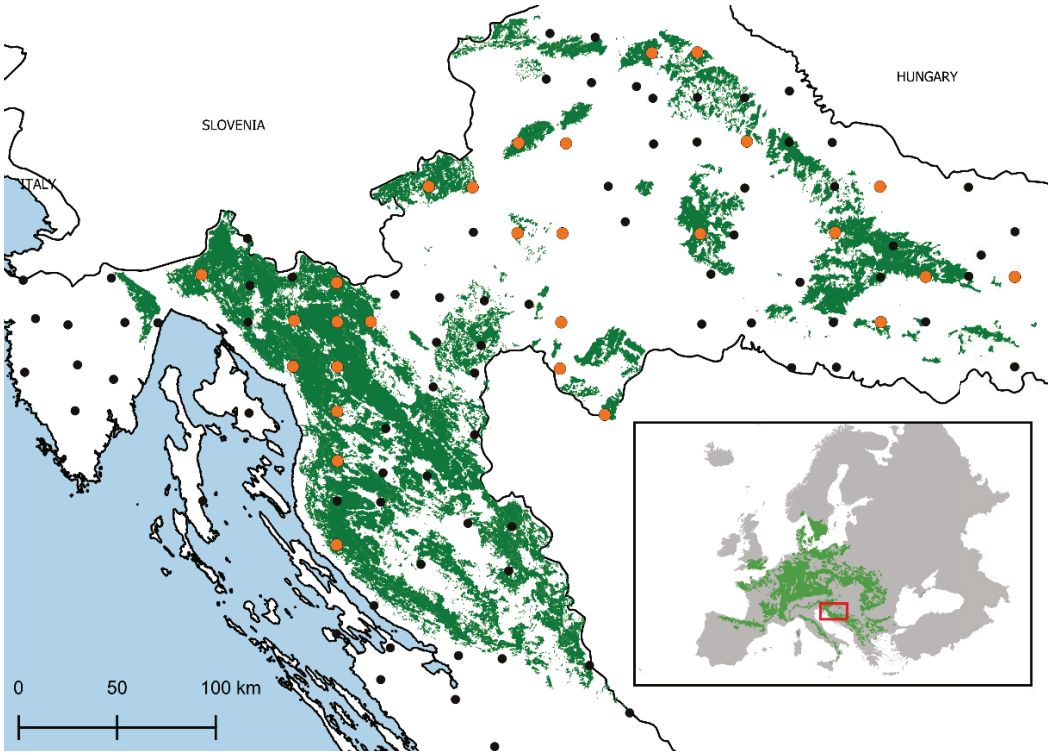

Figure 3. Location of research plots in the context of the distribution of European beech in Europe [66]. Selected Level I ICP Forests monitoring plots (orange dots); remaining Level I plots in Croatian (black dots); distribution of European beech forests in Croatia [67] (green polygon).

4.2. Defoliation Assessment and Crown Vitality Indicators

Defoliation of European beech trees on the selected plots was assessed annually between mid-July and mid-August from 1996 to 2017, in 5% classes from 0 to 100%, according to the ICP Forests Manual [12]. Assessments of tree crowns was performed in comparison with the absolute reference tree. For this study, two crown vitality indicators were calculated and used as response variables: (i) the mean current year crown defoliation DEF_i on plot i, and (ii) the change in the mean current year crown defoliation on plot i compared to the previous year assessment ΔDEF_i. Mean values of crown vitality parameters at the plot level were used, since the values of all predictor variables could only be obtained at the plot level. Additionally, comparison of defoliation variability within and between plots showed that it was lower within plots than between plots.

4.3. Soil Sampling and Analysis

Soil sampling was performed during the summer of 2019 on five points located within each of the research plots. One point was located within each of the four groups of trees that are assessed for defoliation, and an additional fifth point was located in the centre of each research plot. Soil samples were taken with a pedological drill from a depth of 0–10 cm, 10–20 cm, 20–40 cm, and 40–80 cm. Collected samples were pooled according to the sampling depth. Soil chemical parameters were analysed according to standard protocols and methods (Table S2).

4.4. Climate Data

Climate monitoring stations are generally situated at considerable distances from the research plots. Therefore, the data they provide are not always representative of the research locations. To overcome this, we used gridded data produced by regression kriging (RK), which is a hybrid method of interpolation carried out in four steps [68]. The method was validated with leave-one-out cross-validation, while the root mean square error (RMSE) was calculated between observed and interpolated values. Mean RMSEs are for mean monthly temperature from 0.5 °C to 0.9 °C, for minimum temperature from 1.1 °C to 1.5 °C, for maximum temperature from 0.7 °C to 1.1 °C, and for precipitation from 18 to 30 mm, averaged by months.

Mean monthly temperature (T), minimum (Tmin) and maximum (Tmax) monthly temperature, and monthly sum of precipitation (P) from the gridded dataset on 1 km spatial resolution for Croatia [69] were used to calculate yearly values, as well as the Palmer Drought Severity Index (scPDSI) [70] and Standardized Precipitation Evapotranspiration Index (SPEI) [71]. Lower values of scPDSI and SPEI indicate a stronger drought intensity while higher values indicate a higher degree of humidity. SPEI was calculated on a time scale of 3, 6, and 12 months.

4.5. Data Analysis

The trend of defoliation and defoliation change was estimated according to Sen's slope [72], while the significance of a trend was tested by the Mann–Kendall test [73,74] with a significance level of $p \leq 0.05$. Both methods are suitable for data with asymmetric distribution and in this case are significantly more accurate compared to the simple linear regression model [75]. Spatial stratification of defoliation plot-wise trends were examined by calculating the degree of spatial stratified heterogeneity using the q-statistics method [76] and the spatial autocorrelation coefficient, Moran's I [77].

To model the impact of site factors and climate conditions on crown vitality indicators, we used linear mixed effects models (LMM) [78]. Prior to adding climate predictors, a default model was fitted:

$$\begin{aligned} &\mathrm{DEF}_{it} = \mathrm{Year}_t + \mathrm{StandAge}_{it} + \mathrm{Elevation}_i \\ &\mathrm{SamplePlot}_i \sim \mathrm{N}(0,\ \sigma^2) \end{aligned} \quad (1)$$

where DEF_{it} is the mean crown defoliation of European beech trees for sample plot $i = 1, \ldots, n$ and for year $t = 1, \ldots, 22$, averaged over all trees at sample plot i. $\mathrm{SamplePlot}_i$ is the random intercept, which is assumed to be normally distributed with mean 0 and variance σ^2. To account for different number of trees on each plot, weights $1/\alpha_{\mathrm{it}}$ were introduced, where αit is the number of trees assessed at plot i and year t. Since defoliation represents an estimated percentage and due to the LMM requirements, mean defoliation values were divided by 100 before model fitting. First order autocorrelative term was introduced to account for temporal autocorrelation in the model. Seidling [46] states that the serial correlation of European beech that appears over a five-year period is not as distinct as in other species studied, which is contrary to our data. Ignoring serial correlation in model fitting leads to overestimated random effects and to the inflation of the empirical Type I error rates [79], therefore it is crucial to account for this during model fitting of defoliation data.

Due to high kurtosis, The Lambert W $\times$ F function [80] was applied to transform ΔDEF data to a normal distribution. Afterward, the same approach to the base model build up was applied as with DEF data, except that the first order autocorrelative term was left out since the data did not display serial correlation.

The final model selection process was based on diagnostic diagrams and a procedure defined by Johnson and Omland [81]. Spearman's correlation coefficient (*rho*) was calculated between the crown vitality indicators and each quantitative environmental variable in order to obtain an overview of possible impacts. Of the potential independent variables, those that explain most of the variation of crown vitality indicators were selected with

a recursive feature elimination approach (RFE) implemented within the random forest algorithm [82]. Selected variables which were linearly correlated with other variables and had a variance inflation factors VIF > 5, a commonly used threshold in detecting multicollinearity [83], were identified. The identified collinear variables with the lower value according to the Akaike Information Criteria (AIC) [84] were retained for further model development. This subset of uncorrelated environmental variables was used as predictor variables for developing the final models. All analyses were conducted in an R programming environment [85].

Supplementary Materials: The following are available online at https://www.mdpi.com/article/10.3390/plants11060730/s1, References [86–91] are cited in the Supplementary Materials. Figure S1. Linear regression fits (black lines) and kernel smoothing functions (colour lines) for one-year smoothed mean monthly temperature, monthly precipitation sum and mean monthly SPEI data (grey lines) on the research plots during the vegetation period., Figure S2. Distribution of 28 research plots by stand age, altitude, and orientation, Table S1. Additional site factor variables and data sources, Table S2. Descriptive statistics of soil chemical properties from 28 research plots and the applied methods of analysis

Author Contributions: Conceptualization, M.O., I.S. and N.P.; Formal analysis, M.O.; Investigation, M.O.; Methodology, M.O.; Project administration, M.O., I.S. and N.P.; Resources, N.P. and M.P.T.; Supervision, N.P. and D.U.; Visualization, M.O.; Writing—original draft, M.O., I.S. and N.P.; Writing—review and editing, M.O., I.S., N.P., M.M., M.P.T., M.J., P.R., V.T., L.L. and D.U. All authors have read and agreed to the published version of the manuscript.

Funding: This work has been fully supported by Croatian Science Foundation under the project VitaClim (IP-2018-01-5222).

Institutional Review Board Statement: Not applicable.

Informed Consent Statement: Not applicable.

Data Availability Statement: The data presented in this study are available on request from the corresponding author. The data are not publicly available due to legal reasons.

Acknowledgments: We highly appreciate the work of researchers and technicians of the Croatian Forest Research Institute that participated in field research and laboratory analysis for this study.

Conflicts of Interest: The authors declare no conflict of interest.

References

1. Centritto, M.; Tognetti, R.; Leitgeb, E.; Střelcová, K.; Cohen, S. Above Ground Processes: Anticipating Climate Change Influences. In *Forest Management and the Water Cycle: An Ecosystem-Based Approach*; Bredemeier, M., Cohen, S., Godbold, D.L., Lode, E., Pichler, V., Schleppi, P., Eds.; Springer: Dordrecht, The Netherlands, 2011; pp. 31–64.
2. Trumbore, S.; Brando, P.; Hartmann, H. Forest health and global change. *Science* **2015**, *349*, 814–818. [CrossRef] [PubMed]
3. Stocker, T.F.; Qin, D.; Plattner, G.-K.; Alexander, L.V.; Allen, S.K.; Bindoff, N.L.; Bréon, F.-M.; Church, J.A.; Cubasch, U.; Emori, S.; et al. Technical Summary. In *Climate Change 2013: The Physical Science Basis. Contribution of Working Group I to the Fifth Assessment Report of the Intergovernmental Panel on Climate Changep*; Stocker, T.F., Qin, D., Plattner, G.-K., Tignor, M., Allen, S.K., Boschung, J., Nauels, A., Xia, Y., Bex, V., Midgley, P.M., Eds.; Cambridge University Press: Cambridge, UK; New York, NY, USA, 2013.
4. De Vries, W.; Dobbertin, M.H.; Solberg, S.; van Dobben, H.F.; Schaub, M. Impacts of acid deposition, ozone exposure and weather conditions on forest ecosystems in Europe: An overview. *Plant Soil* **2014**, *380*, 1–45. [CrossRef]
5. Ferretti, M.; Waldner, P.; Verstraeten, A.; Schmitz, A.; Michel, A.; Žlindra, D.; Marchetto, A.; Hansen, K.; Pitar, D.; Gottardini, E.; et al. Criterion 2: Maintenance of Forest Ecosystem Health and Vitality. In *FOREST EUROPE, 2020: State of Europe's Forests 2020*; Ministerial Conference on the Protection of Forests in Europe—Liaison Unit Bratislava: Zvolen, Slovak Republic, 2020.
6. Brang, P. *Sanasilva-Bericht 1997: Zustand und Gefährdung des Schweizer Waldes-eine Zwischenbilanz nach 15 Jahren Waldschadenforschung*; Bundesamt für Umwelt Wald und Landschaft; Eidgenössische Forschungsanstalt: Birmensdorf, Switzerland, 1998.
7. Cherubini, P.; Battipaglia, G.; Innes, J.L. Tree Vitality and Forest Health: Can Tree-Ring Stable Isotopes Be Used as Indicators? *Curr. For. Rep.* **2021**, *7*, 69–80. [CrossRef]
8. Gottardini, E.; Cristofolini, F.; Cristofori, A.; Pollastrini, M.; Camin, F.; Ferretti, M. A multi-proxy approach reveals common and species-specific features associated with tree defoliation in broadleaved species. *For. Ecol. Manag.* **2020**, *467*, 118151. [CrossRef]
9. De Vries, W.; Klap, J.M.; Erisman, J.W. Effects of environmental stress on forest crown condition in Europe. Part I: Hypotheses and approach to the study. *Water Air Soil Pollut.* **2000**, *119*, 317–333. [CrossRef]

10. De Marco, A.; Proietti, C.; Cionni, I.; Fischer, R.; Screpanti, A.; Vitale, M. Future impacts of nitrogen deposition and climate change scenarios on forest crown defoliation. *Environ. Pollut.* **2014**, *194*, 171–180. [CrossRef]
11. Dobbertin, M. Tree growth as indicator of tree vitality and of tree reaction to environmental stress: A review. *Eur. J. For. Res.* **2005**, *124*, 319–333. [CrossRef]
12. Eichhorn, J.; Roskams, P.; Potočić, N.; Timmermann, V.; Ferretti, M.; Mues, V.; Szepesi, A.; Durrant, D.; Seletković, I.; Schroeck, H.-W.; et al. Part IV: Visual Assessment of Crown Condition and Damaging Agents. Version 2020-3. In *Manual on Methods and Criteria for Harmonized Sampling, Assessment, Monitoring and Analysis of the Effects of Air Pollution on Forests*; Centre, U.I.F.P.C., Ed.; Thünen Institute of Forest Ecosystems: Eberswalde, Germany, 2020; p. 49 + Annex.
13. Landmann, G. Forest decline and air pollution effects in the French mountains: A synthesis. In *Forest Decline and Atmospheric Deposition Effects in the French Mountains*; Springer: Berlin/Heidelberg, Germany, 1995; pp. 407–452.
14. Ghosh, S.; Innes, J.L.; Hoffmann, C. Observer Variation as a Source of Error in Assessments of Crown Condition Through Time. *For. Sci.* **1995**, *41*, 235–254. [CrossRef]
15. Innes, J.L.; Landmann, G.; Mettendorf, B. Consistency of observations of forest tree defoliation in three European countries. *Environ. Monit. Assess.* **1993**, *25*, 29–40. [CrossRef]
16. Johnson, J.; Jacob, M. Monitoring the effects of air pollution on forest condition in Europe: Is crown defoliation an adequate indicator? *Iforest—Biogeosci. For.* **2010**, *3*, 86–88. [CrossRef]
17. Eickenscheidt, N.; Wellbrock, N. Consistency of defoliation data of the national training courses for the forest condition survey in Germany from 1992 to 2012. *Environ. Monit. Assess.* **2014**, *186*, 257–275. [CrossRef] [PubMed]
18. Ferretti, M.; Bussotti, F.; Cenni, E.; Cozzi, A. Implementation of Quality Assurance Procedures in the Italian Programs of Forest Condition Monitoring. *Water Air Soil Pollut.* **1999**, *116*, 371–376. [CrossRef]
19. Wulff, S. The Accuracy of Forest Damage Assessments—Experiences from Sweden. *Environ. Monit. Assess.* **2002**, *74*, 295–309. [CrossRef]
20. Ferretti, M.; König, N.; Rautio, P.; Sase, H. Quality assurance (QA) in international forest monitoring programmes: Activity, problems and perspectives from East Asia and Europe. *Ann. For. Sci.* **2009**, *66*, 403. [CrossRef]
21. Leuschner, C.; Ellenberg, H. *Ecology of Central European Forests: Vegetation Ecology of Central Europe*; Springer International Publishing: Cham, Switzerland, 2017; Volume 1, pp. 1–971.
22. Duncker, P.S.; Raulund-Rasmussen, K.; Gundersen, P.; Katzensteiner, K.; De Jong, J.; Ravn, H.P.; Smith, M.; Eckmullner, O.; Spiecker, H. How Forest Management affects Ecosystem Services, including Timber Production and Economic Return: Synergies and Trade-Offs. *Ecol. Soc.* **2012**, *17*, 17. [CrossRef]
23. Zimmermann, J.; Hauck, M.; Dulamsuren, C.; Leuschner, C. Climate Warming-Related Growth Decline Affects *Fagus sylvatica*, But Not Other Broad-Leaved Tree Species in Central European Mixed Forests. *Ecosystems* **2015**, *18*, 560–572. [CrossRef]
24. Simon, J.; Dannenmann, M.; Pena, R.; Gessler, A.; Rennenberg, H. Nitrogen nutrition of beech forests in a changing climate: Importance of plant-soil-microbe water, carbon, and nitrogen interactions. *Plant Soil* **2017**, *418*, 89–114. [CrossRef]
25. Beniston, M.; Stephenson, D.B.; Christensen, O.B.; Ferro, C.A.T.; Frei, C.; Goyette, S.; Halsnaes, K.; Holt, T.; Jylhä, K.; Koffi, B.; et al. Future extreme events in European climate: An exploration of regional climate model projections. *Clim. Chang.* **2007**, *81*, 71–95. [CrossRef]
26. Giorgi, F. Climate change hot-spots. *Geophys. Res. Lett.* **2006**, *33*, 113–128. [CrossRef]
27. Gajić-Čapka, M.; Cindrić, K.; Pasarić, Z. Trends in precipitation indices in Croatia, 1961–2010. *Theor. Appl. Climatol.* **2015**, *121*, 167–177. [CrossRef]
28. Zaninović, K.; Gajić-Čapka, M. Changes in Components of the Water Balance in the Croatian Lowlands. *Theor. Appl. Climatol.* **2000**, *65*, 111–117. [CrossRef]
29. Spinoni, J.; Antofie, T.; Barbosa, P.; Bihari, Z.; Lakatos, M.; Szalai, S.; Szentimrey, T.; Vogt, J. An overview of drought events in the Carpathian Region in 1961–2010. *Adv. Sci. Res.* **2013**, *10*, 21–32. [CrossRef]
30. Lorenz, M.; Fischer, R. Pan-European Forest Monitoring: An Overview. In *Developments in Environmental Science*; Volume Forest Monitoring—Methods for Terrestrial Investigations in Europe with an Overview of North America and Asia; Marco Ferretti, R.F., Ed.; Elsevier: Amsterdam, The Netherlands, 2013; p. 14.
31. Zierl, B. A simulation study to analyse the relations between crown condition and drought in Switzerland. *For. Ecol. Manag.* **2004**, *188*, 25–38. [CrossRef]
32. Seidling, W.; Ziche, D.; Beck, W. Climate responses and interrelations of stem increment and crown transparency in Norway spruce, Scots pine, and Common beech. *For. Ecol. Manag.* **2012**, *284*, 196–204. [CrossRef]
33. Ferretti, M.; Nicolas, M.; Bacaro, G.; Brunialti, G.; Calderisi, M.; Croisé, L.; Frati, L.; Lanier, M.; Maccherini, S.; Santi, E.; et al. Plot-scale modelling to detect size, extent, and correlates of changes in tree defoliation in French high forests. *For. Ecol. Manag.* **2014**, *311*, 56–69. [CrossRef]
34. De la Cruz, A.C.; Gil, P.M.; Fernández-Cancio, Á.; Minaya, M.; Navarro-Cerrillo, R.M.; Sánchez-Salguero, R.; Grau, J.M. Defoliation triggered by climate induced effects in Spanish ICP Forests monitoring plots. *For. Ecol. Manag.* **2014**, *331*, 245–255. [CrossRef]
35. Seletković, I.; Potočić, N.; Ugarković, D.; Jazbec, A.; Pernar, R.; Seletković, A.; Benko, M. Climate and relief properties influence crown condition of common beech (*Fagus sylvatica* L.) on the Medvednica massif. *Period. Biol.* **2009**, *111*, 435–441.
36. Potočić, N.; Seletković, I.; Ugarković, D.; Jazbec, A.; Mikac, S. The influence of climate properties on crown condition of Common beech (*Fagus sylvatica* L.) and *Silver fir* (*Abies alba* Mill.) on Velebit. *Period. Biol.* **2008**, *110*, 145–150.

37. Ognjenović, M.; Levanič, T.; Potočić, N.; Ugarković, D.; Indir, K.; Seletković, I. Interrelations of various tree vitality indicators and their reaction to climatic conditions on a european beech (*Fagus sylvatica* L.) plot. *Šumar. List* **2020**, *144*, 351–365. [CrossRef]
38. Sousa-Silva, R.; Verheyen, K.; Ponette, Q.; Bay, E.; Sioen, G.; Titeux, H.; Van de Peer, T.; Van Meerbeek, K.; Muys, B. Tree diversity mitigates defoliation after a drought-induced tipping point. *Glob. Chang. Biol.* **2018**, *24*, 4304–4315. [CrossRef]
39. Augustin, N.H.; Musio, M.; von Wilpert, K.; Kublin, E.; Wood, S.N.; Schumacher, M. Modeling Spatiotemporal Forest Health Monitoring Data. *J. Am. Stat. Assoc.* **2009**, *104*, 899–911. [CrossRef]
40. Cindrić, K.; Telišman Prtenjak, M.; Herceg-Bulić, I.; Mihajlović, D.; Pasarić, Z. Analysis of the extraordinary 2011/2012 drought in Croatia. *Theor. Appl. Climatol.* **2016**, *123*, 503–522. [CrossRef]
41. Carnicer, J.; Coll, M.; Ninyerola, M.; Pons, X.; Sánchez, G.; Peñuelas, J. Widespread crown condition decline, food web disruption, and amplified tree mortality with increased climate change-type drought. *Proc. Natl. Acad. Sci. USA* **2011**, *108*, 1474–1478. [CrossRef] [PubMed]
42. Timmermann, V.; Potočić, N.; Ognjenović, M.; Kirchner, T. *Tree Crown Condition in 2019*; Thünen Institute: Eberswalde, Germany, 2020.
43. Klap, J.M.; Oude Voshaar, J.H.; De Vries, W.; Erisman, J.W. Effects of Environmental Stress on Forest Crown Condition in Europe. Part IV: Statistical Analysis of Relationships. *Water Air Soil Pollut.* **2000**, *119*, 387–420. [CrossRef]
44. Vitale, M.; Proietti, C.; Cionni, I.; Fischer, R.; De Marco, A. Random Forests Analysis: A Useful Tool for Defining the Relative Importance of Environmental Conditions on Crown Defoliation. *Water Air Soil Pollut.* **2014**, *225*, 1992. [CrossRef]
45. Seidling, W. Signals of summer drought in crown condition data from the German Level I network. *Eur. J. For. Res.* **2007**, *126*, 529–544. [CrossRef]
46. Seidling, W. Crown condition within integrated evaluations of Level II monitoring data at the German level. *Eur. J. For. Res.* **2004**, *123*, 63–74. [CrossRef]
47. Ling, K.A.; Power, S.A.; Ashmore, M.R. A Survey of the Health of *Fagus sylvatica* in Southern Britain. *J. Appl. Ecol.* **1993**, *30*, 295–306. [CrossRef]
48. Eichhorn, J.; Icke, R.; Isenberg, A.; Paar, U.; Schönfelder, E. Temporal development of crown condition of beech and oak as a response variable for integrated evaluations. *Eur. J. For. Res.* **2005**, *124*, 335–347. [CrossRef]
49. Ewald, J. Ecological background of crown condition, growth and nutritional status of *Picea abies* (L.) Karst. in the Bavarian Alps. *Eur. J. For. Res.* **2005**, *124*, 9–18. [CrossRef]
50. Graf Pannatier, E.; Dobbertin, M.; Schmitt, M.; Thimonier, A.; Waldner, P. Effects of the drought 2003 on forests in Swiss Level II plots. In Proceedings of the Symposium: Forests in a Changing Environment—Results of 20 Years ICP Forests Monitoring, Göttingen, Germany, 25–28 October 2006; pp. 125–135.
51. Bréda, N.; Huc, R.; Granier, A.; Dreyer, E. Temperate forest trees and stands under severe drought: A review of ecophysiological responses, adaptation processes and long-term consequences. *Ann. For. Sci.* **2006**, *63*, 625–644. [CrossRef]
52. Filewod, B.; Thomas, S.C. Impacts of a spring heat wave on canopy processes in a northern hardwood forest. *Glob. Chang. Biol.* **2014**, *20*, 360–371. [CrossRef] [PubMed]
53. Zweifel, R.; Steppe, K.; Sterck, F.J. Stomatal regulation by microclimate and tree water relations: Interpreting ecophysiological field data with a hydraulic plant model. *J. Exp. Bot.* **2007**, *58*, 2113–2131. [CrossRef] [PubMed]
54. Peñuelas, J.; Hunt, J.M.; Ogaya, R.; Jump, A.S. Twentieth century changes of tree-ring δ13C at the southern range-edge of *Fagus sylvatica*: Increasing water-use efficiency does not avoid the growth decline induced by warming at low altitudes. *Glob. Chang. Biol.* **2008**, *14*, 1076–1088. [CrossRef]
55. Allen, C.D.; Macalady, A.K.; Chenchouni, H.; Bachelet, D.; McDowell, N.; Vennetier, M.; Kitzberger, T.; Rigling, A.; Breshears, D.D.; Hogg, E.H.; et al. A global overview of drought and heat-induced tree mortality reveals emerging climate change risks for forests. *For. Ecol. Manag.* **2010**, *259*, 660–684. [CrossRef]
56. Ogaya, R.; Peñuelas, J.; Asensio, D.; Llusià, J. Chlorophyll fluorescence responses to temperature and water availability in two co-dominant Mediterranean shrub and tree species in a long-term field experiment simulating climate change. *Environ. Exp. Bot.* **2011**, *73*, 89–93. [CrossRef]
57. Dreesen, F.E.; De Boeck, H.J.; Janssens, I.A.; Nijs, I. Summer heat and drought extremes trigger unexpected changes in productivity of a temperate annual/biannual plant community. *Environ. Exp. Bot.* **2012**, *79*, 21–30. [CrossRef]
58. Shao, H.-B.; Chu, L.-Y.; Jaleel, C.A.; Zhao, C.-X. Water-deficit stress-induced anatomical changes in higher plants. *Comptes Rendus Biol.* **2008**, *331*, 215–225. [CrossRef]
59. Perry, T.O. Dormancy of Trees in Winter. *Science* **1971**, *171*, 29–36. [CrossRef]
60. McDowell, N.G.; Allen, C.D. Darcy's law predicts widespread forest mortality under climate warming. *Nat. Clim. Chang.* **2015**, *5*, 669–672. [CrossRef]
61. Eschrich, W.; Burchardt, R.; Essiamah, S. The induction of sun and shade leaves of the European beech (*Fagus sylvatica* L.): Anatomical studies. *Trees* **1989**, *3*, 1–10. [CrossRef]
62. Uemura, A.; Ishida, A.; Nakano, T.; Terashima, I.; Tanabe, H.; Matsumoto, Y. Acclimation of leaf characteristics of *Fagus* species to previous-year and current-year solar irradiances. *Tree Physiol.* **2000**, *20*, 945–951. [CrossRef] [PubMed]
63. McDowell, N.; Pockman, W.T.; Allen, C.D.; Breshears, D.D.; Cobb, N.; Kolb, T.; Plaut, J.; Sperry, J.; West, A.; Williams, D.G.; et al. Mechanisms of plant survival and mortality during drought: Why do some plants survive while others succumb to drought? *New Phytol.* **2008**, *178*, 719–739. [CrossRef]

64. Eickenscheidt, N.; Augustin Nicole, H.; Wellbrock, N. Spatio-temporal modelling of forest monitoring data: Modelling German tree defoliation data collected between 1989 and 2015 for trend estimation and survey grid examination using GAMMs. *iForest—Biogeosci. For.* **2019**, *12*, 338–348. [CrossRef]
65. Ferretti, M.; Fischer, R.; Mues, V.; Granke, O.; Lorenz, M.; Seidling, W.; Nicolas, M. Part II: Basic design principles for the ICP Forests Monitoring Networks. Version 2020-2. In *Manual on Methods and Criteria for Harmonized Sampling, Assessment, Onitoring and Analysis of the Effects of Air Pollution on Forests*; Centre, U.I.F.P.C., Ed.; Thünen Institute of Forest Ecosystems: Eberswalde, Germany, 2020; p. 33 + Annex.
66. Caudullo, G.; Welk, E.; San-Miguel-Ayanz, J. Chorological maps for the main European woody species. *Data Brief* **2017**, *12*, 662–666. [CrossRef] [PubMed]
67. Pravilnik o Vrstama Stanišnih Tipova, Karti Staništa, Ugroženim i Rijetkim Stanišnim Tipovima te o Mjerama za Očuvanje Stanišnih Tipova NN 7/2006. Available online: https://narodne-novine.nn.hr/clanci/sluzbeni/2006_01_7_156.html (accessed on 24 January 2022).
68. Perčec Tadić, M. Gridded Croatian climatology for 1961–1990. *Theor. Appl. Climatol.* **2010**, *102*, 87–103. [CrossRef]
69. Perčec Tadić, M.; Pasarić, Z.; Guijarro, J.A. Croatian High-Resolution Monthly Gridded Data Set of Homogenised Surface Air Temperature (*Manuscript submitted*). *Theor. Appl. Climatol.* **2022**.
70. Palmer, W.C. *Meteorological Drought*; US Department of Commerce, Weather Bureau: Washington, DC, USA, 1965; Volume 45, p. 58.
71. Vicente-Serrano, S.M.; Beguería, S.; López-Moreno, J.I. A Multiscalar Drought Index Sensitive to Global Warming: The Standardized Precipitation Evapotranspiration Index. *J. Clim.* **2010**, *23*, 1696–1718. [CrossRef]
72. Sen, P.K. Estimates of the Regression Coefficient Based on Kendall's Tau. *J. Am. Stat. Assoc.* **1968**, *63*, 1379–1389. [CrossRef]
73. Mann, H.B. Nonparametric tests against trend. *Econometrica* **1945**, *13*, 245–259. [CrossRef]
74. Kendall, M.G. *Rank Correlation Methods*; Griffin: Oxford, UK, 1948.
75. Wilcox, R.R. *Fundamentals of Modern Statistical Methods: Substantially Improving Power and Accuracy*; Springer: New York, NY, USA, 2010.
76. Wang, J.-F.; Zhang, T.-L.; Fu, B.-J. A measure of spatial stratified heterogeneity. *Ecol. Indic.* **2016**, *67*, 250–256. [CrossRef]
77. Bivand, R.S.; Pebesma, E.J.; Gomez-Rubio, V.; Pebesma, E.J. *Applied Spatial Data Analysis with R*; Springer: New York, NY, USA, 2013; Volume 2.
78. Laird, N.M.; Ware, J.H. Random-Effects Models for Longitudinal Data. *Biometrics* **1982**, *38*, 963–974. [CrossRef] [PubMed]
79. LeBeau, B. Impact of serial correlation misspecification with the linear mixed model. *J. Mod. Appl. Stat. Methods* **2016**, *15*, 21. [CrossRef]
80. Goerg, G.M. The Lambert Way to Gaussianize Heavy-Tailed Data with the Inverse of Tukey's *h* Transformation as a Special Case. *Sci. World J.* **2015**, *2015*, 909231. [CrossRef]
81. Johnson, J.B.; Omland, K.S. Model selection in ecology and evolution. *Trends Ecol. Evol.* **2004**, *19*, 101–108. [CrossRef]
82. Breiman, L. Random Forests. *Mach. Learn.* **2001**, *45*, 5–32. [CrossRef]
83. Thompson, C.G.; Kim, R.S.; Aloe, A.M.; Becker, B.J. Extracting the Variance Inflation Factor and Other Multicollinearity Diagnostics from Typical Regression Results. *Basic Appl. Soc. Psychol.* **2017**, *39*, 81–90. [CrossRef]
84. Akaike, H. A new look at the statistical model identification. *IEEE Trans. Autom. Control.* **1974**, *19*, 716–723. [CrossRef]
85. R Core Team. *R: A Language and Environment for Statistical Computing*; R Foundation for Statistical Computing: Vienna, Austria, 2016.
86. Shumway, R.H.; Stoffer, D.S.; Stoffer, D.S. *Time Series Analysis and Its Applications*; Springer: Berlin/Heidelberg, Germany, 2000; Volume 3.
87. EEA. European Digital Elevation Model (EU-DEM), Version 1.1, European Environment Agency (EEA). 2016. Available online: https://land.copernicus.eu/imagery-in-situ/eu-dem/eu-dem-v1.1?tab=metadata (accessed on 24 January 2022).
88. *ISO-13878*; Soil Quality—Determination of Total Nitrogen Content by Dry Combustion ("Elemental Analysis"). ISO: Geneva, Switzerland, 1998.
89. Egnér, H.; Riehm, H.; Domingo, W.R. Untersuchungen über die chemische Bodenanalyse als Grundlage für die Beurteilung des Nährstoffzustandes der Böden. II. Chemische Extraktionsmethoden zur Phosphor-und Kaliumbestimmung. *K. Lantbr. Ann.* **1960**, *26*, 199–215.
90. Škorić, A. *Priručnik za Pedološka Istraživanja*; Fakultet Poljoprivrednih Znanosti: Zagreb, Croatia, 1985.
91. *ISO-10390*; Soil Quality—Determination of pH. ISO: Geneva, Switzerland, 2005.

plants

MDPI

Article

Effects of Climate on Douglas-fir (*Pseudotsuga menziesii* (Mirb.) Franco) Growth Southeast of the European Alps

Tom Levanič [1,2,*] and Hana Štraus [3]

[1] Department of Forest Yield and Silviculture, Slovenian Forestry Institute, Večna Pot 2, SI-1000 Ljubljana, Slovenia
[2] Faculty of Mathematics, Natural Sciences and Information Technologies, University of Primorska, Glagoljaška 8, SI-6000 Koper, Slovenia
[3] Department of Forestry and Renewable Forest Resources, Biotechnical Faculty, University of Ljubljana, Večna Pot 83, SI-1000 Ljubljana, Slovenia; hana.straus@bf.uni-lj.si
* Correspondence: tom.levanic@gozdis.si

Abstract: Douglas-fir (*Pseudotsuga menziesii* (Mirb.) Franco) is a non-native tree species in Slovenia with the potential to partially replace Norway spruce in our native forests. Compared to spruce, it has several advantages in terms of volume growth, wood quality and tolerance to drought. This is important given the changing climate in which spruce is confronted with serious problems caused by increasing temperatures and drought stress. At three sites (one on non-carbonate bedrock and deep soils, and two on limestone with soil layers of varying depths), 20 Douglas-fir and 20 spruce per site were sampled in order to compare their radial growth response to climate and drought events. The radial growth of Douglas-fir exceeds that of spruce by about 20% on comparable sites. It is more responsive to climate than spruce. Above-average temperatures in February and March have a significant positive effect on the radial growth of Douglas-fir. In recent decades, above-average summer precipitation has also had a positive influence on the radial growth of Douglas-fir. Compared to spruce, Douglas-fir is less sensitive to extreme drought events. Our results indicate that Douglas-fir may be a good substitute for spruce in semi-natural managed forest stands in Slovenia. The planting of Douglas-fir should be allowed in Slovenian forests, but the proportion of it in forest stands should be kept lower than is the case with spruce today.

Keywords: climate change; climate response; drought; radial increment; dendrochronology

Citation: Levanič, T.; Štraus, H. Effects of Climate on Douglas-fir (*Pseudotsuga menziesii* (Mirb.) Franco) Growth Southeast of the European Alps. *Plants* **2022**, *11*, 1571. https://doi.org/10.3390/plants11121571

Academic Editor: Nenad Potočić

Received: 25 May 2022
Accepted: 12 June 2022
Published: 14 June 2022

1. Introduction

Climate change is having a major impact on the world's ecosystems. Owing to the longevity of trees, forest ecosystems cannot quickly adapt to changes in the environment. In Europe, climate change is mainly reflected in increasing temperatures (0.85 °C increase from 1880 to 2012) [1], more frequent droughts and more extreme weather events [2]. As a result, higher mortality of individual tree species has already been observed in some forest ecosystems due to drought stress and related factors [3]. Norway spruce (*Picea abies* (L.) Karst), one of the most economically important tree species in Europe, has been the most affected. Slovenia has also experienced massive spruce dieback in recent years due to climate change, natural disasters and the spread of bark beetles. Empirically-based random forest models show that the area of potential spruce sites in Slovenia will decrease in the future [4], and that deciduous forests will slowly replace coniferous forests [5]. As the proportion of spruce in the growing stock decreases, the economic benefits of the forest are expected to decrease, and significant changes in the wood processing industry are also expected. In order to maintain the socio-economic functions of forests, it is necessary to find, among other things, tree species that possess wood properties similar to those of spruce, and that are more resistant and resilient to extreme climatic conditions and drought.

An important limiting factor for the future growth of species will most likely be a lack of accessible water [3].

One way to mitigate the negative consequences of spruce dieback is by introducing other species, such as Douglas-fir (*Pseudotsuga menziesii* (Mirb.) Franco), to close-to-nature forests as a partial replacement for Norway spruce [6]. Due to its fast growth and high-quality wood, Douglas-fir is the most common non-native tree species in many European countries, including Slovenia. Currently, the planting of Douglas-fir is prohibited in Slovenia (Official Gazette of the Republic of Slovenia, No. 96/04), although it was planted in the past and today accounts for 0.5% of the growing stock [7].

The natural distribution range of Douglas-fir extends along the entire Pacific coast of North America, from British Columbia to Mexico. It thrives in a wide range of climatic conditions, but proliferates best in habitats with high humidity and deep, aerated soils [8]. In Slovenia, as in the rest of the central Europe, it grows best at altitudes ranging from 500 to 1000 m above sea level in the belt of beech and silver fir–beech forests [9]). It requires high humidity and a moist, well-aerated and deep soil for rapid growth. It grows poorly in shallow limestone soils and in compacted soils with standing water [10].

Douglas-fir originates from an environment with warm, dry summers, and therefore is physiologically better adapted to a lack of water in the soil compared to Norway spruce. Small leaf stomata, heavily waxed needles and an effective stomata regulating mechanism allow Douglas-fir to use water sparingly, and maintain a positive photosynthetic ratio [11]. Compared to Norway spruce, the root system of Douglas-fir is deeper, which makes it more resistant to drought and windthrow [12]. Resistance to different climatic factors largely depends on the variety and provenance of the species [13]. Despite these physiological adaptations, extreme droughts in recent years have also resulted in needle shed, crown reduction and mortality of Douglas-fir trees in France [14]. Various sources have also noted that the growth of Douglas-fir has also been negatively affected, especially in the late winter months, as it is sensitive to frost [15–17].

Previous studies have shown that the impact of Douglas-fir on European forest ecosystems is comparable to that of native conifers [18], and is less than that of other non-native species [19]. It has the greatest impact when planted in monocultures over large areas, making plantations particularly problematic. Its impact on the soil is also small and difficult to determine due to the complexity of the various factors affecting soil chemistry. The root system is deeper than that of spruce, which reduces competition for nutrients in the rhizosphere. It also appears to be more resistant to drought and the negative effects of climate change in general than spruce. Under suitable conditions, it is potentially invasive in some parts of Europe [20,21], but studies indicate that its invasive potential is not likely to increase due to climate change, as the shallow root system of young trees is vulnerable to drought conditions [19].

Currently, Douglas-fir is not troubled by many pests in Europe, although in its natural habitats in North America, it is affected by a wide variety of pests, including some very damaging and destructive insects (e.g., Douglas-fir tussock moth (*Orgyia pseudotsugata* McDunnough), Douglas-fir beetle (*Dendroctonus pseudotsugae*, Hopkins) and Western spruce bud worm (*Choristoneura occidentalis* Freeman)) [22].

Little is known about the growth of Douglas-fir and its response to climate in Slovenia. The aim of the study was therefore to (1) investigate the radial growth of Douglas-fir on sites with different productivity; (2) analyse the climatic factors that significantly influence the growth of Douglas-fir in order to identify potentially critical meteorological factors for its radial growth and growth in general; (3) compare the response of Douglas-fir and spruce to climatic factors on sites with different productivity; (4) analyse the response of Douglas-fir in years with markedly dry and hot summers and compare it to the response of Norway spruce; and (5) determine whether Douglas-fir can be a good substitute for spruce, and whether replacement of Norway spruce is necessary and appropriate due to spruce's declining vitality caused by climate change.

2. Results

2.1. Radial Growth of Douglas-Fir and Norway Spruce on Three Sites

The radial growth of Douglas-fir and Norway spruce was studied on three different locations with different bedrock and soil depths. Basic information about age, diameter at breast height (DBH) and average width of the annual increment is presented in Table 1. Douglas-fir trees on the studied sites generally have a larger DBH than Norway spruce trees, with radial increments similarly higher in Douglas-fir than in Norway spruce (Table 1).

Table 1. Basic data on the analysed Douglas-fir and Norway spruce trees on all three sites (PO-1, PO-2 and CE). TRW—tree-ring width, DBH—diameter at breast height measured with a diameter tape, Std. dev.—standard deviation.

Location	Tree Species	Age (Years)	DBH (cm)	Std. Dev. DBH (cm)	TRW * (mm)	Std. Dev. TRW (mm)
CE	Douglas-fir	70	69.60	9.51	4.73	0.986
	Norway spruce	71	52.20	4.89	3.48	1.29
PO-1	Douglas-fir	79	75.56	9.39	3.74	1.34
	Norway spruce	96	57.06	7.53	2.40	1.03
PO-2	Douglas-fir	45	49.33	5.87	4.53	1.79
	Norway spruce	121	59.84	11.66	2.17	0.75

* Tree-ring width is the average of the tree-ring width measurements from two cores per tree.

Douglas-fir on site CE, which is characterised by non-carbonate bedrock and deep soil, clearly outperforms Norway spruce. On this site, both tree species are growing in the same forest stand with the same bedrock and soil depth. Radial growth was comparable in the period 1940–1990, but in the period 1990–2020 the radial growth of Douglas-fir on site CE was significantly greater than that of Norway spruce. Moreover, while the radial growth of Norway spruce declined after 1998, Douglas-fir's radial increment slowly increased (Figure 1).

On limestone bedrock and at variable soil depths of the Dinaric Karst, Douglas-fir exhibits variable performance in comparison to spruce. In deeper soils on site PO-1, there is very little difference between the radial growth of Douglas-fir and Norway spruce; both tree species grow more or less similarly and respond to environmental factors in the same way. There is a slight difference in radial growth in favour of Douglas-fir, but it is not statistically significant. The radial growth of Douglas-fir has been decreasing in the last decade and is equal to that of Norway spruce (Figure 1).

On site PO-2 (also Dinaric Karst) with shallow soil and limestone bedrock, the radial growth of Douglas-fir is higher than that of Norway spruce, regardless of the fact that the spruce trees there are older than the Douglas-fir trees. Both species show a similar response to environmental factors. We observed a decrease in the radial growth of Douglas-fir after 1998, with the same decrease also visible in Norway spruce. A recovery in the radial growth of Douglas-fir was observed after 2013. A similar recovery is also visible in Norway spruce, but it is much smaller in terms of absolute numbers (Figure 1).

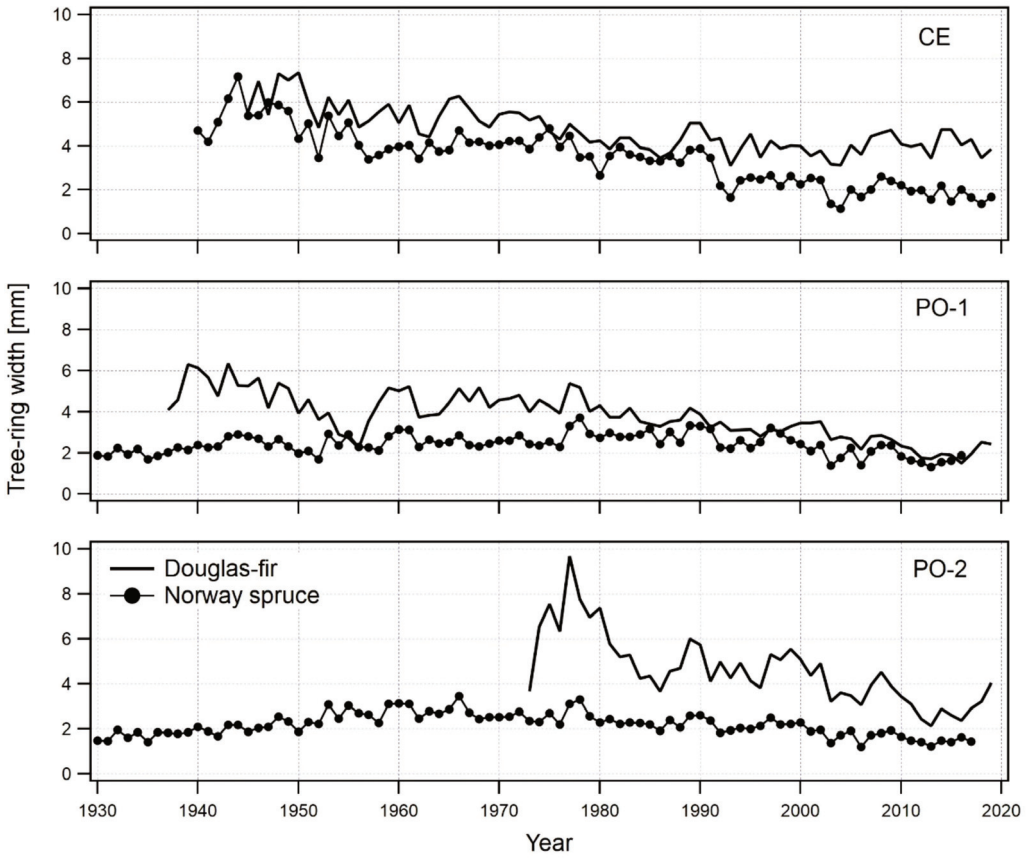

Figure 1. Comparison of tree-ring width chronologies for Douglas-fir and Norway spruce per site. Norway spruce chronologies on PO-1 and PO-2 sites are two years shorter since the samples were collected two years earlier.

2.2. Climate–Growth Relationship of Douglas-fir

The general growth response of Douglas-fir and Norway spruce to climate differs significantly (Figure 2), with Douglas-fir having a much clearer radial growth response to climate than Norway spruce. The above-average radial growth of Douglas-fir is significantly associated with above-average winter temperatures, particularly in February and March, while that of Norway spruce is correlated with above-average precipitation in the summer months, specifically June and July. Above-averages temperature in June and July have a negative impact on the radial growth of Norway spruce and no statistically significant impact on that of Douglas-fir.

In contrast to the general response of trees to climatic factors in the growing season, Douglas-fir is particularly sensitive to above-average temperatures in February and March. Higher than average temperatures in February and March have a positive influence on radial growth for the growing season that follows. This influence on radial growth was observed on all studied sites; however, on PO-1 this relationship was visible but not significant. The highest correlations between radial growth and February–March temperatures were found on the most productive site CE, followed by PO-2 and PO-1 (Figure 2, left panel).

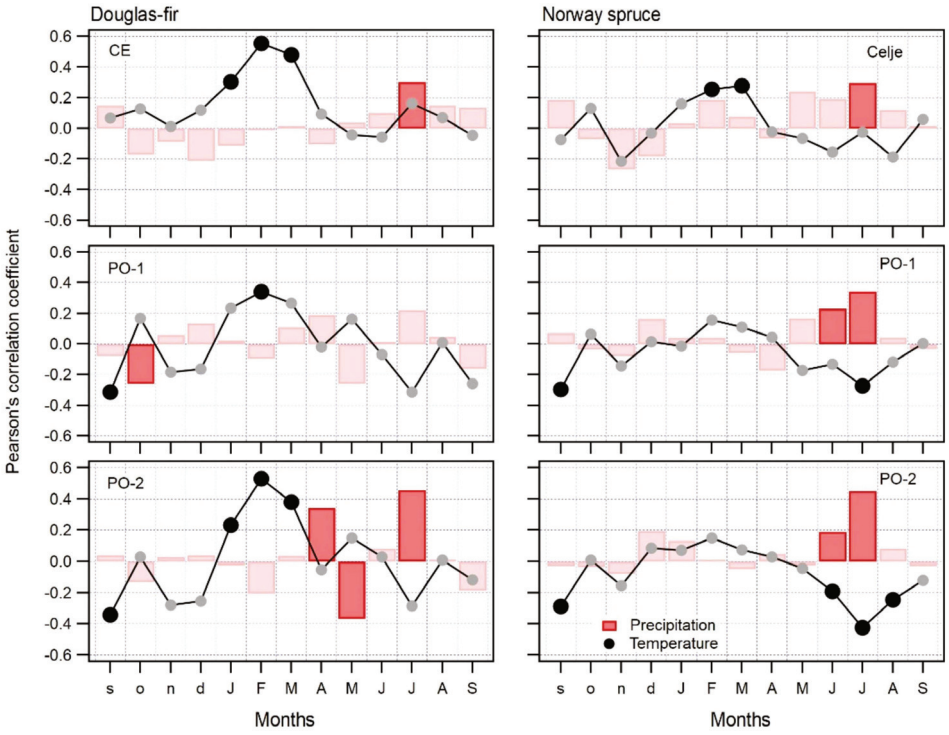

Figure 2. Climate–growth response of Douglas-fir (**left** side panel) and Norway spruce (**right** side panel).

On the least productive and drier site PO-2, precipitation in the growing season also plays important role, especially the lack of precipitation in July, which is indicated by a high positive correlation. A similar response was also observed on site CE, where the correlation is smaller but still significant. On site PO-1, we found a low but still significant negative correlation with above-average precipitation in the previous October. As the interpretation of such a relationship is difficult, we believe that it is just an artefact of the bootstrapped calculation of the correlation coefficient. Additionally, on site PO-2 we found a significant positive effect of precipitation on the radial growth of Douglas-fir in April and a negative effect on it in May (Figure 2, left panel). It seems that above-average precipitation in April has a beneficial influence on the radial growth of Douglas-fir, while above-average temperature in May has a negative influence on radial growth of Norway spruce. It is quite possible that above-average precipitation in May relates to cold air intrusion, which often brings very low temperatures and even snow in the first half of May.

The dependence of spruce on February and March temperatures is significant only on the most productive site CE, while on sites PO-1 and PO-2, we found a significant response of radial growth to climate only in the summer months. Specifically, on the productive PO-1 site, above-average temperature in July has a negative influence on radial growth, while on the least productive site PO-2, above-average temperatures in June, July and August have a significant negative impact on radial growth (Figure 2, right panel).

Precipitation plays a more important role in the radial growth of Norway spruce than temperature. Above-average precipitation in June and July has a positive effect on tree-ring width on PO-1 and PO-2 sites, while on site CE only above-average precipitation in July has a positive influence on tree-ring width (Figure 2, right panel).

The combination of the positive impact of precipitation and negative impact of temperature means that the radial growth of Norway spruce on the least productive site PO-2 and, to some degree, also on the more productive sites CE and PO-1, is negatively affected by a hot and dry climate in the summer months (Figure 2, right panel).

Both studied tree species have a radically different response to climate. For Douglas-fir, February and March are important months for radial growth in the subsequent growth

period. If February and March temperatures are above average, we can expect higher radial growth, and vice versa. Precipitation has less influence on the radial growth of Douglas-fir, most likely as a result of its deep root system. Compared to Douglas-fir, Norway spruce is not as sensitive to winter temperatures. However, above-average precipitation in June and July and above-average temperature in July have a positive and negative influence, respectively. As a result of its shallow root system, Norway spruce is more susceptible to hot and dry summers than Douglas-fir, regardless of site productivity.

Analysis of the radial growth response to climate using bootstrapped moving window correlation provides insight into the temporal response of the studied trees to climate, and into the response of trees to changing climatic conditions over time. This is particularly important given that some climatic factors might have become more significant and some less significant over time. Additionally, by means of temporal analysis with moving window correlation (Appendices A and B), it is also possible to determine whether the radial growth response differs from the general tree-ring width response to climate (as in Figure 2), and whether responses become stable over time or not.

There are important differences between Douglas-fir and Norway spruce with respect to temporal response. The temporal response of Douglas-fir to temperature on all studied sites is clear, statistically significant and stable over time. Above-average temperatures in February and March are important drivers of Douglas-fir growth: warmer late winter months are associated with higher radial increments in the summer months.

The temporal stability of the precipitation signal in Douglas-fir is less pronounced. Only precipitation in July seems to play a role in the higher radial increment on the least productive and most drought-exposed site PO-2, which is expected as this site was selected because of its location on a ridge and its shallow soil. On sites CE and PO-1, precipitation plays some role in July, but is less important and not statistically significant (see Appendix A).

The temporal response of Norway spruce is less pronounced than that of Douglas-fir. On the most productive site CE, above-average March temperature has had an influence on radial growth in the last three decades, and July precipitation has had an influence on radial growth in the last two decades. We also observed that the climate–growth relationship has not been stable over time, and that statistical significance is achieved only occasionally.

On the productive site PO-1 (limestone bedrock on deep soil), the influence of July precipitation on the radial growth of Norway spruce has been stable over time, and its importance has been increasing. June precipitation has also gained importance in the last three decades. The influence of temperature on the radial growth of spruce on site PO-1 is statistically significant in July, but the values are not very high.

On the least productive site PO-2 (limestone bedrock, shallow soil), precipitation in July played an important role throughout the entire study period. The temporal stability of the signal is well defined and moving correlations are high. We also observed a temporally stable negative influence of above-average temperature in July. This means that Norway spruce trees on site PO-2 are negatively affected by the occurrence of drought, and that drought is becoming more pronounced (see Appendix B).

2.3. Douglas-Fir Response in Extreme Years

The response in extreme years, whether they were extremely hot and dry or cold and wet, indicates the ability or adaptability of a tree species to cope with climatic extremes. Even if we do not find statistically significant correlations with climate data for a tree species, which is quite common in the case of lowland oaks [23,24], this does not mean that a tree species does not respond to climate. When we record a weak climatic response of a tree species, or when we are interested in how a tree species could respond through adjustments in the radial increment in harsher climate conditions, it is useful to consider the response in extreme climatic conditions (e.g., hot and dry summers). We analysed pointer years for both tree species on all three sites; however, in this paper we present only

the analysis of pointer years for Douglas-fir, and only basic comparisons with respect to the Norway spruce response.

Douglas-fir has fewer negative pointer years compared to spruce, so it is slightly more tolerant to a lack of precipitation in summer, probably due to its deeper root system. From typical dry and hot years, such as 1976, 1980, 1992, 2003, 2013 and 2015, which were detected in spruce at all studied sites, only one negative pointer year (2003) was detected in Douglas-fir on the PO-1 and PO-2 sites. On the other hand, we detected a pointer year in Douglas-fir that was not found in spruce, specifically 1962, where 100% of the trees on two sites (trees on PO-2 were too young to detect that year) responded with a drop in radial increment (Figure 3).

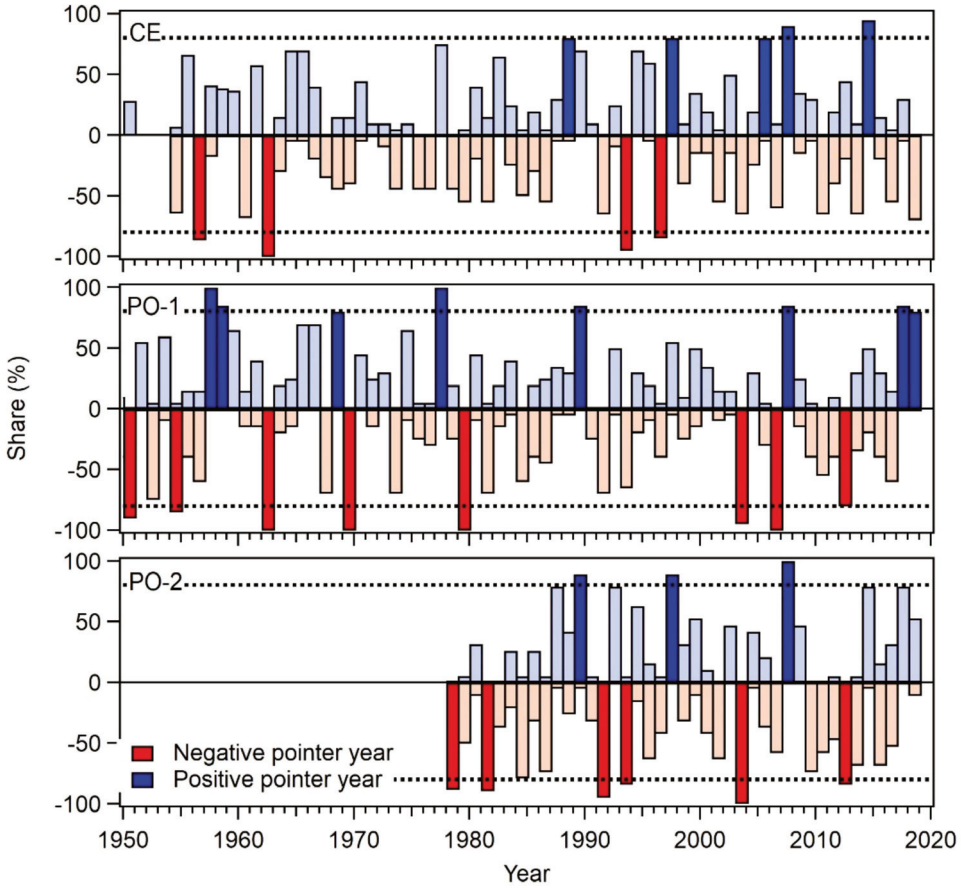

Figure 3. Positive and negative pointer years for Douglas-fir on all three studied sites. The horizontal dashed line represents the 80% threshold for a year to be qualified as a positive or negative pointer year. Emphasised colours indicate significant pointer years with more than 80% of at least 13 trees in a particular year showing an increase or decrease in tree-ring width compared to the previous year.

The following negative pointer years were found on at least two sites for Douglas-fir: 1962, 1993, 2003 and 2012 (Figure 3 and Table 2). In these years, the temperatures in February and March were always below the long-term average, and the winter months were drier with less precipitation in comparison with the long-term average.

Table 2. Common negative pointer years for Douglas-fir on sites PO-1, PO-2 and CE (source of meteorological data: https://meteo.arso.gov.si/met/sl/climate/current/last-12-months/archive/ accessed on 3 February 2022).

Year	Temperature	Precipitation	Sites
Common to all three sites			
No common negative pointer years			
Common to two sites			
1956	February and part of March extremely cold across Europe	No data available	PO-1 and CE, trees on PO-2 too young
1962	Very cold March, close to the long-term record low, below-average temperatures in the first half of the year (including July)	Above-average amount of precipitation between January and July	PO-1 and CE, trees on PO-2 too young
1993	February and March very cold, close to the long-term low, other months close to the long-term average	Below-average amount of precipitation between January and July, absence of snow	PO-2 and CE
2003	February very cold, March within the long-term average, May–August significantly above the long-term average	Entire year very dry, all but late autumn months below the long-term average	PO-1 and PO-2
2012	February very cold, March very warm, June–September notably above the long-term average	January–March very dry, April–July within the long-term average, August dry	PO-1 and PO-2

On site CE with a more continental climate, we also found 1956 to be a negative pointer year. Since this year was not in our local meteorological archives, we checked on-line sources. It turned out that the winter of 1956 was one of the coldest winters in Europe, with temperatures below −24 °C in Basel, Switzerland and −12 °C in Marseille, France [25,26]. Temperatures in February and March were well below average, which had a negative impact on radial growth in the 1956 growing season. The overall winter situation was very similar, if not more extreme, to that in 1962.

In Douglas-fir, we also found four positive pointer years common to at least two sites: 1989, 1997, 2005 and 2007 (Figure 3 and Table 3). A common feature of the positive pointer years is that the key months for future growth, specifically February and March, were always warmer than average, and the monthly precipitation was within or slightly above the long-term average. None of the positive pointer years were particularly cold in the winter or dry in the summer.

One pointer year was common to both studied tree species: the negative pointer year of 2003. That year was one of the hottest and driest ever recorded in Europe. When such a common pointer year occurs in tree-rings, it is important to determine what the weather conditions were during that year such that the same response was observed in the two physiologically different tree species.

The year 2003 was a markedly negative year for many tree species across Europe, including Douglas-fir and Norway spruce [27]; a drought dragged on until September 2003, when monthly rainfall reached the long-term average for the first time in that year. January and July were slightly below the long-term average, while all other months were very dry, with very little or no precipitation. The small amount of precipitation in July was insufficient to compensate for the lack of precipitation in the previous months. Temperatures in 2003 started with below-average values in January, February and March, but then rose to well above the long-term average between April and August.

In 2003, Douglas-fir was mainly influenced by below-average temperatures in February, the month which has a key effect on the growth of Douglas-fir in the same year. Spruce, however, was negatively affected by a lack of precipitation in the first eight months of the year, including the very dry winter and dry summer months, which are key factors in the radial growth of Norway spruce. Therefore, both tree species responded uniformly with a small radial increment, but for different reasons (Table 2).

Table 3. Common positive pointer years for Douglas-fir on sites PO-1, PO-2 and CE (source of meteorological data: https://meteo.arso.gov.si/met/sl/climate/current/last-12-months/archive/ accessed 3 February 2022).

Year	Temperature	Precipitation	Sites
Common to three sites			
2007	Slightly above-average temperature between January and July, then within the long-term average	Precipitation in the entire year within the long-term average with the exception of a very dry April	PO-1, PO-2 and CE
Common to two sites			
1989	February and March temperatures above average, summer temperatures below average	April with above-average amount of precipitation, June–July average and August close to the long-term maximum of precipitation for August	PO-1 and PO-2
1997	February and March temperatures above average	Amount of precipitation in the period February–April above average, later within the long-term average	PO-2 and CE

3. Discussion

3.1. Radial Growth of Douglas-Fir and Norway Spruce on Three Sites

On average, the radial growth of Douglas-fir on three locations in Slovenia always surpassed the growth of Norway spruce, regardless of site productivity. On the most productive non-carbonate site, the average radial increment of Douglas-fir was 4.73 mm and that of Norway spruce was 3.48 mm. On the two limestone bedrock sites, Douglas-fir grew better than Norway spruce; however, on site PO-1 there was no major difference between the two species: 3.74 mm for Douglas-fir and 2.40 mm for Norway spruce. On site PO-2, the difference was similar to the most productive site: 4.53 mm vs. 2.17 mm in favour of Douglas-fir.

Studies done on Douglas-fir in provenance trials with as many as eighteen coastal Douglas-fir provenances [13] showed a radial increment comparable to that of Douglas-fir on sites SE of the Alps. Douglas-firs in the provenance trial had a radial increment ranging between 3.47 mm and 4.42 mm. Douglas-fir from Slovenian sites ranked among the better-growing Douglas-firs when compared with those from provenance trials.

Results from the studies in mixed (Scots pine, European larch, Douglas-fir and black pine) even-aged plantations in Switzerland [3] showed that Douglas-fir is performing well in mixed stands, and that its radial increment is superior to that of other tree species. When comparing the radial increment of Douglas-fir from the trial in Switzerland with that from sites in Slovenia, we found that Douglas-fir grew better on sites in Slovenia, with the exception of PO-1, where the radial increment was slightly below that in Switzerland.

In a study by Vitali et al. [28] from the Black Forest, where the radial increment of Douglas-fir was studied in a three-species intermixed Douglas-fir, Norway spruce and silver fir forest, it was determined that Douglas-fir had the highest radial increment of all three studied species. In comparison with Douglas-fir from sites in Slovenia where the combination of Douglas-fir, Norway spruce and silver fir is very common in the close-to-nature forests of the Karst region, we found that the radial increments of Douglas-fir were not as high but very close to those recorded in the Black Forest.

On Czech forest sites, where Douglas-fir was introduced to forest stands at the end of the 19th and in the 20th centuries [17], researchers carried out a study on 18 sites and concluded that the average radial increment was rather small. In the best case it reached 3.66 mm, and in the worst case it was 1.44 mm. These are far below our findings, and it appears that the productivity of the site where Douglas-fir was planted in Czechia is lower than that in Slovenia.

It seems that the radial increments of Douglas-fir are relatively high in regions with predominantly humid climates (e.g., Slovenia, Southern Germany, parts of Switzerland,

The Netherlands), and lower in countries with a typical continental climate with colder and drier winters (e.g., Czechia). Our research supports this postulation, given that Douglas-fir is sensitive to very cold (and dry) winter months (typical of a continental climate), which results in a smaller radial increment in the vegetation period that follows this paper and [13,17,28,29].

3.2. Climate–Growth Relationship of Douglas-Fir and Comparison to Norway Spruce

Our study shows that the radial increment of Douglas-fir is higher when late winter is mild. On all studied sites, above-average temperature in February is highly correlated with higher radial increment. On two sites, CE and PO-2, above-average temperature in March is also highly correlated with higher radial increment. Precipitation, in general and in any part of the year, is not as important as winter temperatures, although we found some significant correlations with precipitation on sites CE and PO-2 (Figure 2 and Appendix A). However, correlation values for precipitation were lower in comparison with those for temperature. In comparison with Norway spruce, Douglas-fir seems to be more tolerant to above-average summer temperatures, although we assessed that precipitation plays an important role in July, particularly in hot and dry years.

The climate response of Douglas-fir in its natural distribution range in North America (Pacific coast in the USA and Canada) varies across the entire area of distribution. Douglas-fir populations growing in relatively warm and dry climates in Canada have growth patterns correlated mostly with annual precipitation, whereas populations growing in wet and cold climates at high elevations have growth patterns correlated with snowfall, winter and annual temperatures, and ocean–atmosphere climate systems. The strongest response was found in populations growing at climatic extremes [29,30]. A study by Restaino et al. [31] on western Douglas-fir forests in the USA showed that Douglas-fir growth was positively correlated with precipitation and negatively correlated with temperature in the growing season, which is a typical response pattern not only of Douglas-fir but also of many other tree species.

When comparing our results to those from natural Douglas-fir stands in North America, we only found similarities in the climate-growth response with Douglas-fir populations growing in North America's high-elevation wet and cold climates, where a warmer and more humid late winter-early spring resulted in a better radial increment. Since Douglas-fir seed was imported from North America, we can assume that the seeds for some of the older Douglas-fir populations in Slovenia may have come from such regions in N. America [32].

When comparing the climate–growth response of Douglas-fir in Slovenia with that of planted Douglas-fir in different locations in Europe, we found that the climate–growth response on several sites across Europe was comparable. Vejpustkova et al. [17] came to almost identical conclusions with respect to the radial growth of Douglas-fir in Czechia (NE of our sites). The most critical months for Douglas-fir growth were not the summer months but the winter months of January and February. They also found that precipitation in July and August had a positive effect on radial growth. Our observations regarding the response of Douglas-fir to above-average precipitation in summer months are not as conclusive as those from Czechia. Douglas-fir in Slovenia responds positively to July precipitation; however, this response is not as great as in the case of Czechia. An in-depth analysis of the temporal stability of the precipitation signal in the TRW of Douglas-fir on sites in Slovenia showed that precipitation in July is gaining in importance. This is critical, and suggests that climate is changing in such a way that trees need to adapt to new, potentially drier conditions.

Castaldi et al. [16] investigated the climate–growth relationships of Douglas-fir on two contrasting sites in Italy (W and SW of the sites in Slovenia, and on the southern side of the Alps): a Mediterranean area in southern Italy, and a cooler, moister site in the northern Apennines. They found that temperatures in February and March play a positive role in the growth of Douglas-fir on both sites. At the site in northern Italy, Douglas-fir also responds negatively to late summer temperatures and positively to spring–summer precipitation,

which is very similar to our findings. The temporal stability of the climate signal in the two Italian Douglas-fir stands showed that the correlation between radial growth and February temperature is stable over time on the northern site and less so on the southern one. Castaldi et al. [16] also found that precipitation on the northern site is becoming increasingly important. This is highly comparable to the results from Slovenia, which indicate the gradually increasing importance of the July precipitation on the majority of the studied sites (Appendix A). The increasing dependency of Douglas-fir on above-average summer precipitation may possibly have a significant impact on the productivity, and may potentially increase mortality of Douglas-fir in the future.

A study on the climate–growth response of Douglas-fir on 26 forest sites in NW Poland [15], locations north of our sites and north of the Alps, showed that January–March temperature had a statistically significant influence on the growth of Douglas-fir. Principal component analysis revealed that the first component (January–March temperature) explained more than 60% of the entire variability. The second principal component related to precipitation in the summer months accounted for only 8% of the variability. This means that although precipitation plays a role in tree-ring formation, its influence is rather small. This response to precipitation is similar to the response of Douglas-fir to precipitation in Slovenia.

Based on our results and those from different studies across Europe, we can conclude that the climate signal in Douglas-fir tree-rings is comparable over a wide geographical area and diverse climate zones (Figure 4). This indicates that Douglas-fir prefers two main types of climates in Europe: (1) cold to temperate winters, no dry season and (2) warm but not hot summers (types Dfb and CfB after Köppen-Geiger climate classification).

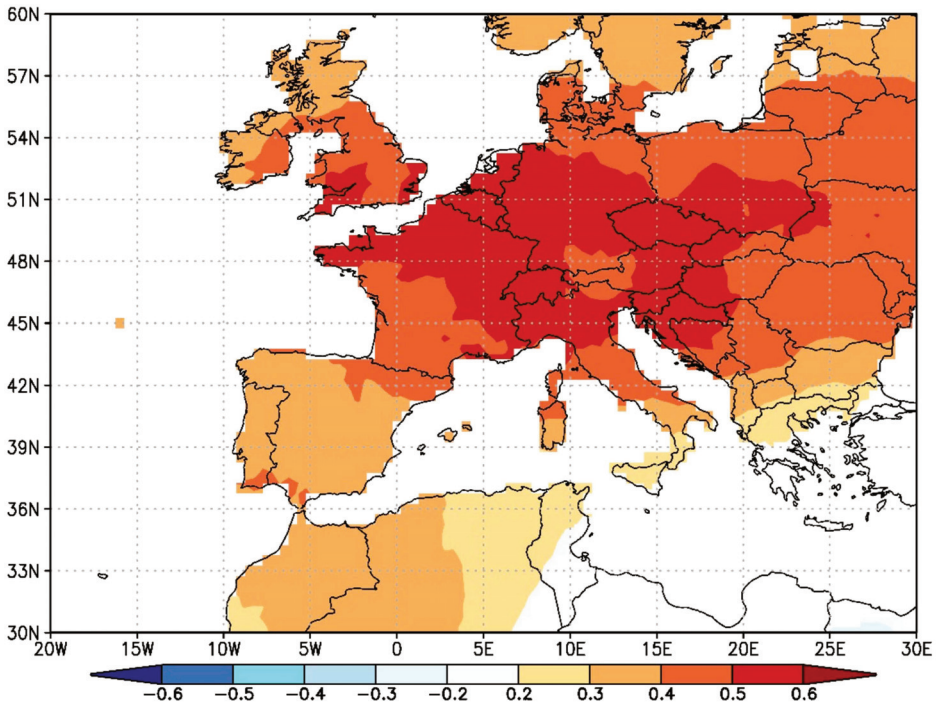

Figure 4. Spatial point correlation between averaged February and March temperatures (1937–2019) and combined Douglas-fir tree-ring chronology for Slovenia. The map shows the spatial extent of Douglas-fir climate–growth signal from Slovenia.

An analysis of the spatial extent of the Douglas-fir climate signal, specifically the response of the TRW to February and March temperatures, showed a very coherent and widespread climate signal. This is quite rare in European tree species, with only a few (e.g., silver fir, larch and partially pedunculate oak) displaying such a widespread climate signal. This climate signal also corresponds well with both of the above-mentioned climate types.

3.3. Douglas-Fir Response in Extreme Years

The response of trees in extreme years, and especially in extremely warm and dry years, provides insight into a tree species' response to extreme climatic conditions and its plasticity. Douglas-fir's natural area of distribution is characterised by a wide range of climate conditions, parent materials, aspects and slopes, and soil textures and sites [20]. It grows best in deep, moist and well-drained soil at mid-elevations with plenty of rainfall. It has a deep root system which can retrieve soil water from deeper layers of the soil. This is in contrast to Norway spruce, which has a shallower root system and is therefore more sensitive to drought.

Pointer years [33] are associated with favourable or unfavourable growing conditions in a certain year. They are a good representation of the common response of trees in a certain year to a common environmental or climatic driver that causes the formation of a wide or narrow tree-ring. In the context of this research, we only focus on negative pointer years in Douglas-fir and Norway spruce and compare them between species and with pointer years detected in Douglas-fir on the European scale.

Based on the literature and our studies, Douglas-fir has not had many negative pointer years between 1900 and the present. In our study, we found five negative pointer years on two out of three sites (trees on one site were too young to capture during pre-1970 pointer years). All negative pointer years in Slovenia were associated with very cold and dry winter months. Two were also associated with very hot and dry summers (1993 and 2003) (Table 2). Some, but not all, extreme years were European wide (e.g., 1956, 2003 or 2013). The year 2003 seems to be negative pointer year for Douglas-fir across Europe. Several authors report that year as being critical for tree growth in general, and for Douglas-fir specifically [3,13,14,17,28]. The year 1976 was also a very warm and dry year in many parts of Europe, but not in Slovenia. We could not detect this pointer year in any of the studied tree species.

Positive pointer years in the tree rings of Douglas-fir in Slovenia are all associated with a mild winter, especially in February, and with an average amount of precipitation throughout the growing season.

The response of trees in extreme years not only shows how trees respond in extreme years, but also how trees will possibly respond to a warmer and drier climate (as predicted by climate models) in the future [34]. Based on pointer-year analysis, we can conclude that the growth response of Douglas-fir in extreme years mainly depends on the winter temperature (February) and on a sufficient amount of precipitation in the peak summer months (July and August). Taking into account different climate change scenarios for Europe [35], we can anticipate that with increasing temperature and, in the best case, stable precipitation patterns, Douglas-fir will have difficulty maintaining high growth rates at increasing vapour-pressure deficits.

4. Materials and Methods

4.1. Sampling Locations

Douglas-fir samples were collected at three locations in Slovenia: Postojna 1 (PO-1-DF), Postojna 2 (PO-2-DF) and Celje (CE-DF)—see Figure 5. Research site Postojna 1 is located on a slope with an eastern exposure on pronounced Karst terrain. Research site Postojna 2 is located on Karst terrain on a ridge with shallow soil and northern exposure, and research site Celje is located on deep soil with a northern exposure. The reason for selecting research plots with such diverse stand conditions is to study the response of the same two tree species in different stand conditions.

We also collected Norway spruce samples for reference on three locations with similar ecological characteristics and as close as possible to the Douglas-fir sites: Ravnik (PO-1-NS), Verd (PO-2-NS) and Celje (CE-NS)—see Table 4 and Figure 5.

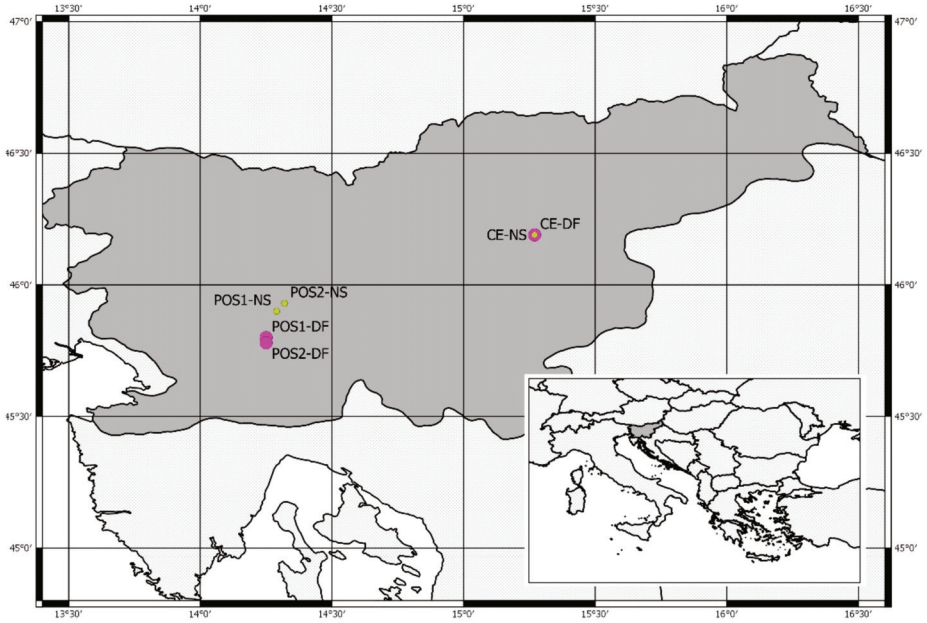

Figure 5. Sampling locations of Douglas-fir (DF) and Norway spruce (NS) in Slovenia (large map) and the location of Slovenia in the wider regional context (smaller map, bottom right).

Table 4. Site characteristics and sample replication for Douglas-fir and Norway spruce sample pool.

Douglas-fir			
	Postojna-1	*Postojna-2*	*Celje*
Local site name	Mačkovc	Golobičevec	Pečovnik
	PO-1-DF	PO-2-DF	CE-DF
Coordinates	N 42.57°, E 20.03°	N 42.63°, E 19.85°	N 46.19°, E 15.27°
Elevation	584–682 m	670–790 m	465–650 m
Slope	16°	18°	25°
Exposition	E	N	N
Soil type	Brown soil on limestone	Shallow brown soil on limestone	Deep brown soils on silicate
Number of cores for tree-ring analysis		40 cores (20 trees) each plot	
Norway spruce			
Local site name	Ravnik	Verd	Pečovnik
	PO-1-NS	PO-2-NS	CE-NS
Coordinates	N 45.90°, E 14.29°	N 45.93°, E 14.32°	N 46.19°, E 15.27°
Elevation	655–795 m	535–700 m	465–650 m
Slope	20°	25°	25°
Exposition	SW	SE	N
Soil type	Brown soil on limestone	Shallow brown soil on limestone	Deep brown soils on silicate
Number of cores for tree-ring analysis		40 cores (20 trees) each plot	

4.2. Sample Collection and Tree-Ring Width Analysis

For the tree-ring width (TRW) analysis, we sampled 20 trees per each location and tree species, which resulted in a total of 60 sampled trees for Douglas-fir and 60 sampled trees for Norway spruce. From each tree we took two 5-millimetre cores, for a total of 240 cores, 120 cores per tree species. All sampled trees were healthy, co-dominant trees with no visible signs of stem damage or any kind of declining tree vitality. Cores were stored in plastic holders and transported to the laboratory.

Once in the laboratory, the cores were dried and then glued onto wooden holders, and sanded with progressively finer sanding paper (up to 800 grit) on an industrial belt sander in order to achieve a highly polished surface and excellent visibility of tree rings. Polished cores were scanned using the ATRICS image capturing system [36]. Core images were then transferred to CooRecorder and CDendro programs (Cybis, Sweden) for measuring and cross-checking. Finally, absolute dating was done in the PAST-5 program (SCIEM, Austria).

Individual TRW series were standardized to remove long-term trends [37] using a 67% cubic smoothing spline with a 50% frequency cut-off in the *dplR* library [38,39] of the R program [40]. Departures of the measured values from the regression curve were calculated as the quotient between the measured tree-ring width and fitted value, resulting in a dimensionless index with a mean of 1. The purpose of this step is to remove factors that are not connected with climate, such as tree age and the effects of stand dynamics [37]. Index values were pre-whitened using an autoregressive model that was selected based on the minimum Akaike criterion, and were combined across all series using a biweight robust estimation of the mean in order to exclude the influence of outliers. The *dplR* produces two types of chronologies: standardized (STD) and residual (RES). In this research, we used the STD chronology, which is a robust estimate of the arithmetic mean and contains autocorrelation [37].

4.3. Meteorological Data

We used climate data from two sources: local and gridded climate data. The local data source was too brief for statistical evaluation of the climate–growth relationship; therefore, we used it only as a comparison for the gridded data to see whether the gridded data represent local climate conditions reasonably well.

As a local source of meteorological data, we used the data from two meteorological stations: Postojna (period 1961–2019, N 45° 47′, E 14° 15′, 743 m a.s.l.) and Celje (period 1977–2019, N 46° 12′, E 15° 16′, 688 m a.s.l.). Gridded meteorological data were obtained for two grid cells, one for sites Postojna 1 and 2 (PO-1, PO-2) and one for Celje (CE), from the Climate Research Unit of the University of East Anglia (Norwich, UK) TS 4.03 database (period 1901–2019, spatial resolution 0.5 × 0.5°) [41] (Figure 6).

Comparison of the two data sets showed that the station data indicated a slightly warmer and drier climate compared to the CRU TS 4.03 data set. Summer precipitation minima are larger in the station data set than in the gridded one. Despite some minor differences for the overlapping period, gridded data were used for the analysis presented in the Results section.

The climate of the studied region ranges from transitional sub-Mediterranean-continental to continental. Sites PO-1 and PO-2 have a transitional sub-Mediterranean-continental climate with 1727 mm precipitation per year and an average yearly temperature of 7.9 °C. In this type of climate, there is a high amount of precipitation in the period between September and December (702 mm), with the temperature in this period ranging between 0 °C and 10 °C; January and February are the coldest months, with temperatures below zero and a relatively large amount of snow. According to the long-term average, February is also the driest month (101 mm of precipitation), and January is the coldest month in the entire year (−1.6 °C). A potential lack of precipitation can occur in July and August, although the long-term average shows that this occurs infrequently. The average monthly temperature during the growing season is between 11.7 °C in May and 13.4 °C in September, with a peak in July (17.2 °C). The climate in the PO-1 and PO-2 regions has changed in the last 3 decades. The average monthly temperature has increased to 16.3 °C in June (+1.3 °C), 18.4 °C in July (+1.2 °C) and 18.1 °C in August (+1.4 °C). The precipitation regime has also changed. Late autumn and early winter peaks are more pronounced, with an increase of between 15 and 25 mm/month (Figure 6).

Site CE has a continental climate with 1298 mm of precipitation per year and an average yearly temperature of 8.7 °C. On average, 660 mm of precipitation is recorded during the growing season (May–September). The average yearly temperature of the

coldest month, January, is −1.4 °C, and the hottest month, July, is 18.2 °C. June is the wettest month, with 146 mm of precipitation. Drought may occur in July and August. The climate in the CE region has changed in the last three decades as well. The average monthly temperature in all months has increased and the monthly sum of precipitation has decreased. In general, the average yearly temperature is 1 °C higher and the yearly amount of precipitation is 58 mm lower than in previous decades (Figure 6).

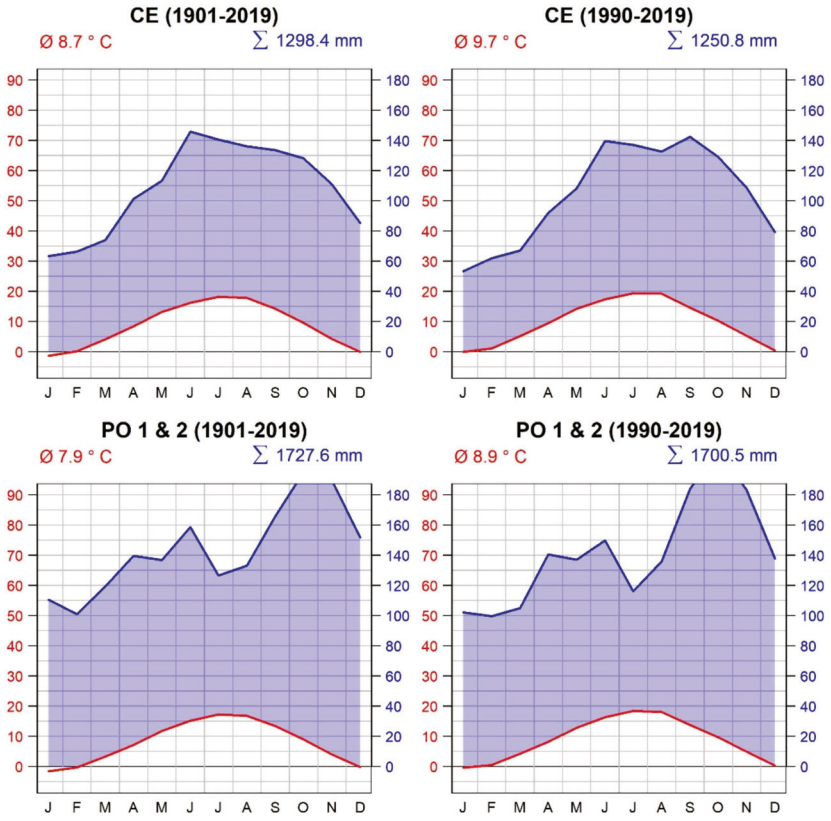

Figure 6. Climate diagrams for the sampling locations CE (**top**) and PO-1 and PO-2 (**bottom**). Sampling locations PO-1 and PO-2 are close to each other; therefore, the same climate data set is used. Climate diagrams are based on CRU TS 4.03 gridded climate data. The **left** panel (**top** and **bottom**) shows the entire period of available meteorological data (1901–2020), while the **right** panel (**top** and **bottom**) shows only the last 30 years (1990–2020) for all three sites.

4.4. Analysis of the Climate–Growth Relationship

After de-trending, TRW chronologies were compared to average monthly temperatures and to the monthly sum of precipitation using a bootstrapped correlation coefficient calculation in the *treeclim* library [42] of the R program [40]. Several combinations of monthly temperature and precipitation data were tested against the tree-ring widths of each studied tree species, in order to find the best possible combination of influential climate variables. A 25-year window with a one-year overlap for the calculation of the bootstrapped correlation between monthly temperature and precipitation and tree-ring widths of both studied species was used to assess the temporal stability of the climate–growth relationship.

Pointer year analysis was done for each tree species on all three locations. We used standard criteria for pointer year selection, as described in Schweingruber et al. [33]. A year was recognized as a pointer year when 80% of at least 13 trees per site and species responded with an increase or decrease in tree-ring width in comparison to the prior year.

In the analysis, we used monthly gridded temperature and precipitation data (0.5 × 0.5° grid) from the CRU TS database [41], available at the KNMI Climate Explorer

website [43,44]. Statistical analysis was done in R libraries *dplR* [38] and *treeclim* [42], and graphs were created using IgorPRO.

5. Conclusions

Based on our research and comparisons with other studies across Europe and North America, we can conclude that:

- Douglas-fir is more drought tolerant than Norway spruce, and as such is better adapted to increasing temperatures and more frequent occurrences of drought events in Slovenia. In part, this relates to its deeper root system than that of Norway spruce, and hence better accessibility to deeper lying water.
- The positive response of Douglas-fir to warmer and wetter winter months is beneficial, as winters are not as cold as they used to be. However, the combination of cold and dry winters and hot and dry summers have negative effects on Douglas-fir radial growth. These effects are similar to the effects of a hot and dry summer on Norway spruce radial growth. Both tree species respond in the same way with a significant decrease in radial increment.
- Douglas-fir is not very sensitive to lack of precipitation in the summer months, but temporal analysis of the correlation between tree- ring widths and summer precipitation at sites in Slovenia shows an increasing importance of summer precipitation (especially precipitation in June and July), suggesting that precipitation may become a growth-limiting factor for Douglas-fir in the future.
- The positive response in radial growth of Douglas-fir to warmer and wetter winter months is not limited to sites in Slovenia; its spatial outreach is much wider, extending throughout western and central Europe as well as in the northern parts of the Balkan and Apennine Peninsulas.
- From the climate–growth point of view, it seems that Douglas-fir can be a good substitute for Norway spruce in part of the current mixed forest stands in Slovenia; however, this is not only a climate–growth related issue. The successful introduction of Douglas-fir into Slovenian, close-to-nature managed forests is also a forest management and legislative problem. As a potentially invasive alien species, Douglas-fir is not allowed to be planted in Slovenian forests, and knowledge about Douglas-fir tending and management is still limited.
- Responses in extremely dry years (e.g., 2003) have shown that Douglas-fir can survive shorter dry periods on drought-prone sites, such as the High Karst in Slovenia (permeable limestone bedrock, shallow soil), but in the long term it is not advisable to plant Douglas-fir on drought-prone sites, especially considering current climate change.

Author Contributions: Conceptualization, T.L.; methodology, T.L.; formal analysis, T.L. and H.Š.; resources, T.L.; writing—original draft preparation, T.L. and H.Š.; visualization, T.L. and H.Š.; supervision, T.L. All authors have read and agreed to the published version of the manuscript.

Funding: This research was funded by the Slovenian Research Agency—research core funding No. P4-0107 Program research group "Forest Biology, Ecology and Technology", and research grants J4-8216 "Mortality of lowland oak forests—consequence of lowering underground water or climate change?", and V4-1614 "Adaptive management with spruce forests in Slovenia" (in part funded by the Slovene Ministry of Agriculture, Forestry and Food). Hana Štraus acknowledges the financial support of the Pahernik Foundation of the Department of Forestry and Renewable Forest Resources at the Biotechnical Faculty.

Data Availability Statement: Tree-ring width data for Douglas-fir and Norway spruce are available on the Mendeley Data repository under Levanic, Tom (2022), "Douglas-fir and Norway spruce tree-ring data from three sites in Slovenia", Mendeley Data, V1, https://doi.org/10.17632/32zydvmzjd.1 (accessed on 3 February 2022).

Acknowledgments: Permission to work in the community forests within the Municipality of Celje was granted to us by the Municipality of Celje (Valentina Glinšek). In the field, we were assisted by foresters from the Slovenia Forest Service, OE Celje Robert Hostnik and Robert Hedl. Permission to work in the forests of OE Postojna was granted to us by the company Slovenian State Forests (SIDG) (Tomi Ivanič) and Slovenia Forest Service (ZGS) (Frenk Prelc). We are also grateful to Robert Krajnc and Samo Stopar for their help in the field and in the laboratory.

Conflicts of Interest: The authors declare no conflict of interest.

Appendix A

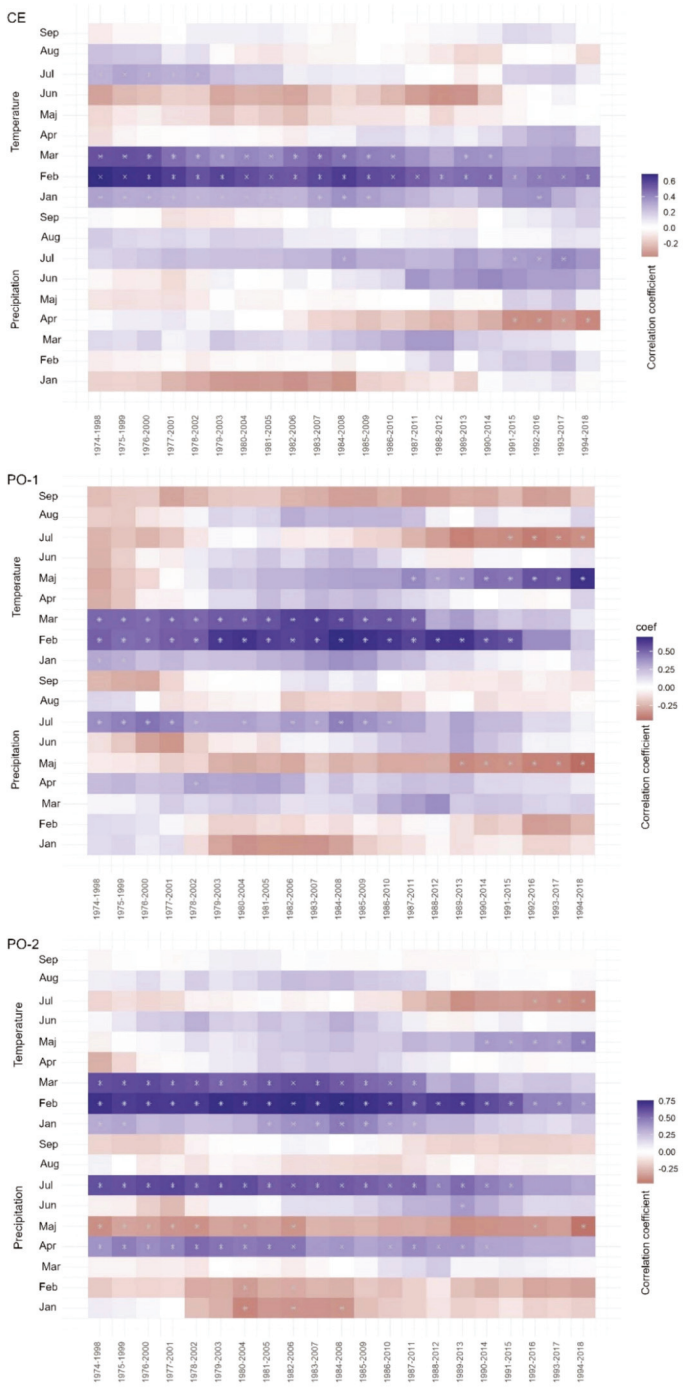

Figure A1. Moving correlations between Douglas-fir tree-ring width and average monthly temperature and monthly precipitation totals for the 1974–2018 period for all three sites. The width of the moving window is 25 years with an overlap of one year.

Appendix B

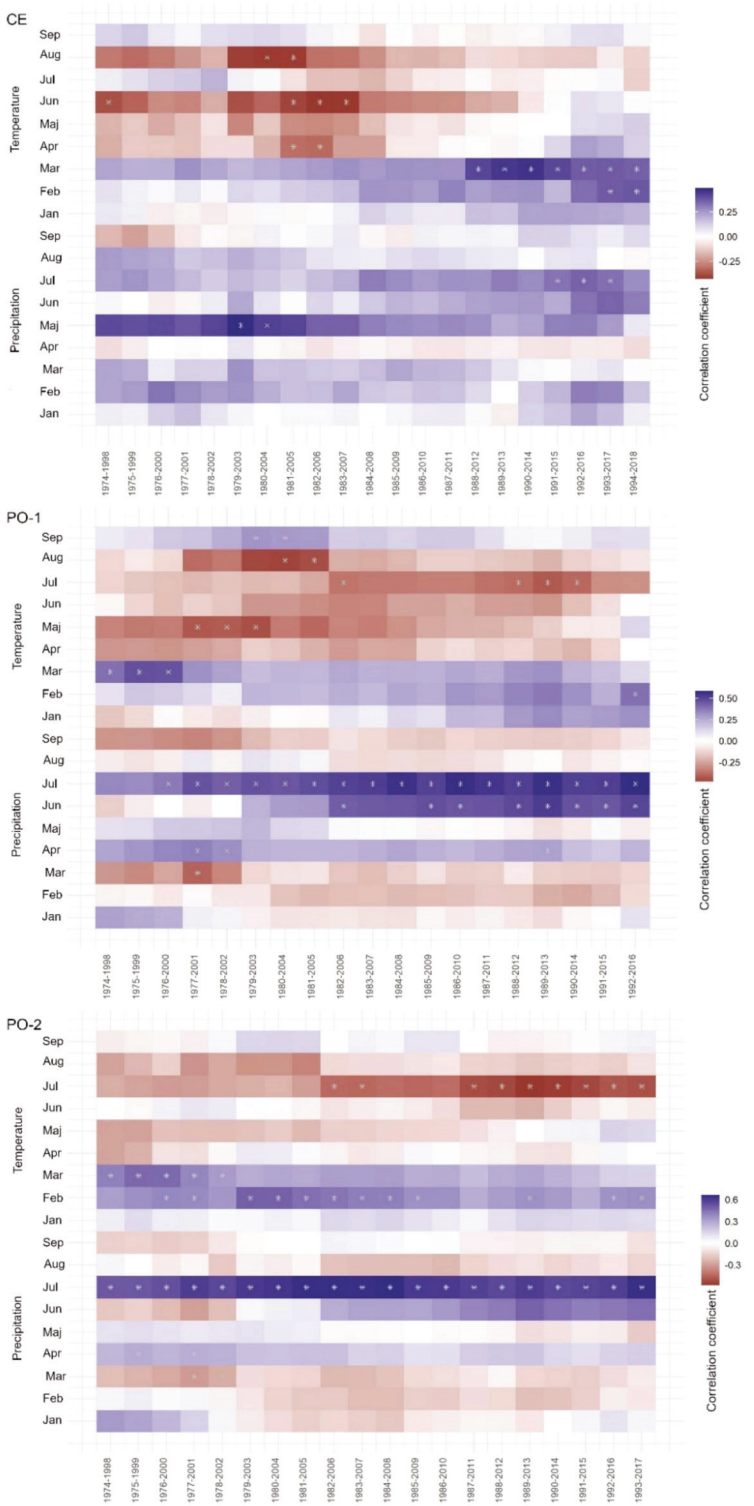

Figure A2. Moving correlations between Norway spruce tree-ring width and average monthly temperature and monthly precipitation totals for the 1974–2018 period for all three sites. The width of the moving window is 25 years with an overlap of one year.

References

1. Pachauri, R.K.; Meyer, L.A. (Eds.) *IPCC, 2014: Climate Change 2014: Synthesis Report. Contribution of Working Groups I, II and III to the Fifth Assessment Report of the Intergovernmental Panel on Climate Change*; IPCC: Geneva, Switzerland, 2014; p. 151.
2. Lindner, M.; Maroschek, M.; Netherer, S.; Kremer, A.; Barbati, A.; Garcia-Gonzalo, J.; Seidl, R.; Delzon, S.; Corona, P.; Kolström, M.; et al. Climate change impacts, adaptive capacity, and vulnerability of European forest ecosystems. *For. Ecol. Manag.* **2010**, *259*, 698–709. [CrossRef]
3. Eilmann, B.; Rigling, A. Tree-growth analyses to estimate tree species' drought tolerance. *Tree Physiol.* **2012**, *32*, 178–187. [CrossRef]
4. Levanič, T.; Kutnar, L.; Kobler, A.; Marinšek, A.; Čater, M.; Božič, G.; Westergren, M.; De Groot, M.; Jevšenak, J.; Stopar, S. *Obvladovanje Tveganj pri Gospodarjenju s Smreko v Gozdovih Slovenije: Zaključno Poročilo Projekta V4-1614*; Gozdarski Inštitut Slovenije: Ljubljana, Slovenia, 2019; p. 121.
5. Kutnar, L.; Kobler, A.; Bergant, K. Vpliv podnebnih sprememb na pričakovano prostorsko prerazporeditev tipov gozdne vegetacije. *Zb. Gozdarstva Lesar.* **2009**, *89*, 33–42.
6. Brus, R.; Kutnar, L. Drevesne vrste za obnovo gozdov po naravnih motnjah v Sloveniji. In Proceedings of the GOZD IN LES: Sistemski problemi obnove gozdov, Ljubljana, Slovenia, 24 November 2016.
7. Kutnar, L.; Pisek, R. Tujerodne in invazivne drevesne vrste v gozdovih Slovenije. *Gozdarski Vestn.* **2013**, *71*, 402–417.
8. Lavender, D.P.; Hermann, R.K. *Douglas-fir: The Genus Pseudotsuga*; Forest Research Publications Office, Oregon State University: Corvallis, OR, USA, 2014.
9. Wraber, M. Gozdna vegetacijska slika in gozdnogojitveni problemi Prekmurja. *Gozdarski Vestn.* **1951**, *23*, 1–52. (In Slovene language)
10. Brus, R. *Drevesne Vrste na Slovenskem (2. Izdaja)*; Samozaložba: Ljubljana, Slovenia, 2012; p. 406.
11. Lassoie, J.P.; Salo, D.J. Physiological response of large Douglas-fir to natural and induced soil water deficits. *Can. J. For. Res.* **1981**, *11*, 139–144. [CrossRef]
12. Nadezhdina, N.; Urban, J.; Čermák, J.; Nadezhdin, V.; Kantor, P. Comparative study of long-term water uptake of Norway spruce and Douglas-fir in Moravian upland. *J. Hydrol.* **2014**, *62*, 1–6. [CrossRef]
13. Eilmann, B.; de Vries, S.M.G.; den Ouden, J.; Mohren, G.M.J.; Sauren, P.; Sass-Klaassen, U. Origin matters! Difference in drought tolerance and productivity of coastal Douglas-fir (Pseudotsuga menziesii (Mirb.)) provenances. *For. Ecol. Manag.* **2013**, *302*, 133–143. [CrossRef]
14. Sergent, A.-S.; Rozenberg, P.; Bréda, N. Douglas-fir is vulnerable to exceptional and recurrent drought episodes and recovers less well on less fertile sites. *Ann. For. Sci.* **2014**, *71*, 697–708. [CrossRef]
15. Feliksik, E.; Wilczynski, S. Dendroclimatic regions of Douglas-fir (Pseudotsuga menziesii (Mirb.) Franco) in western and northern Poland. *Dendrobiology* **2004**, *52*, 9–15.
16. Castaldi, C.; Marchi, M.; Vacchiano, G.; Corona, P. Douglas-fir climate sensitivity at two contrasting sites along the southern limit of the European planting range. *J. For. Res.* **2020**, *31*, 2193–2204. [CrossRef]
17. Vejpustková, M.; Čihák, T. Climate Response of Douglas Fir Reveals Recently Increased Sensitivity to Drought Stress in Central Europe. *Forests* **2019**, *10*, 97. [CrossRef]
18. Schmid, M.; Pautasso, M.; Holdenrieder, O. Ecological consequences of Douglas-fir (Pseudotsuga menziesii) cultivation in Europe. *Eur. J. For. Res.* **2014**, *133*, 13–29. [CrossRef]
19. Wohlgemut, T.; Hafner, J.; Holterman, A.; Moser, B.; Nehring, S.; Rigling, A. Impact of Douglas-fir on forests and open land habitats. In *Douglas-fir—An Option for Europe*; Spiecker, H., Lindner, M., Schuler, J., Eds.; European Forest Institute: Joensu, Finland, 2019; Volume 9, pp. 57–62.
20. Da Ronch, F.; Caudullo, G.; de Rigo, D. Pseudotsuga menziesii in Europe: Distribution, habitat, usage and threats. In *European Atlas of Forest Tree Species*; San-Miguel-Ayanz, J., de Rigo, D., Caudullo, G., Houston Durrant, T., Mauri, A., Eds.; Publication Office of the European Union: Luxembourg, 2016; pp. 146–147.
21. Tschopp, T.; Holderegger, R.; Bollmann, K. Auswirkungen der Douglasie auf die Waldbiodiversität. *Schweiz. Z. Fur Forstwes.* **2015**, *166*, 9–15. [CrossRef]
22. Möller, K.; Heydeck, P. Risikopotenzial und akute Gefährdung der Douglasie—Biotische und abiotische Faktoren. In *Die Douglasie im Nordostdeutschen Tiefland—Chancen und Risiken im Klimawandel*; Engel, J., Ed.; Eberswalder Forstliche Schriftenreihe; Ministerium für Infrastruktur und Landwirtschaft des Landes Brandenburg: Eberswalde, Germany, 2009; Volume 43, pp. 49–58.
23. Levanič, T.; Čater, M. Povezave med klimatskimi dejavniki, osutostjo krošnje in debelinskim prirastkom pri dobu (*Quercus robur* L.) v vzhodni Sloveniji. In Proceedings of the Podnebne Spremembe—Vpliv na Gozd in Gozdarstvo, Ljubljana, Slovenija, 12–13 April 2007; pp. 429–443.
24. Levanič, T.; Čater, M.; McDowell, N.G. Associations between growth, wood anatomy, carbon isotope discrimination and mortality in a Quercus robur forest. *Tree Physiol.* **2011**, *31*, 298–308. [CrossRef]
25. Andrews, F.J. The weather circulation of February 1956 (Including a discussion of persistent blocking and severe weather in Europe). *Mon. Weather Rev.* **1956**, *84*, 66–74. [CrossRef]
26. Dizerens, C.; Lenggenhager, S.; Schwander, M.; Buck, A.; Foffa, S. The 1956 Cold Wave in Western Europe. In *Historical Weather Extremes in Reanalyses*; Brönnimann, S., Ed.; Geographica Bernensia G92; Institute of Geography at the University of Bern: Bern, Switzerland, 2017; pp. 101–111.

27. Kohler, M.; Sohn, J.; Nägele, G.; Bauhus, J. Can drought tolerance of Norway spruce (Picea abies (L.) Karst.) be increased through thinning? *Eur. J. For. Res.* **2010**, *129*, 1109–1118. [CrossRef]
28. Vitali, V.; Büntgen, U.; Bauhus, J. Silver fir and Douglas-fir are more tolerant to extreme droughts than Norway spruce in south-western Germany. *Glob. Change Biol.* **2017**, *23*, 5108–5119. [CrossRef]
29. Griesbauer, H.P.; Scott Green, D. Assessing the climatic sensitivity of Douglas-fir at its northern range margins in British Columbia, Canada. *Trees* **2010**, *24*, 375–389. [CrossRef]
30. Griesbauer, H.P.G.P.; Green, D.S.S. Regional and ecological patterns in interior Douglas-fir climate–growth relationships in British Columbia, Canada. *Can. J. For. Res.* **2010**, *40*, 308–321. [CrossRef]
31. Restaino, C.M.; Peterson, D.L.; Littell, J. Increased water deficit decreases Douglas-fir growth throughout western US forests. *Proc. Natl. Acad. Sci. USA* **2016**, *113*, 9557–9562. [CrossRef]
32. Hintsteiner, W.J.; van Loo, M.; Neophytou, C.; Schueler, S.; Hasenauer, H. The geographic origin of old Douglas-fir stands growing in Central Europe. *Eur. J. For. Res.* **2018**, *137*, 447–461. [CrossRef]
33. Schweingruber, F.H.; Eckstein, D.; Serre Bachet, F.; Braker, O.U. Identification, presentation and interpretation of event years and pointer years in dendrochronology. *Dendrochronologia* **1990**, *8*, 9–38.
34. Temperature and Precipitation Climate Impact Indicators from 1970 to 2100 Derived from European Climate Projections. 2021. Available online: https://cds.climate.copernicus.eu/cdsapp#!/dataset/sis-hydrology-meteorology-derived-projections?tab=overview (accessed on 10 March 2021). [CrossRef]
35. IPPC. IPCC 2021: Summary for Policymakers. In *Climate Change 2021: The Physical Science Basis. Contribution of Working Group I to the Sixth Assessment Report of the Intergovernmental Panel on Climate Change*; Cambridge University Press: Cambridge, UK; New York, NY, USA, 2021; pp. 3–32.
36. Levanič, T. ATRICS—A new system for image acquisition in dendrochronology. *Tree-Ring Res.* **2007**, *63*, 117–122. [CrossRef]
37. Cook, E.R. Time Series Analysis Approach to Tree Ring Standardization. Ph.D. Thesis, University of Arizona, Tucson, AZ, USA, 1985.
38. Bunn, A.G. A dendrochronology program library in R (dplR). *Dendrochronologia* **2008**, *26*, 115–124. [CrossRef]
39. Bunn, A.G. Statistical and visual crossdating in R using the dplR library. *Dendrochronologia* **2010**, *28*, 251–258. [CrossRef]
40. R-Core-Team. *R: A Language and Environment for Statistical Computing*; R Foundation for Statistical Computing: Vienna, Austria, 2019.
41. Harris, I.; Osborn, T.J.; Jones, P.; Lister, D. Version 4 of the CRU TS monthly high-resolution gridded multivariate climate dataset. *Sci Data* **2020**, *7*, 109. [CrossRef]
42. Zang, C.; Biondi, F. treeclim: An R package for the numerical calibration of proxy-climate relationships. *Ecography* **2015**, *38*, 431–436. [CrossRef]
43. Trouet, V.; Van Oldenborgh, G.J. KNMI Climate Explorer: A web-based research tool for high-resolution paleoclimatology. *Tree-Ring Res.* **2013**, *69*, 3–14. [CrossRef]
44. Van Oldenborgh, G.J. *KNMI Climate Explorer*; Koninklijk Netherlands Meteorologisch Institut (KNMI): De Bilt, The Netherlands, 1999.

plants

MDPI

Article

Species-Level Differences in Osmoprotectants and Antioxidants Contribute to Stress Tolerance of *Quercus robur* L., and *Q. cerris* L. Seedlings under Water Deficit and High Temperatures

Marko Kebert [1], Vanja Vuksanović [2], Jacqueline Stefels [3], Mirjana Bojović [4], Rita Horák [5], Saša Kostić [1], Branislav Kovačević [1], Saša Orlović [1], Luisa Neri [6], Massimiliano Magli [6] and Francesca Rapparini [6,*]

1 Institute of Lowland Forestry and Environment, University of Novi Sad, Antona Čehova 13d, 21000 Novi Sad, Serbia; kebertm@uns.ac.rs (M.K.); sasa.kostic@uns.ac.rs (S.K.); branek@uns.ac.rs (B.K.); sasao@uns.ac.rs (S.O.)
2 Faculty of Agriculture, University of Novi Sad, Trg Dositeja Obradovića 8, 21000 Novi Sad, Serbia; vanja.vuksanovic@polj.uns.ac.rs
3 Groningen Institute for Evolutionary Life Sciences, University of Groningen, P.O. Box 11103, 9700 CC Groningen, The Netherlands; j.stefels@rug.nl
4 Faculty of Ecological Agriculture, Educons University, Vojvode Putnika 87, 21208 Sremska Kamenica, Serbia; mirjana.bojovic@educons.edu.rs
5 Teacher Training Faculty in the Hungarian Language, University of Novi Sad, Subotica, Štrosmajerova 11, 24000 Subotica, Serbia; rita.horak@magister.uns.ac.rs
6 Institute of BioEconomy (IBE), Department of Bio-Agrifood Science (DiSBA), National Research Council (CNR), Via P. Gobetti 101, I-40129 Bologna, Italy; luisa.neri@ibe.cnr.it (L.N.); massimiliano.magli@ibe.cnr.it (M.M.)
* Correspondence: francesca.rapparini@ibe.cnr.it

Citation: Kebert, M.; Vuksanović, V.; Stefels, J.; Bojović, M.; Horák, R.; Kostić, S.; Kovačević, B.; Orlović, S.; Neri, L.; Magli, M.; et al. Species-Level Differences in Osmoprotectants and Antioxidants Contribute to Stress Tolerance of *Quercus robur* L., and *Q. cerris* L. Seedlings under Water Deficit and High Temperatures. *Plants* **2022**, *11*, 1744. https://doi.org/10.3390/plants11131744

Academic Editor: Nenad Potočić

Received: 30 May 2022
Accepted: 27 June 2022
Published: 30 June 2022

Abstract: The general aim of this work was to compare the leaf-level responses of different protective components to water deficit and high temperatures in *Quercus cerris* L. and *Quercus robur* L. Several biochemical components of the osmotic adjustment and antioxidant system were investigated together with changes in hormones. *Q. cerris* and *Q. robur* seedlings responded to water deficit and high temperatures by: (1) activating a different pattern of osmoregulation and antioxidant mechanisms depending on the species and on the nature of the stress; (2) upregulating the synthesis of a newly-explored osmoprotectant, dimethylsulphoniopropionate (DMSP); (3) trading-off between metabolites; and (4) modulating hormone levels. Under water deficit, *Q. cerris* had a higher antioxidant capacity compared to *Q. robur*, which showed a lower investment in the antioxidant system. In both species, exposure to high temperatures induced a strong osmoregulation capacity that appeared largely conferred by DMSP in *Q. cerris* and by glycine betaine in *Q. robur*. Collectively, the more stress-responsive compounds in each species were those present at a significant basal level in non-stress conditions. Our results were discussed in terms of pre-adaptation and stress-induced metabolic patterns as related to species-specific stress tolerance features.

Keywords: Fagaceae; osmolytes; antioxidant; phytohormones; trade-off mechanisms; stress marker; oxidative stress

1. Introduction

Increasing air temperature and frequent summer drought events [1] will affect not only the health status, vitality, morphological, and physiological traits of different woody species but also their biochemical traits and even xeric distributional limits [2].

The prime response of plants to environmental constraints such as drought, high light, salinity, heavy metals or extreme temperatures is a reduction in net CO_2 assimilation due to stomatal, mesophyll, and biochemical limitations [3–6]. This in turn results in an excess of light energy absorbed by chloroplasts relative to the capacity for photosynthesis and a consequent increase in the formation of reactive oxygen species (ROS, e.g., singlet oxygen, superoxide anion, hydrogen peroxide, and hydroxyl radicals [7–9].

Low amounts of ROS may have an important role in stress-signaling pathways, while high amounts of ROS detrimentally affect all biomolecules including lipids, proteins, DNA, and RNA, leading to oxidative stress and even to a programmed cell death [10].

Oxidative stress occurs when the production of excess ROS is not counterbalanced by the antioxidant defense system, so that unquenched ROS remains sustained to cause further reactions and oxidize biomolecules [10].

To counteract oxidative stress, plants activate a complex antioxidant network of enzymes (e.g., superoxide dismutases, ascorbate peroxidases, and catalases) and non-enzymatic compounds (e.g., ascorbate, glutathione, flavonoids, carotenoids, and phenolics) to defend plant cells [7,11] by controlling the production/scavenging of ROS. In addition, antioxidants can not only directly quench ROS activity, but they can also play an indirect role such as hormone-mediated signaling, upregulating primary defense genes, and activating secondary defense genes [12].

One central non-enzymatic component of the antioxidant system of plants is glutathione (GSH: γ-glutamyl-cysteinyl-glycine), the most abundant low molecular weight thiol which enhances plant tolerance to different abiotic stresses [13–15] acting either as a chemical antioxidant, a substrate of antioxidative enzymes, or as a substance for biotransformation of xenobiotics through the conjugation process [16]. The enhancement of responses of glutathione levels, glutathione turnover, and redox state in woody species under stress conditions results in an increased antioxidative capacity depending on plant species [13,17]. Among other potential stress markers in plants, flavonoids seem to be very efficient in drought and heat alleviation since many of them exhibit antioxidant properties against ROS [15,18]. Another important group of phenolic compounds are the condensed tannins (CT), particularly abundant in different organs of woody plants [19]. Quantity, composition, localization, and extent of polymerization of tannins are highly climate dependent [20]; however, there is still a lack of specific investigations on the impact of high temperatures and drought on their accumulation in oak species under controlled conditions.

When water is limited or temperatures are elevated, plants increase the production of osmotically active substances that have been associated with drought- and thermotolerance [15,21]. The enhanced accumulation of proline is regarded as protective response of plant metabolism against these stresses in many species [5,22]. Although glycine betaine (GB) is the most studied quaternary ammonium compound with defensive functions [23], however, there is insufficient knowledge about its production in woody tree species. Unlike the abovementioned N-containing osmolytes, little consideration has been given to the protective role of the tertiary sulphonium compound dimethylsulphoniopropionate (DMSP) in plant tolerance to abiotic stress [24], especially in woody species. The role of DMSP in plants was related to osmotic control and adjustments [25,26] and to antioxidant properties [27]. Although DMSP has recently been detected and quantified in leaves of 15 woody plant species, including *Quercus* (Kebert et al., unpublished data), its response to drought and heat stress in woody species was never examined.

To achieve a more complete understanding of the defense response to water deficit and high temperatures in the studied oak species, it is crucial to examine changes in the key phytohormones indole-3-acetic acid (IAA) and abscisic acid (ABA). They, indeed, play a pivotal role as developmental regulators under optimal growth conditions and in photoprotection of the photosynthetic apparatus under various stress conditions [28].

Under water limiting conditions, ABA is an important molecule in conveying the signals about water deficit from the soil to the roots and, in turn, from root to shoot, as it was proven that there is a special correlation between increased xylem sap ABA amounts and reduced stomatal conductance during water deficit [6,28].

The interaction between phytohormones and the components of the plant protection systems have been shown when plants are exposed to water deficit (i.e., ABA and xanthophyll cycle) [28]. Stress responsiveness of these hormones varies greatly depending on species/genotype [29,30], and their metabolic adjustments could reveal different species sensitivity and tolerance to stress conditions as previously shown in oaks, including *Q.*

cerris [31]. In addition, potential cross-talk among phytohormones and proline has been suggested to occur in oaks [31].

Variation in the stress response of protective compounds is associated with differences in physiological plant performance and survival; however, the identification of species-specific metabolic sensitivities may provide early biochemical markers such as osmotic adjustments or antioxidant protection indicators that are informative for woody species tolerance to stress [32,33]. *Quercus* genus (*Fagaceae* family) includes more than 400 deciduous, evergreen, and shrub species [34]. Their responses to water deficit and heat stress are highly variable [35], and their interspecific variation in capacity to cope with these climate changes has not been elucidated [36]. Among the economically and ecologically most important deciduous oak tree species in Europe, the Turkey oak *Q. cerris* and the pedunculate oak *Q. robur* show similar ecological growing conditions but different leaf functional traits of protective systems (i.e., antioxidative and ormoregulative; Table 1). *Q. cerris* belongs to the group of the so-called 'nemoro-Mediterranean oaks' which occupy a xeric habitat [37]. The distributional range of this oak species extends from southern Europe to Asia Minor [38,39], and it is particularly present in the Balkan and Italian Peninsulas [36]. *Q. robur* is more widely distributed in Europe under a temperate-nemoral climate [39] (www.euforgen.org (accessed on 29 May 2022)). *Q. cerris* is known to be more drought tolerant than *Q. robur*, and recent studies evidence that both species are climate-sensitive as shown by the radial growth and stable carbon isotope records [40]. In particular, as predicted by climate scenarios, pedunculate oak is the most endangered *Quercus* species in the Balkan region, more than other *Quercus* species, including Turkey oak [41].

Although *Q. cerris* and *Q. robur* have developed effective protective mechanisms at both physiological and biochemical levels to counteract drought and heat stress [36], species-specific strategies involving antioxidant and osmoregulation systems have not yet been well elucidated, especially at the seedling stage and under high temperature stress (Table 1). In particular, the non-enzymatic antioxidants of *Q. robur* young plants were poorly investigated under both limiting soil water [42–46] and air warming conditions [44,45], generally only through the measurements of the ascorbate/glutathione system. Similarly, the osmotic adjustment of this oak species in response to both stresses has not been studied in depth [44,45]. The protective response of young plants of *Q. Cerris* has been investigated only under drought conditions and by examining only the accumulation of carotenoids among the non-enzymatic antioxidants and of proline among the compatible solutes [46].

When investigating the osmotic adjustment and production of antioxidants, however, the stress response of the protective components might vary from species to species or depend on the nature of the stress [32,33]. Generally, tolerant species are characterized by higher levels of protective metabolites, such as antioxidants and compatible solutes, under non-stress conditions and/or accumulate them in large amounts when stress occurs [47]. Therefore, the characterization of constitutive levels of protective compounds under optimal growth conditions may provide key information to assess the functional changes of these metabolites under stress conditions. In addition, the magnitude of stress-induced variations can reveal differences among genotypes, as species-dependent responses of protective compounds generally do not rely on the accumulation of a specific compound [47].

Table 1. Responses to different biochemical components of the plant defense system to single drought or high temperature stress in young trees of *Q. robur* and *Q. cerris*.

Plant Species	Plant Age	Growth Conditions	Stress Design	Response to Drought	Response to High Temperature	Literature
Q. robur	10 weeks	Potted plants under controlled conditions	Drought: withholding water for about 21 days	↓ Redox ratio of ascorbate and glutathione ↑ MDA ↓ Carotenoids		Schwanz and Polle, 2001
Q. robur	5 years	Potted plants in greenhouse	Drought: withholding water to reach soil moisture level of 13%	↑ Carbohydrates (hexoses) and polyols ↑ Proline and Proline derivatives ‖ Glycine betaine		Spieß et al., 2012
Q. robur	3–5 years	Potted plants under controlled conditions	Drying-rewetting cycles (reduced irrigation for about 20 and 30 days) High temperature (+1/2 °C compared to controlled conditions)	↑ Proline, GABA ↑ Glutathione ‖ Total and Reduced Ascorbate ‖ Cysteine and γ-glutamyl cysteine	‖ Proline, GABA ‖ Glutathione ‖ Total and Reduced Ascorbate ‖ Cysteine and γ-glutamyl cysteine	Hu et al., 2013
Q. robur	3–5 years	Potted plants under controlled conditions	Drying-rewetting cycles (reduced irrigation for about 20 and 30 days) High temperature (+1/2 °C compared to controlled conditions)	↑ Total and specific amino acids-N and Glutamine	‖ Total and specific amino acids-N	Hu et al., 2015
Q. cerris	3 years	Potted plants in greenhouse under controlled conditions	Drought (daily irrigation with 30% effective evapotranspiration for 2 weeks)	↑ Proline, MDA ↑ Chlorophylls ‖ Carotenoids (xantophylls)		Cotrozzi et al., 2015
Q. cerris	3 years	Potted plants in greenhouse under controlled conditions	Drought (daily irrigation with 20% effective evapotranspiration for 2 weeks)	↑ Proline, MDA ↑ Carotenoids, chlorophylls, β-carotene, α-tocopherol, ABA ‖ Carbohydrates (hexoses)		Cotrozzi et al., 2016

↑: increased; ↓: decreased; ‖: unchanged.

Differences in stress responsiveness of various defense metabolic traits may also be driven by the functional relationship (i.e., overlapping and complementary roles) between the individual metabolites contributing to the antioxidative and/or osmoprotective capacity of the plants [48,49]. Likewise, competition for mutual precursors between the synthesis of different compounds (i.e., proline vs. GSH or carotenoids vs. isoprenoids) may affect the endogenous levels of protective metabolites under stress conditions [17,50]. Therefore, the increase in investment in some components of the protection system can come at a cost to investments in the biosynthesis of other biochemical components if limiting resources are occurring, as during unfavorable conditions [51].

Therefore, the general aim of this work was to characterize the leaf-level capacity of antioxidant production and/or osmotic adjustments of *Q. cerris* and *Q. robur* in response to soil water deficit and increasing air temperatures through the measurements of a suite of different physiochemical parameters, including a newly-explored protective compound with a multifunctional role (i.e., DMSP). The examined seedlings from both species are expected to employ protective mechanisms to counteract oxidative stress under the applied stress conditions as the photosynthetic gas exchanges were reduced in response to the applied drought and heat stress on the same plants used for the present experiment [46,52,53]. The more specific objectives were to compare the constitutive and stress-induced changes in antioxidants, osmoprotectants, and phytohormones of the two oak species and to identify common and specific responses to drought and high temperatures.

The following hypotheses were tested:

1. The drought and heat stresses result in specific changes in the production of both individual and/or pattern of osmoprotectants and antioxidants.
2. Species-specific constitutive levels of antioxidants, osmoprotectants, and hormones predispose the studied oak species differently to unfavorable environmental conditions.
3. The magnitude of the examined biochemical responses to both stresses depends on the species-specific features and on the nature of stress.
4. Functional and metabolic relationships among the various metabolites contribute to the physiological performance and stress tolerance capacity of the investigated oak species.

By focusing on the plant capacity of osmotic adjustment and antioxidant production, our information on specific metabolic sensitivities of the investigated oak species to the applied abiotic stresses may provide early biochemical markers that are informative of woody species tolerance to stress [7,32]. Indeed, in forest management, both at the nursery and the field level, there is a need to identify measurable traits that predict susceptibility/resilience of species towards the ongoing climate change in light of the new concept of climate-smart-forestry-based monitoring systems [54].

2. Results

2.1. Effect of Drought and Heat Stress on Osmolyte and DMSP Accumulation

Proline (PRO) content was significantly affected by species and treatment (Table S1; Two-way ANOVA Species, Treatment $p < 0.001$), with the treatment effect explaining about 75% of variation (based on sum of square values). Indeed, differences between species were observed only when plants were well-watered and under ambient temperatures (Controls-C; Figure 1A).

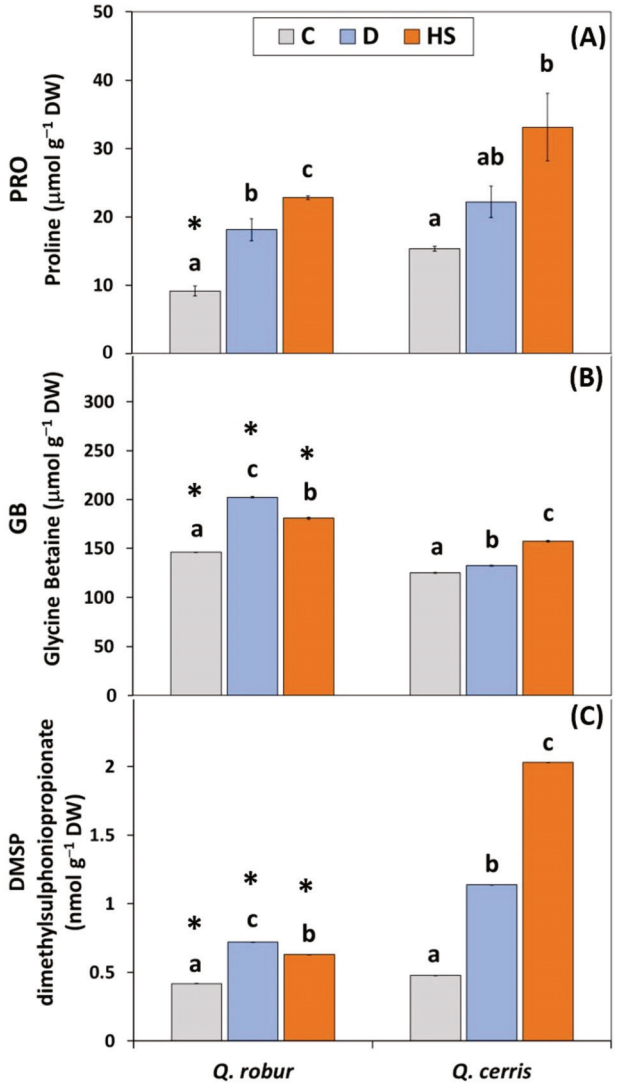

Figure 1. Changes in: (**A**) proline (PRO; µmol g^{-1} DW); (**B**) glycine betaine (GB; µmol g^{-1} DW); and (**C**) dimethylsulphoniopropionate (DMSP; nmol g^{-1} DW) content in leaves of *Quercus robur* and *Q. cerris*. Treatments: C: control plants under well-watered soil conditions to maintain SWC (Soil Water Content) in the range of 32–38% and daily air temperature of 25–28 °C; D: drought-stressed plants by withholding soil water for 12 days until the SWC reached values of ca. 9–11%; HS: heat-stressed plants after 6-days exposure to daily temperatures ranging between 33–47 °C. Different lowercase letters indicate significant differences among treatments within each species, while asterisks indicate significant differences between the two oak species within each treatment after one-way ANOVA with Tukey's honestly significant difference (HSD) post hoc test ($p \leq 0.05$). Data represent the mean ± standard deviation.

When oak seedlings experienced both stress conditions (water deficit-D, high temperatures-HS), a significant increase in PRO level occurred relative to control values, independent of species. In both *Quercus* species, the response of PRO to elevated temperatures was higher compared with that measured under water deficit, a pattern especially evident in *Q. cerris* (ca. 2.2-fold relative to control values in HS vs. 1.4-fold in D).

Although glycine betaine (GB) content in leaves was significantly affected by species and treatment (Table S2; Two-way ANOVA Species, Treatment $p < 0.001$), in contrast to proline, the effect of species was the largest (based on *F* and Sum of square values). Both constitutive and stress-induced leaf levels of GB were significantly higher in *Q. robur* than in *Q. cerris* (Figure 1B). The interaction between the main effects was highly significant (Two-

way ANOVA Species*Treatment $p < 0.001$). Indeed, the GB content increased in response to water scarcity, but the extent of the increase was species-specific: *Q. robur* showed a stronger response to water deficit (ca. 38% relative to control) in GB levels compared to *Q. cerris* (ca. 6% relative to control). Elevated temperatures induced a significant and similar increase in GB levels in both oak species (about 24% relative to control).

Similar to GB, dimethylsulphoniopropionate (DMSP) content in leaves was significantly affected by species and treatment (Table S2; Two-way ANOVA Species, Treatment $p < 0.001$), and the effect of species was the largest (based on *F* and Sum of square values). Differences between species in leaf DMSP content were significantly evident both under control conditions and when seedlings experienced stress conditions, with leaf levels of *Q. cerris* significantly higher than those of *Q. robur* (Figure 1C). Examined oaks species showed increasing patterns of DMSP changes after exposure to both stresses, but the extent of the response depended on the species (Two-way ANOVA Species*Treatment $p < 0.001$). In *Q. cerris*, DMSP content markedly increased in response to water deficit and, especially, to high temperatures (about 2.4 and 4.2-fold relative to control values in D and HS, respectively). Differently, in *Q. robur*, the increase to both stress conditions compared to the control levels were significant but less dramatic (ca. < 1.7-fold relative to control values under both D and HS).

2.2. Effects of Water Deficit and High Temperatures on the Antioxidant Defense System

Leaf lipid peroxidation, measured as amount of malondialdehyde (MDA), was significantly and largely affected by treatment (Figure 2A; Table S2; Two-way ANOVA Treatment $p < 0.001$) according to *F* values. The MDA content increased in response to water scarcity and high air temperatures, but within each species the extent of the increase was dependent on the nature of the stress. In *Q. robur*, the MDA levels were higher under elevated temperatures than under water deficit, while in *Q. cerris* they were similar.

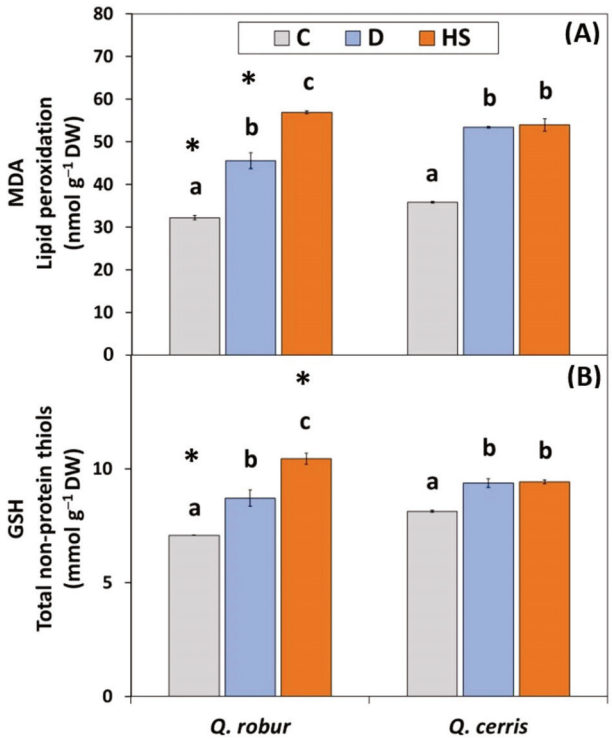

Figure 2. (**A**) Lipid peroxidation measured as levels of malondialdehyde (MDA; nmol g^{-1} DW) and (**B**) total non-thiol compounds measured as reduced glutathione (GSH; nmol g^{-1} DW) in leaves of *Q. robur* and *Q. cerris*. Abbreviations of the treatments, mean separation, and statistical treatments are as shown in Figure 1. Data represent the mean ± standard deviation.

Similar to MDA, the treatment factor mainly affected the levels of total non-protein thiols measured as reduced glutathione (GSH; Table S2; Two-way ANOVA Treatment $p < 0.001$) that increased in response to water deficit and high temperatures (Figure 2B). The response to the applied treatments was dependent on species (Table S2; Two-way ANOVA Species*Treatment $p < 0.001$). In particular, the response of GSH to high temperatures was two-fold higher in *Q. robur* compared to *Q. cerris* (47% vs. 16% relative to controls, respectively). Similar to MDA, after exposure to stresses, the GSH levels in the most responsive species (i.e., *Q. robur*) were higher under elevated temperature than under water deficit conditions.

Overall, the antioxidant capacity was significantly affected by treatment, and the interaction between treatment and species was significant (Table S2; Two-way ANOVA Treatment $p < 0.001$ for ABTS, DPPH, FRAP, Species*Treatment $p < 0.01$ for ABTS, $p < 0.001$ for DPPH and FRAP). The increasing effect of water deficit on the measured parameters was significantly pronounced in *Q. cerris* (Figure 3; about 52% and 25% relative to controls for DPPH and FRAP), while in *Q. robur* this stress treatment either marginally affected or did not affect most of these parameters. Similar to water deficit response, the antioxidant capacity was responsive to high temperatures in *Q. cerris*, while it was not affected in *Q. robur*.

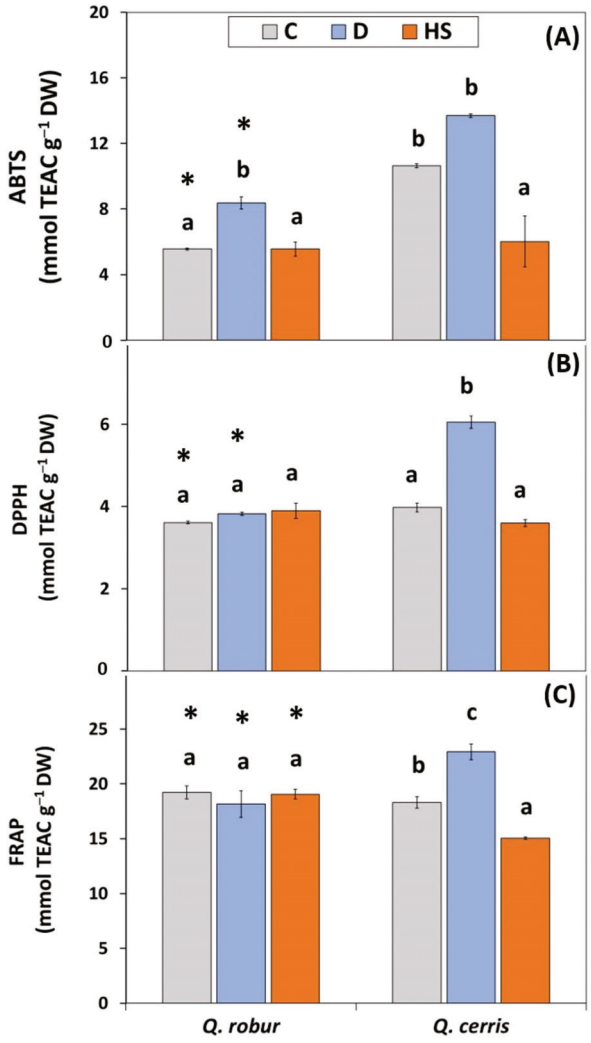

Figure 3. Total antioxidant capacity (mmol TEAC g^{-1} DW) measured by: (**A**) ABTS; (**B**) DPPH; and (**C**) FRAP assay in leaves of *Q. robur* and *Q. cerris*. Abbreviations of the treatments, mean separation, and statistical treatments are as shown in Figure 1. Data represent the mean ± standard deviation.

The total phenolic content (TPC) was significantly affected by species and treatment (Table S2; Two-way ANOVA Treatment $p < 0.001$, species $p < 0.01$) as well by their interaction (Species*Treatment $p < 0.001$). Similar to the overall antioxidant capacity, only in *Q. cerris* was this component of the antioxidant defense system significantly responsive to water deficit and high temperatures, both conditions inducing an increase or a decrease compared to control plants, respectively (Figure 4A).

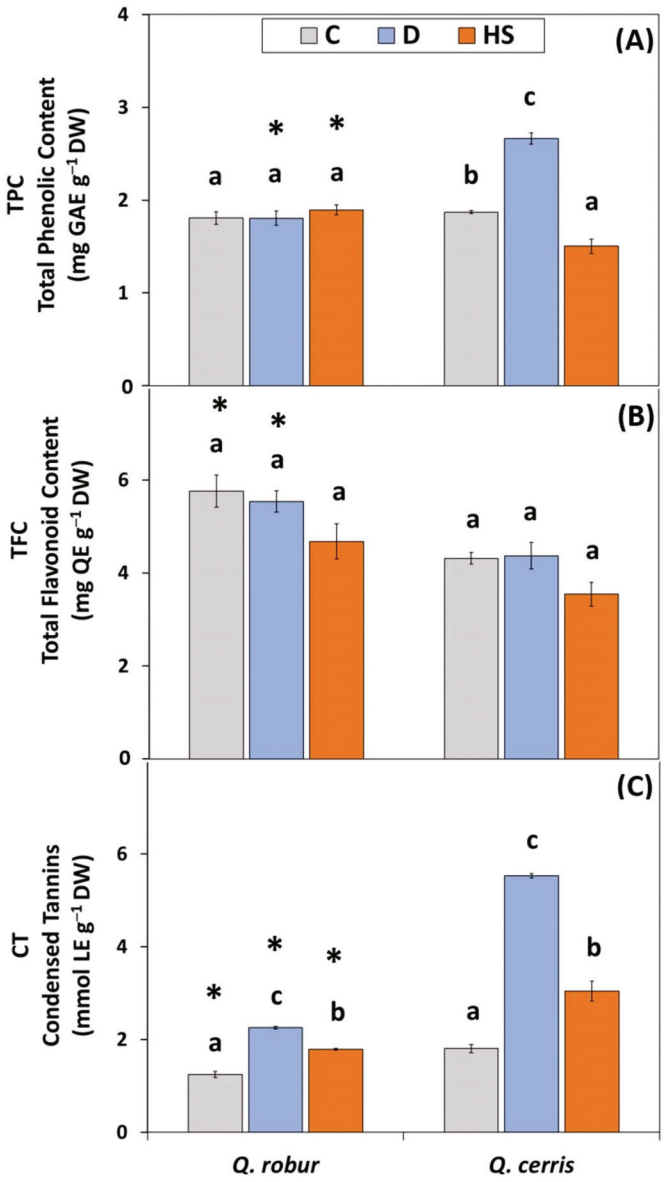

Figure 4. (**A**) Total phenolic content (TPC; mg GAE g^{-1} DW); (**B**) total flavonoid content (TFC; mg QE g^{-1} DW); and (**C**) condensed tannins (CT; mg LE g^{-1} DW) in leaves of *Q. robur* and *Q. cerris*. Abbreviations of the treatments, mean separation, and statistical treatments are as shown in Figure 1. Data represent the mean ± standard deviation.

The main effect of species on total flavonoid content (TFC; Table S2; Two-way ANOVA Species $p < 0.001$) was shown by *Q. robur* having a significantly higher constitutive content of these compounds than *Q. cerris* (Figure 4B). This species-specific difference was maintained under stress conditions. Indeed, in each species, TFC was not significantly altered by water scarcity or elevated temperatures, confirming the lower relevance of the treatment effect based on the *F* values of two-way ANOVA analysis.

The basal level of condensed tannins (CT) under control conditions was higher in *Q. cerris* than in *Q. robur* (Figure 4C). In both oak species, CT increased in response to water scarcity and high temperatures, but the extent of the increase depended on the species and the nature of the stress (Table S2; Two-way ANOVA Species*Treatment $p < 0.001$). The increasing effect of water deficit on CT was significantly more pronounced in *Q. cerris* (3-fold relative to control) than in *Q. robur* (1.8-fold). After exposure to high temperatures, in *Q. cerris* there was again a more significant increase of CT than in *Q. robur*. In both oak species, water deficit-related changes were significantly stronger than those induced by high temperatures relative to controls.

2.3. Leaf Nitrogen and Sulfur Status in Response to Water Deficit and High Temperatures

Overall, the leaf nitrogen (N) and sulfur (S) content was affected by both stress conditions, but the effect depended on the species (Table S2; Two-way ANOVA Species*Treatment $p < 0.001$ for N and $p < 0.01$ and S). In *Q. robur*, soil water deficit and elevated air temperatures induced a decrease of N and S content, while in *Q. cerris*, both stress conditions either slightly affected or did not affect the leaf content of N and S, respectively (Table S2).

2.4. Changes in Leaf IAA and ABA Levels Induced by Soil Drying Conditions and High Temperatures

Under control conditions, both oak species were characterized by comparable leaf levels of indole-3-acetic acid (IAA; Figure 5A; ca. 382 ng g^{-1} DW). Water deficit induced a significant accumulation of IAA in *Q. cerris*, but not in *Q. robur*. Elevated temperatures did not affect IAA concentrations in both species.

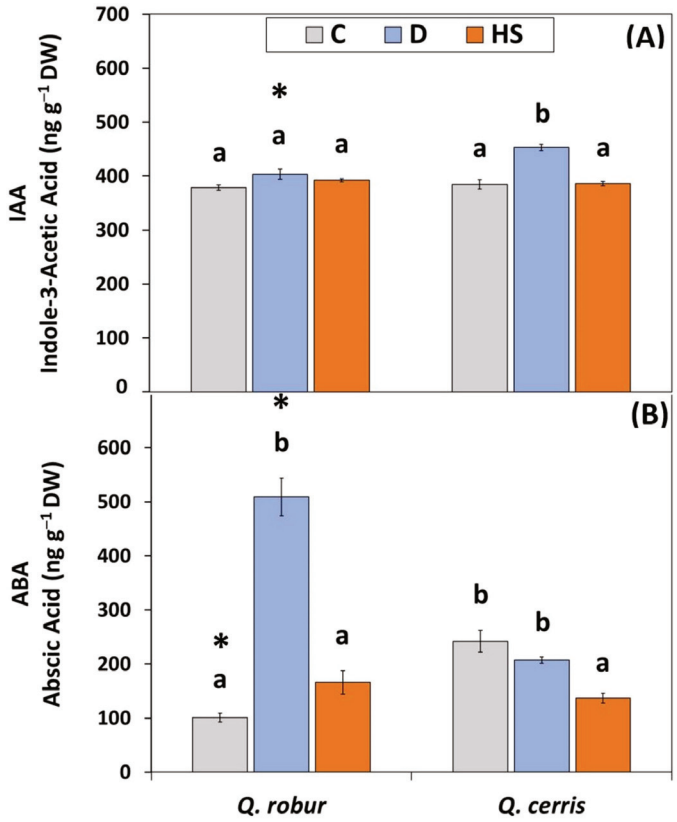

Figure 5. (**A**) Free indole-3-acetic acid (IAA; ng g^{-1} DW) and (**B**) abscisic acid (ABA; ng g^{-1} DW) content in leaves of *Q. robur* and *Q. cerris*. Abbreviations of the treatments, mean separation, and statistical treatments are as shown in Figure 1. Data represent the mean ± standard deviation.

Different from IAA, the leaf constitutive ABA levels were significantly higher in *Q. cerris* than in *Q. robur* (Figure 5B; 242 ng g^{-1} DW vs. 101 ng g^{-1} DW, respectively). The observed effects of stress treatment on ABA concentrations depended on the species (Table S2; Two-way ANOVA Treatment, Species*Treatment $p < 0.001$). Indeed, in response to water deficit, ABA levels increased in *Q. robur* (ca. five-fold compared to controls), while they did not change in *Q. cerris*. By contrast, after exposure to high temperatures, ABA content slightly increased in *Q. robur* (*t*-test $p < 0.05$), while it was significantly reduced in *Q. cerris* (ca. 44% relative to controls).

2.5. PCA Analysis

To test if species shared a common or specific pattern of response to the imposed stress conditions, a principal component analysis (PCA) was run on the full data set (n = 90 cases/270 observations), and an acceptable solution was reached when two principal components described 72.0% of the total variance of the original data set (Figure 6).

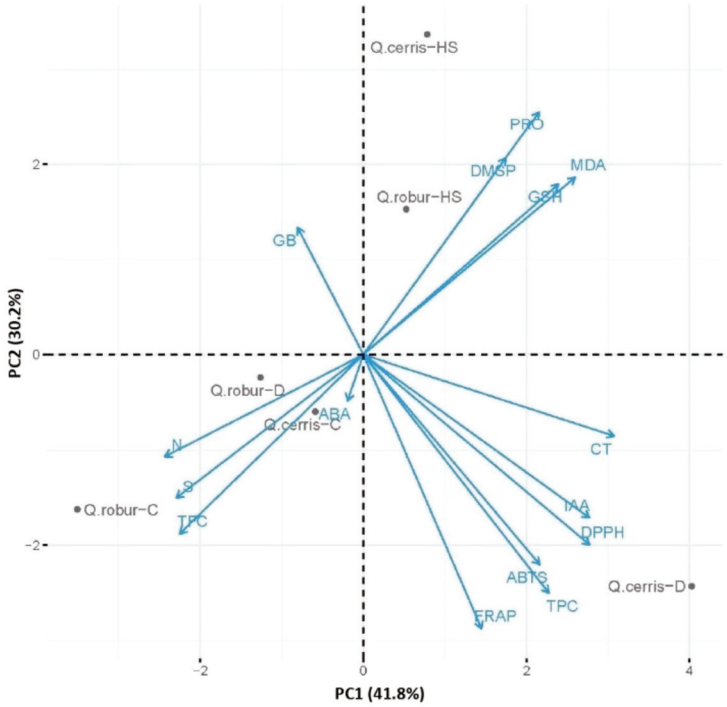

Figure 6. Principal component analysis (PCA) on a correlation matrix including all the biochemical parameters for control I drought-stressed (D) and high-temperatures-stressed (HS) plants of *Quercus cerris* (Q. cerris) and *Quercus robur* (Q. robur). TPC: total phenolic content; TFC: total flavonoid content; CT: condensed tannins; MDA: lipid peroxidation measured as levels of malondialdehyde; GSH: total non-thiol compounds measured as reduced glutathione; ABTS: total antioxidant capacity measured by ABTS assay; DPPH: total antioxidant capacity measured by DPPH assay; FRAP: total antioxidant capacity measured by FRAP assay; PRO: free proline; GB: glycine-betaine content; DMSP: dimethylsulphoniopropionate; IAA: free indole-3-acetic acid; ABA: abscisic acid; S: sulfur; N: nitrogen.

As expected, component 1 (PC1) captured the highest variance within the data (41.8% of the observed variance) and mostly accounted for differences between species as evidenced by the greater effect of species on PC1 than that of the treatment according to *F* values of Two-way ANOVA (Table S3). In particular, species-specific differences were evident across drought-stressed samples, with PC1 strongly discriminating the water-deficit-stressed samples of *Q. cerris* from those of *Q. robur*.

PC1 segregated species mainly according to a combination of antioxidant components and hormonal contribution. The response of *Q. cerris* to water deficit mainly corresponds to high loadings of the highly correlated antioxidant parameters (FRAP, ABTS, and DPPH), total phenolic (TPC), total condensed tannins (CT), and IAA content. The opposite position of GB to antioxidant systems is associated with *Q. robur* stressed plants, that are also characterized by high levels of TFC, N, and S and reveals that this species under water deficit conditions is marginally characterized by the activation of the antioxidant systems, while mainly relying on accumulation of the specific osmolyte (GB) or specific antioxidants (i.e., flavonoids).

Component 2 (PC2) was responsible for 30.2% of the observed variance and mostly reflected the effect of the treatment factor that was greater than that of species on PC2 compared to PC1 (*F* values of Two-way ANOVA; Table S3). Indeed, PC2 scores clearly separate the response to water deficit from the one induced by high temperatures for both *Quercus* species. In both oak species, exposure to high temperatures appeared a relevant source of variance in the data, which indicates a significant change of metabolism under these stress conditions. The significant interaction term (Species*Treatment) highlighted that such a response pattern of PC2 was dependent on species-specific differences. Indeed, PC2 captured the effect of elevated temperatures in each species by clearly separating the heat-treated samples from their controls, with *Q. cerris* showing better performance compared to *Q. robur*. High scores in this component correspond to high loadings of oxidative stress markers (MDA, GSH) and of osmoprotectants (PRO, DMSP), indicating in both species a strong activation of osmoregulation under high temperatures.

2.6. Heat Map with Bi-Cluster Analysis

Hierarchical clustering heat map analysis showed differences between oak species and between the metabolites in response to water deficit and high temperatures (Figure 7).

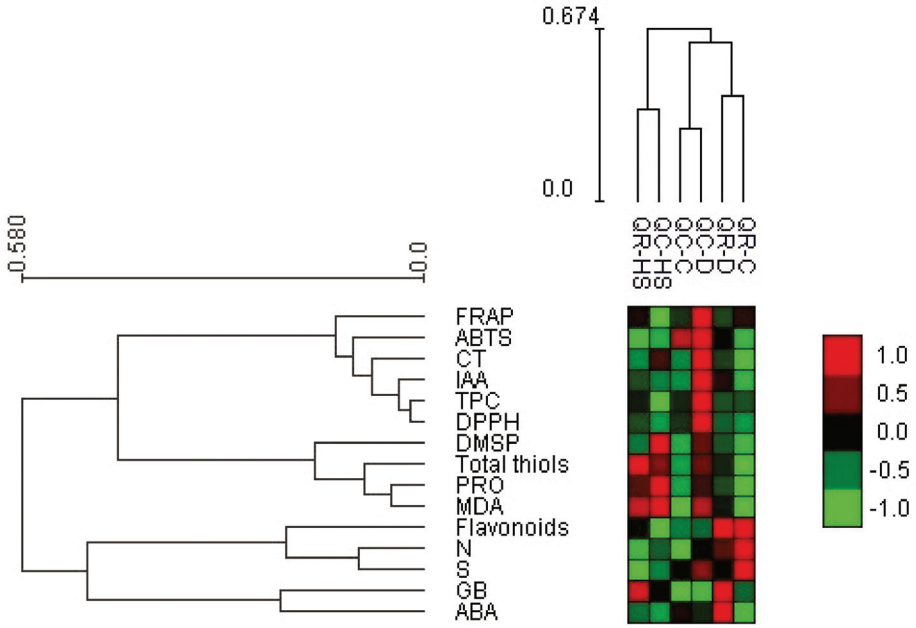

Figure 7. Heat map with bi-cluster analysis where red squares represent highly significant correlation of applied treatment and inspected parameter, while green squares present low interaction assessed according to corresponding Pearson's coefficient. See legend of Figures 1 and 6 for abbreviations of the treatments and parameters.

The species-specific response to water scarcity was evidenced by the drought-treated samples of each oak species being clustered distant. Under this stress condition, the heat map data clearly indicated that some metabolic responses were specifically induced in

each oak species. In particular, the typical response of *Q. robur* to water deficit involves the upper cluster in the metabolite hierarchy that contained GB and ABA. This species was also characterized by maintaining under this stress condition enriched flavonoid reserves that were comparable to those under pre-stressed conditions. The distinct response of *Q. cerris* to water deficit involved the lower metabolite cluster, including phenolics, tannins, and parameters indicative of antioxidant capacity (FRAP, ABTS, DPPH).

The clustering of samples showed that in both *Quercus* species the biochemical response to elevated temperatures differed from the correspondent responses to water deficit. In contrast to water deficit, the high-temperature-treated samples of the two oak species were very close and displayed a positive correlation with the metabolite cluster that includes oxidative stress markers and osmolytes, reflecting the above described PCA observations. Under high temperature conditions, slight differences between oak species were related to the magnitude of changes in proline and GSH, while a distinguished upregulation of specific osmoprotectants was evident (i.e., GB and DMSP in *Q. robur* and *Q. cerris*, respectively).

2.7. Correlation Analysis

Findings by PCA and heat map cluster analysis almost completely matched the relationships between metabolites suggested by the correlation coefficients (Figure 8). For example, a high significant and positive correlation was found among oxidative stress markers (GSH, MDA) and osmolytes (DMSP and PRO) with correlation coefficients ranging from 0.73 to 0.80. Similar elevated correlation coefficients (i.e., ranging from 0.72 up to 0.95) were significantly found ($p < 0.001$) among the antioxidant parameters (DPPH, ABTS) and the content of phenolics and tannins.

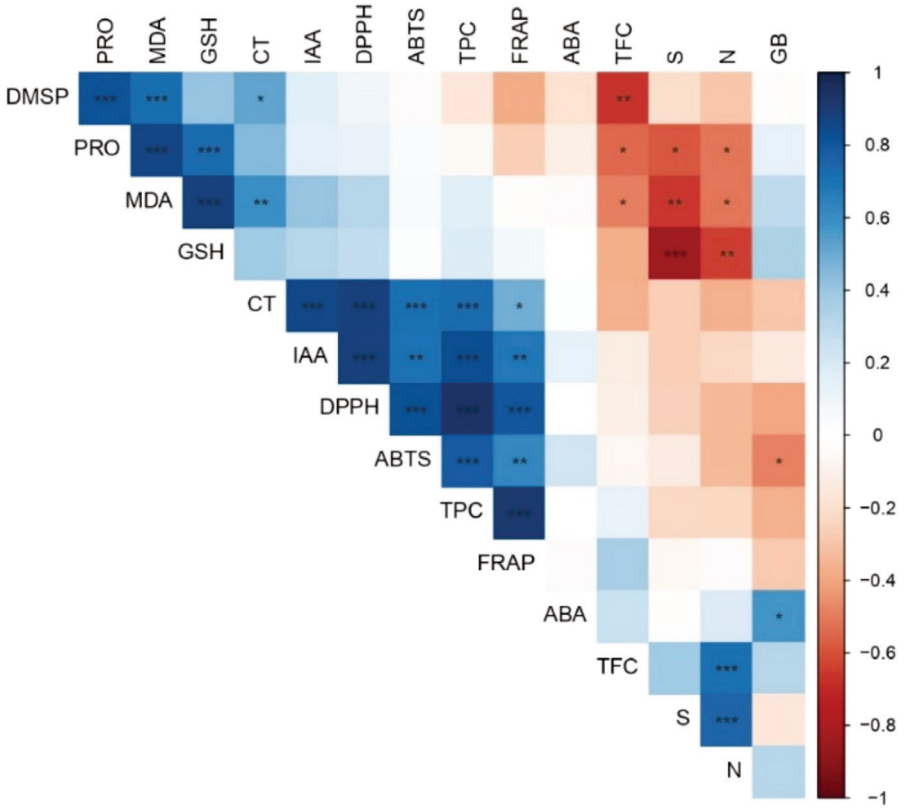

Figure 8. Pearson's coefficient of correlation matrix of the examined parameters in *Q. robur* and *Q. cerris* leaves *. See legend of Figure 6 for abbreviations of parameters. The strength of the correlation is indicated by color saturation. Significance values are indicated as: * $p < 0.05$; ** $p < 0.01$; *** $p < 0.001$.

The observed negative correlations among total flavonoid content (TFC) and the amount of both PRO and DMSP is consistent with PCA results (i.e., opposite position of TFC to PRO and DMSP) and with the heat map data. Taken together, the observations further underline that an increase of osmolyte content under high temperatures is associated with a decrease in flavonoid content.

Interestingly, most of the parameters related to the antioxidant defense system (i.e., CT, TPC, ABTS, DPPH, FRAP) showed a significantly high and positive correlation with the IAA content, with correlation coefficients ranging from 0.69 to 0.89.

The parameters CT, TPC, and those of the antioxidant capacity (FRAP, DPPH, and ABTS) similarly covariate, showing that they are part of the same antioxidant system. High significant and positive correlations among DPPH, TEAC, and FRAP indicate that these parameters use the same mechanism of antioxidant action since practically all of them measure antioxidant capacity that employs an electron transfer (ET) mechanism, which is thoroughly explained by different authors [55,56]. These assays use the assumption that antioxidant capacity is equal to the reducing capacity of extracts [55].

3. Discussion

Quercus species have been widely studied in response to environmental stress conditions [40,57]. However, the discrimination of antioxidative and osmoregulation traits among species is still not well established, especially in young trees and under air warming conditions (Table 1).

Our findings show that Turkey oak (*Q. cerris*) and pedunculate oak (*Q. robur*) seedlings responded to the applied soil water deficit and high air temperature conditions by (Figure 9): (1) increasing differently the levels of several components of their osmoregulation and antioxidative defense system depending on the species and the nature of the stress; (2) upregulating the synthesis of the newly-explored metabolite dimethylsulphoniopropionate (DMSP); (3) trading-off between multifaceted components of the protection system; and (4) modulating the synthesis of stress-related (ABA) and developmental-related (IAA) hormones.

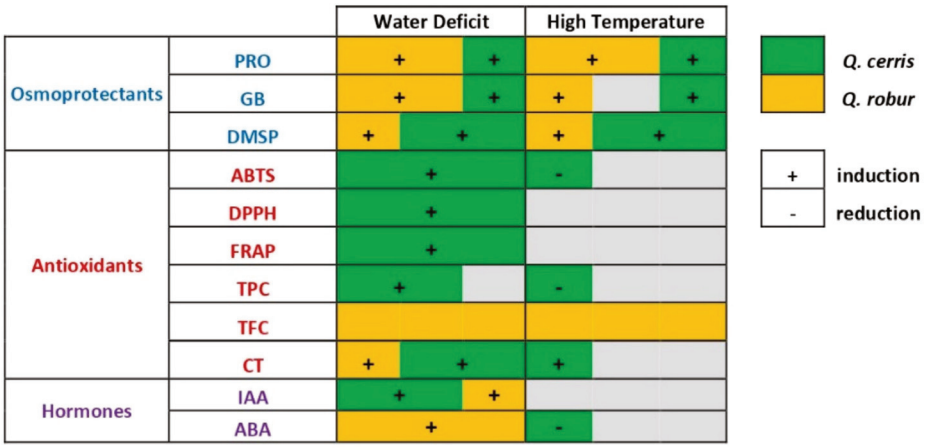

Figure 9. Schematic representation of the soil-water-deficit and high-air-temperatures-induced changes in leaf level content of osmoprotectants, antioxidants, and hormones in *Q. cerris* and *Q. robur*. The size of the boxes reflects the relative induction or reduction of one species compared with the other. See legend of Figure 6 for abbreviations of the parameters.

The occurrence of oxidative stress in leaves of both species under both soil water deficit and high air temperature conditions (i.e., increased membrane lipid peroxidation), is consistent with similar results in *Quercus* [58], including *Q. cerris* and *Q. robur* (Table 1) [42,59,60]. However, the low level of lipid peroxidation, together with the increasing response pattern of mostly biochemical parameters to both stress conditions, suggest an acclimation to oxidative stress for the examined species [61].

Tolerance to the imposed stress conditions was evident in previous measurements of the physiological status on the same plants used for the present experiment [46,52,53]. Although under soil water deficit, a reduced leaf CO_2 assimilation and stomatal conductance was detected, the photosynthetic rates were still rather high (ca. 7–9 μmol m^{-2} s^{-1} in *Q. cerris* and ca. 9–16 μmol m^{-2} s^{-1} in *Q. robur*) [46,53,62,63]. Similarly, thermotolerance of the investigated species was revealed by the maintenance of significant photosynthetic functionality, together with the lack of irreversible damage to the photosynthetic apparatus (i.e., photoinhibition of the PSII) even at the highest temperature (47 °C; [52,64]).

3.1. Species-Specific Accumulation of Osmotically Active Substances Is Induced Differently by Drought and Elevated Temperatures

Under both water deficit and high temperatures, the significant positive covariation between the levels of osmoprotectant proline and DMSP and those of the oxidative stress markers MDA and GSH indicated that an active osmoregulation took place to limit oxidative damage.

When water is limited and a decrease of stomatal conductance occurs together with an increase in diffusive resistance to CO_2, plants can rely on mechanisms of osmotic adjustment as a strategy for maintaining turgor at low leaf water potentials and reducing osmotic potential through the accumulation of compatible solutes in plant leaves [65]. After a drought period similar to that applied in the present study (i.e., within 15 days), acclimation of oak seedlings generally involves osmotic adjustment [66]. The observed increased content of proline is a widely prevalent response to drought due to its multiple functions [22], as previously reported in young trees of *Q. cerris* [59,60,67] (Table 1; Cotrozzi et al., 2016; 2017) and in seedlings of *Q. robur* under soil water regimes (soil moisture ranging between 15-25%) similar to the present study [43,68] (Table 1; Spieß et al., 2012).

Our findings show that the expected water deficit induction of other osmolytes is characterized by a different extent of the response depending on species, as particularly evidenced by PCA and bi-cluster analysis. In *Q. robur*, glycine betaine showed higher constitutive levels and was more drought-responsive than in *Q. cerris*, suggesting a relevant function of this N-containing compound in building drought tolerance of the former species. On the other hand, osmoregulation of *Q. cerris* appears largely conferred by the S-analog of glycine betaine, namely dimethylsulphoniopropionate (DMSP), which shows higher basal pools and water deficit-induced increases of this osmolyte compared to *Q. robur*. Among the metabolically compatible osmolytes, the role of DMSP is revealed for the first time in the *Quercus* species. This crucial component of sulfur metabolism has scarcely been investigated, especially in woody species [69,70]. The detected DMSP levels occurred at a concentration range (nmol g^{-1} DW) similar to that previously reported in leaves of other species [70–72]. The accumulation of DMSP in response to soil water deficit, especially evident in *Q. cerris*, is consistent with previous findings of drought-induced DMSP production in herbaceous species [70,72]. DMSP has been proposed as having a multifunctional role in response to reduced water availability, acting not only as osmoprotectant, but also as antioxidant and overflow for excess energy, thus protecting the photosynthetic machinery from stress injury [69,70].

When oak seedlings were exposed to high temperatures, a strong osmoregulation capacity was mostly involved and enhanced, independent of species, as clearly evidenced by PCA and bi-cluster analysis. Under these stress conditions, the higher oxidative pressure (i.e., elevated MDA and GSH values) was concomitant to a higher accumulation of osmolytes, in particular of proline, compared to the correspondent changes under soil water deficit. This amino acid acts as an effective ROS scavenger in the protection against denaturation and in the stabilization of membrane and subcellular structures [73,74]. Despite the general pronounced induction of osmoregulation in both species when exposed to high temperatures, heat stress impact each species differently as clearly shown by heat map analysis. Similar to the impact of water deficit on osmolyte levels, under high temperatures the stress tolerance of the examined *Quercus* species appears to rely on the major contri-

bution of specific molecules. In *Q. robur*, the pronounced heat-induced oxidative stress is counteracted by sustained and elevated pools of glycine betaine, while in *Q. cerris* the marked accumulation of DMSP appears to play a major role. The protective role of glycine betaine is well recognized under temperature stress [75], while the function of DMSP in thermal tolerance is still unknown, its role being understood only in response to osmotic stresses (i.e., water scarcity or salinity; [72,76,77]).

Taken together, it is worth noting that within each species the magnitude of the stress-induced responses of osmolytes is dependent on the nature of stress. In *Q. cerris*, the specific DMSP changes to high air temperatures were particularly higher than those to water deficit. On the other hand, in *Q. robur* the typical glycine betaine response to soil water deficit was stronger than under the high temperature treatment.

When seedlings were exposed to high temperatures, the marked increase of N- and S-containing osmolytes (i.e., proline and DMSP) was associated with decreased (*Q. robur*) or almost unchanged (*Q. cerris*) levels of leaf inorganic N and S. These findings suggest that in *Q. robur* the enhanced formation of osmolytes may be at the expense of leaf structural N and S, as previously found in oaks [45,78], while in *Q. cerris*, changes in whole plant distribution of inorganic N and S may occur.

3.2. Foliar Antioxidant Defense Systems Are Activated by Drought but Less by Heat

In both oak species, the concomitant and highly correlated increase of foliar MDA and total non-protein thiols (i.e., GSH) under the applied stress conditions can be considered indirect evidence of plant activation of antioxidant responses as previously found in these species (Table 1). However, the induction of individual constituents of the antioxidant system can differ depending on species [79,80] as previously shown in oaks [36,44,45,81] also at molecular level [82].

In *Q. cerris* seedlings, the enhanced antioxidant capacity of leaves in response to soil water deficit can be attributed to the specific accumulation of phenolic compounds and to the higher responsiveness of tannins compared to *Q. robur*. Indeed, these correlated antioxidant components support the occurrence of a concerted defense action involving antioxidant function when water availability is scarce, while highlighting a typical response pattern of *Q. cerris*. Likewise, the slight decrease or no significant changes in the antioxidant capacities of *Q. robur* leaves under soil water deficit was associated with the lack of phenolic accumulation. The less efficient antioxidant defense, in terms of both radical scavenging activity and concentrations of some antioxidants, of *Q. robur* agrees with previous findings obtained on the same oak species and under similar conditions of moderate and relatively short drought stress [43].

When plants were exposed to high air temperatures, a species-specific response of tannins was evident and similar to that observed under soil water deficit, with *Q. cerris* exhibiting a higher responsiveness of these antioxidants to both stress conditions than *Q. robur*. Drought- and heat-induced increasing patterns of foliar tannins have been found in other woody species under stress conditions [83], and our findings confirm that leaf content of tannins is highly species-dependent [84]. Similar to the detected changes of specific osmolytes, we cannot exclude that composition or single metabolites belonging to the classes of phenolics, tannins, or flavonoids respond differently to the imposed stress conditions, depending on species. In addition, we are aware that the analysis of the enzymatic component would provide a more robust understanding of the differential role of the antioxidant machinery in stress tolerance of both *Quercus* species to each specific environmental stressor.

3.3. Tolerance to Soil Water Deficit and High Temperature May Rely on Compensation Mechanisms

Collectively, our findings suggest that under the applied environmental stress conditions a potential and slight trade-off or compensation mechanism may have occurred between the measured components of the antioxidant defense system [17,85]. Protective compounds, such as proline, glycine betaine, and DMSP, play a major role as osmoprotec-

tants but also may act as antioxidants. Therefore, the observed enhancement of proline, glycine betaine, and DMSP in response to both stress conditions could make the activation of other components of the antioxidant defense system less necessary. For example, in both oak species under elevated temperatures, results of PCA analysis together with the general negative correlation between proline and flavonoids may indicate a functional trade-off between these components of the same protective systems. This mechanism may also explain the lack of activation of an antioxidant capacity in *Q. robur* when the investment on other antioxidant components such as flavonoids is sustained. Taken together, these results are also in agreement with previous results suggesting similar compensation mechanisms in other *Quercus* species [86] including *Q. robur* [44].

The marked increase of DMSP in response to the imposed stress conditions appears interesting as this sulfur compound has a metabolic pathway and a functional relationship interacting with that of another protective compound, namely isoprene [70,87], which acts as an antioxidant under drought and thermal stress in several woody species [88] including *Quercus* [89]. Although we did not measure isoprene emission rates of the examined seedlings, the well-established different isoprene emission ability of the two oak species (i.e., *Q. robur* is a high isoprene emitter, *Q. cerris* is a low isoprene emitter; [90]) could further explain their distinct activation of the examined protection systems. In particular, a metabolic trade-off between DMSP and isoprene synthesis may in part justify the high production of DMSP measured in the low isoprene emitter *Quercus cerris*. On the other hand, the minor response of DMSP under high temperatures in the high isoprene emitter *Q. robur* could be partially explained by a trade-off mechanism produced between DMSP and isoprene not only in term of resource allocation for their respective synthesis, but also as a consequence of the antioxidant function of isoprene that in turn can have a potential negative consequence on other traits [51]. Indeed, it has been suggested that the isoprene ability to protect the photosynthetic apparatus [91] can decrease the oxidative load on other leaf protective components [92]. The strong isoprene emission rates of *Q. robur* leaves under high temperatures [93] further support the possibility of the proposed compensation mechanism. Likewise, the lack of induction of leaf antioxidants when *Q. robur* plants were exposed to water deficit is consistent with a reduced requirement for an increased response of other antioxidants, as previously reported in other isoprene-emitting species [92,94] including oaks [89]. However, the influence of isoprene emission capacity on the activation of antioxidants is still controversial [91,95], and further experiments should be designed specifically to explore this hypothesis.

3.4. Drought and Heat Stress Impact the Hormone Balance Differently

Soil water deficit triggered the increase in leaf IAA concentrations in both species but particularly in *Q. cerris*. The strong and significant positive correlations between the extent of IAA response and that of several antioxidants was particularly evident in *Q. cerris* while almost lacking in *Q. robur*. These results suggest that in Turkey oak an enhanced leaf IAA content can contribute to an improved stress tolerance in accordance with findings reported in other woody species under drought conditions [96]. Auxins are recognized to have an impact on photosynthesis with an enhancement of drought tolerance [97].

On the other hand, the increased leaf ABA concentrations in *Q. robur* are an expected plant response to soil water deficit [98,99] including woody species [99,100]. Leaf ABA accumulation is frequently linked with drought tolerance as this hormone plays a key regulatory function in controlling stomatal aperture, in regulating stress-related genes, and in stress signaling [98,99]. The lack of ABA response to drought observed in *Q. cerris* could reflect the moderate stomatal control of transpiration of this anisohydric tree species when subjected to soil water deficit [101]. On the other hand, the high leaf ABA constitutive levels observed in *Q. cerris* may be an important adaptive feature for water conservation in drought-tolerant trees [102].

High temperature conditions did not influence the endogenous leaf concentrations of IAA in both oak species. The role of IAA in heat tolerance is still controversial. Although it is

generally assumed that heat results in an increase in IAA content [103], the lack of responses of IAA levels to high temperatures in our study might be explained by the dynamic nature of IAA. Indeed, in model plants, growth temperature can alter IAA turnover rates and biosynthetic route without a correlated change in its absolute levels [65].

The ABA decrease observed in *Q. cerris* in response to high temperatures might result from substrate competition for common precursors between the biosynthesis of this phytohormone and photosynthetic pigments as previously found under stress conditions [50,104]. After exposure to high temperatures, significant changes in the antioxidant carotenoids were found on the same plants of the present study [52], reflecting a typical response to oxidative stress in several species [85,89] including *Quercus* [42,59,81,105]. Additional explanations of the lack of ABA induction under the applied temperature stress conditions can also rely on the increased stomatal conductance of the same seedlings as a possible consequence of the unlimited water supply [52]. Overall, we cannot exclude that the hormonal balance between the stress-related ABA and the developmental-related IAA, rather than the activities of each single hormone, might contribute coordinately to the tolerance to drought and heat [106].

4. Materials and Methods

4.1. Plant Material and Experimental Design

Experiments were conducted using seedlings of pedunculate oak (*Quercus robur*) and Turkey oak (*Quercus cerris*) as at that developmental stage plants are more sensitive to environmental stresses than adult trees. Therefore, seedlings are more likely to express differences due to water deficit or high temperatures stress, providing relevant information on the tolerance characteristics of the investigated species. Acorns of both oak species were collected from a natural oak population at Morović, which is the largest natural pedunculate oak forest in Serbia. Seeds were germinated in vermiculite in a climate chamber at 25 °C, 80% humidity. Seedlings were transferred to 5 L Micherlich pots filled with loamy fluvisol soil. Soil properties were as follows: pH 8.1 in H_2O, (7.6 in KCl), 21.9 mg g^{-1} humus, 1.32 mg g^{-1} nitrogen, 10.52 mg g^{-1} Mg, 12.68 mg g^{-1} Ca, 7.5 mg g^{-1} K_2O, and 124.5 mg g^{-1} $CaCO_3$. Plants were grown for 3 months (April to June) in semi-controlled conditions (ambient temperature between 25–30 °C) at the greenhouse of the Faculty of Science, Department for Biology and Ecology at the University of Novi Sad, Novi Sad (Serbia). Plants were watered to the soil's maximum water capacity by replacing the amount of water transpired every day until the onset of the experiment.

Soil water content (SWC) was determined daily by drying soil samples (1 g) at 105 °C for approximately 48 h until constant mass was reached and expressed as volume percentages (% vol) according to the formula:

$$\text{SWC } [\%] = \frac{\text{mass of water}}{\text{mass of dry soil}} \times 100\%$$

After determining SWC, the Mitscherlich pots were filled with soil. The plants were grown for 90 days under optimal water supply conditions (they were filled every other day, with SWC ranging from 29 to 38% vol). The day before the start of the treatment, all plants in the Mitscherlich pots were irrigated to the maximum, and the mass of each pot was measured at the maximum substrate moisture. Three-month-old plants (each with 5 to 10 leaves, without side branches) were subjected to treatments.

The experiment consisted of four treatments with a randomized block design as follows:

(1) Control (C): plants were well-watered daily to maintain SWC in the range of 32–38% and were grown at ambient temperature (daytime temperature: 25–28 °C; nighttime: 10–14 °C);
(2) Drought (D): plants were water stressed by withholding water for 12 days until the SWC reached values of ca. 9–11%. The duration of the drought treatment was chosen

to induce an almost natural, reversible drought stress, thus allowing the plant enough time to acclimate and to recover [52,63];

(3) Heat stress (HS): plants were exposed to daily air temperatures ranging between 33–47 °C (night temperatures were about 25–30 °C), using a small enclosure chamber in the greenhouse for 6 days [64]. During the heat treatment, plants were regularly watered to maintain the soil's maximum water capacity, and the daily air temperature was continuously monitored with thermo-sensors.

4.2. Measurements of Osmolytes' Accumulation:

Proline (PRO) concentration was estimated spectrophotometrically at 520 nm after the reaction of proline with ninhydrin reagent by using a rapid colorimetric method described by [107]. Glycine-betaine (GB), as the predominant quaternary ammonium compound (QAC), was quantified using the precipitation method of QAC-periodide complexes in an acid medium [108]. Dimethylsulphoniopropionate (DMSP) content was quantified by measuring the volatile compound dimethyl sulfide (DMS) released after basic hydrolysis from leaf material and swept out into a proton transfer reaction mass spectrometer (PTR-MS, Ionicon, GmbH, Innsbruck, Austria) as thoroughly described by Stefels [109]. All osmolyte data were calculated on a DW basis.

4.3. Assays of Antioxidant Defense Systems

Fully developed leaves of *Q. robur* and *Q. cerris* were sampled from each treatment, frozen, and grinded in liquid nitrogen and later lyophilized in a freeze dryer at −80 °C prior to analysis. For the different chemical analyses, either freeze-dried material was used directly, or extracts in ethanol or phosphate-buffered saline (PBS; 0.1 M KH_2PO_4, KOH, pH = 7) were prepared. Ethanolic extracts were prepared in 2 mL test tubes by mixing around 0.1 g of powdered freeze-dried leaf material with 2 mL of ethanol (96%). Samples were vigorously vortexed and then centrifuged for 30 min at 13,200 rpm at 4 °C. The supernatant was used for the determination of total phenolic and total flavonoid contents, as well as for the quantification of the antioxidant activity of plant extracts by three different methods (see below). Extracts obtained by mixing 0.1 g of plant material with 2 mL of PBS buffer were used for the determination of total non-protein thiol and malondialdehyde (MDA).

Therefore, to investigate the antioxidant capacity of the selected plant species, the following non-enzymatic biochemical parameters were measured. The response of the antioxidant system was investigated through the estimation of several components of the oxidative stress: oxidative damage and antioxidant defenses (i.e., total antioxidant capacity against radical attack and endogenous levels of non-enzymatic antioxidants):

(1) Lipid peroxidation was measured as malondialdehyde (MDA) equivalent which is the secondary end-product of the oxidation of polyunsaturated fatty acids. Determination of MDA was carried out using the acid-catalyzed complexation reaction between MDA and thiobarbituric acid [110]; results are expressed as nmol MDA equivalents on a DW basis.

(2) Total non-protein thiol compounds were measured according to a modified colorimetric assay based on measuring the absorbance of yellow Ellman's reagent (5,5′-dithiobis-(2-nitrobenyoic acid; DTNB) reduced by sulfhydryl compounds at 413 nm. After construction of the calibration curve where we used reduced glutathione (GSH) as standard, total non-protein thiol compounds were expressed as GSH equivalents on a DW basis [111].

(3) Trolox® Equivalent Antioxidant Capacity (TEAC) was estimated with the 2,2′-azinobis-(3-ethylbenzothiozoline-6-sulfonic acid) (ABTS) assay based on the capability of the ethanolic extract to scavenge ABTS radicals [112]. Data were expressed as TEAC on a DW basis.

(4) The 2,2-di-phenyl-1-picrylhydrazyl (DPPH) radical scavenging assay was also applied to measure the antioxidant activity level of ethanolic extracts expressed as TEAC on a DW basis [113].
(5) The Ferric Reducing Antioxidant Power (FRAP) assay was performed to estimate the ability of the plant extract to reduce the ferric 2, 4, 6-tripyridyl-S-triazine complex $[Fe^{3+}\text{-}(TPTZ)_2]^{3-}$ to the intensively blue-colored ferrous complex $(Fe^{2+}\text{-}(TPTZ)_2]^{2-}$ in acidic medium [114]. Data are expressed as TEAC on a DW basis.
(6) Total phenolic content (TPC) was measured by the Folin–Ciocalteu method [115]. Data are expressed as mg of Gallic Acid Equivalents (GAE) on a DW basis.
(7) Total flavonoid content (TFC) was measured by the aluminum chloride colorimetric method [116]. Data are expressed as mg of Quercetin Equivalent (QE) on a DW basis.
(8) Condensed tannins (CT) content was determined from methanolic extracts by using the butanol-HCl-Fe (III) method [117]. Data were expressed as leucocyanidin equivalents (LE) on a DW basis.

4.4. Elemental Analysis of Inorganic Nitrogen and Sulfur

The total content of inorganic nitrogen (N) and sulfur (S) were determined from freeze-dried and powdered oak leaf samples (5–10 mg) with a CHNS analyzer, model Elemental VARIO EL III [118].

4.5. Determination of Leaf Indol-3-Acetic Acid (IAA) and Abscisic Acid (ABA)

A highly reproducible extraction and purification procedure developed for leaf material of woody species was adapted from [4]. Phytohormones (IAA and ABA) were extracted from freeze-dried leaf samples with an extraction mixture (65:35, isopropanol: 0.2 M imidazole buffer, *v*/*v*, pH 7.0) and spiked with isotopically labeled internal standards $[^{13}C_6]$ IAA and $[^{2}H_4]$ ABA (OlChemIm Ltd., Olomouc, Czech Republic). Extracts were purified by using a 3 mL bed volume Quaternary Amine (Strata SAX, Phenomenex, CA, USA) solid phase extraction (SPE) columns, and later, the aqueous phase was additionally purified by using 3 mL volume C_{-18} (STRATA C_{-18}, Phenomenex, CA, USA) SPE columns, whereas IAA and ABA were finally eluted with acetonitrile, evaporated to dryness, and re-suspended in 100 µL methanol. Derivatization of methanolic extracts was carried out with freshly prepared diazomethane [119]. The methylated product was dried under a stream of N_2 and resuspended in ethyl acetate for analysis by gas chromatography coupled with mass spectrometry (GC-MS, model 7890A-5975C, Agilent Technologies, Santa Clara, CA, USA) in split-less mode [120,121]. Methyl esters of plant hormones were separated on an HP1 capillary column (60 m × 0.25 mm, 0.25 µm film thickness, Agilent, Santa Clara, CA, USA) using He as the carrier gas and temperature program as it was described in [4]. IAA and ABA were determined by using the Selected Ion Monitoring (SIM) mode, and final concentrations were calculated by calculating the ratios between corresponding peak and internal standard peak, peak area of m/z 130/136 and m/z 189/195 for IAA, and m/z 190/194 and 162/166 for ABA, according to the principles of isotope dilution [65,121].

4.6. Statistical Analysis

All statistical analyses were run with R studio software (R Studio, Boston, MA, USA). Prior to analysis, Shapiro–Wilk and Levene's tests were performed to evaluate normality and homogeneity of variance of all response variables. Log (x) or Log(x + 1) transformations were applied to some data (ABTS, FRAP, DPPH) to account for violation of assumptions of normal distribution and homogeneity of variance. To determine the overall significances between groups, two-way factorial analysis of variance (two-way ANOVA) was used with species and treatments as factors. The statistical significance of the differences in the means were determined: (i) across treatments within each species, and (ii) across species within each treatment using Tukey's honest significant difference (HSD) post hoc test for multiple comparisons when the one-way analysis of variance (ANOVA) indicated significant differences ($p \leq 0.05$). Pearson's correlation analysis was conducted to explore

the associations between the examined parameters. A principal component analysis (PCA) was used to identify patterns of variations of the examined parameters across species and treatments. Before performing the PCA, the values of each parameter were standardized. A two-way ANOVA was also performed on the scores of the PC explaining the highest proportion of variance (i.e., PC1 and PC2) to test the effect of the factor species and treatment and their interaction on the extracted collective variables. Grouping of treatments and measured traits was examined by hierarchical cluster analysis. Expander 7 was used to create a heat map with bi-cluster analysis based on corresponding Pearson's coefficient. All graphical representations were carried out using R package. All statistical tests were based on three independent repetitions (individual seedlings) for each treatment and species.

5. Conclusions

In summary, when seedlings of pedunculate oak (*Q. robur*) and Turkey oak (*Quercus cerris*) experience soil water deficit and high air temperatures they activate a different pattern of osmoregulation and antioxidant mechanisms to counteract and minimize oxidative stress depending on the species and on the nature of the stress.

In particular, our results on the investigated biochemical mechanisms of protection of the quite drought tolerant and xeric-adapted *Q. cerris* show that its tolerance to soil water deficit might mainly rely on the control of the antioxidant defense system, while its thermotolerance can be partially explained by a high ability to modulate osmolyte production that appeared largely conferred by DMSP. In *Q. robur*, tolerance to the applied soil water deficit and high temperature conditions appears to depend to a certain extent on the highest induction of glycine betaine together with an intrinsic reserve of defensive components.

It is worth noting that in each species, the compounds present at a significant basal level in non-stress conditions are also those more responsive when stresses are applied, as for tannins and DMSP in *Q. cerris*, and for glycine betaine in *Q. robur*. This pattern suggests that the intrinsic pool of those specific metabolites that are constitutively available in each species, may entail a higher ability of these species to activate a prompt and fine-tuned defensive response when oxidative stress occurs. If these response patterns of components of the protection system indicate that the metabolism of the studied oaks is prepared for unfavorable conditions according to [47], they reveal a species-specific metabolic pre-adaptation to these environmental constraints that contributes to the stress tolerance of these oak species.

Additional experiments are needed to elucidate the function of metabolites such as DMSP and isoprenoids that have a multifunctional protective role and are interconnected with other defense mechanisms.

Supplementary Materials: The following supporting information can be downloaded at: https://www.mdpi.com/article/10.3390/plants11131744/s1, Table S1: Results of two-way ANOVA for the effects of species (*Q. robur* and *Q. cerris*), treatment (control, soil water withholding, and high air temperatures), and their interaction (Species*Treatment) on the listed parameters measured at leaf level. Significance values are indicated as: ns, non-significant $p > 0.05$; * $p \leq 0.05$; ** $p \leq 0.01$; *** $p \leq 0.001$, Table S2: Leaf total nitrogen (N) and sulfur (S) content in leaves (% dry weight; mean $\pm$ standard deviation) of *Q. robur* and *Q. cerris* seedlings. See the legend of Figure 1 for abbreviations of the treatments. Different small letters indicate significant differences across the different treatments for each species. Asterisks indicate significant differences between the two oak species within each treatment, Tukey's honestly significant difference (HSD) post hoc test ($p \leq 0.05$), Table S3: Results of the two-way ANOVA (*F* and *p* values) for the first and second principal components (PC1 and PC2, respectively) were extracted. The main effect of species, treatment, and the first-order interaction (*Species* x *Treatment*) are shown. The factor effect was considered significant at $p < 0.05$.

Author Contributions: Conceptualization and design, M.B., F.R., R.H. and M.K.; methodology, M.K., F.R. and V.V.; validation, F.R. and M.K.; biochemical analysis of antioxidants, osmolytes, inorganic ions: M.K., V.V. and J.S.; hormone analysis: M.K. and F.R.; data curation: F.R., B.K. and M.M.; data interpretation: F.R. and M.K.; visualization and statistical analysis: F.R., S.K. and M.M.; writing—draft

preparation: F.R. and M.K.; writing and reviewing final version: F.R. and M.K.; editing: L.N., F.R., M.K. and J.S.; project administration, S.O., M.K. and F.R.; funding acquisition S.O., M.K. and F.R. All authors have read and agreed to the published version of the manuscript.

Funding: This research was supported by the PROMIS project "MYCOCLIMART" No. 6066613 funded by Science Fund of the Republic of Serbia; Life + European project "GAIA" (Green Areas Inner-cities Agreement—http://www.lifegaia.eu (accessed on 30 December 2010); LIFE09 ENV/IT/000074); grant from the COST Action "STReESS" (Studying Tree Responses to extreme Events: A SynthesiS; COST-STSM-FP1106-11208).

Institutional Review Board Statement: Not applicable.

Informed Consent Statement: Not applicable.

Data Availability Statement: Not applicable.

Acknowledgments: We are grateful to L.J. de Kok of the Groningen Institute for Evolutionary Life Sciences (GELIFES), Groningen (The Netherlands) for his scientific support to the overall investigations and to prof. Milan Borišev and Nataša Nikolić from Faculty of Science, University of Novi Sad for help in conceptualization.

Conflicts of Interest: The authors declare no conflict of interest.

References

1. Edenhofer, O.; Pichs-Madruga, R.; Sokona, Y.; Minx, J.C.; Farahani, E.; Kadner, S.; Seyboth, K.; Adler, A.; Baum, I.; Brunner, S.; et al. *Climate Change 2014: Mitigation of Climate Change*; Cambridge University Press: Cambridge, UK, 2015.
2. Madrigal-González, J.; Herrero, A.; Ruiz-Benito, P.; Zavala, M.A. Resilience to Drought in a Dry Forest: Insights from Demographic Rates. *For. Ecol. Manag.* **2017**, *389*, 167–175. [CrossRef]
3. Takahashi, S.; Badger, R.M. Photoprotection in plants: A new light on photosystem II damage. *Trends Plant Sci.* **2011**, *16*, 53–60. [CrossRef] [PubMed]
4. Kebert, M.; Rapparini, F.; Neri, L.; Bertazza, G.; Orlović, S.; Biondi, S. Copper-Induced Responses in Poplar Clones Are Associated with Genotype- and Organ-Specific Changes in Peroxidase Activity and Proline, Polyamine, ABA, and IAA Levels. *J. Plant Growth Regul.* **2017**, *36*, 131–147. [CrossRef]
5. Khaleghi, A.; Naderi, R.; Brunetti, C.; Maserti, B.E.; Salami, A.S.; Babalar, M. Morphological, physiochemical and antioxidant responses of *Maclura pomifera* to drought stress. *Sci. Rep.* **2019**, *9*, 1–12. [CrossRef] [PubMed]
6. Bhusal, N.; Han, S.G.; Yoon, T.M. Impact of drought stress on photosynthetic response, leaf water potential, and stem sap flow in two cultivars of bi-leader apple trees (*Malus*× *domestica* Borkh.). *Sci. Hortic.* **2019**, *246*, 535–543. [CrossRef]
7. Pintó-Marijuan, M.; Munné-Bosch, S. Photo-oxidative stress markers as a measure of abiotic stress-induced leaf senescence: Advantages and limitations. *J. Exp. Bot.* **2014**, *65*, 3845–3857. [CrossRef]
8. Cruz de Carvalho, M.H. Drought stress and reactive oxygen species: Production, scavenging and signaling. *Plant Signal. Behav.* **2007**, *3*, 156–165. [CrossRef]
9. Pospíšil, P. Production of Reactive Oxygen Species by Photosystem II as a Response to Light and Temperature Stress. *Front. Plant Sci.* **2016**, *7*, 1950. [CrossRef]
10. Mittler, R. ROS are good. *Trends Plant Sci.* **2017**, *22*, 11–19. [CrossRef]
11. Morales, M.; Munné-Bosch, S. Oxidative Stress: A Master Regulator of Plant Trade-Offs? *Trends Plant Sci.* **2016**, *21*, 996–999. [CrossRef]
12. Kwak, J.M.; Nguyen, V.; Schroeder, J.I. The role of reactive oxygen species in hormonal responses. *Plant Physiol.* **2006**, *141*, 323–329. [CrossRef]
13. Tausz, M.; Grill, D. The Role of Glutathione in Stress Adaptation of Plants. In Proceedings of the Plant Adaptation to Stress, Kuiper Haren, The Netherlands, 25 June 1999.
14. Hasanuzzaman, M.; Nahar, K.; Anee, T.I.; Fujita, M. Glutathione in Plants: Biosynthesis and Physiological Role in Environmental Stress Tolerance. *Physiol. Mol. Biol. Plants* **2017**, *23*, 249–268. [CrossRef]
15. Khanna-Chopra, R.; Semwal, V.K. Ecophysiology and Response of Plants Under High Temperature Stress. In *Plant Ecophysiology and Adaptation under Climate Change: Mechanisms and Perspectives I*; Springer: Singapore, 2020; pp. 295–329. [CrossRef]
16. Biswal, U.C.; Raval, M.K. *Significance of Glutathione to Plant Adaptation to the Environment*; Springer Science & Business Media: New York, NY, USA, 2001; Volume 2. [CrossRef]
17. Rennenberg, H.; Loreto, F.; Polle, A.; Brilli, F.; Fares, S.; Beniwal, R.S.; Gessler, A. Physiological Responses of Forest Trees to Heat and Drought. *Plant Biol.* **2006**, *8*, 556–571. [CrossRef]
18. Ballizany, W.L.; Hofmann, R.W.; Jahufer, M.Z.Z.; Barrett, B.A. Variation for Constitutive Flavonols and Morphological Traits in a New White Clover Population. *Environ. Exp. Bot.* **2014**, *105*, 65–69. [CrossRef]

19. Constabel, C.P.; Yoshida, K.; Walker, V. Diverse ecological roles of plant tannins: Plant defense and beyond. *Recent Adv. Polyphen. Res.* **2014**, *4*, 115–142.
20. Top, S.M.; Preston, C.M.; Dukes, J.S.; Tharayil, N. Climate Influences the Content and Chemical Composition of Foliar Tannins in Green and Senesced Tissues of Quercus Rubra. *Front. Plant Sci.* **2017**, *8*, 423. [CrossRef]
21. Ruiz-Sánchez, M.; Aroca, R.; Muñoz, Y.; Polón, R.; Ruiz-Lozano, J.M. The Arbuscular Mycorrhizal Symbiosis Enhances the Photosynthetic Efficiency and the Antioxidative Response of Rice Plants Subjected to Drought Stress. *J. Plant Physiol.* **2010**, *167*, 862–869. [CrossRef]
22. Kishor, P.K.; Sangam, S.; Amrutha, R.N.; Laxmi, P.S.; Naidu, K.R.; Rao, K.S.; Rao, S.; Reddy, K.J.; Theriappan, P.; Sreenivasulu, N. Regulation of proline biosynthesis, degradation, uptake and transport in higher plants: Its implications in plant growth and abiotic stress tolerance. *Curr. Sci.* **2005**, *88*, 424–438.
23. Chen, T.H.; Murata, N. Glycinebetaine: An effective protectant against abiotic stress in plants. *Trends Plant Sci.* **2008**, *13*, 499–505. [CrossRef]
24. Otte, M.L.; Wilson, G.; Morris, J.T.; Moran, B.M. Dimethylsulphoniopropionate (DMSP) and related compounds in higher plants. *J. Exp. Bot.* **2004**, *55*, 1919–1925. [CrossRef]
25. Stefels, J. Physiological Aspects of the Production and Conversion of DMSP in Marine Algae and Higher Plants. *J. Sea Res.* **2000**, *43*, 183–197. [CrossRef]
26. Slama, I.; Abdelly, C.; Bouchereau, A.; Flowers, T.; Savouré, A. Diversity, distribution and roles of osmoprotective compounds accumulated in halophytes under abiotic stress. *Ann. Bot.* **2015**, *115*, 433–447. [CrossRef]
27. Sunda, W.; Kieber, D.J.; Kiene, R.P.; Huntsman, S. An Antioxidant Function for DMSP and DMS in Marine Algae. *Nature* **2002**, *418*, 317–320. [CrossRef]
28. Gururani, M.A.; Mohanta, T.K.; Bae, H. Current understanding of the interplay between phytohormones and photosynthesis under environmental stress. *Int. J. Mol. Sci.* **2015**, *16*, 19055–19085. [CrossRef]
29. Song, Y.; Ci, D.; Tian, M.; Zhang, D. Comparison of the Physiological Effects and Transcriptome Responses of Populus Simonii under Different Abiotic Stresses. *Plant Mol. Biol.* **2014**, *86*, 139–156. [CrossRef]
30. Zia, R.; Nawaz, M.S.; Siddique, M.J.; Hakim, S.; Imran, A. Plant Survival under Drought Stress: Implications, Adaptive Responses, and Integrated Rhizosphere Management Strategy for Stress Mitigation. *Microbiol. Res.* **2021**, *242*, 126626. [CrossRef]
31. Landi, M.; Cotrozzi, L.; Pellegrini, E.; Remorini, D.; Tonelli, M.; Trivellini, A.; Nali, C.; Guidi, L.; Massai, R.; Vernieri, P.; et al. When "Thirsty" Means "Less Able to Activate the Signalling Wave Trigged by a Pulse of Ozone": A Case of Study in Two Mediterranean Deciduous Oak Species with Different Drought Sensitivity. *Sci. Total Environ.* **2019**, *657*, 379–390. [CrossRef]
32. Bhusal, N.; Lee, M.; Lee, H.; Adhikari, A.; Han, A.R.; Han, A.; Kim, H.S. Evaluation of morphological, physiological, and biochemical traits for assessing drought resistance in eleven tree species. *Sci. Total Environ.* **2021**, *779*, 146466. [CrossRef] [PubMed]
33. Pintó-Marijuan, M.; Munné-Bosch, S. Ecophysiology of invasive plants: Osmotic adjustment and antioxidants. *Trends Plant Sci.* **2013**, *18*, 660–666. [CrossRef] [PubMed]
34. Kesić, L.; Stojnić, S.; Orlović, S.; Pavlović, L.; Lozjanin, R.; Tepavac, A.; Vaštag, E. Variability of the morphological characteristics of pedunculate (*Quercus robur* L.), sessile (*Q. petraea* (Matt.) Lieb.) and Turkey oak (*Q. cerris* L.) acorns. *Topola/Poplar* **2018**, *201*, 187–201.
35. Nixon, K.C. Global and Neotropical Distribution and Diversity of Oak (Genus) and Oak Forests. *Ecol. Conserv. Neotrop. Montane Oak For.* **2006**, *185*, 3–13. [CrossRef]
36. García-Plazaola, J.I.; Hernández, A.; Fernández-Marín, B.; Esteban, R.; Peguero-Pina, J.J.; Verhoeven, A.; Cavender-Bares, J. Photoprotective Mechanisms in the Genus in Response to Winter Cold and Summer Drought. In *Oaks Physiological Ecology. Exploring the Functional Diversity of Genus Quercus L.*; Springer: Cham, Switzerland, 2017; pp. 361–391. [CrossRef]
37. Corcuera, L.; Camarero, J.J.; Gil-Pelegrín, E. Functional groups in *Quercus* species derived from the analysis of pressure–volume curves. *Trees* **2022**, *16*, 465–472. [CrossRef]
38. Simeone, M.C.; Zhelev, P.; Kandemir, G. *Technical Guidelines for Genetic Conservation and Use of Turkey Oak (Quercus cerris)*; EUFORGEN Secretariat: Bonn, Germany, 2019.
39. EUFORGEN European Forest Genetic Resources Programme. Available online: https://www.euforgen.org/ (accessed on 6 May 2022).
40. Kostić, S.; Kesić, L.; Matović, B.; Orlović, S.; Stojnić, S.; Stojanović, D.B. Soil properties are significant modifiers of pedunculate oak (*Quercus robur* L.) radial increment variations and their sensitivity to drought. *Dendrochronologia* **2021**, *67*, 125838. [CrossRef]
41. Stojanović, D.B.; Matović, B.; Orlović, S.; Kržič, A.; Trudić, B.; Galić, Z.; Stojnić, S.; Pekeč, S. Future of the Main Important Forest Tree Species in Serbia from the Climate Change Perspective. *South-East Eur. For. SEEFOR* **2014**, *5*, 117–124. [CrossRef]
42. Hansen, U.; Schneiderheinze, J.; Stadelmann, S.; Rank, B. The α-tocopherol content of leaves of pedunculate oak (*Quercus robur* L.)-variation over the growing season and along the vertical light gradient in the canopy. *J. Plant Physiol.* **2003**, *160*, 91–96. [CrossRef]
43. Spieß, N.; Oufir, M.; Matušíková, I.; Stierschneider, M.; Kopecky, D.; Homolka, A.; Burg, K.; Fluch, S.; Hausman, J.F.; Wilhelm, E. Ecophysiological and transcriptomic responses of oak (*Quercus robur*) to long-term drought exposure and rewatering. *Environ. Exp. Bot.* **2012**, *77*, 117–126. [CrossRef]

44. Hu, B.; Simon, J.; Rennenberg, H. Drought and air warming affect the species-specific levels of stress-related foliar metabolites of three oak species on acidic and calcareous soil. *Tree Physiol.* **2013**, *33*, 489–504. [CrossRef]
45. Hu, B.; Simon, J.; Günthardt-Goerg, M.S.; Arend, M.; Kuster, T.M.; Rennenberg, H. Changes in the dynamics of foliar N metabolites in oak saplings by drought and air warming depend on species and soil type. *PLoS ONE* **2015**, *10*, e0126701. [CrossRef]
46. Bojović, M.; Nikolić, N.; Borišev, M.; Pajević, S.; Horák, R.; Pavlović, L.; Vaštag, E. The effect of drought stress and recovery on pedunculate oak populations grown in semi-controlled conditions. *Topola* **2017**, *200*, 193–207.
47. Krasensky, J.; Jonak, C. Drought, salt, and temperature stress-induced metabolic rearrangements and regulatory networks. *J. Exp. Bot.* **2012**, *63*, 1593–1608. [CrossRef]
48. Niinemets, Ü. Uncovering the hidden facets of drought stress: Secondary metabolites make the difference. *Tree Physiol.* **2016**, *36*, 129–132. [CrossRef]
49. Rennenberg, H.; Herschbach, C. Sulfur Compounds in Multiple Compensation Reactions of Abiotic Stress Responses. *Sulfur Metab. Plants* **2012**, *1*, 203–215. [CrossRef]
50. Owen, S.M.; Peñuelas, J. Opportunistic emissions of volatile isoprenoids. *Trends Plant Sci.* **2005**, *10*, 420–426. [CrossRef]
51. Monaghan, P.; Metcalfe, N.B.; Torres, R. Oxidative stress as a mediator of life history trade-offs: Mechanisms, measurements and interpretation. *Ecol. Lett.* **2009**, *12*, 75–92. [CrossRef]
52. Horak, R.; Župunski, M.; Pajević, S.; Borišev, M.; Arsenov, D.; Nikolić, N.; Orlović, S. Carbon assimilation in oak (*Quercus* spp.) populations under acute and chronic high-temperature stress. *Photosynthetica* **2019**, *57*, 875–889. [CrossRef]
53. Bojović, M.; Nikolić, N.; Borišev, M.; Pajević, S.; Horak, R.; Orlović, S.; Lozjanin, R. The impact of drought on the physiological characteristics of half-sib lines of Turkey oak (*Quercus cerris* L.). *Glas. Sumar. Fak.* **2019**, *119*, 9–32. [CrossRef]
54. Bowditch, E.; Santopuoli, G.; Binder, F.; del Río, M.; La Porta, N.; Kluvankova, T.; Lesinski, J.; Motta, R.; Pach, M.; Panzacchi, P.; et al. What Is Climate-Smart Forestry? A Definition from a Multinational Collaborative Process Focused on Mountain Regions of Europe. *Ecosyst. Serv.* **2020**, *43*, 101113. [CrossRef]
55. Huang, D.; Boxin, O.U.; Prior, R.L. The Chemistry behind Antioxidant Capacity Assays. *J. Agric. Food Chem.* **2005**, *53*, 1841–1856. [CrossRef]
56. Stevanato, R.; Fabris, S.; Momo, F. New enzymatic method for the determination of total phenolic content in tea and wine. *J. Agric. Food Chem.* **2004**, *52*, 6287–6293. [CrossRef]
57. Gil-Pelegrín, E.; Javier, J.; Domingo, P.P.; Editors, S.-K. Oaks Physiological Ecology. In *Exploring the Functional Diversity of Genus Quercus L.*; Springer: Cham, Swizerland, 2017.
58. Ghanbary, E.; Tabari Kouchaksaraei, M.; Zarafshar, M.; Bader, K.F.M.; Mirabolfathy, M.; Ziaei, M. Differential physiological and biochemical responses of *Quercus infectoria* and *Q. libani* to drought and charcoal disease. *Physiol. Plant.* **2020**, *168*, 876–892. [CrossRef]
59. Cotrozzi, L.; Remorini, D.; Pellegrini, E.; Landi, M.; Massai, R.; Nali, C.; Guidi, L.; Lorenzini, G. Variations in physiological and biochemical traits of Oak seedlings grown under drought and ozone stress. *Physiol. Plant.* **2016**, *157*, 69–84. [CrossRef] [PubMed]
60. Cotrozzi, L.; Remorini, D.; Pellegrini, E.; Guidi, L.; Lorenzini, G.; Massai, R.; Nali, C.; Landi, M. Cross-talk between physiological and metabolic adjustments adopted by *Quercus cerris* to mitigate the effects of severe drought and realistic future ozone concentrations. *Forests* **2017**, *8*, 148. [CrossRef]
61. Tausz, M.; Šircelj, H.; Grill, D. The glutathione system as a stress marker in plant ecophysiology: Is a stress response concept valid? *J. Exp. Bot.* **2004**, *55*, 1955–1962. [CrossRef] [PubMed]
62. Vastag, E.; Cocozza, C.; Orlović, S.; Kesić, L.; Kresoja, M.; Stojnić, S. Half-sib lines of pedunculate oak (*Quercus robur L.*) respond differently to drought through biometrical, anatomical and physiological traits. *Forests* **2020**, *11*, 153. [CrossRef]
63. Stojnić, S.; Kovačević, B.; Kebert, M.; Vaštag, E.; Bojović, M.; Nedić, M.S.; Orlovic, S. The use of physiological, biochemical and morpho-anatomical traits in tree breeding for improved water-use efficiency of *Quercus robur* L. *For. Syst.* **2019**, *28*, 5. [CrossRef]
64. Dascaliuc, A.; Ralea, T.; Cuza, P. Influence of heat shock on chlorophyll fluorescence of white oak (*Quercus pubescens* Willd.) leaves. *Photosynthetica* **2007**, *45*, 469–471. [CrossRef]
65. Rapparini, F.; Tam, Y.Y.; Cohen, J.D.; Slovin, J.P. Indole-3-Acetic Acid Metabolism in *Lemna Gibba* Undergoes Dynamic Changes in Response to Growth Temperature. *Plant Physiol.* **2002**, *128*, 1410–1416. [CrossRef]
66. Blum, A. Osmotic Adjustment Is a Prime Drought Stress Adaptive Engine in Support of Plant Production. *Plant Cell Environ.* **2017**, *40*, 4–10. [CrossRef]
67. Deligöz, A.; Bayar, E. Drought stress responses of seedlings of two oak species (*Quercus cerris* and *Quercus robur*). *Turk. J. Agric. For.* **2018**, *42*, 114–123. [CrossRef]
68. Xiong, S.; Wang, Y.; Chen, Y.; Gao, M.; Zhao, Y.; Wu, L. Effects of drought stress and rehydration on physiological and biochemical properties of four oak species in China. *Plants* **2022**, *11*, 679. [CrossRef]
69. Trossat, C.; Rathinasabapathi, B.; Weretilnyk, E.A.; Shen, T.L.; Huang, Z.H.; Gage, D.A.; Hanson, A.D. Salinity promotes accumulation of 3-dimethylsulfoniopropionate and its precursor S-methylmethionine in chloroplasts. *Plant Physiol.* **1998**, *116*, 165–171. [CrossRef]
70. Haworth, M.; Catola, S.; Marino, G.; Brunetti, C.; Michelozzi, M.; Riggi, E.; Avola, G.; Cosentino, S.L.; Loreto, F.; Centritto, M. Moderate Drought Stress Induces Increased Foliar Dimethylsulphoniopropionate (DMSP) Concentration and Isoprene Emission in Two Contrasting Ecotypes of Arundo Donax. *Front. Plant Sci.* **2017**, *8*, 1016. [CrossRef]

71. Ausma, T.; Kebert, M.; Stefels, J.; de Kok, L.J. DMSP: Occurrence in Plants and Response to Salinity in *Zea mays*. In *Sulfur Metabolism in Higher Plants-Fundamental, Environmental and Agricultural Aspects*; Springer: New York, NY, USA, 2017; pp. 87–91. [CrossRef]
72. Catola, S.; Ganesha, S.D.K.; Calamai, L.; Loreto, F.; Ranieri, A.; Centritto, M. Headspace-Solid Phase Microextraction Approach for Dimethylsulfoniopropionate Quantification in *Solanum lycopersicum* Plants Subjected to Water Stress. *Front. Plant Sci.* **2016**, *7*, 1257. [CrossRef]
73. Szabados, L.; Savouré, A. Proline: A multifunctional amino acid. *Trends Plant Sci.* **2010**, *15*, 89–97. [CrossRef]
74. Hossain, M.A.; Li, Z.G.; Hoque, T.S.; Burritt, D.J.; Fujita, M.; Munné-Bosch, S. Heat or Cold Priming-Induced Cross-Tolerance to Abiotic Stresses in Plants: Key Regulators and Possible Mechanisms. *Protoplasma* **2018**, *255*, 399–412. [CrossRef]
75. Sakamoto, A.; Murata, N. The role of glycine betaine in the protection of plants from stress: Clues from transgenic plants. *Plant Cell Environ.* **2002**, *25*, 163–171. [CrossRef]
76. Mulholland, M.M.; Otte, M.L. The effects of nitrogen supply and salinity on DMSP, glycine betaine and proline concentrations in leaves of *Spartina anglica*. *Aquat. Bot.* **2002**, *72*, 193–200. [CrossRef]
77. Thariath, D.V.; Divakaran, D.; Chenicherry, S. Influence of salinity on the dimethylsulphoniopropionate production from *Prymnesium simplex*. *Sustain. Environ. Res.* **2019**, *29*, 1–8. [CrossRef]
78. Ionescu, M.; Edu, E.M.; Mihalache, M.; Ciuvat, L.A. Study on carbon, nitrogen and sulfur in litter *Quercus robur*, *Tilia* sp., *Carpinus betulas*, and *Fagus sylvatica*. *Sci. Pap.-Ser. A Agron.* **2013**, *56*, 48–50.
79. Smirnof, N. The role of active oxygen in the response of plants to water deficit and desiccation. *New Phytol.* **1993**, *125*, 27–58. [CrossRef]
80. 80. Cherit-Hacid, F.; Derridij, A.; Moulti-Mati, F.; Mati, A. Drought stress effect on some biochemical and physiological parameters; accumulation on total polyphenols and flavonoids in leaves of two provenance seedling Pistacia lentiscus. *Int. J. Res. Appl. Nat. Soc. Sci.* **2015**, *3*, 127–138.
81. Schwanz, P.; Polle, A. Differential stress responses of antioxidative systems to drought in pendunculate oak (*Quercus robur*) and maritime pine (*Pinus pinaster*) grown under high CO_2 concentrations. *J. Exp. Bot.* **2001**, *52*, 133–143. [CrossRef]
82. Madritsch, S.; Wischnitzki, E.; Kotrade, P.; Ashoub, A.; Burg, A.; Fluch, S.; Brüggemann, W.; Sehr, E.M. Elucidating drought stress tolerance in European oaks through cross-species transcriptomics. *G3-Genes Genom Genet.* **2019**, *10*, 3181–3199. [CrossRef]
83. Jamieson, M.A.; Schwartzberg, E.G.; Raffa, K.F.; Reich, P.B.; Lindroth, R.L. Experimental Climate Warming Alters Aspen and Birch Phytochemistry and Performance Traits for an Outbreak Insect Herbivore. *Glob. Chang. Biol.* **2015**, *21*, 2698–2710. [CrossRef]
84. Ahmed, Z.B.; Yousfi, M.; Viaene, J.; Dejaegher, B.; Demeyer, K.; Mangelings, D.; Heyden, Y. Vander Seasonal, Gender and Regional Variations in Total Phenolic, Flavonoid, and Condensed Tannins Contents and in Antioxidant Properties from *Pistacia atlantica* ssp. Leaves. *Pharm. Biol.* **2017**, *55*, 1185–1194. [CrossRef]
85. Munné-Bosch, S. The role of α-tocopherol in plant stress tolerance. *J. Plant Physiol.* **2005**, *162*, 743–748. [CrossRef]
86. Saunier, A.; Ormeño, E.; Havaux, M.; Wortham, H.; Ksas, B.; Temime-Roussel, B.; Blande, J.D.; Lecareux, C.; Mévy, J.P.; Bousquet-Mélou, A. Resistance of Native Oak to Recurrent Drought Conditions Simulating Predicted Climatic Changes in the Mediterranean Region. *Plant Cell Environ.* **2018**, *41*, 2299–2312. [CrossRef]
87. Monson, R.K.; Jones, R.T.; Rosenstiel, T.N.; Schnitzler, J.P. Why only some plants emit isoprene. *Plant Cell Environ.* **2013**, *36*, 503–516. [CrossRef]
88. Sharkey, T.D.; Yeh, S. Isoprene emission from plants. *Annu. Rev. Plant Biol.* **2001**, *52*, 407–436. [CrossRef]
89. Peñuelas, J.; Munné-Bosch, S. Isoprenoids: An Evolutionary Pool for Photoprotection. *Trends Plant Sci.* **2005**, *10*, 166–169. [CrossRef] [PubMed]
90. Kesselmeier, J.; Staudt, M. Biogenic Volatile Organic Compounds (VOC): An Overview on Emission, Physiology and Ecology. *J. Atmos. Chem.* **1999**, *33*, 23–88. [CrossRef]
91. Pollastri, S.; Baccelli, I.; Loreto, F. Isoprene: An Antioxidant Itself or a Molecule with Multiple Regulatory Functions in Plants? *Antioxidants* **2021**, *10*, 684. [CrossRef] [PubMed]
92. Vickers, C.E.; Gershenzon, J.; Lerdau, M.T.; Loreto, F. A unified mechanism of action for volatile isoprenoids in plant abiotic stress. *Nat. Chem. Biol.* **2009**, *5*, 283–291. [CrossRef]
93. Li, Z.; Ratliff, E.A.; Sharkey, T.D. Effect of temperature on postillumination isoprene emission in oak and poplar. *Plant Physiol.* **2011**, *155*, 1037–1046. [CrossRef]
94. Behnke, K.; Kleist, E.; Uerlings, R.; Wildt, J.; Rennenberg, H.; Schnitzler, J.P. RNAi-Mediated Suppression of Isoprene Biosynthesis in Hybrid Poplar Impacts Ozone Tolerance. *Tree Physiol.* **2009**, *29*, 725–736. [CrossRef]
95. Monson, R.K.; Weraduwage, S.M.; Rosenkranz, M.; Schnitzler, J.P.; Sharkey, D.T. Leaf Isoprene Emission as a Trait That Mediates the Growth-Defense Tradeoff in the Face of Climate Stress. *Oecologia* **2021**, *197*, 885–902. [CrossRef]
96. De Diego, N.; Saiz-Fernández, I.; Rodríguez, J.L.; Pérez-Alfocea, P.; Sampedro, M.C.; Barrio, R.J.; Lacuesta, M.; Moncaleán, P. Metabolites and hormones are involved in the intraspecific variability of drought hardening in radiata pine. *J. Plant Physiol.* **2015**, *188*, 64–71. [CrossRef]
97. Müller, M.; Munné-Bosch, S. Hormonal impact on photosynthesis and photoprotection in plants. *Plant Physiol.* **2021**, *185*, 1500–1522. [CrossRef]
98. Müller, M.; Munné-Bosch, S. Ethylene Response Factors: A Key Regulatory Hub in Hormone and Stress Signaling. *Plant Physiol.* **2015**, *169*, 32–41. [CrossRef]

99. Verma, V.; Ravindran, P.; Kumar, P.P. Plant Hormone-Mediated Regulation of Stress Responses. *BMC Plant Biol.* **2016**, *16*, 1–10. [CrossRef]
100. Long, A.; Zhang, J.; Yang, L.-T.; Ye, X.; Lai, N.-W.; Tan, L.-L.; Lin, D.; Chen, L.-S. Effects of Low PH on Photosynthesis, Related Physiological Parameters, and Nutrient Profiles of Citrus. *Front. Plant Sci.* **2017**, *8*, 185. [CrossRef] [PubMed]
101. Nardini, A.; Lo Gullo, M.A.; Salleo, S. Competitive Strategies for Water Availability in Two Mediterranean *Quercus* Species. *Plant Cell Environ.* **1999**, *22*, 109–116. [CrossRef]
102. Aasamaa, K.; Sõber, A.; Hartung, W.; Niinemets, Ü. Rate of stomatal opening, shoot hydraulic conductance and photosynthetic characteristics in relation to leaf abscisic acid concentration in six temperate deciduous trees. *Tree Physiol.* **2002**, *22*, 267–276. [CrossRef] [PubMed]
103. Li, F.; Zhan, D.; Xu, L.; Han, L.; Zhang, X. Antioxidant and Hormone Responses to Heat Stress in Two Kentucky Bluegrass Cultivars Contrasting in Heat Tolerance. *J. Am. Soc. Hortic. Sci.* **2014**, *139*, 587–596. [CrossRef]
104. Rasulov, B.; Bichele, I.; Laisk, A.; Niinemets, Ü. Competition between Isoprene Emission and Pigment Synthesis during Leaf Development in Aspen. *Plant Cell Environ.* **2014**, *37*, 724–741. [CrossRef]
105. Munné-Bosch, S.; Peñuelas, J.; Asensio, D.; Llusià, J. Airborne Ethylene May Alter Antioxidant Protection and Reduce Tolerance of Holm Oak to Heat and Drought Stress. *Plant Physiol.* **2004**, *136*, 2937–2947. [CrossRef]
106. Weiss, D.; Ori, N.; Smith, R.H. Update on Cross Talk between Gibberellin and Other Hormones Mechanisms of Cross Talk between Gibberellin and Other Hormones. *Plant Physiol.* **2007**, *144*, 1240–1246. [CrossRef]
107. Bates, L.S.; Waldren, R.P.; Teare, I.D. Rapid Determination of Free Proline for Water-Stress Studies. *Plant Soil* **1973**, *39*, 205–207. [CrossRef]
108. Grieve, C.M.; Grattan, S.R. Rapid assay for determination of water soluble quaternary ammonium compounds. *Plant Soil* **1983**, *70*, 303–307. [CrossRef]
109. Stefels, J.; Carnat, G.; Dacey, J.W.H.; Goossens, T.; Elzenga, J.T.M.; Tison, J.L. The Analysis of Dimethylsulfide and Dimethylsulfoniopropionate in Sea Ice: Dry-Crushing and Melting Using Stable Isotope Additions. *Mar. Chem.* **2012**, *128–129*, 34–43. [CrossRef]
110. Hodges, D.M.; DeLong, J.M.; Forney, C.F.; Prange, R.K. Improving the Thiobarbituric Acid-Reactive-Substances Assay for Estimating Lipid Peroxidation in Plant Tissues Containing Anthocyanin and Other Interfering Compounds. *Planta* **1999**, *207*, 604–611. [CrossRef]
111. De Kok, L.J.; Buwalda, F.; Bosma, W. Determination of cysteine and its accumulation in spinach leaf tissue upon exposure to excess sulfur. *J. Plant Physiol.* **1988**, *133*, 502–505. [CrossRef]
112. Miller, N.J.; Rice-Evans, C.A. Factors Influencing the Antioxidant Activity Determined by the $ABTS^{\bullet+}$ Radical Cation Assay. *Free Radic. Res.* **1997**, *26*, 195–199. [CrossRef]
113. Arnao, M.B. Some Methodological Problems in the Determination of Antioxidant Activity Using Chromogen Radicals: A Practical Case. *Trends Food Sci Technol.* **2000**, *11*, 419–421. [CrossRef]
114. Benzie, I.F.F.; Strain, J.J. The Ferric Reducing Ability of Plasma (FRAP) as a Measure of "Antioxidant Power": The FRAP Assay. *Anal. Biochem.* **1996**, *239*, 70–76. [CrossRef]
115. Kim, D.O.; Jeong, S.W.; Lee, C.Y. Antioxidant Capacity of Phenolic Phytochemicals from Various Cultivars of Plums. *Food Chem.* **2003**, *81*, 321–326. [CrossRef]
116. Chang, C.C.; Yang, M.H.; Wen, H.M.; Chern, J.C. Estimation of total flavonoid content in propolis by two complementary colorimetric methods. *J. Food Drug Anal.* **2002**, *10*, 178–182. [CrossRef]
117. Porter, L.J.; Hrstich, L.N.; Chan, B.G. The Conversion of Procyanidins and Prodelphinidins to Cyanidin and Delphinidin. *Phytochemistry* **1985**, *25*, 223–230. [CrossRef]
118. Karthikeyan, R.; Kumaravel, S. Study on Phenolic content, Antioxidant Activity and CHNS elemental analysis of *Amorphophallus sylvaticus*. *Int. J. Agric. Life Sci.* **2016**, *2*, 12–17.
119. Cohen, J.D. Convenient Apparatus for the Generation of Small Amounts of Diazomethane. *J. Chromatogr. A* **1984**, *303*, 193–196. [CrossRef]
120. Ruiz, K.B.; Rapparini, F.; Bertazza, G.; Silva, H.; Torrigiani, P.; Biondi, S. Comparing salt-induced responses at the transcript level in a salares and coastal-lowlands landrace of quinoa (*Chenopodium quinoa* Willd). *Environ. Exp. Bot.* **2017**, *139*, 127–142. [CrossRef]
121. Cohen, J.D.; Baldi, J.P.; Slovin, S.P. A new internal standard for quantitative mass spectral analysis of indole-3-acetic acid in plants. *Plant Physiol.* **1987**, *80*, 14–19. [CrossRef]

plants

MDPI

Article

Are Foliar Nutrition Status and Indicators of Oxidative Stress Associated with Tree Defoliation of Four Mediterranean Forest Species?

Lucija Lovreškov [1], Ivana Radojčić Redovniković [2,*], Ivan Limić [3], Nenad Potočić [1], Ivan Seletković [1], Mia Marušić [1], Ana Jurinjak Tušek [2], Tamara Jakovljević [1,*] and Lukrecija Butorac [3]

[1] Croatian Forest Research Institute, Cvjetno Naselje 41, 10450 Jastrebarsko, Croatia
[2] Faculty of Food Technology and Biotechnology, University of Zagreb, Pierottijeva 6, 10000 Zagreb, Croatia
[3] Institute for Adriatic Crops and Karst Reclamation, Put Duilova 11, 21000 Split, Croatia
* Correspondence: irredovnikovic@pbf.hr (I.R.R.); tamaraj@sumins.hr (T.J.)

Abstract: Mediterranean forest ecosystems in Croatia are of very high significance because of the ecological functions they provide. This region is highly sensitive to abiotic stresses such as air pollution, high sunlight, and high temperatures alongside dry periods; therefore, it is important to monitor the state of these forest ecosystems and how they respond to these stresses. This study was conducted on trees in situ and focused on the four most important forest species in the Mediterranean region in Croatia: pubescent oak (*Quercus pubescens* Willd.), holm oak (*Quercus ilex* L.), Aleppo pine (*Pinus halepensis* Mill.) and black pine (*Pinus nigra* J. F. Arnold.). Trees were selected and divided into two groups: trees with defoliation of >25% (defoliated) and trees with defoliation of ≤25% (undefoliated). Leaves and needles were collected from selected trees. Differences in chlorophyll content, hydrogen peroxide content, lipid peroxidation and enzyme activity (superoxide dismutase, catalase, ascorbate peroxidase, non-specific peroxidase), and nutrient content between the defoliated and undefoliated trees of the examined species were determined. The results showed that there were significant differences for all species between the defoliated and undefoliated trees for at least one of the examined parameters. A principal component analysis showed that the enzyme ascorbate peroxidase can be an indicator of oxidative stress caused by ozone. By using oxidative stress indicators, it is possible to determine whether the trees are under stress even before visual damage occurs.

Keywords: antioxidative enzymes; chlorophyll; defoliated trees; hydrogen peroxide; lipid peroxidation; nutrient concentration; oxidative stress; *Pinus* spp.; *Quercus* spp.; undefoliated trees

Citation: Lovreškov, L.; Radojčić Redovniković, I.; Limić, I.; Potočić, N.; Seletković, I.; Marušić, M.; Jurinjak Tušek, A.; Jakovljević, T.; Butorac, L. Are Foliar Nutrition Status and Indicators of Oxidative Stress Associated with Tree Defoliation of Four Mediterranean Forest Species?. *Plants* **2022**, *11*, 3484. https://doi.org/10.3390/plants11243484

Academic Editor: Aneta Helena Baczewska-Dąbrowska

Received: 31 October 2022
Accepted: 9 December 2022
Published: 13 December 2022

1. Introduction

Various abiotic stresses such as ground-level ozone (O_3), intense drought, and acid compounds strongly limit the growth of plants in the Mediterranean region [1,2]. These ecosystems are affected by the combined influence of local, regional, and long-distance pollution caused by human activities [3–8]. Additionally, these factors tend to be the main cause of the decline in forest vitality and productivity [2,9–12]. For example, abiotic stress caused by ground-level ozone, which is phytotoxic to plants and harmful to humans, can cause chlorosis and necrosis [13,14]. Additionally, nitrogen deposition can have a positive influence on forest productivity but can also cause forest degradation through acidification and nutrient deficiency. Changes to the frequency and intensity of climatic extremes (e.g., heat waves, precipitation, and storms) are also among the various factors that can have a serious impact on forest health and vitality. [4,15,16]. Proper forest monitoring is therefore essential to document their conditions and to investigate the effects of—and relationship with—stress factors [17].

Crown defoliation is a commonly used indicator of acute stress that is defined as the loss of leaves in the assessable crown compared to a reference tree, and it is observed regardless of the cause of foliage loss [18,19]. In field conditions, it is difficult to confirm if defoliation is a consequence of one particular stress factor because many factors simultaneously influence the tree balance [20]. Plants adapt to survive, and the allocation of resources (nutrients) at the cost of losing leaves is one of the known plant defense mechanisms [21]. However, leaf loss is still used as a health indicator in Europe according to the methodology of the International Co-operative Program on Assessment and Monitoring of Air Pollution Effects on Forests (ICP Forests) [18]. One of the main factors of forest health and functioning is the circulation of nutrients between the soil and plants [22]. The concentration of biogenic elements and their relationships in the leaves of forest trees are important indicators of their functioning and provide insight into the state of nutrition. Macronutrients such as nitrogen (N), phosphorus (P), potassium (K), calcium (Ca), and magnesium (Mg) are important parts of plant metabolism. Nitrogen is one of the most important macronutrients required by plants. All proteins that are part of the structure of chlorophyll consist of nitrogen-containing amino acids [23]. Due to its role in the production of chlorophyll and specific proteins such as ribulose-1,5-bisphosphate carboxylase (RuBisCO), which is responsible for the uptake of CO_2, nitrogen is a crucial element for the development of the photosynthetic process and vegetative growth of a plant [23]. Nitrogen deficiency can decrease the photosynthetic activity and longevity of leaves. Generally, nutrient deficiency, a source of abiotic stress, can cause increased hydrogen peroxide (H_2O_2) and lipid peroxidation (LPO) depending on the plant species [24]. Enzyme activity tends to increase as a result of increased H_2O_2 and LPO [24]. Macronutrient deficiencies disrupt plant metabolism and functions including various physiological or metabolic activities that increase the production of reactive oxygen species (ROS) in organisms. The excess production of ROS causes oxidative stress in plants [24]. The lack of these nutrients generally manifests as chlorosis, necrosis, defoliation, and lower growth and productivity, which can eventually lead to plant death [18,25–27]. In such conditions, plant defense mechanisms play a very important role, especially in maintaining the normal functionality and survival of a plant [28]. Changes in the environment trigger plant defense mechanisms, which remove the undesirable products created because of oxidative stress. These products are called ROS, and their production is a consequence of aerobic metabolism [29]. Accumulation of ROS can cause cell damage such as lipid peroxidation (LPO), protein damage, and membrane destruction leading to cell death. These effects manifest themselves in various ways such as leaf yellowing, chlorosis, and necrosis [29,30]. To prevent the damage caused by the oxidation of essential molecules (proteins, DNA, RNA, and lipids) inside a cell, the ROS are neutralized by special molecules, enzymes, and antioxidants. Antioxidant enzymes include superoxide dismutase (SOD), ascorbate peroxidase (APX), catalase (CAT), and peroxidase (POD), which are part of the defense mechanism for removing ROS [25]. The first line of defense is SOD which converts superoxide (O_2^-) to H_2O_2, whereas POD, CAT, and APX decompose H_2O_2 to water (H_2O) [31,32]. The biochemical response of the plant depends on the environment in which it grows, the sources of stress that affect it, and the type of plant [33].

Considering various sources of abiotic stress and the fragility of Mediterranean ecosystems, there is an increasing need to improve the knowledge of Mediterranean forest ecosystems, especially in Croatia where few epidemiological studies have been conducted under Mediterranean field conditions [7,8,34]. This study was focused on four of the most widespread and most important forest tree species of the Mediterranean region: pubescent oak (*Quercus pubescens* Willd.), holm oak (*Quercus ilex* L.), Aleppo pine (*Pinus halepensis* Mill.), and black pine (*Pinus nigra* J. F. Arnold.). We conducted field observations and visual assessment of crown condition (defoliation) and complemented these observations with measurements of stress indicators, including chlorophyll content (Chl), H_2O_2, LPO, and antioxidative enzyme activities, including those of SOD, CAT, POD, and APX. Our aim was to test whether foliar nutrition status and the indicators of oxidative stress were associated

with tree defoliation. Differences in foliar nutrition status and oxidative stress indicators between trees with defoliation of >25% (defoliated) and trees with defoliation of ≤25% (undefoliated) were tested. Furthermore, using a principal component analysis (PCA) we investigated whether the oxidative stress indicators were associated with defoliation and environmental variables to determine if they could be used as early indicators of forest tree health.

2. Results and Discussion

2.1. Foliar Nutrition Status of Four Selected Mediterranean Species

A common problem occurring in the Mediterranean region is nutrient deficiency [35]. Nutrient deficiency is considered an abiotic stress because it can cause irregular plant development, which leads to (among other things) defoliation [36]. For example, Ferretti et al. [37] determined that common beech trees with crown defoliation over 25% have an imbalance of N with K and Ca. Thus, to gain insight into the nutrient status of our examined species, the concentration of nutrients (N, P, K, Ca, and Mg) was determined for selected undefoliated and defoliated trees.

The nutrient concentrations (N, P, K, Ca, and Mg) in the leaves and needles of pubescent oak, holm oak, Aleppo pine, and black pine are shown in Table 1. Plant nutrition was generally in an optimal range with a few exceptions [38]. As expected, we identified significant differences in nutrient concentrations among species. However, regarding holm oak (K) and Aleppo pine trees (Ca and Mg), the nutrient status of the defoliated trees was in the low nutritional range (except for undefoliated trees for Mg) (Table 1).

Table 1. Concentrations of nutrients (N, P, K, Ca, and Mg) in the leaves and needles of pubescent oak, holm oak, Aleppo pine and black pine for defoliated and undefoliated trees. Results are expressed as mean values (n = 3). Values marked in bold show a statistically significant difference between defoliated and undefoliated trees for the same species according to the Student's t-test (* $p < 0.05$). The colors indicate the concentrations of the elements: red—high; green—optimal; yellow—low [38].

Species	Category	N mg g^{-1}	P mg g^{-1}	K mg g^{-1}	Ca mg g^{-1}	Mg mg g^{-1}
Pubescent oak	Undefoliated trees (≤25%)	16.95	1.22	6.62	10.72	1.23
	Defoliated trees (>25%)	16.95	**1.75** *	**7.50** *	**14.66** *	**1.97** *
Holm oak	Undefoliated trees (≤25%)	13.30	0.99	**6.26** *	6.21	1.22
	Defoliated trees (>25%)	12.15	0.99	3.17	6.72	1.42
Aleppo pine	Undefoliated trees (≤25%)	11.14	1.34	3.99	**8.41** *	1.65
	Defoliated trees (>25%)	10.88	1.33	3.96	4.03	1.70
Black pine	Undefoliated trees (≤25%)	10.11	1.20	4.98	**5.24** *	1.30
	Defoliated trees (>25%)	9.69	**1.51** *	**6.36** *	2.52	1.22

A nutrient imbalance can occur due to various external influences on plants [10,36,39]. One of the most phytotoxic abiotic factors today is ozone [10,40]. Nitrogen plays an important role in regulating plant sensitivity to ozone; i.e., with a sufficient amount of the N nutrient, plants can neutralize higher amounts of ozone without causing damage to the plant tissue [41]. The addition of P can cause an increase in tree biomass and an increase in ozone tolerance but only when the amount of nitrogen is low [41]. A study in northern Spain reported that P was higher in more defoliated beech trees [42]. In our study, a significantly higher concentration of P was found in the defoliated pubescent oak trees and black pine trees compared to the undefoliated trees. Furthermore, a previous study on sampled leaves of the Persian oak found that the concentrations of Ca increased with increased drought [43]. Potočić et al. [44] found that drought caused low needle Ca concentrations in Silver fir trees of all defoliation classes. Calcium and K have a common role in the regulation of water in trees [45]. During the dry period, cell division and leaf growth are reduced due to reduced cell turgor. There is also a decrease in the rate of photosynthesis because the intake of CO_2 is limited during drought conditions, which subsequently limits the growth of leaves [43]. Thus, due to the increase in defoliation, the remaining green leaves of trees in categories with higher degrees of defoliation must absorb

a greater amount of Ca to perform vital activities such as photosynthesis. In our study, this same process could be observed in the undefoliated pubescent oak and Aleppo pine trees as a defense mechanism. It is possible that the trees may have also been under stress due to environmental conditions in the Mediterranean region, such as high concentrations of ozone and a large amount of nitrogenous and acidic compounds [7,8,34]. Although the results showed a mostly optimal concentration of nutrients (Table 1), various factors affect the resistance of the examined species, and the concentration of nutrients could not be considered as a potential cause of stress in the tested species.

2.2. Content of Chl, H_2O_2, and MDA in Four Selected Mediterranean Species

Chlorophyll content depends on various sources of abiotic and biotic stresses, such as ozone, atmospheric and soil pollution [46,47], stress intensity and duration [39,46], and plant nutritional status, especially the status of nitrogen as a major component of chlorophyll [23,48]. In our study, the content of chlorophyll a (Chl-a), chlorophyll b (Chl-b) and total chlorophyll (Chl-tot) was determined (Table 2). Different contents of chlorophyll were identified, depending on the species. In oak species, a significantly higher Chl-tot content was found in the undefoliated trees, whereas in black pine, significantly more Chl-tot was found in the defoliated trees. For Chl-a, significant differences were found between the defoliated and undefoliated trees for pubescent oak, holm oak, and black pine. For Chl-b, significant differences were found for holm oak and Aleppo pine. Higher Chl-a, Chl-b, and Chl-tot contents were found in the undefoliated oak trees. However, higher Chl-a, Chl-b, and Chl-tot contents were found in pine defoliated trees.

Table 2. Content of photosynthetic pigments in the leaves and needles (Chl-a, Chl-b, and Chl-tot), hydrogen peroxide (H_2O_2), and malondialdehyde (MDA) of pubescent oak, holm oak, Aleppo pine, and black pine for the defoliated and undefoliated trees. Results are expressed as mean ± SD (n = 3). Values marked in bold show a statistically significant difference between the defoliated and undefoliated trees of a plant species according to the Student's t-test (* $p < 0.05$).

Species	Category	Chl-a μg g^{-1} FW	Chl-b μg g^{-1} FW	Chl-tot μg g^{-1} FW	H_2O_2 nmol g^{-1} FW	MDA nmol g^{-1} FW
Pubescent oak	Undefoliated trees (≤25%)	**1503.93 ± 53.84 ***	366.39 ± 36.32	**1870.32 ± 90.16 ***	44.04 ± 12.88	**84.10 ± 7.33 ***
	Defoliated trees (>25%)	1302.68 ± 57.91	347.22 ± 35.22	1649.90 ± 93.13	39.4 ± 5.67	48.95 ± 4.13
Holm oak	Undefoliated trees (≤25%)	**1673.62 ± 69.47 ***	**466.84 ± 42.40 ***	**2140.46 ± 111.87 ***	0.03 ± 0.01	93.65 ± 7.57
	Defoliated trees (>25%)	1387.09 ± 55.64	357.96 ± 24.75	1745.05 ± 80.39	0.02 ± 0.00	**140.63 ± 6.16 ***
Aleppo pine	Undefoliated trees (≤25%)	406.74 ± 119.81	123.81 ± 25.77	530.55 ± 145.85	0.58 ± 0.09	16.49 ± 3.65
	Defoliated trees (>25%)	562.72 ± 104.72	**250.47 ± 34.61 ***	813.19 ± 139.33	0.61 ± 0.2	**31.60 ± 4.31 ***
Black pine	Undefoliated trees (≤25%)	666.30 ± 23.50	221.35 ± 13.81	887.65 ± 37.31	**0.89 ± 0.21 ***	27.76 ± 5.06
	Defoliated trees (>25%)	**795.59 ± 8.42 ***	241.20 ± 26.52	**1034.79 ± 34.94 ***	0.32 ± 0.06	24.57 ± 4.41

The content of H_2O_2 was only significantly different between the defoliated and undefoliated trees for the black pine species. A higher content of H_2O_2 was found in the undefoliated trees of all species except for the Aleppo pine trees. Furthermore, significantly different contents of MDA were found for all species except black pine. The results showed a higher MDA content in the undefoliated trees of pubescent oak and black pine but a lower MDA content in the undefoliated trees of holm oak and Aleppo pine (Table 2).

In the literature, there have not been many similar studies conducted in field conditions due to the complex relationship between trees and various environmental variables. Most studies were performed in controlled conditions [33,39,47,49]. However, some of the results obtained in this study can be compared to the previous results obtained under controlled conditions.

Studies have found that the content of photosynthetic pigments is affected by the most influential factors in the Mediterranean region: ozone, nutrient deficiency, and drought [33,39,47]. Drought leads to reductions in chlorophyll, especially if other sources of stress, such as ozone, are involved. Furthermore, it was found that during stressful conditions, deciduous species focused on the synthesis of chlorophyll and the maintenance of photosynthesis to create enough energy for reproduction during the growing season [49]. On the other hand, evergreen species were more focused on preservation, which resulted in lower growth (lower photosynthesis), thus suggesting that their goal was leaf survival (up to two years). Therefore, evergreen species invest more energy in extending leaf life and less energy in chlorophyll formation [49]. In our study, significantly lower contents of Chl-a, Chl-b, and Chl-tot were found in the defoliated trees of the holm oak species (Table 2). For the pine species, a significantly higher content of chlorophyll was found in the defoliated trees (Table 2), suggesting that the pine species were investing energy in chlorophyll synthesis. Pines are known to shed their needles as a defense mechanism to protect themselves from drought and other stresses [3,50]. Due to their lack of leaf surface, pines invested energy into the synthesis of chlorophyll to compensate for this loss. Accordingly, higher chlorophyll content was found in the defoliated trees. Nutrients such as nitrogen (one of constituents of chlorophyll) were not considered to cause differences in chlorophyll concentrations between the defoliated and undefoliated trees, as the N concentrations in both tree groups were in the optimal range (Table 1).

Under stress-free conditions, the H_2O_2 that is created inside a cell via cell metabolism serves as a signaling molecule [32]. However, during stressful conditions, H_2O_2 is produced in excessive amounts and causes damage inside cells [29]. The H_2O_2 contents found in our study are listed in Table 2. Significant differences in H_2O_2 contents were determined between the defoliated and undefoliated black pine trees, but the other species did not show any significant differences. Furthermore, H_2O_2 is one of the main precursors of LPO. Lipid peroxidation occurs when damage is caused to the cell membrane as a result of intense oxidative stress and insufficient removal of the ROS [29]. As a consequence of this damage to the lipid membrane, MDA is produced [32]. For holm oak and Aleppo pine, a significantly higher content of MDA was found in the defoliated trees than in the undefoliated trees (Table 2). For pubescent oak, a significantly lower content of MDA was found in the undefoliated than in the defoliated trees. For holm oak and Aleppo pine, significantly greater differences in MDA were found in the defoliated trees than in the undefoliated trees. Interestingly, a significant difference in H_2O_2 content was only found in black pine. Furthermore, no significant difference in MDA content was found for this species, demonstrating that black pine efficiently removed H_2O_2 in both the defoliated and undefoliated trees (Table 2).

A study on holm oak saplings examined the influence of ozone and salinity and demonstrated lipid peroxidation after exposure to the aforementioned sources of stress, revealing significant difference compared with plants that were exposed to one or both sources of stress [2]. Furthermore, the results of research on oak species (*Quercus brantii* Lindl.) showed that an increase in drought stress caused an increase in MDA content and resulted in an increase in Ca content in the leaves [43]. In our study, no significant differences in the content of MDA between the undefoliated and defoliated black pine trees were found, but significant differences were found for all other species. These results indicated that the content of H_2O_2 activated defense mechanisms in the undefoliated trees and that these mechanisms were already activated in the defoliated trees, which resulted in no significant differences in the content of MDA. Our recent research has shown that all the examined species are under oxidative stress due to the high ozone concentrations determined on all four plots [7].

2.3. Activity of Antioxidative Enzymes in Four Selected Mediterranean Species

For the optimal growth and development of a plant in a changing environment, it is essential to neutralize ROS production [25]. The results of enzyme activity in the leaves and needles of the defoliated and undefoliated trees are shown in Figure 1. Significant differences in SOD activity were only found between the undefoliated and defoliated black pine trees. Higher SOD activity was found in the defoliated black pine trees, whereas SOD activity was lower in the undefoliated black pine trees (Figure 1a). CAT activity showed significant differences between the undefoliated and defoliated trees for all species except for the holm oak. The results showed higher CAT activities in the defoliated holm oak and Aleppo pine trees and vice versa for the pubescent oak and black pine trees (Figure 1b). Significant differences in POD activity were only recorded between the undefoliated and defoliated black pine trees. As shown in Figure 1c, higher POD activities were found in the defoliated holm oak and Aleppo pine trees and vice versa for the pubescent oak and black pine trees. Significant differences in APX activity were found between the undefoliated and defoliated trees for all species except for holm oak. Higher APX activities were determined in the undefoliated trees of all species except the holm oak trees (Figure 1d).

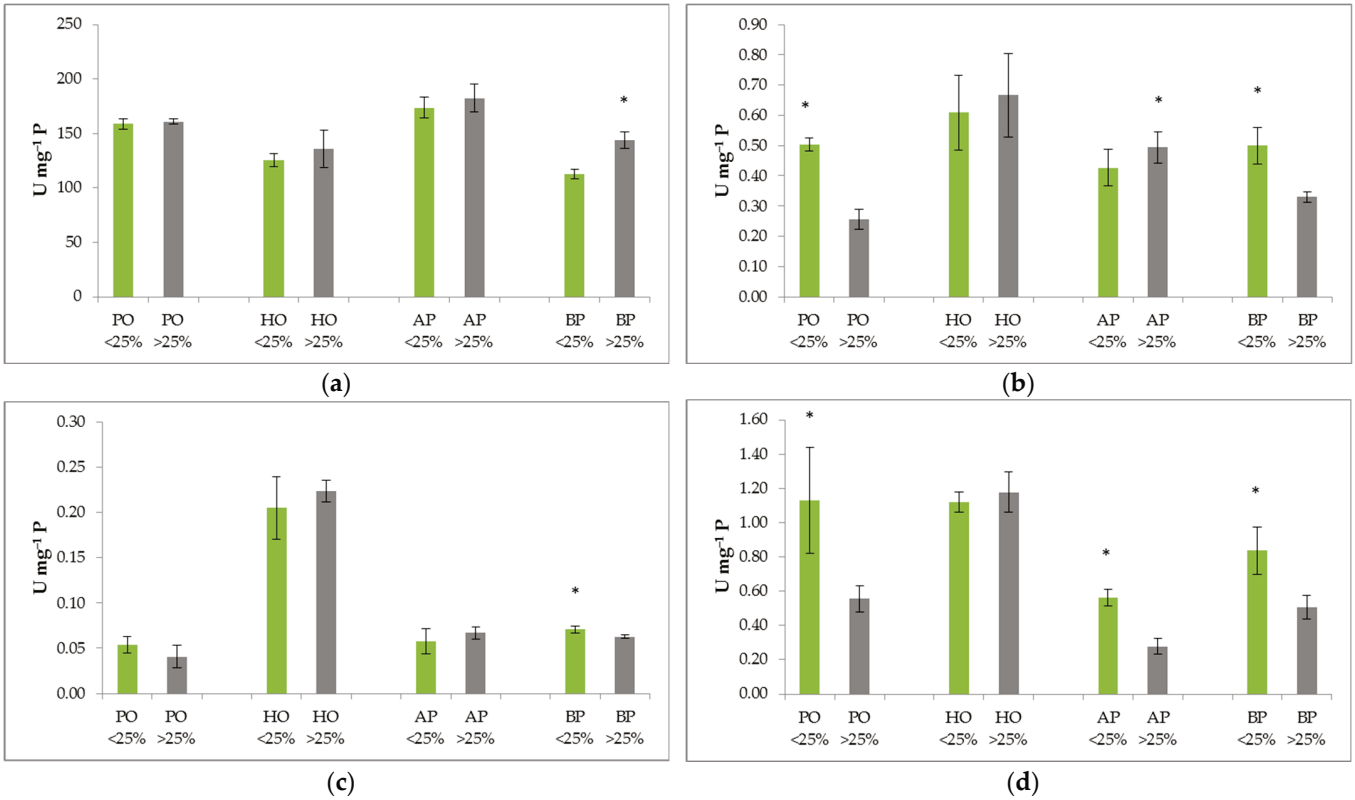

Figure 1. Activity of (**a**) superoxide dismutase (SOD), (**b**) catalase (CAT), (**c**) peroxidase (POD), and (**d**) ascorbate peroxidase (APX) in the leaves and needles of defoliated (defoliation of >25%, grey) and undefoliated (defoliation of ≤25%, green) pubescent oak (PO), holm oak (HO), Aleppo pine (AP), and black pine (BP) trees. Results are expressed as mean ± S. D. (n = 3). Values marked with a star (*) show a statistically significant difference between defoliated and undefoliated trees for a given species according to the Student's t-test (* $p < 0.05$).

In our study, the significant differences in H_2O_2 and SOD activity between the undefoliated and defoliated black pine trees suggest that the main product of ROS is a superoxide radical. Similar conclusions were also drawn during research on the pubescent oak species [33]. The role of the antioxidant enzyme SOD is to directly catalyze superoxide radicals to H_2O_2 [33,51]. In our study, the accumulated H_2O_2 activated the enzymes

CAT, POD, and APX (Figure 1). In a controlled environment, adding ozone to chambers containing the black ash (*Fraxinus ornus* L.) was found to increase the amount of ROS and, consequently, the activity of the SOD and CAT enzymes [52]. In our study, many factors could influence the activation of defense mechanisms in the examined species, such as nitrogen and acidic compounds of atmospheric deposition, high ozone concentrations, and high temperatures [7,8].

According to the obtained results, only the activation of the APX enzyme could be considered an indicator of stress for the examined species. This suggests that the APX enzyme activity could be used to determine whether a plant is under stress even before visual damage occurs. Therefore, it is important to monitor undefoliated trees and defoliated trees to be able to react in a timely manner with the aim of preserving these sensitive forest ecosystems.

2.4. Relationship between Defoliation, Oxidative Stress Indicators, and Environmental Variables

In our previous investigations, we examined the effects of air pollution on the condition of the forest ecosystem by analyzing tree vitality and obtained interesting results [7,8,34]. For example, higher levels of N, acid compounds, and ozone concentrations were measured in dominant forest species along the Adriatic coast [7,8,34]. The highest percentages of defoliated trees were found for the pubescent oak, Aleppo pine, and black pine plots [8]. Based on these findings, the relationship between defoliation, oxidative stress indicators, and environmental variables was tested using a PCA analysis to gain insight into the behavior of an individual species in response to external influences.

A principal component analysis was carried out to analyze the relationship between the spatial distribution patterns of the indicators of oxidative stress and environmental conditions for the four investigated tree species separated into two groups: defoliated and undefoliated trees (Figure 2). In this analysis, the indicators of oxidative stress included APX, CAT, Chl-a, Chl-b, Chl-tot, H_2O_2, MDA, POD, and SOD, whereas the environmental conditions included ozone (O_3), air temperature (T), air relative humidity (RH), solar radiation (Rad) and soil water content at different depths: SWC1 = 0–7 cm, SWC2 = 7–28 cm, SWC3 = 28–100 and SWC > 100 cm, and rain. For the analyzed combinations of variables, the first two principal components (PCs) accounted for 99.99% of the total variance. In Figure 2, the positive correlation between variables is greater when the variable representative points are close to one another and the circle, whereas the negative correlation is greater when the points are distant from the circle's center and the circle. The variable representative points are uncorrelated when they are orthogonal to the center of the circle. Our results show that the correlations between stress indicators and antioxidants, environmental conditions, and soil water content differ for the different tree species and defoliation states. APX (which catalyzes the reduction of H_2O_2 to water) was found to be positively correlated with SWC1 and SWC2, whereas POD was found to be positively correlated with rain and RH in the undefoliated pubescent oak trees. On the other hand, for the defoliated pubescent oak trees, APX was positively correlated with O_3 concentration. Furthermore, for the undefoliated holm oak trees, APX was positively correlated with RH, SWC, Rad, and T; for the undefoliated Aleppo pine trees, APX was positively correlated with SWC1, SWC2, and SWC3; and for the undefoliated black pine trees, APX was positively correlated with O_3 concentration. APX release could be a potential defense mechanism of the selected species against the oxidative stress caused by high ozone concentrations on the examined plots. The separation of SWC4 from the other SWC1-3 variables was due to a difference in water content depending on soil depth and season. In southern Europe, the upper soil layer dries out faster than the deeper layers during the warm and dry seasons [53]. The lack of a clear relationship between the stress indicators and environmental variables of the defoliated and undefoliated trees of the examined species could partially be due to a complex relationship between trees and their surroundings. The PCA revealed that the MDA concentration was positively correlated with O_3 concentration for the undefoliated pubescent oak, holm oak, and black pine trees. The MDA concentration

was also positively correlated with RH and rain for the undefoliated Aleppo pine trees. A plant can reach a state of oxidative stress due to various external influences (biotic and abiotic), and air pollutants are one of the main abiotic factors that cause oxidative stress in forest ecosystems. Therefore, we expected to find differences in the response to oxidative stress because this study was conducted on four different forest species. In this study, the biochemical analysis showed that possible damage could occur. The results of the oxidative stress indicators showed that the examined species were under stress. In field conditions, various sources of stress could cause the activation of defense mechanisms in these four species. Higher chlorophyll content in the undefoliated oak trees suggests an investment of energy into chlorophyll synthesis. More chlorophyll was found in the defoliated pine trees, suggesting the investment of energy into survival. The accumulated H_2O_2 caused lipid peroxidation, which was confirmed by the presence of MDA in all species. The principal component analysis identified different responses depending on the tree species and on the defoliated or undefoliated status.

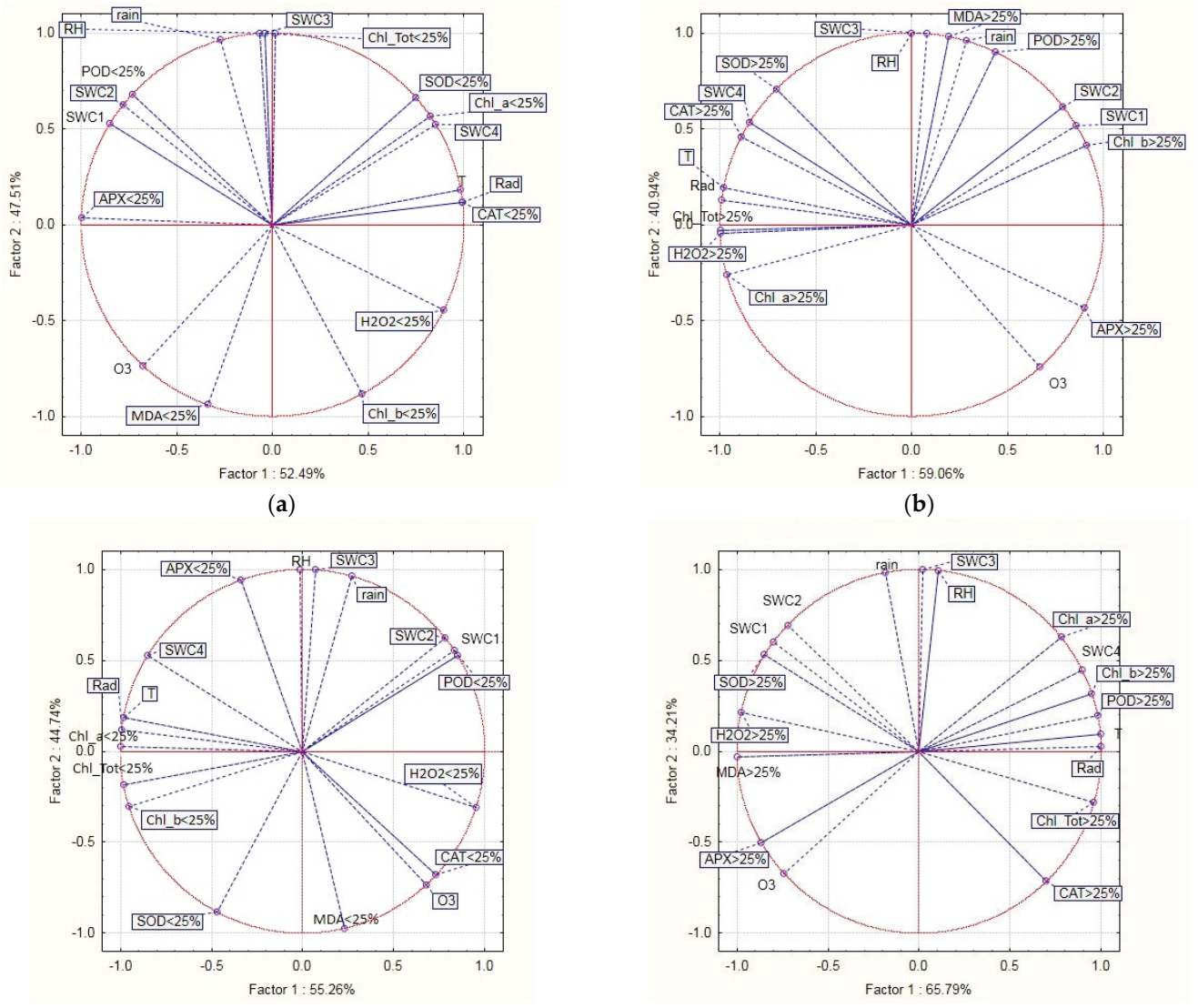

Figure 2. *Cont.*

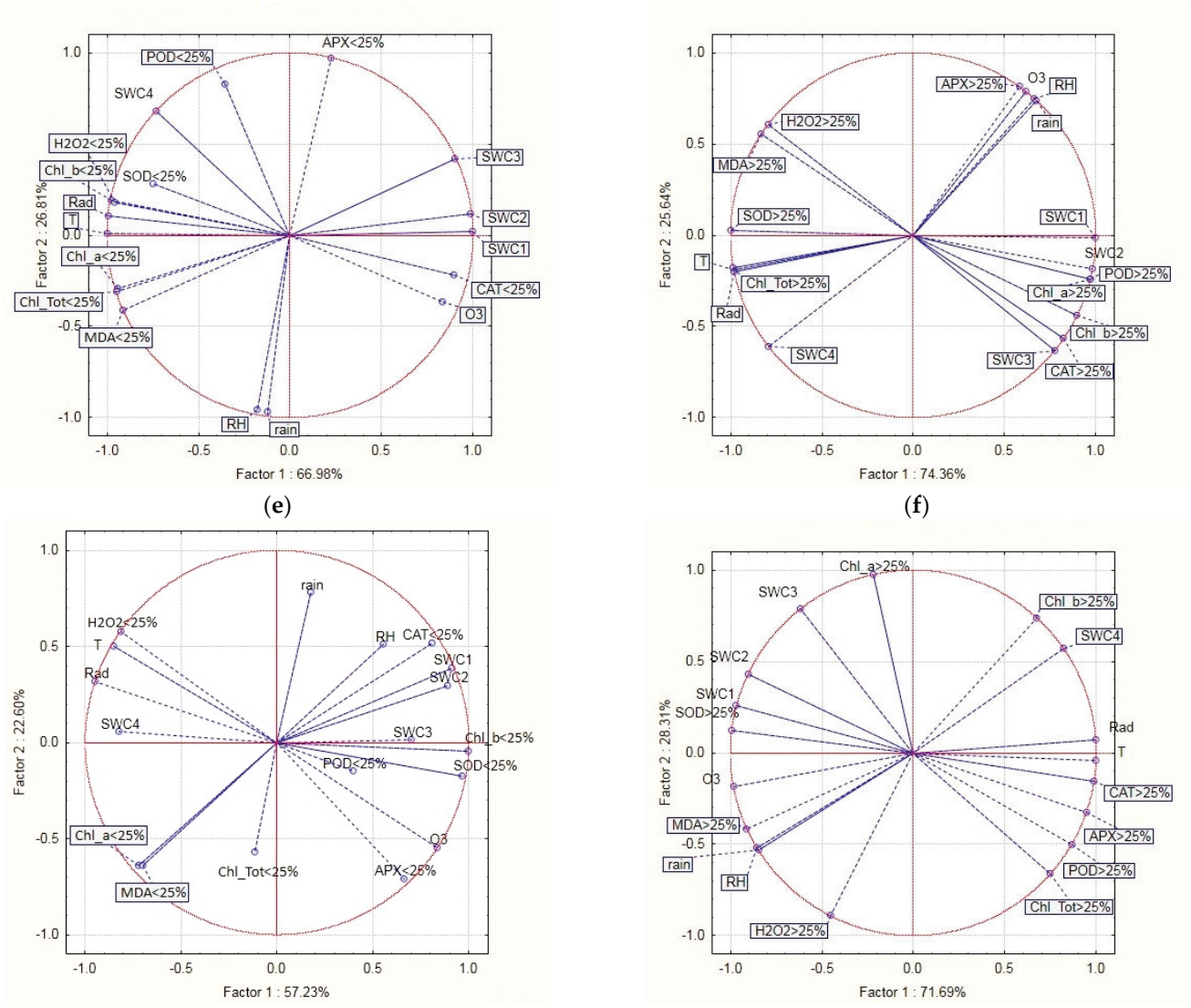

Figure 2. Principal component analysis (PCA) biplot of the physiological data and environmental variables for undefoliated (<25%) and defoliated (>25%) trees in four Mediterranean forest species: (**a**) pubescent oak (<25%); (**b**) pubescent oak (>25%); (**c**) holm oak (<25%); (**d**) holm oak (>25%); (**e**) Aleppo pine (<25%); (**f**) Aleppo pine (>25%); (**g**) black pine (<25%); (**h**) black pine (>25%). APX—ascorbate peroxidase; CAT—catalase; Chl_a—chlorophyll a; Chl_b—chlorophyll b; Chl_Tot—total chlorophyll; H_2O_2—hydrogen peroxide; MDA—malondialdehyde; O_3—ground-level ozone; POD—peroxidase; Rad—solar radiation; rain—rain; RH—relative humidity; SOD—superoxide dismutase; SWC1—soil water content at 0–7 cm; SWC2—soil water content at 7–28 cm; SWC3—soil water content at 28–100 cm; SWC4—soil water content > 100 cm; T—temperature.

3. Materials and Methods

3.1. Selected Plots

Measurements were obtained from different Mediterranean forest ecosystems of the Eastern Adriatic coast in four plots. The most common broadleaf species in this part of the Mediterranean are *Quercus pubescens* Wild. (pubescent oak) and *Quercus ilex* L. (holm oak) in the Istria region and *Pinus halepensis* Mill. (Aleppo pine) and *Pinus nigra* J. F. Arnold. (black pine) in the Dalmatia region [54]. A detailed description of the plots can be found in [7,8].

3.2. Crown Condition Assessment and Collection of Leaves and Needles

The defoliation status of the selected sample trees was assessed annually by trained and experienced personnel in 2017 and 2018 [18]. After the assessment, trees were divided into two categories: defoliated (defoliation > 25%) and undefoliated (defoliation $\leq$ 25%) trees. A threshold of 25% is traditionally used to distinguish between "healthy" and "damaged" trees [18,55]. Defoliation of >25% is also reflected by a distinct change in the functional leaf traits and other indicators of tree health [55]. From these two categories, three trees of each species were randomly selected and sampled. Collected leaves and needles were harvested in late summer when the leaves were fully developed. Leaves were harvested off the upper light-exposed portion of the crown at 2–4 m height [18]. Collected samples were used for analyses of nutrient content and oxidative stress indicators.

3.3. Foliar Nutrition Analysis

Plant samples used in the foliar nutrition analysis were oven-dried at 80 °C for 24 h. Approximately 0.3 g of sub-samples were digested using a mixture of 30% H_2O_2 and 65% HNO_3 for plants and 0.3 g of the elemental analyzer (LECO CNS-2000, St. Joseph, MI, USA) [56]. The concentration of nutrients was determined as follows: N using an elemental analyzer P with a spectrophotometer (LaboMed UV-VIS, Los Angeles, CA, USA) and Ca, P, Mg, and K using an atomic absorption spectrophotometer (Perkin Elmer AAS AAnalyst 700, Waltham, MA, USA) [56].

3.4. Estimation of Chlorophylls

Leaves or needles (0.1 g) were homogenized using a mortar and pestle in 10 mL of chilled 80 % acetone. The chlorophyll extract was refrigerated at 4 °C for 24 h. The samples were then centrifuged at 4000× *g* for 10 min, and the absorbance of the supernatant was measured using a spectrophotometer (LaboMed UV-VIS) at 663 nm and 645 nm. The content of photosynthetic pigments is expressed as µg of photosynthetic pigments per gram of fresh weight of leaves or needles (µg g^{-1} FW) [57].

3.5. Evaluation of Lipid Peroxidation (LPO) and Hydrogen Peroxide (H_2O_2)

Leaves or needles (0.2 g) were homogenized using a mortar and pestle in 2 mL of 0.1% thiobarbituric acid (TBA). The extracts were centrifuged at 10,000× *g* for 20 min, and the resulting supernatants were used to determine lipid peroxidation and H_2O_2.

The level of lipid peroxidation in the leaves and needles of the selected species was evaluated by measuring malondialdehyde (MDA) using the thiobarbituric acid method, which yields a colored product [58]. A mixture of supernatant and 0.5% thiobarbiturate acid (TBA) in 20% trichloroacetic acid (TCA) was heated at 95 °C for 30 min and then cooled in an ice bath. After centrifugation at 10,000× *g* for 10 min, the absorbance of the supernatant was read at 532 nm, and the correction for unspecific turbidity was conducted by subtracting the absorbance at 600 nm on the LaboMed UV-VIS. A total of 0.25% TBA in 10% TCA served as the blank. The MDA content was calculated according to its extinction coefficient of 155 mM^{-1} cm^{-1} and expressed as nmol g^{-1} FW [58,59].

To determine hydrogen peroxide (H_2O_2), a 100 mM potassium phosphate buffer and potassium iodide were added to the supernatant. The absorbance of the mixture was read at 390 nm on the LaboMed UV-VIS. The molar extinction coefficient for H_2O_2 is 0.28 μM^{-1} cm^{-1}, and the amount of H_2O_2 is expressed as µmol per gram of fresh weight of leaves or needles (µmol g^{-1} FW) [58,59].

3.6. Antioxidant Enzyme Extraction and Assay

For the enzyme analysis, 0.2 g of leaves or needles were homogenized in an ice bath with the addition of polyvinyl polypyrrolidone (PVPP) in a 100 mM potassium phosphate (K_2HPO_4/KH_2PO_4) buffer solution, pH 7.0, that included 1 mM EDTA and L-ascorbic acid using a pre-chilled mortar and pestle. The homogenates were centrifuged at 15,000× *g* and

4 °C for 20 min. The supernatant was used for the enzyme activity and protein content assays [59]. All analyses were completed using a LaboMed UV-VIS spectrophotometer.

The total soluble protein contents of the enzyme extracts were estimated according to Bradford [60]. A 40 µL sample of the supernatant was added to 1.2 mL of Bradford reagent followed by incubation in a dark room for 15 min. The absorbance of the supernatant was read at 595 nm. The protein content was expressed in mg protein g^{-1} FW.

The activity of superoxide dismutase (SOD) was determined by measuring the inhibition of the photochemical reduction of nitro blue tetrazolium (NBT) using the method of Beauchamp [61]. An aliquot of enzyme extract was added to a reaction mixture containing a 50 mM potassium phosphate (KPO_4) buffer (pH 7.8), 13 mM methionine, 75 mM NBT, 2 mM riboflavin, and 0.1 mM ethylenediaminetetraacetic acid. The test tubes were shaken, and the enzymatic reaction was started by turning on the 36 W fluorescent lamp. The increase in absorbance due to formazan formation was read at 560 nm. One unit of SOD activity was defined as the amount of enzyme that inhibits the NBT photoreduction by 50%. The activity of SOD is expressed as a unit (U) mg^{-1} protein [59].

The catalase (CAT) activity was determined using the decomposition of H_2O_2 and was measured spectrophotometrically [62]. The decrease in absorbance was assessed at 240 nm in a quartz cuvette. The reaction mixture contained 50 mM KPO_4 buffer (pH 7.0), 10 mM H_2O_2, and an enzyme extract. Catalase activity is expressed as U mg^{-1} protein [58,59].

Ascorbate peroxidase (APX) activity was measured according to the method of Ambriović-Ristov et al. [58]. A suitable enzyme extract aliquot was added to the reaction mixture containing 0.5 mM ascorbate and 0.12 mM H_2O_2 in a 50 mM phosphate buffer (pH 7.0). APX activity was determined according to the decrease in absorbance of ascorbate at 290 nm (ε = 2.8 mM^{-1} cm^{-1}). The activity of APX is expressed as U mg^{-1} protein [59].

The nonspecific peroxidase (POD) activity was measured according to the method of Chance and Maehly [63]. The reaction mixture contained a 50 mM phosphate buffer (pH 7), 5 mM H_2O_2, 18 mM guaiacol, and a suitable enzyme extract aliquot. POD activity was estimated according to the increase in the absorbance of oxiguaiacol at 470 nm (ε = 26.6 mM^{-1} cm^{-1}) and is expressed as U mg^{-1} protein [59].

3.7. Statistical Analysis

Data were analyzed using the STATISTICA software (version 10.0, StatSoft Inc., Tulsa, OK, USA, 2011). The results presented are the mean ± SD. Differences between the means were analyzed using an ANOVA followed by the post hoc Tukey's test. A significant difference was considered at the level of $p < 0.05$. Prior to the statistical analysis, the normality of the data was evaluated using the Kolmogorov–Smirnov test implemented in STATISTICA. The *p*-values of the analyzed datasets were not significant, so the assumption of normality was accepted. The homogeneity of variance was assessed using the Levene's test implemented in STATISTICA. The *p*-values of the analyzed datasets were higher than 0.05, indicating a homogeneity of variance. Data in the text, Tables and Figures were expressed as mean ± standard deviation (±SD), and error bars in the Figures indicate standard deviation. A principal component analysis (PCA) was carried out to identify the parameters that best describe the physiological performance of oxidative stress upon environmental conditions for the four tree species divided into defoliated (defoliation > 25%) and undefoliated trees using the STATISTICA software. Environmental data (i.e., ozone (O_3), air temperature (T), air relative humidity (RH), solar radiation (Rad) and soil water content at different depths: SWC1 = 0–7 cm, SWC2 = 7–28 cm, SWC3 = 28–100 and SWC > 100 cm, and rain) were derived from ERA5 [64]. The variables were extracted from the gridded ERA5 dataset with a spatial resolution of about 33 km at the site location using bilinear interpolation.

4. Conclusions

This study focused on the oxidative stress indicators in four Mediterranean forest species. Considering the presence of ROS due to the stressful conditions present in the field, we found significant differences at the leaf level for all species between the defoliated

and undefoliated trees for at least one of the examined parameters. After examining the biochemical indicators of oxidative stress, it is possible to determine whether a tree is in a state of stress before visual damage occurs. It was difficult to conclude which factors influenced the activation of the defense mechanisms of the examined species due to the small number of published studies carried out in the field and due to the many variables that can simultaneously affect a plant. Due to the small number of studies in the field and due to the many variables, that can simultaneously affect a plant, it is difficult to conclude which factors influenced the activation of the defense mechanisms of the examined species, and more studies like this are highly desirable. The long-term, field-based monitoring of environmental variables and forest health indicators at the same time could provide insight into the behavior of an individual species in response to external influences.

Author Contributions: Conceptualization, L.L., I.R.R. and T.J.; methodology, L.L., I.R.R., T.J., L.B., N.P. and I.S.; formal analysis, L.L., I.L. and A.J.T.; investigation, L.L.; resources, T.J.; writing—original draft preparation, L.L.; writing—review and editing, L.L., I.R.R., T.J., A.J.T., L.B., I.L., N.P., I.S. and M.M.; visualization, L.L. and A.J.T.; supervision, I.R.R. and T.J.; project administration, T.J. All authors have read and agreed to the published version of the manuscript.

Funding: This research was fully supported by the Croatian Science Foundation under the project IP-2016-06-3337 "Assessment of Atmospheric Deposition and Ozone levels in Mediterranean Forest ecosystems (DepOMedFor)". The work of PhD students Lucija Lovreškov and Ivan Limić has been fully supported by the "Young researchers' career development project—training of doctoral students" of the Croatian Science Foundation funded by the European Union from the European Social Fund.

Data Availability Statement: Not applicable.

Acknowledgments: We are grateful to all the operators who performed sampling in the field and analyses in the laboratory, particularly Dragan Jakšić, Monika Hlebić, and Renata Tubikanec from the Croatian Forest Research Institute for their activity in the laboratory.

Conflicts of Interest: The authors declare no conflict of interest.

References

1. Cuttelod, A.; García, N.; Malak, D.A.; Temple, H.J.; Katariya, V. The Mediterranean: A Biodiversity Hotspot under Threat. In *Wildlife in a Changing World—An Analysis of the 2008 IUCN Red List of Threatened Species*; IUCN: Gland, Switzerland, 2009; Volume 89, p. 9.
2. Guidi, L.; Remorini, D.; Cotrozzi, L.; Giordani, T.; Lorenzini, G.; Massai, R.; Nali, C.; Natali, L.; Pellegrini, E.; Trivellini, A.; et al. The Harsh Life of an Urban Tree: The Effect of a Single Pulse of Ozone in Salt-Stressed *Quercus ilex* Saplings. *Tree Physiol.* **2017**, *37*, 246–260. [CrossRef] [PubMed]
3. Sicard, P.; Dalstein-Richier, L. Health and Vitality Assessment of Two Common Pine Species in the Context of Climate Change in Southern Europe. *Environ. Res.* **2015**, *137*, 235–245. [CrossRef] [PubMed]
4. de Vries, W.; Dobbertin, M.H.; Solberg, S.; van Dobben, H.F.; Schaub, M. Impacts of Acid Deposition, Ozone Exposure and Weather Conditions on Forest Ecosystems in Europe: An Overview. *Plant Soil* **2014**, *380*, 1–45. [CrossRef]
5. Šiljković, Ž.; Mamut, M. Forest Fires in Dalmatia. *Bull. Geogr. Socio-Econ. Ser.* **2016**, *32*, 117–130. [CrossRef]
6. Anav, A.; De Marco, A.; Friedlingstein, P.; Savi, F.; Sicard, P.; Sitch, S.; Vitale, M.; Paoletti, E. Growing Season Extension Affects Ozone Uptake by European Forests. *Sci. Total Environ.* **2019**, *669*, 1043–1052. [CrossRef] [PubMed]
7. Jakovljević, T.; Lovreškov, L.; Jelić, G.; Anav, A.; Popa, I.; Fornasier, M.F.; Proietti, C.; Limić, I.; Butorac, L.; Vitale, M.; et al. Impact of Ground-Level Ozone on Mediterranean Forest Ecosystems Health. *Sci. Total Environ.* **2021**, *783*, 147063. [CrossRef]
8. Jakovljević, T.; Marchetto, A.; Lovreškov, L.; Potočić, N.; Seletković, I.; Indir, K.; Jelić, G.; Butorac, L.; Zgrablić, Ž.; De Marco, A.; et al. Assessment of Atmospheric Deposition and Vitality Indicators in Mediterranean Forest Ecosystems. *Sustainability* **2019**, *11*, 6805. [CrossRef]
9. Allen, C.D.; Macalady, A.K.; Chenchouni, H.; Bachelet, D.; McDowell, N.; Vennetier, M.; Kitzberger, T.; Rigling, A.; Breshears, D.D.; Hogg, E.H.; et al. A Global Overview of Drought and Heat-Induced Tree Mortality Reveals Emerging Climate Change Risks for Forests. *For. Ecol. Manag.* **2010**, *259*, 660–684. [CrossRef]
10. Proietti, C.; Anav, A.; De Marco, A.; Sicard, P.; Vitale, M. A Multi-Sites Analysis on the Ozone Effects on Gross Primary Production of European Forests. *Sci. Total Environ.* **2016**, *556*, 1–11. [CrossRef]
11. Zhang, L.; Hoshika, Y.; Carrari, E.; Cotrozzi, L.; Pellegrini, E.; Paoletti, E. Effects of Nitrogen and Phosphorus Imbalance on Photosynthetic Traits of Poplar Oxford Clone under Ozone Pollution. *J. Plant Res.* **2018**, *131*, 915–924. [CrossRef]

12. Cotrozzi, L.; Remorini, D.; Pellegrini, E.; Landi, M.; Massai, R.; Nali, C.; Guidi, L.; Lorenzini, G. Variations in Physiological and Biochemical Traits of Oak Seedlings Grown under Drought and Ozone Stress. *Physiol. Plant.* **2016**, *157*, 69–84. [CrossRef] [PubMed]
13. De Marco, A.; Proietti, C.; Anav, A.; Ciancarella, L.; D'Elia, I.; Fares, S.; Fornasier, M.F.; Fusaro, L.; Gualtieri, M.; Manes, F.; et al. Impacts of Air Pollution on Human and Ecosystem Health, and Implications for the National Emission Ceilings Directive: Insights from Italy. *Environ. Int.* **2019**, *125*, 320–333. [CrossRef] [PubMed]
14. Sicard, P.; Augustaitis, A.; Belyazid, S.; Calfapietra, C.; de Marco, A.; Fenn, M.; Bytnerowicz, A.; Grulke, N.; He, S.; Matyssek, R.; et al. Global Topics and Novel Approaches in the Study of Air Pollution, Climate Change and Forest Ecosystems. *Environ. Pollut.* **2016**, *213*, 977–987. [CrossRef] [PubMed]
15. Alonso, R.; Elvira, S.; González-Fernández, I.; Calvete, H.; García-Gómez, H.; Bermejo, V. Drought Stress Does Not Protect *Quercus ilex* L. from Ozone Effects: Results from a Comparative Study of Two Subspecies Differing in Ozone Sensitivity. *Plant Biol.* **2014**, *16*, 375–384. [CrossRef] [PubMed]
16. Proietti, C.; Fornasier, M.F.; Sicard, P.; Anav, A.; Paoletti, E.; De Marco, A. Trends in Tropospheric Ozone Concentrations and Forest Impact Metrics in Europe over the Time Period 2000–2014. *J. For. Res.* **2021**, *32*, 543–551. [CrossRef]
17. Ferretti, M.; Fischer, R. *Forest Monitoring: Methods for Terrestrial Investigations in Europe with an Overview of North America and Asia*; Ferretti, M., Fischer, R., Eds.; Newnes: Oxford, UK, 2013.
18. Eichhorn, J.; Roskams, P.; Potočic, N.; Timmermann, V.; Ferretti, M.; Mues, V.; Szepesi, A.; Durrant, D.; Seletković, I.; Schröck, H.; et al. Part IV: Visual Assessment of Crown Condition and Damaging Agents. In *Manual on Methods and Criteria for Harmonized Sampling, Assessment, Monitoring and Analysis of the Effects of Air Pollution on Forests*; Thünen Institute of Forest Ecosystems: Eberswalde, Germany, 2020; p. 49 + Annex.
19. Landmann, G. Forest Decline and Air Pollution Effects in the French Mountains: A Synthesis. In *Forest Decline and Atmospheric Deposition Effects in the French Mountains*; Springer: Berlin/Heidelberg, Germany, 1995; pp. 407–452.
20. Johnson, J.; Jacob, M. Monitoring the Effects of Air Pollution on Forest Condition in Europe: Is Crown Defoliation an Adequate Indicator? *iForest-Biogeosci. For.* **2010**, *3*, 86–88. [CrossRef]
21. Le Roncé, I.; Toïgo, M.; Dardevet, E.; Venner, S.; Limousin, J.-M.; Chuine, I. Resource Manipulation through Experimental Defoliation Has Legacy Effects on Allocation to Reproductive and Vegetative Organs in *Quercus ilex*. *Ann. Bot.* **2020**, *126*, 1165–1179. [CrossRef]
22. Braun, S.; Schindler, C.; Rihm, B. Foliar Nutrient Concentrations of European Beech in Switzerland: Relations with Nitrogen Deposition, Ozone, Climate and Soil Chemistry. *Front. For. Glob. Chang.* **2020**, *3*, 33. [CrossRef]
23. Wang, N.; Fu, F.; Wang, H.; Wang, P.; He, S.; Shao, H.; Ni, Z.; Zhang, X. Effects of Irrigation and Nitrogen on Chlorophyll Content, Dry Matter and Nitrogen Accumulation in Sugar Beet (*Beta vulgaris* L.). *Sci. Rep.* **2021**, *11*, 16651. [CrossRef]
24. Tewari, R.K.; Yadav, N.; Gupta, R.; Kumar, P. Oxidative Stress Under Macronutrient Deficiency in Plants. *J. Soil Sci. Plant Nutr.* **2021**, *21*, 832–859. [CrossRef]
25. Bhatla, S.C.; Lal, M.A. *Plant Physiology, Development and Metabolism*; Springer: New Delhi, India, 2018; ISBN 9811320233.
26. Guo, W.; Nazim, H.; Liang, Z.; Yang, D. Magnesium Deficiency in Plants: An Urgent Problem. *Crop J.* **2016**, *4*, 83–91. [CrossRef]
27. Jonard, M.; Fürst, A.; Verstraeten, A.; Thimonier, A.; Timmermann, V.; Potočić, N.; Waldner, P.; Benham, S.; Hansen, K.; Merilä, P.; et al. Tree Mineral Nutrition Is Deteriorating in Europe. *Glob. Chang. Biol.* **2015**, *21*, 418–430. [CrossRef] [PubMed]
28. Hasanuzzaman, M.; Bhuyan, M.H.M.B.; Zulfiqar, F.; Raza, A.; Mohsin, S.M.; Al Mahmud, J.; Fujita, M.; Fotopoulos, V. Reactive Oxygen Species and Antioxidant Defense in Plants under Abiotic Stress: Revisiting the Crucial Role of a Universal Defense Regulator. *Antioxidants* **2020**, *9*, 681. [CrossRef] [PubMed]
29. Sharma, P.; Jha, A.B.; Dubey, R.S.; Pessarakli, M. Reactive Oxygen Species, Oxidative Damage, and Antioxidative Defense Mechanism in Plants under Stressful Conditions. *J. Bot.* **2012**, *2012*, 217037. [CrossRef]
30. Schwanz, P.; Polle, A. Antioxidative Systems, Pigment and Protein Contents in Leaves of Adult Mediterranean Oak Species (*Quercus pubescens* and *Q. ilex*) with Lifetime Exposure to Elevated CO_2. *New Phytol.* **1998**, *140*, 411–423. [CrossRef]
31. Gill, S.S.; Anjum, N.A.; Gill, R.; Yadav, S.; Hasanuzzaman, M.; Fujita, M.; Mishra, P.; Sabat, S.C.; Tuteja, N. Superoxide Dismutase—Mentor of Abiotic Stress Tolerance in Crop Plants. *Environ. Sci. Pollut. Res.* **2015**, *22*, 10375–10394. [CrossRef]
32. Gill, S.S.; Tuteja, N. Reactive Oxygen Species and Antioxidant Machinery in Abiotic Stress Tolerance in Crop Plants. *Plant Physiol. Biochem.* **2010**, *48*, 909–930. [CrossRef]
33. Contran, N.; Günthardt-Goerg, M.S.; Kuster, T.M.; Cerana, R.; Crosti, P.; Paoletti, E. Physiological and Biochemical Responses of *Quercus pubescens* to Air Warming and Drought on Acidic and Calcareous Soils. *Plant Biol.* **2013**, *15*, 157–168. [CrossRef]
34. Lovreškov, L.; Limić, I.; Butorac, L.; Jakovljević, T. Nitrogen Deposition in Different Mediterranean Forest Types along the Eastern Adriatic Coast. *South-East Eur. For.* **2021**, *12*, 115–122. [CrossRef]
35. Bobbink, R.; Hettelingh, J.P. Effects of Nitrogen Deposition on Woodland, Forest and Other Wooded Land (EUNIS Class G). In *Review and Revision of Empirical Critical Loads and Dose–Response Relationships*; RIVM Report 680359002; National Institute for Public Health and the Environment: Bilthoven, The Netherlands, 2011; pp. 135–171.
36. Taiz, L.; Zeiger, E.; Møller, I.M.; Murphy, A. *Plant Physiology and Development*; Sinauer Associates Incorporated: New York, NY, USA, 2018; ISBN 9781605357454.

37. Ferretti, M.; Calderisi, M.; Marchetto, A.; Waldner, P.; Thimonier, A.; Jonard, M.; Cools, N.; Rautio, P.; Clarke, N.; Hansen, K.; et al. Variables Related to Nitrogen Deposition Improve Defoliation Models for European Forests. *Ann. For. Sci.* **2015**, *72*, 897–906. [CrossRef]
38. Fürst, A.; Kowalska, A.; Brunialti, G.; Clarke, N.; Cools, N.; De Vos, B.; Derome, J.; Derome, K.; Ferretti, M.; Jakovljević, T.; et al. Part XVI: Quality Assurance and Control in Laboratories. In *Manual on Methods and Criteria for Harmonized Sampling, Assessment, Monitoring and Analysis of the Effects of Air Pollution on Forests*; Thünen Institute of Forest Ecosystems: Eberswalde, Germany, 2020; p. 48.
39. Cotrozzi, L.; Pellegrini, E.; Guidi, L.; Landi, M.; Lorenzini, G.; Massai, R.; Remorini, D.; Tonelli, M.; Trivellini, A.; Vernieri, P.; et al. Losing the Warning Signal: Drought Compromises the Cross-Talk of Signaling Molecules in *Quercus ilex* Exposed to Ozone. *Front. Plant Sci.* **2017**, *8*, 1020. [CrossRef] [PubMed]
40. Cailleret, M.; Ferretti, M.; Gessler, A.; Rigling, A.; Schaub, M. Ozone Effects on European Forest Growth—Towards an Integrative Approach. *J. Ecol.* **2018**, *106*, 1377–1389. [CrossRef]
41. Zhang, L.; Hoshika, Y.; Carrari, E.; Badea, O.; Paoletti, E. Ozone Risk Assessment Is Affected by Nutrient Availability: Evidence from a Simulation Experiment under Free Air Controlled Exposure (FACE). *Environ. Pollut.* **2018**, *238*, 812–822. [CrossRef] [PubMed]
42. Amores, G.; Bermejo, R.; Elustondo, D.; Lasheras, E.; Santamaría, J.M. Nutritional Status of Northern Spain Beech Forests Wate 4915. *Water. Air. Soil Pollut.* **2006**, *177*, 227–238. [CrossRef]
43. Azim Nejad, Z.; Badehian, Z.; Rezaei Nejad, A.; Bazot, S. Do Soil Properties and Ecophysiological Responses of Oak (*Quercus brantii* Lindl.) Correlate with the Rate of Dieback? *Trees* **2021**, *35*, 1639–1650. [CrossRef]
44. Potočić, N.; Ćosić, T.; Pilaš, I. The Influence of Climate and Soil Properties on Calcium Nutrition and Vitality of Silver Fir (*Abies alba* Mill.). *Environ. Pollut.* **2005**, *137*, 596–602. [CrossRef] [PubMed]
45. Raghavendra, A.S. *Photosynthesis: A Comprehensive Treatise*; Raghavendra, A.S., Ed.; Cambridge University Press: Cambridge, UK, 2000.
46. Agathokleous, E.; Feng, Z.; Peñuelas, J. Chlorophyll Hormesis: Are Chlorophylls Major Components of Stress Biology in Higher Plants? *Sci. Total Environ.* **2020**, *726*, 138637. [CrossRef]
47. Landi, M.; Cotrozzi, L.; Pellegrini, E.; Remorini, D.; Tonelli, M.; Trivellini, A.; Nali, C.; Guidi, L.; Massai, R.; Vernieri, P.; et al. When "Thirsty" Means "Less Able to Activate the Signalling Wave Trigged by a Pulse of Ozone": A Case of Study in Two Mediterranean Deciduous Oak Species with Different Drought Sensitivity. *Sci. Total Environ.* **2019**, *657*, 379–390. [CrossRef]
48. Bassi, D.; Menossi, M.; Mattiello, L. Nitrogen Supply Influences Photosynthesis Establishment along the Sugarcane Leaf. *Sci. Rep.* **2018**, *8*, 2327. [CrossRef]
49. Takashima, T.; Hikosaka, K.; Hirose, T. Photosynthesis or Persistence: Nitrogen Allocation in Leaves of Evergreen and Deciduous Quercus Species. *Plant Cell Environ.* **2004**, *27*, 1047–1054. [CrossRef]
50. Poyatos, R.; Aguadé, D.; Galiano, L.; Mencuccini, M.; Martínez-Vilalta, J. Drought-Induced Defoliation and Long Periods of near-Zero Gas Exchange Play a Key Role in Accentuating Metabolic Decline of Scots Pine. *New Phytol.* **2013**, *200*, 388–401. [CrossRef] [PubMed]
51. Mittler, R.; Vanderauwera, S.; Gollery, M.; Van Breusegem, F. Reactive Oxygen Gene Network of Plants. *Trends Plant Sci.* **2004**, *9*, 490–498. [CrossRef] [PubMed]
52. Fusaro, L.; Palma, A.; Salvatori, E.; Basile, A.; Maresca, V.; Asadi Karam, E.; Manes, F. Functional Indicators of Response Mechanisms to Nitrogen Deposition, Ozone, and Their Interaction in Two Mediterranean Tree Species. *PLoS ONE* **2017**, *12*, e0185836. [CrossRef] [PubMed]
53. Anav, A.; Proietti, C.; Menut, L.; Carnicelli, S.; De Marco, A.; Paoletti, E. Sensitivity of Stomatal Conductance to Soil Moisture: Implications for Tropospheric Ozone. *Atmos. Chem. Phys.* **2018**, *18*, 5747–5763. [CrossRef]
54. Prpić, B.; Pernar, R.; Jurjević, P.; Milković, I.; Vrebčević, M.; Petreš, S. Kartiranje Općekorisnih Funkcija Šuma u Sredozemlju. In *Šume Hrvatskog Sredozemlja*; Matić, S., Ed.; Akademija Šumarskih Znanosti: Zagreb, Croatia, 2011; pp. 288–294. ISBN 978-953-985715-6.
55. Gottardini, E.; Cristofolini, F.; Cristofori, A.; Pollastrini, M.; Camin, F.; Ferretti, M. A Multi-Proxy Approach Reveals Common and Species-Specific Features Associated with Tree Defoliation in Broadleaved Species. *For. Ecol. Manag.* **2020**, *467*, 118151. [CrossRef]
56. Rautio, P.; Fürst, A.; Stefan, K.; Raitio, H.; Bartels, U. Part XII: Sampling and Analysis of Needles and Leaves. In *Manual on Methods and Criteria for Harmonized Sampling, Assessment, Monitoring and Analysis of the Effects of Air Pollution on Forests*; Thünen Institute of Forest Ecosystems: Eberswalde, Germany, 2020; p. 19.
57. Arnon, D.I. Copper Enzymes in Isolated Chloroplasts. Polyphenoloxidase in Beta Vulgaris. *Plant Physiol.* **1949**, *24*, 1–15. [CrossRef]
58. Ambriović-Ristov, A.; Brozović, A.; Bruvo Mađarić, B.; Ćetković, H.; Herak Bosnar, M.; Hranilović, D.; Katušić Hećimović, S.; Meštrović Radan, N.; Mihaljević, S.; Slade, N.; et al. *Metode u Molekularnoj Biologiji*; Institut Ruđer Bošković: Zagreb, Croatia, 2007; ISBN 9789536690725.
59. Radojčić Redovniković, I.; De Marco, A.; Proietti, C.; Hanousek, K.; Sedak, M.; Bilandžić, N.; Jakovljević, T. Poplar Response to Cadmium and Lead Soil Contamination. *Ecotoxicol. Environ. Saf.* **2017**, *144*, 482–489. [CrossRef]
60. Bradford, M.M. A Rapid and Sensitive Method for the Quantitation of Microgram Quantities of Protein Utilizing the Principle of Protein-Dye Binding. *Anal. Biochem.* **1976**, *72*, 248–254. [CrossRef]
61. Beauchamp, C.; Fridovich, I. Superoxide Dismutase: Improved Assays and an Assay Applicable to Acrylamide Gels. *Anal. Biochem.* **1971**, *44*, 276–287. [CrossRef]

62. Aebi, H. Catalase in Vitro. In *Methods in Enzymology*; Elsevier: Amsterdam, The Netherlands, 1984; Volume 105, pp. 121–126, ISBN 0076-6879.
63. Chance, B.; Maehly, A.C. Assay of Catalases and Peroxidases. In *Methods in Enzymology*; Academic Press: New York, NY, USA, 1955; Volume 2, pp. 764–775, ISBN 0076-6879.
64. Hersbach, H.; Bell, B.; Berrisford, P.; Hirahara, S.; Horányi, A.; Muñoz-Sabater, J.; Nicolas, J.; Peubey, C.; Radu, R.; Schepers, D.; et al. The ERA5 Global Reanalysis. *Q. J. R. Meteorol. Soc.* **2020**, *146*, 1999–2049. [CrossRef]

plants

MDPI

Article

Dynamics Changes in Basal Area Increment, Carbon Isotopes Composition and Water Use Efficiency in Pine as Response to Water and Heat Stress in Silesia, Poland

Barbara Sensuła [1,*] and Sławomir Wilczyński [2]

[1] Institute of Physics-Center for Science and Education, The Silesian University of Technology, Konarskiego 22B, 44-100 Gliwice, Poland
[2] Department of Forest Ecosystem Protection, the University of Agriculture in Krakow, Al. 29 Listopada 46, 31-425 Kraków, Poland
* Correspondence: barbara.sensula@polsl.pl; Tel.: +48-322372035

Abstract: Trees can be used as archives of changes in the environment. In this paper, we present the results of the analysis of the impact of water stress and increase in air temperature on BAI and carbon stable isotopic composition and water use efficiency of pine. Dendrochronological methods together with mass spectrometry techniques give a possibility to conduct a detailed investigation of pine growing in four industrial forests in Silesia (Poland). Detailed analysis-based bootstrap and moving correlation between climatic indices (temperature, precipitation, and Standardized Precipitation-Evapotranspiration Index) and tree parameters give the chance to check if the climatic signals recorded by trees can be hidden or modified over a longer period of time. Trees have been found to be very sensitive to weather conditions, but their sensitivity can be modified and masked by the effect of pollution. Scots pine trees at all sites systematically increased the basal area increment (BAI) and the intrinsic water use efficiency (iWUE) and decreased $\delta^{13}C$ in the last century. Furthermore, their sensitivity to the climatic factor remained at a relatively high level. Industrial pollution caused a small reduction in the wood growth of pines and an increase in the heterogeneity of annual growth responses of trees. The main factors influencing the formation of wood in the pines were thermal conditions in the winter season and pluvial conditions in the previous autumn, and also in spring and summer in the year of tree ring formation. The impact of thermal and pluvial conditions in the year of tree ring formation has also been reflected in the isotopic composition of tree rings and water use efficiency. Three different scenarios of trees' reaction link to the reduction of stomata conductance or changes in photosynthesis rate as the response to climate changes in the last 40 years have been proposed.

Keywords: pine; BAI; isotopes; iWUE; water and thermal stress; SPEI; Poland

Citation: Sensuła, B.; Wilczyński, S. Dynamics Changes in Basal Area Increment, Carbon Isotopes Composition and Water Use Efficiency in Pine as Response to Water and Heat Stress in Silesia, Poland. *Plants* **2022**, *11*, 3569. https://doi.org/10.3390/plants11243569

Academic Editor: Nenad Potočić

Received: 29 October 2022
Accepted: 6 December 2022
Published: 17 December 2022

1. Introduction

In recent decades, it has been observed that a significant problem of increase in temperature and decrease in precipitation is responsible for the drought period in most ecosystems all around the world. Scientists have used many different indices and different archives have been examined to monitor the impact of water stress on forest stands [1–8]. Pines and their tree ring properties can be used as archives of the change in the environment in which the tree has been growing. The climatic changes and the anthropogenic effect can be recorded, e.g., in the width of the tree ring, and its isotopic and elemental composition [1–13].

It is well-known that the influence of seasonal fluctuation in temperature and water stress, which reduces the stomata conductance, changes the photosynthetic rates, and has an impact on tree-ring width, stable isotopic composition, and thus on water use efficiency. Several models of stable carbon isotope variation during photosynthesis (e.g., [3])

describe fractionation that occurs due to diffusion in air and stomatal conductance, and fractionation caused by carboxylation (discrimination by RuBisCO). The pathway and associated fractionation of carbon isotopes in CO_2 during photosynthesis and respiration have been described in detail [2,3,6,12,13]. Through photosynthesis, plants convert CO_2 and H_2O to saccharides $(C_6H_{12}O_6)_n$, using light, and release oxygen into the atmosphere. Tree adaptation and its sensitivity to climate change can be studied using statistical methods, including bootstrap correlation and moving correlation functions [11,14]. The comparison of dynamic variation in tree ring width and stable carbon isotopic composition, and thus in the relationship between stomata conductance (g) and photosynthesis rate (A), and thus in water use efficiency iWUE (iWUE = A/g) of trees with variability of climatic factors examines how trees react and adapt to climate changes, including water stress and increased air temperature increase [9,15,16]. Previous analysis has shown that climatic signals can be modified or masked by human activities (for example, an increase in the emission of pollution) that have an impact on the ecosystem in which the tree is grown. The input of pollutants into the atmosphere has increased significantly since the middle of the twentieth century as a result of the increase in industrial activities in the world. Since the 1980s, pro-ecological policy and pro-ecological investments were implemented in most of the factories in Poland. The further reduction of the emission of contamination in Silesia was associated with restrictive governmental regulations on emissions according to EU legislation.

To date, despite interest in research on trees as bioindicators, few studies have considered the influence of climate on pine stands and stable isotopic composition of trees growing in forests localized in highly populated and industrialized parts of southern Poland- in Silesia, e.g., [7,8,14,17–20]. This study explores, for the first time, the interaction between tree properties and the index: Standardized Precipitation-Evapotranspiration Index (SPEI) [21–24]. The aim of this work is to broaden our understanding of spatial and temporal variations in BAI, carbon isotope fractionation, and iWUE associated with water balance and increased temperature. Therefore, we investigate the relation between seasonal fluctuation in the amount of precipitation and potential evapotranspiration and the response of trees to these changes in the selected region.

Annual wood growth can be considered a measure of the sensitivity of trees to pressure from various environmental factors, including climatic conditions [25]. An important factor that influences the variation in stem growth in trees is changing weather conditions from year to year [26]. One of the parameters for the vitality of trees can be, for example, the increment of the basal area, which provides information about the amount of wood deposited by trees. Dendrochronological methods can be used, for example, to demonstrate the influence of individual climatic elements on the growth of wood, that is, the vitality of trees [27]. However, industrial pollution often reduces the vitality of trees, the growth of trees, and their sensitivity to meteorological factors, and increases the heterogeneity of their annual growth responses [28–32]. Most of the dendrochronological studies of tree rings evaluate changes in radial stem growth, which in coniferous species is characterized by a clear decrease with age, which may obscure the true causes of changes in tree condition. Unlike radial growth, basal area increment (BAI) in healthy trees is characterized by a long-term upward trend with age, reaching its peak at several dozen years of age [33]. In particular, we investigate whether BAI is a sensitive indicator of tree vigor.

The purpose of these studies was to investigate the sensitivity of the pine population to temperature and precipitation in four forest areas in Silesia influenced by industrial pollution. The annual variation of the basal area increment, $\delta^{13}C$, and iWUE were used as the indicators of the tree's response to climate change, when there was a strong increase in industrial activities in the investigated area.

2. Results

Figure 1 shows dynamic changes in the average monthly temperature and the amount of precipitation in the investigated area. The period from 1951 to 2012 was characterized in

the regional climate records by an annual mean temperature range of 6.5 to 10.5 °C) and a mean annual precipitation range of 360 to 870 mm.

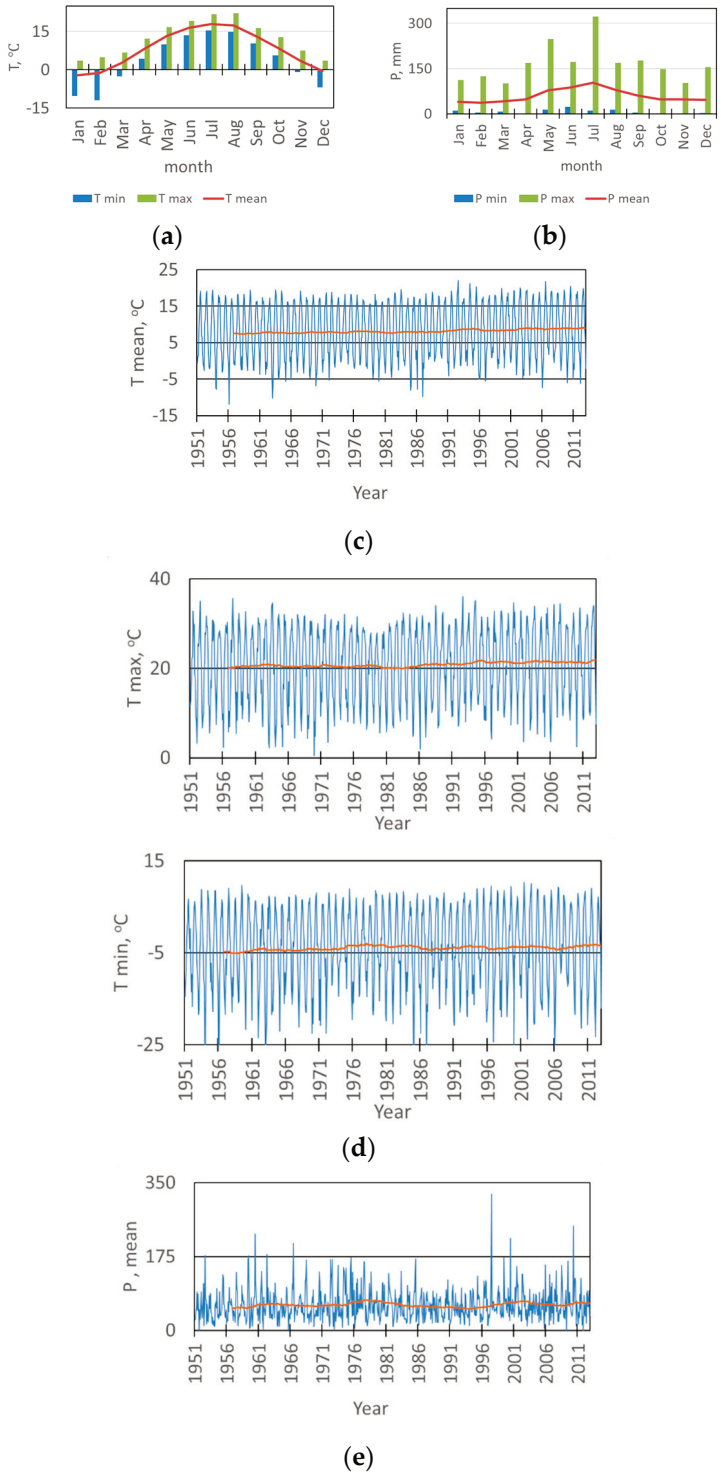

Figure 1. Trends and intraannual variation in air temperature (T) and amount of precipitation (P) mean value (mean) and extremes (max-maximum, min-minimum) (**a**,**b**) and comparison of time series, and trends in the total amount of precipitation and mean, maximum (max) and minimal (min) air temperature, respectively, orange lines indicate a trend of 5-year mean of average temperature (**c**), maximal and minimal temperature (**d**) and the sum of precipitation (**e**), in the investigated area (1950–2012).

Figures 2 and 3 provide an overview of the data from the SPEI Global Drought Monitor related to the climatic water balance, including a comparison of time series, means, extremes, and trends. The threshold and symbology for the SPEI were used according to the Global Operational Support Team [24]. To detect drought episodes, it is possible to use SPEI, which takes into account the intensity and duration of drought episodes. The idea behind SPEI is to compare the maximum possible atmospheric evaporation demand with current water supplies. The SPEIbase v2.0 database is based on the FAO-56 Penman–Monteith equation [21–23]. Negative SPEI values represent a rainfall deficit below average precipitation and high potential evapotranspiration. Dry episodes begin when the SPEI value is below or equal to −1.0. Positive SPEI values indicate that rainfall surpluses are higher than median rainfall and that potential evapotranspiration is low. The wet periods start when the SPEI value is above or equal to 1.0, and end when the value becomes negative.

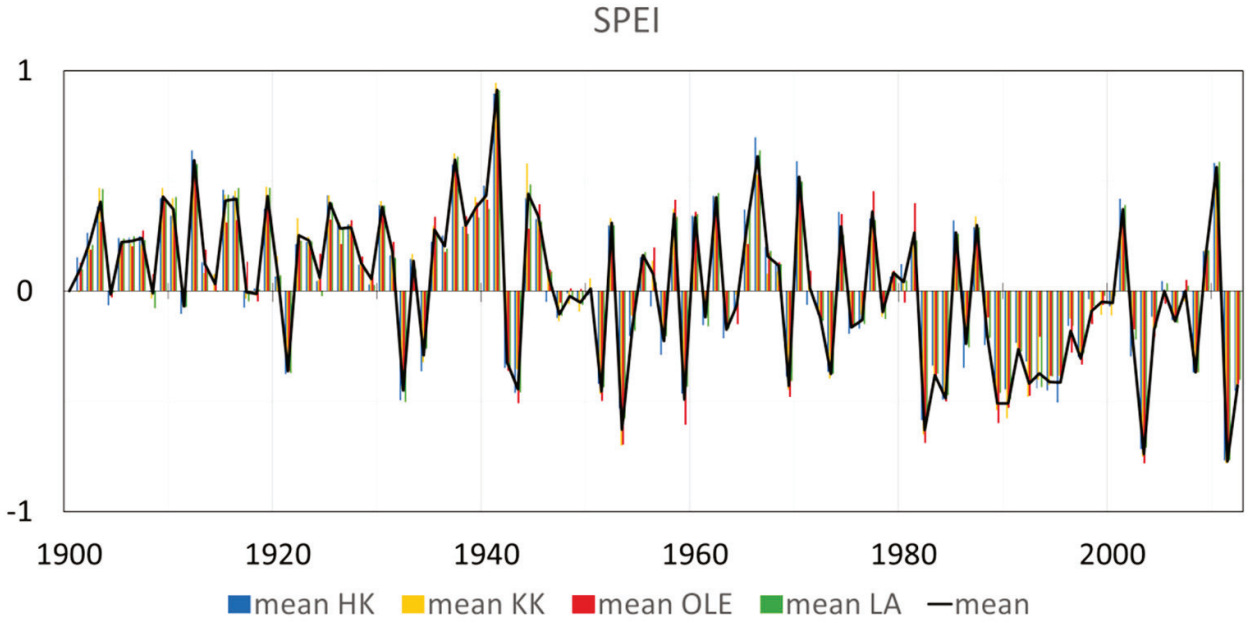

Figure 2. Comparison of time series and trends of annual mean SPEI between 4 investigated sites in Poland: HK-Dabrowa Górnicza, LA-Łaziska Górne, KK-Kędzierzyn Koźle, OLE-Olesno. Based on the data set [23,24].

In the last century, the dynamic changes in SPEI can be seen in Figure 3. In the first two decades of the twentieth century, only a few times have the mean SPEI been lower than 0, and this period was rather moisture. In the next six decades, from 1920–1980, much more often the SPEI has been less than 0, so dry periods seem to occur more frequently. Since the 1980s, more frequent and longer dry period, including extremely and exceptionally dry, has been observed. (Figures 2 and 3).

2.1. δ^{13} C and iWUE and Climate Changes

Figure 4 shows a clear trend of decreasing the value of δ^{13}C value, Figure 4b shows an increase in iWUE.

The tests revealed weak and significant correlations between T, P, SPEI, and δ^{13}C, iWUE. The results of the moving correlation tests presented in Figure 5 are useful in analyzing the temporal stability of the significant relationships between the selected parameters. The results confirm that there is a high correlation between climatic factors and carbon isotopic composition and iWUE and a high positive or negative relationship between them can be observed over the investigated period of time, whereas the other may be visible only for a short period of time, while the others might be hazardous. At this time, we cannot

exclude that some results of the response of trees to climate change may be masked by the anthropopression in this region.

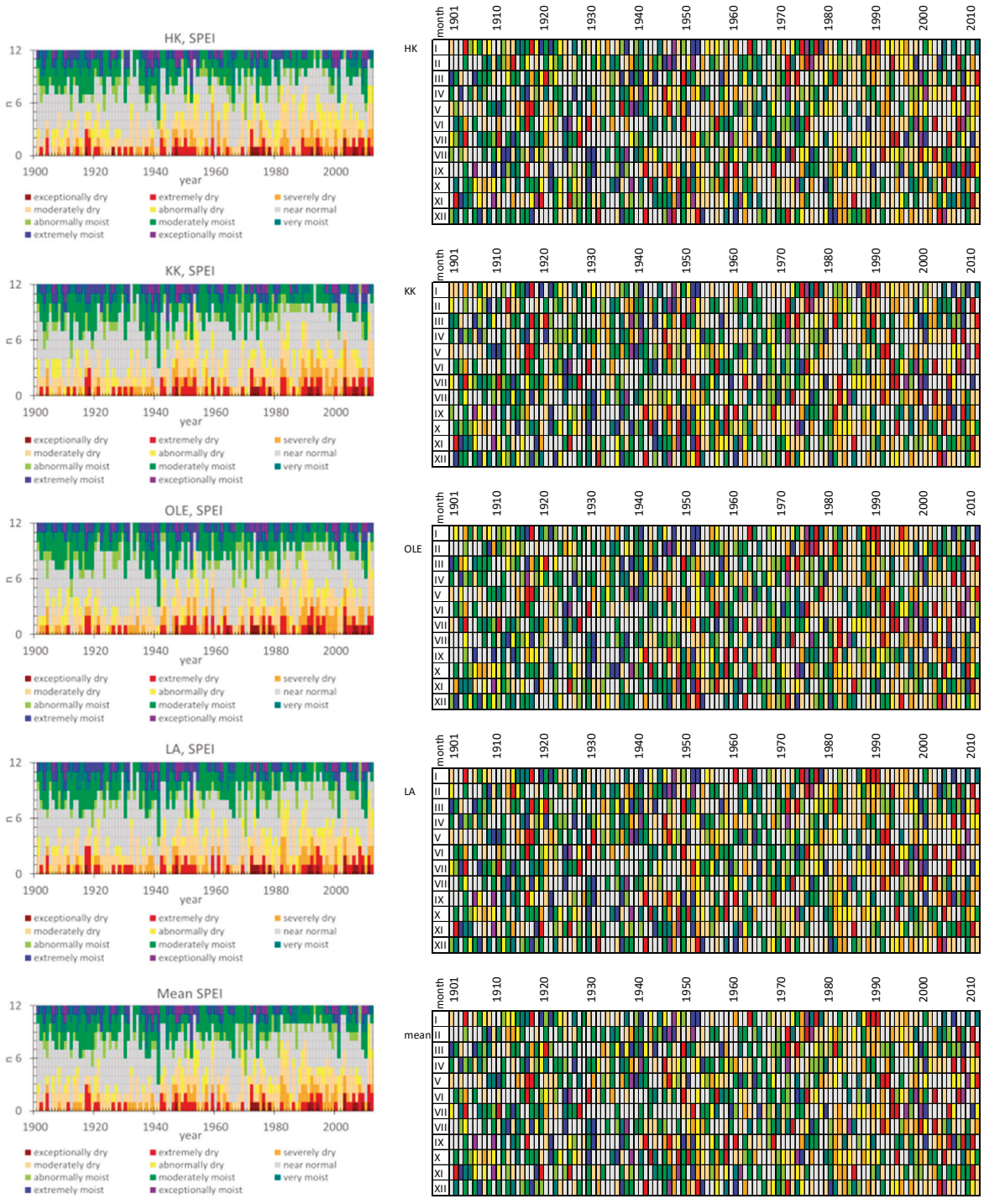

Figure 3. Graphical analysis of SPEI in the investigated area (HK-Dabrowa Górnicza, LA-Łaziska Górne, KK-Kędzierzyn Koźle, OLE-Olesno and mean SPEI value in Silesia region) since 1900–2012. Comparison of time series, means, extremes, and trends of monthly SPEI (**a**) the number of months in each year (1900–2012) with the division to 11 types of the period depends on SPEI (**b**) the temporal distribution of variation in SPEI over each year since 1900–2012. The comparison according to the threshold and symbology for the SPEI [24], and data [23].

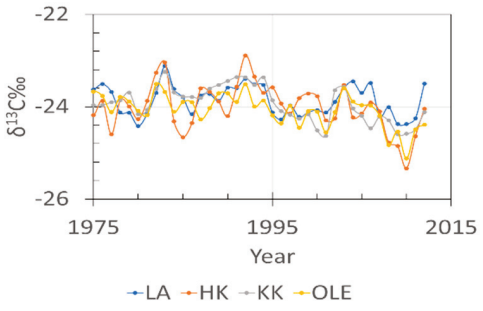

(**a**)

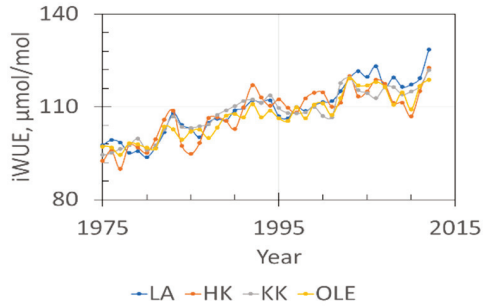

(**b**)

Figure 4. Changes in carbon stable isotope composition of tree rings (**a**) and iWUE (**b**) in pine grown in four forests in Silesia (Poland): HK-Dabrowa Górnicza, LA-Łaziska Górne, KK-Kędzierzyn Koźle, OLE-Olesno.

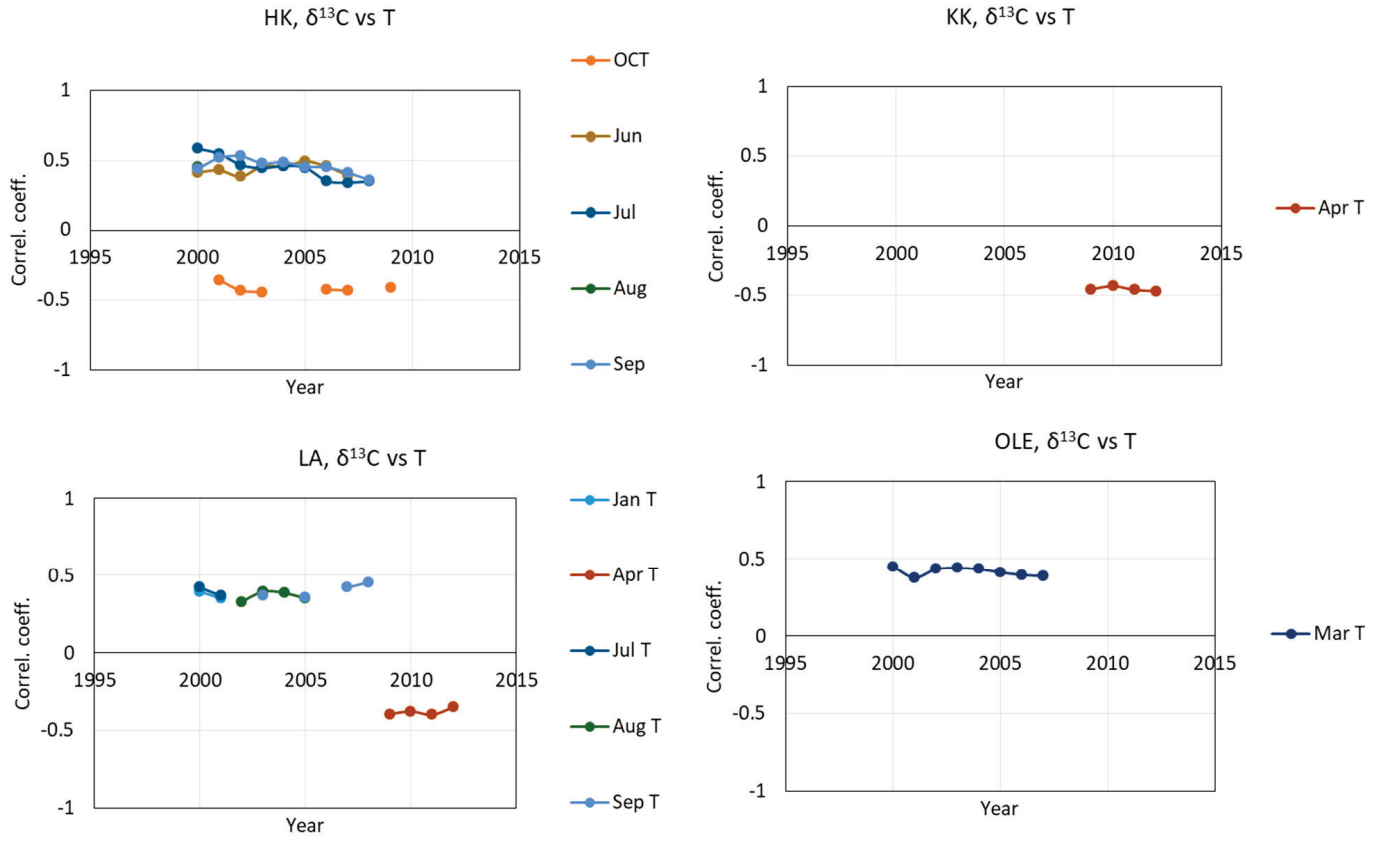

(**a**)

Figure 5. *Cont.*

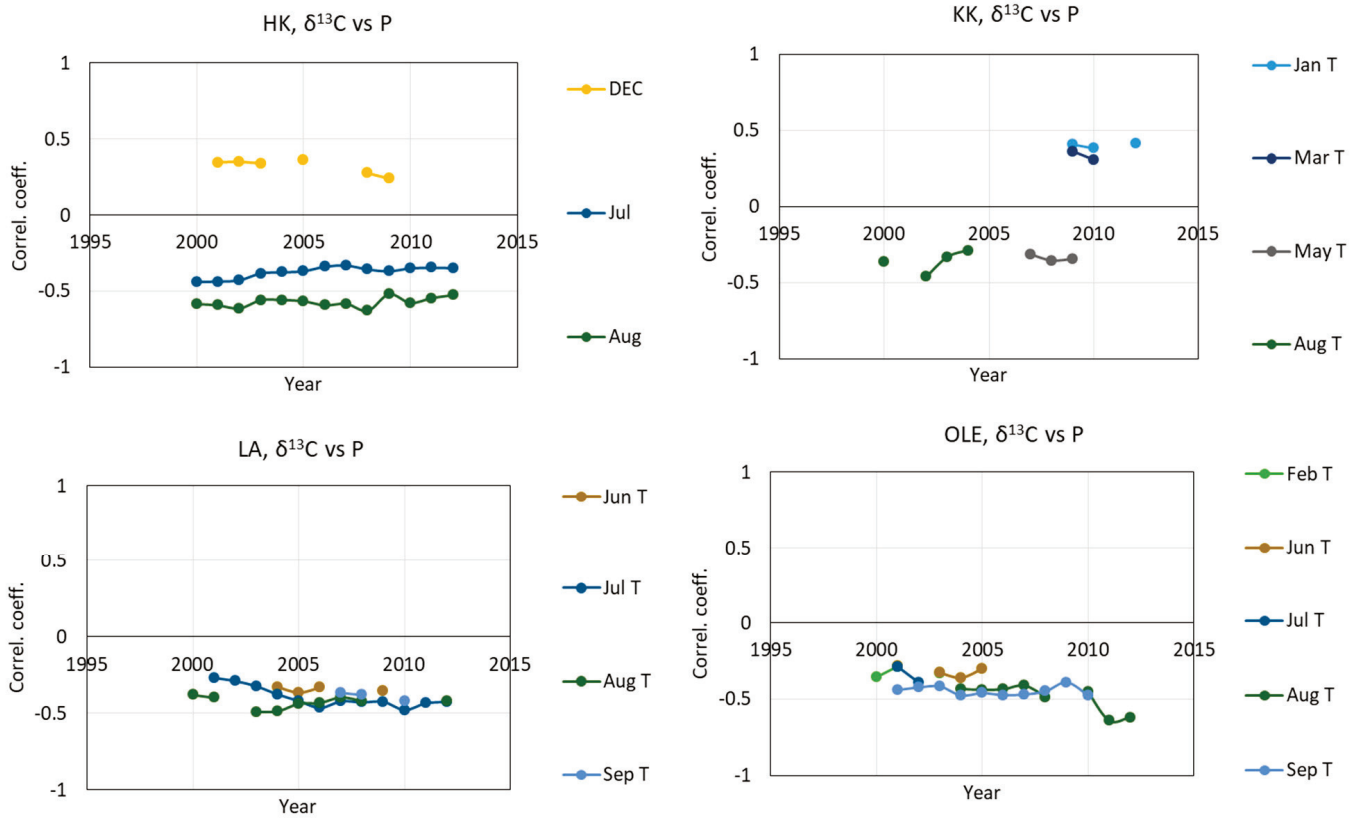

(**b**)

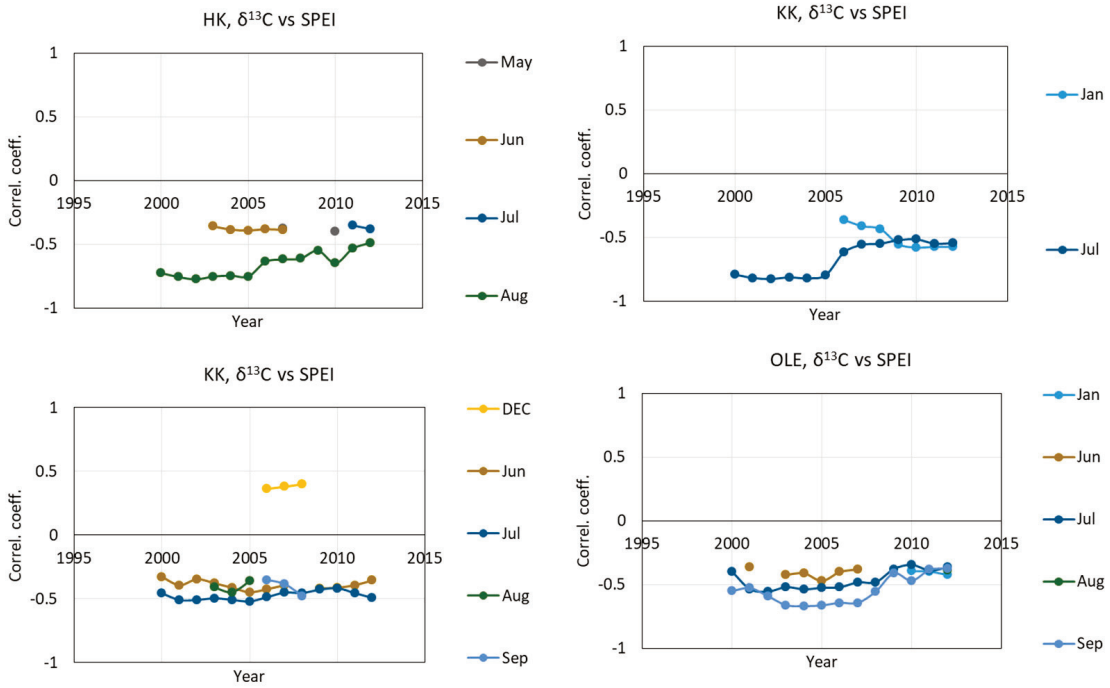

(**c**)

Figure 5. *Cont.*

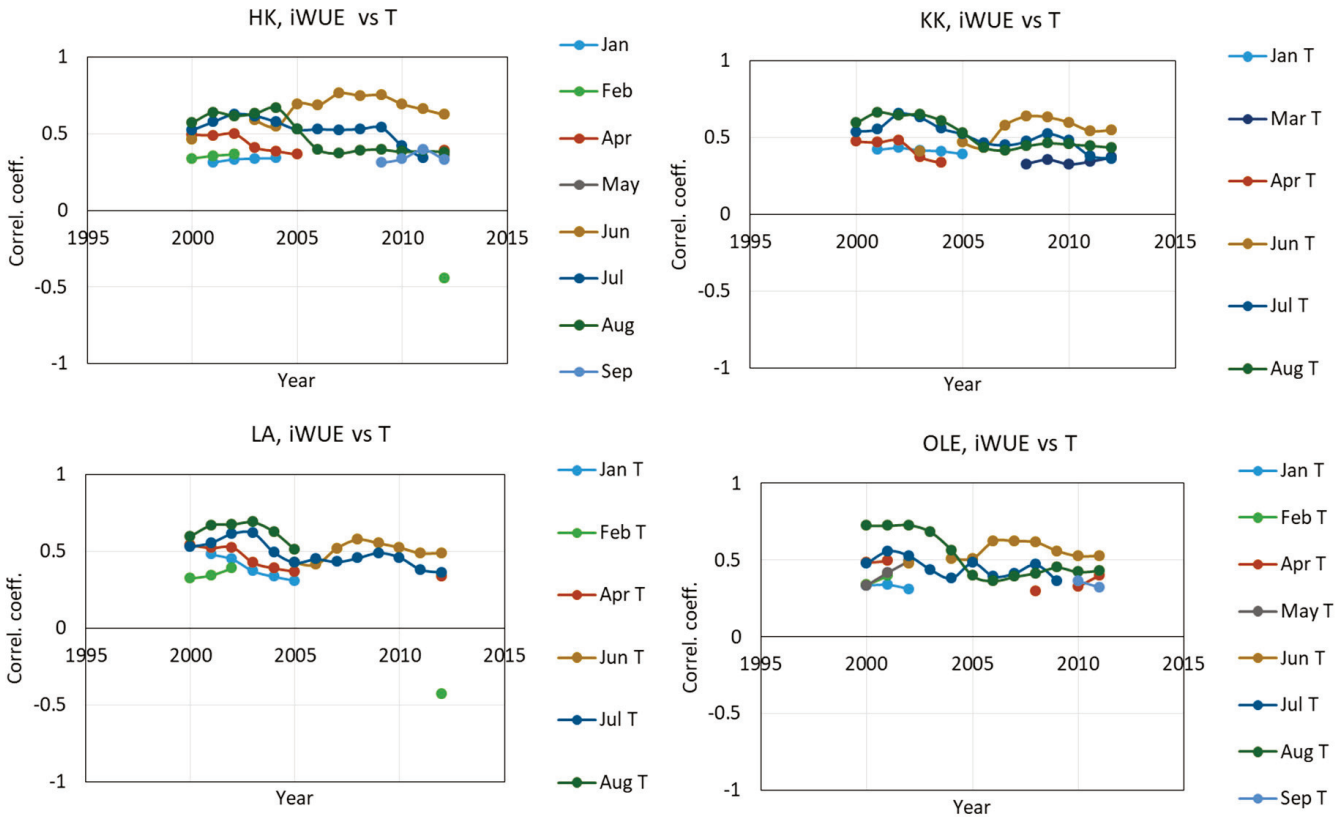

(**d**)

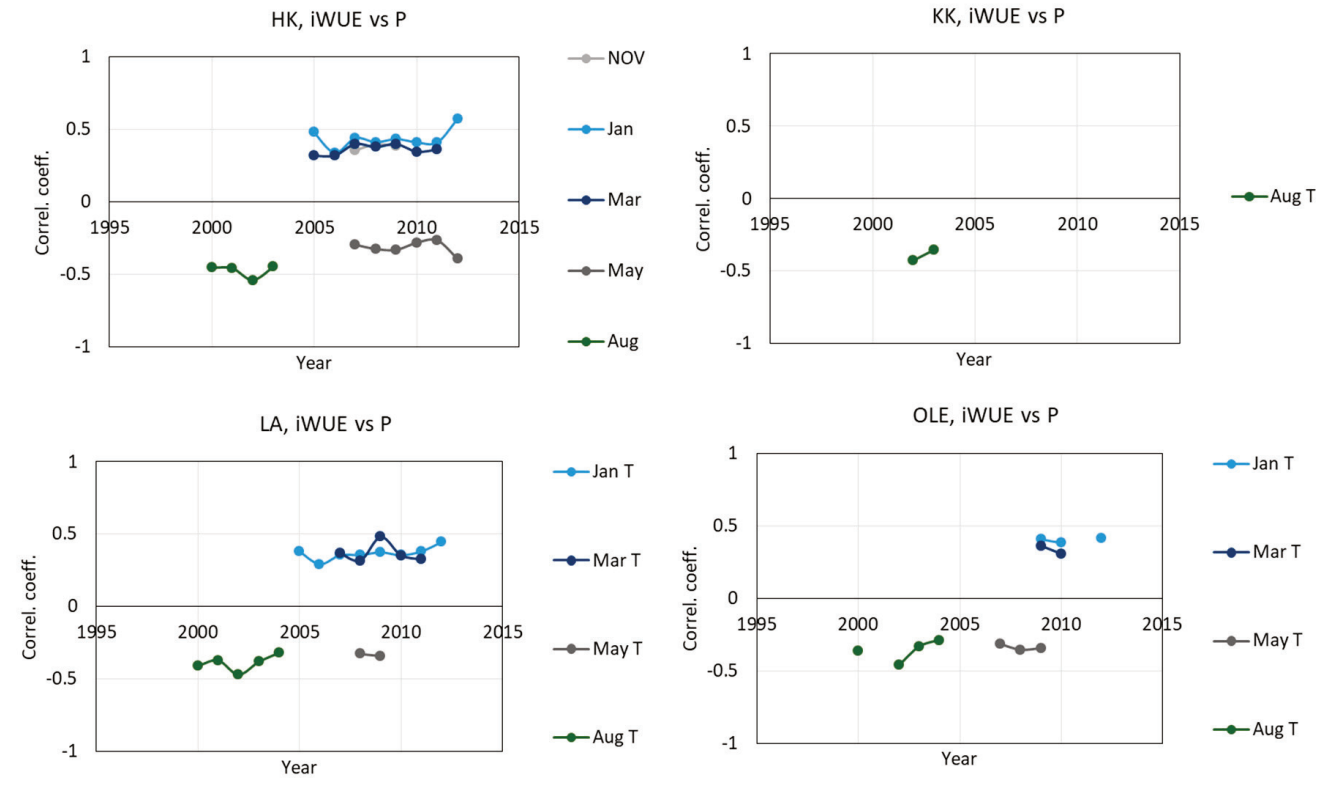

(**e**)

Figure 5. *Cont.*

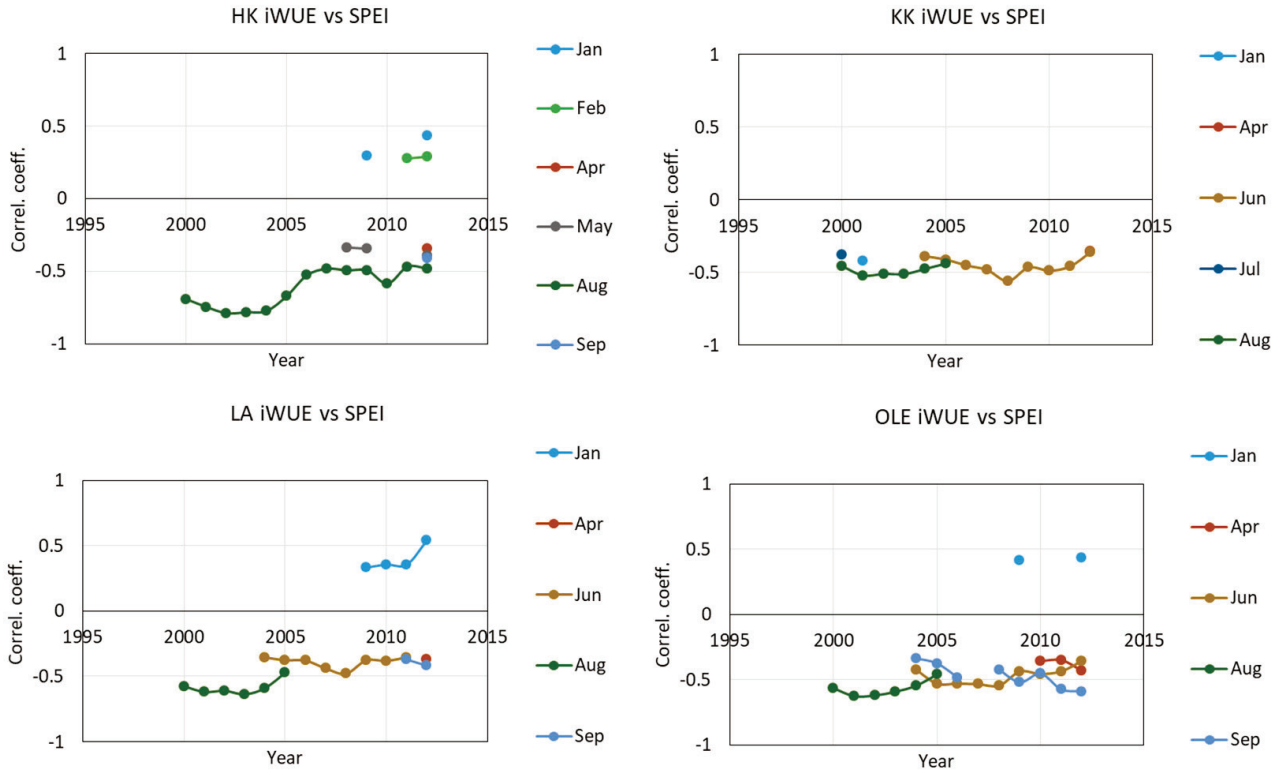

(f)

Figure 5. The impact of climate changes on fractionation of carbon isotopes in pine grown in four forests in Silesia (Poland): HK-Dabrowa Górnicza, LA-Łaziska Górne, KK-Kędzierzyn Koźle, OLE-Olesno. Relationship between $\delta^{13}C$ and monthly mean air temperature (T) (**a**), monthly sum of precipitation (P) (**b**), standardized precipitation−evapotranspiration index (SPEI) (**c**) and iWUE between monthly mean air temperature (**d**), monthly sum of precipitation (**e**) and standardized precipitation-evapotranspiration index (**f**). The results of the temporal stability test of the correlation between climatic parameters and $\delta^{13}C$ and iWUE based on the bootstrap correlation and the moving interval correlation (base length 26 years, last year was indicated on the $x-$axis). The investigated period of time was from September (capital letter) of the previous year until September of a given year, $p < 0.05$, investigated cover period of time: 1975–2012).

Figure 5a,b shows the coefficient correlation between $\delta^{13}C$ and temperature and precipitation, respectively. Figure 5c reveals a relationship between $\delta^{13}C$ and SPEI. Figure 5d,e shows a strong correlation between iWUE and temperature and precipitation, respectively. Figure 5f reveals a relationship between iWUE and SPEI.

In general, a negative relationship of $\delta^{13}C$ with precipitation in July and September has been observed, whereas some positive relationship has been observed with the amount of precipitation in winter. However, a negative relationship of $\delta^{13}C$ with temperature in March and a April and positive relationship with temperature in September has been observed. Comparing $\delta^{13}C$ with SPEI, a strong significant correlation with SPEI in July has been observed. Most trees show a strong correlation with different summer months (June, July, August, and September). The lower value of SPEI corresponds to an increase in $\delta^{13}C$ in trees.

The analysis of iWUE gives the possibility to investigate the impact of climate factors on carbon isotopic composition by removing the effect of depletion of $^{13}CO_2$ in the air caused by fossil fuel combustion.

The temporal stability tests of the correlation between iWUE and air temperature, amount of precipitation, and SPEI results show a significant relationship, in most of the

investigated sites, with temperature in June, July, and August. Interestingly, there are also differences in sensitivity. The strength of this relationship has not been constant and has been modified over an investigated period of time. The correlation between iWUE and temperature is surprising in the last years—where the relationship with spring seems to start significantly. The relationship between winter temperatures (February) is probably a risk. However, this significant relationship between iWUE and temperature in February was noted in two sites. The results of moving correlation tests suggest that iWUE may be affected by the amount of precipitation in winter and spring (January and March), where a positive correlation has been observed, and with precipitation in August (negative relationship). In the last period of time also, the sum of precipitation in May seems to be significant.

The results of moving correlation tests presented in Figure 5 show the strong positive relationship between iWUE and SPEI in summer, in June, August, and September.

2.2. Long- and Short-Term Basal Area Increment

The site chronologies of basal area increments (BAI) are characterized not only by clear short-term variability but also by long-term variation (Figure 6). The chronologies had a similar long-term pattern. The BAI gradually increased with the age of the trees and peaked mostly after several decades. We see long-term BAI growth at all sites. The similarity of annual changes in BAI in 18 pine populations was also relatively high (Figure 6). The variation in BAI from year to year is mainly the result of the effects of climate conditions on trees. Therefore, it can be assumed that the climate signal contained in the chronologies of 18 pine populations was similar during the period studied. The indexed chronologies (BAII) show a strongly reduced long-term variation, while short-term variation is highlighted (Figure 7). MS values indicate high annual sensitivity of trees and strong climatic signals contained in the site BAI chronologies during the period considered. The mean sensitivity (MS) of 18 BAI chronologies in the period 1930–2012 ranged from 0.175 to 0.239, which can be considered relatively high values. The sensitivity of the pines remained relatively high even during periods of high industrial pollution, i.e., the 1960s, 1970s, and 1980s (Figure 8). However, it should be emphasized that pines slightly reduced basal area increments in the 1970s and 1980s (Figure 6), and the heterogeneity of annual increment responses increased. This is evident from the lack of pointer years in the 1970s and 1980s (Figure 9). Before and after this period, homogeneity was much higher. This was probably a consequence of the strong increase in industrial pollution.

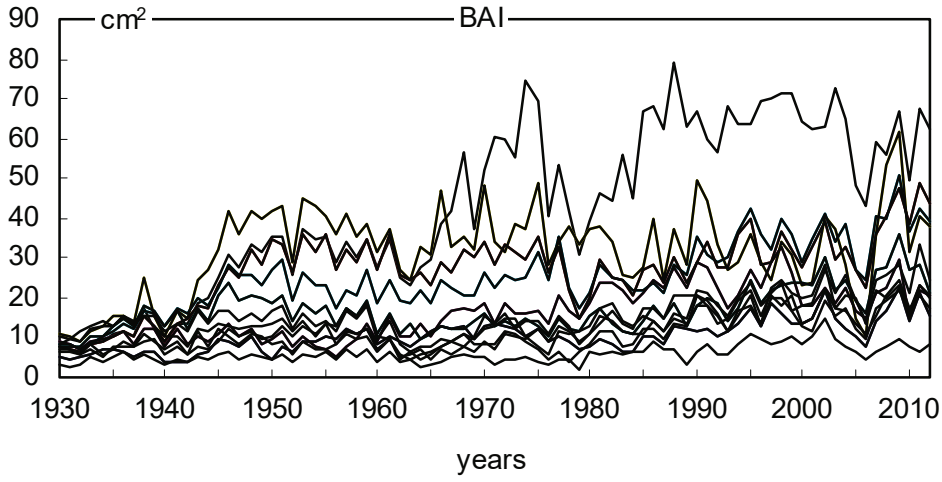

Figure 6. Eighteen site chronologies of basal area increment.

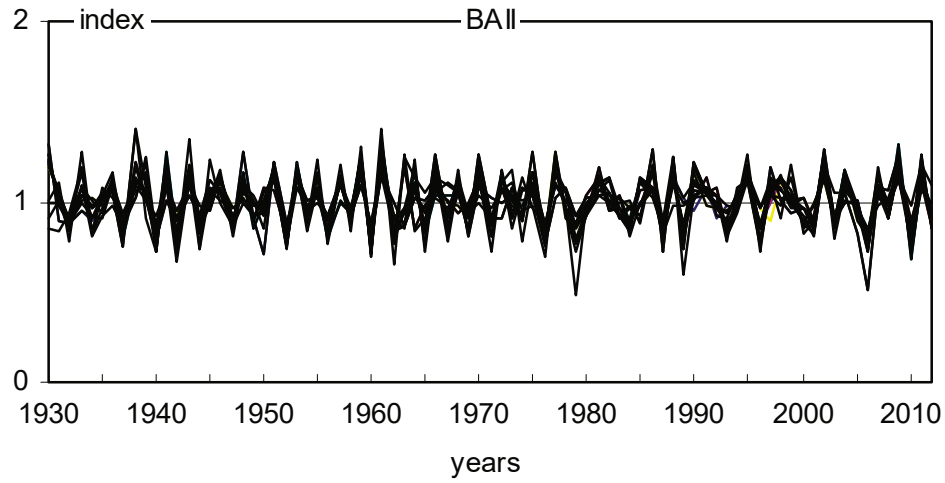

Figure 7. Eighteen site indexed chronologies.

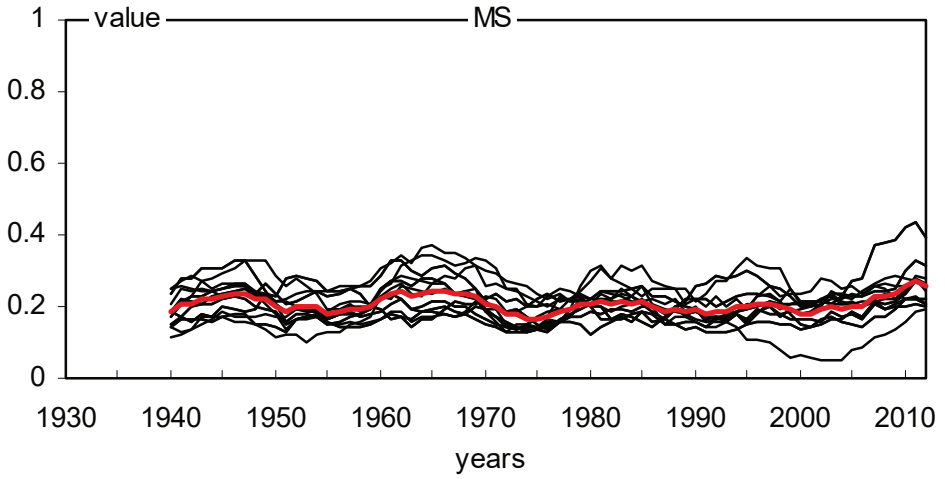

Figure 8. Ten-year running values of MS index. The consecutive MS values are plotted at the end of each 10-year period; the first period ranged from 1931 to 1940 and the last period from 2003 to 2012. The average MS values are marked with a red line.

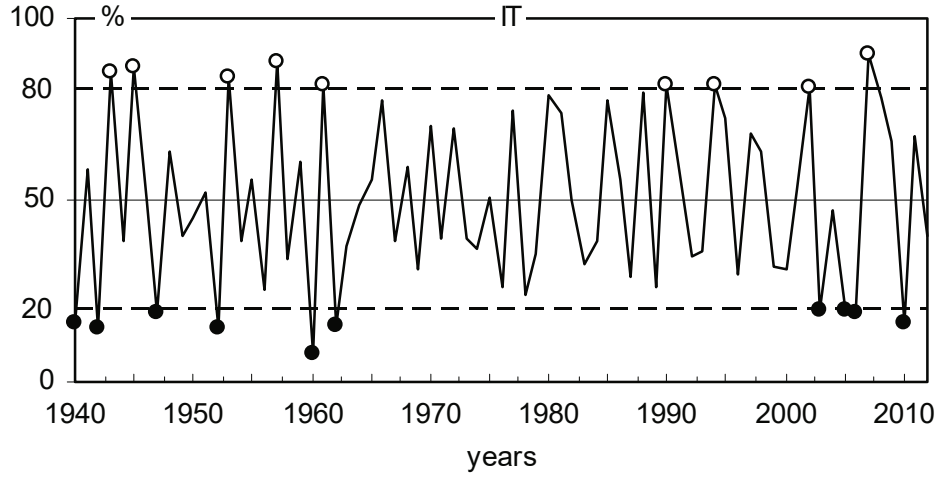

Figure 9. Regional chronology of IT indices and positive (white dots) and negative (black dots) pointer years.

2.3. BAI, Climate Conditions, and Pointer Years

A total of 18 site-indexed chronologies (BAII) were correlated with the climate parameters (Figure 10). The relationship between BAI and air temperature in February and March, as well as precipitation in the previous September, and current May and July, was very similar in all pine populations (Figure 10). These correlations are confirmed by the analysis of the climatic conditions in the positive and negative pointer years (Figure 11). The positive pointer years were characterized by high precipitation in September of the previous year, a warm and short winter, low precipitation in May, and high precipitation in June and July in the year of tree-ring formation. In the negative pointer years, the climatic conditions were opposite (Figure 11).

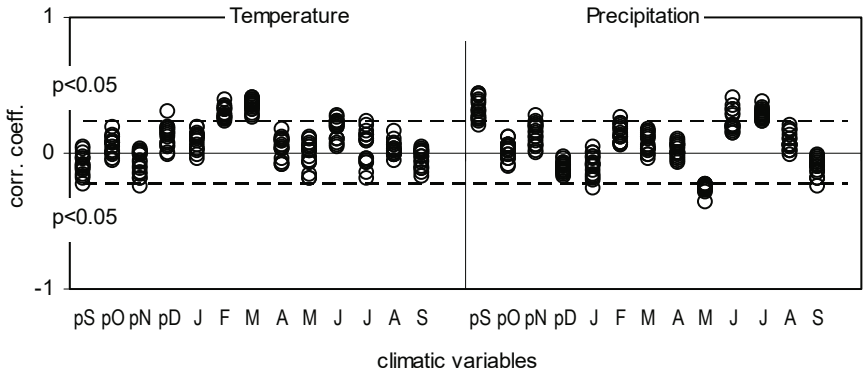

Figure 10. Correlation coefficients between 18 site indexed chronologies (BAII) and mean monthly temperature and precipitation, from September of the previous year (pS) to September of the current year (S).

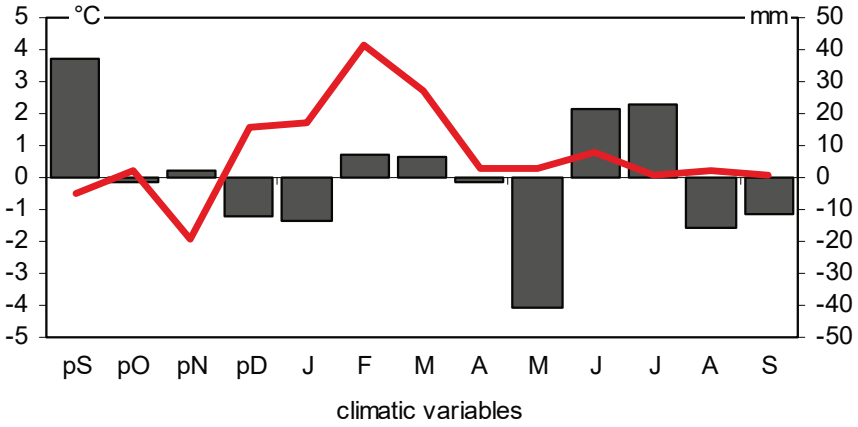

Figure 11. The climatic diagram. Differences in mean monthly temperature (red line) and precipitation (black bars) between the negative and positive pointer years.

3. Discussion

3.1. Climatic Factors That Influence the Basal Area Increment

The study area can be considered homogeneous in terms of annual BAI changes in pine trees. Interestingly, the pine populations show a similar sensitivity to climatic conditions even in period of high pollution. However, the heterogeneity of their annual incremental responses increased in this period. This is evidenced by the lack of pointer years. In recent years, there has been an increase in MS, and pointer years have reappeared. This may indicate the increasing sensitivity of pines to climatic conditions. The climatic conditions of the current and the previous year influence tree growth in temperate and boreal zones [27]). This is also the case with Scots pine, as shown by the results of dendroclimatic studies [34–38]. An important factor that affects the increase in the basal area increment

of studied Scots pine was the precipitation conditions in September in the year before the current growing season. The high precipitation in this month had a positive effect on wood growth in the following year. Scot pines usually finish their wood growth at the end of August or at the beginning of September [39]. The trees concentrate on accumulating reserve substances that affect the vitality of the trees during the winter period [27]. In turn, sunny weather in September affects the high number of generative organ buds [40,41], and flowering and a lot of cones with seeds in the next spring have a negative impact on wood growth [42]. On the other hand, the cloudy and wet weather in September influences the amount of vegetative buds, and therefore the number of new shoots and needles in the next spring is high [42]. Therefore, the assimilation area and the production of auxins increase, accelerating the cambial division and increasing wood increment. Our results confirm that high precipitation in September has a positive effect on the basal area increment of pines in the following year.

The results of our study show that warm and short winters also positively influence the condition and wood increment of 18 Scots pine populations. In the temperate zone, bud break and division of the vascular cambium occur after winter. These processes are temperature-dependent [43,44]. The results of many studies show that the earlier onset of wood cell formation in Scots pine trees is related to a higher air temperature at the beginning of the growing season [45–48]. Interestingly, the dry weather in May had a similar positive effect on the basal area of the pines. These correlations are confirmed in other dendroclimatic studies in pines [35,38,49]. Low precipitation due to lack of cloud cover increases the inflow of direct solar radiation, which warms shoots and needles. The positive effects on the increase in the basal area increment of the pines were also caused by high precipitation in summer, mainly in July in the year of tree-ring formation. It causes a prolongation of the period of intensive divisions of the vascular cambium and the formation of large-diameter cells. The water deficit in summer often leads to earlier termination of cambium activity in conifers [48–50]. Therefore, summer droughts are the factor that limits wood growth, which has been observed in the pines throughout their range [51–58].

3.2. The Impact of Climatic Changes on $\delta^{13}C$, iWUE

The decrease in $\delta^{13}C$ in trees and the increase in iWUE since 1975–2012 in each sampling site can be explained by isotopic fractionation in the air or the response of the plant to changes in plant physiology due to changes in the ecosystem, for example, changes in weather conditions or water stress and limitation of access to the water. It could be due to climatic changes and also due to the fractionation of $\delta^{13}C$ in atmospheric CO_2, which originates from different sources. This phenomenon has been reported by [11–13]. It is evident that the emission of CO_2 from fossil fuel combustion is depleted by $^{13}CO_2$. In consequence, mixing natural and anthropogenic CO_2 in the atmosphere modified the level of $^{13}CO_2$ in the atmosphere and a global trend of decrease $\delta^{13}C$ in the air was observed. Coal was the main fuel in the region, accounting for 83% of the total CO_2 emissions from fossil fuels in 1950. Recently, gas fuels have increased significantly, and since the late 1990s, gas fuel emissions have exceeded coal emissions. Increased CO_2 significantly reduces the $\delta^{13}C$ in the atmosphere. The current $\delta^{13}C$ is about $-8‰$.

Other investigations [1–3,9–13,15–20] conclude from their analyzes that also different climatic factors, tree physiology, and carbon isotope fractionation that occurs due to diffusion in air and carboxylation-causing stomatal conductance, and fractionation (discrimination by RuBisCO) have an influence on carbon isotopic composition of plants. Furthermore, previous isotopic research conducted in this research area focused primarily on single climate factors that influence the isotopic composition of selected saccharides in three of the four forests investigated in the current studies.

It can be observed that the variation in $\delta^{13}C$ and iWUE can be associated with different climatic factors such as precipitation or temperature and can be correlated with SPEI. In most cases, the impact of the weather conditions of the previous year has not been observed.

The findings in current studies confirm those of earlier studies, such as the climatic factor having an impact on the carbon isotopic composition of tree rings. The results indicate that, in general, $\delta^{13}C$ has been positively correlated with the temperature in summer and negatively correlated with the temperature in summer, and negatively correlated with the amount of precipitation in winter and spring and positively with the precipitation in summer. iWUE has been positively correlated with temperature; the highest correlation was observed with temperature in June, July, and August. When comparing iWUE with the monthly amount of rain, it can be observed that prior to 2003, there was a strong correlation with precipitation in August (negative correlation), and a positive correlation between iWUE and the amount of precipitation in January and March seems to be more significant in the last decades.

Dynamic changes in photosynthesis rate and stomata conductance may be affected by different environmental factors. On the one hand, taking into account pollution emissions in this area, it cannot be excluded that until the 1990s, photosynthesis could be limited due to pollution and toxic substances in the air that could be toxic to plants; thus, trees absorbed less CO_2 from the air by leaves during photosynthesis. On the other hand, the decreasing trend in SPEI suggested that in this region the drought episodes seem to be significant and more frequent, so in consequence, trees could react against water transpiration from the leave by modification of stomata conductance. So, more frequent and more extremely dry periods in the last decades might be reflected in dynamic changes in pine stomata conductivity due to water deficit and thus in carbon stable isotope composition and iWUE variations.

By comparing the results of the variations in moisture over the past century, moderate, very moist, and exceptionally wet months were observed in the last decades. These results can be explained by the fact that the high value of SPEI can usually be associated with short and intensive rain that could cause floods. In effect, water could not be captured by the soil. The decrease in SPEI associated with dry and water deficit periods corresponds to the summer time in Poland. The relationship of $\delta^{13}C$ and iWUE with the climatic parameters and SPEI is certainly due to the fact that throughout the year, in Poland, in summer, the most intensive but also very short raining episodes are in summer, and the soil cannot save and retain the water or the water evaporates very quickly due to the high temperature. The increase in iWUE may be associated with a variation in the photosynthesis rate or a change in stomata conductance. A more detailed analysis of iWUE [9,15,16] taking into account changes in the photosynthesis rate (A) and changes in the conductances of the stomata (g) give a possibility to create the hypothesis of the reaction of the different scenario of plants as a response to environmental changes. These scenarios of dynamic changes in iWUE may be possible with a different probability. The iWUE may increase if:

1. The photosynthesis rate increases significantly and the stomata conductance is at the same level or does not significantly
2. The photosynthesis rate is constant, and the stomata conductance is reduced.
3. The photosynthesis rate decreases and the stomata conductance is reduced, but stomata conductance reduction is a much more significant process than a reduction in photosynthesis speed.

These results need to be interpreted with caution because, at this moment, it is hard to say which scenario is the most likely one. Taking into account that (i) in the air there is a lot of CO_2, and trees have access to CO_2, and currently, the pollution emission from industry is much lower than in the 1960–1980s, so current conditions are more favorable for photosynthesis and that (ii) SPEI reach much lower value so the reaction of trees will be associated with reduction of stomata conductance to avoid rapid water evaporation, in our opinion scenario 2 or 3 is the most probable. But to confirm this hypothesis a further more detailed analysis should be conducted.

The effect of drought and water stress on pine production in the southern part of Poland is evident. As a consequence of these strong rains, the soil could not restore water

for a longer period of time. As a consequence, it has been possible to observe the water deficit that could be responsible for plant reactions against water stress.

4. Materials and Methods

4.1. Study Area

18 pine stands in the following in the forest close to the following cities Dąbrowa Górnicza near steelwork "Huta Katowice" (HK; 50°20′29.7″ N 19°17′04.8″ E), Kędzierzyn-Koźle near chemical factories (KK, 50°18′20″ N 18°15′27″ E), and Łaziska near heat and power station (LA; 50°07′58.0″ N 18°50′47.1″ E) and one reference site (OLE, 50°52′37″ N, 18°25′15″ E) was under dendrochronological investigation (Figure 12). The sampling sites were located at different distances from industrial factories (from 1 to 20 km from the factories). The comparison site was 100 km from industrial factories. On the basis of dendrochronological results, a representative site from each region was isotopically investigated. Selection based on the length and size of the reduction in tree rings width during the most industrialized period of time in Poland [19]. This limitation of the analysis was due to costs and time-limited projects.

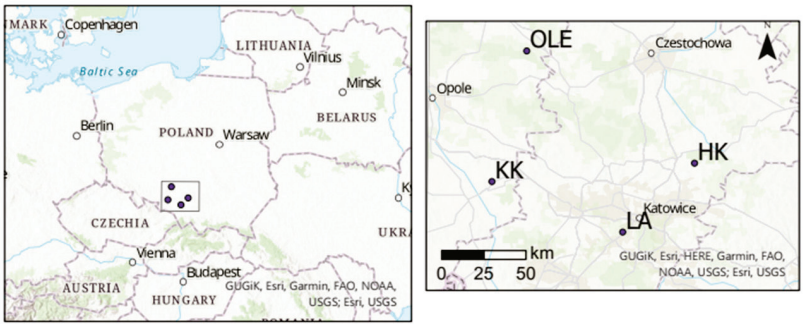

Figure 12. Sampling sites-forests closed to Dąbrowa Górnicza (HK: 50°24′ N 19°28′ E); Kędzierzyn-Koźle (KK: 50°20′ N 18°19′ E), Łaziska (LA: 50°8′ N; 18°53′ E) and a reference site (OLE).

Meteorological data from the meteorological stations in Katowice (50.96° N 19.01° E) and Opole (50.67° N 17.93° E) were provided by the Polish Institute of Meteorology and Water Management (IMGWPIB). The SPEI data was downloaded from the SPEI Global Drought Monitor [21–24].

Using the threshold and symbology for the SPEI https://bennyistanto.github.io/gost-climate/indices/spei.html accessed on 1 October 2022), it is possible to conduct detailed analysis and compare time series, means, extremes, and trends of monthly SPEI with the division to 11 types of period: exceptionally dry for SPEI below or equal to −2.00; extremely dry for SPEI range from −2.00 to −1.50; severely dry for SPEI range from −1.50 to −1.20; moderately dry for SPEI range from −1.20 to −0.70; abnormally dry for SPEI range from −0.70 to −0.50; near normal for SPEI range from −0.50 to +0.50; abnormally moist for SPEI range from +0.50 to +0.70; moderately moist for SPEI range from +0.70 to +1.20; very moist for SPEI range from +1.20 to +1.50; extremely moist for SPEI range from +1.50 to +2.00; exceptionally moist for SPEI equal and above 2.00.

Dendrochronological analyzes cover a period of time from 1900–2012. The relationship between precipitation, temperature, and BAI was analyzed for the period of time between 1951 and 2012, while the relationship between precipitation, temperature, and drought index (SPEI), $\delta^{13}C$, and iWUE was analyzed for the period of time between 1975 and 2012.

4.2. Dendrochronological Analysis

In each of the 18 tree stands (sites), a total of 15 dominant and co-dominant Scots pine trees were selected for this study. The age of trees was about 100 years old. Two increment cores were taken from each tree at 1.3 m above the ground. The cores were sanded and scanned in a resolution of 2400 DPI. The widths of the tree rings in cores were

then measured to the nearest 0.01 mm using CooRecorder and CDendro 7.8 software [58]. The quality of the measurement data and the cross-dating was checked with the COFECHA program [59]. For each tree in each year, the mean tree-ring width was calculated as

$$r = (r_1 + r_2)/2 \quad (1)$$

based on radious r_1 and r_2.

The annual basal area increment (BAI) was calculated from the average radius values as follows;

$$BAIi = \pi r_i^2 - \pi r_{i-1}^2 \quad (2)$$

where: r_i is the radius increment of the stem in the year i and r_{i-1} is the radius increment in the previous year.

For each site, the annual BAI of 15 trees sampled in each year was averaged. In this way, the BAI chronologies of the sites were created. In addition, the BAI series of each tree was subjected to indexing and autoregressive modeling using the ARSTAN program [58]. The program twice fits a negative exponential curve or trend line to each BAI series. The BAI indices (BAII) for each year are calculated using the following formula.

$$BAII_i = R_i/Y_i \quad (3)$$

where R_i is the BAI in the year i and Y_i is the value of a fitted curve in the year i.

Subsequently, each indexed series was subjected to autoregressive modeling to eliminate autocorrelation. This removed trends, long-term fluctuations, and autocorrelation in the BAI series. Consequently, each tree was represented by an individual BAI and an indexed chronology (BAII). For each pine stand, BAI and BAII chronology was developed based on 15 tree chronologies. The average relative difference in radial increment of the trees was evaluated using mean sensitivity (MS) [27]. The MS values were calculated for the period 1931–2012 and for 10-year periods. The MS determines the sensitivity of trees to short-term environmental stimuli, mainly climate. Correlation coefficients were calculated for each site indexed chronology (BAII) and climate parameters (mean monthly temperature and total monthly precipitation from the previous September to September in the year of tree-ring formation). Furthermore, IT indicators (interval trend indices) were calculated for all (270 = 18 sites × 15 trees) BAI series [60];

$$IT = 100 \cdot m/n\ (\%) \quad (4)$$

where: m, the number of trees where BAI in the current year is greater than BAI in the previous year, n, the total number of trees studied.

A higher value of IT corresponds to a higher degree of homogeneity of the incremental response of trees in a given year. IT equal to 100% means that all trees increased BAI compared to the previous year. IT equal to 0% means that all trees decreased BAI compared to the previous year. IT equal to 50% means that half of the trees decreased BAI compared to the previous year and half of the trees increased BAI. The climatic conditions in the years of positive (IT > 80%) and negative (IT < 20%) pointer years were compared to identify the climatic factors that contributed to the occurrence of the pointer years.

4.3. Isotopic Analysis

The isotopic chronologies were based on a pooled-ring approach, with 10 trees per each of the four sites (LA, HK, KK, OLE). The sites were chosen during previous research that was immediately related to the current studies [7,8,17–20].

The isotopic composition of the α-cellulose, extracted using the standard procedure [15,18–21,61] was measured in triplicate samples by IRMS (Isoprime, GV Instruments,

Manchester, UK) at the Institute of Physics of the Silesian University of Technology, Poland, and reported with the delta notation in respect to the international standard (VPDB):

$$\delta = (R_{sample}/R_{standard} - 1)\cdot 1000, \text{ ‰}. \quad (5)$$

where R_{sample} and $R_{standard}$ are the molar fractions of $^{13}C/^{12}C$ the sample and the standard, respectively. The calibration was performed using an internal standard (C-3 and C-5, IAEA for $\delta^{13}C$, standard deviations for each triplicate sample were less than 0.3‰).

To calculate iWUE on the basis of $\delta^{13}C$ in pine and in air, we used the formula according to [3,61]

$$\Delta^{13}C = \frac{\delta^{13}C_{air} - \delta^{13}C_{pine}}{1 + \frac{\delta^{13}C_{pine}}{1000}} \quad (6)$$

$$\Delta^{13}C = a + (b - a)\frac{c_i}{c_a} \quad (7)$$

$$iWUE = \frac{A}{g} = c_a\left[1 - \frac{c_i}{c_a}\right]0.625 \quad (8)$$

where c_i is intercellular CO_2 concentration, c_a is ambient CO_2 concentration, a = ~4.4‰ is the discrimination against $^{13}CO_2$ during CO_2 diffusion through the stomata, and b = ~27‰ is the discrimination associated with carboxylation.

In this study, a detailed analysis of the sensitivity to variations in air temperature has been carried out, and the sum of precipitation and possible evapotranspiration has been carried out using the bootstrap correlation and the correlation of the moving interval, DendroClim2022 [62] (base length of 26 years, the investigated period of time was September of the previous year until September of the given year, $p < 0.05$, period of time: 1975–2012). Although the variation in SPEI for each of the investigated sites is evident but not very significant, a local value of SPEI was taken into account in a more detailed analysis of the influence of climate on selected pine stands in four forests.

5. Conclusions

The results of this study provide information on the stem growth of Scots pine trees in 18 pine stands growing in polluted areas. The pines studied are sensitive to the various climatic factors that occur in the previous and current year of tree-ring formation. The most important factors that affected the increase in the basal area of Scots pine were pluvial conditions in the previous autumn and current spring, and thermal conditions in the winter of the year in which the annual rings were formed. The increasingly warm winters could have a positive effect on the growth of Scots pine in the future. On the other hand, the factor limiting their wood growth will be the ever-decreasing precipitation in summer. Industrial pollution caused only a small reduction in the wood growth of pines and an increase in the heterogeneity of their growth responses. This fact did not have a strong influence on the relationships between the BAI and climate conditions.

The main factors influencing carbon isotopic fractionation in pines were thermal and pluvial conditions in different seasons of the year of tree ring formation. This study confirms that the carbon isotope composition provides a useful measure of integrated water use efficiency (iWUE) of pines and, together with BAI can be used to classify the tolerance to the drought of pines growing in the industrial forest area.

SPEI analysis confirmed that there could be a different scenario of the dynamic tree response to water stress. Father detailed analysis should be conducted to confirm which of two scenarios is more probable: or (1) constant photosynthesis rate and reduction of stomata conductivity (2) decrease in the photosynthesis rate and reduction in the stomata conductivity, in the case where stomata conductance reduction is much stronger than photosynthesis rate limitation.

Author Contributions: Conceptualization, Methodology, Validation, Formal Analysis, Isotopic and SPEI investigation, Writing—Original Draft Preparation, Review and Editing, Visualization, Supervision, Project Administration, Funding Acquisition, B.S. Conceptualization: Methodology, Validation, Formal Analysis, Dendrochronologic and Dendroclimatic investigation, Writing—Original Draft Preparation, Review and Editing, Visualization, Supervision, S.W. All authors have read and agreed to the published version of the manuscript.

Funding: This research was part of the BIOPOL project entitled: 'Trees as bioindicators of industrial air pollution during the implementation of the pro-environmental policy in the Silesia region', funded by the National Science Center and allocated on the basis of decision number DEC-2011/03/D/ST10/05251.

Data Availability Statement: Not applicable.

Acknowledgments: The authors express their gratitude to all the people from the Silesian University of Technology who contributed to making these investigations possible.

Conflicts of Interest: The authors declare that they have no conflict of interest. The sponsors had no role in the design of the study; in the collection, analyses, or interpretation of data; in the writing of the manuscript; or in the decision to publish the results.

References

1. Savard, M.M. Tree-ring stable isotopes and historical perspectives on pollution: An overview. *Environ. Pollut.* **2010**, *158*, 2007–2013. [CrossRef] [PubMed]
2. Ferrio, J.; Voltas, J.; Araus, J. Use of carbon isotope composition in monitoring environmental changes. *Manag. Environ. Qual.* **2003**, *14*, 82–98. [CrossRef]
3. Farquhar, G.D.; Lloyd, L. Carbon and oxygen isotope effects in the exchange of carbon dioxide between plants and the atmosphere. In *Stable Isotopes and Plant Carbon-Water Relations*; Ehrelinger, J.R., Hall, A.E., Farquhar, G.D., Eds.; Academic Press: New York, NY, USA, 1993; pp. 47–70.
4. Malik, I.; Danek, M.; Marchwińska-Wyrwał, E.; Danek, T.; Wistuba, M.; Krąpiec, M. Scots pine (*Pinus sylvestris* L.) growth suppression and adverse effects on human health due to air pollution in the Upper Silesian Industrial District (USID), Southern Poland. *Water Air Soil Pollut.* **2012**, *223*, 3345–3364. [CrossRef] [PubMed]
5. Dmuchowski, W.; Bytnerowicz, A. Monitoring environmental pollution in Poland by chemical analysis of Scots pine (*Pinus sylvestris* L.) needles. *Environ. Pollut.* **1995**, *87*, 87–104. [CrossRef]
6. Białobok, S. *Outline of Physiology of Scots Pine (Zarys Fizjologii Sosny Zwyczajnej)*, 1st ed.; SORUS: Poznań, Poland; Kórnik, Poland, 1976; pp. 1–613.
7. Sensuła, B.; Wilczyński, S.; Monin, L.; Allan, M.; Pazdur, A.; Fagel, N. Variations of tree ring width and chemical composition of wood of pine growing in the area nearby chemical factories. *Geochronometria* **2017**, *44*, 226–239. [CrossRef]
8. Sensuła, B.; Fagel, N.; Michczyński, A. Radiocarbon, trace elements and Pb isotope composition of pine needles from a highly industrialized region in southern Poland. *Radiocarbon* **2021**, *63*, 713–726. [CrossRef]
9. Ehrelinger, J.R.; Hall, A.E.; Farquhar, G.D. *Stable Isotopes and Plant Carbon-Water Relation*, 1st ed.; Academic Press: New York, NY, USA, 1993; pp. 1–555.
10. Leavitt, S.; Long, A. Stable carbon isotopes as a potential supplemental tool in dendrochronology. *Tree Ring Bull.* **1982**, *42*, 49–56.
11. McCarroll, D.; Gagen, M.H.; Loader, N.J.; Robertson, I.; Anchukaitis, K.J.; Los, S.; Young, G.H.F.; Jalkanen, R.; Kirchhefer, A.; Waterhouse, J.S. Correction of tree ring stable carbon isotope chronologies for changes in the carbon dioxide content of the atmosphere. *Geochim. Cosmochim. Acta* **2009**, *73*, 1539–1547. [CrossRef]
12. Craig, H. Carbon-13 in plants and the relationship between carbon-13 and carbon-14 variations in nature. *J. Geol.* **1954**, *62*, 115–149. [CrossRef]
13. Keeling, C.D.; Chin, J.F.S.; Whorf, T.P. Increased activity of northern vegetation inferred from atmospheric CO_2 measurements. *Nature* **1996**, *382*, 146–149. [CrossRef]
14. Sensuła, B.; Michczyński, A.; Piotrowska, N.; Wilczyński, S. Anthropogenic CO_2 Emission Records in Scots Pine Growing in the Most Industrialized Region of Poland from 1975 to 2014. *Radiocarbon* **2018**, *60*, 1041–1053. [CrossRef]
15. Gagen, M.; Finsinger, W.; Wagner-Cremer, F.; McCarroll, D.; Loader, N.; Robertson, I.; Jalkanen, R.; Young, G.; Kirchhefer, A. Evidence of changing intrinsic water-use efficiency under rising atmospheric CO_2 concentrations in Boreal Fennoscandia from sub-fossil leaves and tree ring δ13C ratios. *Glob. Chang. Biol.* **2011**, *17*, 1064–1072. [CrossRef]
16. Scheidegger, Y.; Saurer, M.; Bahn, M.; Siegwolf, R. Linking stable oxygen and carbon isotopes with stomatal conductance and photosynthetic capacity: A conceptual model. *Oecologia* **2000**, *125*, 350–357. [CrossRef] [PubMed]
17. Sensuła, B.; Wilczyński, S.; Opała, M. Tree growth and climate relationship: Dynamics of scots pine (*Pinus sylvestris* L.) growing in the near-source region of the combined heat and power plant during the development of the pro-ecological strategy in Poland. *Water Air Soil Pollut.* **2015**, *226*, 220. [CrossRef] [PubMed]

18. Sensuła, B.; Wilczyński, S. Climatic signals in tree-ring width and stable isotopes composition of *Pinus sylvestris* L. Growing in the industrialized area nearby Kędzierzyn-Koźle. *Geochronometria* **2017**, *44*, 240–255. [CrossRef]
19. Sensuła, B.; Wilczyński, S. Tree-ring widths and the stable isotope composition of pine tree-rings as climate indicators in the most industrialised part of Poland during CO_2 elevation. *Geochronometria* **2018**, *45*, 130–145. [CrossRef]
20. Sensula, B.; Opala, M.; Wilczynski, S.; Pawelczyk, S. Long- and short-term incremental response of *Pinus sylvestris* L. from industrial area nearby steelworks in Silesian Upland, Poland. *Dendrochronologia* **2015**, *36*, 1–12. [CrossRef]
21. Vicente-Serrano, S.M.; Beguería, S.; López-Moreno, J.I. A Multi-scalar drought index sensitive to global warming: The Standardized Precipitation Evapotranspiration Index—SPEI. *J. Clim.* **2010**, *23*, 1696–1718. [CrossRef]
22. Allen, R.G.; Pereira, L.S.; Raes, D.; Smith, M. *Crop Evapotranspiration: Guidelines for Computing Crop Requirements*; FAO Irrigation and Drainage Paper; FAO: Rome, Italy, 1998; p. 56.
23. SPEI Database. Available online: https://spei.csic.es/spei_database_2_7 (accessed on 24 October 2022).
24. World Bank Group GOST Climate. Available online: https://bennyistanto.github.io/gost-climate/indices/spei.html (accessed on 24 October 2022).
25. Eckstein, D.; Schweingruber, F. Dendrochronologia—A mirror for 25 years of tree-ring research and a sensor for promising topics. *Dendrochronologia* **2009**, *27*, 7–13. [CrossRef]
26. Hughes, M.K.; Swetnam, T.W.; Diaz, H.F. Dendroclimatology progress and prospects. In *Development in Paleoenvironmental Research*; Springer: Dordrecht, The Netherlands, 2011; p. 11.
27. Fritts, H.C. *Tree Rings and Climate*; Academic Press: London, UK, 1976; pp. 1–567.
28. Juknys, R.; Stravinskiene, V.; Vencloviene, J. Tree-ring analysis for the assessment of anthropogenic changes and trends. *Environ. Monit. Assess.* **2002**, *77*, 81–97. [CrossRef]
29. Wilczyński, S. The variation of tree−ring widths of Scots pine (*Pinus sylvestris* L.) affected by air pollution. *Eur. J. For. Res.* **2006**, *125*, 213–219. [CrossRef]
30. Elling, W.; Dittmar, C.; Pfaffelmoser, K.; Rotzer, T. Dendroecological assessment of the complex causes of decline and recovery of the growth of silver fir (*Abies alba* Mill.) in Southern Germany. *For. Ecol. Manag.* **2009**, *257*, 1175–1187. [CrossRef]
31. Stravinskiene, V.; Bartkevicius, E.; Plausinyte, E. Dendrochronological research of Scots pine (*Pinus sylvestris* L.) radial growth in vicinity of industrial pollution. *Dendrochronologia* **2013**, *31*, 179–186. [CrossRef]
32. Sensuła, B.; Wilczyński, S. Records of Anthropogenic Pollution in Silesia Captured in Scots Pine Tree Rings: Analysis by Radiocarbon, Stable Isotopes, and Basal Area Increment Analysis. *Water Air Soil Pollut.* **2022**, *233*, 143. [CrossRef]
33. Wilczyński, S. Record of the changes in environment by Scots pine and Jack pine trees. *Sylwan* **2020**, *164*, 583–593. [CrossRef]
34. Lindholm, M.; Timonen, M.; Meriläinen, J. Extracting mid-summer temperatures from ring-width chronologies of living pines at the northern forest limit in Fennoscandia. *Dendrochronologia* **1996**, *14*, 99–113.
35. Wilczyński, S.; Skrzyszewski, J. The climatic signal in tree-rings of Scots pine (*Pinus sylvestris* L.) from foot-hills of the Sudetic Mountains, southern Poland. *For. Cent.* **2002**, *121*, 15–24. [CrossRef]
36. Tuovinen, M. Response of tree−ring width and density of *Pinus sylvestris* to climate beyond the continuous northern forest line in Finland. *Dendrochronologia* **2005**, *22*, 83–91. [CrossRef]
37. Helama, S.; Mielikäinen, K.; Timonen, M.; Herva, H.; Tuomenvirta, H.; Veneäläinen, A. Regional climatic signals in Scots pine growth with insights into snow and soil associations. *Dendrobiology* **2013**, *70*, 27–34. [CrossRef]
38. Juknys, R.; Augustaitis, A.; Vencloviene, J.; Kliučius, A.; Vitas, A.; Bartkevičius, E.; Jurkonis, N. Dynamic response of tree growth to changing environmental pollution. *Eur. J. For. Res.* **2014**, *133*, 713–724. [CrossRef]
39. Ermich, K. Studies on the seasonal course of the radial increment of *Pinus silvestris* L. and *Quercus robur* L. *Acta Soc. Bot. Pol.* **1959**, *28*, 15–63. [CrossRef]
40. Andersson, E. Cone and Seed Studies in Norway Spruce (*Picea abies* (L.) Karst). In *Studia Forestalia Suecica*; Skogshögskolan: Stockholm, Sweden, 1965; p. 23.
41. Fober, H. Relation between climatic factors and Scots pine (*Pinus sylvestris* L.) cone crops in Poland. *Arbor. Kórnickie* **1976**, *21*, 367–374.
42. Chałupka, W.; Giertych, M.; Królikowski, Z. The effect of cone crops on growth in Scot pine on tree diameter increment. *Arbor. Kórnickie* **1976**, *21*, 361–366.
43. Hanninen, H.; Tanino, K. Tree seasonality in a warming climate. *Trends Plant Sci.* **2011**, *16*, 412–416. [CrossRef]
44. Rossi, S.; Morin, H.; Deslauriers, A.; Plourde, P.Y. Predicting xylem phenology in back spruce under climate warming. *Glob. Chang. Biol.* **2011**, *17*, 614–625. [CrossRef]
45. Rossi, S.; Deslauriers, A.; Anfodillo, T.; Carraro, V. Evidence of threshold temperatures for xylogenesis in conifers at high altitudes. *Oecologia* **2007**, *152*, 1–12. [CrossRef]
46. Gruber, A.; Zimmermann, J.; Wieser, G.; Oberhuber, W. Effects of climate variables on intra-annual stem radial increment in *Pinus cembra* along the alpine treeline ecotone. *Ann. For. Sci.* **2009**, *66*, 503. [CrossRef]
47. Swidrak, I.; Gruber, A.; Kofler, W.; Oberhuber, W. Effects of environmental conditions on onset of xylem growth in *Pinus sylvestris* under drought. *Tree Physiol.* **2011**, *31*, 483–493. [CrossRef]
48. Oberhuber, W.; Gruber, A.; Kofler, W.; Swidrak, I. Radial stem growth in response to microclimate and soil moisture in a drought-prone mixed coniferous at an inner Alpine site. *Eur. J. Res.* **2014**, *133*, 467–479. [CrossRef]

49. Richter, K.; Eckstein, D.; Holmes, R.L. The dendrochronological signal of the pine trees, *Pinus* sp. in Spain. *Tree-Ring Bull.* **1991**, *51*, 1–13.
50. Pilcher, P.; Oberhuber, W. Radial growth response of coniferous forest trees in an inner Alpine environment to heat-wave in 2003. *For. Ecol. Manag.* **2007**, *242*, 1513–1523.
51. Thabeet, A.; Vennetier, M.; Gadbin-Henry, C.; Denelle, N.; Roux, M.; Caraglio, Y.; Vila, B. Response of *Pinus sylvestris* L. to recent climatic events in the French Mediterranean region. *Trees* **2009**, *23*, 843–853. [CrossRef]
52. Irvine, J.; Perks, M.P.; Magnani, F.; Grace, J. The response of *Pinus sylvestris* to drought: Stomatal control of transpiration and hydraulic conductance. *Tree Physiol.* **1998**, *18*, 393–402. [CrossRef] [PubMed]
53. Cinnirella, S.; Magnani, F.; Saracino, A.; Borghetti, M. Response of a mature *Pinus laricio* plantation to a three-year restriction of water supply: Structural and functional acclimation to drought. *Tree Physiol.* **2002**, *22*, 21–30. [CrossRef] [PubMed]
54. Pensa, M.; Salminen, H.; Jalkanen, R. A 250-year-long height-increment chronology for Pinus sylvestris at the northern coniferous timberline: A novel tool for reconstructing past summer temperatures? *Dendrochronologia* **2005**, *22*, 75–81. [CrossRef]
55. Gruber, A.; Strobl, S.; Veit, B.; Oberhuber, W. Impact of drought on the temporal dynamics of wood formation in *Pinus sylvestris*. *Tree Physiol.* **2010**, *30*, 490–501. [CrossRef]
56. Cook, E.R.; Holmes, R.L. User's manual for program ARSTAN. In *Tree−Ring Chronologies of Western North America: California, Eastern Oregon a Northern Great Basin*; Chronology; Holmes, R.L., Adams, R.K., Fritts, H.C., Eds.; Laboratory of Tree-Ring Research, University of Arizona: Tucson, AZ, USA, 1986; Volume 6, pp. 50–56.
57. Pålnäsvägen, Sweden. Available online: https://www.cybis.se (accessed on 24 October 2022).
58. Holmes, R.L. Computer-assisted quality control in tree-ring dating and measurement. *Tree-Ring Bull.* **1983**, *43*, 69–78.
59. Green, J. Wood cellulose. In *Methods in Carbohydrate Chemistry 3*; Whistler, R.L., Ed.; Academic Press: New York, NY, USA, 1963; pp. 9–21.
60. Schweingruber, F.H.; Eckstein, D.; Serre-Bachet, F.; Bräker, O.U. Identification, presentation and interpretation of event years and pointer years in dendrochronology. *Dendrochronologia* **2009**, *8*, 9–38.
61. Saurer, M.; Spahni, R.; Frank, D.C.; Joos, F.; Leuenberger, M.; Loader, N.J.; McCarroll, D.; Gagen, M.; Poulter, B.; Siegwolf, R.T.W.; et al. Spatial variability and temporal trends in water-use efficiency of European forests. *Glob. Chang. Biol.* **2014**, *20*, 3700–3712. [CrossRef]
62. Biondi, F. Evolutionary and moving response functions in dendroclimatology. *Dendrochronologia* **1997**, *15*, 139–150.

plants

MDPI

Article

Do Different Tree-Ring Proxies Contain Different Temperature Signals? A Case Study of Norway Spruce (*Picea abies* (L.) Karst) in the Eastern Carpathians

Andrei Popa [1,2], Ionel Popa [1,3,*], Cătălin-Constantin Roibu [4] and Ovidiu Nicolae Badea [1,2]

1 National Institute for Research and Development in Forestry 'Marin Drăcea', 007190 Bucharest, Romania
2 Faculty of Silviculture and Forest Engineering, Transilvania University of Brașov, 500036 Brașov, Romania
3 Center for Mountain Economy (CE–MONT), 725700 Vatra Dornei, Romania
4 Forest Biometrics Laboratory, Faculty of Forestry, 'Stefan cel Mare' University of Suceava, 720229 Suceava, Romania
* Correspondence: popaicas@gmail.com

Abstract: One of the most important proxy archives for past climate variation is tree rings. Tree-ring parameters offer valuable knowledge regarding how trees respond and adapt to environmental changes. Trees encode all environmental changes in different tree-ring parameters. In this study, we analyzed how air temperature is encoded in different Norway spruce tree-ring proxies along an altitude gradient in an intramountain valley of the Carpathians. The study area, in the Gheorgheni region, Romania (Eastern Carpathians), has a mountain climate with a frequent temperature inversion in winter. The climate–growth relationship was analyzed for two contrasting altitudes: low elevation, i.e., below 1000 m a.s.l., and high elevation, i.e., above 1500 m a.s.l. Two local weather stations, one in the valley and the other on the upper part of the mountains, provide daily temperatures (Joseni—750 m a.s.l. and Bucin—1282 m a.s.l.). The bootstrap Pearson correlation between cumulative daily temperature data and three tree-ring proxies (tree-ring width—TRW, basal area increment—BAI, and blue intensity—BI) was computed for each series. The results show that elevation modulates the climate response pattern in the case of BI, and remains relatively similar for TRW and BAI. The winter temperature's positive influence on spruce growth was observed in both TRW and BAI chronologies. Additionally, the BAI chronology highlights a positive relationship with summer temperature. The highest correlation coefficient ($r = 0.551$, $p < 0.05$, $n = 41$) was recorded between BI residual chronology from high elevation series and summer/autumn temperature from the upper-part weather station for a cumulative period of 59 days (the second half of August to the beginning of October). Our results show that, for this intramountain valley of the Eastern Carpathians, different tree-ring proxies capture different climate signals.

Keywords: climate–growth relationship; climate signal; tree-ring width; basal area increment; blue intensity; daily climatic data

Citation: Popa, A.; Popa, I.; Roibu, C.-C.; Badea, O.N. Do Different Tree-Ring Proxies Contain Different Temperature Signals? A Case Study of Norway Spruce (*Picea abies* (L.) Karst) in the Eastern Carpathians. *Plants* **2022**, *11*, 2428. https://doi.org/10.3390/plants11182428

Academic Editor: Nenad Potočić

Received: 9 August 2022
Accepted: 13 September 2022
Published: 17 September 2022

Publisher's Note: MDPI stays neutral with regard to jurisdictional claims in published maps and institutional affiliations.

1. Introduction

Tree growth is driven by multiple factors, and climatic conditions represent one of the main drivers of wood accumulation [1,2]. Changes in climatic conditions (e.g., temperature rise, precipitation decrease) and higher frequencies of extreme events (e.g., heat waves, long periods of drought) induce stress on trees and forest stands, with negative ecological and economic effects [3,4]. All these environmental changes are encoded in different tree-ring parameters.

In the context of climate change, increasing efforts have been made to understand and assess the effect of environmental change on forest ecosystems [5]. Knowledge and mitigation of climate-change impacts represent a central goal for forest management systems [6–10].

Dendrochronological studies analyzing how trees are influenced by climate and how tree species adapt to new climate conditions also provide a record of the past climate [1,2,11]. Tree rings can be used as an important proxy to highlight annual climate variations [12]. The main tree-ring proxy used in dendrochronology is tree-ring width (TRW). However, in some cases, TRW does not provide a strong and robust climate signal compared to other tree-ring parameters such as maximum latewood density (MXD) or stable isotopes [13–18]. Usually, to ascertain MXD, expensive equipment is required, and there are logistical limitations. A relatively new parameter (image-based blue reflectance—blue intensity, BI) has been developed to respond to these limitations [19–21]. BI is a proxy that represents measured reflected light in specific wavelengths of the color spectrum. Studies have shown a strong correlation (over r = 0.95, $p < 0.05$) between BI and MXD [19–24]. BI has a stronger climate signal in temperature-limited ecosystems compared to TRW and is less sensitive to disturbances [24,25]. Based on these findings, there is potential for BI to be used as a substitute for MXD. However, the basal area increment (BAI) represents a two-dimensional measurement, specifically on the surface of the tree ring. The basal area increment is more related to the biomass increment of the tree and stand productivity [26,27]. Moreover, BAI is a suitable proxy that can preserve low and medium-frequency growth variability [28,29].

Norway spruce (*Picea abies* (L.) Karst) is one of the dominant coniferous species at both the Romanian and European levels [30]. On a large scale, Norway spruce is managed in monocultures due to its high productivity and ability to grow at high rates inside and outside of natural areas, with significant economic advantages [31]. Monoculture management, which focuses mainly on wood production, is prone to more issues compared to mixed-forest management, which focuses on both productivity and biodiversity, with higher stand resistance and resilience [8,32,33]. Generally, Norway spruce growth is driven by summer temperature in mountainous areas and by precipitation at lower elevations [34–39]. Spruce has demonstrated high sensitivity to extreme events such as drought or heatwaves [40–42].

In mountainous areas, due to alternating slopes and valleys, it is possible to have a regional climate modulated by a local topography [43]. The particular local climate specific to the intramountain valleys of the Carpathians can induce different climate responses of tree species (in our case, Norway spruce) compared with general patterns observed in mountainous regions.

In this study, we aimed to determine the climate signals captured in three tree proxies (TRW, BAI, and BI) of Norway spruce in an intramountain valley in the Eastern Carpathians along an altitudinal gradient. The specific research questions were:

- How does air temperature modulate Norway spruce growth in an intramountain valley of the Carpathians?
- Is the correlation between temperature and the investigated tree-ring parameters stable through time?

2. Results and Discussion

2.1. Description of Chronologies

The individual age of sampled trees varies from 68 years to 135 years with a mean chronologies age of 98 years, with insignificant differences between low- and high-elevation chronologies (Table 1). The average growth rate is 1.96 mm·year^{-1}, and ranges from 1.77 mm·year^{-1} (high elevation) to 2.16 mm·year^{-1} (low elevation). A reduction in tree growth with increasing elevation is expected, being the consequence of temperature decrease and shortening of the growing season [34,44].

Table 1. Basis statistics for the six chronologies: TRW—tree-ring width; BAI—basal area increment; BI—blue intensity; AGR—average growth rate (mm year^{-1} for TRW, mm^2 year^{-1} for BAI, and no unit for BI); SD—standard deviation; Rbar—series intercorrelation; Mean sens—mean sensitivity; Auto corr.—serial autocorrelation.

Tree Ring Proxy	Series Length			AGR ± SD	Rbar	Mean Sens	Auto Corr.
	Mean	Min	Max				
Low Elevation Chronologies							
TRW	95	79	135	2.16 ± 0.53	0.304	0.176	0.869
BAI				1445.7 ± 614.7	0.299	0.211	0.773
BI				2.27 ± 0.17	0.146	0.063	0.548
High Elevation Chronologies							
TRW	101	68	133	1.77 ± 0.54	0.335	0.150	0.857
BAI				1003.6 ± 541.6	0.333	0.163	0.844
BI				2.15 ± 0.20	0.287	0.077	0.459

Common variance, expressed by the mean series intercorrelation (Rbar) with values around 0.3 for all tree-ring proxies except for BI at the low elevation, reflects a medium climatic control of Norway spruce growth in the study area. The mean sensitivity of the analyzed chronologies showed lower interannual variability for BI chronologies compared to TRW or BAI chronologies. Low mean-sensitivity values are typical for Norway spruce growing in optimal climatic conditions [35]. Lower values for mean sensitivity of BI chronologies have also been recorded for Norway spruce in other regions [45,46] or for other species from the *Picea*, *Abies* genus [45,47,48]. The temporal memory, expressed by serial autocorrelation of raw data, is highest in the case of TRW and lowest for BI.

The TRW, BAI, and BI index chronologies were truncated for the period 1978–2019 to overlap with the climatic data (Figure 1). The expressed population signal (EPS) for the analyzed period exceeds the threshold of 0.85 [49] for all chronologies.

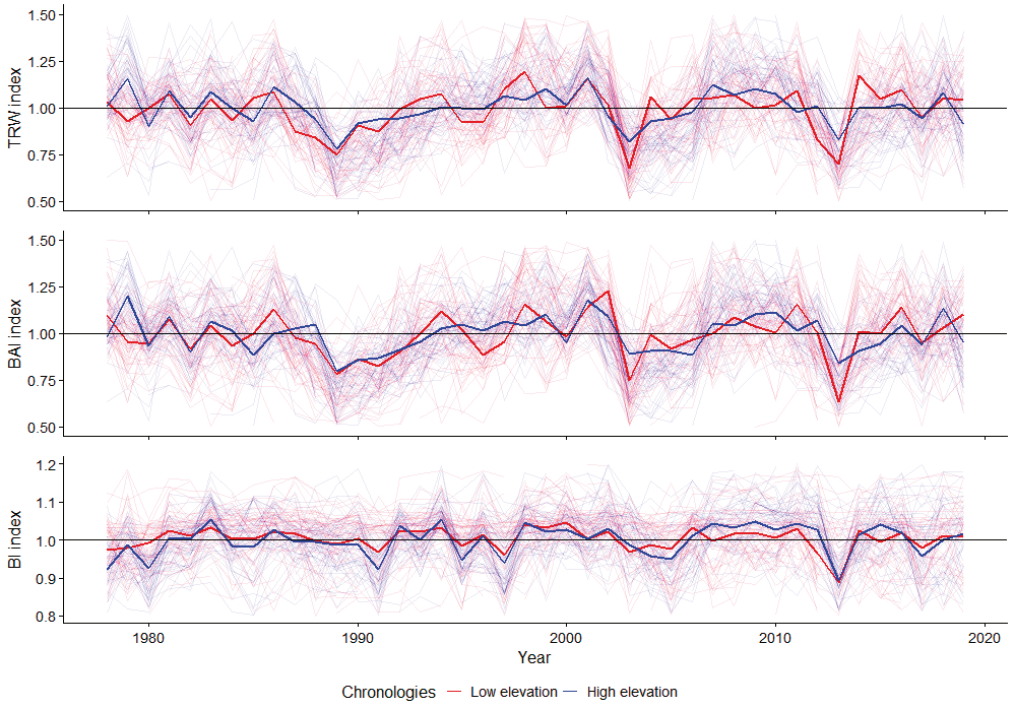

Figure 1. Norway spruce TRW, BAI, and BI residual index series chronologies for 1978–2019 (the shadowed line represents the individual series and the thicker line represents the master chronologies).

2.2. Climate–Growth Relationships for Three Tree-Ring Parameters

The TRW residual index chronologies correlate positively with winter temperatures (cumulative windows width starting from 21 to 120 days) (Figure 2). The correlation coefficient between high-elevation TRW index chronology and mean temperature from the up-hill weather station (Bucin) has the highest value (r = 0.494, $p < 0.05$, $n = 41$) with the 3 December–18 January period. The low-elevation TRW index chronology has the highest correlation (r = 0.485, $p < 0.05$, $n = 41$) with the 1 November–12 February mean temperature from the up-hill weather station. Regarding the correlation between the TRW residuals index and the winter air temperature from the valley weather station, the maximum correlations were lower (r= 0.442, $p < 0.05$, $n = 41$—high-elevation chronology and r = 0.435, $p < 0.05$, $n = 41$—low-elevation chronology).

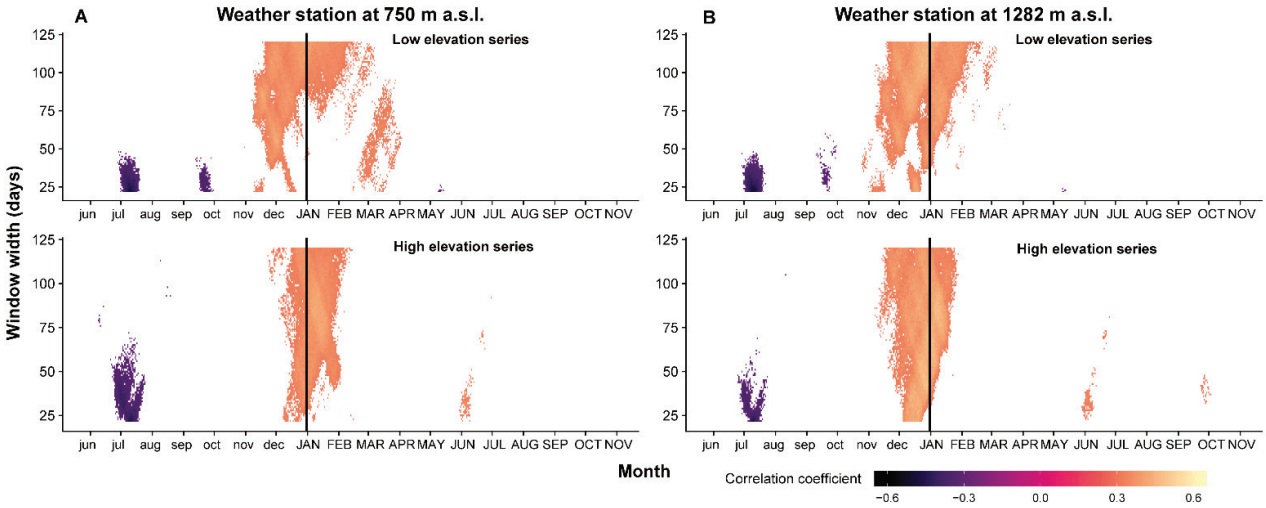

Figure 2. Correlation between TRW residual index chronologies and cumulative daily temperature from valley weather station (Joseni) (**A**) and from up-hill weather station (Bucin) (**B**) (vertical black line represents the limit between previous (with lowercase) and current (with uppercase) year).

Moreover, the TRW residual index chronology from low-elevation sites shows a positive and significant correlation with spring temperature (recorded in the valley) from March to April (r = 0.374, $p < 0.05$, $n = 41$). For both chronologies, low and high elevation, a negative correlation between TRW residual index and mean temperatures is present in the previous vegetation season, in July. The maximum negative correlation between TRW residual index chronologies and previous summer temperature varies from r = −0.502 ($p < 0.05$, $n = 41$) for low-elevation series (temperature from the up-hill weather station) to r = −0.462 ($p < 0.05$, $n = 41$) for high-elevation series (temperature from the up-hill weather station). A significant negative correlation between TRW index chronology and temperature in the previous autumn is present only at low-elevation sites, regardless of the weather station.

A positive correlation between the TRW index and December temperatures has also been reported for other forests in the Eastern Carpathians [50]. In mountainous regions, and mainly at high elevation, the growth of Norway spruce is usually positively correlated with summer temperatures [35,37,38,50–52]. The positive correlation between TRW index chronologies and winter temperatures at an elevation above 1500 m a.s.l. is not a common dendroclimatic pattern for Norway spruce. The possible explanation for this climate–growth relationship could be related to temperature inversion with a high frequency during winter.

Generally, the air temperature is characterized by a decreasing gradient proportional to the elevation [53]. The average gradient for decreasing air temperature with the increase in elevation, in mountainous areas, is 0.6 °C/100 m [54]. Temperature inversions are phenomena caused by the abnormal variation of the radiative heat balance induced by terrain fragmentation, depth of valleys, and local topographical peculiarities [55–57]. Temperature

inversions are a common occurrence in intramountain valleys, especially in the Eastern Carpathians [56,58]. Thermal inversion leads to cold-air stagnation at the bottom of the valleys, which favors fog formation with a significant impact on both human health and vegetation growth [59]. At the same time, the upper part of the slopes benefits from higher global radiation and warmer air mass with positive effects on vegetation and soil conditions.

Due to the temperature inversion phenomenon or mild winters, a higher air temperature in the cold season can lead to faster snow melt and higher soil temperature. These factors have a positive influence on cambium reactivation and apical growth in the spring, decreasing the risk of tissue freezing and even creating a low probability of xylem embolism in the spring [60–62]. These hypotheses could offer a possible explanation for the positive and significant correlation between temperatures in the winter and TRW index chronologies.

A negative correlation between TRW index series and temperature from the previous vegetation season has been observed in other Eastern Carpathian sites [50], Tatra Mountains [38,63], in the timberline in East-Central Europe [37,64], and in the Alps [65]. This correlation highlights a sensitivity of Norway spruce growth to the previous year's temperature. Increasing summer temperatures may induce a reduction in the growth of spruce in the next year. This temporal memory of growth can be linked with structural carbohydrate dynamics and extending the growing season in previous years [51], and is supported by high values of first order autocorrelation (Table 1). The correlation of growth with the previous year temperature highlighted the importance of the carryover effects of climate variability, such as photosynthetic gain and storage of assimilates [1,66]. Moreover, a warm summer promotes the flowering of spruce, which is associated with a decrease in growth in the next year [67]. Hansen and Beck [68] highlight that the carbohydrates accumulated in previous autumn are depleted in spring. Also, the dynamics of spruce reserves involve an accumulation of lipids in summer which are metabolized during the autumn [69].

The BAI residual index chronology correlation pattern differs depending on elevation (Figure 3). The correlation between high-elevation BAI index chronology and winter temperatures recorded at the up-hill weather station is significant and has a higher value for the period of 26 November to 18 February. Interestingly, the positive correlation between winter–spring temperatures and the BAI index chronology from a low elevation is no longer significant when the temperatures are considered from the up-hill weather station. Regarding the high-elevation BAI index chronology, the correlation patterns with respect to the mean temperatures from both weather stations are similar. In the case of the winter period, the correlation with temperatures from the valley weather station is significant for longer cumulative window lengths.

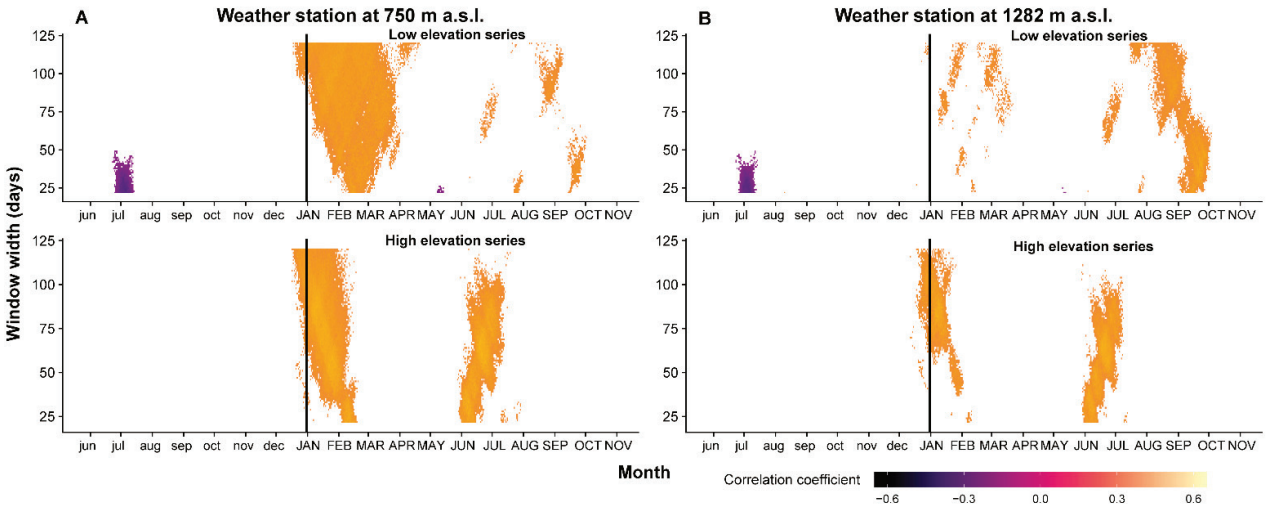

Figure 3. Correlation between BAI residual index chronologies and cumulative daily temperature from valley weather station (Joseni) (**A**) and from up-hill weather station (Bucin) (**B**) (vertical black line represents the limit between previous (with lowercase) and current (with uppercase) year).

Compared to the dendroclimatic pattern of TRW, a positive relationship with summer temperature was observed for BAI. The highest correlation was recorded between the BAI chronology from the high elevation and cumulative temperatures from the valley weather station from 17 May to 22 July ($r = 0.468$, $p < 0.05$, $n = 41$). A positive correlation with summer temperature on the current year's wood accumulation is logical for high-altitude chronology, since temperature is a limiting factor for these habitats [35]. A negative correlation ($r = -0.507$, $p < 0.05$, $n = 41$) between BAI residual chronology from lower sites and previous summer temperatures is significant for cumulative periods of 29 days (second half of June to the middle of July) for both weather stations. The authors of [51] point out that higher temperatures during the summer can induce a high rate of respiration with negative effects on carbohydrate reserves used in the first phase of growth of the next year. The photosynthetic gain during the previous summer has a strong effect on current year ring width [67,70].

A clear pattern of positive and significant correlation coefficient between temperature and BI chronologies was found only for the high-elevation chronology (Figure 4). The highest correlation between the BI residual chronology from high-elevation series and summer/autumn from the up-hill station is 0.551, $p < 0.05$, $n = 41$ for cumulative windows of 59 days (second half of August to the beginning of October). An unusual correlation was found between the BI index and winter temperature from the valley weather station. This may be a false-positive correlation because it is less likely that winter temperature has a strong influence on the wood density of latewood. The correlation between low-elevation BI chronology and mean temperature from the previous summer is negative and significant ($r = -0.481$, $p < 0.05$, $n = 41$) for a cumulative window of 28 days; that is, 19 June–17 July. No significant correlation between BI index and previous year temperature was noted in the case of the high-elevation chronology.

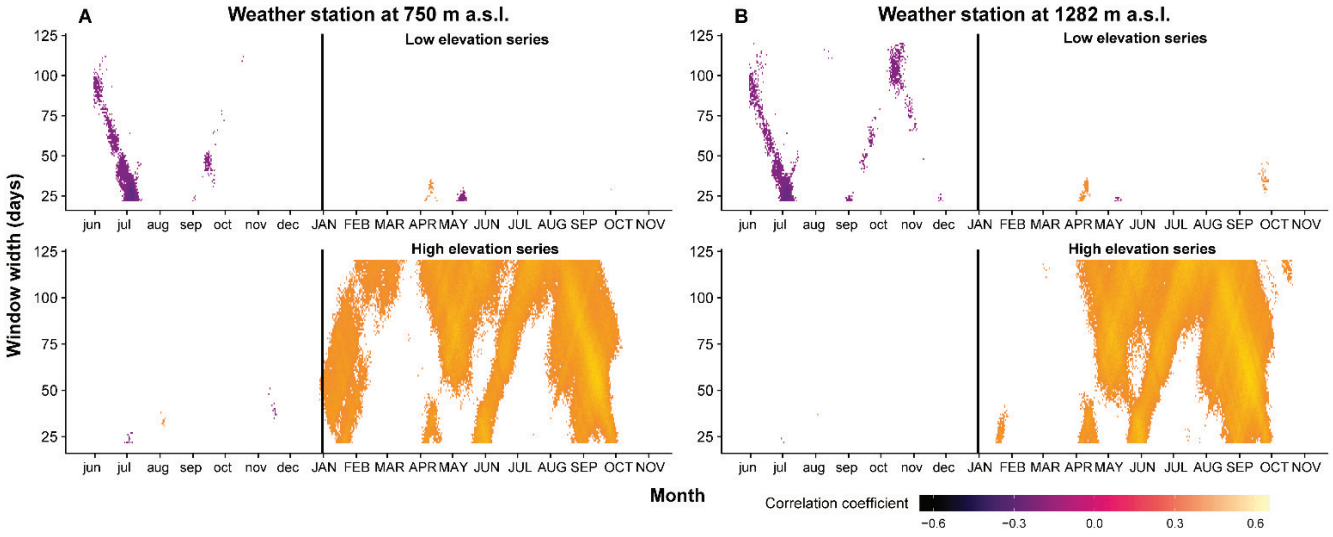

Figure 4. Correlation between BI residual index chronologies and cumulative daily temperature from valley weather station (Joseni) (**A**) and from up-hill weather station (Bucin) (**B**) (vertical black line represents the limit between previous (with lowercase) and current (with uppercase) year).

In contrast, at low elevation, the BI chronology shows almost no significant correlation with current year temperatures. This suggests that at elevations below 1000 m, in this intramountain valley, the late-summer temperature is not a limiting factor in the thickening and lignification of cell walls of Norway spruce. This can be linked to a longer growing season at lower-altitude sites and a higher stand productivity [35]. The highest correlation between tree-ring parameters and temperature has been reported for BI chronologies from the high elevation. These BI correlation patterns show that thickening of the secondary cellular wall and the lignification process at high altitude are driven by the late-summer

temperature [71]. The negative relationship with the previous year's temperature can be explained by the trade-offs in the carbohydrate allocation for seed production, increment and formation of buds, with significant effects on nutrients reserves available for next year's growing start [72,73]. It has already been reported in the literature that BI chronologies, as surrogates for maximum latewood density, express a stronger relationship with climate compared to TRW at sites where the temperature is the most limiting factor [16,20,74–76].

Tree-ring width or basal area increment are tree-ring proxies containing aggregated information about the climate conditions throughout the whole growth season, and about disturbances. Meanwhile, the blue intensity contains information about the second part of the growing season. The combination of these three tree-ring proxies can offer an integrated perspective on the climate–growth relationship.

2.3. Time Stability of Climate–Growth Relationship

The time stability correlation between TRW, BAI, and BI residual chronologies and temperature from the up-hill weather station was assessed using the cumulative window with the highest correlation coefficient. It was preferred to assess the time stability for windows with the highest correlations despite different periods between low and high elevation chronologies. The periods with the highest correlations may be the most relevant for assessing the climate sensitivity of Norway spruce. In the case of TRW, for the low-elevation series, the highest correlation was for the interval between 31 October and 18 February and, in the case of the high-elevation series, for the period between 5 December and 14 January. The time variation pattern of the correlation has evident temporal shifts, mainly in the second part of the analyzed period (Figure 5A). For the high-elevation chronology, the correlation has an increasing general trend with a small decrease around 1992 and stabilization after 2000. Contrary to the low-elevation chronology, the correlation intensity increased until the 1989–2003 period. After that, a slight decrease was recorded, with robust stability in time in the last years. The correlation between the low-elevation TRW chronology and temperature from the up-hill weather station is lower than the correlation recorded for high-elevation sites for most of the periods analyzed.

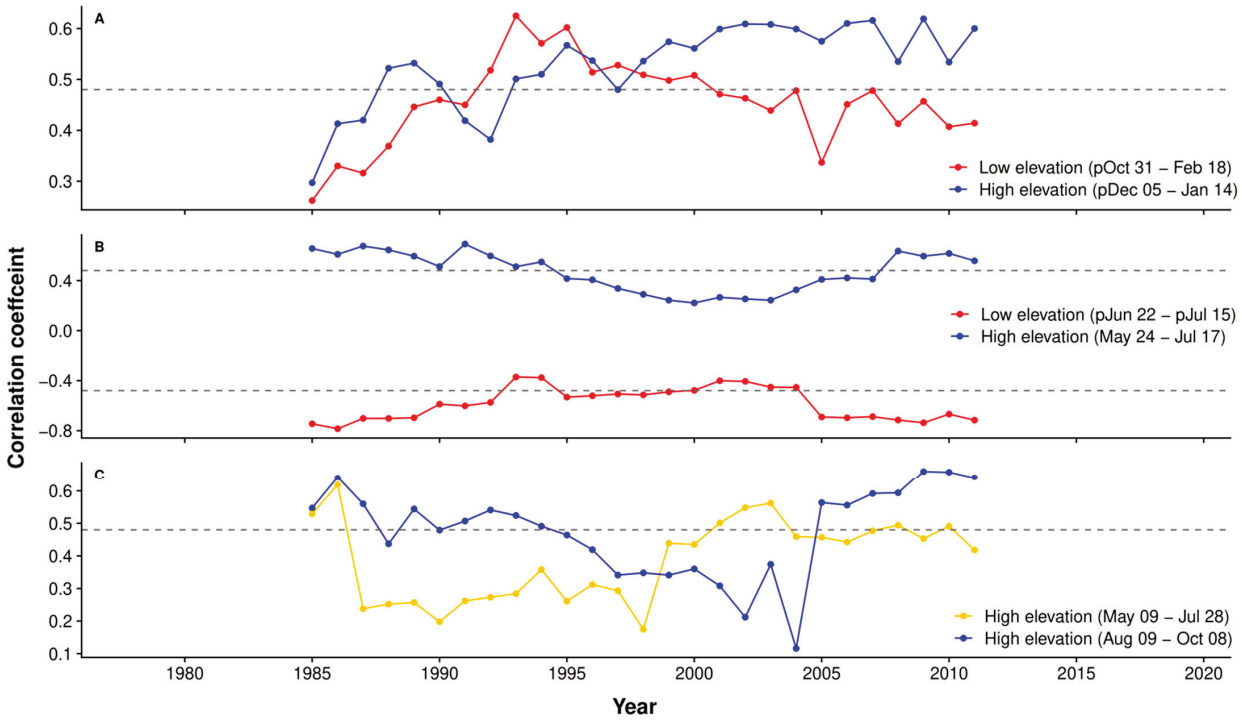

Figure 5. The 15-year running correlations between air temperature and tree-ring proxies ((**A**)—tree-ring width; (**B**)—basal area increment; (**C**)—blue intensity). The legend contains the site location and period (with the dashed line representing a significant correlation coefficient for $p < 0.05$, $n = 15$).

The stability of correlation between the BAI chronology from upper sites and growing season temperatures (24 May to 17 July) is stable in time with a slight decrease around the 2000s (Figure 5B). The correlation coefficient for the entire period is r = 0.441, with a minimum correlation of r = 0.298 for the period 1995–2009. Similarly, for lower sites, the BAI chronology moving correlation with previous summer temperatures (22 June to 15 July) records a reduction of the intensity in the middle of the analyzed periods, which is statistically non-significant. The decrease in correlation highlights a temporal instability in the climate sensitivity of BAI for both elevations, which has also been reported in other Norway spruce sites around Europe [34,44].

The time stability for BI correlation with air temperature was checked only for the high-elevation chronology (Figure 5C). Two periods were analyzed, one in the first part of the growing season (9 May to 28 July) and one in the late part (9 August to 8 October). The correlation between the temperature at the beginning of the growing season and BI index chronology has lower values in the first part of the analyzed period. The correlation is stable in time and significant only after the 1997–2010 period. The temperature from the last part of the growing season leads to a constant decrease in time of the correlation with the BI residual chronology, followed by a significant increase after 2004.

The running correlation for a 15-year period highlights the non-stationary correlation between TRW, BAI, and BI index chronologies, and air temperature. The continuous climate change leads to different responses of trees to temperature.

3. Materials and Methods

3.1. Study Area

The study was carried out in the Gheorgheni region, a large intramountain valley in the center of the Eastern Carpathians (Romania). The altitude in the study region ranges from 700 m a.s.l. to 1770 m a.s.l. The study area is located between 46°37′ N, 25°25′ E and 46°50′ N, 25°36′ E (Figure 6). The general geology of the study area is represented by a volcanogenic–sedimentary complex.

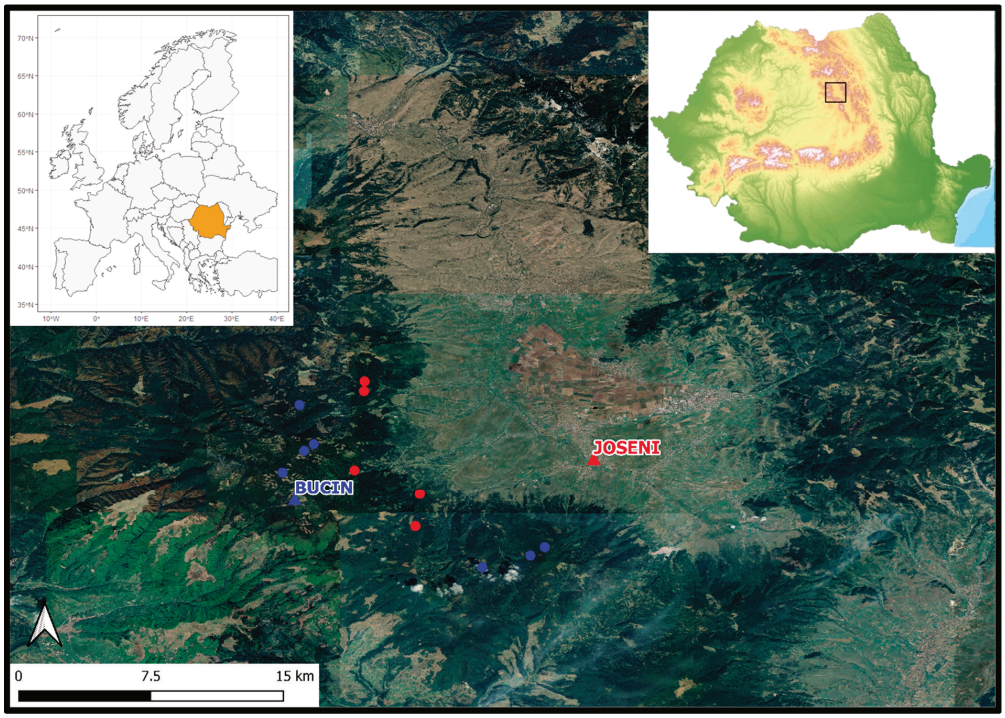

Figure 6. The study localization—with blue the high elevation sites, up-hill weather station, and with red the low elevation sites, valley weather station (image source: https://geoportal.ancpi.ro (accessed on 1 August 2022); https://earth.google.com (accessed on 1 August 2022)).

All the forests in the study area are managed forests, even-aged, and the Norway spruce is the main species. The forests belong to private and community owners and are managed by Gheorgheni Forest District manly in a high forest silvicultural system (clear-cutting system and shelterwood system).

In the study area mean annual temperature varies from 6.0 °C at the lower part of the valley to 4.8 °C at higher elevations (Figure 7). The average amount of annual precipitation is 542 mm at 750 m a.s.l. and 1004 mm in the upper part of the valley. The coldest month is January (the mean temperature at the lower part of the valley is −6.4 °C and −5.7 °C at higher elevations) and the warmest is July (the mean temperature at the lower part of the valley is 16.6 °C and 14.1 °C at up-hill weather station). The month with the most precipitation is June with 130 mm in the upper part of the valley and 90 mm at the lower part. The study area is characterized by frequent thermal inversion [59]. January is the month with the highest average of days with temperature inversion (13.8 days) followed by December (12.9 days) and November (11.9 days). During the spring/summer months, on average, less than 1–2 days with temperature inversion were recorded.

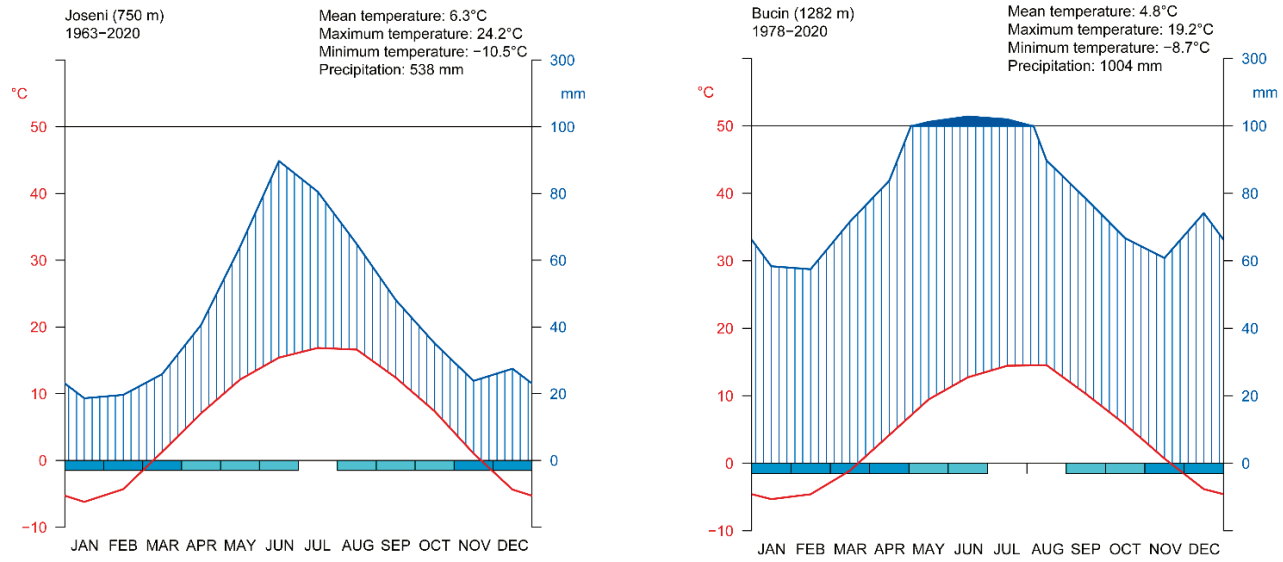

Figure 7. Climate diagrams according with Walter and Leith [77] for the local weather stations in the study area (valley station on the right and up-hill station on the left). The red line represents the variations of the mean monthly temperatures, the blue line represents the variations of the monthly precipitation, the blue hatched area represents the humid period, and the blue filled area represents the wet period. The bar in the lower part suggests the indication of months where frost is likely.

The climate diagrams according to Walter and Leith were created in R using the climatol package [78].

3.2. Sample Collection and Data Processing

To investigate the effect of altitude on the Norway spruce, climate response increment cores from 12 locations were collected: five locations at low elevation (altitude varied from 880 m a.s.l. to 1020 m a.s.l.) and seven locations at high elevation (altitude varied from 1510 m a.s.l. to 1630 m a.s.l.). In each plot, 15 to 20 dominant and healthy trees were selected to extract increment cores. By applying a sampling strategy, we selected mature trees, and the limitation of the analysis period to available temperature data ensured the exclusion of the juvenile growth part from the climate–growth relationship analysis. One core per tree was extracted using a 5-mm-diameter Pressler borer at breast height (i.e., 1.3 m). For each sampled tree, 2 perpendicular breast-height diameters (DBH) were measured with a forest caliper. The mean of these two diameters was used to compute the BAI. All three tree-ring proxies (TRW, BAI, and BI) were measured/calculated for the same cores. A subset of

50 cores for each altitude level (high and low elevations), were selected for measurements and analysis. In order to obtain reliable BI measurements, we selected only cores with no discoloration due to fungi, no gaps due to broken cores, and with parallel rings, as well as from cores containing pith or those that allowed easy determination of any missing rings.

Increment cores were dried, mounted on wooden supports, and sanded with successive sanding grits (from 80 grit to 400 grit) to ensure the flatness of the sanded surface and ring boundaries' visibility. Sandpaper of 400 grains/mm^2, according to [79], can assure the quality of BI measurements. After sanding, cores were scanned at 1200 DPI using an Epson Expression 12,000 XL scanner to measure TRW and BI. The scanning resolution (1200 DPI) used in this study represents the scanner's hardware optical resolution, and we did not use an interpolation algorithm that could affect the BI measurements [79].

Norway spruce is a coniferous species with no visible differences between heartwood and sapwood. Based on this characteristic of spruce wood, it is possible to measure latewood blue reflectance without any chemical treatments [22,80–82]. To measure latewood blue reflectance, the standard protocol was followed [21,23]. Window parameter settings were adjusted according to [21]. The measured values of blue reflectance were transformed into blue intensity (BI) using Equation (1):

$$x_{i(adj)} = 2.56 - \frac{x_i}{100} \quad (1)$$

where x_i represents the raw BI value for the year i; the constant 2.56 is used to ensure that all the values of BI are positive (all the possible values for x_i are from 0 to 255). The inversion step was computed in CooRecorder 9.6 [83].

The tree-ring measurements (TRW and BI) were computed using CooRecorder software on scanned images [83]. No missing or false rings were observed.

The BAI was reconstructed for each ring individually and adjusted according to the mean DBH of each tree. The DBH of each tree (i) and for each year (t) was reconstructed by subtracting the doubled radial growth in the year t from the DBH in the year t. The calculation starts with the DBH measured in the year of coring (Equation (2)) [84].

$$DBH_{i(t-1)} = DBH_{i(t)} - 2 \times TRW_{i(t)} \quad (2)$$

Based on the annual reconstructed DBH, the BAI for each tree was calculated using the following equation:

$$BAI_t = \frac{\pi}{4} \times \left(DBH_t^2 - DBH_{t-1}^2 \right) \quad (3)$$

The BAI was calculated using an iterative function in R [85].

The measured individual series were cross-dated visually using TSAP-Win software [86]. COFECHA software was used for statistically cross-dating and measurement checking using correlation analysis of detrended 50-year intervals with a 25-year overlap [87,88].

A cubic smoothing spline function with a 50% frequency cutoff at 30 years was used to eliminate the age trend and any other disturbance signals in TRW and BAI chronologies [89,90]. According to [21], for the BI value, there is a possible increase in the juvenile period due to the transformation from blue reflectance to blue intensity. Because of this, the detrending of the BI series was made by fitting a Hugershoff curve to raw measurements [89].

For each analyzed tree-ring parameter, 2 chronologies were developed, one for low elevation and the second for high elevation. Indices were computed as the ratio between raw measurements and fitted values. In order to eliminate the autocorrelation that was still present in the standard index series, an autoregressive model was applied. In the analyses, we used the residual index chronologies obtained by bi-weight mean without variance stabilization. The chronologies quality and proprieties were assessed by calcu-

lating the classical dendrochronological statistics parameters as mean sensitivity, mean series intercorrelation, first-order autocorrelation, and expressed population signal. The mean sensitivity highlights the change in year-to-year tree growth [1]. The mean series intercorrelation (known as R-bar) and expressed population signal (known as EPS) express the signal strength in the analyzed chronologies and the common variability [49,89]. The carry-over effect of the previous year's climate condition on the current year's growth can be assessed by first-order autocorrelation [1,2]. The detrending, chronology development, and statistical parameters were computed using the dplR package on R software [91].

3.3. Climatic Dataset

Two local weather stations, Joseni (750 m a.s.l.)—valley weather station—and Bucin (1282 m a.s.l.)—up-hill weather station—provided the climatic data (daily mean temperature) (Figures 6 and 7). Climatic data are available from 1963 at the Joseni weather station and from 1978 at the Bucin weather station. Therefore, the analyzed interval was limited to the common period, 1978–2019.

3.4. Climate–Growth Relationship Assessment

The availability of local daily air temperature data in the study area allowed us to analyze the climate–growth relationship on a cumulative daily scale [92]. Using the monthly temperature data, a common practice in dendroclimatology [89], to investigate the relationship between climate and tree growth conduce to a signal lost because of the artificial split of year in months, without any physiological bases [92,93]. The tree photosynthesis and wood increment are continuous processes and require more flexible time windows to investigate the relationship between tree growth and climate. The bootstrapped (n = 1000 replications) Pearson correlation between the TRW, BAI, and BI residual index chronologies and cumulative daily mean temperature was calculated [94,95]. Bootstrap samples were selected randomly with replacement from the entire interval (1978–2019) [96]. The significance of the bootstrapped correlation coefficient, at $p < 0.05$, was established according with [97]. The daily temperatures were aggregated in moving time windows of 21 days to 120 days starting from June in the previous year of growth to October of the current growing season. The time stability of correlations was checked for running windows with a length of 15 years, moved by one year [96]. The correlation between residual index chronologies and cumulative daily temperatures and time stability were computed using the dendroTools package in R [98].

4. Conclusions

Our results show that each tree-ring proxy contains a different climate signal. In the studied intramountain valley in the Eastern Carpathians, the growth of Norway spruce is influenced by winter temperatures, and signals demonstrating this are present in both TRW and BAI chronologies. The presence of temperature inversions can explain the unusual correlation pattern. The TRW and winter temperature correlation is unstable through time for both elevations, with evident temporal shifts after 1996. The highest correlations for TRW were obtained for cumulative windows of 45 days at high elevation and for cumulative windows of 113 days for low elevation; both cumulative windows are centered at the beginning of January. The BAI at high elevation contains a strong temperature signal from the middle of the growing season. In the case of BI, a clear climatic signal was observed only for the high-elevation chronology for cumulative windows starting in the second half of August to the beginning of October. The preliminary results obtained in this study need to be replicated for other intramountain valleys in the Carpathians to confirm the change in the general dendroclimatic pattern (growth driven by summer temperature) due to specific local climate modulated by thermal inversions.

Author Contributions: Conceptualization, A.P. and I.P.; methodology, A.P. and I.P.; software, A.P.; formal analysis, A.P.; investigation, A.P. and I.P.; resources, A.P. and I.P.; data curation, A.P. and I.P.; visualization, A.P. and C.-C.R.; writing—original draft preparation, A.P.; writing—review and editing, I.P., C.-C.R. and O.N.B.; supervision, I.P. and O.N.B.; project administration, I.P.; funding acquisition, I.P. and O.N.B. All authors have read and agreed to the published version of the manuscript.

Funding: A.P., I.P. and O.N.B. were supported by a grant of the Ministry of Research, Innovation and Digitization, CNCS-UEFISCDI, project number PN-III-P4-PCE-2021–1002, within PNCDI III and from project CresPerfInst (contract 34PFE/30.12.2021). C-C.R. was supported by a grant of the Ministry of Research, Innovation and Digitization, CNCS-UEFISCDI, project number PN-III-P1-1.1-TE-2021-1419, within PNCDI III.

Institutional Review Board Statement: Not applicable.

Informed Consent Statement: Not applicable.

Data Availability Statement: The data presented in this study are available on a reasonable request from the corresponding author.

Acknowledgments: Permission to work in the forests from the Gheorgheni area was granted to us by the Gheorgheni Forest District (Arnold Horvath). We want to thank to Mihai Balabașciuc for help in the field and in the laboratory. We would like to thank the reviewers for all valuable comments and suggestions, which helped us to improve the quality of the manuscript.

Conflicts of Interest: The authors declare no conflict of interest.

References

1. Fritts, H. *Tree Rings and Climate*; Elsevier: Amsterdam, The Netherlands, 1976; ISBN 0323145280.
2. Speer, J.H. *Fundamentals of Tree-Ring Research*; University of Arizona Press: Tucson, AZ, USA, 2010; ISBN 0816526842.
3. Kramer, K.; Leinonen, I.; Loustau, D. The importance of phenology for the evaluation of impact of climate change on growth of boreal, temperate and Mediterranean forests ecosystems: An overview. *Int. J. Biometeorol.* **2000**, *44*, 67–75. [CrossRef]
4. Lindner, M.; Maroschek, M.; Netherer, S.; Kremer, A.; Barbati, A.; Garcia-Gonzalo, J.; Seidl, R.; Delzon, S.; Corona, P.; Kolström, M.; et al. Climate change impacts, adaptive capacity, and vulnerability of European forest ecosystems. *For. Ecol. Manag.* **2010**, *259*, 698–709. [CrossRef]
5. European Environment Agency. *European Forest Ecosystems: State and Trends*; Publications Office of European Union: Luxembourg, 2016.
6. Bigler, C.; Veblen, T.T. Increased early growth rates decrease longevities of conifers in subalpine forests. *Oikos* **2009**, *118*, 1130–1138. [CrossRef]
7. Di Filippo, A.; Pederson, N.; Baliva, M.; Brunetti, M.; Dinella, A.; Kitamura, K.; Knapp, H.D.; Schirone, B.; Piovesan, G. The longevity of broadleaf deciduous trees in Northern Hemisphere temperate forests: Insights from tree-ring series. *Front. Ecol. Evol.* **2015**, *3*, 46. [CrossRef]
8. Lindenmayer, D.B.; Franklin, J.F. *Conserving Forest Biodiversity: A Comprehensive Multiscaled Approach*; Island Press: Washington, DC, USA, 2002; ISBN 1559639350.
9. Pretzsch, H.; Biber, P.; Schütze, G.; Uhl, E.; Rötzer, T. Forest stand growth dynamics in Central Europe have accelerated since 1870. *Nat. Commun.* **2014**, *5*, 4967. [CrossRef]
10. Vitali, V.; Büntgen, U.; Bauhus, J. Seasonality matters—The effects of past and projected seasonal climate change on the growth of native and exotic conifer species in Central Europe. *Dendrochronologia* **2018**, *48*, 1–9. [CrossRef]
11. Parobeková, Z.; Sedmáková, D.; Kucbel, S.; Pittner, J.; Jaloviar, P.; Saniga, M.; Balanda, M.; Vencurik, J. Influence of disturbances and climate on high-mountain Norway spruce forests in the Low Tatra Mts., Slovakia. *For. Ecol. Manag.* **2016**, *380*, 128–138. [CrossRef]
12. Jones, P.D.; Briffa, K.R.; Osborn, T.J.; Lough, J.M.; van Ommen, T.D.; Vinther, B.M.; Luterbacher, J.; Wahl, E.R.; Zwiers, F.W.; Mann, M.E.; et al. High-resolution palaeoclimatology of the last millennium: A review of current status and future prospects. *Holocene* **2009**, *19*, 3–49. [CrossRef]
13. Büntgen, U.; Frank, D.C.; Nievergelt, D.; Esper, J. Summer Temperature Variations in the European Alps, a.d. 755–2004. *J. Clim.* **2006**, *19*, 5606–5623. [CrossRef]
14. Schweingruber, F.; Fritts, H.; Bräker, O.; Drew, L.; Schär, E. The X-ray technique as applied to dendroclimatology. *Tree Ring Bull.* **1978**, *38*, 61–91.
15. Wilson, R.; Anchukaitis, K.; Briffa, K.R.; Büntgen, U.; Cook, E.; D'Arrigo, R.; Davi, N.; Esper, J.; Frank, D.; Gunnarson, B.; et al. Last millennium northern hemisphere summer temperatures from tree rings: Part I: The long term context. *Quat. Sci. Rev.* **2016**, *134*, 1–18. [CrossRef]
16. Nagavciuc, V.; Roibu, C.-C.; Ionita, M.; Mursa, A.; Cotos, M.-G.; Popa, I. Different climate response of three tree ring proxies of Pinus sylvestris from the Eastern Carpathians, Romania. *Dendrochronologia* **2019**, *54*, 56–63. [CrossRef]

17. Nagavciuc, V.; Kern, Z.; Ionita, M.; Hartl, C.; Konter, O.; Esper, J.; Popa, I. Climate signals in carbon and oxygen isotope ratios of *Pinus cembra* tree-ring cellulose from the Călimani Mountains, Romania. *Int. J. Clim.* **2020**, *40*, 2539–2556. [CrossRef]
18. Koprowski, M.; Duncker, P. Tree ring width and wood density as the indicators of climatic factors and insect outbreaks affecting spruce growth. *Ecol. Indic.* **2012**, *23*, 332–337. [CrossRef]
19. McCarroll, D.; Pettigrew, E.; Luckman, A.; Guibal, F.; Edouard, J.-L. Blue Reflectance Provides a Surrogate for Latewood Density of High-latitude Pine Tree Rings. *Arct. Antarct. Alp. Res.* **2002**, *34*, 450–453. [CrossRef]
20. Campbell, R.; McCarroll, D.; Loader, N.J.; Grudd, H.; Robertson, I.; Jalkanen, R. Blue intensity in *Pinus sylvestris* tree-rings: Developing a new palaeoclimate proxy. *Holocene* **2007**, *17*, 821–828. [CrossRef]
21. Rydval, M.; Larsson, L.-Å.; McGlynn, L.; Gunnarson, B.E.; Loader, N.J.; Young, G.H.F.; Wilson, R. Blue intensity for dendroclimatology: Should we have the blues? Experiments from Scotland. *Dendrochronologia* **2014**, *32*, 191–204. [CrossRef]
22. Björklund, J.A.; Gunnarson, B.E.; Seftigen, K.; Esper, J.; Linderholm, H.W. Blue intensity and density from northern Fennoscandian tree rings, exploring the potential to improve summer temperature reconstructions with earlywood information. *Clim. Past* **2014**, *10*, 877–885. [CrossRef]
23. Campbell, R.; McCarroll, D.; Robertson, I.; Loader, N.J.; Grudd, H.; Gunnarson, B. Blue Intensity In Pinus sylvestris Tree Rings: A Manual for A New Palaeoclimate Proxy. *Tree-Ring Res.* **2011**, *67*, 127–134. [CrossRef]
24. Wilson, R.; Rao, R.; Rydval, M.; Wood, C.; Larsson, L.-Å.; Luckman, B.H. Blue Intensity for dendroclimatology: The BC blues: A case study from British Columbia, Canada. *Holocene* **2014**, *24*, 1428–1438. [CrossRef]
25. Björklund, J.A.; Gunnarson, B.E.; Seftigen, K.; Esper, J.; Linderholm, H.W. Is Blue Intensity Ready to Replace Maximum Latewood Density as a Strong Temperature Proxy? A Tree-Ring Case Study on Scots Pine from Northern Sweden. *Clim. Past Discuss.* **2013**, *9*, 5227–5261. [CrossRef]
26. Biondi, F. Comparing tree-ring chronologies and repeated timber inventories as forest monitoring tools. *Ecol. Appl.* **1999**, *9*, 12. [CrossRef]
27. West, P. Use of diameter increment and basal area increment in tree growth studies. *Can. J. For. Res.* **1980**, *10*, 71–77. [CrossRef]
28. Biondi, F.; Qeadan, F. A Theory-Driven Approach to Tree-Ring Standardization: Defining the Biological Trend from Expected Basal Area Increment. *Tree-Ring Res.* **2008**, *64*, 81–96. [CrossRef]
29. Han, Y.; Wang, Y.; Liu, B.; Huang, R.; Camarero, J.J. Moisture mediates temperature-growth couplings of high-elevation shrubs in the Tibetan plateau. *Trees* **2022**, *36*, 273–281. [CrossRef]
30. Caudullo, G.; Tinner, W.; de Rigo, D. *Picea abies* in Europe: Distribution, habitat, usage and threats. In *European Atlas of Forest Tree Species*; Publication Office of EU: Luxembourg, 2016.
31. Klimo, E.; Hager, H.; Kulhavý, J. *Spruce Monocultures in Central Europe: Problems and Prospects*; European Forest Institute Joensuu: Joensuu, Finland, 2000; Volume 33.
32. Paquette, A.; Messier, C. The effect of biodiversity on tree productivity: From temperate to boreal forests: The effect of biodiversity on the productivity. *Glob. Ecol. Biogeogr.* **2011**, *20*, 170–180. [CrossRef]
33. Schütz, J.-P.; Götz, M.; Schmid, W.; Mandallaz, D. Vulnerability of spruce (*Picea abies*) and beech (*Fagus sylvatica*) forest stands to storms and consequences for silviculture. *Eur. J. For. Res* **2006**, *125*, 291–302. [CrossRef]
34. Bošel'a, M.; Sedmák, R.; Sedmáková, D.; Marušák, R.; Kulla, L. Temporal shifts of climate–growth relationships of Norway spruce as an indicator of health decline in the Beskids, Slovakia. *For. Ecol. Manag.* **2014**, *325*, 108–117. [CrossRef]
35. Levanič, T.; Gričar, J.; Gagen, M.; Jalkanen, R.; Loader, N.J.; McCarroll, D.; Oven, P.; Robertson, I. The climate sensitivity of Norway spruce [*Picea abies* (L.) Karst.] in the southeastern European Alps. *Trees* **2009**, *23*, 169–180. [CrossRef]
36. Mäkinen, H.; Nöjd, P.; Kahle, H.-P.; Neumann, U.; Tveite, B.; Mielikäinen, K.; Röhle, H.; Spiecker, H. Radial growth variation of Norway spruce (*Picea abies* (L.) Karst.) across latitudinal and altitudinal gradients in central and northern Europe. *For. Ecol. Manag.* **2002**, *171*, 243–259. [CrossRef]
37. Ponocná, T.; Spyt, B.; Kaczka, R.; Büntgen, U.; Treml, V. Growth trends and climate responses of Norway spruce along elevational gradients in East-Central Europe. *Trees* **2016**, *30*, 1633–1646. [CrossRef]
38. Savva, Y.; Oleksyn, J.; Reich, P.B.; Tjoelker, M.G.; Vaganov, E.A.; Modrzynski, J. Interannual growth response of Norway spruce to climate along an altitudinal gradient in the Tatra Mountains, Poland. *Trees* **2006**, *20*, 735–746. [CrossRef]
39. Koprowski, M.; Zielski, A. Dendrochronology of Norway spruce (*Picea abies* (L.) Karst.) from two range centres in lowland Poland. *Trees* **2006**, *20*, 383–390. [CrossRef]
40. Lebourgeois, F.; Rathgeber, C.B.K.; Ulrich, E. Sensitivity of French temperate coniferous forests to climate variability and extreme events (*Abies alba*, *Picea abies* and *Pinus sylvestris*). *J. Veg. Sci.* **2010**, *21*, 364–376. [CrossRef]
41. Pichler, P.; Oberhuber, W. Radial growth response of coniferous forest trees in an inner Alpine environment to heat-wave in 2003. *For. Ecol. Manag.* **2007**, *242*, 688–699. [CrossRef]
42. Van der Maaten-Theunissen, M.; Kahle, H.-P.; van der Maaten, E. Drought sensitivity of Norway spruce is higher than that of silver fir along an altitudinal gradient in southwestern Germany. *Ann. For. Sci.* **2013**, *70*, 185–193. [CrossRef]
43. Barry, R.G. *Mountain Weather and Climate*; Psychology Press: London, UK, 1992; ISBN 0415071135.
44. Kolář, T.; Čermák, P.; Trnka, M.; Žid, T.; Rybníček, M. Temporal changes in the climate sensitivity of Norway spruce and European beech along an elevation gradient in Central Europe. *Agric. For. Meteorol.* **2017**, *239*, 24–33. [CrossRef]

45. Begović, K.; Rydval, M.; Mikac, S.; Čupić, S.; Svobodova, K.; Mikoláš, M.; Kozák, D.; Kameniar, O.; Frankovič, M.; Pavlin, J.; et al. Climate-growth relationships of Norway Spruce and silver fir in primary forests of the Croatian Dinaric mountains. *Agric. For. Meteorol.* **2020**, *288–289*, 108000. [CrossRef]
46. Kaczka, R.J.; Spyt, B.; Janecka, K.; Beil, I.; Büntgen, U.; Scharnweber, T.; Nievergelt, D.; Wilmking, M. Different maximum latewood density and blue intensity measurements techniques reveal similar results. *Dendrochronologia* **2018**, *49*, 94–101. [CrossRef]
47. Tsvetanov, N.; Dolgova, E.; Panayotov, M. First measurements of Blue intensity from Pinus peuce and Pinus heldreichii tree rings and potential for climate reconstructions. *Dendrochronologia* **2020**, *60*, 125681. [CrossRef]
48. Schwab, N.; Kaczka, R.; Janecka, K.; Böhner, J.; Chaudhary, R.; Scholten, T.; Schickhoff, U. Climate Change-Induced Shift of Tree Growth Sensitivity at a Central Himalayan Treeline Ecotone. *Forests* **2018**, *9*, 267. [CrossRef]
49. Wigley, T.M.; Briffa, K.R.; Jones, P.D. On the average value of correlated time series, with applications in dendroclimatology and hydrometeorology. *J. Appl. Meteorol. Climatol.* **1984**, *23*, 201–213. [CrossRef]
50. Sidor, C.G.; Popa, I.; Vlad, R.; Cherubini, P. Different tree-ring responses of Norway spruce to air temperature across an altitudinal gradient in the Eastern Carpathians (Romania). *Trees* **2015**, *29*, 985–997. [CrossRef]
51. Bouriaud, O.; Popa, I. Comparative dendroclimatic study of Scots pine, Norway spruce, and silver fir in the Vrancea Range, Eastern Carpathian Mountains. *Trees* **2009**, *23*, 95–106. [CrossRef]
52. Leonelli, G.; Pelfini, M. Influence of climate and climate anomalies on norway spruce tree-ring growth at different altitudes and on glacier responses: Examples from the central italian alps. *Geogr. Ann. Ser. A Phys. Geogr.* **2008**, *90*, 75–86. [CrossRef]
53. Apăvaloae, M.; Apostol, L.; Pîrvulescu, I. Inversiunile termice din culoarul Moldovei (sectorul Câmpulung Moldovenesc–Frasin) și influența lor asupra poluării atmosferei. *Sci. Ann. "Stefan Cel Mare" Univ. Geogr. Ser.* **1994**, 5.
54. Ahrens, C.D. *Meteorology Today: An Introduction to Weather, Climate, and the Environment*; Cengage Learning Canada, Inc.: Toronto, ON, Canada, 2015; ISBN 0176728333.
55. Apăvaloae, M.; Pîrvulescu, I.; Apostol, L. Caracteristici ale inversiunilor termice din Podișul Fălticenilor. *Lucr. Semin. Geogr. "Dimitrie Cantemir"* **1987**, 8.
56. Ciutea, A.; Jitariu, V. Thermal inversions identification through the analysis of the vegetation inversions occurred in the forest ecosystems from the Eastern Carpathians. *Present Environ. Sustain. Dev.* **2020**, *14*, 29–42. [CrossRef]
57. Ichim, P.; Apostol, L.; Sfîcă, L.; Kadhim-Abid, A.-L.; Istrate, V. Frequency of Thermal Inversions Between Siret and Prut Rivers in 2013. *Present Environ. Sustain. Dev.* **2014**, *8*, 267–284. [CrossRef]
58. Sfîcă, L.; Nicuriuc, I.; Niță, A. Boundary Layer Temperature Stratification as Result of Atmospheric Circulation within the Western Side of Brașov Depression. In Proceedings of the 2019 Air and Water Components of the Environment Conference, Cluj-Napoca, Romania, 22–24 March 2019; pp. 53–64.
59. Palffy, E. Temperature inversion in the Csik basin. *Acta Clim.* **1995**, *28*, 41–45.
60. Mayr, S.; Schmid, P.; Beikircher, B.; Feng, F.; Badel, E. Die hard: Timberline conifers survive annual winter embolism. *New Phytol.* **2020**, *226*, 13–20. [CrossRef] [PubMed]
61. Rossi, S.; Deslauriers, A.; Anfodillo, T.; Carraro, V. Evidence of threshold temperatures for xylogenesis in conifers at high altitudes. *Oecologia* **2007**, *152*, 1–12. [CrossRef] [PubMed]
62. Rossi, S.; Rathgeber, C.B.K.; Deslauriers, A. Comparing needle and shoot phenology with xylem development on three conifer species in Italy. *Ann. For. Sci.* **2009**, *66*, 206. [CrossRef]
63. Buntgen, U.; Frank, D.C.; Kaczka, R.J.; Verstege, A.; Zwijacz-Kozica, T.; Esper, J. Growth responses to climate in a multi-species tree-ring network in the Western Carpathian Tatra Mountains, Poland and Slovakia. *Tree Physiol.* **2007**, *27*, 689–702. [CrossRef] [PubMed]
64. Putalová, T.; Vacek, Z.; Vacek, S.; Štefančík, I.; Bulušek, D.; Král, J. Tree-ring widths as an indicator of air pollution stress and climate conditions in different Norway spruce forest stands in the Krkonoše Mts. *Cent. Eur. For. J.* **2019**, *65*, 21–33. [CrossRef]
65. Leal, S.; Melvin, T.M.; Grabner, M.; Wimmer, R.; Briffa, K.R. Tree-ring growth variability in the Austrian Alps: The influence of site, altitude, tree species and climate. *Boreas* **2007**, *36*, 426–440. [CrossRef]
66. Matisons, R.; Elferts, D.; Krišāns, O.; Schneck, V.; Gärtner, H.; Wojda, T.; Kowalczyk, J.; Jansons, Ā. Nonlinear Weather–Growth Relationships Suggest Disproportional Growth Changes of Norway Spruce in the Eastern Baltic Region. *Forests* **2021**, *12*, 661. [CrossRef]
67. Selås, V.; Piovesan, G.; Adams, J.M.; Bernabei, M. Climatic factors controlling reproduction and growth of Norway spruce in southern Norway. *Can. J. For. Res.* **2002**, *32*, 9. [CrossRef]
68. Hansen, J.; Beck, E. Seasonal changes in the utilization and turnover of assimilation products in 8-year-old Scots pine (*Pinus sylvestris* L.) trees. *Trees* **1994**, *8*, 172–182. [CrossRef]
69. Holl, W. Seasonal Fluctuation of Reserve Materials in the Trunkwood of Spruce [*Picea abies* (L.) Karst.]. *J. Plant Physiol.* **1985**, *117*, 355–362. [CrossRef]
70. Kozlowski, T.T.; Pallardy, S.G. *Growth Control in Woody Plants*; Elsevier: Amsterdam, The Netherlands, 1997; ISBN 0080532683.
71. Gindl, W.; Grabner, M.; Wimmer, R. The influence of temperature on latewood lignin content in treeline Norway spruce compared with maximum density and ring width. *Trees* **2000**, *14*, 409–414. [CrossRef]
72. Hacket-Pain, A.; Ascoli, D.; Berretti, R.; Mencuccini, M.; Motta, R.; Nola, P.; Piussi, P.; Ruffinatto, F.; Vacchiano, G. Temperature and masting control Norway spruce growth, but with high individual tree variability. *For. Ecol. Manag.* **2019**, *438*, 142–150. [CrossRef]

73. Matisons, R.; Elferts, D.; Krišāns, O.; Schneck, V.; Gärtner, H.; Bast, A.; Wojda, T.; Kowalczyk, J.; Jansons, Ā. Non-linear regional weather-growth relationships indicate limited adaptability of the eastern Baltic Scots pine. *For. Ecol. Manag.* **2021**, *479*, 118600. [CrossRef]
74. Akhmetzyanov, L.; Sánchez-Salguero, R.; García-González, I.; Buras, A.; Dominguez-Delmás, M.; Mohren, F.; den Ouden, J.; Sass-Klaassen, U. Towards a new approach for dendroprovenancing pines in the Mediterranean Iberian Peninsula. *Dendrochronologia* **2020**, *60*, 125688. [CrossRef]
75. Fuentes, M.; Salo, R.; Björklund, J.; Seftigen, K.; Zhang, P.; Gunnarson, B.; Aravena, J.-C.; Linderholm, H.W. A 970-year-long summer temperature reconstruction from Rogen, west-central Sweden, based on blue intensity from tree rings. *Holocene* **2018**, *28*, 254–266. [CrossRef]
76. Știrbu, M.-I.; Roibu, C.-C.; Carrer, M.; Mursa, A.; Unterholzner, L.; Prendin, A.L. Contrasting Climate Sensitivity of Pinus cembra Tree-Ring Traits in the Carpathians. *Front. Plant Sci.* **2022**, *13*, 855003. [CrossRef] [PubMed]
77. Walter, H.; Lieth, H. *Klimadiagramm-Weltatlas: Von Heinrich Walter Und Helmut Lieth*; Gustav Fischer Verlag Jena: Jena, Germany, 1967.
78. Guijarro, J.A.; Guijarro, M.J.A. Package 'Climatol'. 2019. Available online: https://cran.r-project.org/web/packages/climatol/climatol.pdf (accessed on 20 April 2020).
79. Babst, F.; Frank, D.; Büntgen, U.; Nievergelt, D.; Esper, J. Effect of sample preparation and scanning resolution on the Blue Reflectance of *Picea abies*. *TRACE Proc.* **2009**, *7*, 188–195.
80. Björklund, J.; Gunnarson, B.E.; Seftigen, K.; Zhang, P.; Linderholm, H.W. Using adjusted Blue Intensity data to attain high-quality summer temperature information: A case study from Central Scandinavia. *Holocene* **2015**, *25*, 547–556. [CrossRef]
81. Wilson, R.; D'Arrigo, R.; Andreu-Hayles, L.; Oelkers, R.; Wiles, G.; Anchukaitis, K.; Davi, N. Experiments based on blue intensity for reconstructing North Pacific temperatures along the Gulf of Alaska. *Clim. Past* **2017**, *13*, 1007–1022. [CrossRef]
82. Wilson, R.; Anchukaitis, K.; Andreu-Hayles, L.; Cook, E.; D'Arrigo, R.; Davi, N.; Haberbauer, L.; Krusic, P.; Luckman, B.; Morimoto, D.; et al. Improved dendroclimatic calibration using blue intensity in the southern Yukon. *Holocene* **2019**, *29*, 1817–1830. [CrossRef]
83. Maxwell, R.S.; Larsson, L.-A. Measuring tree-ring widths using the CooRecorder software application. *Dendrochronologia* **2021**, *67*, 125841. [CrossRef]
84. Bosela, M.; Tumajer, J.; Cienciala, E.; Dobor, L.; Kulla, L.; Marčiš, P.; Popa, I.; Sedmák, R.; Sedmáková, D.; Sitko, R.; et al. Climate warming induced synchronous growth decline in Norway spruce populations across biogeographical gradients since 2000. *Sci. Total Environ.* **2021**, *752*, 141794. [CrossRef] [PubMed]
85. R Core Team. *R: A Language and Environment for Statistical Computing*; R Foundation for Statistical Computing: Vienna, Austria, 2022.
86. Rinn Tech. *TSAPWin Scientific: Time Series Analysis and Presentation for Dendrochronology and Related Applications*; Rinn Tech: Heidelberg, Germany, 2012.
87. Holmes, R. Computer assisted quality control. *Tree-Ring Bull* **1983**, *43*, 69–78.
88. Grissino-Mayer, H.D. Evaluating crossdating accuracy: A manual and tutorial for the computer program COFECHA. *Tree Ring Res.* **2001**, *57*, 205–221.
89. Cook, E.R.; Kairiukstis, L.A. *Methods of Dendrochronology: Applications in the Environmental Sciences*; Springer Science & Business Media: Berlin/Heidelberg, Germany, 1990; ISBN 9401578796.
90. Schweingruber, F.H. *Tree Rings: Basics and Applications of Dendrochronology*; Springer Science & Business Media: Berlin/Heidelberg, Germany, 1989; ISBN 9400912730.
91. Bunn, A.G. A dendrochronology program library in R (dplR). *Dendrochronologia* **2008**, *26*, 115–124. [CrossRef]
92. Jevšenak, J. Daily climate data reveal stronger climate-growth relationships for an extended European tree-ring network. *Quat. Sci. Rev.* **2019**, *221*, 105868. [CrossRef]
93. Beck, W.; Sanders, T.G.M.; Pofahl, U. CLIMTREG: Detecting temporal changes in climate–growth reactions—A computer program using intra-annual daily and yearly moving time intervals of variable width. *Dendrochronologia* **2013**, *31*, 232–241. [CrossRef]
94. Efron, B.; Tibshirani, R. Bootstrap methods for standard errors, confidence intervals, and other measures of statistical accuracy. *Stat. Sci.* **1986**, *1*, 54–75. [CrossRef]
95. Guiot, J. The bootstrapped response function. *Tree-Ring Bull* **1991**, *51*, 39–41.
96. Biondi, F.; Waikul, K. DENDROCLIM2002: A C++ program for statistical calibration of climate signals in tree-ring chronologies. *Comput. Geosci.* **2004**, *30*, 303–311. [CrossRef]
97. Dixon, P. Bootstrap resampling. In *The Encyclopedia of Environmetrics*; El-Shaarawi, A.H., Piegorsch, W.W., Eds.; Springer: Berlin/Heidelberg, Germany, 2001.
98. Jevšenak, J.; Levanič, T. dendroTools: R package for studying linear and nonlinear responses between tree-rings and daily environmental data. *Dendrochronologia* **2018**, *48*, 32–39. [CrossRef]

plants

MDPI

Article

Impact of an Extremely Dry Period on Tree Defoliation and Tree Mortality in Serbia

Goran Češljar [1,*], Filip Jovanović [2], Ljiljana Brašanac-Bosanac [3], Ilija Đorđević [1], Suzana Mitrović [3], Saša Eremija [2], Tatjana Ćirković-Mitrović [2] and Aleksandar Lučić [4]

[1] Department of Spatial Regulation, GIS and Forest Policy, Institute of Forestry, 11030 Belgrade, Serbia; djordjevic_ika@yahoo.com
[2] Department of Forest Establishment, Silviculture and Ecology, Institute of Forestry, 11030 Belgrade, Serbia; filip.a.jovanovic@gmail.com (F.J.); sasaeremija@gmail.com (S.E.); tanjacirk@gmail.com (T.Ć.-M.)
[3] Department of Environmental Protection and Improvement, Institute of Forestry, 11030 Belgrade, Serbia; brasanlj@yahoo.com (L.B.-B.); mitrovicsuzana79@gmail.com (S.M.)
[4] Department of Genetics, Plant Breeding, Seed and Nursery Production, Institute of Forestry, 11030 Belgrade, Serbia; aleksandar.lucic@gmail.com
* Correspondence: cesljargoran@gmail.com

Abstract: This paper presents research results on forest decline in Serbia. The results were obtained through monitoring defoliation of 34 tree species at 130 sample plots during the period from 2004 to 2018. This research aimed to determine whether the occurrence of defoliation and tree mortality were caused by drought. Defoliation was assessed in 5% steps according to the International Co-operative Programme on Assessment and Monitoring of Air Pollution Effects on Forests (ICP Forests) methodology. All the trees recorded as dead were singled out, and annual mortality rates were calculated. To determine changes in air temperature and precipitation regimes during the study period, we processed and analysed climatic data related to air temperature and precipitation throughout the year and in the growing season at 28 main weather stations in Serbia. Tree mortality patterns were established by classifying trees into three groups. The first group of trees exhibited a gradual increase in defoliation during the last few years of monitoring, with dying as the final outcome. The second group was characterised by sudden death of trees. The third group of trees reached a higher degree of defoliation immediately after the first monitoring year, and the trees died after several years. Tree mortality rates were compared between years using the Standardised Precipitation Evaporation Index (SPI) and the Standardised Precipitation Evapotranspiration Index (SPEI), the most common methods used to monitor drought. The most intensive forest decline was recorded during the period from 2013 to 2016, when the largest percentage of the total number of all trees died. According to the annual mortality rates calculated for the three observation periods (2004–2008, 2009–2013, and 2014–2018) the highest forest decline rate was recorded in the period from 2014 to 2018, with no statistically significant difference between broadleaved and coniferous tree species. As the sample of coniferous species was small, the number of sample plots should be increased in order to achieve better systematic forest condition monitoring in Serbia. The analysis of the relationship between defoliation and climatic parameters proved the correlation between them. It was noted that the forest decline in Serbia was preceded by an extremely dry period with high temperatures from 2011 to 2013, supporting the hypothesis that it was caused by drought. We therefore conclude that these unfavourable climatic conditions had serious and long-term consequences on forest ecosystems in Serbia.

Keywords: defoliation; forest decline; extreme climate events; drought; tree mortality

Citation: Češljar, G.; Jovanović, F.; Brašanac-Bosanac, L.; Đorđević, I.; Mitrović, S.; Eremija, S.; Ćirković-Mitrović, T.; Lučić, A. Impact of an Extremely Dry Period on Tree Defoliation and Tree Mortality in Serbia. *Plants* **2022**, *11*, 1286. https://doi.org/10.3390/plants11101286

Academic Editor: Nenad Potočić

Received: 21 February 2022
Accepted: 6 May 2022
Published: 11 May 2022

1. Introduction

Forest ecosystems and forest vitality are directly affected by rising mean annual temperatures, changing precipitation dynamics and quantity, and extreme weather events

of increasing and varying frequency and timing [1]. The impact of the changing climate on forests results from the complex interaction of meteorological factors and soil [2]. One of the effects of global warming is increasing risk of drought, the stress of which has a negative effect on forests [3]. The effects of prolonged and intense drought affect all parts of the environment. Droughts develop slowly, and often go unnoticed until they become visible to the naked eye. The slow manifestation and long duration of droughts often make their quantification very difficult [4]. Their main characteristics, such as onset, duration, and severity, are not easily or quickly detectable [5]. Drought should not be confused with aridity, which represents a permanent trait of a dry climate. Droughts affect all the components of the water cycle, resulting in a deficit of soil moisture and a decrease in the levels of groundwaters, brooks, and rivers. As they study precipitation and temperature as meteorological input variables, our investigations deal with meteorological drought and its influence on forest decline. Meteorological drought is the primary cause of drought. Other types of droughts (agricultural, hydrological, groundwater, and socioeconomic) describe the secondary effects of droughts on certain ecological and economic components [6].

Droughts and drought periods are not exclusively related to arid areas, such as the Mediterranean region; they can occur in areas that, while according to their climate characteristics are not considered at risk, can be affected by prolonged droughts (e.g., Central and Western Europe). Numerous studies have focused on drought periods occurring in Europe, regardless of the usual climatic conditions prevailing in these parts of the continent [5,7–13]. Furthermore, many authors have indicated that drought and drought periods can affect various species of trees and types of forests in general [1,3,10,14–20]. Drought events (heat followed by a lack of precipitation) increase tree mortality, which in turn disturbs the overall functioning of forest ecosystems. Therefore, tree mortality data are considered a prerequisite for a more comprehensive understanding of the complex interactions between climate and forests [21–28]. Several drought periods were registered in Serbia in the last decade, with certain years characterised as extremely dry [29].

Climate impacts can trigger defoliation processes in various types of forests [14]. Defoliation of tree crowns is the most widely used parameter for the assessment of forest vitality [30–33]. The percentage of tree damage is determined based on the visual assessment of the lack of assimilation organs (i.e., percentage of defoliation). Defoliation may indicate various stress factors, and can be caused by numerous biotic, abiotic, and human factors which affect trees either individually or through their interaction. It essentially reveals the actual condition of forests and is considered to be an indicator of the balance between a tree and its environment [34]. Stand age has a significant impact on the occurrence of defoliation [35–37]. In line with this, large and old trees should show increasing mortality, while the mortality of young trees should show a decreasing rate [38]. Although tree mortality is a natural process, several studies have pointed to increasing mortality rates due to climate change [15,39].

Following its introduction as an indicator of forest condition (ICP Forests) in the early 1980s [40], defoliation has been used as a main indicator [41]. Tree defoliation assessed in 5% steps is a useful parameter in predicting year-to-year tree mortality [42]. It is defined as the loss of leaves in broadleaves or needles in conifers compared to a reference tree, i.e., a healthy tree without any defoliation symptoms in the immediate vicinity of the assessed tree or an imaginary tree with no loss of leaves/needles. Defoliation is assessed regardless of the cause of the loss of leaves or needles. As the assessment is subjective, it has to be repeated and verified in order to provide uniform and accurate results.

Defoliation may be caused by various stress factors, including weather conditions such as extreme air temperatures and precipitation as well as insect or fungal attacks, air pollution, acid rain, etc. Variations in defoliation at the annual level are completely reversible, and are associated with fluctuations in climatic factors [43]. They may be caused either by temporary impacts (e.g. defoliating insects) or inaccurate measurements. Therefore, results are typically focused on long-term trends. Furthermore, according to previous research studies based on defoliation monitoring, the variability in the number of

sampled trees due to felling, removal of dead trees, and their replacement with new ones does not distort study results over the years [44]. Monitoring networks are an essential source of data needed to predict changes in ecosystems [45].

However, from the very beginning studies have emphasised that defoliation is not a good indicator of forest condition [46]. The same attitude can be noted in recent studies [47] and even in the latest findings [48]. Previous authors have suggested that defoliation is a more useful indicator when combined with other indicators [30]. However, a large number of researchers consider defoliation the best indicator of forest vitality, and use it in their research [32,33,49–51].

Led by claims that defoliation cannot be used as the main indicator of forest condition, we accessed the internal ICP Forests database on each individual tree in order to resolve this dilemma. This database is a kind of "health history form" that allowed us to trace the chronological chain of events in the recent or distant past of each tree and monitor the course of defoliation over the years. The long-term trend of monitoring the defoliation of individual trees allowed us to determine the reasons for their die-back and correlate them with the mass forest declines which in fact occurred in the territory of the Republic of Serbia [52]. Except for a few research studies [53–56], defoliation has not been described in detail as an indicator of forest condition in Serbia in previous research. Furthermore, the method of chronological monitoring and classifying each dead tree by groups relative to defoliation trends was applied in our study for the first time. We wanted to determine whether defoliation trends follow the trends of extended extreme drought and the way prolonged drought events affect defoliation. We aimed to study the differences in tree responses before, during, and after the drought. In order to address these issues, we conducted research at all permanent sample plots of the ICP Forests network in Serbia. We included all tree species present on sample plots, as our main goal was to investigate the impact of drought on the occurrence of defoliation and tree mortality as a final outcome. In addition, in order to study the differences in the response to drought of broadleaved and coniferous species and trees at different altitudes, these groups of species and sample plots were analysed separately.

2. Results

2.1. Forest Decline and Die-Back of Individual Trees in Serbia

Increasing defoliation is one of the first symptoms of the die-back of individual trees. Therefore, it is very important to monitor its intensity in order to determine its causes. The largest number of dead trees with 100% defoliation was registered in 2014, which amounted to 29% of the total number of dead trees in the research period (2004–2018). This year was followed by 2013 with 11.7%, 2015 with 11%, and 2016 with 9%, while the remaining years had similar values, ranging from 2% to 7% of dead trees (Figure S1). The largest number of dead trees can be classified in the first group (the trees with a gradual increase in defoliation) and the second group of trees with “sudden” tree death. Compared to the number of trees that died in the whole fifteen-year research period (2004–2018), these two groups had the greatest number of trees in the period from 2013 to 2016. In only four years, 60.7% of the total number of all trees died. This statement is illustrated in the graph presented in Figure 1. It shows the trend of mortality of individual trees in the entire research period. A sharp increase in the number of dead trees can be seen in the period from 2013 to 2016, after which this number decreases. Such observations were made both in the immediate vicinity and further away from the sample plots, as noted by researchers in their field records.

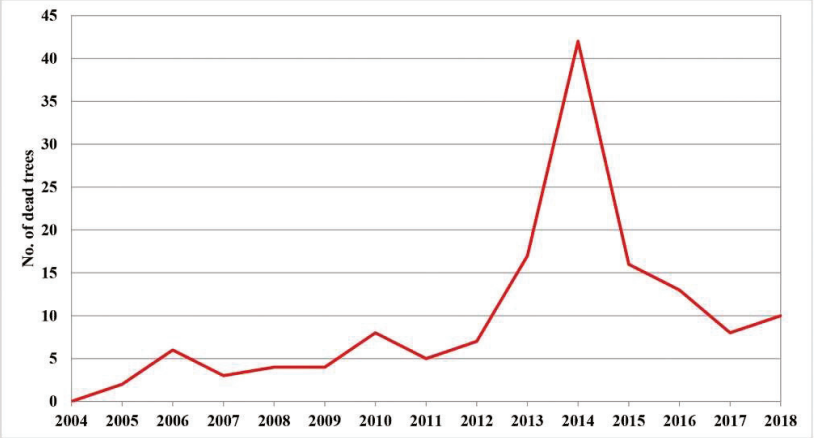

Figure 1. Tree mortality in the Republic of Serbia (2004–2018) (data not shown).

Looking at localities with a large number of dead trees, it is evident that trees died either in the same year or in two consecutive years (Table S1). We registered the damage that may be related to climatic conditions where it deviated from the normal values in many parameters. Special attention was paid to damage from unknown causes, ie., damage with a cause that could not be determined with certainty during assessment (e.g., death of whole trees or die-back of their parts). According to the results of our analysis of the data on defoliation related to damage from unknown causes in the years when the damage significantly deviated from normal (i.e., 2011 to 2014), the percentage of trees of all species with damage from unknown causes amounted to 4.8% in 2011, while it was 5.6% in 2012 (the highest), 4.6% in 2013, and 4.4% in 2014. The percentage of this damage in the stated period was higher than the percentage of damage caused by human activity or abiotic factors (Figure S2). We rejected the impact of stand age on defoliation because the average numbers of dead trees did not differ significantly between different stand age categories (results not shown). The influence of biotic factors (insects and fungi) on tree die-back was rejected due to the high percentage of trees that died suddenly (Table S1, Group II). It amounted to 41% of the total number of dead trees. This was further indicated by trees whose defoliation increased in several consecutive years (Table S1, Group I), when unfavorable climatic conditions were at their peak and the number of these trees was 39%. Only one-fifth or 20% of dead trees (Table S1, Group III) had a higher percentage of defoliation over many years. Their defoliation was most commonly caused by fungi, which eventually resulted in the death of the tree.

Based on the defoliation monitoring data (trees with defoliation of 100% were considered dead), annual mortality rates were calculated for the territory of Serbia in three observation periods (2004–2008, 2009–2013, and 2014–2018). The results of the descriptive and nonparametric statistics for the annual mortality rates of the monitored trees in three observation periods are presented in Table 1. The medians of the annual mortality rates were 0.000, 0.000, and 0.003 for the observation periods of 2004–2008, 2009–2013, and 2014–2018, respectively. According to the Kruskal–Wallis test (KWt), there is a statistically significant difference at the 95% confidence level (p = 0.00) between the medians that represent the three observation periods. The median plot (Figure 2) shows that the median of the annual mortality rate for the third observation period (2014–2018), which took place after the drought period from 2011 to 2013, was higher than the medians obtained for the previous two observation periods (2004–2008 and 2009–2013). The annual mortality rates did not differ significantly between coniferous and broadleaved trees or forests at different altitudes (Tables S2 and S3; Figures S3 and S4).

Table 1. Descriptive and nonparametric statistics for the annual mortality rates of trees monitored in the territory of Serbia for three observation periods. M—median; MAD—median absolute deviation; MIN—minimum value; MAX—maximum value; KWt—Kruskal-Wallis test.

Period of Observation	Sample Size	M	MAD	MIN	MAX	Average Rank in KWt	Test Statistic	*p*-Value
2004–2008	34	0.000	0.000	0.000	0.018	41.294	10.7105	0.0047
2009–2013	34	0.000	0.000	0.000	0.028	51.235		
2014-2018	34	0.003	0.003	0.000	0.492	61.971		

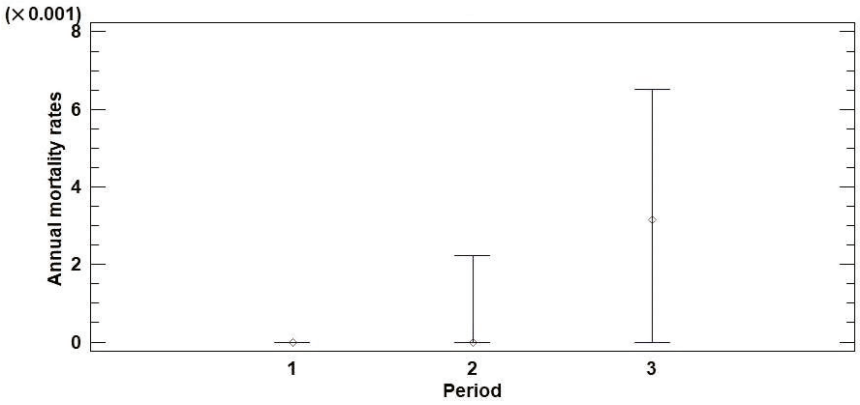

Figure 2. Median plot with 95% confidence intervals for the annual mortality rates of trees monitored in the territory of Serbia in three observation periods: (1) 2004–2008, (2) 2009–2013, and (3) 2014–2018.

2.2. Extreme Climate Events and Forest Decline

Extreme climate events have undoubtedly affected forest ecosystems in the entire territory of Serbia (Tables S4–S7). Several extreme climate events were recorded in the research period [57]. They significantly contributed to the progressive increase of mortality (dying) of both individual trees and large forest areas in Serbia.

The analysis of the annual averages for the whole of Serbia shows that the period from 2011 to 2013 was continuously warm (Table S4). The mean annual air temperature in the growing season was the highest in 2012 (Table S5).

The lowest precipitation average in the research period was registered in 2011 (Table S6). This year was considered to be extremely dry, with the amount of precipitation below 500 mm, which is the limit for declaring drought [58]. The extremely dry 2011 was followed by extremely low and extremely high air temperatures in 2012, a year with the continuously lowest average amount of precipitation. While the following year, 2013, was dry again (especially in the growing season), it was followed by the highest amount of precipitation on record in 2014 (Tables S4–S7). Based on general characteristics related to the amount of precipitation during the growing season in 2011, the entire territory of Serbia was affected by severe and extreme drought (Table S7). Figure 3 shows the drought intensity based on the SPI and SPEI during the growing season (SPI-6 and SPEI-6, Figure 3a), i.e., from April to September 2004 to 2018, in the Republic of Serbia. Drought events of greater or lesser intensity occurred several times during the research period. However, the drought that lasted for two consecutive growing seasons (2011 and 2012) had long-term consequences for forest ecosystems. If we supplement this finding with the annual data on moisture conditions in the territory of Serbia (SPI-12 and SPEI-12), we can see that the lack of precipitation was even more intense outside the growing season (2011–2012) (Figure 3b). This is important to note because the drought began in the autumn of 2011, which according to SPI was categorised as the year with the most extreme drought (SPI ≤ -2). In no previous year had the drought period lasted as long or been as intense (three consecutive years, considering both the growing season and the whole year). In addition to the reduced

amount of precipitation, the increased temperature significantly contributed to the severity of the dry period. The temperature had a strong impact on the intensity of drought during 2011 and 2012, as can be seen in Figure 3a,b. Figure 3a (SPEI-6) points to the significant influence of temperature that, together with the reduced amount of precipitation in the growing season, makes it the longest period of drought in the research period.

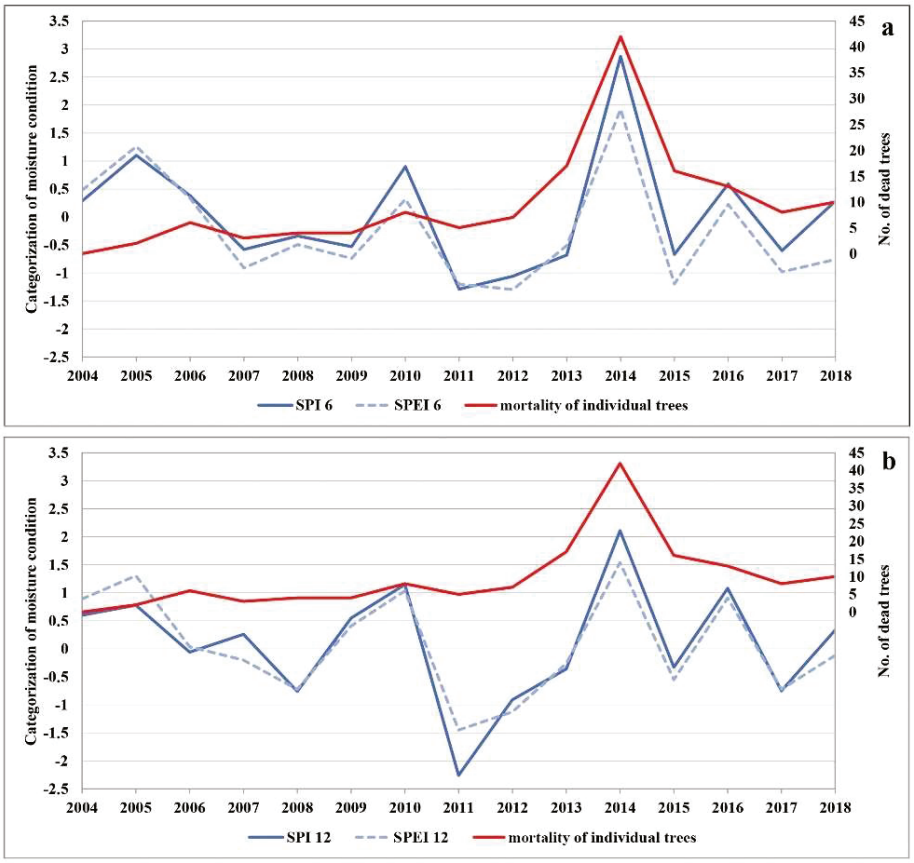

Figure 3. The comparison of (**a**) SPI-6 and SPEI-6 and (**b**) SPI-12 and SPEI-12 with the number of dead trees.

Based on the above, we compared the SPI-6 and SPEI-6 as well as the SPI-12 and SPEI-12 with the number of dead trees in the research period (Figure 3a,b). Having in mind that reduced soil moisture disturbs the growth and development of plants, we compared the trend of defoliation with tree mortality in certain years. We found clear indications that the trend of increasing defoliation began with the onset of the drought period in 2011. It continued over the next two years (2012 and 2013) and reached its peak in 2014, when the largest number of dead trees was recorded. This is further confirmed by the three distinct groups of trees (Table S1) and by the correlation between the trees in Groups I and II and drought years (2011–2013).

Because moisture and temperature conditions vary with altitude, we further analysed the conditions at individual localities based on the SPI and SPEI (Figure 4a,b). We decided to present the SPI and SPEI on a twelve-month basis, as the results indicated that the drought was present the whole year round and not just in the growing season. The SPI was calculated for the major weather stations, i.e., localities in the north (Palić, 102 m above sea level), west (Zlatibor, 1028 m above sea level), east (Negotin, 42 m above sea level), and south (Vranje, 432 m above sea level) in order to confirm the impact of drought regardless of altitude. The observations made at the main weather stations separately [57] revealed deviations in the amount of precipitation, which were conditioned by, among other things, the altitude. However, the amount of precipitation was typically far below the annual

average at all major weather stations in 2011 and 2012, and according to the SPI criteria they all ranged from severe to extreme or even exceptional drought (Figure 4a). On the other hand, for the SPEI we calculated time series at a single grid cell according to coordinates in the north, west, east, and south of the country. Similar conditions were found to prevail at high and low altitudes. As can be seen in the Supplementary Materials Table S1, these conditions strongly contributed to mortality in the following years regardless of altitude and tree species.

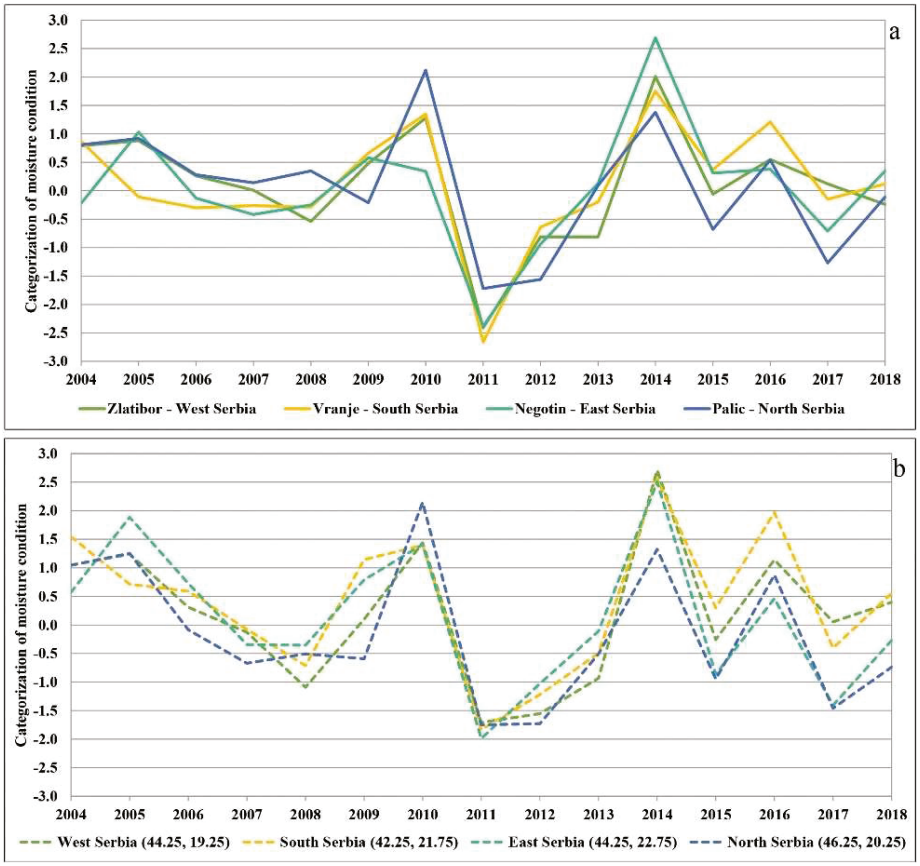

Figure 4. (**a**) SPI-12 for the four major weather stations in the north, west, east, and south of Serbia; (**b**) SPEI-12 for time series in the north, west, east, and south of Serbia.

3. Discussion

Forest decline and die-back of individual trees are long-lasting processes and, in many cases they are not triggered at the same time as the unfavourable factor that disturbs the growth and development of a tree or the entire forest ecosystem. However, a large number of trees in Serbia died suddenly in the period from 2013 to 2016 (Table S1) without previous visible symptoms of defoliation and regardless of stand age, which stresses the severity, i.e., adverse effect of climate conditions that in this case imply extreme climate events in the form of prolonged drought.

According to "Srbijašume", the State Enterprise dealing with forest management, the forest decline in this period has been the most massive forest decline during the monitoring period of forest conditions in the forestry sector of the Republic of Serbia. The long-lasting drought caused a massive forest decline in the whole territory of the Republic of Serbia, affecting an area of 13,885.00 ha. Die-back of individual trees was recorded in an area of 12,084.19 ha and die-back of groups of trees in an area of 1800.81 ha, while the deadwood volume amounted to 81,631.61 m^3 [52].

The majority of broadleaved and coniferous trees that died in the period from 2012 to 2016 fell into the categories of intense defoliation and dead trees. As can be seen in

Supplementary Tables S8 and S9, conifers showed intense defoliation in 2013 due to initial physiological weakening by drought followed by an attack of bark beetles. Unlike conifers, broadleaved trees had already been affected by intense defoliation in 2012. Seidling [35] similarly observed that certain tree species (conifers) reacted a year later than broadleaved trees, i.e., defoliation was detected a year later. This can be explained by the fact that defoliation is more noticeable in broadleaved trees than conifers, whose needles remain on the branches for a time after dying-back. Looking back at the climate framework, conifers show greater drought resistance than broadleaved trees, i.e., conifers are more resistant to the freezing and thawing cycle than broadleaved trees [59]. On the other hand, coniferous tree species are susceptible to attacks of secondary pests such as bark beetles, which attack physiologically weakened trees, and drought is assumed to be the crucial trigger of symptoms [60]. However, our statistical analysis showed that the highest forest decline was recorded in the period from 2014 to 2018, and annual mortality rates did not differ significantly between coniferous and broadleaved tree species. Although the number of main tree species on sample plots corresponded to the share of the same species in the forest cover on the territory of Serbia, the sample of coniferous tree species was small. Therefore, in order to achieve a better representation of these species, the number of sample plots should be increased. Air temperature and precipitation are the key factors in the growth and development of plants. For a plant to survive, these climate factors have to be at least at a certain minimum level, especially in the growing season [61,62]. Major parts of Serbia have a continental precipitation regime, with higher quantities in warmer part of the year [63]. Increasing amounts of precipitation enhance the growth of vegetation, while deficiency in precipitation over an extended period of time leads to drought as the most common cause of damage and die-back of individual trees and large forest areas [64]. Unfavourable climate, especially the lack of precipitation during the growing season, air temperatures above multi-annual averages (Tables S4–S7), and prolonged and frequent drought periods have had serious and long-term consequences on forest ecosystems in Serbia. Similar observations have been stated by domestic authors [53–55,65–70], whose research confirms the negative impacts of climate change and extreme climate events on the growth, development, and vitality of forest tree species and forest ecosystems as a whole.

In the last decade alone, Europe had several extremely hot and dry summers [71–76]. The data of the European Environment Agency (EEA) [77] showing drought periods and the areas affected throughout Europe can serve as a good indicator of the drought distribution. Thus, the Republic of Serbia had six periods without rainfall followed by high temperatures (i.e., drought). A study by Spinioni et al. [78] compiles a pan-European list of past drought events for the period from 1950 to 2012, with Europe divided into thirteen regions according to country borders and geographic and climatic characteristics. Regarding the Balkan countries (Albania, Bosnia and Herzegovina, Croatia, Montenegro, FYR Macedonia, Serbia, and Slovenia), the period from 2007 to 2009 was stated to be the longest drought period in terms of duration (number of months), while the period from 2011 to 2012 was the most severe in terms of drought and its effects, which coincides with our research results. These scenarios can be confirmed on websites that provide data on drought periods worldwide [79,80]. Several authors have analysed the relationship between tree mortality and drought based on tree mortality maps in Europe over a thirty-year period (1986–2016) [28]. These maps clearly show that 2012 and 2013 had the most intense drought and highest tree canopy mortality, which was the case in the wider area of Serbia as well [28,81]. Technical reports [82] based on data submitted by the countries participating in the ICP Forests Programme contain overviews of the state of European forests based on the monitoring of sample plots at the annual level. Other countries that were affected by drought in 2011 and 2012 (e.g., Croatia and Hungary) stated an increase in defoliation in this period and stressed climate conditions (i.e., drought) as the most obvious reasons for the increase. They warned that the damage could be much greater than was shown by research at the time. Furthermore, the report of the Intergovernmental Panel on Climate Change [83] highlighted the impact of extreme climate events such

as heatwaves and droughts that significantly increase the exposure and vulnerability of certain ecosystems.

4. Conclusions

Based on our analysis of monitoring data on tree defoliation in Serbia over a fifteen-year period (2004–2018), it can be concluded that the damage caused by the registered extreme climate events occurred gradually and periodically after several consecutive dry years. However, it was of very high intensity and affected the entire territory of Serbia. It increased significantly in the period from 2013 to 2016. At first, defoliation was recorded as the impact of an unknown cause; however, the correlation with the number of dead and dying trees and climate characteristics in the research period revealed the causes. Due to extreme weather conditions, the tolerance threshold of certain tree species was exceeded, which eventually led to their gradual die-back and death regardless of stand age or the influence of biotic factors. The years preceding the ones with the most extensive tree mortality in Serbia (2013–2016) recorded mortality events of both individual trees and large forest complexes. However, there had not previously been such an intensive die-back with clear linking causes. The period from 2011 to 2013 showed the greatest stress on plants recorded during the period of tree vitality monitoring on sample plots. It should be noted that the occurrence of defoliation with ultimate die-back was recorded in the areas at both higher and lower altitudes. Although these higher-altitude areas are usually categorised as humid, they recorded a desert climate type in the above-stated years with extreme climate events. Furthermore, die-back was detected in both broadleaved and coniferous tree species, with the difference that defoliation was more easily observed in broadleaves. Our statistical analysis showed that the highest forest decline was recorded in the period from 2014 to 2018 and that annual mortality rates did not differ significantly between coniferous and broadleaved trees or among sites at different altitudes.

After many years of researching the impact of various factors on forest ecosystems, we have become aware of many advantages of the continuous monitoring method performed at a large number of sample plots. Monitoring of phenomena and processes over a long period and on a large number of specimens enables more precise identification of the real causes of forest decline. If symptoms found on selected trees can be diagnosed in their immediate surroundings, it is easier to draw conclusions on the causes of die-back. However, although the number of main tree species on sample plots coresponds to the share of the same species in forest cover on the territory of Serbia, for certain species (particularly conifers) the sample in the present study was small. Thus, to achieve better representation of these species and better forest condition monitoring, the number of sample plots should be increased.

Based on the results of this research, it can be concluded that unfavourable climate conditions, primarily the lack of precipitation, rising air temperatures, and increasingly frequent and long dry periods, had serious and long-term consequences on forest ecosystems in Serbia.

5. Materials and Methods

5.1. Study Area and Data Preparation

The total number of dead trees was determined based on the data collected in the territory of the Republic of Serbia within the International Cooperative Programme on Assessment and Monitoring of Air Pollution Effects on Forests (ICP Forests) [40]. The research was conducted over a period from 2004 to 2018 on all 130 sample plots established at the intersections of 16 × 16 km and 4 × 4 km (Figure 5). This network is located at 0 to 1600 m above sea level. The center of each sample plot was marked and six trees were selected in each cardinal direction, resulting in 24 trees in each sample plot [84]. The main criterion in the selection of trees for condition monitoring within the network of sample plots was the absence of any significant mechanical damage. Mechanical injuries make trees susceptible to attack by insects or fungi that can cause defoliation and eventual die-back,

masking the primary cause. The selected trees had been monitored continuously following the establishment of each sample plot. Any change in the whole tree was detected and recorded and the cause of the damage was identified during the growing season, from the time leaves and needles are fully developed to the beginning of autumn senescence. Monitoring was focused on assimilation organs, as the damage caused by various factors can in most cases be observed on them. The assessment of defoliation included any kind of damage recorded on the examined trees. In most species, the most suitable time to perform observations is from early summer, when leaves or needles are fully formed, to late summer. Out of a total of 3800 trees monitored, the research encompassed an average of 2880 trees per year. The number of trees varied with various factors, such as regular felling, snow breakage, wind breakage, die-back, etc. Of the observed number of trees, the trees that were recorded as dead during the research period were selected and analysed in detail. The trees were then divided into three groups based on the changes in defoliation (Table S1).

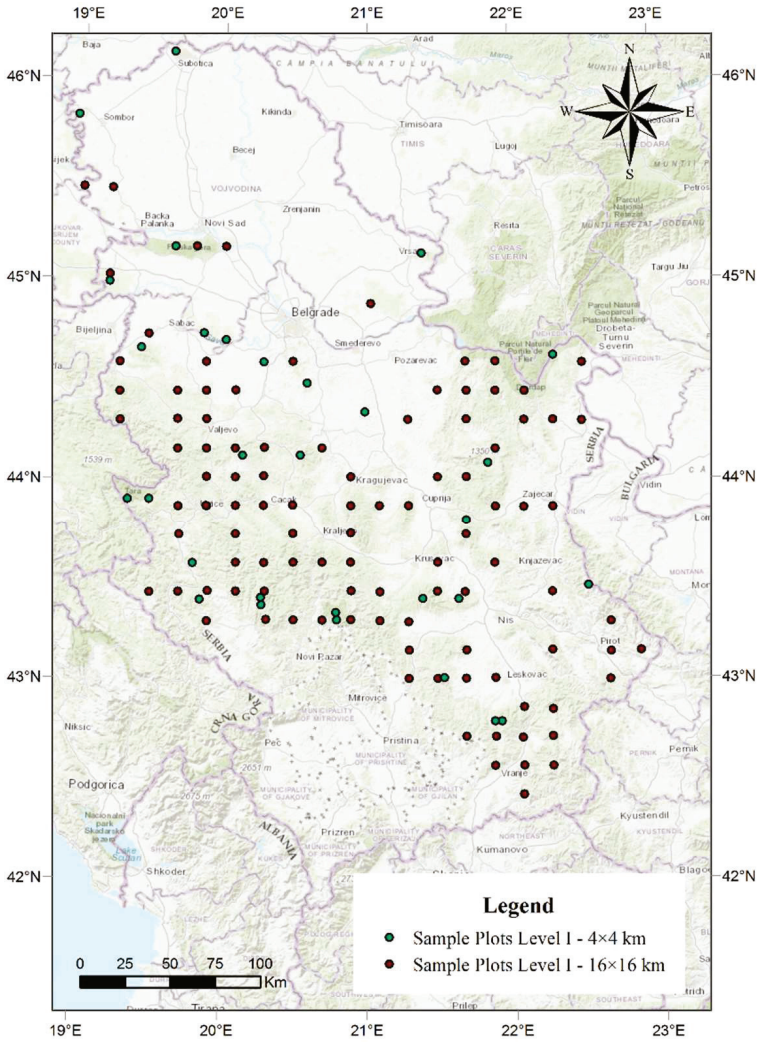

Figure 5. The spatial arrangement of sample plots in the territory of the Republic of Serbia.

The main data on tree species, stand age, and altitude range at the investigated localities are presented in Supplementary Figure S5.

5.2. Defoliation

The principal method was based on the assessment of defoliation as the main parameter of the condition of forests. Defoliation was assessed in 5% steps, for instance 5 (>0–5%), 10 (>5–10%), etc. (Figure 6). The missing leaf mass was assessed compared to healthy trees

growing in the same site and stand conditions and observed regardless of the cause of foliage loss. The method was as previously described in the literature [41].

Figure 6. An illustration of defoliation assessment: (**a**) 10%; (**b**) 25%; (**c**) 65%.

During the research period (2004–2018), defoliation was assessed regardless of its cause. In order to understand the possible cause of death, we singled out all trees recorded as dead during the period (Table S1). The trees were classified into three different groups of trees whose death was caused by defoliation:

I. The first group included trees with no defoliation (class 0) and slight defoliation (class 1) at the beginning of condition monitoring and during most of the years for which defoliation moved to higher classes of defoliation in the last few years, namely, classes 2 (moderate), 3 (severe), and 4 (dead).
II. The second group included trees that died suddenly and moved from class 0 or class 1 to class 4.
III. The third group included trees with higher classes of defoliation that occurred after the first year of monitoring, and which several years later led to their death.

5.3. Climate Characteristics

The non-reactive research method was used for the collection of data on climate characteristics during the research period [85]. The data on mean monthly air temperatures, extreme maximum and minimum air temperatures, and monthly precipitation amounts for the research period (2004–2018) were provided by the Republic Hydrometeorological Service of Serbia (RHSS) for 28 main meteorological stations in Serbia [57]. The data were used to calculate the mean monthly and annual values of the air temperature and precipitation amount for the growing period (April–September). Based on the arithmetical means of monthly values calculated for each year, annual and growing season values were obtained (Tables S4–S7).

According to the applied Köppen and Köppen–Geiger climate classification systems [86,87], Mihajlović, J. [88] distinguished two types of climate in Serbia, namely, temperate (S) and cold (D). A warm temperate rainy (S) climate is present in different variants, with dominant Sfb and Cfa classes, while a cold or boreal snow forest (D) climate is represented by the Dfb, Dfc, and Dfa classes [89].

5.4. Drought Index Quantification

In order to quantify the precipitation deficit for different time intervals, the Standardised Precipitation Index (SPI) was calculated according to McKee et al. [90]. When determining the SPI with precipitation as the only input parameter, we used the precipitation totals from 28 main weather stations of the Republic Hydrometeorological Service of Serbia in the period from 2004 to 2018 [57] to calculate the time series of previous droughts and assess their severity. We calculated the SPI at the semi-annual level (SPI-6) for the growing season (April–September) and the SPI at the annual level (SPI-12). We calculated SPI-6 in the growing season to provide a better representation of the amount of precipitation at the time plants need it most for their growth and development. The results of the SPI for the drought periods were then compared and correlated with the tree defoliation.

We further calculated the Standardised Precipitation Evapotranspiration Index (SPEI) in order to prove the existence of the drought period; SPEI input data included temperature and precipitation [91]. The SPEI data were obtained from the global SPEI database [79] as part of the weather series for the region of Serbia (coordinates: upper left 42.25, 23.25, and lower right 46.25, 18.75). By using air temperature alongside precipitation data, the SPEI allows a broader view of the effects of drought and links them to defoliation. The SPEI was calculated at 6- and 12-month intervals (SPEI-6 and SPEI-12).

This study used the SPI and SPEI as the most common methods for monitoring drought [92–94]. The SPI was used to estimate precipitation deviations from the normal state, while the SPEI included the temperature component in addition to precipitation to obtain a clearer picture of the drought. According to the SPI, a drought event begins when its values are equal to or below −1.0 and ends when the values become positive [90], which is the case with the SPEI as well [91].

5.5. Tree Mortality

Based on the ICP Forests Manual [41], detailed attention was paid to tree mortality in a given year, as the total number of dead trees per plot at any time did not provide information on mortality rates. According to the methodology, dead trees are commonly included in the sample if they are standing. Such trees are categorised as severely defoliated. In our study, these trees were considered dead at the time when intense defoliation (99%) occurred. By doing this, we were able to determine the exact year of die-back of a particular tree. The exact year of mortality was identified, and the results are presented in Supplementary Table S1. The mortality and the number of dead trees per plot are two different issues. Tree mortality was determined according to the year when defoliation was found to be 100% and divided into three groups based on the progression of defoliation. We then determined the connection between the tree mortality rate and the SPI and the SPEI during periods of drought.

5.6. Statistical Analysis

For a total of 3800 trees belonging to 34 species at 130 sites in the Republic of Serbia, annual mortality rates were calculated for three observation periods (2004–2008, 2009–2013, and 2014–2018). These calculations used the data obtained from monitoring defoliation according to the ICP Forests methodology [41]; trees with defoliation of 100% were considered dead. According to Sheil et al. [95], the true annual mortality is defined by the equation $m = 1 - (N_1/N_0)^{1/t}$, where N_0 and N_1 are population counts at the beginning and end of the measurement interval, t. As m is recommended as a standard quantity for comparing annual mortality rates in plant ecology [95], it was adopted as the annual mortality rate in this study. The variation in mortality rates was captured using the mortality rate of each of the 34 tree species analysed as a subpopulation. To calculate m, we used three five-year intervals, because the five-year interval is the most commonly used census interval length (as recommended by Lewis et al. [96]) and maximises intercensus and intersite comparability. Before performing the statistical analysis, data on annual mortality rates were tested for normality. As the assumption that these data were normally

distributed had not been confirmed, the medians (M) were used for both intervals of observation. The median absolute deviation (MAD) was determined for each median, and the comparison and determination of the difference between the medians was carried out using the Kruskal–Wallis test (KWt). All statistical analyses were performed using Statgraphics software (2009; Statpoint Technologies, Inc., Warrenton, VA, USA).

Supplementary Materials: The following supporting information can be downloaded at: https://www.mdpi.com/article/10.3390/plants11101286/s1, Figure S1: Forest decline on sample plots on the territory of the Republic of Serbia in the period from 2004 to 2018.; Figure S2: The percentage of trees of all species with the damage on the sample plots (2011–2014).; Figure S3: Median plot with 95% confidence intervals for the annual mortality rates of broadleaved and conifer tree species monitored in the territory of Serbia in the period of 2014–2018.; Figure S4: Median plot with 95% confidence intervals for the annual mortality rates of trees monitored at different altitude ranges in the territory of Serbia in the period of 2014–2018.; Figure S5: Distribution of 130 Sample plots by tree species, altitude and stand age.; Table S1: Trends in defoliation on trees during the years of research with the final outcome of dying and division into groups.; Table S2: Descriptive and nonparametric statistics for the annual mortality rates of broadleaf and conifer tree species monitored in the territory of Serbia in the period of 2014–2018.; Table S3: Descriptive and nonparametric statistics for the annual mortality rates of trees monitored at different altitude ranges in the territory of Serbia in the period of 2014–2018.; Table S4: Mean annual air temperatures (°C) in Serbia in the period from 2004 to 2018.; Table S5: Mean annual air temperatures (°C) in the growing season in Serbia from 2004 to 2018.; Table S6: Mean precipitation sum (mm) in Serbia in the period from 2004 to 2018.; Table S7: Mean precipitation sum (mm) in the growing season (April–September) in Serbia in the period from 2004 to 2018.; Table S8: Comparative analysis of defoliation in the period 2004–2018—Conifers.; Table S9: Comparative analysis of defoliation in the period 2004–2018—Broadleaves.

Author Contributions: Conceptualization, G.Č.; Data curation, G.Č. and L.B.-B.; Formal analysis, G.Č., and F.J.; Investigation, G.Č., I.Đ., S.M., S.E., T.Ć.-M. and A.L.; Methodology, G.Č. and F.J.; Project administration, G.Č.; Resources, L.B.-B., I.Đ., S.M., S.E., T.Ć.-M. and A.L.; Validation, G.Č., F.J., L.B.-B., I.Đ., S.M., S.E., T.Ć.-M. and A.L.; Visualization, G.Č., F.J., L.B.-B., I.Đ., S.M., S.E., T.Ć.-M. and A.L.; Writing—original draft, G.Č.; Writing—review and editing, G.Č. and F.J. All authors have read and agreed to the published version of the manuscript.

Funding: This research was supported by the Ministry of Education, Science, and Technological Development (Agreement no. 451-03-68/2022-14/200027) and the Ministry of Agriculture, Forestry, and Water Management of the Republic of Serbia's Forest Directorate within the project "Monitoring and Assessment of Air Pollution Impacts and its Effects on Forest Ecosystems in Republic of Serbia—Forest Condition Monitoring" (Agreement no. 401-00-41/2022-10).

Data Availability Statement: All data are included in the manuscript.

Acknowledgments: We highly appreciate the work of all researchers who have participated in field research all these years.

Conflicts of Interest: The authors declare no conflict of interest.

References

1. Bennett, A.; McDowell, N.; Allen, C.; Anderson-Teixeira, K. Larger trees suffer most during drought in forests worldwide. *Nat. Plants* **2015**, *1*, 15139. [CrossRef] [PubMed]
2. Barbeta, A.; Mejia-Chang, M.; Ogaya, R.; Voltas, J.; Dawson, T.; Penuelas, J. The combined effects of a long-term experimental drought and an extreme drought on the use of plant-water sources in a Mediterranean forest. *Glob. Change Biol.* **2015**, *21*, 1213–1225. [CrossRef] [PubMed]
3. Boczoń, A.; Kowalska, A.; Dudzińska, M.; Wróbel, M. Drought in Polish forests in 2015. *Pol. J. Environ. Stud.* **2016**, *25*, 1857–1862. [CrossRef]
4. Wilhite, D.A. *Drought and Water Crises: Science, Technology, and Management Issues*; Taylor and Francis: Boca Raton, FL, USA, 2005; 406p.
5. Dai, A. Drought under global warming: A review. *WIREs Clim. Change* **2011**, *2*, 45–65. [CrossRef]
6. Spinoni, J.; Naumann, G.; Vogt, J.; Barbosa, P. *Meteorological Droughts in Europe: Events and Impacts—Past Trends and Future Projections*; EUR 27748 EN; Publications Office of the European Union: Luxembour, 2016. [CrossRef]

7. Bradford, R.B. Drought Events in Europe. In Drought and Drought Mitigation in Europe. *Adv. Nat. Technol. Hazard. Res.* **2000**, *14*, 7–20. [CrossRef]
8. Fink, A.H.; Brucher, T.; Kruger, A.; Leckebusch, G.; Pinto, J.; Ulbrich, U. The 2003 European summer heatwaves and drought–synoptic diagnosis and impacts. *Weather* **2004**, *59*, 209–216. [CrossRef]
9. Gil-Pelegrín, E.; Peguero-Pina, J.J.; Camarero, J.J.; Fernández-Cancio, A.; Navarro-Cerrillo, R. Drought and forest decline in the Iberian Peninsula: A simple explanation for a complex phenomenon? In *Droughts: Causes, Effects and Predictions*; Sánchez, J.M., Ed.; Nova Science Publishers: New York, NY, USA, 2008; pp. 27–68.
10. Jentsch, A.; Beierkuhnlein, C. Research frontiers in climate change: Effects of extreme meteorological events on ecosystems. *Comptes Rendus Geosci.* **2008**, *340*, 621–628. [CrossRef]
11. Bissolli, P.; Ziese, M.; Pietzsch, S.; Finger, P.; Friedrich, K.; Nitsche, H.; Obregón, A. *Drought Conditions in Europe in the Spring of 2012*; Report; Deutscher Wetterdienst (DWD): Offenbach, Germany, 2012; pp. 1–30.
12. Spinoni, J.; Antofie, T.; Barbosa, P.; Bihari, Z.; Lakatos, M.; Szalai, S.; Szentimrey, T.; Vogt, J. An overview of drought events in the Carpathian Region in 1961–2010. *Adv. Sci. Res.* **2013**, *10*, 21–32. [CrossRef]
13. Stahl, K.; Kohn, I.; Blauhut, V.; Urquijo, J.; De Stefano, L.; Acácio, V.; Dias, S.; Stagge, J.; Tallaksen, L.; Kampragou, E.; et al. Impacts of European drought events: Insights from an international database of text-based reports. *Nat. Hazard. Earth Sys.* **2016**, *16*, 801–819. [CrossRef]
14. De la Cruz, A.; Gil, P.; Fernández-Cancio, A.; Minaya, M.; Navarro-Cerrillo, R.; Sánchez-Salguero, R.; Grau, J.M. Defoliation triggered by climate induced effects in Spanish ICP Forests monitoring plots. *For. Ecol. Manag.* **2014**, *331*, 245–255. [CrossRef]
15. Allen, C.D.; Macalady, A.K.; Chenchouni, H.; Bachelet, D.; McDowell, N.; Vennetier, M.; Kitzberger, T.; Rigling, A.; Breshears, D.D.; Hogg, E.H.; et al. A global overview of drought and heat-induced tree mortality reveals emerging climate change risks for forests. *For. Ecol. Manag.* **2010**, *259*, 660–684. [CrossRef]
16. Lindner, M.; Maroschek, M.; Netherer, S.; Kremer, A.; Barbati, A.; Garcia-Gonzalo, J.; Seidl, R.; Delzon, S.; Corona, P.; Kolström, M.; et al. Climate change impacts, adaptive capacity, and vulnerability of European forest ecosystems. *For. Ecol. Manag.* **2010**, *259*, 698–709. [CrossRef]
17. Carnicer, J.; Coll, M.; Ninyerola, M.; Pons, X.; Sánchez, G.; Peñuelas, J. Widespread crown condition decline, food web disruption, and amplified tree mortality with increased climate change-type drought. *Proc. Natl. Acad. Sci. USA* **2011**, *108*, 1474–1478. [CrossRef] [PubMed]
18. Martínez-Vilalta, J.; Lloret, F.; Breshears, D.D. Drought-induced forest decline: Causes, scope and implication. *Biol. Lett.* **2012**, *8*, 689–691. [CrossRef]
19. Sánchez-Salguero, R.; Camarero, J.J.; Carrer, M.; Gutiérrez, E.; Alla, A.Q.; Andreu-Hayles, L.; Hevia, A.; Koutavas, A.; Martínez-Sancho, E.; Nola, P.; et al. Climate extremes and predicted warming threaten Mediterranean Holocene firs forests refugia. *Proc. Natl. Acad. Sci. USA* **2017**, *114*, E10142–E10150. [CrossRef]
20. Zhang, Q.; Shao, M.; Jia, X.; Wei, X. Relationship of climatic and forest factors to drought-and heat-induced tree mortality. *PLoS ONE* **2017**, *12*, e0169770. [CrossRef]
21. Neumann, M.; Mues, V.; Moreno, A.; Hasenauer, H.; Seidl, R. Climate variability drives recent tree mortality in Europe. *Glob. Change Biol.* **2017**, *23*, 4788–4797. [CrossRef]
22. Choat, B.; Brodribb, T.J.; Brodersen, C.R.; Duursma, R.A.; López, R.; Medlyn, B.E. Triggers of tree mortality under drought. *Nature* **2018**, *558*, 531–539. [CrossRef]
23. Hartmann, H.; Schuldt, B.; Sanders, T.G.M.; Macinnis-Ng, C.; Boehmer, H.J.; Allen, C.D.; Bolte, A.; Crowther, T.W.; Hansen, M.C.; Medlyn, B.E.; et al. Monitoring global tree mortality patterns and trends. Report from the VW symposium 'Crossing scales and disciplines to identify global trends of tree mortality as indicators of forest health'. *New Phytol.* **2018**, *217*, 984–987. [CrossRef]
24. Senf, C.; Pflugmacher, D.; Zhiqiang, Y.; Sebald, J.; Knorn, J.; Neumann, M.; Hostert, P.; Seidl, R. Canopy mortality has doubled in Europe's temperate forests over the last three decades. *Nat. Commun.* **2018**, *9*, 4978. [CrossRef]
25. Anderegg, W.R.L.; Anderegg, L.D.L.; Kerr, K.L.; Trugman, A.T. Widespread drought-induced tree mortality at dry range edges indicates that climate stress exceeds species' compensating mechanisms. *Glob. Change Biol.* **2019**, *25*, 3793–3802. [CrossRef] [PubMed]
26. Caudullo, G.; Barredo, J.I. A georeferenced dataset of drought and heat-induced tree mortality in Europe. *One Ecosyst.* **2019**, *4*, e37753. [CrossRef]
27. DeSoto, L.; Cailleret, M.; Sterck, F.; Jansen, S.; Kramer, K.; Robert, E.M.R.; Aakala, T.; Amoroso, M.M.; Bigler, C.; Camarero, J.J.; et al. Low growth resilience to drought is related to future mortality risk in trees. *Nat. Commun.* **2020**, *11*, 545. [CrossRef] [PubMed]
28. Senf, C.; Buras, A.; Zang, C.S.; Rammig, A.; Seidl, R. Excess forest mortality is consistently linked to drought across Europe. *Nat. Commun.* **2020**, *11*, 6200. [CrossRef] [PubMed]
29. Republic Hydrometeorological Service of Serbia (RHSS) Annual Climate Characteristics for the Territory of Serbia, Republic Hydrometeorological Service of Serbia, Belgrade. Available online: http://www.hidmet.gov.rs/eng/meteorologija/klimatologija_produkti.php (accessed on 31 March 2022).
30. Pollastrini, M.; Feducci, M.; Bonal, D.; Fotelli, M.; Gessler, A.; Grossiord, G.; Guyot, V.; Jactel, H.; Nguyen, D.; Radoglou, K.; et al. Physiological significance of forest tree defoliation: Results from a survey in a mixed forest in Tuscany (central Italy). *For. Ecol. Manag.* **2016**, *361*, 170–178. [CrossRef]

31. Sousa-Silva, R.; Verheyen, K.; Ponette, Q.; Bay, E.; Sioen, G.; Titeux, H.; Van de Peer, T.; Van Meerbeek, K.; Muys, B. Tree diversity mitigates defoliation after a drought-induced tipping point. *Glob. Change Biol.* **2018**, *24*, 4304–4315. [CrossRef]
32. Gottardini, E.; Cristofolini, F.; Cristofori, A.; Pollastrini, M.; Camin, F.; Ferretti, M. A multi-proxy approach reveals common and species-specific features associated with tree defoliation in broadleaved species. *For. Ecol. Manag.* **2020**, *467*, 118151. [CrossRef]
33. Ferretti, M.; Bacaro, G.; Brunialti, G.; Calderisi, M.; Croisé, L.; Frati, L.; Nicolas, M. Tree canopy defoliation can reveal growth decline in mid-latitude temperate forests. *Ecol. Indic.* **2021**, *127*, 107749. [CrossRef]
34. Bussoti, F.; Pollastrini, M. Traditional and novel indicators of climate change impacts on European forest trees. *Forests* **2017**, *8*, 137. [CrossRef]
35. Seidling, W. Signals of summer drought in crown condition data from the German Level I network. *Eur. J. For. Res.* **2007**, *126*, 529–544. [CrossRef]
36. Fabiánek, P.; Hellebrandová, K.; Čapek, M. Monitoring of defoliation in forest standsof the Czech Republic and its comparison with results of defoliation monitoring in other European countries. *J. For. Sci.* **2012**, *58*, 193–202. [CrossRef]
37. Eickenscheidt, N.; Augustin, N.H.; Wellbrock, N. Spatio-temporal modelling of forest monitoring data: Modelling German tree defoliation data collected between 1989 and 2015 for trend estimation and survey grid examination using GAMMs. *iForest* **2019**, *12*, 338–348. [CrossRef]
38. Etzold, S.; Ziemińska, K.; Rohner, B.; Bottero, A.; Bose, A.; Ruehr, N.K.; Zingg, A.; Rigling, A. One Century of Forest Monitoring Data in Switzerland Reveals Species- and Site-Specific Trends of Climate-Induced Tree Mortality. *Front. Plant Sci.* **2019**, *10*, 1–19. [CrossRef] [PubMed]
39. McDowell, N.; Allen, C.D.; Anderson-Teixeira, K.; Brando, P.; Brienen, R.; Chambers, J.; Christoffersen, B.; Davies, S.; Doughty, C.; Duqueet, A.; et al. Drivers and mechanisms of tree mortality in moist tropical forests. *New Phytol.* **2018**, *219*, 851–869. [CrossRef]
40. ICP Forests—International Co-operative Programme on Assessment and Monitoring of Air Pollution Effects on Forests. Available online: http://icp-forests.net/ (accessed on 31 January 2022).
41. Eichhorn, J.; Roskams, P.; Potočić, N.; Timmermann, V.; Ferretti, M.; Mues, V.; Szepesi, A.; Durrant, D.; Seletković, I.; Schröck, H.-W.; et al. Part IV Visual Assessment of Crown Condition and Damaging Agents. In *ICP Forests Manual*; Version 2020-3; Thünen Institute of Forest Ecosystems: Eberswalde, Germany, 2020; pp. 5–54. Available online: https://storage.ning.com/topology/rest/1.0/file/get/9995547265?profile=original (accessed on 31 January 2022).
42. Dobbertin, M.; Brang, P. Crown defoliation improves tree mortality models. *For. Ecol. Manag.* **2001**, *141*, 271–284. [CrossRef]
43. Ferretti, M.; Nicolas, M.; Bacaro, G.; Brunialti, G.; Calderisi, M.; Croisé, L.; Frati, L.; Lanier, M.; Maccherini, S.; Santi, E.; et al. Plot-scale modelling to detect size, extent, and correlates of changes in tree defoliation in French high forests. *For. Ecol. Manag.* **2014**, *311*, 56–69. [CrossRef]
44. Lorenz, M.; Fischer, R.; Becher, G.; Mues, V.; Granke, O.; Braslavskaya, T.; Bobrinsky, A.; Clarke, N.; Lachmanová, Z.; Lukina, N.; et al. Work Report, Institute for World Forestry. Forest Condition in Europe. Technical Report of ICP Forests. 2009. Available online: https://www.icp-forests.org/pdf/TR2009.pdf (accessed on 31 January 2022).
45. Nicolas, M.; Jolivet, C.; Jonard, M. How monitoring networks contribute to the understanding and to the management of soil and forest ecosystems? *Rev. For. Fr.* **2014**, *66*, 95–103. [CrossRef]
46. Innes, J.L. Forest health surveys—A critique. *Environ Pollut.* **1988**, *54*, 1–15. [CrossRef]
47. Johnson, J.; Jacob, M. Monitoring the effects of air pollution on forest condition in Europe: Is crown defoliation an adequate indicator? *iForest* **2010**, *3*, 86–88. [CrossRef]
48. Cherubini, P.; Battipaglia, G.; Innes, J.L. Tree Vitality and Forest Health: Can Tree-Ring Stable Isotopes Be Used as Indicators? *Curr. For. Rep.* **2021**, *7*, 69–80. [CrossRef]
49. De Vries, W.; Klap, J.M.; Erisman, J.W. Effects of environmental stress on forest crown condition in Europe. Part I: Hypotheses and approach to the study. *Water Air Soil Pollut.* **2000**, *119*, 317–333. [CrossRef]
50. De Marco, A.; Proietti, C.; Cionni, I.; Fischer, R.; Screpanti, A.; Vitale, M. Future impacts of nitrogen deposition and climate change scenarios on forest crown defoliation. *Environ. Pollut.* **2014**, *194*, 171–180. [CrossRef] [PubMed]
51. Ognjenović, M.; Seletković, I.; Potočić, N.; Marušić, M.; Tadić, M.P.; Jonard, M.; Rautio, P.; Timmermann, V.; Lovreškov, L.; Ugarković, D. Defoliation Change of European Beech (*Fagus sylvatica* L.) Depends on Previous Year Drought. *Plants* **2022**, *11*, 730. [CrossRef] [PubMed]
52. Jančić, G. Sušenje šuma—Uzroci sušenja i mere sanacije. *Revija Šume* **2013**, *120*, 10–11. Available online: https://srbijasume.rs/ssume/wp-content/uploads/2021/02/Sume_120.pdf (accessed on 31 January 2022).
53. Češljar, G.; Nevenić, R.; Bilibajkić, S.; Stefanović, T.; Gagić Serdar, R.; Đorđević, I.; Poduška, Z. Viability of trees on bio-indicator plots Level 1 in Republic of Serbia in 2013. *Sustain. For.* **2013**, *67/68*, 69–78.
54. Češljar, G.; Gagić Serdar, R.; Đorđević, I.; Poduška, Z.; Stefanović, T.; Bilibajkić, S.; Nevenić, R. Analysis of types of damages at the sample plots of Level 1 in 2013 at the territory of the Republic of Serbia. *Sustain. For.* **2014**, *69/70*, 63–71. [CrossRef]
55. Češljar, G.; Đorđević, I.; Brašanac-Bosanac, L.; Eremija, S.; Mitrović, S.; Ćirković-Mitrović, T.; Lučić, A. Determination of forest decline due to the action of dominant stress factor through monitoring of defoliation—Case study of Maljen, Serbia. *Agric. For.* **2021**, *67*, 211–226. [CrossRef]
56. Drekić, M.; Poljaković-Pajnik, L.; Orlović, S.; Kovačević, B.; Vasić, V.; Pilipović, A. Results of multiannual monitoring of tree crown condition. *Poplar* **2014**, *193/194*, 23–35.

57. Republic Hydrometeorological Service of Serbia (RHSS). Meteorological Yearbook—Climatological Data. Republic Hydrometeorological Service of Serbia, Belgrade. Available online: http://www.hidmet.gov.rs/latin/meteorologija/klimatologija_godisnjaci.php (accessed on 31 March 2022).
58. Rakićević, T. Klimatsko rejoniranje SR Srbije. In *Zbornik Radova Geografskog Instituta "Jovan Cvijić"*; SANU: Beograd, Srbija, 1980; Knjiga 27; pp. 29–42.
59. Augusto, L.; Davies, T.J.; Delzon, S.; De Schrijver, A. The enigma of the rise of angiosperms: Can we untie the knot? *Ecol. Lett.* **2014**, *17*, 1326–1338. [CrossRef]
60. Hentschel, R.; Rosner, S.; Kayler, Z.E.; Andreassen, K.; Børja, I.; Solberg, S.; Tveito, O.E.; Priesack, E.P.; Gess-ler, A. Norway spruce physiological and anatomical predisposition to dieback. *For. Ecol. Manag.* **2014**, *322*, 27–36. [CrossRef]
61. Hacket-Pain, A.J.; Cavin, L.; Friend, A.D.; Jump, A.S. Consistent limitation of growth by high temperature and low precipitation from range core to southern edge of European beech indicates widespread vulnerability to changing climate. *Eur. J. For. Res.* **2016**, *135*, 897–909. [CrossRef]
62. Devi, N.M.; Kukarskih, V.V.; Galimova, A.A.; Mazepa, V.S.; Grigoriev, A.A. Climate change evidence in tree growth and stand productivity at the upper treeline ecotone in the Polar Ural Mountains. *For. Ecosyst.* **2020**, *7*, 7. [CrossRef]
63. Republic Hydrometeorological Service of Serbia (RHSS). Basic Climate Characteristics for the Territory of Serbia. Republic Hydrometeorological Service of Serbia, Belgrade. Available online: https://www.hidmet.gov.rs/eng/meteorologija/klimatologija_srbije.php (accessed on 1 May 2022).
64. Gazol, A.; Camarero, J.J. Compound climate events increase tree drought mortality across European forests. *Sci. Total Environ.* **2022**, *816*, 151604. [CrossRef] [PubMed]
65. Popović, T.; Radulović, E.; Jovanović, M. Koliko nam se menja klima, kakva će biti naša buduća klima? *EnE05—Konf. Zivotn. Sred. Ka Evropi. Beogr.* **2005**, 212–218. Available online: http://www.sepa.gov.rs/download/5_web.pdf (accessed on 10 January 2022).
66. Vukovic, A.; Vujadinovic, M.; Rendulic, S.; Djurdjevic, V.; Ruml, M.; Babic, V.; Popovic, D. Global warming impact on climate change in Serbia for the period 1961–2100. *Therm. Sci.* **2018**, *22*, 2267–2280. [CrossRef]
67. Stojanović, D.B.; Orlović, S.; Zlatković, M.; Kostić, S.; Vasić, V.; Miletić, B.; Kesić, L.; Matović, B.; Božanić, D.; Pavlović, L.; et al. Climate change within Serbian forests: Current state and future perspectives. *Poplar* **2021**, *208*, 39–56. [CrossRef]
68. Stanković, Z.; Govedar, Z.; Kapović, M.; Hrkić, Z. Climate Change Impact on Forest Vegetation in Republic of Srpska. In Proceedings of the International Scientific Conference "Forest Ecosystems and Climate Changes", Belgrade, Serbia, 9–10 March 2010; Institute of Forestry: Belgrade, Serbia, 2010; Volume 1, pp. 21–25. Available online: http://www.forest.org.rs/pdf/konferencije/PROCEEDINGS-Vol1-FOREST-ECOSYSTEMSAND-CLIMATE-CHANGES.pdf (accessed on 10 January 2022).
69. Brašanac-Bosanac, L.; Filipović, D.; Ćirković-Mitrović, T. Measurements for the adaptation of forest ecosystems on negative impacts of climate change in Serbia. *Fresen. Environ. Bull. Ger.* **2011**, *20*, 2653–2660.
70. Ćirković-Mitrović, T.; Popović, V.; Brašanac-Bosanac, L.; Rakonjac, L.; Lučić, A. The impact of climate elements on the diameter increment of Austrian pine (*Pinus nigra* Arn.) in Serbia. *Arch. Biol. Sci.* **2013**, *65*, 161–170. [CrossRef]
71. Ciais, P.; Reichstein, M.; Viovy, N.; Granier, A.; Ogée, J.; Allard, V.; Aubinet, M.; Buchmann, N.; Bernhofer, C.; Carrara, A.; et al. Europe-wide reduction in primary productivity caused by the heat and drought in 2003. *Nature* **2005**, *437*, 529–533. [CrossRef]
72. Barriopedro, D.; Fischer, E.M.; Luterbacher, J.; Trigo, R.M.; García-Herrera, R. The hot summer of 2010: Redrawing the temperature record map of Europe. *Science* **2011**, *332*, 220–224. [CrossRef]
73. Hanel, M.; Rakovec, O.; Markonis, Y.; Máca, P.; Samaniego, L.; Kyselý, J.; Kumar, R. Revisiting the recent European droughts from a long-term perspective. *Sci. Rep.* **2018**, *8*, 9499. [CrossRef] [PubMed]
74. Hari, V.; Rakovec, O.; Markonis, Y.; Hanel, M.; Kumar, R. Increased future occurrences of the exceptional 2018–2019 Central European drought under global warming. *Sci. Rep.* **2020**, *10*, 12207. [CrossRef] [PubMed]
75. Liu, X.; He, B.; Guo, L.; Huang, L.; Chen, D. Similarities and differences in the mechanisms causing the European summer heatwaves in 2003, 2010, and 2018. *Earth's Future* **2020**, *7*, e2019EF001386. [CrossRef]
76. Büntgen, U.; Urban, O.; Krusic, P.J.; Rybníček, M.; Kolář, T.; Kyncl, T.; Ač, A.; Koňasová, E.; Čáslavský, J.; Esper, J.; et al. Recent European drought extremes beyond Common Era background variability. *Nat. Geosci.* **2021**, *14*, 190–196. [CrossRef]
77. European Environment Agency—EEA. Available online: https://www.eea.europa.eu/data-and-maps/figures/main-drought-events-in-europe (accessed on 10 January 2022).
78. Spinonia, J.; Naumannb, G.; Vogta, J.V.; Barbosaa, P. The biggest drought events in Europe from 1950 to 2012. *J. Hydrol Reg. Stud.* **2015**, *3*, 509–524. [CrossRef]
79. Standardized Precipitation Evapotranspiration Index (SPEI) Database. Available online: http://sac.csic.es/spei/database.html (accessed on 31 January 2022).
80. Global Integrated Drought Monitoring and Prediction System (GIDMaPS). Available online: http://drought.eng.uci.edu/ (accessed on 31 January 2022).
81. Senf, C.; Seidl, R. Mapping the forest disturbance regimes of Europe. *Nat. Sustain.* **2020**, *4*, 63–70. [CrossRef]
82. Technical Report of ICP Forests 2013: Forest Condition in Europe. Available online: https://www.icp-forests.org/pdf/TR2013.pdf (accessed on 31 January 2022).
83. Intergovernmental Panel on Climate Change. Climate Change—IPCC 2014, Synthesis Report, Summary for Policymakers. Available online: https://www.ipcc.ch/site/assets/uploads/2018/02/AR5_SYR_FINAL_SPM.pdf (accessed on 31 January 2022).

84. Ferretti, M.; Fischer, R.; Mues, V.; Granke, O.; Lorenz, M.; Seidling, W.; Nicolas, M. 2020: Part II: Basic Design Principles for the ICP Forests Monitoring Networks. Version 2020-2. In *Manual on Methods and Criteria for Harmonized Sampling, Assessment, Monitoring and Analysis of the Effects of Air Pollution on Forests*; UNECE ICP Forests Programme Co-Ordinating Centre, Ed.; Thünen Institute of Forest Ecosystems: Eberswalde, Germany, 2020; pp. 33 + Annex. Available online: http://icp-forests.net/page/icp-forests-manual (accessed on 31 March 2022).
85. Neuman, W.L. *Social Research Methods: Qualitative and Quantitative Approaches*, 6th ed.; Part one; Pearson Inc.: London, UK, 2006; pp. 1–79.
86. Köppen, W.P. Klassification der Klimate nach Temperatur, Niederschlag und Jahreslauf. *Petermanns Geog. Mitt.* **1918**, *64*, 243–248.
87. Koppen, W.P.; Koppen, W. Das geographisca system der klimate. In *Handbuch der Klimatologie*; Koppen, W., Geiger, G.C., Eds.; Gebr. Borntraeger: Berlin, Germany, 1936; pp. 1–44.
88. Mihajlović, J. Application of Recent Climate Classifications for the Climate Regionalization of Serbia. PhD Thesis, University of Belgrade, Faculty of Geography, Belgrade, Serbia, 2018; pp. 1–368. Available online: https://nardus.mpn.gov.rs/handle/123456789/10657 (accessed on 30 April 2022).
89. Kottek, M.; Grieser, J.; Beck, C.; Rudolf, B.; Rubel, F. World Map of the Koppen-Geiger climate classification updated. *Meteorol. Z.* **2006**, *15*, 259–263. [CrossRef]
90. McKee, T.B.; Doesken, N.J.; Kleist, J. The relationship of drought frequency and duration to time scales. Proceedings of the Eighth Conference on Applied Climatology. Boston MA. *Am. Meteorol. Soc.* **1993**, *17*, 179–184.
91. Vicente-Serrano, S.M.; Beguería, S.; López-Moreno, J.I. A Multi-scalar drought index sensitive to global warming: The Standardized Precipitation Evapotranspiration Index—SPEI. *J. Clim.* **2010**, *23*, 1696–1718. [CrossRef]
92. Tirivarombo, S.; Osupile, D.; Eliasson, P. Drought Monitoring and Analysis: Standardised Precipitation Evapotranspiration Index (SPEI) and Standardised Precipitation Index (SPI). *Phys. Chem. Earth Parts A/B/C* **2018**, *106*, 1–10. [CrossRef]
93. Tefera, A.S.; Ayoade, J.O.; Bello, N.J. Comparative analyses of SPI and SPEI as drought assessment tools in Tigray Region, Northern Ethiopia. *SN Appl. Sci.* **2019**, *1*, 1265. [CrossRef]
94. Pei, Z.; Fang, S.; Wang, L.; Yang, W. Comparative analysis of drought indicated by the SPI and SPEI at various timescales in Inner Mongolia, China. *Water* **2020**, *12*, 1925. [CrossRef]
95. Sheil, D.; Burslem, D.F.R.P.; Alder, D. The interpretation and misinterpretation of mortality rate measures. *J. Ecol.* **1995**, *83*, 331–333. [CrossRef]
96. Lewis, S.L.; Phillips, O.L.; Sheil, D.; Vinceti, B.; Baker, T.R.; Brown, S.; Graham, A.W.; Higuchi, N.; Hilbert, D.W.; Laurance, W.F.; et al. Tropical forest tree mortality, recruiting and turnover rates: Calculation, interpretation and comparison when census intervals vary. *J. Ecol.* **2004**, *92*, 929–944. [CrossRef]

plants

MDPI

Article

Metal- and Organ-Specific Response to Heavy Metal-Induced Stress Mediated by Antioxidant Enzymes' Activities, Polyamines, and Plant Hormones Levels in *Populus deltoides*

Marko Kebert [1,*], Saša Kostić [1], Vanja Vuksanović [2], Anđelina Gavranović Markić [3], Biljana Kiprovski [4], Martina Zorić [1] and Saša Orlović [1]

[1] Institute of Lowland Forestry and Environment, University of Novi Sad, Antona Čehova 13d, 21000 Novi Sad, Serbia
[2] Faculty of Agriculture, University of Novi Sad, Trg Dositeja Obradovića 8, 21000 Novi Sad, Serbia
[3] Division for Genetics, Forest Tree Breeding and Seed Science, Croatian Forest Research Institute, Cvjetno Naselje 41, HR-10450 Jastrebarsko, Croatia
[4] Institute of Field and Vegetable Crops, National Institute of the Republic of Serbia, Maksima Gorkog 30, 21000 Novi Sad, Serbia
* Correspondence: kebertmarko@gmail.com

Abstract: Besides anthropogenic factors, climate change causes altered precipitation patterns that indirectly affect the increase of heavy metals in soils due to hydrological effects and enhanced leaching (i.e., Cd and Ni), especially in the vicinity of mines and smelters. Phytoextraction is a well-known, powerful "green" technique for environmental clean-up that uses plants to extract, sequester, and/or detoxify heavy metals, and it makes significant contributions to the removal of persistent inorganic pollutants from soils. Poplar species, due to their growth features, high transpiration rate, large biomass, and feasible reproduction represent great candidates for phytoextraction technology. However, the consequences of concomitant oxidative stress upon plant metabolism and the mechanism of the poplar's tolerance to heavy metal-induced stress are still not completely understood. In this study, cuttings of poplar species (*Populus deltoides* W. Bartram ex Marshall) were separately exposed to two heavy metals (Cd^{2+} and Ni^{2+}) that were triple the maximum allowed amount (MAA) (according to national legislation). The aim of the study was to estimate the effects of heavy metals on: (I) the accumulation of free and conjugated polyamines, (II) plant hormones (including abscisic acid-ABA and indole-3-acetic acid-IAA), and (III) the activities of different antioxidant enzymes at root and leaf levels. By using the selected ion monitoring (SIM) mode of gas chromatography with mass spectrometry (GC/MS) coupled with the isotopically labeled technique, amounts of ABA and IAA were quantified, while polyamine amounts were determined by using high-performance liquid chromatography (HPLC) with fluorometric detection after derivatization. The results showed that *P. deltoides* responded to elevated concentrations of heavy metals in soils by exhibiting metal- and organ-specific tolerance. Knowledge about tolerance mechanisms is of great importance for the development of phytoremediation technology and afforestation programs for polluted soils.

Keywords: cadmium; nickel; phytoremediation; plant hormones; polyamines; poplar; *Populus deltoides*

Citation: Kebert, M.; Kostić, S.; Vuksanović, V.; Gavranović Markić, A.; Kiprovski, B.; Zorić, M.; Orlović, S. Metal- and Organ-Specific Response to Heavy Metal-Induced Stress Mediated by Antioxidant Enzymes' Activities, Polyamines, and Plant Hormones Levels in *Populus deltoides*. *Plants* **2022**, *11*, 3246. https://doi.org/10.3390/plants11233246

Academic Editor: Nenad Potočić

Received: 31 October 2022
Accepted: 22 November 2022
Published: 26 November 2022

1. Introduction

Two major global environmental problems—future climate change and heavy metal (HM) pollution—are cross-linked and co-dependent. Some climate scenarios predict altered precipitation patterns with an increasing trend of precipitation of up to 30% before 2030, which may result in increased heavy metal mobility and HM leaching into groundwater (depending on HM solubility) [1,2]. This is especially threatening due to the non-biodegradable, hazardous, and persistent nature of heavy metals that lead to their accumulation in the soil

above allowed amounts and at toxic levels [3]. Although some heavy metals are essential for plants and humans in low amounts, their cumulative effects and biomagnification phenomenon (or the significant increase of metal content through the food chain as trophic levels rise) make them dangerous to animal and human health as they bioaccumulate in higher amounts [4–6].

Cadmium (Cd^{2+}), in particular, accumulates in the human body (primarily in the kidneys), and it has a negative impact on many organs due to its high toxicity, causing pulmonary emphysema, renal tubular damage, and kidney stones [7]. Whereas nickel (Ni^{2+}) has the potential to cause severe allergies, lung fibrosis, and even lung and nasal cancer by causing epigenetic alternation [8].

Although many HM in soils slithogenic origins, with some HM released during pedogenesis, two of the most notorious heavy metals, Cd and Ni, primarily enter the soil through anthropogenic activities, such as wastewater irrigation, zinc mining, automobile exhaust smoke, fossil fuel combustion, electroplating, industrial waste, pigments metal alloys, industrial or municipal waste, or excessive application of HM containing pesticides or synthetic phosphate fertilizers [5,9,10]. In addition, the recent overconsumption of electronic products has resulted in the increasing trend of electronic waste as a significant source of HM contamination and soil overload [11–13]. High amounts of toxic HM pollute the environment due to crude and unscientific e-waste recycling procedures (such as mechanical separation, hydrometallurgical, pyrometallurgy, etc.), particularly in the case of Ni-Cd batteries and their carcinogenic electrolytic waste, which make significant contributions to the leaching of toxic HMs in soils [14,15]. Therefore, there is an urgent and critical need for the development of new technologies for HMs clean-up from the environment since old traditional methods, such as excavation, heat treatment, electroremediation, chemical precipitation, metal leaching, and soil washing or replacement, are all rather expensive and invasive [16,17].

Phytoremediation refers to an environmentally friendly, aesthetically pleasing, and low-cost technology that uses plants (as well as their associated microbes) as solar-powered pumps to uptake, sequester, and/or detoxify organic or inorganic pollutants (including HMs, organic contaminants, radionuclides, antibiotics, pesticides, and even explosives such as trinitrotoluene, etc.) from various mediums (including soil, water, and air) and translocate them into harvestable parts [18–20]. Specifically, the process of soil restoration of HMs by plants is called phytoextraction [21,22], and it is the best-known technique of phytoremediation besides phytostabilization, phytodegradation, rhizofiltration, and phytovolatilization [16]. Although phytoremediation has been known for decades, it is still an emerging technique since upcoming climate change will impose new demands and necessitate new adjustments and improvements in terms of sustainability [18]. Crispr-Cas9, a new generation of plant genome editing technologies, provides tools for the rapid improvement of phytoremediation technology by designing genome engineered metallicolous plants with improved heat and drought tolerance, specifically for the purpose of sustainable phytoremediation [23]. Although many herbaceous plants (e.g., *Dysphania botrys*, *Lotus corniculatus*, *Lotus hispidus*, *Plantago lanceolata*, *Trifolium repens*, and *Medicago lupulina*) exhibit metallophyte behavior and are efficient regarding metal accumulation and translocation [24], wooden plant species are more appropriate for phytoremediation due to their large biomass production [25]. Poplars and willows are particularly suitable for phytoextraction because they are fast-growing species with high transpiration indices, easy propagation technology, and a deep rooting system, as well as a high ability to accumulate and translocate essential and non-essential HMs into aerial parts [26–29].

Recently, the entire genome of *Populus trichoderma* has been sequenced, making poplars especially appealing candidates for genome editing toward HM stress tolerance and further investigation of its potential to act as an efficient phytoremediator [23,30]. In this study, we used eastern cottonwood (*Populus deltoides* W. Bartram ex Marshall) clone PE19/66 to investigate Ni and Cd effects on *P. deltoides* biochemical properties since it has been shown to be particularly tolerant to copper by accumulating high amounts of proline (PRO) and

abscisic acid (ABA) in its leaves and roots and high amounts of polyamines in its roots during HM induced stress [31].

Understanding the underlying mechanisms of HM stress tolerance is critical for the further development of phytoremediation techniques, the selection of the most suitable clones, and potential gene targeting and editing. Through evolution, plants evolved their entire machinery to combat HM pollution, and they created/employed strategies and mechanisms to sequester and detoxify HM in order to reduce their toxicity [32–34]. Cd has no known biological functions in higher plants and does not participate in redox reactions, but it does contribute to oxidative damage, protein carbonylation, and lipid peroxidation, and it is extremely toxic to plants due to its high affinity for protein sulfhydryl groups, thus causing the inhibition of many enzymes [35,36]. In contrast, nickel is a structural component of many enzymes, including glyoxylases, peptide-deformylases, methyl-CoM reductases, and several types of superoxide-dismutases and hydrogenases [37]. Excess Ni causes Ni-toxicity, and symptoms (such as leaf chlorosis, plant root growth inhibition, and decreased photosynthesis and respiration) may appear, and Ni also disrupts mineral nutrition, water relations, and sugar transport [38]. Heavy metals, such as Cd and Ni, are uptaken by roots via the apoplastic (passive diffusion) or symplastic (active transport by root plasma membrane transporters for essential elements with low selectivity) pathways, where they form complexes with different chelating agents and are then immobilized in cell walls and vacuoles where detoxification occurs, either by conjugating with glutathione (GSH) or cysteine-rich peptides, such as phytochelatins (PC) or metallothioneins (MS) [39,40]. Heavy metal ions and essential metal ions have a similar radius and charge; therefore, heavy metals can impair the uptake and transport of essential metals like calcium and magnesium [41].

Since heavy metals cause oxidative stress in plants by increasing the production of reactive oxygen species (ROS), the activation of ROS scavenging enzymes, such as superoxide dismutase (SOD), catalase (CAT), ascorbate peroxidase (Apx), glutathione reductase (GR), thioredoxin, and the peroxy-redoxin family of proteins, is one of the first lines of defense [31,42,43]. In addition to enzymatic, antioxidant defense also includes non-enzymatic ROS scavengers, such as ascorbate and glutathione, carotenoids, tocopherols, quinones, lipoic acid, phenolic compounds, polyamines, etc. [44,45].

Polyamines have a variety of regulatory roles in plant cells due to their antioxidant and polycationic nature, and as important abiotic stress markers, they modulate plant tolerance to HM through the direct scavenging of ROS or the activation of antioxidant machinery, or they act as signal molecules to activate ABA or H_2O_2 stress-responsive pathways [46–48]. Their protective role in HM stress has already been proposed, and increasing patterns of both free and conjugated polyamines (such as putrescine, spermidine, and spermine) have been reported as a poplars response to copper and zinc, but to the best of the authors' knowledge, they have not been examined in response to nickel and cadmium [31,49,50].

Although it is well known that abscisic acid (ABA), which is an important plant stress hormone, and indole-3-acetic acid (IAA), which is a developmental hormone, are involved in the perception and signaling of excess HMs by roots, these hormones also affect plant growth and regulate the antioxidant defense system in the presence of HMs [31,51,52]. In particular, their exogenous application prevents the negative effects of excess HM on plant growth and overall fitness [53,54]. Still, little is known about how Ni and Cd affect endogenous plant hormone levels and distribution in *P. deltoides*.

Therefore, the main aim of the study was to investigate how excess amounts of Cd and Ni in soil affect *P. deltoides* responses at root and leaf levels, regarding:

- ✓ The metal content (calcium and magnesium), translocation (TF), and bioconcentration factors (BCF) in *P. deltoides* clone Pe19/66;
- ✓ The activities of different ROS scavenging enzymes, such as guaiacol peroxidase, glutathione reductase, and superoxide dismutase;

- ✓ Total antioxidant and reducing activities (estimated by biochemical assays DPPH and FRAP, respectively) and radical scavenger capacity (against NO and OH radicals), as well as total polyphenol compounds (TPC) accumulation; and
- ✓ Endogenous hormone levels (ABA and IAA), as well as plant hormone, regulators-polyamines content (putrescine, spermine, and spermidine) that is both free and conjugated.

2. Results

2.1. Metal and Non-Metal Contents, Translocation (TF), and Bioconcentration Factors (BCF)

The results regarding the contents of root and shoot uptake of metal content, calcium and magnesium levels, and bioconcentration and translocation in *P. deltoides* clone 19/66 leaves and roots are presented in Table 1.

Table 1. Metal and non-metal accumulation (mean ± SD), bioconcentration, and translocation factors of Ni and Cd in *P. deltoides* clone Pe19/66.

	Ni	**Cd**
Root metal accumulation (mg kg^{-1})	152.77 ± 8.01	17.46 ± 2.46
Leaf metal accumulation (mg kg^{-1})	23.36 ± 0.75	31.98 ± 2.52
Leaf calcium accumulation (mg kg^{-1})	11.86 ± 0.60	10.70 ± 0.29
Root calcium accumulation (mg kg^{-1})	8.24 ± 1.16	7.22 ± 0.97
Leaf magnesium accumulation (mg kg^{-1})	9.07 ± 0.29	8.35 ± 0.23
Root magnesium accumulation (mg kg^{-1})	5.55 ± 0.55	6.49 ± 0.99
Root bioconcentration factor (rBCF)	0.75	1.97
Aboveground bioconcentration factor (aBCF)	0.18	5.02
Translocation factor (TF)	24.62	261.8
Leaf nitrogen content (mg g^{-1})	19.9 ± 3.3	15.3 ± 1.4
Root nitrogen content (mg g^{-1})	9.75 ± 3.2	6.77 ± 1.2
Leaf carbon content (mg g^{-1})	420.5 ± 13.3	417.3 ± 12.5
Root carbon content (mg g^{-1})	391.3 ± 27.8	344.4 ± 10.8

2.2. The Effects of Cd and Ni on Antioxidant Enzymes Activities in Poplar Leaves and Roots

Activities of POD, SOD, and GR were significantly higher in the leaves than in the roots of the tested poplar plants (Figure 1). POD activity in the poplar leaves was 30% lower in the Cd (9 ppm) treatment compared with the unpolluted control, while GR activity was 57% lower in the *P. deltoides* plants under Cd treatment compared with the untreated controls (Figure 1a,c). The highest level of SOD (377.7 SOD g^{-1} FW) activity was observed in the leaves of *P. deltoides* treated with Cd (9 ppm) (Figure 1b). *P. deltoides* cuttings treated with Ni (150 ppm) had significantly higher foliar POD activity (242.4 POD g^{-1} FW). There was no statistically significant difference in SOD and GR activities in roots treated with Ni (150 ppm) when compared to those from the untreated control, contrary to the activity of POD, which was significantly higher in Ni-treated roots (Figure 1).

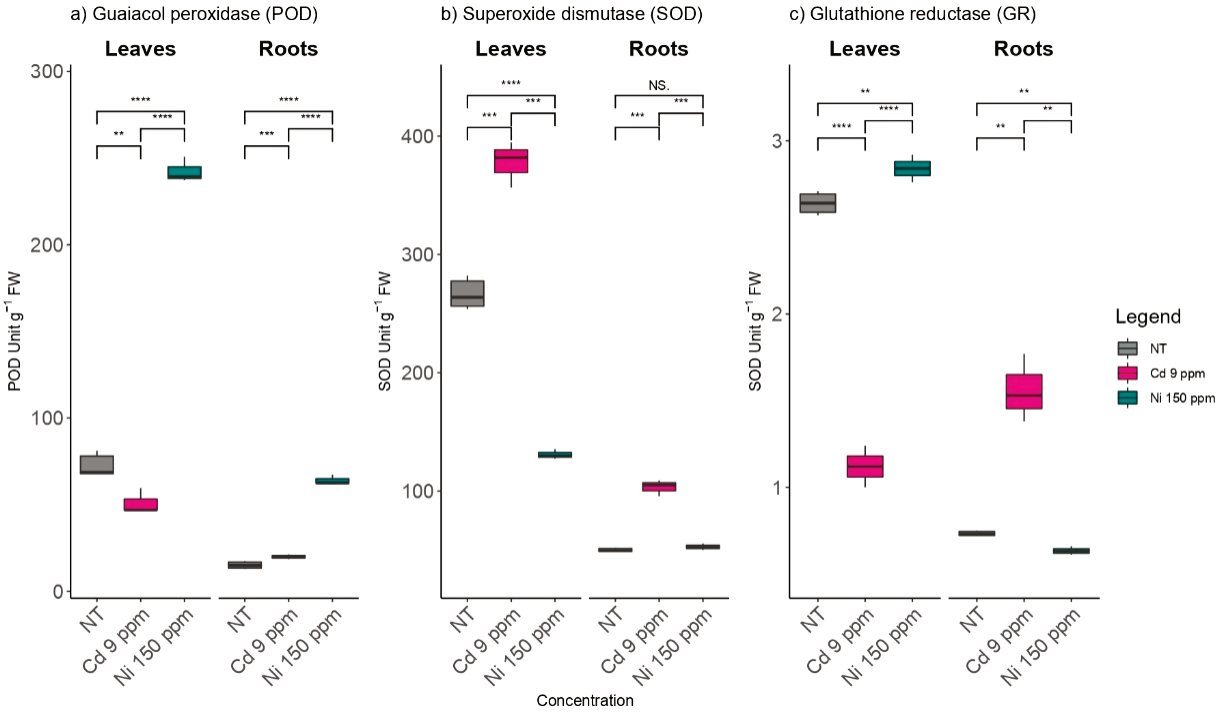

Figure 1. The effects of elevated Cd and Ni soil contents on (**a**) guaiacol peroxidase (POD); (**b**) superoxide dismutase (SOD), and (**c**) glutathione reductase (GR) activities at root and leaf levels using NT-non treated soil. Cd 9 ppm-soil was supplemented to 9 mg Cd kg^{-1} of soil DW and Ni 150 ppm-soil was supplemented to 150 mg Ni kg^{-1} of soil DW. Significance levels: (NS) non-significant versus significant (**) < 0.01; (***) < 0.001, and (****) < 0.0001.

2.3. The Effects of Cd and Ni on the Antioxidant Capacity of Poplar Leaves and Roots

The highest scavenging capacity against DPPH radicals (64.9%) was measured in the extracts of poplar roots grown in the soil treated with Cd (9 ppm). In general, a significantly higher scavenging capacity against DPPH radicals was detected in the leaf extracts of *P. deltoides* from all the examined treatments compared to the control, both in the extracts of the roots and in the leaves (Figure 2a). Scavenger capacity against NO radical indicates that the ability to neutralize NO radicals increases under the influence of Ni and Cd ions since the values for NO scavenger capacity ranged from 17% in the extracts of the roots from the control up to 74.1% in the extracts of the leaves from the plants grown using the treatment with Cd (9 ppm) (Figure 2b). Cd treatment at a concentration of 9 ppm did not affect the ability of *P. deltoides* leaves and root extracts to neutralize OH radicals, yet plants treated with 150 ppm Ni had a significantly higher capacity compared to those from the control (Figure 2c). The ability of leaves extracts to neutralize NO and OH radicals were more affected by the Ni treatment (150 ppm), while the ability to neutralize DPPH radicals was more affected by treatment with Cd (9 ppm) (Figure 2a–c).

After the application of Ni and Cd in amounts that were three times higher than the MAA, there was an increase in LP intensity in both the roots and the leaves (Figure 2d). The highest LP intensity was observed in the poplar leaves grown using the treatment with Cd (9 ppm) (139.9 nmol MDA g^{-1} DW). In general, MDA accumulation was higher in the leaves than in the roots, but the difference in MDA content was higher in the roots when control and treatments were compared. Also, Ni treatment had a greater effect on MDA accumulation than Cd treatment.

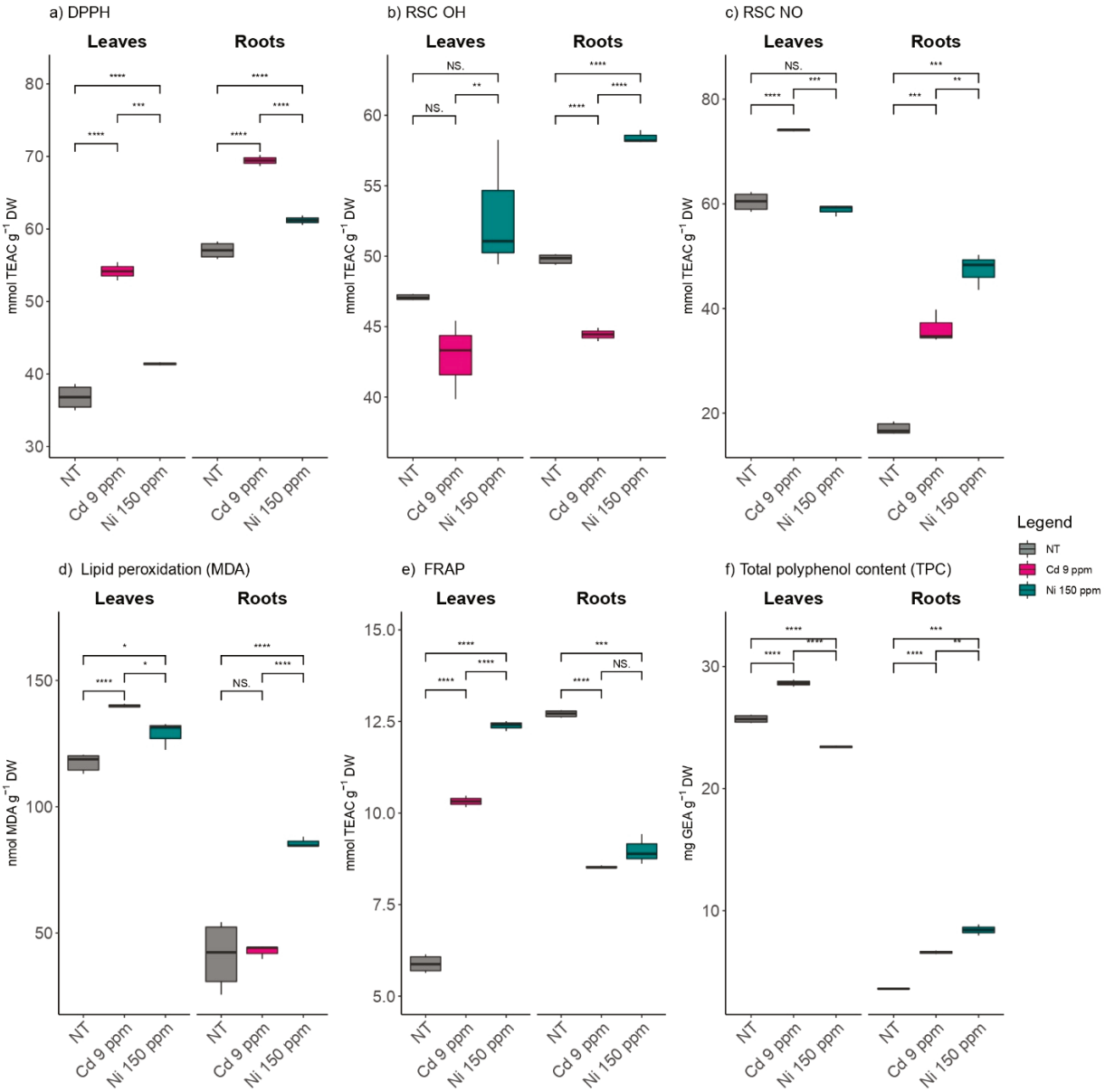

Figure 2. The effects of elevated Cd and Ni soil contents on radical scavenger activities against (**a**) DPPH, (**b**) OH, and (**c**) NO radicals, as well as (**d**) lipid peroxidation, (**e**) ferric reducing antioxidant power (FRAP), and (**f**) total polyphenol content (TPC) at root and leaf levels using NT-non treated soil. Cd 9 ppm-soil was supplemented to 9 mg Cd kg^{-1} of soil DW and Ni 150 ppm-soil was supplemented to 150 mg Ni kg^{-1} of soil dry weight. Significance levels: (NS) non-significant versus significant (*) < 0.05; (**) < 0.01; (***) < 0.001; and (****) < 0.0001.

The reducing capacity of the *P. deltoides* leaves extracts increased by 100% in Ni (150 ppm) and Cd (9 ppm) treatments compared with the control, while the reducing capacity of the roots extracts decreased by about 30% compared with the control (Figure 2e).

The content of polyphenol compounds (TPC) in poplar leaves ranged from 23.4 mg GAE g^{-1} DW (Ni 150 ppm) to 28.6 mg GAE g^{-1} DW (Cd 9 ppm). The highest TPC content was measured in the leaves of the plants from the Cd treatment (9 ppm), and the lowest was detected in the roots of the plants grown using the control media. Significantly higher values of TPC under the influence of Ni ions (150 ppm) were measured in poplar roots compared with the control (Figure 2f).The increase in the content of phenolic compounds was more pronounced in the roots than in the leaves.

2.4. The Effects of Cd and Ni on Plant Hormones and Hormone Regulators Content

The content of abscisic acid increased under the influence of both applied metals, (Ni and Cd increased by 100% and 114%, respectively), whereas the levels of abscisic acid detected in the roots did not differ significantly under the metal treatments (Figure 3a). The constitutive levels of abscisic acid in the roots of the untreated plants were higher than in the leaves.

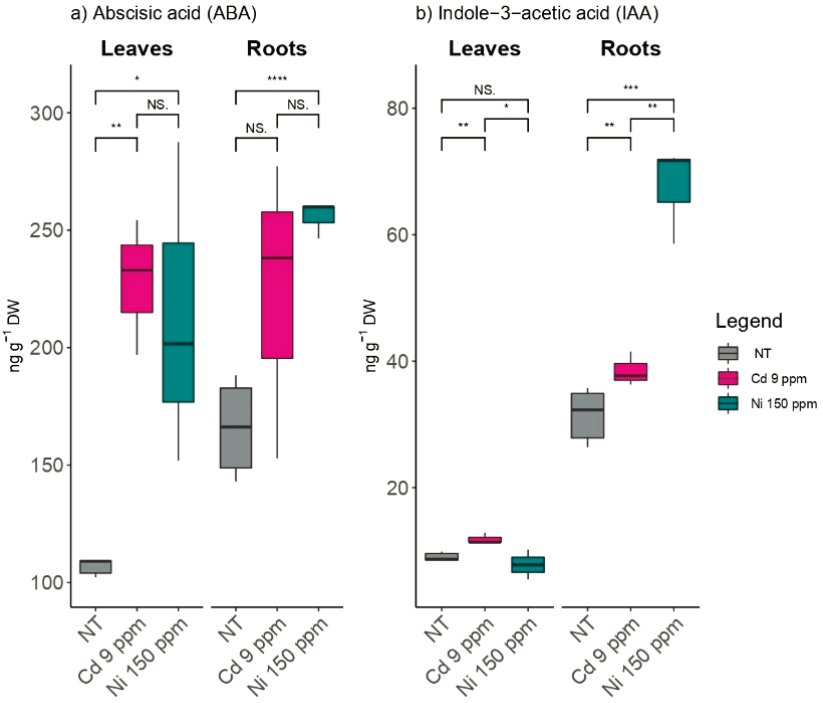

Figure 3. The effects of elevated Cd and Ni soil contents on amounts of plant hormones, (**a**) abscisic acid (ABA), and (**b**) indole-3-acetic acid (IAA) at root and leaf levels using NT-non treated soil. Cd 9 ppm-soil was supplemented to 9 mg Cd kg^{-1} of soil DW and Ni 150 ppm-soil was supplemented to 150 mg Ni kg^{-1} of soil DW. Significance levels: (NS) non-significant versus significant (*) < 0.05; (**) < 0.01; (***) < 0.001; and (****) < 0.0001.

Similarly, the roots had a significantly higher content of indole-3-acetic acid than the leaves (Figure 3b). The nickel treatment significantly increased IAA levels in the roots, but there were no significant changes in foliar IAA under either treatment.

The *P. deltoides* clone Pe19/66 showed a wide range of polyamine responses to different heavy metals (Cd and Ni) in terms of polyamines contents (including putrescine-PUT, spermidine-SMD, and spermine-SPM) in their free and conjugated forms and in organ (root and leaf) defined/related responses (Figure 4). Putrescine was the most abundant polyamine in both the free and conjugated fractions, with SPM being the least abundant in the analyzed *P. deltoides* clone. *P. deltoides* exposed to increased Ni concentrations resulted in a significant increase in PUT and SPM at the root level, but no significant changes in SPD levels occurred. At the leaf level, a different pattern was observed. Ni induced a significant reduction in SPD when compared to non-treated controls, whereas foliar PUT and SPM did not change under the influence of Ni ions. When exposed to excess Ni, all conjugated polyamines increased significantly at the root level, while at the leaf level, conjugated SPD decreased and foliar conjugated PUT and SPM increased slightly compared to untreated controls. Under Cd treatment, all free polyamines exhibited significant declining trends in both inspected organs compared to non-treated controls, with the exception of SPD at the root level, which remained unchanged compared to non-treated controls. Under Cd effects, all conjugated polyamines decreased at the root level compared to untreated *P. deltoides*,

whereas foliar conjugated PUT and SPM increased compared to untreated controls, and conjugated SPD remained unchanged.

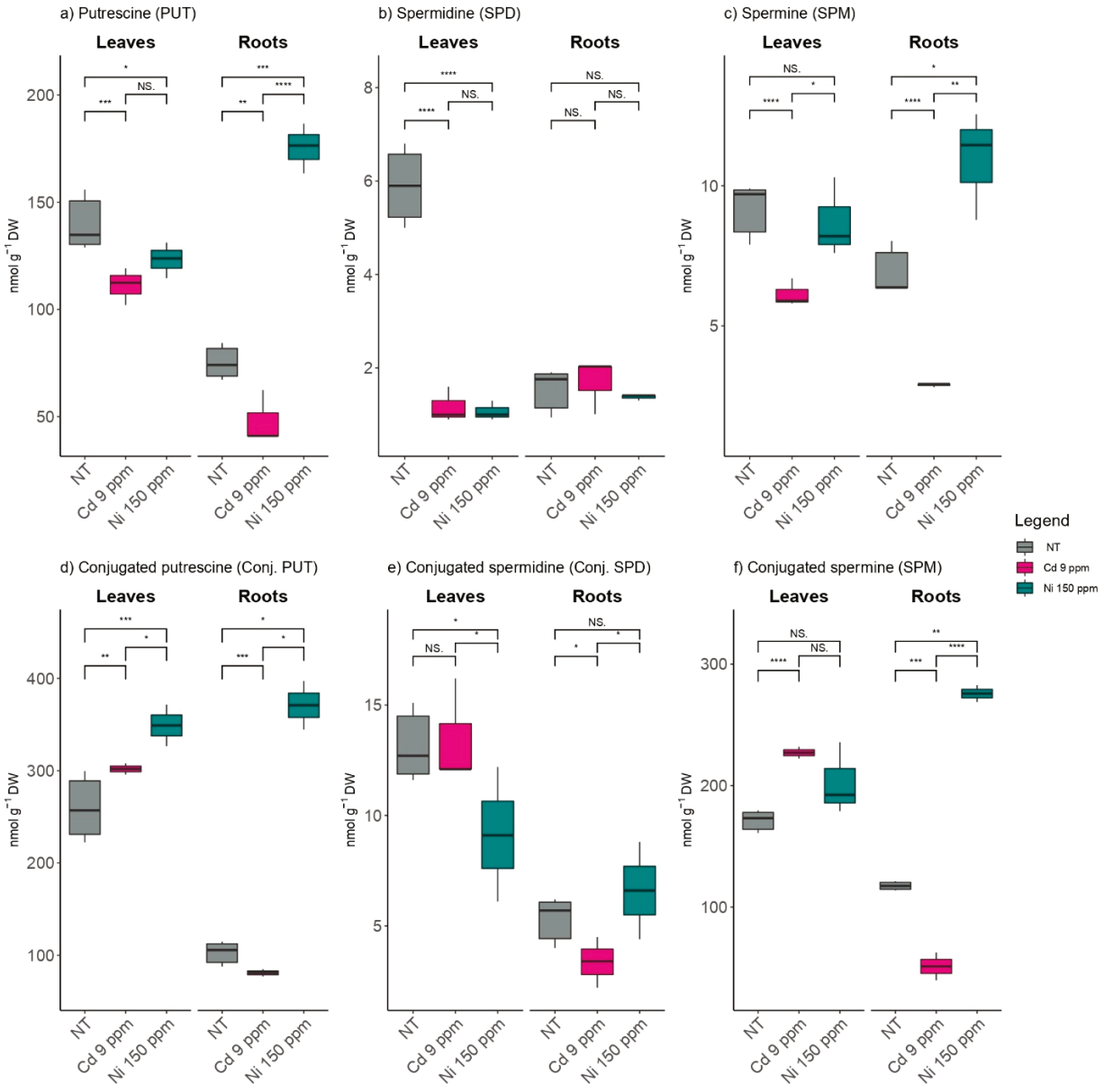

Figure 4. The effects of elevated Cd and Ni soil contents on amounts of accumulated free polyamines ((**a**) putrescine-PUT, (**b**) spermidine-SPD, and (**c**) spermine-SPM), as well as conjugated polyamines ((**d**) conjugated putrescine-conj. PUT, (**e**) conjugated spermidine-conj. SPD, and (**f**) conjugated spermine-conj. SPM) at root and leaf levels using NT-non treated soil. Cd 9 ppm-soil was supplemented to 9 mg Cd kg^{-1} of soil dry weight and Ni 150 ppm-soil was supplemented to 150 mg Ni kg^{-1} of soil DW. Significance levels: (NS) non-significant versus significant (*) < 0.05; (**) < 0.01; (***) < 0.001; and (****) < 0.0001.

2.5. The Principal Component and Correlation Analysis

The Principal Component Analysis (PCA) of analyzed parameters (metabolites, enzymatic activities, radical scavenger activities, and metal content) separately for root (Figure 5a) and leaves (Figure 5b) samples showed differences in organ-specific manner to heavy metal stressors. In both analyzed organs, the first two principal components (PC) described mostly all sample variation (root: 99.28% and leaf: 99.89%). In the root samples

(Figure 5a), parameters associated with PC1 (LP < N < POD < HM conc. < IAA < Put < Conj. Put) defined Ni induced stress, while parameters defined by PC2 (RSD DPPH < SOD < GR < Spd) were defined by Cd induced stress responses. In contrast, analyzed parameters in leaf samples showed that parameters associated with PC2 (POD < N < C < Conj. Put < RSC OH < Ca < Mg) defined Ni induced stress. Opposite to the parameter distribution in Figure 5a for root samples, Cd induced stressors were defined by both PCs, mostly with parameters which defined enzyme activity and hormonal status, particularly with parameters RSC NO < IAA < TPC < SOD < RSD DPPH. Firstly, non-treated control samples were closely distributed on both PCAs, while treated samples were obviously removed from each other as well as from the control samples. Different PCAs and correlation matrix patterns that define different relations among analyzed parameters indicate organ specific responses to elevated soil HM amounts.

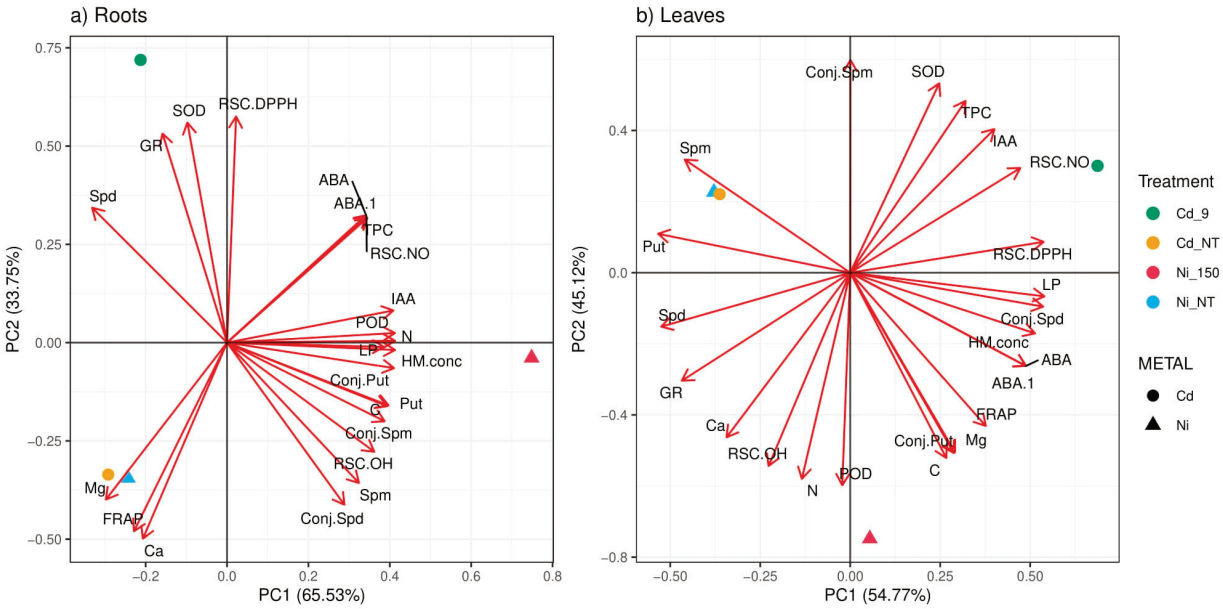

Figure 5. Principal Component Analyses (PCA) with treatment and heavy metal treatment as a dependent variable separately using root (**a**) and leaf (**b**) samples. Treatments include: Cd 9 (*P. deltoides* grown in soil supplemented with 9 ppm Cd); Cd_NT (poplar cuttings grown in non-treated soil); Ni 150 (poplar cuttings grown in soil supplemented with 150 ppm of Ni); and Cd_NT (poplar cuttings grown in Cd non-treated soil). The following abbreviations examined parameters. TPC: total phenolic content; FRAP: ferric reducing antioxidant power; LP: lipid peroxidation; SPD: spermidine; SPM: spermine; PUT: putrescine; SOD: superoxide dismutase; POD: guaiacol peroxidase; GR: glutathione reductase; ABA: abscisic acid; IAA: indole-3-acetic acid; and DPPH: 2,2-Diphenyl-1-picrylhydrazyl radical.

Heavy metal root content positively correlated with almost all the measured parameters. We noted the strongest correlations between heavy metal content from roots with N and C contents, TPC and LP, enzymatic activities, hormonal status (ABA and IAA), and free polyamine content (PUT and SPM), as well as all conjugated forms of polyamines, and with parameters of antioxidant defense system (RSC NO and RSC OH). Root HM contents had a strong, negative correlation with SPD. In contrast to the roots, heavy metal contents in the leaves did not exhibit a uniform response. Although a majority of parameters showed a positive correlation, all inspected polyamines (PUT, SPD, and SPD) expressed negative correlations to HMs content.

Plant hormones (ABA and IAA) measured in both organs (leaves and roots) exhibited similar relation patterns as other analyzed parameters. We noted that ABA from root tissue was strongly and positively correlated with parameters of enzymatic activity and

parameters of antioxidant defense system, such as TPC, LP, POD, and RSC NO, as well as with heavy metal content. In contrast, root levels of ABA were negatively correlated with FRAP values, Ca, and Mg contents, while the correlation with polyamines was missing. Root amounts of IAA showed similar patterns, such as ABA, with all parameters measured in the root tissue. Foliar plant hormones (ABA and IAA) obtained strong correlations with HM content applied using the treatments as well as with Mg and C content, FRAP values, LP activity, and conjugated forms of polyamines. In contrast, foliar ABA exhibited a strong negative correlation with free polyamines (PUT, SPM, and SPD) (Figure 6a).

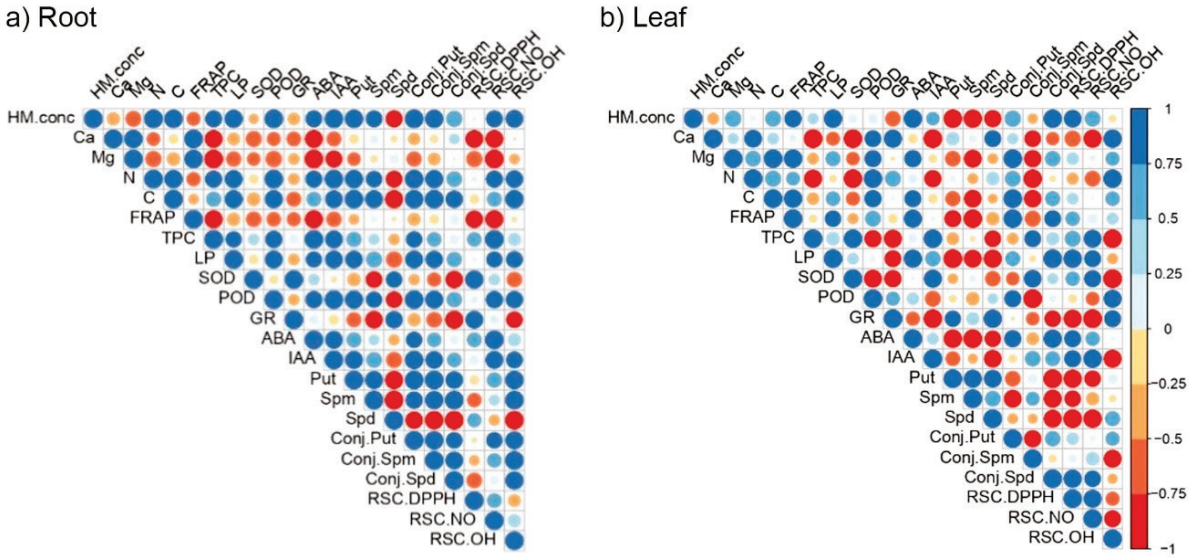

Figure 6. Pearson's correlation matrix of all analyzed parameters for roots (**a**) and leaves (**b**) exposed to increased levels of Ni and Cd. The following abbreviations examined the parameters. TPC: total phenolic content; FRAP: ferric reducing antioxidant power; LP: lipid peroxidation; SPD: spermidine; SPM: spermine; PUT: putrescine; SOD: superoxide dismutase; POD: guaiacol peroxidase; GR: glutathione reductase; ABA: abscisic acid; IAA: indole-3-acetic acid; and DPPH: 2,2-Diphenyl-1-picrylhydrazyl radical.

Within polyamines detected from the root tissue, PUT and SPM showed similar correlation patterns as other examined parameters, contrary to SPD patterns. Likewise, PUT and SPM had strong mutual correlation at the root level. To expand, PUT and SPD in roots were positively correlated with applied amounts of heavy metals, C and N contents, and their conjugated forms, as well as with RSC OH and POD, while negative correlations were noted among PUT and SPM with SOD, Gr, and SPD. We observed opposite patterns of correlation among PUT, SPD and SPM at the leaf level compared with the root tissues, which contributed to the hypothesis of organ-specific responses to increased heavy metal content. At the leaf level, polyamines established numerous negative correlations, like those with HM contents, LP, ABA, RSC DPPH, and RSC NO, as well as conjugated forms of SPD (Figure 6b). Conjugated forms of polyamines exhibited different correlation patterns compared to their free forms extracted from leaves.

Parameters of the antioxidant defense system in roots (RSC NO and RSC OH) had similar relations as other analyzed parameters. The stronger positive correlations were noted with Ca, N, and C contents compared with LP, POD, IAA, and polyamines (PUT and SPM). This trend was opposite to the established correlations with parameters such as GR and SPD, which exposed negative correlation patterns only with RSC OH in the roots. Ambiguous and inconsistent patterns of antioxidant defense system correlations were detected at the leaf level. The most positive relationship was observed between RSC OH and Ca, N, and POD, while RSC NO negatively correlated with TPC, SOD, and IAA in poplar leaves (Figure 6a).

3. Discussion

3.1. The Effects of Cd and Ni on the Antioxidant Defense System

Heavy metals, in addition to influencing enzyme expression, also alter enzyme catalytic function due to their strong binding affinity to sulfhydryl or other groups from the enzyme's active center, resulting in lower enzyme activity or even complete inhibition [55]. Heavy metals can interfere with the function of many enzymes and even displace important metal ions from active sites, resulting in altered activities or the loss of activity [56]. Excessive heavy metal amounts in plants cause oxidative stress which stimulates activities or upregulates expression patterns of defense antioxidant enzymes, such as superoxide dismutase (SOD) and glutathione reductase (GR) [57,58]. The results provided in this study reveal that the change in Ni content in poplar root extract had no effect on the activity of SOD and GR, but the results also confirm that Ni ions have stimulating effects on POD activity. In contrast, Cd ions boost the activity of SOD, POD, and GR in poplar leaf extracts. It was reported previously that Cd influences enzyme activity in poplars, resulting in higher activities of ascorbate peroxidase, glutathione peroxidase, and catalase in roots [59]. Since Ni is not a redox-active element, it is not expected to have a direct impact on the generation of reactive oxygen species; however, this property allows Ni ions to indirectly interact with a large number of antioxidant enzymes, such as superoxide dismutase (SOD), catalase (CAT), glutathione peroxidase (GSH-Px), glutathione reductase (GR), guaiacol peroxidase (GPx), and ascorbate peroxidase (Apx) [60]. The activity of antioxidant enzymes varies depending on the time of exposure, the type of treatment, and the species and plant organs involved [61]. According to Gajewska and Sklodowska [62], SOD and CAT activities decreased significantly in wheat leaves after treatment with 100 mM Ni for three, six, and nine days, while glutathione peroxidase (GSH-Px), guiacol peroxidase (POD), and ascorbate peroxidase (Apx) activities increased. However, the same authors [63] reported that exposing peas (*Pisum sativum*) to nickel ions for 14 days (concentrations of 10, 100, and 200 mM) reduced SOD activity in both shoots and roots, which is in accordance with our findings for poplar clone PE19/66.

The results of the experiment show an increase in total polyphenol content in response to higher Ni and Cd ion concentrations. Similarly, a metal induced increase of total phenolics was reported for other plant species, such as corn [64], cress (*Lepidium sativum*) [65], Scots Pine (*Pinus sylvestris*) [66], and wheat (*Triticum sp*.) [67]. Furthermore, the content of phenolic chemicals increases in poplar as a result of Cd exposure. A concentration of 200 µM caused a 47% increase in phenolic compounds in the roots of *Populus deltoides* and a 38–168% increase in the bark of *Populus* ×*euramericana*, *Populus nigra*, and *Populus popularis*, while in the leaves of *Populus nigra,* phenolic content was 67% higher compared to control plants [59]. Phenolic compounds increase plant tolerance to various abiotic stress factors, such as temperature fluctuations, the presence of heavy metals [68], and water deficit [69,70], in addition to their importance in allelopathic relationships and herbivore defense [71]. Furthermore, other publications revealed that the total polyphenolic content of many plants reduced during abiotic stresses [72–75]. The defensive role of phenolic compounds is attributed to the photoprotective, osmoregulatory, and mostly antioxidant properties of these compounds [76]. According to the study's findings, higher phenolic compound contents in roots and leaves reveals a greater ability to remove ROS. Increased Ni and Cd ion concentrations (three times higher than the MAA) increase the antioxidant capacity of treated poplar clones. There is an increase in the ability to neutralize DPPH radicals under the influence of Ni ions at a concentration of 150 ppm. This is most likely due to the activation of antioxidant defense, which is manifested via the increased biosynthesis of secondary metabolites under stressed conditions caused by Ni ions. Kebert et al. [77] investigated oxidative stress in the leaves of poplar clones Pe19/66, B229 (*P. deltoides*), and Panonnia (*P.* ×*euramericana*) after field exposure to a mixture of heavy metals (Ni, Cd, and Pb), herbicides, diesel fuel, and combined treatment with diesel and heavy metals. The authors stated that heavy metal treated poplar leaves had higher antioxidant capacity than the control group and identified clone B229 as the most tolerant to the treatments used.

In addition, Cd induced stress activated the *Brassica juncea* antioxidative defense system [78]. However, the findings of a study about the toxic effects of cadmium on *Brassica rapa* var. *turnip* discovered that Cd treated plants had lower antioxidant activity [79]. The findings of this study reveal that the ferric reducing antioxidant power (FRAP) of poplar root and leaves extracts is increased when it is exposed to high levels of Ni and Cd. Furthermore, Kebert et al. [77] demonstrated that there is an increase in poplar leaf reducing capacity (estimated by FRAP assay) due to the exposure of plants to stress caused by heavy metals, pesticides, and/or diesel in the soil. The results of the FRAP test on the antioxidant capacity in basil (*Ocimum basilicum*) leaves revealed that the antioxidant capacity increased with a treatment of Ni 500 pp and that antioxidant capacity decreased as Ni content increased [80].

The results obtained in this research indicate that the amounts of measured malondialdehyde (MDA) in poplar leaves and roots increases with an increase of the Ni and Cd ions concentration. Previously published research revealed that the process of lipid peroxidation is enhanced in higher plants under situations of oxidative stress produced by heavy metals. As a result of heavy metal exposure, the amounts of MDA, as an end product of lipid peroxidation, increased in peas [81], different genotypes of rye (*Secale cereale*) [82], sunflower (*Helianthus annuus*) [83], *Arabidopsis thaliana* [84], nodules of soybean (*Glycine max* L.) [85], spring barley (*Hordeum vulgare* L.) [86], and citrus (*Citrus aurantium* L.) [87], which is consistent with the results of this research.

3.2. HM Induced Stress Affected Plant Developmental and Stress Hormones (IAA and ABA)

Abscisic acid (ABA) is a multifunctional phytohormone that has been linked with tolerance to adverse environmental conditions, and its signaling pathway is a key regulator of abiotic stress response in plants, including heavy metal induced stress [31,88–90]. It has been proposed that ABA accumulation and the regulation of ABA biosynthetic gene expression contribute to heavy metal tolerance without affecting growth [91]. The beneficial effects of ABA are associated with its ability to cause stomata closure and to regulate hydraulic conductivity during drought stress or during significant osmotic changes, such as those caused by HM [92]. Furthermore, ABA is involved in the regulation of genes encoding biosynthetic enzymes of different osmoprotective compounds, such as proline and glycine betaine [93,94]. The accumulation of ABA and proline is crucial in the development of tolerance to Cd ions, indicating the networking of signaling pathways in conditions of abiotic stress caused by water deficit and an increased content of heavy metals [95]. Improved tolerance in HM-stressed plant species has also been linked to exogenous ABA application [54]. In contrast, the endogenous levels of plant hormones changes after poplar plants are exposed to a high amount of Cd and Ni in the soil and tissue accumulation of this metal. The significant increase of ABA levels at the root level found in this study could be associated with the important role of this hormone in stress perception and root–shoot signal transduction that enables the transfer of information about increased contents of heavy metals in the soil to the shoots [96]. Our findings about increasing ABA root content are consistent with those found in *Phaseolus vulgaris* under Ni induced stress [97]. When plants are exposed to an excess of Cd ions, they exhibit symptoms of general plant stress, such as decreased leaf elongation and growth and decreased cell size (ethylene response), and symptoms of water deficit, such as decreased stomatal conductance and transpiration, which represent a typical ABA response since it is well known that toxic trace metals impair plants' water balance [98–100]. Our findings show that Cd treatment increases ABA levels by 117% which aligns with previous studies that confirmed Cd induced ABA and ethylene biosynthesis in roots [101–105].

Furthermore, recent findings in Mung bean (*Vigna radiata*) after exogenous application of ABA during Cd stress demonstrated that ABA plays a role in HM tolerance via the regulation of antioxidant machinery [98]. This finding is consistent with the high positive correlations among ABA, total phenolic content, and peroxidase activity at the root level found in this study. Transpiration, on the other hand, stimulates Cd ion transport

to the shoots, and exogenous ABA application reduces this transport [106,107]. ABA-mediated osmotic stress and ABA-mediated signaling pathways induced by excess Cd ions resulted in an increased expression of metallothionein in peas, indicating the existence of signaling crosstalk between drought and Cd induced stress [108]. Depending on the applied concentation, Ni ions can stimulate and inhibit the activities of enzymes involved in the metabolism of plant hormones. Thus, under the influence of 50 µmol $NiCl_2$, the activity of indole-3-acetic acid oxidase in *O. sativa* seedlings significantly increased, while at higher concentrations of Ni ions, the enzymatic activity of this enzyme significantly decreased [109]. In our study, slightly increased root levels of IAA under both elevated Ni and Cd ions are present, while there are no significant changes in IAA at the leaf level. In contrast to our findings, arsenic (As) decreased levels of three auxins, including IAA, NAA, and indole-3-butyric acid (IBA), occurred in *Brassica juncea* [110], whereas short-term cadmium exposure also reduced IAA levels in the root tips of barley *(Hordeum vulgare)* [111].

3.3. Polyamines Exhibited Metal and Organ Specific Responses to HM-Induced Stress

Polyamines, as ubiquitous polycationic antioxidants, have been shown to be mediators of increased heavy metal tolerance in numerous plant species by mitigating the toxic effects of heavy metals in plants [112]. Their protective role is based on their high antioxidant and strong ROS scavenger capacity, and therefore their ability to regulate redox homeostasis during oxidative stress caused by heavy metals [113,114], and also on their ability to act as metal chelators [115]. During their catabolism, polyamines generate hydrogen peroxide, allowing them to modulate entire ROS signaling pathways [116], but they can also activate plant antioxidant defense machinery, specifically affecting the gene expression of ROS scavenging enzymes [117,118]. As positively charged compounds, they have a high affinity for binding to negatively charged biomolecules, such as DNA or lipid membranes, increasing their stability and inhibiting lipid peroxidation, while also having a high affinity for binding to ionic channels and regulating ion homeostasis and ion transport in plants [119,120]. Depending on their charge (Spm^{4+} > Spd^{3+} > Put^{2+}), polyamines block fast-activating vacuolar cation channels which gives them the ability to modulate salt stress tolerance in plants and heavy metal induced stress through modulation of metal transporters [121]. Increased tolerance to heavy metal induced stress has been linked to plants' ability to increase endogenous levels of specific polyamines [31,122] or to the exogenous application of Pas during exposure to elevated heavy metal amounts in soil [123]. In our study, after long-term exposure to high Ni and Cd soil levels, polyamines exhibit organ- and metal-specific responses, with mostly decreasing patterns of free polyamines with increasing Cd levels and increasing patterns of free polyamines during nickel induced stress. Increasing polyamine patterns during Ni induced stress in poplar clone Pe19/66 are consistent with findings of increased foliar SPD and SPM levels in *Amaranthus paniculatus* plants during Ni induced oxidative stress [124], whereas significantly increased PUT levels were reported in *Brassica napus* under excess Ni accumulation [125]. Increased endogenous levels of PAs were also detected in the tissue culture of the commercial white poplar clone 'Villafranca' (*Populus alba*) after exposure to elevated Zn and Cu contents [49] and in poplar clones M1 (*Populus* × *euramericana*), PE19/66, and B229 (*Populus deltoides*) exposed to elevated soil Cu content [31]. Furthermore, elevated Zn amounts were found to increase the expression of the polyamine biosynthetic genes PaADC and PaODC in poplar leaves [49], while the addition of polyamines decreased the expression of genes encoding metallothionein type 2 (*PoMT2*) during Zn induced stress in *Plantago ovata* [126]. Tobacco (*Nicotiana tabacum*) leaves treated with $CdCl_2$ showed increasing patterns of all free and conjugated polyamines, which contrasts with our finding that elevated Cd amounts reduce the main foliar and root polyamines in poplar [127]. When Mung bean was exposed to increased Cd content, putrescine levels increased, but spermidine and spermine levels decreased, which is consistent with our findings [128], whereas cadmium increased the enzyme activities of polyamine biosynthetic enzymes (ADC, ODC, SPMS, and SPDS) in *Oryza sativa* [129]. Mitigating effects of the exogenous application of SPD, SPM, and PUT

during heavy metal induced stress were reported in wheat exposed to increased lead [130] and cadmium levels [131], which resulted in beneficial effects of polyamines, increased plant tolerance to heavy metals, and reduced metal phytotoxicity.

Conjugated polyamines or phenylamides (PhA) are amides formed of aliphatic (e.g., putrescine, spermidine, or spermine) or aromatic (e.g., tyramine and tryptamine) polyamines and hydroxycimetic acids (most commonly caffeic, ferulic, and *p*-coumaric acid) [132]. As polyamines covalently linked to phenylpropanoids, phenylamides have the combined chemical properties of both components, providing them with a wide range of biochemical and metabolic actions, particularly related to free radical scavenging, so there are particularly involved in plant response to elevated heavy metal contents [46]. Because of the high levels of phenylpropanoids in poplars, these conjugated polyamines were abundant in poplar tissues [133]. In this study, all examined conjugated polyamines increased significantly at the root level when exposed to excess nickel, while conjugated polyamines prominently declined in both inspected organs after Cd treatment. These findings for cadmium response in poplar contrast to elevated amounts of conjugated polyamines found in *Hydrocharis dubia* when spermidine was applied exogenously to mitigate Cd induced stress [134]. Furthermore, when the same poplar clone was exposed to long-term effects of excess copper levels, increasing patterns of conjugated polyamines were observed, demonstrating the importance of conjugated polyamines in heavy metal tolerance in poplars [31].

4. Materials and Methods

4.1. Experimental Design and Sampling

In the experiment, 10 dm^3 pots with sandy fluvisol soil were used (see Table 2). The substrate was artificially contaminated by separately adding Cd $(NO_3)_2$ and Ni $(NO_3)_2$ to final contents of 9 mg kg^{-1} Cd and 150 mg kg^{-1} Ni. The control substrate was not artificially contaminated. After the stabilization of the metal content via natural microbiological activity (which took eight weeks), non-rooted cuttings of *P. deltoides* clone PE 19/66 were planted in the spring in pots (including four cuttings in three replicates per treatment and the control) and grown in a greenhouse under semi-controlled conditions. The plants received regular irrigation and monthly additions of Hoagland's solution. After five months of the experiment, one portion of the plant material (the leaves and roots) was used when it was fresh for the preparation of buffer extracts, while the second was frozen in liquid nitrogen and lyophilized to analyze plant hormones and the hormone regulator, and the third and fourth were dried at room temperature for radical scavenger capacity and TPC analyses and in the oven at 70 °C for the determination of metals content to achieve a constant weight, respectively.

Table 2. Chemical properties and particle size composition of the soil used in the experiment.

Horizon	Depth (cm)	pH (in H_2O)	Humus (%)	$CaCO_2$ (%)	Particle Size Composition					
					Coarse Sand (>0.2)	Fine Sand (0.2–0.02)	Silt (0.02–0.002)	Clay (<0.002)	Total Sand (>0.02)	Total Clay (<0.02)
Ap	0–30	7.55	2.64	17.08	0.5	37.4	40.4	21.7	37.9	62.1
I	30–58	7.91	1.58	19.56	0.3	45.9	34.8	19.0	46.2	53.8
II	58–72	8.08	1.00	16.06	0.3	71.0	15.9	12.8	71.3	28.7
III Geo	72–110	8.22	1.09	19.10	1.9	40.5	37.7	19.9	42.4	57.6
IV Geo	110–175	8.53	0.46	15.93	2.5	88.5	1.5	7.5	91.0	9.0

4.2. Metal Content, Translocation (TF), and Bioconcentration Factors (BCF)

Using a microwave-assisted digestion system (model Milestone, D series), 300 mg of oven-dried and crushed plant material were digested with 10 mL of nitric acid and 2 mL of 30% *w/v* hydrogen peroxide and then diluted to 25 mL with deionized water.

The samples were then processed using an Atomic Absorption Spectrophotometer (model FS AAS240/GTA120, Varian, California, CA, USA) and the acetylene/air burner flame technique with an atomization temperature of approximately 2300 °C. The contents of Mg, Ca, Cd, and Ni were determined at 285.2, 422.7, 228, and 232 nm, respectively, and expressed in mg kg^{-1} dry weight (DW) of plant material. All analyses of metal accumulation were performed in three biological and two technical replicates.

4.3. Activities of Antioxidant Enzymes, Radical Scavenger Capacity, Lipid Peroxidation Intensity and Content of Total Polyphenol Compounds

To prepare buffer extracts of leaf and root samples for the measurement of antioxidant enzymes activities (POD, SOD, and GR), lipid peroxidation intensity (LP) and ferric reducing antioxidant power (FRAP test), 250 mg of fresh plant material was mixed with 2 mL of a 50 mM K-phosphate buffer (pH 7.0) using a ground glass homogenizer centrifuged at 15,000× *g*, and after separation of the supernatants, some were used for further analyses.

Seventy percent ethanol in a ratio of 1:10 (*w/v*) was added to 20 mg of air-dried plant material, and after centrifugation at 15,000× *g*, supernatants were used to test radical scavenger capacity (RSC) against DPPH, OH, NO radicals, and TPC.

All mentioned parameters were determined spectrophotometrically using a MultiScan spectrophotometer (Thermo Fisher Scientific, model Multiscan, Santa Clara, GO, CA).

(A) Enzymes activities (POD, SOD, and GR)

Guaiacol peroxidase (GPOD, EC 1.11.1.7) activity was measured according to Zimmerlin et al. [135] with minor modifications. Buffer extracts, as a source of POD, were added to the reaction medium with 0.1 M acetate buffer (pH 7.0) and 10 mM guaiacol as POD substrate. After the addition of 0.1 mM H_2O_2, the increase in the absorbance was measured at 436 nm over 2 min. The enzyme activity was calculated using the extinction coefficient for tetraguaiacol (e = 25.6 mM^{-1} cm^{-1}) and expressed as enzyme units (U) g^{-1} FW, where one unit (U) represented the quantity of the enzyme that catalyzes the conversion of 1 µmol of substrate per min.

Superoxide dismutase (SOD) activity was determined by inhibiting the photochemical reduction of nitro blue tetrazolium (NBT) to formazan, which is a blue product of NBT reduction with superoxide anion ($O2^{\bullet -}$) [136]. Buffer extracts, as a source of SOD, were added to the reaction medium with 0.1 M K-phosphate buffer (pH 7.8), 13 mM methionine, 75 µM NBT, 0.1 mM EDTA, and 2 µM riboflavin. After the illumination of the samples using a fluorescent lamp for 10 min, a change in color was measured at 560 nm. The enzyme activity was defined as the amount of enzyme that inhibits NBT reduction by 50% at 25 °C and expressed as U g^{-1} FW.

Glutathione reductase (GR) activity was assayed using the Carlberg and Mannervik's procedure [137]. Buffer extracts, as a source of GR, were added to the reaction medium with 100 mM phosphate buffer (pH 7), 1 mM GSSG, 1 mM EDTA, and 0.1 mM NADPH. Glutathione-dependent oxidization of NADPH was monitored for 2 min at 340 nm. The extinction coefficient was 6.22 mmol L^{-1} cm^{-1}. The enzyme activity was expressed as U g^{-1} FW.

(B) Assays of Antioxidant Defense Systems

The DPPH-scavenging activity was determined according to Arnao et al.'s method [138] based on the reaction of the transformation of purple (λ_{max} = 515 nm) DPPH-radical (2,2-diphenyl-1-picrylhydrazyl) into reduced yellow form DPPH-H after incubation at 30 °C for 30 min in the dark.

Neutralization of the hydroxyl radical ($OH^{\bullet}$) was determined by monitoring the degradation reaction of 2-deoxy-D-ribose in the presence of free $OH^{\bullet}$ radicals generated in the Fe^{2+}/H_2O_2 system [139]. One of the final products of this reaction was malonyldialdehyde (MDA) which was determined spectrophotometrically with the help of a thiobarbiturate test (TBA test) at 532 nm.

Nitric oxide ($NO^{\bullet}$) radical inhibition was calculated using the Griess Illosvory diazotization process and the method developed by Hensley et al. [140]. The chromophore's absorbance was measured at 546 nm.

The total antioxidant power was measured using the FRAP assay [141] based on the reduction of Fe^{3+}-TPTZ to Fe^{2+}-TPTZ leading to a change in the reaction medium to a dark blue color with maximum absorbance at 593 nm.

Different concentrations of Trolox (6-Hydroxy-2,5,7,8-tetramethylchroman-2-carboxylic acid), which is a hydrophilic analog of vitamin E, were used as a standard in previously mentioned methods. Radical scavenger capacity against DPPH, OH, and NO radicals, as well as ferric reducing antioxidant power-FRAP were calculated using a standard curve and expressed as nmol of Trolox equivalents per g of fresh and dry weight of plant material (nmol TEAC g^{-1} FW/DW), depending on the extract used in the assay.

The intensity of lipid peroxidation (LP) was determined based on the content of malondialdehyde (MDA) as an end product of LP [142]. Absorbance was measured at 532 nm after incubation of the reaction medium (with the buffer extract and a solution containing 20% trichloroacetic acid and 0.5% 2-thiobarbituric acid) at 95 °C for 30 min. MDA amounts (determined by its molar extinction coefficient, 155 mM L^{-1} cm^{-1}) were expressed as nmol MDA per gram fresh weight (nmol MDA g^{-1} FW).

The content of total phenolic (TPC) was estimated using the Folin–Ciocalteu assay according to a method developed by Singleton et al. [143] at 725 nm. The standard calibration curve was plotted using gallic acid and expressed as mg of gallic acid equivalents per g of dry weight of plant material (mg GAE g^{-1} DW).

4.4. Plant Hormones and Hormone Regulators Content

(A) Plant hormone analysis (ABA and IAA)

Freeze-dried leaves and roots weighing between 0.1 and 0.2 g DW were extracted using a solution of 65:35 isopropanol and 0.2 M imidazole buffer (pH 7.0). As an internal standard, [^{13}C6]IAA and [^{2}H4]ABA were added to the reaction mediums for the quantitative mass-spectral analysis of abscisic acid (ABA) and indole-3-acetic acid (IAA) in poplar leaves and roots. After overnight isotope equilibration, the analyses were performed according to Chen et al. [144] and Rapparini et al. [145] using gas chromatography-mass spectrometry-single ion monitoring (GC-MS-SIM) as described by Baraldi et al. [146]. The results of ABA and IAA quantification were expressed as ng g^{-1} DW.

(B) Polyamines determination

Plant tissues (approx. 20 mg DW of freeze-dried material) were extracted with 10 volumes of 4% perchloric acid (PCA). The homogenate was kept for 1 h on ice and then centrifuged at 15,000× *g* for 30 min. Aliquots of the supernatants and standard solutions of putrescine (PUT), spermidine (SPD), and spermine (SPM) were derivatized with dansylchloride as described by Scaramagli et al. [147]. Dansylated derivatives were extracted with toluene, dried, and resuspended in acetonitrile prior to HPLC analysis. Aliquots of the supernatant were subjected to acid hydrolysis (6 N HCl overnight at 110 °C) in order to release PAs from their PCA-soluble conjugates. Released PAs were derivatized and analyzed as described above. PAs were separated and quantified with HPLC (Jasco, Tokyo, Japan) using a reverse phase C_{18} column (Spherisorb ODS2, 5-µm particle diameter, 4.6 × 250 mm, Waters, Wexford, Ireland) and a programmed acetonitrile-water step gradient. The results of PAs quantification were expressed as nmol g^{-1} DW. The conjugated PAs amounts were calculated as the difference of total PAs in the hydrolyzed supernatants and the amounts of the free PAs in the nonhydrolyzed supernatants.

4.5. Elemental Analysis of Nitrogen and Carbon Content

The contents of nitrogen (N) and carbon (C) in freeze-dried powdered poplar leaf material were determined using a CHN analyzer (model Elemental VARIO EL III, Hanau,

Germany) coupled with a thermo-conductivity detector by using the manufacturer's instructions. Acetanilide was used as a standard compound.

4.6. Statistics

Descriptive statistics, two factorial ANOVA, the *t*-test, principal component analysis (PCA), and Pearson correlation statistical techniques were employed. In two-way ANOVA, heavy metals (Ni and Cd) and plant organs (root and leaf) were used as factors, which were interpreted using the Fisher (F) test and their statistical significance levels. The *t*-test results were visually represented on a box plot diagram. The R programming environment was used for all statistical data processing (R Core Team). The "*rstatix*" R package [148] was used to calculate descriptive statistics and run two-way ANOVA and t-tests, while the "*ggplot2*" R package [149] was used for other visual representations. We used three levels of statistical significance throughout the paper denoted as (*) 0.05, (**) 0.01, (***) 0.001, and (****) 0.0001.

5. Conclusions

This study represents one of the first findings regarding the ability of the tested *P. deltoides* clone PE19/66 to be used for the phytoremediation of nickel and cadmium from soil. The study was designed to follow the effects of artificially applied heavy metals on poplar biological responses at the root and leaf levels. Tracking antioxidant, metabolic, and ROS enzymatic poplar biological responses and elevated nickel and cadmium soil amounts revealed a high metal- and -organ specificity. *P. deltoides* clone 19/66 showed an ambiguous response to different heavy metals, whereas polyamines showed mostly decreasing patterns of free polyamines in response to increased cadmium levels and increasing patterns of free polyamines in response to nickel induced stress. As a result of elevated nickel and cadmium soil contents, there was a significant increase in antioxidant activities, phenolic content, and ABA amounts at the poplar root level, confirming the role of this hormone in stress perception and signal transduction. These findings could be useful to develop afforestation programs for heavy metal-polluted habitats.

Author Contributions: Conceptualization, M.K. and B.K.; methodology, M.K., B.K., A.G.M. and M.Z.; statistical analysis and software, S.K.; formal analysis, M.K., V.V., and M.Z.; writing—original draft preparation, M.K.; writing—review and editing, B.K., S.O., M.Z., V.V., A.G.M. and S.K.; visualization, S.K.; supervision, S.O. and B.K.; funding acquisition, M.K. and S.K. All authors have read and agreed to the published version of the manuscript.

Funding: This study was funded by the Provincial Secretariat for Higher Education and Scientific Research through the project 'Influence of specific factors in urban environment on alley trees vitality' (Contract No. 142-451-2558/2021-01/2) and by the Ministry of Education, Science and Technological Development of the Republic of Serbia (Contract No. 451-03-68/2022-14/200197 and 451-03-68/2022-14/200117).

Acknowledgments: We are grateful to Stefania Biondi from the Department of Biological, Geological, and Environmental Sciences at the University of Bologna, Italy. She deserves special recognition for her supervision and guidance during polyamine quantification. Furthermore, a special thanks goes to senior researcher dr Francessca Rapparini from the Institute of BioEconomy (IBE), National Research Council (CNR), Bologna, Italy for her selfless help and dedication during the plant hormone analysis.

Conflicts of Interest: The authors declare no conflict of interest.

References

1. Yang, W.; Zhao, F.; Wang, Y.; Ding, Z.; Yang, X.; Zhu, Z. Differences in Uptake and Accumulation of Copper and Zinc by Salix Clones under Flooded versus Non-Flooded Conditions. *Chemosphere* **2020**, *241*, 125059. [CrossRef]
2. Oyewo, O.A.; Adeniyi, A.; Bopape, M.F.; Onyango, M.S. Chapter 4—Heavy Metal Mobility in Surface Water and Soil, Climate Change, and Soil Interactions. In *Climate Change and Soil Interactions*; Prasad, M.N.V., Pietrzykowski, M., Eds.; Elsevier: Amsterdam, The Netherlands, 2020; pp. 51–88. [CrossRef]

3. Zafar-ul-Hye, M.; Naeem, M.; Danish, S.; Fahad, S.; Datta, R.; Abbas, M.; Rahi, A.A.; Brtnicky, M.; Holátko, J.; Tarar, Z.H.; et al. Alleviation of Cadmium Adverse Effects by Improving Nutrients Uptake in Bitter Gourd through Cadmium Tolerant Rhizobacteria. *Environments* **2020**, *7*, 54. [CrossRef]
4. Shah, K.; Nongkynrih, J.M. Metal Hyperaccumulation and Bioremediation. *Biol. Plantarum.* **2007**, *51*, 618–634. [CrossRef]
5. Ali, H.; Khan, E.; Ilahi, I. Environmental Chemistry and Ecotoxicology of Hazardous Heavy Metals: Environmental Persistence, Toxicity, and Bioaccumulation. *J. Chem.* **2019**, *2019*, e6730305. [CrossRef]
6. Singh, D.J.; Kalamdhad, A. Effects of Heavy Metals on Soil, Plants, Human Health and Aquatic Life. *Int. J. Res. Chem. Environ.* **2011**, *1*, 15–21.
7. Mahajan, P.; Kaushal, J. Role of Phytoremediation in Reducing Cadmium Toxicity in Soil and Water. *J. Toxicol.* **2018**, *2018*, e4864365. [CrossRef] [PubMed]
8. Genchi, G.; Carocci, A.; Lauria, G.; Sinicropi, M.S.; Catalano, A. Nickel: Human Health and Environmental Toxicology. *Int. J. Environ. Res. Public Health* **2020**, *17*, 679. [CrossRef]
9. Dixit, P.; Mukherjee, P.K.; Ramachandran, V.; Eapen, S. Glutathione Transferase from Trichoderma Virens Enhances Cadmium Tolerance without Enhancing Its Accumulation in Transgenic Nicotiana Tabacum. *PLoS ONE* **2011**, *6*, e16360. [CrossRef] [PubMed]
10. Rao, K.S.; Mohapatra, M.; Anand, S.; Venkateswarlu, P. Review on Cadmium Removal from Aqueous Solutions. *Int. J. Eng. Sci. Technol.* **2010**, *2*, 81–103. [CrossRef]
11. Chen, M.; Ogunseitan, O.A.; Wang, J.; Chen, H.; Wang, B.; Chen, S. Evolution of Electronic Waste Toxicity: Trends in Innovation and Regulation. *Environ. Int.* **2016**, *89–90*, 147–154. [CrossRef]
12. Chen, M.; Qin, X.; Zeng, G.; Li, J. Impacts of Human Activity Modes and Climate on Heavy Metal "Spread" in Groundwater Are Biased. *Chemosphere* **2016**, *152*, 439–445. [CrossRef]
13. Kumar, P.; Fulekar, M.H. Multivariate and Statistical Approaches for the Evaluation of Heavy Metals Pollution at E-Waste Dumping Sites. *SN Appl. Sci.* **2019**, *1*, 1506. [CrossRef]
14. Moreira, T.F.M.; Santana, I.L.; Moura, M.N.; Ferreira, S.A.D.; Lelis, M.F.F.; Freitas, M.B.J.G. Recycling of Negative Electrodes from Spent Ni-Cd Batteries as CdO with Nanoparticle Sizes and Its Application in Remediation of Azo Dye. *Mater. Chem. Phys.* **2017**, *195*, 19–27. [CrossRef]
15. Arya, S.; Kumar, S. E-Waste in India at a Glance: Current Trends, Regulations, Challenges and Management Strategies. *J. Clean. Prod.* **2020**, *271*, 122707. [CrossRef]
16. Nedjimi, B. Phytoremediation: A Sustainable Environmental Technology for Heavy Metals Decontamination. *SN Appl. Sci.* **2021**, *3*, 286. [CrossRef]
17. Habibul, N.; Chen, J.-J.; Hu, Y.-Y.; Hu, Y.; Yin, H.; Sheng, G.-P.; Yu, H.-Q. Uptake, Accumulation and Metabolization of 1-Butyl-3-Methylimidazolium Bromide by Ryegrass from Water: Prospects for Phytoremediation. *Water Res.* **2019**, *156*, 82–91. [CrossRef]
18. Kafle, A.; Timilsina, A.; Gautam, A.; Adhikari, K.; Bhattarai, A.; Aryal, N. Phytoremediation: Mechanisms, Plant Selection and Enhancement by Natural and Synthetic Agents. *Environ. Adv.* **2022**, *8*, 100203. [CrossRef]
19. Sun, Y.; Zhou, Q.; Wang, L.; Liu, W. The Influence of Different Growth Stages and Dosage of EDTA on Cd Uptake and Accumulation in Cd-Hyperaccumulator (*Solanum Nigrum* L.). *Bull. Environ. Contam. Toxicol.* **2009**, *82*, 348–353. [CrossRef] [PubMed]
20. Baker, A.J.M.; McGrath, S.P.; Reeves, R.D.; Smith, J.A.C. Metal Hyperaccumulator Plants: A Review of the Ecology and Physiology of a Biological Resource for Phytoremediation of Metal-Polluted Soils. In *Phytoremediation of Contaminated Soil*; Terry, N., Vangronsveld, J., Banuelos, G., Eds.; CRC Press: Boca Raton, FL, USA, 1999; pp. 85–107.
21. Suman, J.; Uhlik, O.; Viktorova, J.; Macek, T. Phytoextraction of Heavy Metals: A Promising Tool for Clean-Up of Polluted Environment? *Front. Plant Sci.* **2018**, *9*, 1476. [CrossRef] [PubMed]
22. Garbisu, C.; Alkorta, I. Phytoextraction: A Cost-Effective Plant-Based Technology for the Removal of Metals from the Environment. *Bioresour. Technol.* **2001**, *77*, 229–236. [CrossRef] [PubMed]
23. Sarma, H.; Islam, N.F.; Prasad, R.; Prasad, M.N.V.; Ma, L.Q.; Rinklebe, J. Enhancing Phytoremediation of Hazardous Metal(Loid)s Using Genome Engineering CRISPR–Cas9 Technology. *J. Hazard. Mater.* **2021**, *414*, 125493. [CrossRef]
24. Matanzas, N.; Afif, E.; Díaz, T.E.; Gallego, J.R. Phytoremediation Potential of Native Herbaceous Plant Species Growing on a Paradigmatic Brownfield Site. *Water Air Soil Pollut.* **2021**, *232*, 290. [CrossRef]
25. Yıldırım, K.; Kasım, G.Ç. Phytoremediation Potential of Poplar and Willow Species in Small Scale Constructed Wetland for Boron Removal. *Chemosphere* **2018**, *194*, 722–736. [CrossRef] [PubMed]
26. Malá, J.; Cvrčková, H.; Máchová, P.; Dostál, J.; Šíma, P. Heavy Metal Accumulation by Willow Clones in Short-Time Hydroponics. *J. For. Sci.* **2010**, *56*, 28–34. [CrossRef]
27. Greger, M.; Landberg, T. Use of Willow in Phytoextraction. *Int. J. Phytoremed.* **1999**, *1*, 115–123. [CrossRef]
28. Zacchini, M.; Pietrini, F.; Mugnozza, G.S.; Iori, V.; Pietrosanti, L.; Massacci, A. Metal Tolerance, Accumulation and Translocation in Poplar and Willow Clones Treated with Cadmium in Hydroponics. *Water Air Soil Pollut.* **2008**, *197*, 23. [CrossRef]
29. Pajević, S.; Borišev, M.; Nikolić, N.; Krstić, B.; Pilipović, A.; Orlović, S. Phytoremediation Capacity of Poplar (*Populus* spp.) and Willow (*Salix* spp.) Clonesin Relation to Photosynthesis. *Arch. Biol. Sci.* **2009**, *61*, 239–247. [CrossRef]
30. Wullschleger, S.D.; Weston, D.J.; DiFazio, S.P.; Tuskan, G.A. Revisiting the Sequencing of the First Tree Genome: Populus Trichocarpa. *Tree Physiol.* **2013**, *33*, 357–364. [CrossRef] [PubMed]

31. Kebert, M.; Rapparini, F.; Neri, L.; Bertazza, G.; Orlović, S.; Biondi, S. Copper-Induced Responses in Poplar Clones Are Associated with Genotype- and Organ-Specific Changes in Peroxidase Activity and Proline, Polyamine, ABA, and IAA Levels. *J. Plant Growth Regul.* **2017**, *36*, 131–147. [CrossRef]
32. Luo, J.-S.; Zhang, Z. Mechanisms of Cadmium Phytoremediation and Detoxification in Plants. *Crop. J.* **2021**, *9*, 521–529. [CrossRef]
33. Ge, W.; Jiao, Y.Q.; Sun, B.L.; Qin, R.; Jiang, W.S.; Liu, D.H. Cadmium-Mediated Oxidative Stress and Ultrastructural Changes in Root Cells of Poplar Cultivars. *S. Afr. J. Bot.* **2012**, *83*, 98–108. [CrossRef]
34. Li, S.; Yang, D.; Tian, J.; Wang, S.; Yan, Y.; He, X.; Du, Z.; Zhong, F. Physiological and Transcriptional Response of Carbohydrate and Nitrogen Metabolism in Tomato Plant Leaves to Nickel Ion and Nitrogen Levels. *Sci. Hortic.* **2022**, *292*, 110620. [CrossRef]
35. Chaoui, A.; El Ferjani, E. Effects of Cadmium and Copper on Antioxidant Capacities, Lignification and Auxin Degradation in Leaves of Pea (*Pisum sativum* L.) Seedlings. *Comptes Rendus Biol.* **2005**, *328*, 23–31. [CrossRef]
36. Haider, F.U.; Liqun, C.; Coulter, J.A.; Cheema, S.A.; Wu, J.; Zhang, R.; Wenjun, M.; Farooq, M. Cadmium Toxicity in Plants: Impacts and Remediation Strategies. *Ecotoxicol. Environ. Saf.* **2021**, *211*, 111887. [CrossRef]
37. Shahzad, B.; Tanveer, M.; Rehman, A.; Cheema, S.A.; Fahad, S.; Rehman, S.; Sharma, A. Nickel; Whether Toxic or Essential for Plants and Environment—A Review. *Plant Physiol. Biochem.* **2018**, *132*, 641–651. [CrossRef] [PubMed]
38. Seregin, I.V.; Kozhevnikova, A.D.; Davydova, M.A.; Bystrova, E.I.; Schat, H.; Ivanov, V.B. Role of Root and Shoot Tissues of Excluders and Hyperaccumulators in Nickel Transport and Accumulation. *Dokl. Biol. Sci.* **2007**, *415*, 295–297. [CrossRef] [PubMed]
39. Cobbett, C.; Goldsbrough, P. Phytochelatins and Metallothioneins: Roles in Heavy Metal Detoxification and Homeostasis. *Annu. Rev. Plant Biol.* **2002**, *53*, 159–182. [CrossRef] [PubMed]
40. Zimeri, A.M.; Dhankher, O.P.; McCaig, B.; Meagher, R.B. The Plant MT1 Metallothioneins Are Stabilized by Binding Cadmiums and Are Required for Cadmium Tolerance and Accumulation. *Plant Mol. Biol.* **2005**, *58*, 839–855. [CrossRef] [PubMed]
41. Singh, R.; Gautam, N.; Mishra, A.; Gupta, R. Heavy Metals and Living Systems: An Overview. *Indian J. Pharmacol.* **2011**, *43*, 246–253. [CrossRef] [PubMed]
42. Valko, M.; Morris, H.; Cronin, M.T.D. Metals, Toxicity and Oxidative Stress. *Curr. Med. Chem.* **2005**, *12*, 1161–1208. [CrossRef] [PubMed]
43. Mittler, R.; Vanderauwera, S.; Gollery, M.; Van Breusegem, F. Reactive Oxygen Gene Network of Plants. *Trends Plant Sci.* **2004**, *9*, 490–498. [CrossRef] [PubMed]
44. Danouche, M.; El Ghachtouli, N.; El Baouchi, A.; El Arroussi, H. Heavy Metals Phycoremediation Using Tolerant Green Microalgae: Enzymatic and Non-Enzymatic Antioxidant Systems for the Management of Oxidative Stress. *J. Environ. Chem. Eng.* **2020**, *8*, 104460. [CrossRef]
45. Santovito, G.; Trentin, E.; Gobbi, I.; Bisaccia, P.; Tallandini, L.; Irato, P. Non-Enzymatic Antioxidant Responses of Mytilus Galloprovincialis: Insights into the Physiological Role against Metal-Induced Oxidative Stress. *Comp. Biochem. Physiol. C Toxicol. Pharmacol.* **2021**, *240*, 108909. [CrossRef]
46. Velikova, V.B.; Edreva, A.M.; Tsonev, T.D.; Jones, H.G. Singlet Oxygen Quenching by Phenylamides and Their Parent Compounds. *Z. Naturforsch. C* **2007**, *62*, 833–838. [CrossRef]
47. Mandal, C.; Ghosh, N.; Maiti, S.; Das, K.; Gupta, S.; Dey, N.; Adak, M.K. Antioxidative Responses of Salvinia (*Salvinia natans* Linn.) to Aluminium Stress and It's Modulation by Polyamine. *Physiol. Mol. Biol. Plants* **2013**, *19*, 91–103. [CrossRef] [PubMed]
48. Minocha, R.; Majumdar, R.; Minocha, S.C. Polyamines and Abiotic Stress in Plants: A Complex Relationship. *Front. Plant Sci.* **2014**, *5*, 175. [CrossRef]
49. Franchin, C.; Fossati, T.; Pasquini, E.; Lingua, G.; Castiglione, S.; Torrigiani, P.; Biondi, S. High Concentrations of Zinc and Copper Induce Differential Polyamine Responses in Micropropagated White Poplar (*Populus alba*). *Physiol. Plant.* **2007**, *130*, 77–90. [CrossRef]
50. Castiglione, S.; Todeschini, V.; Franchin, C.; Torrigiani, P.; Gastaldi, D.; Cicatelli, A.; Rinaudo, C.; Berta, G.; Biondi, S.; Lingua, G. Clonal Differences in Survival Capacity, Copper and Zinc Accumulation, and Correlation with Leaf Polyamine Levels in Poplar: A Large-Scale Field Trial on Heavily Polluted Soil. *Environ. Pollut.* **2009**, *157*, 2108. [CrossRef]
51. Song, Y.; Ci, D.; Tian, M.; Zhang, D. Comparison of the Physiological Effects and Transcriptome Responses of Populus Simonii under Different Abiotic Stresses. *Plant Mol. Biol.* **2014**, *86*, 139–156. [CrossRef] [PubMed]
52. Gangwar, S.; Singh, V.P. Indole Acetic Acid Differently Changes Growth and Nitrogen Metabolism in *Pisum sativum* L. Seedlings under Chromium (VI) Phytotoxicity: Implication of Oxidative Stress. *Sci. Hortic.* **2011**, *129*, 321–328. [CrossRef]
53. Elobeid, M.; Polle, A. Interference of Heavy Metal Toxicity with Auxin Physiology. In *Metal Toxicity in Plants: Perception, Signaling and Remediation*; Gupta, D., Sandalio, L., Eds.; Springer: Berlin/Heidelberg, Germany, 2012; pp. 249–259.
54. Asgher, M.; Khan, M.I.R.; Anjum, N.A.; Khan, N.A. Minimising Toxicity of Cadmium in Plants-Role of Plant Growth Regulators. *Protoplasma* **2015**, *252*, 399–413. [CrossRef]
55. Schwitzguébel, J.-P.; van der Lelie, D.; Baker, A.; Glass, D.; Vangronsveld, J. Phytoremediation: European and American Trends. Successes, Obstacles and Needs. *J. Soils Sediments* **2002**, *2*, 91–99. [CrossRef]
56. Sharma, R.K.; Agrawal, M. Biological Effects of Heavy Metals: An Overview. *J. Environ. Biol.* **2005**, *26*, 301–313.
57. Drążkiewicz, M.; Skórzyńska-Polit, E.; Krupa, Z. Response of the Ascorbate–Glutathione Cycle to Excess Copper in *Arabidopsis thaliana* (L.). *Plant Sci.* **2003**, *164*, 195–202. [CrossRef]

58. Wang, H.; Shan, X.; Wen, B.; Zhang, S.; Wang, Z. Responses of Antioxidative Enzymes to Accumulation of Copper in a Copper Hyperaccumulator of Commoelina Communis. *Arch. Environ. Contam. Toxicol.* **2004**, *47*, 185–192. [CrossRef] [PubMed]
59. He, J.; Ma, C.; Ma, Y.; Li, H.; Kang, J.; Liu, T.-X.; Polle, A.; Peng, C.; Luo, Z.-B. Cadmium Tolerance in Six Poplar Species. *Environ. Sci. Pollut. Res. Int.* **2012**, *20*, 163–174. [CrossRef] [PubMed]
60. Hao, F.; Wang, X.; Chen, J. Involvement of Plasma-Membrane NADPH Oxidase in Nickel-Induced Oxidative Stress in Roots of Wheat Seedlings. *Plant Sci.* **2006**, *170*, 151–158. [CrossRef]
61. del Carmen, E.M.; Souza, V.; Bucio, L.; Hernández, E.; Damián-Matsumura, P.; Zaga, V.; Gutiérrez-Ruiz, M.C. Cadmium Induces Alpha(1)Collagen (I) and Metallothionein II Gene and Alters the Antioxidant System in Rat Hepatic Stellate Cells. *Toxicology* **2002**, *170*, 63–73. [CrossRef] [PubMed]
62. Gajewska, E.; Skłodowska, M. Effect of Nickel on ROS Content and Antioxidative Enzyme Activities in Wheat Leaves. *Biometals* **2007**, *20*, 27–36. [CrossRef] [PubMed]
63. Gajewska, E.; Skłodowska, M. Antioxidative Responses and Proline Level in Leaves and Roots of Pea Plants Subjected to Nickel Stress. *Acta Physiol. Plant.* **2005**, *27*, 329–340. [CrossRef]
64. Kısa, D.; Elmastaş, M.; Öztürk, L.; Kayır, Ö. Responses of the Phenolic Compounds of Zea Mays under Heavy Metal Stress. *Appl. Biol. Chem.* **2016**, *59*, 813–820. [CrossRef]
65. Torres, J.; Barrientos, E.; Wrobel, K.; Wrobel, K. Effect of Cadmium (Cd(II)), Selenium (Se(IV)) and Their Mixtures on Phenolic Compounds and Antioxidant Capacity in Lepidium Sativum. *Acta Physiol. Plant.* **2014**, *35*, 431–441. [CrossRef]
66. Schützendübel, A.; Schwanz, P.; Teichmann, T.; Gross, K.; Langenfeld-Heyser, R.; Godbold, D.L.; Polle, A. Cadmium-Induced Changes in Antioxidative Systems, Hydrogen Peroxide Content, and Differentiation in Scots Pine Roots. *Plant Physiol.* **2001**, *127*, 887–898. [CrossRef]
67. Díaz, J.; Bernal, A.; Pomar, F.; Merino, F. Induction of Shikimate Dehydrogenase and Peroxidase in Pepper (*Capsicum annuum* L.) Seedlings in Response to Copper Stress and Its Relation to Lignification. *Plant Sci.* **2001**, *161*, 179. [CrossRef]
68. Hale, K.L.; Tufan, H.A.; Pickering, I.J.; George, G.N.; Terry, N.; Pilon, M.; Pilon-Smits, E.A.H. Anthocyanins Facilitate Tungsten Accumulation in Brassica. *Physiol. Plant* **2002**, *116*, 351–358. [CrossRef]
69. Vuksanović, V.; Kovačević, B.; Stojnić, S.; Kebert, M.; Kesić, L.; Galović, V.; Orlović, S. Variability of Tolerance of Wild Cherry Clones to PEG-Induced Osmotic Stress in Vitro. *iForest* **2022**, *15*, 265. [CrossRef]
70. Król, A.; Amarowicz, R.; Weidner, S. Changes in the Composition of Phenolic Compounds and Antioxidant Properties of Grapevine Roots and Leaves (*Vitis vinifera* L.) under Continuous of Long-Term Drought Stress. *Acta Physiol. Plant.* **2014**, *36*, 1491–1499. [CrossRef]
71. Solecka, D.; Kacperska, A. Phenylpropanoid Deficiency Affects the Course of Plant Acclimation to Cold. *Physiol. Plant.* **2003**, *119*, 253–262. [CrossRef]
72. Kisa, D.; Kayir, O.; Saglam, N.; şahin, S.; Öztürk, L.; Elmastaş, M. Changes of Phenolic Compounds in Tomato Associated With The Heavy Metal Stress. *Bartın Univ. Int. J. Nat. Appl. Sci.* **2019**, *2*, 35–43.
73. Vuksanović, V.; Kovaćević, B.; Kebert, M.; Katanić, M.; Pavlović, L.; Kesić, L.; Orlović, S. Clone Specificity of White Poplar (*Populus alba* L.) Acidity Tolerance in Vitro. *Fresenius Environ. Bull.* **2019**, *28*, 8307–8313.
74. Puente-Garza, C.A.; Meza-Miranda, C.; Ochoa-Martínez, D.; García-Lara, S. Effect of in Vitro Drought Stress on Phenolic Acids, Flavonols, Saponins, and Antioxidant Activity in Agave Salmiana. *Plant Physiol. Biochem.* **2017**, *115*, 400–407. [CrossRef]
75. Hamooh, B.T.; Sattar, F.A.; Wellman, G.; Mousa, M.A.A. Metabolomic and Biochemical Analysis of Two Potato (*Solanum tuberosum* L.) Cultivars Exposed to In Vitro Osmotic and Salt Stresses. *Plants* **2021**, *10*, 98. [CrossRef]
76. Gould, K.S.; Neill, S.O.; Vogelmann, T.C. A Unified Explanation for Anthocyanins in Leaves? *Adv. Bot. Res.* **2002**, *37*, 167–192.
77. Kebert, M.; Trudić, B.; Stojnić, S.; Orlović, S.; Štajner, D.; Popović, B.; Galić, Z. Estimation of Antioxidant Capacities of Poplar Clones Involved in Phytoremediation Processes. In Proceedings of the STREPOW International Workshop, Andrevlje-Novi Sad, Serbia, 23–24 February 2011.
78. Kapoor, D.; Kaur, S.; Bhardwaj, R. Physiological and Biochemical Changes in *Brassica juncea* Plants under Cd-Induced Stress. *BioMed Res. Int.* **2014**, *2014*, e726070. [CrossRef] [PubMed]
79. Siddiqui, M.M.; Abbasi, B.H.; Ahmad, N.; Ali, M.; Mahmood, T. Toxic Effects of Heavy Metals (Cd, Cr and Pb) on Seed Germination and Growth and DPPH-Scavenging Activity in Brassica Rapa Var. Turnip. *Toxicol. Ind. Health* **2014**, *30*, 238–249. [CrossRef] [PubMed]
80. Georgiadou, E.C.; Kowalska, E.; Patla, K.; Kulbat, K.; Smolińska, B.; Leszczyńska, J.; Fotopoulos, V. Influence of Heavy Metals (Ni, Cu, and Zn) on Nitro-Oxidative Stress Responses, Proteome Regulation and Allergen Production in Basil (*Ocimum basilicum* L.) Plants. *Front. Plant Sci.* **2018**, *9*, 862. [CrossRef] [PubMed]
81. Metwally, A.; Safronova, V.I.; Belimov, A.A.; Dietz, K.-J. Genotypic Variation of the Response to Cadmium Toxicity in *Pisum sativum* L. *J. Exp. Bot.* **2005**, *56*, 167–178. [CrossRef]
82. Wu, F.B.; Zhang, G.P.; Dominy, P. Four Barley Genotypes Respond Differently to Cadmium: Lipid Peroxidation and Activities of Antioxidant Capacity. *Environ. Exp. Bot.* **2003**, *50*, 67–78. [CrossRef]
83. Groppa, M.D.; Tomaro, M.L.; Benavides, M.P. Polyamines as Protectors against Cadmium or Copper-Induced Oxidative Damage in Sunflower Leaf Discs. *Plant Sci.* **2001**, *161*, 481. [CrossRef]
84. Cho, U.-H.; Seo, N.-H. Oxidative Stress in Arabidopsis Thaliana Exposed to Cadmium Is Due to Hydrogen Peroxide Accumulation. *Plant Sci.* **2005**, *168*, 113–120. [CrossRef]

85. Balestrasse, K.B.; Gallego, S.M.; Tomaro, M.L. Cadmium-Induced Senescence in Nodules of Soybean (*Glycine max* L.) Plants. *Plant Soil* **2004**, *262*, 373–381. [CrossRef]
86. Juknys, R.; Vitkauskaitė, G.; Račaitė, M.; Venclovienė, J. The Impacts of Heavy Metals on Oxidative Stress and Growth of Spring Barley. *Open Life Sci.* **2012**, *7*, 299–306. [CrossRef]
87. Giannakoula, A.; Therios, I.; Chatzissavvidis, C. Effect of Lead and Copper on Photosynthetic Apparatus in Citrus (*Citrus aurantium* L.) Plants. The Role of Antioxidants in Oxidative Damage as a Response to Heavy Metal Stress. *Plants* **2021**, *10*, 155. [CrossRef] [PubMed]
88. Bartels, D.; Sunkar, R. Drought and Salt Tolerance in Plants. *Crit. Rev. Plant Sci.* **2005**, *24*, 23–58. [CrossRef]
89. Tuteja, N. Abscisic Acid and Abiotic Stress Signaling. *Plant Signal. Behav.* **2007**, *2*, 135–138. [CrossRef] [PubMed]
90. Danquah, A.; de Zelicourt, A.; Colcombet, J.; Hirt, H. The Role of ABA and MAPK Signaling Pathways in Plant Abiotic Stress Responses. *Biotechnol. Adv.* **2014**, *32*, 40–52. [CrossRef]
91. Choudhary, S.P.; Bhardwaj, R.; Gupta, B.D.; Dutt, P.; Gupta, R.K.; Biondi, S.; Kanwar, M. Epibrassinolide Induces Changes in Indole-3-Acetic Acid, Abscisic Acid and Polyamine Concentrations and Enhances Antioxidant Potential of Radish Seedlings under Copper Stress. *Physiol. Plant.* **2010**, *140*, 280–296. [CrossRef] [PubMed]
92. Yamasaki, H.; Cohen, M.F. NO Signal at the Crossroads: Polyamine-Induced Nitric Oxide Synthesis in Plants? *Trends Plant Sci.* **2006**, *11*, 522–524. [CrossRef]
93. Shevyakova, N.I.; Cheremisina, A.I.; Kuznetsov, V.V. Phytoremediation Potential of Amaranthus Hybrids: Antagonism between Nickel and Iron and Chelating Role of Polyamines. *Russ. J. Plant Physiol.* **2011**, *58*, 634–642. [CrossRef]
94. Kishor, P.K.; Sangam, S.; Amrutha, R.N.; Laxmi, P.S.; Naidu, K.R.; Rao, K.S.; Rao, S.; Reddy, K.J.; Theriappan, P.; Sreenivasulu, N. Regulation of Proline Biosynthesis, Degradation, Uptake and Transport in Higher Plants: Its Implications in Plant Growth and Abiotic Stress Tolerance. *Curr. Sci. India* **2005**, *88*, 424–438.
95. Siripornadulsil, S.; Traina, S.; Verma, D.P.S.; Sayre, R.T. Molecular Mechanisms of Proline-Mediated Tolerance to Toxic Heavy Metals in Transgenic Microalgae. *Plant Cell* **2002**, *14*, 2837–2847. [CrossRef] [PubMed]
96. Raghavendra, A.S.; Gonugunta, V.K.; Christmann, A.; Grill, E. ABA Perception and Signalling. *Trends Plant Sci.* **2010**, *15*, 395–401. [CrossRef] [PubMed]
97. Bishnoi, N.R.; Sheoran, I.S.; Singh, R. Influence of Cadmium and Nickel on Photosynthesis and Water Relations in Wheat Leaves of Different Insertion Level. *Photosynthetica* **1993**, *28*, 473–479.
98. Li, S.-W.; Leng, Y.; Feng, L.; Zeng, X.-Y. Involvement of Abscisic Acid in Regulating Antioxidative Defense Systems and IAA-Oxidase Activity and Improving Adventitious Rooting in Mung Bean [*Vigna radiata* (L.) Wilczek] Seedlings under Cadmium Stress. *Environ. Sci. Pollut. Res. Int.* **2014**, *21*, 525–537. [CrossRef] [PubMed]
99. Haag-Kerwer, A.; Schäfer, H.J.; Heiss, S.; Walter, C.; Rausch, T. Cadmium Exposure in Brassica Juncea Causes a Decline in Transpiration Rate and Leaf Expansion without Effect on Photosynthesis. *J. Exp. Bot.* **1999**, *50*, 1827–1835. [CrossRef]
100. Perfus-Barbeoch, L.; Leonhardt, N.; Vavasseur, A.; Forestier, C. Heavy Metal Toxicity: Cadmium Permeates through Calcium Channels and Disturbs the Plant Water Status. *Plant J.* **2002**, *32*, 539–548. [CrossRef] [PubMed]
101. Sanità di Toppi, L.; Lambardi, M.; Pazzagli, L.; Cappugi, G.; Durante, M.; Gabbrielli, R. Response to Cadmium in Carrot in Vitro Plants and Cell Suspension Cultures. *Plant Sci.* **1998**, *137*, 119–129. [CrossRef]
102. Chen, S.L.; Kao, C.H. Glutathione Reduces the Inhibition of Rice Seedling Root Growth Caused by Cadmium. *Plant Growth Regul.* **1995**, *16*, 249–252. [CrossRef]
103. Hollenbach, B.; Schreiber, L.; Hartung, W.; Dietz, K.J. Cadmium Leads to Stimulated Expression of the Lipid Transfer Protein Genes in Barley: Implications for the Involvement of Lipid Transfer Proteins in Wax Assembly. *Planta* **1997**, *203*, 9–19. [CrossRef] [PubMed]
104. Sanità Di Toppi, L.; Lambardi, M.; Pecchion, N.; Pazzagli, L.; Durante, M.; Gabbrielli, R. Effects of Cadmium Stress on Hairy Roots of Daucus Carota. *J. Plant Physiol.* **1999**, *154*, 385–391. [CrossRef]
105. Chen, C.T.; Chen, L.-M.; Lin, C.C.; Kao, C.H. Regulation of Proline Accumulation in Detached Rice Leaves Exposed to Excess Copper. *Plant Sci.* **2001**, *160*, 283–290. [CrossRef] [PubMed]
106. Rubio, M.I.; Escrig, I.; Martinez-Cortina, C.; Lopez-Benet, F.J.; Sanz, A. Cadmium and Nickel Accumulation in Rice Plants. Effects on Mineral Nutrition and Possible Interactions of Abscisic and Gibberellic Acids. *Plant Growth Regul.* **1994**, *14*, 151–157. [CrossRef]
107. Salt, D.E.; Rauser, W.E. MgATP-Dependent Transport of Phytochelatins Across the Tonoplast of Oat Roots. *Plant Physiol.* **1995**, *107*, 1293–1301. [CrossRef] [PubMed]
108. Muñoz, F.J.; Dopico, B.; Labrador, E. A CDNA Encoding a Proline-Rich Protein from Cicer Arietinum. Changes in Expression during Development and Abiotic Stresses. *Physiol. Plant.* **1998**, *102*, 582–590. [CrossRef]
109. Das, P.; Samantaray, S.; Rout, G.R. Studies on Cadmium Toxicity in Plants: A Review. *Environ. Pollut.* **1997**, *98*, 29–36. [CrossRef] [PubMed]
110. Srivastava, S.; Srivastava, A.K.; Suprasanna, P.; D'Souza, S.F. Identification and Profiling of Arsenic Stress-Induced MicroRNAs in *Brassica juncea*. *J. Exp. Bot.* **2013**, *64*, 303–315. [CrossRef] [PubMed]
111. Zelinová, V.; Alemayehu, A.; Bočová, B.; Huttová, J.; Tamás, L. Cadmium-Induced Reactive Oxygen Species Generation, Changes in Morphogenic Responses and Activity of Some Enzymes in Barley Root Tip Are Regulated by Auxin. *Biologia* **2015**, *70*, 356–364. [CrossRef]

112. Bhardwaj, R.; Sharma, I.; Handa, N.; Kapoor, D.; Kaur, H.; Gautam, V.; Kohli, S. Role of polyamines in stress management. In *Plant Adaptation to Environmental Changes: Significance of Amino Acids and Their Derivatives*; Anjum, N.A., Gill, S.S., Gill, R., Eds.; CABI Publishers: Wallingford, CT, USA, 2014; pp. 245–265.
113. Saha, J.; Brauer, E.K.; Sengupta, A.; Popescu, S.C.; Gupta, K.; Gupta, B. Polyamines as Redox Homeostasis Regulators during Salt Stress in Plants. *Front. Environ. Sci.* **2015**, *3*, 21. [CrossRef]
114. Benavides, M.P.; Groppa, M.D.; Recalde, L.; Verstraeten, S.V. Effects of Polyamines on Cadmium- and Copper-Mediated Alterations in Wheat (*Triticum aestivum* L) and Sunflower (*Helianthus annuus* L) Seedling Membrane Fluidity. *Arch. Biochem. Biophys.* **2018**, *654*, 27–39. [CrossRef]
115. Shevyakova, N.I.; Il'ina, E.N.; Stetsenko, L.A.; Kuznetsov, V.V. Nickel Accumulation in Rape Shoots (*Brassica napus* L.) Increased by Putrescine. *Int. J. Phytoremediation* **2011**, *13*, 345–356. [CrossRef] [PubMed]
116. Pottosin, I.; Velarde-Buendía, A.M.; Bose, J.; Zepeda-Jazo, I.; Shabala, S.; Dobrovinskaya, O. Cross-Talk between Reactive Oxygen Species and Polyamines in Regulation of Ion Transport across the Plasma Membrane: Implications for Plant Adaptive Responses. *J. Exp. Bot.* **2014**, *65*, 1271–1283. [CrossRef]
117. Velikova, V.; Yordanov, I.; Edreva, A. Oxidative Stress and Some Antioxidant Systems in Acid Rain-Treated Bean Plants: Protective Role of Exogenous Polyamines. *Plant Sci.* **2000**, *151*, 59–66. [CrossRef]
118. Rahman, H.; Sabreen, S.; Alam, S.; Kawai, S. Effects of Nickel on Growth and Composition of Metal Micronutrients in Barley Plants Grown in Nutrient Solution. *J. Plant Nutr.* **2005**, *28*, 393–404. [CrossRef]
119. Hasanuzzaman, M.; Nahar, K.; Fujita, M. Regulatory role of polyamines in growth, development and abiotic stress tolerance in plants. In *Plant Adaptation to Environmental Changes: Significance of Amino Acids and Their Derivatives*; Anjum, N.A., Gill, S.S., Gill, R., Eds.; CABI Publishers: Wallingford, CT, USA, 2014; pp. 157–193.
120. Liu, J.-H.; Wang, W.; Wu, H.; Gong, X.; Moriguchi, T. Polyamines Function in Stress Tolerance: From Synthesis to Regulation. *Front. Plant Sci.* **2015**, *6*, 827. [CrossRef] [PubMed]
121. Brüggemann, L.I.; Pottosin, I.I.; Schönknecht, G. Cytoplasmic Polyamines Block the Fast-Activating Vacuolar Cation Channel. *Plant J.* **1998**, *16*, 101–105. [CrossRef]
122. Pál, M.; Horváth, E.; Janda, T.; Páldi, E.; Szalai, G. Physiological Changes and Defense Mechanisms Induced by Cadmium Stress in Maize. *J. Plant Nutr. Soil Sci.* **2006**, *169*, 239–246. [CrossRef]
123. Chen, L.; Wang, L.; Chen, F.; Korpelainen, H.; Li, C. The Effects of Exogenous Putrescine on Sex-Specific Responses of *Populus cathayana* to Copper Stress. *Ecotoxicol. Environ. Saf.* **2013**, *97*, 94–102. [CrossRef] [PubMed]
124. Pietrini, F.; Iori, V.; Cheremisina, A.; Shevyakova, N.I.; Radyukina, N.; Kuznetsov, V.V.; Zacchini, M. Evaluation of Nickel Tolerance in *Amaranthus paniculatus* L. Plants by Measuring Photosynthesis, Oxidative Status, Antioxidative Response and Metal-Binding Molecule Content. *Environ. Sci. Pollut. Res. Int.* **2015**, *22*, 482–494. [CrossRef]
125. Shevyakova, N.I.; Il'ina, E.N.; Kuznetsov, V.V. Polyamines Increase Plant Potential for Phytoremediation of Soils Polluted with Heavy Metals. *Dokl. Biol. Sci.* **2008**, *423*, 457–460. [CrossRef] [PubMed]
126. Raychaudhuri, S.S.; Pramanick, P.; Talukder, P.; Basak, A. Chapter 6-Polyamines, Metallothioneins, and Phytochelatins—Natural Defense of Plants to Mitigate Heavy Metals. In *Studies in Natural Products Chemistry*; Atta-ur-Rahman, Ed.; Bioactive Natural Products; Elsevier: Amsterdam, The Netherlands, 2021; Volume 69, pp. 227–261.
127. Kuthanová, A.; Gemperlová, L.; Zelenková, S.; Eder, J.; Machácková, I.; Opatrný, Z.; Cvikrová, M. Cytological Changes and Alterations in Polyamine Contents Induced by Cadmium in Tobacco BY-2 Cells. *Plant Physiol. Biochem.* **2004**, *42*, 149–156. [CrossRef] [PubMed]
128. Choudhary, A.; Singh, R.P. Cadmium-Induced Changes in Diamine Oxidase Activity and Polyamine Levels in Vigna Radiata Wilczek Seedlings. *J. Plant Physiol.* **2000**, *156*, 704–710. [CrossRef]
129. Pál, M.; Csávás, G.; Szalai, G.; Oláh, T.; Khalil, R.; Yordanova, R.; Gell, G.; Birinyi, Z.; Németh, E.; Janda, T. Polyamines May Influence Phytochelatin Synthesis during Cd Stress in Rice. *J. Hazard. Mater.* **2017**, *340*, 272–280. [CrossRef] [PubMed]
130. Rady, M.; El-Yazal, M.; Taie, H.; Ahmed, S. Response of Wheat Growth and Productivity to Exogenous Polyamines under Lead Stress. *J. Crop. Sci. Biotechnol.* **2016**, *19*, 363–371. [CrossRef]
131. Rady, M.M.; Hemida, K.A. Modulation of Cadmium Toxicity and Enhancing Cadmium-Tolerance in Wheat Seedlings by Exogenous Application of Polyamines. *Ecotoxicol. Environ. Saf.* **2015**, *119*, 178–185. [CrossRef] [PubMed]
132. Bagni, N.; Tassoni, A. Biosynthesis, Oxidation and Conjugation of Aliphatic Polyamines in Higher Plants. *Amino Acids* **2001**, *20*, 301–317. [CrossRef] [PubMed]
133. Tsai, C.-J.; Harding, S.A.; Tschaplinski, T.J.; Lindroth, R.L.; Yuan, Y. Genome-Wide Analysis of the Structural Genes Regulating Defense Phenylpropanoid Metabolism in Populus. *New Phytol* **2006**, *172*, 47–62. [CrossRef] [PubMed]
134. Yang, H.Y.; Shi, G.X.; Li, W.L.; Wu, W.L. Exogenous Spermidine Enhances Hydrocharis Dubia Cadmium Tolerance. *Russ J. Plant Physiol.* **2013**, *60*, 770–775. [CrossRef]
135. Zimmerlin, A.; Wojtaszek, P.; Bolwell, G.P. Synthesis of Dehydrogenation Polymers of Ferulic Acid with High Specificity by a Purified Cell-Wall Peroxidase from French Bean (*Phaseolus vulgaris* L.). *Biochem. J.* **1994**, *299 Pt 3*, 747–753. [CrossRef] [PubMed]
136. Fridovich, I. Superoxide Radical and Superoxide Dismutases. *Annu. Rev. Biochem.* **1995**, *64*, 97–112. [CrossRef] [PubMed]
137. Carlberg, I.; Mannervik, B. Glutathione Reductase. *Methods Enzymol.* **1985**, *113*, 484–490. [CrossRef] [PubMed]
138. Arnao, M.B. Some Methodological Problems in the Determination of Antioxidant Activity Using Chromogen Radicals: A Practical Case. *Trends Food Sci. Technol.* **2000**, *11*, 419–421. [CrossRef]

139. Halliwell, B.; Gutteridge, J.M.; Aruoma, O.I. The Deoxyribose Method: A Simple "Test-Tube" Assay for Determination of Rate Constants for Reactions of Hydroxyl Radicals. *Anal. Biochem.* **1987**, *165*, 215–219. [CrossRef] [PubMed]
140. Hensley, K.; Mou, S.; Pye, Q.N. Nitrite determination by colorimetric and fluorometric Griess diazotization assays. In *Methods in Pharmacology and Toxicology: Methods in Biological Oxidative Stress*; Hensley, K., Floyd, R.A., Eds.; Humana Press Inc.: Totowa, NJ, USA, 2009; pp. 185–193.
141. Benzie, I.F.; Strain, J.J. The Ferric Reducing Ability of Plasma (FRAP) as a Measure of "Antioxidant Power": The FRAP Assay. *Anal. Biochem.* **1996**, *239*, 70–76. [CrossRef] [PubMed]
142. Devasagayam, T.; Boloor, K.; Ramasarma, T. Methods for Estimating Lipid Peroxidation: An Analysis of Merits and Demerits. *Indian J. Biochem. Biophys.* **2003**, *40*, 300–308. [PubMed]
143. Singleton, V.L.; Orthofer, R.; Lamuela-Raventós, R. Analysis of Total Phenols and Other Oxidation Substrates and Antioxidants by Means of Folin-Ciocalteu Reagent. *Methods Enzymol.* **1999**, *299*, 152–178. [CrossRef]
144. Chen, K.H.; Miller, A.N.; Patterson, G.W.; Cohen, J.D. A Rapid and Simple Procedure for Purification of Indole-3-Acetic Acid Prior to GC-SIM-MS Analysis. *Plant Physiol.* **1988**, *86*, 822–825. [CrossRef] [PubMed]
145. Rapparini, F.; Tam, Y.Y.; Cohen, J.D.; Slovin, J.P. Indole-3-Acetic Acid Metabolism in Lemna Gibba Undergoes Dynamic Changes in Response to Growth Temperature. *Plant Physiol.* **2002**, *128*, 1410–1416. [CrossRef] [PubMed]
146. Baraldi, R.; Bertazza, G.; Bogino, J.; Luna, V.; Bottini, R. Effect of Light Quality on Prunus Cerasus II. Changes in Hormone Levels in Plants Grown under Different Light Conditions. *Photochem. Photobiol.* **1995**, *62*, 800–803. [CrossRef]
147. Scaramagli, S.; Biondi, S.; Capitani, F.; Gerola, P.; Altamura, M.M.; Torrigiani, P. Polyamine Conjugate Levels and Ethylene Biosynthesis: Inverse Relationship with Vegetative Bud Formation in Tobacco Thin Layers. *Physiol. Plant.* **1999**, *105*, 366–375. [CrossRef]
148. Kassambara, A. *Pipe-Friendly Framework for Basic Statistical Tests [R Package Rstatix Version 0.7.0]*; Free Software Foundation Inc.: Boston, MA, USA, 2021.
149. Wickham, H. Ggplot2. *WIREs Comput. Stat.* **2011**, *3*, 180–185. [CrossRef]

plants

MDPI

Article

The Effect of Environmental Factors on the Nutrition of European Beech (*Fagus sylvatica* L.) Varies with Defoliation

Mladen Ognjenović [1], Ivan Seletković [2], Mia Marušić [2,*], Mathieu Jonard [3], Pasi Rautio [4], Volkmar Timmermann [5], Melita Perčec Tadić [6], Miran Lanšćak [2], Damir Ugarković [7] and Nenad Potočić [2]

1 Department of BI, Analytics and Research, Njuškalo Ltd., 10000 Zagreb, Croatia
2 Croatian Forest Research Institute, 10450 Jastrebarsko, Croatia
3 Earth and Life Institute, Université Catholique de Louvain, 1348 Louvain-la-Neuve, Belgium
4 Natural Resources Institute Finland, 00790 Helsinki, Finland
5 Norwegian Institute of Bioeconomy Research, 1433 Ås, Norway
6 Meteorological and Hydrological Service, 10000 Zagreb, Croatia
7 Faculty of Forestry and Wood Technology, University of Zagreb, 10000 Zagreb, Croatia
* Correspondence: miam@sumins.hr

Abstract: Despite being adapted to a wide range of environmental conditions, the vitality of European beech is expected to be significantly affected by the projected effects of climate change, which we attempted to assess with foliar nutrition and crown defoliation, as two different, yet interlinked vitality indicators. Based on 28 beech plots of the ICP Forests Level I network, we set out to investigate the nutritional status of beech in Croatia, the relation of its defoliation and nutrient status, and the effects of environmental factors on this relation. The results indicate a generally satisfactory nutrition of common beech in Croatia. Links between defoliation and nutrition of beech are not very direct or very prominent; differences were observed only in some years and on limited number of plots. However, the applied multinomial logistic regression models show that environmental factors affect the relationship between defoliation and nutrition, as climate and altitude influence the occurrence of differences in foliar nutrition between defoliation categories.

Keywords: tree vitality; foliar composition; stoichiometry; climate change; ICP Forests

Citation: Ognjenović, M.; Seletković, I.; Marušić, M.; Jonard, M.; Rautio, P.; Timmermann, V.; Tadić, M.P.; Lanšćak, M.; Ugarković, D.; Potočić, N. The Effect of Environmental Factors on the Nutrition of European Beech (*Fagus sylvatica* L.) Varies with Defoliation. *Plants* **2023**, *12*, 168. https://doi.org/10.3390/plants12010168

Academic Editor: Aneta Helena Baczewska-Dąbrowska

Received: 31 October 2022
Revised: 7 December 2022
Accepted: 23 December 2022
Published: 30 December 2022

1. Introduction

Meteorological and climate conditions affect vegetation directly and indirectly. Direct effects include responses to temperature; indirect effects occur primarily as soil-mediated phenomena, such as the influence of precipitation on soil moisture regimes [1–4]. Probably the greatest threat to existing forest ecosystems in Europe comes from a changing climate [5]. Extreme climatic events such as droughts are thought to be important in initiating changes in forest ecosystems [6]. According to IPCC [7] predictions, extreme climate events such as heat waves and long-lasting summer droughts will occur more frequently. Such climate changes will negatively impact the stability, structure and biodiversity of forest ecosystems throughout Europe [8]. The region of southeast Europe is one of the most vulnerable regions in Europe when it comes to climate change impacts, primarily through intensified severity and duration of droughts and heat waves. As these impacts should be stronger and faster than on the rest of the continent [9,10] this region is an ideal model for studying the future impact of changing climatic conditions.

A prerequisite for healthy growth and balanced metabolism is the maintenance of adequate concentrations and relatively stable ratios of nutrients in plant tissues [11]. Concentrations of nutrients and their relationships in the leaves of forest trees are important indicators of their functioning. It is crucial to account for nutrient limitation when studying the forest response to climate change [12], as nutritional status has a significant and diverse impact on tree vitality [13]. The concentration of nutrients in leaves depends on many

factors: the amount and distribution of precipitation and the length of the growing season, the presence of nutrients in the soil, ion antagonisms, ion mobility and uptake capacity, etc. [14]. It seems that the nutritional status of European beech (*Fagus sylvatica* L.) is deteriorating: Jonard et al. [12] and Talkner et al. [15] both report on the negative trend in beech phosphorus (P) nutrition; furthermore, trends of concentrations of calcium and magnesium in the foliage of beech trees in Europe were also found to be negative [12]. Nutrient contents of tree foliage, which reflect atmospheric and soil-related influences, are an important part of the UNECE ICP Forests monitoring scheme [16]. Beech forests in Croatia have a very wide edaphic amplitude [17], but baseline data on the chemical composition of foliage in beech stands has so far been missing.

Tree vitality is defined as the ability of a tree to assimilate, to survive stress, to react to changing conditions, and to reproduce [18]. As vitality cannot be measured directly, various indicators can be used to describe it [19]. Crown defoliation is a commonly used tree vitality indicator [20–22], which can be obtained cost-effectively and relatively quickly in field surveys [23]. Defoliation is defined as the loss of needles or leaves in the assessable part of the crown compared to a reference tree [24]. Trees with defoliation above 25% are regarded as considerably defoliated and are thus defined as damaged [25]. A recent study showed that there are significant morphological and, in this context even more importantly, physiological differences in beech leaves between healthy and considerably defoliated trees [22]. Although European beech had the lowest mean defoliation (20.9%) of all main tree species in the ICP Forests 2021 survey, the 20-year trend in mean plot defoliation shows that defoliation of beech is constantly on the rise (3.4% in 20 years), and that larger deviations from this trend can be linked to drought events [26]. A good example is year 2004, when the annual mean plot defoliation was higher than the trend as a result of the drought in the preceding year which affected large parts of Europe [27–29]. In Croatia, the trend in mean defoliation of beech is much steeper with an 8.6 % rise in the period of 1996–2017 [30].

European beech is often mentioned in the context of sensitivity to high temperatures and drought [31,32], as beech grows best in areas marked by moderately warm summers and high quantities of precipitation [33]. Beech forms vast forest communities which provide multiple ecosystem goods and services, and is the dominant tree species in many deciduous forests in Europe under temperate climate conditions [34]. The projected effects of climate change, particularly drought, are expected to significantly affect the vitality of beech, which we attempted to assess with foliar nutrition and crown defoliation, as two different, yet closely interlinked vitality indicators. Although considered a nonspecific indicator of vitality, defoliation appears to depend on the nutritional status of trees. However, research on the relationship between tree defoliation and nutritional status has so far been limited, especially for beech: Jonard et al. [35] found that defoliation was associated with lower concentrations of calcium (Ca) and magnesium (Mg) in beech leaves. A study conducted in Switzerland did not find a link between nitrogen (N) concentrations and defoliation [36], but Ferretti et al. [37] report that the proportion of common beech trees with more than 25% defoliation increases with elevated nitrogen to calcium and potassium (K) ratios in the leaves, indicating that crown status depends on the balance of nutrients in leaves. Toigo et al. [38] found that defoliation increased due to drought effects, while the influence of nutritional status was less consistent. The study by Ognjenović et al. [39] on a limited sample of 26 beech trees showed that defoliation and calcium leaf concentrations show similar susceptibility to drought, but with different responses in time. Obviously, besides the overall tree health condition, the concentration of nutrients in leaves depends on many outside factors. In this context, we set out to better characterize the link between defoliation and foliar nutrition and determine the influence of environmental factors on the foliar composition of beech trees of two distinct defoliation categories, on a large sample of beech-dominated ICP Forests Level I plots in Croatia, with the hypotheses that (I) environmental factors have a significant influence over the defoliation/nutrition relationship and (II) trees with higher defoliation have lower concentrations of nutrients in leaves. In the

process, we investigated whether tree nutrition plays a role in the loss of vitality of beech trees (and vice versa); and if the link between tree nutrition and vitality loss varies from year to year due to interannual climate variations.

2. Results

2.1. Foliar Nutrient Concentrations

Mean N foliar concentrations in the study area level were within normal range [40] in both defoliation categories and across sampling years. Repeated Measures ANOVA indicated that there was no difference in N concentrations between LD and HD trees, while there was a difference between individual years ($F(2, 556) = 30.4$, $p < 0.0001$). In 2018, significantly lower N concentrations were recorded for both defoliation categories compared to 2019 and 2020 (Table 1).

Table 1. Results of Holm pairwise comparisons of foliar nutrient concentrations and sample dry mass within a defoliation category and between sampling years (NS–not significant, * $p < 0.05$, ** $p < 0.01$, *** $p < 0.001$).

Defoliation Category	Year 1	Year 2	N	P	K	Ca	Mg	Sample Dry Mass
LD	2018	2019	***	ns	***	**	***	***
LD	2018	2020	***	***	***	***	ns	*
LD	2019	2020	ns	***	ns	***	*	*
HD	2018	2019	***	***	***	ns	***	***
HD	2018	2020	***	***	***	***	***	***
HD	2019	2020	ns	*	**	***	ns	*

Although there is no significant main effect of defoliation category on P concentrations, the pairwise comparisons between LD and HD trees indicated significant differences in 2019, when LD trees had a higher concentration than HD trees, but not in 2018 and 2020 (Figure 1). Significant differences in P concentrations ($F(2, 556) = 74.9$, $p < 0.001$) were also observed between individual sampling years (Table 1) with a decrease during the study period. However, values of P on the plot level were mostly normal throughout the study period except for the year 2020, when P concentrations were slightly below normal range on 53% of the research plots (Figure S3).

No significant differences were established for potassium (K) between defoliation categories and mean concertation values stayed within the normal range in each year (Figure 1).

Repeated Measures ANOVA showed no significant main effect of defoliation category on Mg concentrations. Nevertheless, pairwise comparisons between LD and HD trees revealed significant differences in 2018, with HD trees having higher Mg concentrations (Figure 1). Mean Mg concentrations were within normal range in each year, although they were lower in 2019 and 2020 compared to 2018 for HD trees.

Similar to other elements, there was no significant main effect of defoliation category on calcium (Ca) concentrations ($F(2, 556) = 3.4$, $p = 0.06$). Pairwise comparisons, however, showed that HD trees in 2018 and 2019 had significantly higher Ca concentrations than LD trees (Figure 1). For these years, values for both groups fall within normal Ca concentration range for beech. In 2020, both categories had significantly higher concentrations than in previous years, bordering on surplus (luxury) values, but no significant difference was found between them (Figure 1).

Although there was no significant main effect of defoliation category on dry leaf mass, the pairwise comparisons between LD and HD trees indicated significant differences in 2018, when LD trees had a higher dry leaf mass than HD trees (Figure 1). However, there was a statistically significant main effect of the sampling year on dry leaf mass ($F(2, 556) = 56.3$, $p < 0.001$) and pairwise comparisons showed differences between all years for both defoliation categories (Table 1).

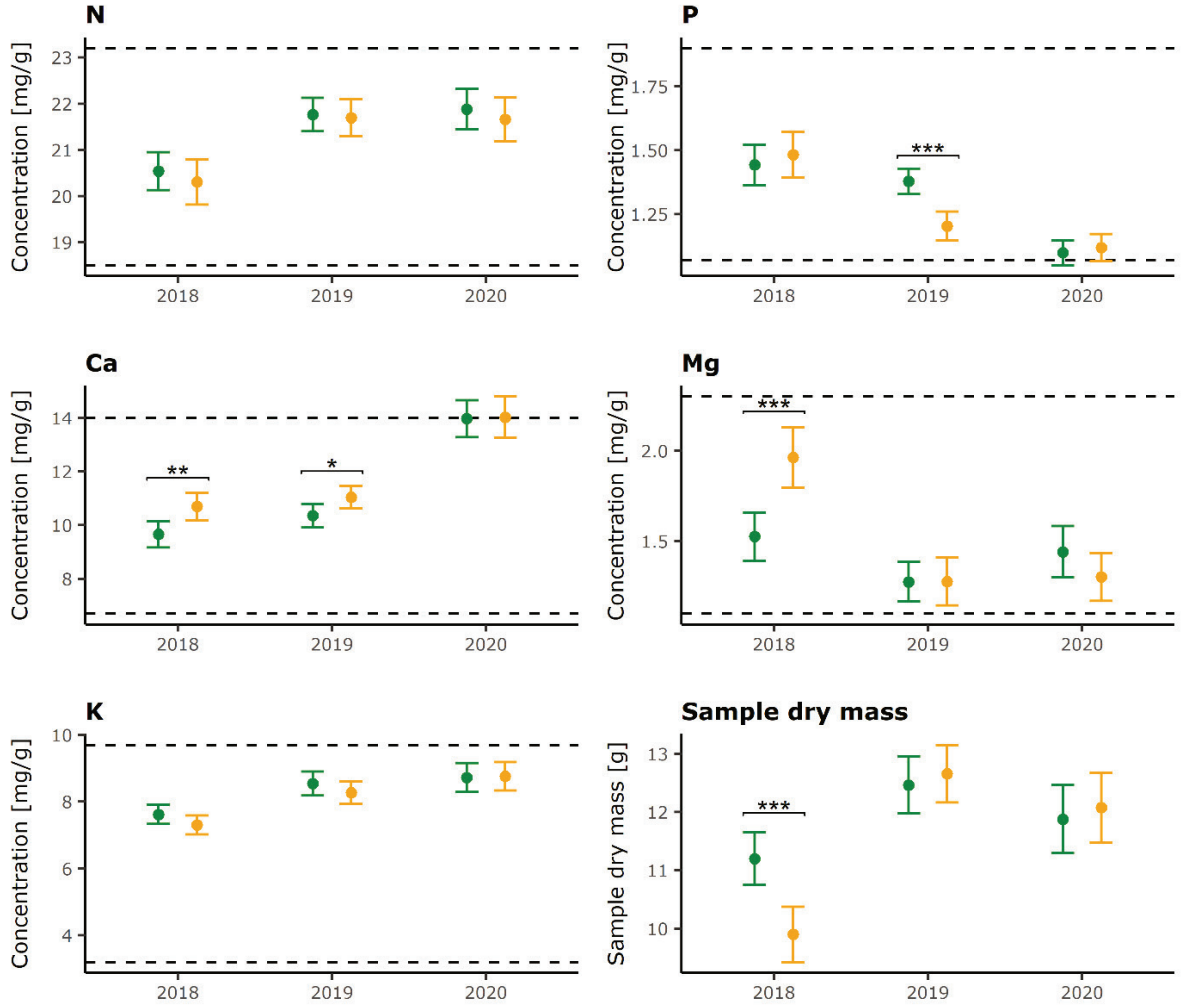

Figure 1. Mean foliar concentrations and sample dry mass (dots) with confidence intervals (vertical bars) for LD (green color) and HD trees (orange color) on all plots within sampling years. Dotted lines represent lower and upper critical value for normal range of foliar N concentrations for common beech according to Mellert and Goettlein [40]. Only significant differences in foliar concentrations between LD and HD categories determined by the Holm–Bonferroni method are indicated (* $p < 0.05$, ** $p < 0.01$, *** $p < 0.001$).

On the plot level, mean Ca concentrations were mostly in the normal range during the first two years, while excessive Ca concentrations were observed on all plots located in the alpine region in 2020 (Figure S5), and most of the alpine region plots had insufficient P concentrations (Figure S3). In the same year, excessive K concentrations were found on eleven plots (39%), most of them located in the continental region (Figure S4). N values are rather plot dependent and relatively stable in time (Figure S2), while Mg concentrations show a very broad range of values, independent of the area, defoliation category, or sampling year (Figure S6)

Overall, the share of plots with differences in foliar concentrations between defoliation categories was relatively low for most elements during the entire sampling period (Table 2). The highest share of plots with differences in foliar concentrations between defoliation categories was determined for Ca (21.4%) in 2018, followed by Mg (17.9%) in the same year.

Table 2. Number of plots with significantly higher foliar concentrations in each defoliation category within sampling years determined by the independent samples *t*-test (total number of plots: 28).

		N	P	K	Ca	Mg
2018	HD higher	1	-	-	6	4
	LD higher	1	-	2	-	1
2019	HD higher	-	-	1	-	2
	LD higher	1	4	1	1	1
2020	HD higher	-	2	1	1	1
	LD higher	2	-	-	-	1

2.2. Foliar Nutrient Ratios

N/P ratios were especially high and above the upper limit for both LD and HD trees in 2020 at the study area level, mostly due to very low P values that approached deficiency values (Figure 2). Repeated Measures ANOVA did not show a significant main effect of defoliation category on N/P ratio. However, pairwise comparison between LD and HD trees indicated significant differences in N/P ratios in 2019, with values out of optimal range for HD trees due to low P concentration values (Figure 2). The main effect of the sampling year was significant ($F(2556) = 13.4$, $p < 0.001$) with an increase in N/P ratio during the monitoring period.

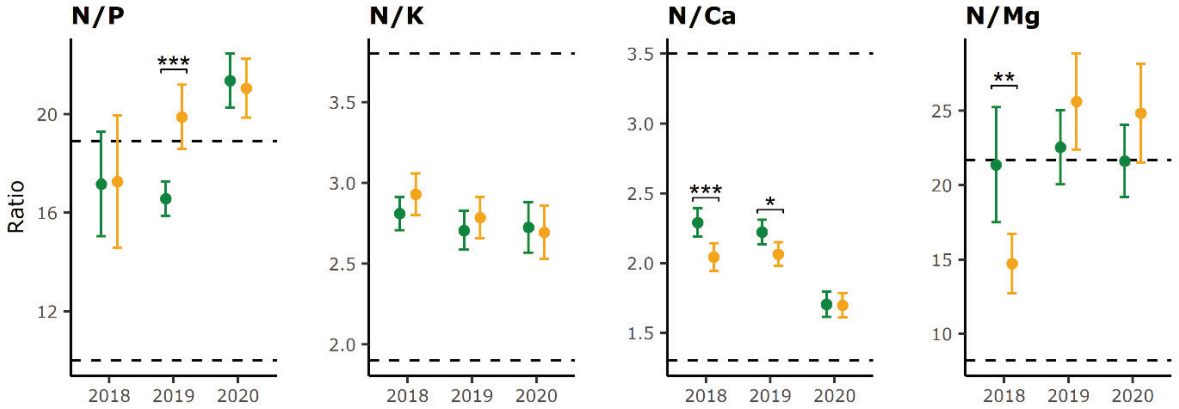

Figure 2. Mean foliar ratios (dots) and confidence intervals (vertical bars) for LD (green color) and HD trees (orange color) on all plots within sampling years. Dotted lines represent lower and upper critical value for normal range of foliar ratios for common beech according to Mellert and Goettlein [40]. Only significant differences in foliar ratios between LD and HD categories determined by the Holm–Bonferroni method are indicated (* $p < 0.05$, ** $p < 0.01$, *** $p < 0.001$).

No significant differences were found for N/K ratio between defoliation groups or sampling years and values were within normal range in all years.

Repeated Measures ANOVA identified a significant main effect of defoliation categories on N/Ca ratios ($F(2556) = 109.9$, $p < 0.0001$). Pairwise comparisons confirmed differences in N/Ca ratios between defoliation groups in 2018 and 2019 (Figure 2). These differences were dictated primarily by Ca concentrations, which showed higher values in HD trees in 2018 and 2019. Sampling year also had a significant effect ($F(2556) = 13.4$, $p < 0.001$) and pairwise comparison established that values within defoliation categories were lower in 2020 compared to 2018 and 2019 (Table 3).

Due to low Mg concentrations in 2019 and 2020, the N/Mg ratios were mostly in the surplus range in those years (Figure 2). No significant effect of defoliation categories on N/Mg ratios was found. However, pairwise comparisons showed a significant difference between LD and HD trees in 2018, with higher values for LD trees.

Table 3. Results of Holm pairwise comparisons of foliar nutrient ratios within a defoliation category and between sampling years (ns–not significant, * $p < 0.05$, *** $p < 0.001$).

Defoliation Category	Year 1	Year 2	N/P	N/K	N/Ca	N/Mg
LD	2018	2019	ns	ns	ns	ns
LD	2018	2020	***	ns	***	ns
LD	2019	2020	***	ns	***	ns
HD	2018	2019	ns	ns	ns	***
HD	2018	2020	*	*	***	***
HD	2019	2020	ns	ns	***	ns

Mean N/P, N/K and N/Ca ratios on the plot level were mostly in normal range during the entire study (Figures S7–S9). However, in 2020, most of the plots located in the alpine biogeographic region had excessive N/P and insufficient N/Ca ratios.

The highest share of plots with differences between defoliation categories (5 out of 28, or 17.9%) was determined for N/Ca in 2018 and N/P in 2019. The share of plots in which we found differences hardly passed 10% for other ratios and years (Table 4).

Table 4. Number of plots with significantly higher foliar ratios in each defoliation category within sampling years determined by the independent samples *t*-test (total number of plots: 28).

		N/P	N/Ca	N/Mg	N/K
2018	HD higher	-	-	1	2
	LD higher	-	5	2	-
2019	HD higher	5	1	1	2
	LD higher	-	2	1	1
2020	HD higher	1	-	-	-
	LD higher	1	2	1	-

2.3. Effects of Environmental Factors on Differences in Foliar Nutrition

While the fitted MLR (multinomial logistic regression) models for N and P did not indicate a significant influence of any of the tested factors, we found that environmental factors influence the occurrence of differences in foliar concentrations of K, Ca, and Mg between defoliation categories.

Altitude (alt) and mean annual temperature (MAT) are the only environmental factors that influence the occurrence of Differences in Foliar Concentrations (DFC) of K. Keeping all other variables constant, the odds for LD trees having higher K concentration is 0.5% higher for every meter increase in altitude. On the other hand, odds are 35% lower for HD trees to have higher K concentrations when the mean temperature increases.

Trees on higher altitudes are more likely to have higher Ca concentrations in HD trees (Table 5). An opposite effect can be seen with mean annual precipitation (MAP) where, keeping all other variables constant, with an increase in precipitation the odds are 90% higher for LD trees and 2% lower for HD trees to have higher Ca concentrations. With increasing maximum temperatures (Tmax) it is 1.3 times likely that HD trees will have significantly higher Ca concentrations.

Beech trees on higher altitudes are also more likely to have higher Mg concentrations in HD trees, but the effect on LD trees is not significant. Keeping all other variables constant, with a 1 °C increase in mean temperature it is 6.6 times likely that HD trees will have higher Mg concentrations, while at the same time the likelihood of LD having higher concentrations is negligible (Table 5).

Table 5. Results of multinomial logistic regression for Differences in Foliar Concentrations (DFC) of potassium, calcium and magnesium and corresponding model AIC. Odds ratios are reported for each environmental factor while the confidence intervals are given in the brackets (* $p < 0.1$, ** $p < 0.05$, *** $p < 0.01$).

Element	Environmental Factor [1]	DFC	
		HD Higher	LD Higher
K	Alt	1.000 (0.996, 1.003)	1.005 *** (1.002, 1.008)
	MAT	0.644 *** (0.480, 0.809)	0.884 (0.659, 1.108)
	AIC	48.042	48.042
Ca	Tmax	1.298 *** (1.112, 1.485)	0.00002 *** (0.00002, 0.00002)
	sand	0.926 (0.809, 1.043)	0.048 *** (0.048, 0.048)
	MAP	0.988 ** (0.977, 0.999)	1.900 *** (1.900, 1.900)
	Alt	1.005 ** (1.001, 1.009)	0.372 *** (0.372, 0.372)
	AIC	56.908	56.908
Mg	MAT	6.578 *** (6.330, 6.826)	1.671 * (1.149, 2.194)
	MAP	1.002 (0.996, 1.007)	1.006 (0.998, 1.015)
	Alt	1.009 *** (1.005, 1.013)	1.001 (0.992, 1.009)
	sand	0.991 (0.885, 1.097)	1.121 ** (1.020, 1.222)
	pH	2.600 ** (1.708, 3.492)	1.015 (−0.815, 2.846)
	AIC	80.311	80.311

Environmental factors [1] Alt—altitude, MAT—Mean Annual Temperature, MAP—Mean Annual Precipitation, sand—soil sand fraction, pH—pH value, AIC—Akaike information criterion.

The results of the fitted MLR models indicate that beech on higher altitudes is less likely to have significant differences in N/P ratios and increasing maximum temperature has the same effect (Table 6). A similar effect of maximum temperatures can be seen for differences in N/Ca. Holding all other variables constant, with an increase in precipitation the odds are 0.6% higher that HD trees will have higher N/P ratios and 0.8% higher N/Mg ratios. When mean temperatures and soil pH increase, it is 2.5 and 3.7 times, respectively, more likely that LD trees will have higher N/Mg ratios. Keeping all other variables constant, with a unit increase in PDSI, i.e., less drought, the odds are 83.5% higher that LD trees will have higher N/Ca ratios. The fitted MLR models for N/K did not indicate a significant influence of any of the tested environmental factors on the occurrence probability of differences in foliar nutrient ratios.

Table 6. Results of multinomial logistic regression for Differences in Foliar Ratios (DFR) of potassium, calcium and magnesium. Odds ratios are reported for each environmental factor while the confidence intervals are given in the brackets (* $p < 0.1$, ** $p < 0.05$, *** $p < 0.01$).

		DFC	
	Environmental Factor [1]	**HD Higher**	**LD Higher**
N/P	**MAP**	1.006 * (1.000, 1.012)	0.989 (0.967, 1.011)
	Tmax	0.820 *** (0.696, 0.943)	0.006 *** (−0.438, 0.449)
	Alt	0.992 ** (0.986, 0.999)	0.960 *** (0.937, 0.983)
	AIC	59.378	59.378
N/Ca	**Tmax**	0.070 *** (−1.553, 1.693)	0.402 *** (0.029, 0.775)
	PDSI	1.401 (−0.956, 3.758)	1.835 ** (1.251, 2.419)
	Ca^{2+}	0.534 (−0.314, 1.381)	0.909 ** (0.829, 0.988)
	MAP	0.996 (0.957, 1.036)	0.993 *** (0.989, 0.998)
	silt	0.741 (−0.353, 1.835)	1.158 * (0.996, 1.319)
	AIC	72.131	72.131
N/Mg	**MAP**	0.999 (0.989, 1.009)	1.008 *** (1.002, 1.014)
	MAT	1.070 (0.648, 1.493)	2.502 *** (2.198, 2.805)
	pH	0.631 (−1.419, 2.681)	3.708 *** (2.770, 4.646)
	SPEI	2.613 (−1.249, 6.474)	0.071 ** (−2.192, 2.333)
	AIC	65.799	65.799

Environmental factors [1] Alt—altitude, MAT—Mean Annual Temperature, Tmax—Mean annual maximum temperature, MAP—Mean Annual Precipitation, silt—soil silt fraction, SPEI—Standardised Precipitation-Evapotranspiration Index, PDSI—Palmer Drought Severity Index, Ca^{2+}—Soil exchangeable calcium, AIC—Akaike information criterion.

3. Discussion

Assessing the nutritional status of trees using the values of element concentrations in needles or leaves is a common diagnostic practice in forestry [40–42]. In Croatia there have been only a few studies into the nutritional status of beech [41,43,44], however these studies were performed on a limited research area. The results obtained in this study indicate a generally satisfactory nutrition of common beech in Croatia. Mean concentrations on the study and plot levels were within the normal range for beech [40]. Similar results were reported by Ognjenović et al. [39] from a long-term monitoring based case study of beech foliar composition on one ICP Forests intensive monitoring plot.

Large deviations from the mean concentration values of longer periods in individual years have been reported for several mineral nutrients [45–47]. In contrast, foliar K concentrations were reported to be relatively stable [39], and this finding is repeated in our study, although concentrations of all investigated elements stayed mostly within limit values [40]. Very similar relationships of N and K to limit values has also been observed in other studies [48,49]. On the other hand, P foliar levels are a reason for concern at the European level [12,15]. While beech P nutrition on a study area level seemed to be sufficient [40], on average 33% of the plots had insufficient P nutrition during the study

period (Figure S3). Additionally, the ratio of nitrogen to phosphorus shows that beech nutrition in 2019 and 2020 was not balanced in this respect, which is partly caused by diminishing P, and partly by increasing N concentrations, respectively.

The fact that we found surplus N/Mg ratios in 2019 and 2020, both due to increasing N and decreasing Mg values, echoes results of other studies that report an unbalanced Mg nutrition on national [48,50] and European level [12].

Excessive Ca concentrations on an extremely high proportion of plots (90%) were determined in a study of beech nutrition in northern Spain, but since no symptoms of unbalanced nutrition have been identified in the field, the authors believe that the deviations of the obtained values may be based on ecological and geological differences between the studied forests and central European forests on the basis of which reference values were obtained [51]. This consideration is consistent with the hypothesis that the optimal leaf composition of each species depends on the specific ecological biogeochemical niche that the species occupies [52]. Taking into account the wide ecological amplitude of common beech, there is a possibility that the optimal range of concentrations of nutrients is adapted to the specific habitat in which a particular stand develops. Thus Sardans and Peñuelas [53] assume that plant species have a certain degree of flexibility in changing stoichiometry in response to changes in environmental conditions such as climate gradients.

Nutritional status and tree crown defoliation, as indicators of vitality, can provide a basis for monitoring the effects of long-term environmental changes on forest ecosystems [22,48]. According to Simon and Wild [54], if the concentration of a certain element remains in the normal range, a decrease in mineral nutrition should be regarded more as a consequence than the cause of damage. If, on the other hand, the concentrations are inadequate, we can suspect nutrition to be the cause of damage. Although we did not find a universal relationship between the defoliation categories and nutritional status of beech trees, subsequent comparisons revealed differences in the element concentrations and ratios for certain years. For instance, we found significantly higher P concentrations in LD trees in year 2019. On the contrary, a study in northern Spain recorded higher P concentrations in more damaged trees [51]. The most pronounced differences in concentrations between defoliation categories were determined for Ca, with HD trees having significantly higher concentrations in 2018 and 2019. Higher concentrations in HD trees were also recorded for Mg in 2018. Conversely, Jonard et al. [35] report that higher defoliation values are associated with lower Ca and Mg concentrations in a liming and P/K fertilization experiment of beech stands in Belgium.

A case study investigating interrelations of various common beech vitality indicators did not find significant links between foliar nutrient concentrations and defoliation [39]. It should be taken into account that (i) the study was performed on a limited area, (ii) element concentrations were mostly within the normal range, and (iii) the range of defoliation values was narrow and seldom exceeded 25%. The lack of association between N concentrations and defoliation values, also recorded in this study, Thimonier et al. [36] attribute to the same kind of limitations. Unlike Ouimet and Moore [55], who observed that an increase in K concentration in needles resulted in a decrease in defoliation in balsam fir stands, we found no significant differences in K concentrations between defoliation categories. Compared to fertilization experiments, the analysis of the nutritional status in natural stands is more demanding due to the high variability of data and the inability to control many factors that may affect the nutritional status. Ewald [56] states heterogeneous environmental conditions as the reason for the lack of significant relationship between nutrient concentrations and spruce defoliation status in a study conducted in Bavaria. On the other hand, with this study we do have a full picture of beech nutritional status in Croatia, including the insight into the significant variations between years and defoliation categories. Significant differences in concentrations only during certain years are not a phenomenon specific to this research alone. High year-to-year variability in nutrient concentrations is characteristic of nutritional studies [15,35,48,57].

The quantification of forest ecosystem response in a climate driven changing environment is fundamental for maintenance, enhancement and restoration of future forest ecosystem goods and services. The results presented in this study are a novel approach in investigating the effects of climate and environmental properties on the defoliation/nutrition relationship. Both tree nutrition and defoliation have been reported to depend on climate properties in various studies. A study by Braun [58] showed that air temperature and precipitation have a considerable impact on the foliar nutrient concentration. Jonard et al. [49] observed a positive relationship between precipitation and foliar Ca concentrations, while insufficient water supply during dry spells have a negative impact on the uptake of calcium, according to Bergmann [59]. Our results indicate that the increase in precipitation is better utilized in low defoliation trees since the odds are 90% higher for LD trees to have higher Ca concentrations with an increase in precipitation. Lukac et al. [60] state that elements with primarily biologically controlled cycles such as nitrogen can show a different reaction to temperature changes than elements whose cycles are controlled by both biological and geological processes (P and K) or predominantly by geological processes (Ca and Mg). Therefore, it is not surprising that we did not determine a significant effect of environmental factors on the occurrence of differences in N concentrations between defoliation categories. A study of beech nutrient dynamics along a precipitation gradient found that N concentrations remain constant with decreasing precipitation while P concentrations increase, resulting in a decrease in N/P ratio [61]. However, in this study increasing precipitation increases the odds of higher N/P ratios in high defoliation trees suggesting a disturbed uptake and utilization of P in beech with higher defoliation.

From our results it becomes quite clear that an unequivocal association of foliar nutrition and crown status should not be expected for beech. It seems plausible that various pressures influence this relationship, affecting the physiological status of beech trees in a multitude of ways. For instance, Gottardini et al. [22] found that various morphological and physiological characteristics of beech leaves and canopy such as leaf volume and photosynthetic activity, had a significant negative association with the extent of damage. Additionally, Ferretti et al. [62] showed that the 25%-defoliation threshold can be a reasonable approximation for tree classification indicated by the effect of slight and moderate variations in defoliation on tree growth, which is in contrast to the results obtained by Tallieu [63]. Highly differing research results on this topic are likely depending on the research area, management practices, climate influences and other unknown factors. Nevertheless, we established that environmental factors, especially climate, influence the occurrence of differences in foliar nutrition between defoliation categories.

4. Materials and Methods

4.1. Study Area and Plot Design

The ICP Forests Level I monitoring plots in Croatia are established on intersections of a 16 × 16 km grid that contain forest cover. These plots do not have a fixed area; rather, 24 trees are chosen for defoliation assessments using a cross-cluster system with six trees in each cluster [64]. Only plots with a minimum of five beech trees in the sample in 2018 were selected to ensure that beech was significantly represented in the mixture of tree species, resulting in total of 28 plots (Figure 3).

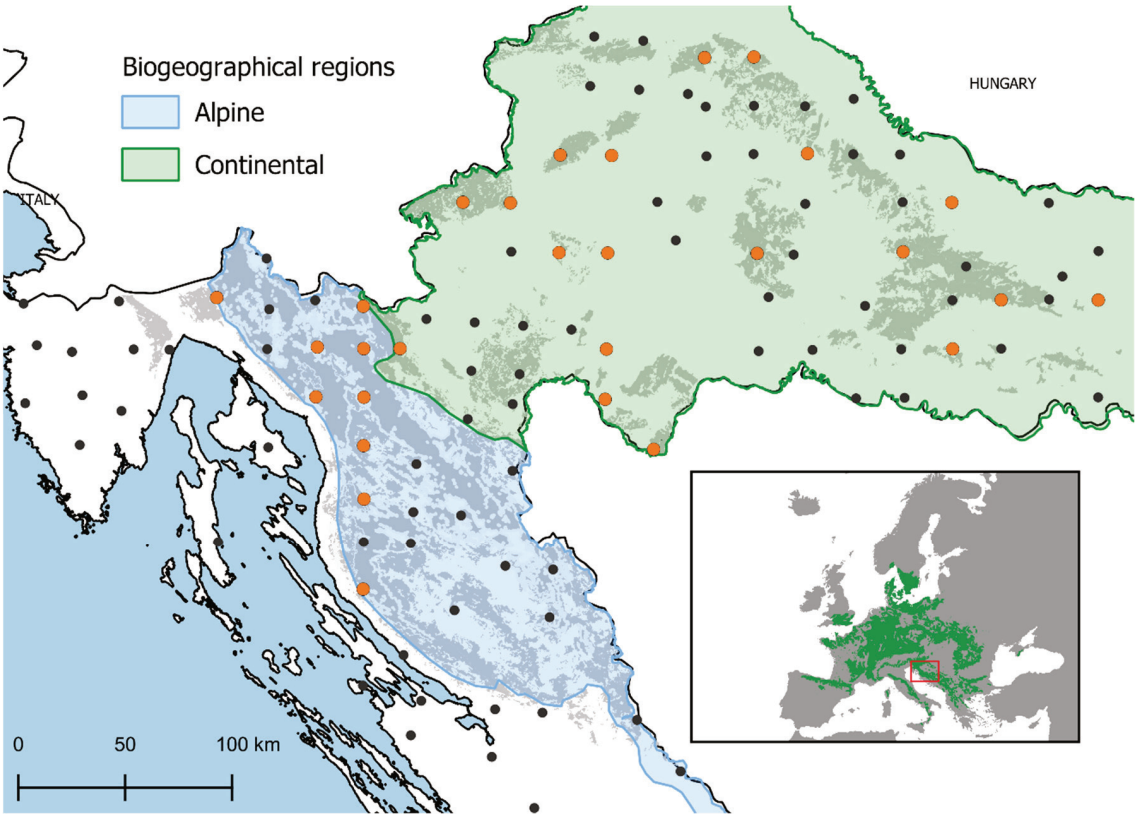

Figure 3. Location of research plots and distribution of European beech in Europe [65]. Selected Level I ICP Forests monitoring plots (orange dots); remaining Level I plots in Croatia (black dots); distribution of European beech forests in Croatia [66] (gray polygon); biogeographic region in the study area (shaded polygon) [67].

4.2. Climate Data

Climate monitoring stations are generally situated at considerable distances from the forest research plots. Therefore, the data they provide are not always representative of the research locations. To overcome this, we used gridded data produced by regression kriging (RK), which is a hybrid method of interpolation carried out in four steps [68,69]. The method was validated with leave-one-out cross-validation, while the root mean square error (RMSE) was calculated between observed and interpolated values. Mean RMSEs are for mean monthly temperature from 0.5 °C to 0.9 °C, for minimum temperature from 1.1 °C to 1.5 °C, for maximum temperature from 0.7 °C to 1.1 °C, and for precipitation from 18 to 30 mm, averaged by months.

Monthly temperature and precipitation values from the gridded dataset on 1 km spatial resolution for Croatia [30] were used to calculate Mean Annual Temperature (MAT), mean annual minimum (Tmin) and mean annual maximum (Tmax) temperature, Mean Annual Precipitation (MAP) as well as the Palmer Drought Severity Index (PDSI) [70] and Standardized Precipitation Evapotranspiration Index (SPEI) [71]. Lower values of scPDSI and SPEI indicate a stronger drought intensity while higher values indicate a higher degree of humidity. SPEI was calculated on a time scale of 3 months.

4.3. Tree Selection Procedures, Foliar Sampling and Analysis

Sampling was conducted annually from 2018 to 2020 during late July and August. At a distance of less than 50 m from the centre of the plot, a stratified sampling of trees based on the percentage of defoliation was carried out, forming two groups of five trees: (i) "LOW DEFOLIATION" (LD) trees with defoliation lower than 25% and (ii) 'HIGH DEFOLIATION' (HD) trees with defoliation higher than 25%. Defoliation assessments were

performed during July and August according to the ICP Forests methodology [24] in steps of 5%, ranging from 0 to 100%. An absolute reference tree, defined as the best/healthiest possible beech tree, was used in the assessments, regardless of local factors that may affect the crown condition. Only dominant or codominant trees were selected, without any wounds or fruiting bodies of fungi on the trunk. In cases when trees changed their defoliation percentage and thus changed their group status (LD/HD), new, replacement trees were selected instead, and the discarded trees were not used in further sampling. Stratified sampling allowed us to circumvent the irregular distribution of tree defoliation status on plots and focus on determining whether concentrations/contents of nutrients in leaves differ in trees of different defoliation categories on each plot. Leaves were sampled from the upper third of the crown using a shotgun rifle or a rope climbing technique [72,73]. Samples from each tree were combined into a composite sample according to fresh weight and analyzed in the Laboratory for Physical and Chemical Testing (LFKI) of the Croatian Forest Research Institute. Upon arrival to the laboratory, samples of plant material were dried at 105 ° C to constant mass, ground in a Fritsch Pulverisette 14 mill and prepared for analysis in a Milestone Ethos One microwave oven [74]. Concentrations of total nitrogen were determined on a Leco CNS 2000 elemental analyzer (LECO, 2000). Phosphorus (P) concentration was determined colorimetrically on a LaboMed UV/VIS spectrophotometer [74], and potassium, calcium and magnesium by atomic absorption on the Perkin-Elmer Aanalyst 700 absorption spectrophotometer [74].

4.4. Soil Sampling and Analysis

Soil sampling was performed in 2019 on five points located within each of the research plots. One point was located within each of the four clusters of trees that are assessed for defoliation during regular monitoring activities, and an additional fifth point was located in the centre of each plot. Soil samples were taken with a pedological drill from a depth of 0–10 cm, 10–20 cm, 20–40 cm, and 40–80 cm. Collected samples were pooled by sampling depth. Soil mechanical properties were determined by [75] and chemical parameters were analysed according to the following protocols and methods:

- soil pH ($CaCl_2$) [76]
- exchangeable K, Ca and Mg according to [77]
- exchangeable acidity (free H^+) according to [78]
- total N with an elemental analyzer Leco CNS 2000 [79]
- available P and K with the AL method [80]; P by spectrophotometry using molybdate blue method, on UV/VIS spectrophotometer LaboMed and K directly from filtrate on flame photometer Buck scientific PFP−7 [81].

4.5. Data Analysis

Descriptive statistics of foliar concentration and ratios were performed for each element. Foliar data distribution was inspected visually and by Shapiro-Wilk test. Slight deviations from normality were determined, especially for potassium, calcium and magnesium. However, studies have shown that slight deviations from normality do not affect the rate of false positive results [82].

Therefore, a two-factor repeated measures analysis of variance (ANOVA) was used to determine the difference in foliar concentrations and ratios between defoliation categories (LD/HD) of common beech on a study area level. The data of all elements met the assumption of homoscedasticity, which was confirmed by Levene's test. The Holm–Bonferroni method [83] was used to perform pairwise comparisons to determine differences in foliar concentrations (i) between LD and HD categories in single years and (iii) across defoliation categories between sampling years.

To determine differences in foliar concentrations and ratios between defoliation categories on a plot level, we used the independent samples t-test [84]. The results were then categorized for each plot and sampling year to reflect three cases: (i) *HD_higher* if HD trees had significantly higher foliar concentrations ($p < 0.05$), (ii) *LD_higher* if LD trees

had significantly higher foliar concentrations ($p < 0.05$) and (iii) *NO_diff* if there were no significant differences in foliar concentrations between defoliation categories, thus creating a variable which represents Differences in Foliar Concentrations or Ratios for each element (DFC/DFR).

Multinomial logistic regression (MLR) was used to determine which environmental factors influence the occurrence probability of a certain DFC/DFR category, except no_dif which was set as the reference category. Separate odds ratios, which are the exponentiation of model coefficients, were determined for all independent variables for each DFC/DFR category. The odds ratio of a coefficient indicates the occurrence probability of either HD or LD trees having significantly higher foliar concentrations over the probability of no difference between defoliation categories (*NO_diff*). An odds ratio > 1 indicates that the occurrence probability of a certain DFC/DFR category relative to the occurrence of *NO_diff* increases as the independent variable increases, whereas an odds ratio < 1 indicates that the occurrence of a certain DFC/DFR category decreases. Of the potential independent variables, those with the highest variable importance were selected with the random forest algorithm [85]. The final model selection process was based on diagnostic diagrams and a procedure defined by Johnson et al. [86]. All analyses were conducted in an R programming environment [87].

5. Conclusions

Our final view is that links between defoliation and nutrition of beech in Croatia are not very direct or very prominent; this can be seen from (I) the fact that differences in nutrition of LD and HD trees were found for only a few nutrients (II) these effects are mostly not universal, but present only in some years and on a limited number of plots and (III) nutrient concentrations mostly stay within normal values regardless of tree defoliation status. However, it is clear that environmental factors, especially climate properties, do affect the relationship between defoliation and nutrition. Discovering mechanisms by which environmental factors affect foliar nutrition should complement current research on the defoliation–nutrition relationships.

Supplementary Materials: The following supporting information can be downloaded at: https://www.mdpi.com/article/10.3390/plants12010168/s1, Figure S1. Comparison of study area climate properties during the vegetation period with the climate normal (1980–2011) of the vegetation period (March -September); Figure S2. Foliar nitrogen concentrations on research plots; Figure S3. Foliar phosphorus concentrations on research plots; Figure S4. Foliar potassium concentrations on research plots; Figure S5. Foliar calcium concentrations on research plots; Figure S6. Foliar magnesium concentrations on research plots; Figure S7. Foliar N/P ratios on research plots; Figure S8. Foliar N/Ca ratios on research plots; Figure S9. Foliar N/K ratios on research plots; Figure S10. Foliar N/Mg ratios on research plots; Figure S11. Defoliation of common beech on research plots; Figure S12. Defoliation of common beech on all plots during the study period.

Author Contributions: Conceptualization, M.O., I.S. and N.P.; methodology, M.O.; formal analysis, M.O.; investigation, M.O., I.S., P.R. and N.P.; resources, N.P.; data curation, M.O.; writing—original draft preparation, M.O., I.S. and N.P.; writing—review and editing, M.O., I.S., M.M., P.R., M.J., V.T., M.L., M.P.T., D.U. and N.P.; visualization, M.O.; supervision, N.P.; project administration, M.O. and M.M.; funding acquisition, M.O., I.S. and N.P. All authors have read and agreed to the published version of the manuscript.

Funding: This work has been fully supported by Croatian Science Foundation under the project VitaClim (IP-2018-01-5222).

Institutional Review Board Statement: Not applicable.

Informed Consent Statement: Not applicable.

Data Availability Statement: The data presented in this study are available on request from the corresponding author. The data are not publicly available due to legal reasons.

Acknowledgments: We highly appreciate the work of researchers and technicians of the Croatian Forest Research Institute that participated in field research and laboratory analysis for this study.

Conflicts of Interest: The authors declare no conflict of interest.

References

1. Centritto, M.; Tognetti, R.; Leitgeb, E.; Střelcová, K.; Cohen, S. Above Ground Processes: Anticipating Climate Change Influences. In *Forest Management and the Water Cycle: An Ecosystem-Based Approach*; Bredemeier, M., Cohen, S., Godbold, D.L., Lode, E., Pichler, V., Schleppi, P., Eds.; Springer: Dordrecht, The Netherlands, 2011; pp. 31–64. ISBN 978-90-481-9834-4.
2. Trumbore, S.; Brando, P.; Hartmann, H. Forest Health and Global Change. *Science* **2015**, *349*, 814–818. [CrossRef]
3. Stocker, T.F.; Qin, D.; Plattner, G.-K.; Alexander, L.V.; Allen, S.K.; Bindoff, N.L.; Bréon, F.-M.; Church, J.A.; Cubasch, U.; Emori, S.; et al. Technical Summary. In *Climate Change 2013: The Physical Science Basis. Contribution of Working Group I to the Fifth Assessment Report of the Intergovernmental Panel on Climate Change*; Stocker, T.F., Qin, D., Plattner, G.-K., Tignor, M., Allen, S.K., Boschung, J., Nauels, A., Xia, Y., Bex, V., Midgley, P.M., Eds.; Cambridge University Press: Cambridge, UK; New York, NY, USA, 2013.
4. de Vries, W.; Dobbertin, M.H.; Solberg, S.; van Dobben, H.F.; Schaub, M. Impacts of Acid Deposition, Ozone Exposure and Weather Conditions on Forest Ecosystems in Europe: An Overview. *Plant Soil* **2014**, *380*, 1–45. [CrossRef]
5. Ferretti, M.; Waldner, P.; Verstraeten, A.; Schmitz, A.; Michel, A.; Žlindra, D.; Marchetto, A.; Hansen, K.; Pitar, D.; Gottardini, E.; et al. Criterion 2: Maintenance of Forest EcosystemHealth and Vitality. In *Forest Europe, 2020: State of Europe's Forests 2020*; Ministerial Conference on the Protection of Forests in Europe—Liaison Unit Bratislava: Zvolen, Slovak Republic, 2020.
6. Zierl, B. A Simulation Study to Analyse the Relations between Crown Condition and Drought in Switzerland. *For. Ecol. Manag.* **2004**, *188*, 25–38. [CrossRef]
7. IPCC. Summary for Policymakers. In *Climate Change 2021: The Physical Science Basis. Contribution of Working Group I to the Fifth Assessment Report of the Intergovernmental Panel on Climate Change*; Masson-Delmotte, V., Zhai, P., Pirani, A., Connors, S.L., Péan, C., Berger, S., Caud, N., Chen, Y., Goldfarb, L., Gomis, M.I., et al., Eds.; Cambridge University Press: Cambridge, UK; New York, NY, USA, 2021; pp. 3–32. [CrossRef]
8. Allen, C.D.; Macalady, A.K.; Chenchouni, H.; Bachelet, D.; McDowell, N.; Vennetier, M.; Kitzberger, T.; Rigling, A.; Breshears, D.D.; Hogg, E.H.; et al. A Global Overview of Drought and Heat-Induced Tree Mortality Reveals Emerging Climate Change Risks for Forests. *For. Ecol. Manag.* **2010**, *259*, 660–684. [CrossRef]
9. Giorgi, F. Climate Change Hot-Spots. *Geophys. Res. Lett.* **2006**, *33*. [CrossRef]
10. Beniston, M.; Stephenson, D.B.; Christensen, O.B.; Ferro, C.A.T.; Frei, C.; Goyette, S.; Halsnaes, K.; Holt, T.; Jylhä, K.; Koffi, B.; et al. Future Extreme Events in European Climate: An Exploration of Regional Climate Model Projections. *Clim. Change* **2007**, *81*, 71–95. [CrossRef]
11. Marschner, H. 9—Functions of Mineral Nutrients: Micronutrients. In *Marschner's Mineral Nutrition of Higher Plants*, 2nd ed.; Academic Press: San Diego, CA, USA, 2002; pp. 313–404. ISBN 978-0-12-473543-9.
12. Jonard, M.; Fürst, A.; Verstraeten, A.; Thimonier, A.; Timmermann, V.; Potočić, N.; Waldner, P.; Benham, S.; Hansen, K.; Merilä, P.; et al. Tree Mineral Nutrition Is Deteriorating in Europe. *Glob. Chang. Biol.* **2015**, *21*, 418–430. [CrossRef]
13. Hallenbarter, D.; Landolt, W.; Bucher, J. Nutrition and Vitality: Phenological Investigation in Forest under Different Fertiliser Treatments. In *Trends in European Forest Tree Physiology Research: Cost Action E6: EUROSILVA*; Springer: Dordrecht, The Netherlands, 2001; pp. 9–12.
14. Kreuzwieser, J.; Gessler, A. Global Climate Change and Tree Nutrition: Influence of Water Availability. *Tree Physiol.* **2010**, *30*, 1221–1234. [CrossRef]
15. Talkner, U.; Meiwes, K.J.; Potočić, N.; Seletković, I.; Cools, N.; De Vos, B.; Rautio, P. Phosphorus Nutrition of Beech (*Fagus sylvatica* L.) Is Decreasing in Europe. *Ann. For. Sci.* **2015**, *72*, 919–928. [CrossRef]
16. Potočić, N.; Timmermann, V.; Ognjenović, M.; Kirchner, T.; Prescher, A.K.; Ferretti, M. *Tree Health Is Deteriorating in the European Forests*; ICP Forests: 2021; Programme Coordinating Centre of ICP Forests, Thünen, Institute of Forest Ecosystems: Eberswalde, Germany, 2021. [CrossRef]
17. Pernar, N.; Bakšić, D. The Soils of Beech Forests. In *Common Beech (Fagus sylvatica L.) in Croatia*; Matić, S., Ed.; Academy of Forestry Sciences: Zagreb, Croatia, 2003; ISBN 953-98571-1-2.
18. Dobbertin, M.; Brang, P. Crown Defoliation Improves Tree Mortality Models. *For. Ecol. Manag.* **2001**, *141*, 271–284. [CrossRef]
19. Cherubini, P.; Battipaglia, G.; Innes, J.L. Tree Vitality and Forest Health: Can Tree-Ring Stable Isotopes Be Used as Indicators? *Curr. For. Rep.* **2021**, *7*, 69–80. [CrossRef]
20. De Vries, W.; Klap, J.M.; Erisman, J.W. Effects of Environmental Stress on Forest Crown Condition in Europe. Part I: Hypotheses and Approach to the Study. *Water. Air. Soil Pollut.* **2000**, *119*, 317–333. [CrossRef]
21. De Marco, A.; Proietti, C.; Cionni, I.; Fischer, R.; Screpanti, A.; Vitale, M. Future Impacts of Nitrogen Deposition and Climate Change Scenarios on Forest Crown Defoliation. *Environ. Pollut.* **2014**, *194*, 171–180. [CrossRef]
22. Gottardini, E.; Cristofolini, F.; Cristofori, A.; Pollastrini, M.; Camin, F.; Ferretti, M. A Multi-Proxy Approach Reveals Common and Species-Specific Features Associated with Tree Defoliation in Broadleaved Species. *For. Ecol. Manag.* **2020**, *467*, 118151. [CrossRef]
23. Dobbertin, M. Tree Growth as Indicator of Tree Vitality and of Tree Reaction to Environmental Stress: A Review. *Eur. J. For. Res.* **2005**, *124*, 319–333. [CrossRef]

24. Eichhorn, J.; Roskams, P.; Potočić, N.; Timmermann, V.; Ferretti, M.; Mues, V.; Szepesi, A.; Durrant, D.; Seletković, I.; Schroeck, H.-W.; et al. Part IV: Visual Assessment of Crown Condition and Damaging Agents. Version 2020-3. In *Manual on Methods and Criteria For harmonized Sampling, Assessment, Monitoring and Analysis of the Effects of Air pollution on Forests*; Thünen Institute of Forest Ecosystems: Eberswalde, Germany, 2020; p. 49. ISBN 978-3-86576-162-0.
25. Lorenz, M. International Co-Operative Programme on Assessment and Monitoring of Air Pollution Effects on Forests-ICP Forests. *Water. Air. Soil Pollut.* **1995**, *85*, 1221–1226. [CrossRef]
26. Timmermann, V.; Potočić, N.; Ognjenović, M.; Kirchner, T. *Tree Crown Condition in 2021. Forest Condition in Europe: The 2022 Assessment. ICP Forests technical Report under the UNECE Convention on Long-Range Transboundary Air Pollution (Air Convention)*; Thünen Institute: Eberswalde, Germany, 2022; pp. 41–55.
27. Ciais, P.; Reichstein, M.; Viovy, N.; Granier, A.; Ogée, J.; Allard, V.; Aubinet, M.; Buchmann, N.; Bernhofer, C.; Carrara, A.; et al. Europe-Wide Reduction in Primary Productivity Caused by the Heat and Drought in 2003. *Nature* **2005**, *437*, 529–533. [CrossRef]
28. Seidling, W. Signals of Summer Drought in Crown Condition Data from the German Level I Network. *Eur. J. For. Res.* **2007**, *126*, 529–544. [CrossRef]
29. Seletković, I.; Potočić, N.; Ugarković, D.; Jazbec, A.; Pernar, R.; Seletković, A.; Benko, M. Climate and Relief Properties Influence Crown Condition of Common Beech (*Fagus sylvatica* L.) on the Medvednica Massif. *Period. Biol.* **2009**, *111*, 435–441.
30. Ognjenović, M.; Seletković, I.; Potočić, N.; Marušić, M.; Tadić, M.P.; Jonard, M.; Rautio, P.; Timmermann, V.; Lovreškov, L.; Ugarković, D. Defoliation Change of European Beech (Fagus Sylvatica L.) Depends on Previous Year Drought. *Plants* **2022**, *11*, 730. [CrossRef]
31. Geßler, A.; Keitel, C.; Kreuzwieser, J.; Matyssek, R.; Seiler, W.; Rennenberg, H. Potential Risks for European Beech (*Fagus Sylvatica* L.) in a Changing Climate. *Trees-Struct. Funct.* **2007**, *21*, 1–11. [CrossRef]
32. Leuschner, C. Drought Response of European Beech (*Fagus sylvatica* L.)—A Review. *Perspect. Plant Ecol. Evol. Syst.* **2020**, *47*, 125576. [CrossRef]
33. Seletković, Z.; Tikvić, I.; Prpić, B. Ekološka Konstitucija Obične Bukve. In *Obična Bukva (Fagus sylvatica L.) u Hrvatskoj*; Matić, S., Ed.; Akademija Šumarskih Znanosti: Zagreb, Croatia, 2003.
34. Bolte, A.; Czajkowski, T.; Cocozza, C.; Tognetti, R.; De Miguel, M.; Pšidová, E.; Ditmarová, L.; Dinca, L.; Delzon, S.; Cochard, H.; et al. Desiccation and Mortality Dynamics in Seedlings of Different European Beech (*Fagus sylvatica* L.) Populations under Extreme Drought Conditions. *Front. Plant Sci.* **2016**, *7*, 751. [CrossRef] [PubMed]
35. Jonard, M.; André, F.; Giot, P.; Weissen, F.; Van der Perre, R.; Ponette, Q. Thirteen-Year Monitoring of Liming and PK Fertilization Effects on Tree Vitality in Norway Spruce and European Beech Stands. *Eur. J. For. Res.* **2010**, *129*, 1203–1211. [CrossRef]
36. Thimonier, A.; Graf Pannatier, E.; Schmitt, M.; Waldner, P.; Walthert, L.; Schleppi, P.; Dobbertin, M.; Kräuchi, N. Does Exceeding the Critical Loads for Nitrogen Alter Nitrate Leaching, the Nutrient Status of Trees and Their Crown Condition at Swiss Long-Term Forest Ecosystem Research (LWF) Sites? *Eur. J. For. Res.* **2010**, *129*, 443–461. [CrossRef]
37. Ferretti, M.; Calderisi, M.; Marchetto, A.; Waldner, P.; Thimonier, A.; Jonard, M.; Cools, N.; Rautio, P.; Clarke, N.; Hansen, K.; et al. Variables Related to Nitrogen Deposition Improve Defoliation Models for European Forests. *Ann. For. Sci.* **2015**, *72*, 897–906. [CrossRef]
38. Toïgo, M.; Nicolas, M.; Jonard, M.; Croisé, L.; Nageleisen, L.M.; Jactel, H. Temporal Trends in Tree Defoliation and Response to Multiple Biotic and Abiotic Stresses. *For. Ecol. Manag.* **2020**, *477*, 118476. [CrossRef]
39. Ognjenović, M.; Levanič, T.; Potočić, N.; Ugarković, D.; Indir, K.; Seletković, I. Interrelations of Various Tree Vitality Indicators and Their Reaction to Climatic Conditions on a European Beech (*Fagus sylvatica* L.) Plot. *Šumarski List* **2020**, *144*, 351–365. [CrossRef]
40. Mellert, K.H.; Göttlein, A. Comparison of New Foliar Nutrient Thresholds Derived from van Den Burg's Literature Compilation with Established Central European References. *Eur. J. For. Res.* **2012**, *131*, 1461–1472. [CrossRef]
41. Seletković, I.; Potočić, N. Stanje Ishrane Obične Bukve (*Fagus sylvatica* L.) i Obične Jele (*Abies alba* Mill.) Na Području Medvednice. *Rad. Šum. Inst. Izvanredno Izd.* **2006**, *9*, 117–125.
42. Raitio, H. Chemical Needle Analysis as a Diagnostic and Monitoring Method. In *Nutrient Uptake and Cycling in Forest Ecosystems*; Nilsson, L.O., Hüttl, R.F., Johansson, U.T., Eds.; Kluwer Academic Publishers: Dordrecht, The Netherlands, 1993; Volume 197–202, ISBN 0792330307.
43. Komlenović, N.; Gračan, J.; Pezdric, N.; Rastovski, P. Utjecaj Polutanata Na Bukove Šume i Kulture Smreke u Sjeverozapadnoj Hrvatskoj. *Šumarski List* **1988**, *112*, 12.
44. Komlenović, N.; Matković, N.; Moćan, D.; Rastovski, P. Unos Onečišćenja Iz Zraka u Šumu Bukve i Jele (Abieti-Fagetum "Dinaricum") u Predjelu Lividrage u Zapadnoj Hrvatskoj. *Šumarski List* **1997**, *121*, 8.
45. Sauter, U. Zeitliche Variationen Des Ernährungszustands Nordbayerischer Kiefernbestände. *Forstwissenschaftliches Cent. Ver. mit Tharandter Forstl. Jahrb.* **1991**, *110*, 13–33. [CrossRef]
46. Prietzel, J.; Kolb, E.; Rehfuess, K.E. Langzeituntersuchung Ehemals Streugenutzter Kiefernökosysteme in der Oberpfalz: Veränderungen von Bodenchemischen Eigenschaften und der Nährelementversorgung der Bestände. *Forstwissenschaftliches Cent. Ver. mit Tharandter Forstl. Jahrb.* **1997**, *116*, 269–290. [CrossRef]
47. Stefan, K.; Fürst, A.; Hacker, R.; Bartels, U. *Forest Foliar Condition in Europe. Results of Large-Scale Foliar Chemistry Surveys.*; European Commission—United Nations/Economic Commission for Europe: Brussels, Belgium, 1997.
48. Duquesnay, A.; Dupouey, J.-L.; Clement, A.; Ulrich, E.; Le Tacon, F. Spatial and Temporal Variability of Foliar Mineral Concentration in Beech (*Fagus Sylvatica*) Stands in Northeastern France. *Tree Physiol.* **2000**, *20*, 13–22. [CrossRef]

49. Jonard, M.; André, F.; Dambrine, E.; Ponette, Q.; Ulrich, E. Temporal Trends in the Foliar Nutritional Status of the French, Walloon and Luxembourg Broad-Leaved Plots of Forest Monitoring. *Ann. For. Sci.* **2009**, *66*, 412. [CrossRef]
50. Amores, G.; Santamaría, J.M. Beech Foliar Chemical Composition: A Bioindicator of Air Pollution Stress. In *Developments in Environmental Science*; Elsevier: Amsterdam, The Netherlands, 2003; Volume 3, pp. 301–313. ISBN 1474-8177.
51. Amores, G.; Bermejo, R.; Elustondo, D.; Lasheras, E.; Santamaría, J.M. Nutritional Status of Northern Spain Beech Forests. *Water Air Soil Pollut.* **2006**, *177*, 227–238. [CrossRef]
52. Penuelas, J.; Sardans, J.; Ogaya, R.; Estiarte, M. Nutrient Stoichiometric Relations and Biogeochemical Niche in Coexisting Plant Species: Effect of Simulated Climate Change. *Polish J. Ecol.* **2008**, *56*, 613–622.
53. Sardans, J.; Peñuelas, J. Tree Growth Changes with Climate and Forest Type Are Associated with Relative Allocation of Nutrients, Especially Phosphorus, to Leaves and Wood. *Glob. Ecol. Biogeogr.* **2013**, *22*, 494–507. [CrossRef]
54. Simon, A.; Wild, A. Mineral Nutrients in Leaves and Bast of Pedunculate Oak (*Quercus robur* L.) at Different States of Defoliation. *Chemosphere* **1998**, *36*, 955–959. [CrossRef]
55. Ouimet, R.; Moore, J.-D. Effects of Fertilization and Liming on Tree Growth, Vitality and Nutrient Status in Boreal Balsam Fir Stands. *For. Ecol. Manag.* **2015**, *345*, 39–49. [CrossRef]
56. Ewald, J. Ecological Background of Crown Condition, Growth and Nutritional Status of *Picea Abies* (L.) Karst. in the Bavarian Alps. *Eur. J. For. Res.* **2005**, *124*, 9–18. [CrossRef]
57. Potočić, N.; Ćosić, T.; Pilaš, I. The Influence of Climate and Soil Properties on Calcium Nutrition and Vitality of Silver Fir (Abies Alba Mill.). *Environ. Pollut.* **2005**, *137*, 596–602. [CrossRef] [PubMed]
58. Braun, S.; Schindler, C.; Rihm, B. Foliar Nutrient Concentrations of European Beech in Switzerland: Relations with Nitrogen Deposition, Ozone, Climate and Soil Chemistry. *Front. For. Glob. Chang.* **2020**, *3*, 33. [CrossRef]
59. Bergmann, W. (Ed.) *Nutritional Disorders of Plants*; Gustav Fischer Verlag: Jena, Germany; Stuttgart, Germany; New York, NY, USA, 1992.
60. Lukac, M.; Calfapietra, C.; Lagomarsino, A.; Loreto, F. Global Climate Change and Tree Nutrition: Effects of Elevated CO_2 and Temperature. *Tree Physiol.* **2010**, *30*, 1209–1220. [CrossRef]
61. Meier, I.C.; Leuschner, C. Nutrient Dynamics along a Precipitation Gradient in European Beech Forests. *Biogeochemistry* **2014**, *120*, 51–69. [CrossRef]
62. Ferretti, M.; Bacaro, G.; Brunialti, G.; Calderisi, M.; Croisé, L.; Frati, L.; Nicolas, M. Tree Canopy Defoliation Can Reveal Growth Decline in Mid-Latitude Temperate Forests. *Ecol. Indic.* **2021**, *127*, 107749. [CrossRef]
63. Tallieu, C.; Badeau, V.; Allard, D.; Nageleisen, L.M.; Bréda, N. Year-to-Year Crown Condition Poorly Contributes to Ring Width Variations of Beech Trees in French ICP Level I Network. *For. Ecol. Manag.* **2020**, *465*, 118071. [CrossRef]
64. Ferretti, M.; Fischer, R.; Mues, V.; Granke, O.; Lorenz, M.; Seidling, W.; Nicolas, M. Part II:Basic Design principlesfor the ICP Forests Monitoring Networks. Version 2020-2. In *Manual on Methods and Criteria for Harmonized Sampling, Assessment, Monitoring and Analysis of the Effects of Air Pollution On forests*; Thünen Institute of Forest Ecosystems: Eberswalde, Germany, 2020; p. 33. ISBN 978-3-86576-162-0.
65. Caudullo, G.; Welk, E.; San-Miguel-Ayanz, J. Chorological Maps for the Main European Woody Species. *Data Br.* **2017**, *12*, 662–666. [CrossRef]
66. Pravilnik o Vrstama Stanišnih Tipova, Karti Staništa, Ugroženim i Rijetkim Stanišnim Tipovima Te o Mjerama Za Očuvanje Stanišnih Tipova NN 7/2006. Available online: https://narodne-novine.nn.hr/clanci/sluzbeni/2006_01_7_156.html (accessed on 14 July 2022).
67. Cervellini, M.; Zannini, P.; Di Musciano, M.; Fattorini, S.; Jiménez-Alfaro, B.; Rocchini, D.; Field, R.; Vetaas, O.R.; Irl, S.D.H.; Beierkuhnlein, C. A Grid-Based Map for the Biogeographical Regions of Europe. *Biodivers. Data J.* **2020**, *8*, e53720. [CrossRef]
68. Perčec Tadić, M. Gridded Croatian Climatology for 1961–1990. *Theor. Appl. Climatol.* **2010**, *102*, 87–103. [CrossRef]
69. Perčec Tadić, M.; Pasarić, Z.; Guijarro, J.A. Croatian High-Resolution Monthly Gridded Data Set of Homogenised Surface Air Temperature. *Theor. Appl. Climatol.* **2022**. [CrossRef]
70. Palmer, W.C. *Meteorological Drought*; US Department of Commerce, Weather Bureau: Washington, DC, USA, 1965; Volume 45.
71. Vicente-Serrano, S.M.; Beguería, S.; López-Moreno, J.I. A Multiscalar Drought Index Sensitive to Global Warming: The Standardized Precipitation Evapotranspiration Index. *J. Clim.* **2010**, *23*, 1696–1718. [CrossRef]
72. Dial, R.; Tobin, S.C. Description of Arborist Methods for Forest Canopy Access and Movement. *Selbyana* **1994**, *15*, 24–37.
73. Jepson, J. *The Tree Climber's Companion*; Beaver Tree Publishing: Longville, MI, USA, 2000.
74. Rautio, P.; Fürst, A.; Stefan, K.; Raitio, H.; Bartels, U. Part XII: Sampling and Analysis of Needles and Leaves. In *Manual on Methods and Criteria for Harmonized Sampling, Assessment, Monitoring and Analysis of the Effects of Air Pollution on Forests*; UNECE, ICP Forests Programme Co-Ordinating Centre: Hamburg, Germany, 2016.
75. *ISO 11277*; Soil Quality—Determination of Particle Size Distribution in Mineral Soil Material. ISO: Geneva, Switzerland, 2020.
76. *ISO-10390*; Soil Quality—Determination of PH. ISO: Geneva, Switzerland, 2005.
77. *ISO-11260*; Soil Quality—Determination of Effective Cation Exchange Capacity and Base Saturation Level Using Barium Chloride Solution4. ISO: Geneva, Switzerland, 1994.
78. *ISO 14254*; Soil Quality—Determination of Exchangeable Acidity Using Barium Chloride Solution as Extractant 2018. ISO: Geneva, Switzerland, 2018.

79. *ISO-13878*; Soil Quality—Determination of Total Nitrogen Content by Dry Combustion ("elemental Analysis") 1998. ISO: Geneva, Switzerland, 1998.
80. Egnér, H.; Riehm, H.; Domingo, W.R. Untersuchungen Über Die Chemische Bodenanalyse Als Grundlage Für Die Beurteilung Des Nährstoffzustandes Der Böden. II. Chemische Extraktionsmethoden Zur Phosphor-Und Kaliumbestimmung. *K. Lantbr. Ann.* **1960**, *26*, 199–215.
81. Škorić, A. *Priručnik Za Pedološka Istraživanja*; Fakultet Poljoprivrednih Znanosti: Zagreb, Croatia, 1985.
82. Lix, L.M.; Keselman, J.C.; Keselman, H.J. Consequences of Assumption Violations Revisited: A Quantitative Review of Alternatives to the One-Way Analysis of Variance F Test. *Rev. Educ. Res.* **1996**, *66*, 579–619. [CrossRef]
83. Holm, S. A Simple Sequentially Rejective Multiple Test Procedure. *Scand. J. Stat.* **1979**, *6*, 65–70.
84. Ross, A.; Willson, V.L. Independent Samples T-Test. In *Basic and Advanced Statistical Tests*; Springer: Rotterdam, The Netherlands, 2017; pp. 13–16.
85. Breiman, L. Random Forests. *Mach. Learn.* **2001**, *45*, 5–32. [CrossRef]
86. Johnson, J.B.; Omland, K.S. Model Selection in Ecology and Evolution. *Trends Ecol. Evol.* **2004**, *19*, 101–108. [CrossRef]
87. R Core Team. *R: A Language and Environment for Statistical Computing*; R Foundation for Statistical Computing: Vienna, Austria, 2016.

plants

MDPI

Article

How Tree Decline Varies the Anatomical Features in *Quercus brantii*

Forough Soheili [1], Hazandy Abdul-Hamid [2,*], Isaac Almasi [3], Mehdi Heydari [1], Afsaneh Tongo [4], Stephen Woodward [5] and Hamid Reza Naji [1,*]

[1] Department of Forest Sciences, Ilam University, Ilam 67187-73654, Iran
[2] Faculty of Forestry and Environment, Universiti Putra Malaysia, Serdang 43400, Selangor, Malaysia
[3] Faculty of Science, Department of Statistics, Razi University, Kermanshah 67144-14971, Iran
[4] Department of Forest Science and Engineering, Sari University of Agricultural Sciences and Natural Resources, Sari 48181-68984, Iran
[5] School of Biological Sciences, University of Aberdeen, Aberdeen AB24 3UU, UK
* Correspondence: hazandy@upm.edu.my (H.A.-H.); h.naji@ilam.ac.ir (H.R.N.); Tel.: +98-911-458-9774 (H.R.N.)

Abstract: Drought has serious effects on forests, especially semi-arid and arid forests, around the world. Zagros Forest in Iran has been severely affected by drought, which has led to the decline of the most common tree species, Persian oak (*Quercus brantii*). The objective of this study was to determine the effects of drought on the anatomical structure of Persian oak. Three healthy and three declined trees were sampled from each of two forest sites in Ilam Forest. Discs were cut at breast height, and three sapwood blocks were taken near the bark of each tree for sectioning. The anatomical characteristics measured included fiber length (FL), fiber wall thickness (FWT), number of axial parenchymal cells (NPC), ray number (RN), ray width (RW), and number of calcium oxalate crystals. Differences between healthy and declined trees were observed in the abundance of NPC and in RN, FL, and FWT, while no differences occurred in the number of oxalate crystals. The decline had uncertain effects on the FL of trees from sites A and B, which showed values of 700.5 and 837.3 μm compared with 592.7 and 919.6 μm in healthy trees. However, the decline resulted in an increase in the FWT of trees from sites A and B (9.33 and 11.53 μm) compared with healthy trees (5.23 and 9.56 μm). NPC, RN, and RW also increased in declined individuals from sites A and B (28.40 and 28.40 mm^{-1}; 41.06 and 48.60 mm^{-1}; 18.60 and 23.20 μm, respectively) compared with healthy trees (20.50 and 19.63 mm^{-2}; 31.60 and 28.30 mm^{-2}; 17.93 and 15.30 μm, respectively). Thus, drought caused measurable changes in the anatomical characteristics of declined trees compared with healthy trees.

Keywords: drought; tree decline; *Quercus brantii*; cellular characteristics; calcium oxalate crystals

Citation: Soheili, F.; Abdul-Hamid, H.; Almasi, I.; Heydari, M.; Tongo, A.; Woodward, S.; Naji, H.R. How Tree Decline Varies the Anatomical Features in *Quercus brantii*. *Plants* **2023**, *12*, 377. https://doi.org/10.3390/plants12020377

Academic Editor: Nenad Potočić

Received: 1 November 2022
Revised: 23 December 2022
Accepted: 29 December 2022
Published: 13 January 2023

1. Introduction

Ongoing global warming is increasing stress in most of the Earth's ecosystems [1]. As the duration, frequency, and intensity of droughts increase, forest productivity decreases and tree mortality rates are expected to increase [2,3].

In forest ecosystems, trees are exposed to a combination of biotic and abiotic stressors that limit their growth potential [4]. Abiotic stressors such as drought weaken tree response to environmental conditions, leading to further damage and, in extreme cases, death [5]. In the last 20–30 years, the effects of climate change have led to an increase in damage to forest ecosystems, reducing the adaptive capacity of plant communities in these ecosystems [6]. Forest decline is a complex destructive phenomenon that leads to declining tree growth and, over time, tree death [7]. The decline is often a result of extreme climatic events, which can also lead to further damage caused by biotic factors [8].

In recent decades, the decline of oak species has been observed throughout the Mediterranean region and is clearly related to dry seasons [9]. Zagros Forest, a semi-arid region

in western Iran, is the largest oak forest in the world with an area of more than 5 million hectares, dominated by Persian oak (*Quercus brantii* L.) [10]. In this forest, oaks help to store and regulate water resources, conserve soil, mitigate climate change, and improve the socioeconomic conditions of human communities [11]. This forest is rich in biodiversity and provides habitat for numerous species of organisms. Since 2000, there have been recurrent droughts in Iran, especially in Zagros Forest, which have led to the disturbing death of trees, mainly Persian oaks. Drought is considered to be the most important influencing factor, followed by reduction in photosynthetic rate, reduction in annual growth increment, weakening of trees, and invasion of fungi and wood beetles [12].

Correlating variations in wood structure and tree defense strategies could help to better understand plant performance, especially in the face of climate change [13,14]. The plant cell wall, a complex macromolecular structure that surrounds and protects the cell contents, is essential to plant survival. Under drought conditions, negative stresses increasingly occur in the xylem due to water stress, causing the thickness of nearby fiber walls to prevent the vessels from imploding under the altered tension [15]. The fluctuations in climatic conditions affect trees and lead to permanent records in the xylem tissue. Therefore, trees can easily be considered as reliable natural documents that reveal past environmental events [16,17]. The xylem parenchymal cells are important for facilitating water conduction, serving as a water reservoir to prevent embolisms and providing osmotic agents to aid in the repair of embolisms [18]. The functions of the parenchyma (axial and ray cells) are (a) storage of water, nonstructural carbohydrates, and mineral elements [19–21]; (b) defense system against decay fungi and pathogens [22]; (c) aid in the transition from sapwood to heartwood [23]; and (d) biomechanical contributor, especially the ray parenchyma [24].

Calcium oxalate crystals form in the cells of many plant species, both monocotyledonous and dicotyledonous plants [25], and their functions include balancing the ionic balance, protecting and defending the plant, and detoxifying potentially harmful chemicals [26–28]. Serdar and Demiray [29] reported an abundance of intracellular crystals with different shapes in three different oaks from Turkey.

Despite the key role of the parenchyma in tree functioning, there is little research on the changes that occur in wood parenchymal cells in response to potential factors that affect their abundance. Morris et al. [30] found that an increase in the average number of parenchymal cells in the xylem occurred as a result of the increase in the annual air temperature. The effect was more pronounced in regions with average annual temperatures above 16 °C. In cold regions, where the total number of parenchymal cells in wood is lower than in the tropics, the role of the parenchyma as a defensive tissue may have a higher priority than other functions [31].

In recent decades, Persian oak forests have shown symptoms of a new phenomenon known as oak decline, most likely caused by drought stress [32]. Understanding the responses of trees to drought could be considered an interesting and active discipline of plant science research [33].

In the absence of specific information on changes in the cell anatomical structure of wood fibers and axial and ray parenchymal cells during drought stress, the work described in this article could provide valuable insights into this aspect of tree–environment interactions. Because all components of wood tissue may respond differently to environmental stress, we hypothesized the role of wood parenchymal cells and the changes in fiber and cell crystal properties during tree response to prolonged drought.

2. Results

2.1. Fiber Biometric Characterization

2.1.1. Fiber Length (FL)

The differences in FL in trees from the two sites and site×decline interactions were significant ($p < 0.01$) in sapwood samples collected near the bark (Table 1). Regarding site A, FL was significantly greater in sapwood near the bark in declined trees (700.5 µm) than in

healthy individuals (592.7 µm). In sapwood tissue samples from site B, FL was significantly shorter in dying trees (837.3 µm) than in healthy trees ($p < 0.05$) (919.6 µm; Figure 1A).

Table 1. Summary of two-way ANOVA of wood anatomical variables in sapwood of healthy and declined *Quercus brantii* affected by drought stress.

		Mean Square					
Source of Variation	**df**	**FL (µm)**	**FWT (µm)**	**NPC (mm^{-1})**	**RN (mm^{-1})**	**RW (µm)**	**NC (mm^{-2})**
Decline	1	0.206 ^{ns}	37.899 **	113.733 **	142.474 **	21.338 **	0.500 ^{ns}
Sites	1	67.690 **	43.954 **	0.308 ^{ns}	2.882 ^{ns}	1.125 ^{ns}	135.380 **
Decline × Sites	1	11.384 **	4.686 *	0.308 ^{ns}	18.871 **	15.213 **	0.30 ^{ns}
Error	116	23,817,771	7.283	18.318	46.643	25.795	22.830

FL, fiber length; FWT, fiber wall thickness; NPC, number of axial parenchymal cells; RN, ray number; RW, ray width; NC, number of crystals. * The mean difference was significant at the 0.05 level. ** The mean difference was significant at the 0.01 level. ns, non-significant.

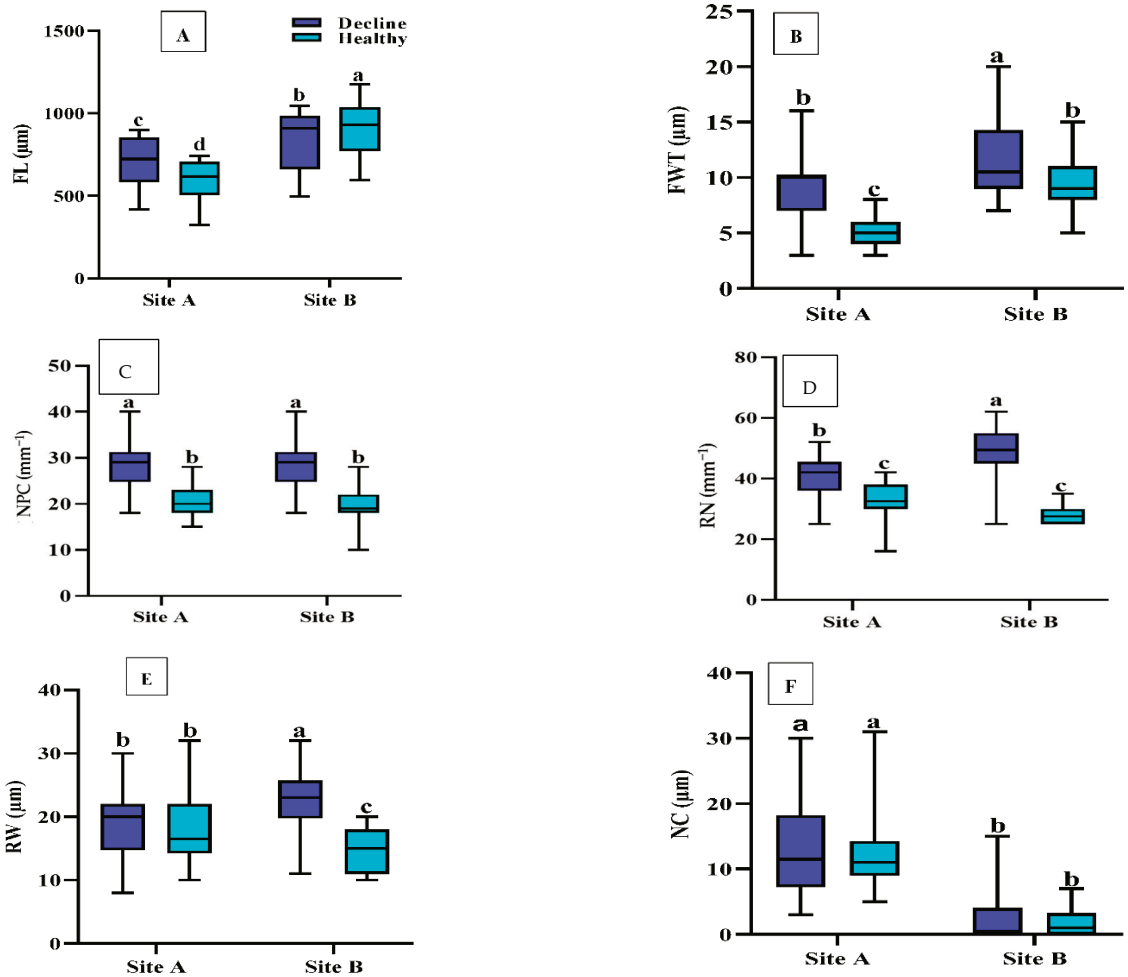

Figure 1. Boxplots of wood anatomy (**A**) FL, fiber length; (**B**) FWT, fiber wall thickness; (**C**) NPC, number of axial parenchymal cells; (**D**) RN, ray number; (**E**) RW, ray width; (**F**) NC, number of crystals) of sapwood from declined and healthy *Quercus brantii* from two sites in Iran. Site A, Dareh-shahr; site B, Ilam. Vertical bar above each column represents standard deviation. Lowercase letters in the boxes indicate significant differences between declined and healthy trees from the two sites (Duncan's multiple range test). The same letters indicate no significant differences ($p < 0.05$).

2.1.2. Fiber Wall Thickness (FWT)

The effects of decline, site, and their interaction on FWT were significant ($p < 0.01$) in sapwood adjacent to the bark (Table 1). FWT was significantly higher ($p < 0.05$) in declined trees from sites A and B (9.33 µm and 11.53 µm, respectively) than in healthy trees from the two sites (5.23 µm and 9.56 µm; Figure 1B).

2.1.3. Number of Axial Parenchymal Cells (NPC)

Decline had significant effects on the NPC ($p < 0.01$) in sapwood near the bark (Table 1). The NPC in fallen trees from sites A and B (28.4 and 28.4 mm^{-2}, respectively) was higher than that in healthy trees (20.5 and 19.6 mm^{-2}; Figure 1C).

2.1.4. Ray Number (RN)

The effects of decline and site × decline interaction on the RN were significant in sapwood near the bark ($p < 0.01$; Table 1). The RN was significantly higher in the sapwood of declined trees (41.06 and 48.60 mm^{-2}) than in healthy trees (31.60 and 28.30 mm^{-2}) from the two sites (Figure 1D).

2.1.5. Ray Width (RW)

RW in sapwood was significantly affected by decline ($p < 0.01$); interactions between decline and site also showed a significant effect on RW ($p < 0.01$; Table 1). RW was significantly higher ($p < 0.01$) in declined trees (23.20 µm) than in healthy trees (15.30 µm) in sapwood near the bark of trees from site B, but no significant differences were observed between declined and healthy trees from site A (Figure 1E).

2.1.6. Number of Crystals (NC)

Crystals were only observed in ray parenchymal cells. Differences in the NC between sites were significant ($p < 0.05$) in sapwood near the bark (Table 1). The NC in declined wood was higher in healthy trees ($p < 0.05$) from the two sites (Figure 2). In addition, the highest NC was observed in a sample from site A (Figure 1F).

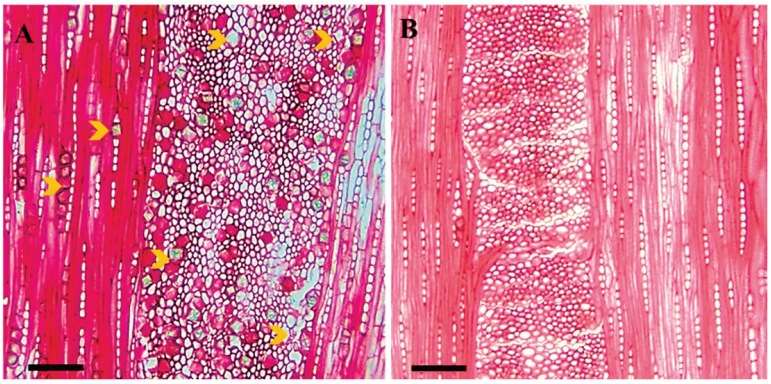

Figure 2. Frequency of crystals in the cells of the ray parenchyma of tangential sections in declined Persian oak wood from two different sampling sites: (**A**) Dareh-shahr, with high numbers, and (**B**) Ilam, with low numbers of crystals. Yellow arrows indicate crystals. Scale bar = 75 µm.

2.1.7. Principal Component Analysis (PCA)

The first and second axes of the PCA explained approximately 34.7 and 28.0% of the variance in sapwood from healthy and declined *Quercus brantii* affected by drought stress at the two sites. For declined oak trees in Dareh-shahr, the most important variables were FWT, RW, RN, and NPC, and the most important trait of healthy trees from the Ilam site was FL. Similarly, in declined trees from the Ilam site, the most important trait was the NC. It was investigated that drought-affected oaks from both climatic regions could be distinguished from healthy trees based on the anatomical characteristics. The RW, RN,

and NPC traits were significantly more distinct and common in declined oak trees than in healthy trees from both the Dareh-shahr and Ilam sites (Figure 3; Table 2).

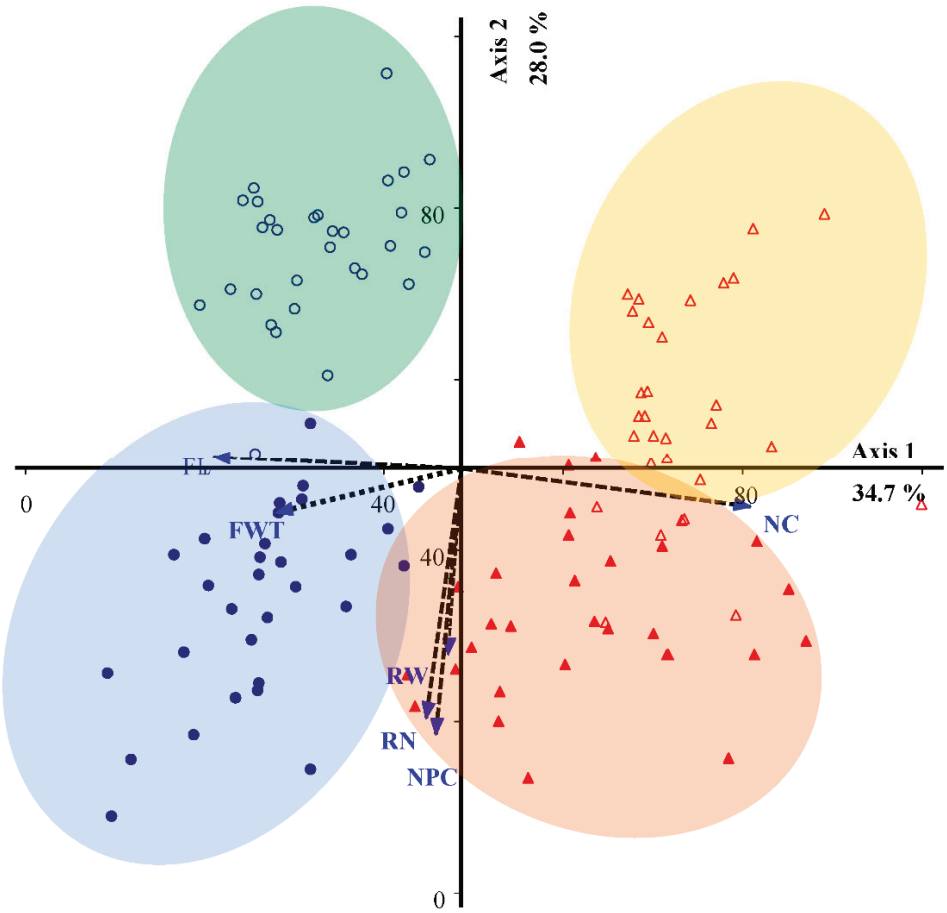

Figure 3. Principal component analysis (PCA) biplot based on correlation matrix of declined and healthy *Quercus brantii*. ▲ Declined trees from Dareh-shahr; △ healthy trees from Dareh-shahr; • declined trees from Ilam; ○ healthy trees from Ilam. Arrows with narrow angles from the axis indicate strong correlations, while a right angle indicates no correlation. The length of the arrow is a measure of the relative importance of the variables. FL, fiber length; FWT, fiber wall thickness; NPC, number of axial parenchymal cells; RN, ray number; RW, ray width; NC, number of crystals.

Table 2. Wood anatomical traits used in the principal component analysis (PCA) on sapwood of healthy and declined *Quercus brantii* affected by drought stress.

Trait	Component	
	Axis 1	**Axis 2**
FL (μm)	−0.746 **	0.167 ^{ns}
FWT (μm)	−0.644 **	−0.315 *
NPC (mm^{-1})	−0.237 ^{ns}	0.770 **
RN (mm^{-1})	−0.280 ^{ns}	−0.748 **
RW (μm)	−0.170 ^{ns}	−0.643 **
NC (mm^{-2})	0.804 **	−0.291 ^{ns}
Eigenvalues	2.431	1.962
% of variance	34.730	28.031

FL, fiber length; FWT, fiber wall thickness; NPC, number of axial parenchymal cells; RN, ray number; RW, ray width; NC, number of crystals. * The mean difference was significant at the 0.05 level. ** The mean difference was significant at the 0.01 level. ns, non-significant.

3. Discussion

Drought, as a severe environmental condition, affects tree growth [34]. To reduce water loss and adapt to drought, some typical changes in physiological processes occur, such as stomatal closure, reduction in photosynthetic assimilation, and cessation of leaf and shoot growth [35]. In addition, Soheili et al. [32] found that the number of earlywood vessels in Persian oaks decreased due to tree decline. These conditions greatly reduce cambial activity and result in strong inhibition of radial growth. This reduction in tree growth is known to be a result of reduced auxin levels [36]. As a result, the growth of the tree stem diameter decreases. As noted by Nola et al. [37], among angiosperms, the genus *Quercus* is more sensitive to drought than other species. This suggests that they may be less competitive under drier conditions in the future.

The influence of drought stress on changes in the anatomical characteristics of *Quercus brantii* wood was studied to determine the effects on living parenchymal cells in sapwood, a subject that has received little attention in the past. The results of this work provide a more solid basis for establishing a functional hypothesis about the role of the parenchyma in wood and the changes in fiber and cell crystal properties during tree response to drought.

Cell wall architecture is important for stress resistance in plants [38,39]. Cell wall synthesis is a flexible component of plant anatomy that can be altered to better cope with the effects of fluctuating biotic and abiotic factors [40]. In this work, according to the FL and FWT values, fibers in sapwood near the bark were shorter and thicker, respectively, in declined trees than in healthy trees (Figures 1A,B and 3). This could lead to higher wood density in declined Persian oaks, as reported in our last publication (Soheili et al. [32]). Previous publications [41,42] suggested that smaller anatomical structures (small- diameter vessels and thinner cell walls) in groups of weakened and dead ash trees (*Fraxinus* spp.) and *Quercus brantii* were due to low activity during the differentiation of the cambium into wood cells. The diameter of earlywood vessels and the area of earlywood vessels were also reduced in Persian oak affected by decline [32]. In addition, Hacke [43] and Wildhagen et al. [44] found that new xylem cells with thicker walls formed under drought compared with unaffected wood. The thickening of cell walls under drought is an important response to improve cell stability and prevent their collapse when pressure on the hydraulic system increases [45].

Environmental stresses such as drought during wood formation affect the size of cells formed subsequently by affecting the rate of cell division and expansion [46]. These physiological changes can sometimes help the plant to adapt to new conditions [47,48]. Naji and Taher Pour [49] stated that abiotic stress, such as a dust storm, can cause significant changes in wood structure, especially fiber properties, in seedlings of Persian oak. Based

on the hypothesis that environmental stress can disrupt the hormonal regulation of wood formation as well as the tree's ability to conduct water [50], it was hypothesized that environmental stress during wood formation leads to structural changes and thus changes in plant properties.

Living parenchymal cells found in the secondary xylem of woody plants can provide a dynamic response to xylem infection and mechanical damage. Furthermore, their role is critical to our understanding of tree defense mechanisms [51]. The xylem parenchyma is known to be a storage compartment in cells [52]. In addition, cells of the ray parenchyma are an important component for the radial water transport between phloem and xylem and for the storage of water, carbohydrates, and other nutrients [53]. Our results suggest that stem ray parenchymal cells respond to long-term environmental conditions such as climate change [54]. Parenchymal cell count (axial and ray) and ray width were greater in declined trees than in healthy trees from the two sites (Figures 1C–E and 3), consistently with the results of previous work on Ulmaceae [55–57]. von Arx et al. [54] found that the abundance of ray parenchymal cells in wood tissue may reflect tree vigor and defense against stress. They are able to transport more nutrients to strengthen the tree.

The role played by parenchymal cells in relation to tree hydraulics and their involvement in tree defense strategy against pathogens is not clearly understood, especially since the two responses are interrelated. Parenchymal cells can indirectly prevent the invasion of decay fungi, for example, by separating air-filled vessels. The associated woody cells can act as a buffer zone by refilling emboli in the vessels or creating a continuous flow of water in the otherwise compromised xylem [58–60]. Tyloses, as balloon-like swellings that usually form when adjacent parenchymal cells invade dead vascular cells, are a consequence of biotic/abiotic stress in trees, especially in ring-porous species with wide vessels such as oaks [61]. This phenomenon was greatly increased in declined Persian oaks when they were affected by drought [32].

Another possible reason for the increase in the average number of axial parenchymal and ray parenchymal cells in the woody tissues of declined trees could be related to the accumulation of antimicrobial compounds such as phytoalexins or phenolic compounds and the deposition of suberin to prevent the spread of fungi [62].

Calcium oxalate crystals (CaOx) are widely distributed in flowering plants, indicating an important role in growth and development processes. It should be noted that Table 1 and Figure 1F show no significant effects of decline on the frequency of crystals in the sapwood of healthy and declined trees. Figure 2 shows the frequency of crystals in the ray parenchyma cells of declined trees from two different sampling sites. An abundance of crystals was also observed in biotically stressed trees. Previous research has shown that the deposition of calcium oxalate crystals is high in the parenchymal cells of trees affected by biotic stress such as wood-destroying fungi [63,64]. Figures 1F and 2 show that the differences in the NC were highly related to the site and not to the effects of drought. Therefore, the causes of the differences in the NC between the different sites could have been due to the differences in the elemental mineral content of the soil or in the soil chemistry [65].

4. Conclusions

Xylem traits help to better understand and predict woody plant responses to climate change on local and global scales. They may also provide an answer to some questions about tree response and performance to changing environmental conditions. Drought stress has major destructive effects on Persian oak (*Quercus brantii*) in Zagros Forest in Iran. Therefore, the work presented here investigated the changes in wood anatomy resulting from drought stress. Previous work on drought-stressed *Q. brantii* has not quantified the effects of this abiotic problem on anatomical characteristics. In general, a decrease in fiber length and an increase in fiber wall thickness were observed in declined wood near the bark. In addition, the number of axial parenchymal and ray parenchymal cells, and the width of the rays were greater in the sapwood of samples from declined trees than in healthy trees. A large number of crystals were present in the ray parenchyma of sapwood

sampled immediately adjacent to the bark, although there were no quantitative differences between declined and healthy trees. Further research combining physiology, morphology, and molecular techniques is needed to better understand the role of the variables studied in this work on tree defense and to evaluate the possible role in resistance to biotic and abiotic stresses. In addition, these results can be used as basic information on the effect of drought stress on anatomical changes in *Q. brantii*, and tree responses and adaptations to environmental stress in the future.

5. Material and Methods

5.1. Study Areas

This study was conducted on Persian oak trees (*Quercus brantii*), both healthy individuals and those affected by drought stress, from two forest sites: Dareh-shahr and Ilam in Zagros Forest, Ilam Province, western Iran (Figure 4). The forest sites are dominated by *Q. brantii* [66]. The main characteristics of the study sites, and the precipitation and temperature data from the nearest meteorological station [67] are tabulated in Table 3. Furthermore, the warmest and coldest months at all three sites are August and January, respectively. The climate classification based on the De Martonne Aridity Index (IDM) is also shown in Table 3.

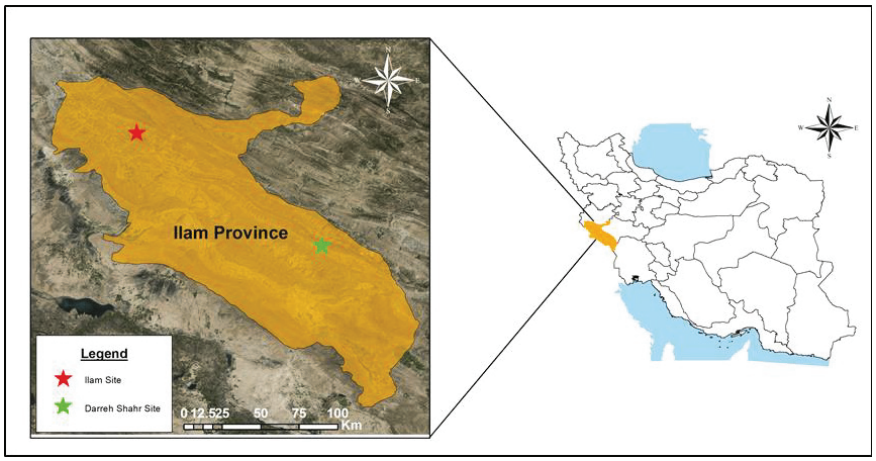

Figure 4. The locations of sampled forests stands on Ilam map, western Iran.

Table 3. Main characteristics of the study sites and the precipitation and temperature data from the nearest meteorological station.

Forest Site	Altitude (m)	Longitude	Latitude	A.M.P (mm)	A.M.T (°C)	Max. T	Min. T	Aridity I.	Soil Type
Dareh-shahr (A)	933	33°3′30″ N	47°19′30″ E	465.1	19.5	44.7	2.6	Semi-arid (16.48)	Sand-loamy
Ilam (B)	1680	33°43′03″ N	46°14′36″ E	582.2	16.9	36.8	0.6	Mediterranean (21.65)	Loam-clay-sandy

A.M.P., Annual Mean Precipitation; A.M.T., Annual Mean Temperature; Max. T., Maximum Monthly Temperature; Min. T., Minimum Monthly Temperature; Aridity I.; De Martonne Aridity Index. The values inside the parentheses show the De Martonne Aridity Index. A.M.P and A.M.T are, respectively, the mean annual precipitations and temperatures for a period of 33 years from 1986 to 2018. Max. T and Min. T. are, respectively, the mean temperatures in the hottest and coldest months for a period of 33 years from 1986 to 2018 (Ilam Meteorological Bureau, 2018). Soil types were reported by Menati et al. [68].

The severity and duration of drought stress were determined using the Standardized Precipitation Index (SPI), as shown in Figure 5. According to Figure 5, the drought began in 2000, and the index was negative and below normal in most years, indicating moderate-to-severe drought.

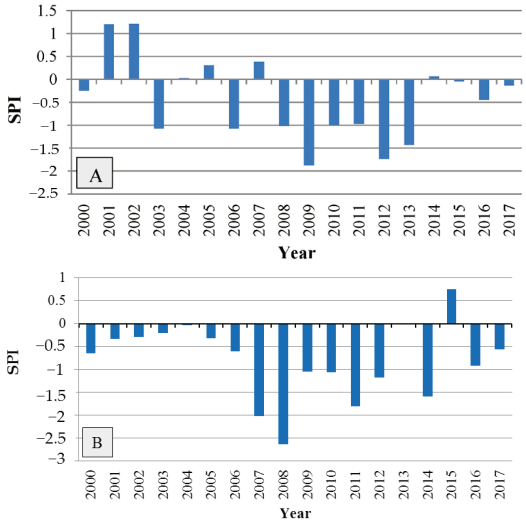

Figure 5. Standardized Precipitation Index (SPI) showing the severity and period of drought at the two sampling sites of Dareh-shahr (**A**) and Ilam (**B**).

5.2. Sampling Method

Due to the protected status of Zagros Forest, the number of trees we could sample from each stand was limited. For the declined trees, sampled discs were taken from the trunks of some trees that had been cut by the Department of Natural Resources of Ilam Province as part of a plan to remove damaged trees from the forest. Three healthy and three completely declined trees were sampled from each stand, i.e., the declined and healthy trees were cut from the same stand. A total of 12 trees with diameters at breast height (DBHs) of 30–40 cm were selected from two stands (see Table 3). To avoid the comparison of individual trees of different sizes and ages, trees were taken from a narrow range of DBHs. A disc approximately five-centimeter thick was taken from each fallen tree at breast height for further study. The discs from declined trees were cut with a chainsaw and then sanded using a flat sanding machine (Makita BO4901). More information on the sampling method can be found in our published paper in the journal *Forests* [32]. The study areas and materials of the current work were similar to those in the published work mentioned above, but the difference between the two was in the number of trees selected for the study. In the study by Soheili et al. [32], we measured some microstructures such as tree ring width, vessel characteristics, and wood density in declined trees to compare the variations in the radial direction from bark to pith; therefore, only six declined trees were selected for the study. However, in the present study, three healthy and three declined trees were chosen from each site for the measurement of the variables explained here. Since this is a protected forest and we did not have permission to fell healthy trees, some core samples were taken with an increment borer (HAGLÖF SWEDEN®®) from each tree at breast height.

5.3. Sample Preparation for Microscopic Investigation

Three small blocks of sapwood attached to the bark, approximately 1 × 1 × 1 cm in size, were cut radially from each disc. Each sample block contained nearly 3–4 annual growth rings. The blocks were labelled with the tree number, location, and class of decline and were fixed in classic fixative FAA according to Ruzin [69] (formaldehyde: ethanol alcohol 95%: Acetic acid; 10%:50%:5% + 35% doubled distilled water). Immediately prior to sectioning, the blocks were softened by heating to 60 °C for 24 h in an oven (Tehran STR).

5.4. Wood Sample Processing and Variable Measurement

Wood sections were prepared with no embedding according to the standard protocols by Gartner and Schweingruber [70]. Tangential sections with a thickness of 15–20 µm were prepared using a rotary microtome (POOYAN MK 1110, Binalood, Iran). Due to the strong

influence of drought on the trees, the growth rings were narrow; therefore, both earlywood and latewood were included in the tangential sections. Sections were stained with 0.1% (*w*/*v*) aqueous safranin (Safranin O; Sigma Aldrich, England) for 5–10 min, rinsed three times in distilled water, and dehydrated with an ethanol series of 60%, 85%, 95%, and absolute for approximately 15 min each. The dehydrated sections were fixed on glass slides with Canada balsam [71] and examined under a light microscope (Olympus, CX22LED; Japan) at 100× and 400× magnifications. The report of magnifications in the text are based on the total magnification of ocular and objective lenses. Images were taken with a digital camera connected to a computer. Measurements were performed using Mosaiv ver. 2.0 software (True Chrome metrics, China). The number of axial parenchymal cells (NPC mm^{-1}), the number of rays (RN mm^{-1}), ray width (RW μm), and the number of crystals (NC mm^{-2}) were measured following the IAWA committee (1989) guidelines in both healthy and declined trees at a magnification of 100×. Crystals were distributed in both ray parenchymal cells and axial parenchymal cells. The number of crystals varied in the cells, as most cells contained no crystals, while some cells had at least one and more. In addition, we considered the number of crystals for counting, and the measurement was performed in fields with an area of 1 mm^2. The fields for measuring the crystals in the parenchymal cells were centered on the locations of sections with no care. This was repeated in some fields to cover all parts of the section [72]. Due to the spindle shape of the ray parenchymal cells, the width was measured in the middle part of the rays. The axial and ray parenchymal cells were measured individually, with 60 counts for each site.

To measure fiber length (FL) and fiber wall thickness (FWT), matchstick-sized pieces of wood were removed from each block with a sharp blade and macerated in a solution of 1.5 g of sodium chlorite in 25 mL of distilled water with 8 drops of glacial acetic acid. The mixture was then placed in a bain-marie water bath at 80 °C for approximately 24 h. The suspension was carefully rinsed several times in distilled water before five drops of Safranin O were added. The free wood fibers were mounted on slides in 30% glycerol and then examined with an Olympus microscope at 100× and 400× magnifications to measure FL and FWT, respectively. Tip-to-tip lengths of undamaged, intact fibers were digitized for measurement. In total, measurements were based on 60 cells in 10 standard fields with an observation area of 1 mm^2 for each site.

5.5. Statistical Analysis

First, we performed the Shapiro–Wilk and Levene's tests to determine whether using ANOVA or non-parametric equivalents. The results showed that the dependent variables were normally distributed and that the variances were homogenous. To examine the separate and combined effects of the factors of the two sites (A and B) and the severity of decline (healthy and declined trees) on the dependent variables, we used two-way ANOVA and Duncan's multiple comparison test methods. The means and standard errors of wood anatomical characteristics between declined and healthy trees from the two sites were calculated. The SPSS ver. 21 statistical software package was used for all statistical analyses. Principal component analysis (PCA) based on the correlation matrix using PC-Ord version 5.0 was used to examine multivariate correlations (i.e., relationships among wood anatomical characteristic traits of declined and healthy trees from the two sites).

Author Contributions: F.S. and H.R.N. carried out the conceptualization of the experiment and wrote the manuscript with support from S.W.; I.A., M.H., and A.T. performed the computations and verified the analytical methods; H.A.-H. confirmed the methodology and helped to supervise the project. All authors have read and agreed to the published version of the manuscript.

Funding: This research was funded by Ilam University, grant number 805-1397-12.

Informed Consent Statement: Not applicable.

Data Availability Statement: The datasets generated for this study are available at: 10.6084/m9.figshare.21438231 (accessed on 30 October 2022).

Conflicts of Interest: The authors declare no conflict of interest.

References

1. IPCC. Summary for policymakers. In *Climate Change: The Physical Science Basis. Contribution of Working Group I to the Fifth Assessment Report of the Intergovernmental Panel on Climate Change*; Stocker, T.F., Qin, D., Plattner, G.K., Tignor, M., Allen, S.K., Boschung, J., Nauels, A., Xia, Y., Bex, V., Midgley, P.M., et al., Eds.; Cambridge University Press: Cambridge, UK; New York, NY, USA, 2013.
2. Allen, C.D.; Macalady, A.K.; Chenchouni, H.; Bachelet, D.; McDowell, N.; Vennetier, M.; Kitzberger, T.; Rigling, A.; Breshears, D.D.; Hogg, E.T.; et al. A global over-view of drought and heat-induced tree mortality reveals emerging climate change risks for forests. *For. Ecol. Manag.* **2010**, *259*, 660–684. [CrossRef]
3. Carnicer, J.; Coll, M.; Ninyerola, M.; Pons, X.; Sanchez, G.; Penuelas, J. Widespread crown condition decline, food web disruption, and amplified tree mortality with increased climate change-type drought. *Proc. Natl. Acad. Sci. USA* **2011**, *108*, 1474–1478. [CrossRef]
4. Ramegowda, V.; Senthil-Kumar, M. The interactive effects of simultaneous biotic and abiotic stresses on plants: Mechanistic understanding from drought and pathogen combination. *J. Plant Physiol.* **2015**, *176*, 47–54. [CrossRef]
5. Garrett, K.; Dendy, S.; Frank, E.; Rouse, M.; Travers, S. Climate change effects on plant disease: Genomes to ecosystems. *Annu. Rev. Phytopathol.* **2006**, *44*, 489–509. [CrossRef] [PubMed]
6. Lindner, M.; Maroschek, M.; Netherer, S.; Kremer, A.; Barbati, A.; Garcia-Gonzalo, J.; Seidl, R.; Delzon, S.; Corona, P.; Kolström, M.; et al. Climate change impacts, adaptive capacity, and vulnerability of European forest ecosystems. *For. Ecol. Manag.* **2010**, *259*, 698–709. [CrossRef]
7. McLaughlin, S.B.; Downing, D.J.; Blasing, T.J.; Cook, E.R.; Adams, H.S. An analysis of climate and competition as contributors to decline of red spruce in high elevation Appalachian forests of the eastern United States. *Oecologia* **1987**, *72*, 487–501. [CrossRef] [PubMed]
8. Colangelo, M.; Camarero, J.J.; Borghetti, M.; Gentilesca, T.; Oliva, J.; Redondo, M.A.; Ripullone, F. Drought and Phytophthora are associated with the decline of oak species in southern Italy. *Front Plant Sci.* **2018**, *9*, 1595. [CrossRef]
9. Desprez-Loustau, M.L.; Marçais, B.; Nageleisen, L.M.; Piou, D.; Vannini, A. Interactive effects of drought and pathogens in forest trees. *Ann. For. Sci.* **2006**, *63*, 597–612. [CrossRef]
10. Sagheb-Talebi, K.; Sajedi, T.; Yazdian, F. Research Institute of Forests and Rangelands. *For. Res. Div.* **2004**, *339*, 28.
11. Salehi, A.; Karltun, L.C.; So¨derberg, U.; Eriksson, L.O. Livelihood dependency on woodland resources in southern Zagros, Iran. *Casp. J. Environ. Sci.* **2010**, *8*, 181–194.
12. Tongo, A.; Jalilvand, H.; Hosseininasr, M.; Naji, H.R. Leaf morphological and physiological variations in response to canopy dieback of Persian Oak (*Quercus brantii* Lindl.). *For. Pathol.* **2021**, *51*, 12671. [CrossRef]
13. Aitken, S.N.; Yeaman, S.; Holliday, J.A.; Wang, T.; Curtis-McLane, S. Adaptation, migration or extirpation: Climate change out comes for tree populations. *Evol. Appl.* **2008**, *1*, 95–111. [CrossRef] [PubMed]
14. Sturrock, R.N.; Frankel, S.J.; Brown, A.V.; Hennon, P.E.; Kliejunas, J.T.; Lewis, K.T.; Worrall, J.J.; Woods, A.J. Climate change and forest diseases. *Plant Pathol.* **2011**, *60*, 133–149. [CrossRef]
15. Baas, P.; Ewers, F.W.; Davis, S.D.; Wheeler, E. A. The evolution of xylem physiology. In *The Evolution of Plant Physiology*; Hemsley, A.R., Poole, I., Eds.; Academic Press: London, UK, 2004; pp. 273–295.
16. Bradley, R.S. Natural archives, changing climates. *Science* **2011**, *7*, 21–25. [CrossRef]
17. Pandey, S. Climatic infuence on tree wood anatomy: A review. *Wood Sci.* **2021**, *67*, 24. [CrossRef]
18. Braun, H.J. The significance of the accessory tissues of the hydrosystem for water shifting as the second principle of water ascent, with some thoughts concerning the evolution of trees. *IAWA Bull.* **1984**, *5*, 275–294. [CrossRef]
19. Trockenbrodt, M. Calcium oxalate crystals in the bark of *Quercus robur*, *Ulmus glabra*, *Populus tremula* and *Betula pendula*. *Ann. Bot.* **1995**, *75*, 281–284. [CrossRef]
20. Pfautsch, S.; Renard, J.; Tjoelker, M.G.; Salih, A. Phloem as capacitor: Radial transfer of water into xylem of tree stems occurs via symplastic transport in ray parenchyma. *Plant Physiol.* **2015**, *167*, 963–971. [CrossRef]
21. Plavcová, L.; Jansen, S. The role of xylem parenchyma in the storage and utilization of non-structural carbohydrates. In *Functional and Ecological Xylem Anatomy*; Hacke, U.G., Ed.; Springer: Basel, Switzerland, 2015; pp. 209–234. [CrossRef]
22. Deflorio, G.; Johnson, C.; Fink, S.; Schwarze, F.M.W.R. Decay development in living sapwood of coniferous and deciduous trees inoculated with six wood decay fungi. *For. Ecol. Manag.* **2008**, *255*, 2373–2383. [CrossRef]
23. Nawrot, M.; Pazdrowski, W.; Szymanski, M. Dynamics of heart-wood formation and axial and radial distribution of sapwood and heartwood in stems of European larch (*Larix decidua* Mill.). *J. For. Sci.* **2008**, *54*, 409–417. [CrossRef]
24. Reiterer, A.; Burgert, I.; Sinn, G.; Tschegg, S. The radial reinforcement of the wood structure and its implication on mechanical and fracture mechanical properties—A comparison between two tree species. *J. Mater. Sci.* **2002**, *37*, 935–940. [CrossRef]
25. Nakata, P.A. Plant calcium oxalate crystal formation, function, and its impact on human health. *Front. Biol.* **2012**, *7*, 254–266. [CrossRef]
26. Franceschi, V.R.; Horner, H.T. Calcium oxalate crystals in plants. *Bot. Rev.* **1980**, *46*, 361–427. [CrossRef]
27. Ruiz, N.; Ward, D.; Saltz, S. Responses of *Pancratium sickenbergeri* to simulated bulb herbivory: Combining defence and tolerance strategies. *J. Ecol.* **2002**, *90*, 472–479. [CrossRef]

28. Volk, G.M.; Lynch-Holm, V.J.; Kostman, T.A.; Goss, L.J.; Franceschi, V.R. The role of druse and raphide calcium oxalate crystals in tissue calcium regulation in *Pistia stratiotes* leaves. *Plant Biol.* **2008**, *4*, 34–45. [CrossRef]
29. Serdar, B.; Demiray, H. Calcium oxalate crystal types in three oak species (*Quercus* L.). *Turkey. Turk. J. Biol.* **2012**, *36*, 386–393.
30. Morris, H.; Plavcová, L.; Cvecko, P.; Fichtler, E.; Gillingham, M.A.F.; Martinez-Cabrera, H.I.; McGlinn, D.J.; Wheeler, E.; Zheng, J.; Ziemińska, K.; et al. A global analysis of parenchyma tissue fractions in secondary xylem of seed plants. *New Phytol.* **2016**, *209*, 1553–1565. [CrossRef]
31. Schwartz, F.W.M.R.; Fink, S.; Deflorio, G. Resistance of parenchyma cells in wood degraded by brown rot fungi. *Mycol Prog.* **2003**, *2*, 26–74. [CrossRef]
32. Soheili, F.; Woodward, S.; Almasi, I.; Abdul-Hamid, H.; Naji, H.N. Variations in Wood Density, Annual Ring Width and Vessel Properties of *Quercus brantii* Affected by Crown Dieback. *Forests* **2021**, *12*, 642. [CrossRef]
33. Lloret, F.; Martinez-Vilalta, J.; Serra-Diaz, J.M.; Ninyerola, M. Relationship between projected changes in future climatic suitability anddemographic and functional traits of forest tree species in Spain. *Clim. Chang.* **2013**, *120*, 449–462. [CrossRef]
34. Polle, A.; Chen, S.L.; Eckert, C.; Harfouche, A. Engineering Drought Resistance in Forest Trees. *Front. Plant Sci.* **2019**, *9*, 1875. [CrossRef]
35. Fischer, U.; Kucukoglu, M.; Helariutta, Y.; Bhalerao, R.P. The Dynamics of Cambial Stem Cell Activity. *Annu. Rev. Plant Biol.* **2019**, *70*, 293–319. [CrossRef] [PubMed]
36. Fischer, U.; Polle, A. Populus responses to abiotic stress. In *Genetics and Genomics of Populus*; Jansson, S., Bhalerao, R., Groover, A., Eds.; Springer: Berlin, Germany, 2010; pp. 225–247. [CrossRef]
37. Nola, P.; Bracco, F.; Assini, S.; von Arx, G.; Castagneri, D. Xylem anatomy of *Robinia pseudoacacia* L. and *Quercus robur* L. is diferently afected by climate in a temperate alluvial forest. *Ann. For. Sci.* **2020**, *77*, 8. [CrossRef]
38. Seifert, G.J.; Blaukopf, C. Irritable walls: The plant extracellular matrix and signaling. *Plant Physiol.* **2010**, *153*, 467–478. [CrossRef]
39. Kesten, C.; Menna, A.; Sánchez-Rodríguez, C. Regulation of cellulose synthesis in response to stress. *Curr. Opin. Plant Biol.* **2017**, *40*, 106–113. [CrossRef]
40. Gaffal, K.H.; Mohnen, D. The structure, function, and biosynthesis of plant cell wall pectic polysaccharides. *Carbohydr. Res.* **2009**, *344*, 1879–1900. [CrossRef]
41. Zweifel, R.; Zimmermann, L.; Zeugin, F.; Newbery, D.M. Intra annual radial growth and water relations of trees: Implications towards a growth mechanism. *J. Exp. Bot.* **2006**, *57*, 1445–1459. [CrossRef] [PubMed]
42. Steppe, K.; Lemeur, R. Effects of ring-porous and diffuse-porous stem wood anatomy on the hydraulic parameters used in a water flow and storage model. *Tree Physiol.* **2007**, *27*, 43–52. [CrossRef]
43. Hacke, U. *Functional and Ecological Xylem Anatomy*; Springer: Berlin/Heidelberg, Germany, 2015; ISBN 978-3-319-15783-2.
44. Wildhagen, H.; Paul, S.; Allwright, M.; Smith, H.K.; Malinowska, M.; Schnabel, S.K.; Paulo, M.J.; Cattonaro, F.; Vendramin, V.; Scalabrin, S.; et al. Genes and Gene Clusters Related to Genotype and Drought-Induced Variation in Saccharification Potential, Lignin Content and Wood Anatomical Traits in Populus Nigra. *Tree Physiol.* **2018**, *38*, 320–339. [CrossRef]
45. Yu, D.; Janz, D.; Zienkiewicz, K.; Herrfurth, C.; Feussner, I.; Chen, S.; Polle, A. Wood Formation under Severe Drought Invokes Adjustment of the Hormonal and Transcriptional Landscape in Poplar. *Int. J. Mol. Sci.* **2021**, *22*, 9899. [CrossRef]
46. Fonti, P.; García-González, I. Earlywood vessel size of oak as potential proxy for spring precipitation in mesic sites. *J. Biogeogr.* **2008**, *35*, 2249–2257. [CrossRef]
47. Eilmann, B.; Weber, P.; Rigling, A.; Eckstein, D. Growth reactions of Pinus sylvestris L. and Quercus pubescens Willd. to drought years at a xeric site in Valais, Switzerland. *Dendrochronologia* **2006**, *23*, 121–132. [CrossRef]
48. Roushani Nia, F.; Naji, H.R.; Bazgir, M.; Naderi, M. Effect of Simulated Dust Storm on some Bio-chemical features of Persian Oak (*Quercus brantii* Lindl.). *Envirn. Eros. Res.* **2018**, *29*, 59–73. (In Farsi)
49. Naji, H.R.; Taher Pour, M. The effect of simulated dust storm on wood development and leaf stomata in *Quercus brantii* L. *Desert* **2019**, *24*, 43–49. [CrossRef]
50. Aloni, R.; Zimmermann, M.H.Z. The control of vessel size and density along the plant axis. A new hypothesis. *Differentiation* **1983**, *24*, 203–208. [CrossRef]
51. Evert, R.F.; Eichhorn, S.E. *Esau's Plant Anatomy: Meristems, Cells, and Tissues of the Plant Body: Their Structure, Function, and Development*; John Wiley and Sons, Inc.: Hoboken, NJ, USA, 2006.
52. Wheeler, E.A.; Bass, P.; Rodgers, S. Variations in dicot wood anatomy: A global analysis based on the Inside Wood database. *IAWAJ.* **2007**, *28*, 229–248. [CrossRef]
53. Hölttä, T.; Vesala, T.; Perämäki, M.; Nikinmaa, E. Refilling of embolised conduits as a consequence of 'Munch water' circulation. *Funct. Plant Biol.* **2006**, *33*, 949–959. [CrossRef] [PubMed]
54. von Arx, G.; Arzac, A.; Olano, J.M.; Fonti, P. Assessing Conifer Ray Parenchyma for Ecological Studies: Pitfalls and Guidelines. *Front. Plant Sci.* **2015**, *6*, 1016. [CrossRef]
55. Safdari, V.; Golchinfar, M. Comparative wood anatomy of Wyche Elm, English Elm, Caucasian Elm and Hackberry. *Iran. J. Wood Pap. Sci. Res.* **2011**, *26*, 564–578. (In Farsi)
56. Torkaman, J.; Ghodskhah Daryaee, M.; Zolghadry, S.H. The Role of Xylem Vessel Size and Ray Traits in Dutch Elm Disease Frequency in Ulmaceae. *J. For. Wood Prod.* **2014**, *67*, 453–462. (In Farsi)

57. Martin, J.A.; Solla, A.; Esteban, L.G. Borderd pit and ray morphology involment in elm resistance to *ophiostoma novo-ulmi*. *Can. J. For. Res.* **2009**, *39*, 420–429. [CrossRef]
58. Schenk, H.J.; Espino, S.; Goedhart, C.M.; Nordenstahl, M.; Martinez-Cabrera, H.I.; Jones, C.S. Hydraulic integration and shrub growth form linked across continental aridity gradients. *Proc. Natl. Acad. Sci. USA* **2008**, *105*, 11248–11253. [CrossRef]
59. Knipfer, T.; Cuneo, I.F.; Brodersen, C.R.; McElrone, A.J. In-situ visualization of the dynamics in xylem embolism formation and removal in the absence of root pressure: A study on excised grapevine stems. *Plant Physiol.* **2016**, *171*, 1024–1036. [CrossRef]
60. Jupa, R.; Plavcová, L.; Gloser, V.; Jansen, S. Linking xylem water storage with anatomical parameters in fivetemperate trees pecies. *Tree Physiol.* **2016**, *36*, 756–769. [CrossRef]
61. Esau, K. *Plant Anatomy*; McGraw-Hill: New York, NY, USA, 1965; p. 567.
62. Biggs, A.R. Occurrence and location of suberin in wound reaction zones in xylem of 17 tree species. *Phytopathology* **1987**, *77*, 718–725. [CrossRef]
63. Schilling, J.S.; Jellison, J. Oxalate regulation by two brown rot fungi decaying oxalate-amended and non-amended wood. *Holzforschung* **2005**, *59*, 681–688. [CrossRef]
64. Hatakka, A.; Hammel, K.E. Fungal Biodegradation of Lignocelluloses. In *Industrial Applications. The Mycota*; Hofrichter, M., Ed.; Springer: Berlin/Heidelberg, Germany, 2011; Volume 10. [CrossRef]
65. Penninckx, V.; Glineur, S.; Gruber, W.; Herbauts, J.; Meerts, P. Radial variations in wood mineral element concentrations: A comparison of beech and pedunculate oak from the Belgian Ardennes. *Ann. For. Sci.* **2001**, *58*, 253–260. [CrossRef]
66. Ghazanfari, H.; Namiranian, M.; Sobhani, H.; Marvi Mohajer, R. Traditional forest management and its application to encourage public participation for sustainable forest management in the northern Zagros Mountains of Kurdistan Province, Iran. *Scand J Forest Res.* **2004**, *19*, 65–71. [CrossRef]
67. Ilam Meteorological Bureau. Available online: http://www.ilammet.ir/ (accessed on 20 August 2018).
68. Menati, T.; Bazgir, M.; Rostaminya, M.; Mahdavi, A. Chemical and physical characteristics of oak forest soils in different climates in Ilam Province. *Iran. J. For.* **2019**, *10*, 449–460.
69. Ruzin, S.E. *Plant Microtechnique and Microscopy*; Oxford University Press: New York, NY, USA, 1999; 336p.
70. Gartner, H.; Schweingruber, F.H. *Microscopic Preparation Techniques for Plant Stem Analysis*; Verlag Dr. Kessel: Remagen, Germany, 2013; p. 78.
71. Camargo, M.A.B.; Marenco, R.A. Density, size and distribution of stomata in 35 rainforest tree species in Central Amazonia. *Acta Amaz.* **2011**, *41*, 205–212. [CrossRef]
72. Meng, Q.; Fu, F.; Wang, J.; He, T.; Jiang, X.; Zhang, Y.; Yin, Y.; Li, N.; Guo, J. Ray Traits of Juvenile Wood and Mature Wood: Pinus massonia and Cunninghamia lanceolata. *Forests* **2021**, *12*, 1277. [CrossRef]

MDPI
St. Alban-Anlage 66
4052 Basel
Switzerland
Tel. +41 61 683 77 34
Fax +41 61 302 89 18
www.mdpi.com

Plants Editorial Office
E-mail: plants@mdpi.com
www.mdpi.com/journal/plants

MDPI
St. Alban-Anlage 66
4052 Basel
Switzerland

Tel: +41 61 683 77 34

www.mdpi.com

ISBN 978-3-0365-7518-6